SEDIMENTOLOGY AND PROVENANCE OF THE DUNNOTTAR AND CRAWTON GROUPS, LOWER OLD RED SANDSTONE, KINCARDINESHIRE, SCOTLAND

Peter David William Haughton B.A.(Mod.)

A thesis submitted for the degree of Doctor of Philosophy at the Department of Geology, University of Glasgow

March 1986.

CONTENTS

The material presented herein is the result of independent research undertaken between October 1982 and March 1986 at the Scottish Universities Research and Reactor Centre (East Kilbride) and the Department of Geology, University of Glasgow. Any published or unpublished results of other workers have been given full acknowledgement in the text.

Peter Haughton.

Peter D.W. Haughton

ACKNOWLEDGEMENTS

The receipt of a University of Glasgow postgraduate scholarship is gratefully acknowledged.

I am grateful to Professor B.E. Leake for the provision of research facilities in the Department of Geology, University of Glasgow.

Dr B.J. Bluck initiated and supervised the project and provided much stimulating discussion and encouragement.

Isotope facilities at the SURRC are supported by NERC.
J.Jocelyn, Fiona McLaren and John Hutchinson provided technical instruction and support.
I am grateful to Dr A.N. Halliday for supervision and useful discussions.
Dr A. Dickin assisted with Pb isotope analyses.
Dr R.M. McIntyre kindly provided K-Ar analyses to complement the present study.

I would like to thank all members of the academic staff and research students of the Department of Geology, University of Glasgow for useful discussion, particularly Professor D.R. Bowes and Dr C. Farrow.
Thanks are also due to the technical staff especially Mr R. Morrison, Mr D. McLean, Mr G. Bruce, Mr D. McIntyre, Mr J. Gallagher and Mr R. McDonald.

I would like to express my gratitude to my parents for their encouragement and moral support.

Finally I would like to thank L. for many hours of much appreciated typing and for her patience and company.
To her I dedicate this thesis.

SUMMARY

The largely conglomeratic Dunnottar and Crawton Groups which make up the lower part of a thick Lower ORS succession developed in the NE Midland Valley of Scotland have been re-investigated. Two contrasting conglomerate lithosomes have been identified. These can be distinguished not only on the basis of their gross structure, but also by their mutually exclusive clast assemblages and contraposed palaeoflows. Conglomerates having an important recycled component and a predominantly northerly and north-easterly derivation are dominated by metaquartzite, psammite and granite detritus. Angular conglomerates of southerly and easterly provenance are of first cycle derivation and include clasts of lithic arenite, metagreywacke, granite, vesicular basalt and rare limestone. Andesitic and dacitic detritus occurs in conglomerates of both northerly and southerly provenance, and also makes up discreet volcanogenic units which comprise a third lithosome type.

The structure of the two conglomerate lithosomes is in both instances consistent with fluvial deposition. The contrasting structure and contraposed dispersal of coeval conglomerates are attributed to deposition on fluvial dominated fans prograding from opposite margins of a small laterally filled basin. The Dunnottar and Crawton Groups are consequently interpreted as having accumulated within a small tectonically active sub-basin (the Crawton Basin) stratigraphically beneath the more extensive Strathmore succession. Some features of the internal fill to this sub-basin are suggestive of deposition within a strike-slip controlled pull-apart basin. The basin overlies and may originally have nucleated on a substantial change in crustal structure, now revealed in the disparate clast assemblages dispersed from opposite margins of the basin. Large granite clasts are an important component in conglomerates with opposed dispersal patterns shed from separate terranes flanking the basin to the north and south. As the plutons from which the granite clasts were derived were emplaced into and interacted with the crust on either margin of the basin, geochemical, chronological and isotopic typing of the granite detritus allow constraints to

be placed on the nature of the inferred transition in crustal structure.

Granite clasts occurring in first-cycle conglomerates of southerly provenance are a unique sample of granites which can no longer be found in outcrop. The clasts were originally derived from a source terrane which during the late-Silurian early-Devonian occupied the east central Midland Valley. Four distinctive granite clast suites can be identified on the basis of field appearance and petrography. The subdivision into suites is substantiated by major and trace element analyses. A wide separation of coherent geochemical trends produced by clasts from each of the suites suggest derivation from separate high-level plutons. Rb-Sr mineral-whole rock isochrons for representative clasts establish an important sediment contribution from tonalite and granodiorite plutons with probable Silurian ages (420 $\pm$ 5 Ma) and low initial $^{87}Sr/^{86}Sr$ ratios (0.7044-0.7055). The Silurian ages indicate that granites of calc-alkaline affinity were emplaced in the Midland Valley at a time when magmatism was suppressed in the Grampian Highlands. The clasts fill a gap in a long history of magmatism within the Midland Valley Zone. They also record an important transition in the style of magmatism from dominantly plutonic to dominantly effusive. The wide range in magma chemistry evident between the clast suites at constant silica is unlike that seen in contemporary late Caledonian granite magmas. Isotopically the three Silurian clast suites appear to be closely related with very similar Pb and Nd isotope compositions and only slight variation in Sr. Significantly the Sr and Nd compositions of the granite clasts are similar to Lower ORS lava compositions. A model involving variable deep level fractionation, possibly linked with the oblique-slip tectonic framework in which the generation and emplacement of the magmas occurred, may account for the unusual chemistry of the clasts.

Granite clasts in northerly derived polycyclic conglomerates are chemically and isotopically distinct from those simultaneously dispersed from the southern margin of the basin. Chemical and isotopic data define an episodic magmatic history for the terrane from which the clasts of northerly provenance were derived. A

suite of c. 460 Ma two-mica granite clasts are distinguished from a late Silurian suite of evolved, fractionated high level granites with intermediate initial $^{87}Sr/^{86}Sr$ ratios (0.706). The magmatic history of the adjacent NE Grampian region bears a striking resemblance to that established for the granite clasts in the contiguous Crawton Basin. This suggests there is unlikely to have been large post-Lower ORS strike-slip displacements between the northern Midland Valley and the Grampian Highlands. As the Highland Border Complex and Grampian Highlands have to be widely separated during the Ordovician, lateral translation and juxtaposition of the terranes during the Silurian is envisaged. The Crawton Basin may have developed during the final approach of the two disparate blocks.

Sedimentary and metasedimentary clasts in conglomerates dispersed from opposite flanks of the basin serve to emphasise the contrast between the two sediment sources. Psammitic clasts of northerly and northeasterly provenance show evidence for an ultimate source in Grampian style metamorphic rocks. The psammitic clasts texturally, petrographically and geochemically resemble Upper Dalradian metasediments of the southern Highlands Group. Rb-Sr mica-whole rock closure ages from psammitic clasts closely parallel those in much of the adjacent Dalradian. Should the clasts have been derived from the Dalradian, the data require that the clasts were sourced from close to the present day erosion surface. Sm-Nd data for southerly derived lithic arenite and metagreywacke clasts denote the former presence of a thick sediment pile which isotopically appears to be unrelated to SULPS. High Cr and Ni abundances in many of the metagreywacke clasts indicate that the sediments originally contained an important ophiolitic component. The bulk crustal residence age of the source which contributed to the Midland Valley sequence was substantially older than that which contributed to SULPS, but not sufficiently old to indicate an ultimate provenance in metamorphic rocks of the Grampian Highlands.

Pb isotopic data for feldspar separates from granite clasts dispersed from opposite flanks of the basin show the basin to overlie a boundary between granites which to the south have more

radiogenic Pb compositions than those to the north. The northerly derived Ordovician and Silurian granite clasts have Pb isotopic compositions which are compatible with a source in granites of the NE Grampian region.

ABBREVIATIONS

CHUR	CHondritic Uniform Reservoir
CU	Coarsening Upwards
CR	Crustal Residence
DI	Differentiation Index
DM	Depleted Mantle
HFS	High Field Strength
LIL	Large Ion Lithophile
LOI	Loss On Ignition
LREE	Light Rare Earth Elements
MCS	Maximum Clast Size
MORB	Mid Oceanic Ridge Basalt
MSWD	Mean Square Weighted Deviate
OIB	Oceanic Island Basalt
ORS	Old Red Sandstone
PAAS	Post Archaean Australian Sediment
REE	Rare Earth Element
SULPS	Southern Uplands Lower Palaeozoic Sediment
SURRC	Scottish Universities Research and Reactor Centre

LIST OF FIGURES

LIST OF TABLES

LIST OF PLATES

CHAPTER ONE

INTRODUCTION

1.1 STRATIGRAPHIC FRAMEWORK

Late Silurian and Devonian sedimentary basins of terrestrial aspect occur widely in the North Atlantic region. Many are associated with unusually high rates of sedimentation and are bounded by faults on which large vertical displacements have occurred (Friend 1969, 1981). It is generally accepted that these basins reflect uplift and sedimentation characteristic of late or post-orogenic tectonism associated with the ending of the Caledonian Orogeny. The term Old Red Sandstone (ORS) has become synonymous with the continental sediments and volcanic rocks filling these basins.

The present study is concerned with aspects of the depositional history and provenance of ORS conglomerates preserved within a small basin associated with a major crustal fracture zone. In addition, the basin is flanked by rocks which are known to have been deformed, metamorphosed and uplifted during the Grampian Orogeny. The structural setting of the basin therefore allows the relationship between sedimentation and late- or post-orogenic tectonism to be examined in some detail.

The sediments considered form part of the extensive ORS deposits exposed in the Strathmore region of Central Scotland(Fig.1.1a). The upper levels of the Strathmore succession can be traced continuously from Stonehaven on the east coast to the Clyde on the west coast. In contrast the lower and older part of the succession is restricted to the north-east where it is well exposed in coastal cliff and foreshore outcrops in Kincardineshire (Fig. 1.2). It is this older and more restricted ORS sequence in Kincardineshire which has been the subject of the research reported in the following chapters.

1.1.1 Regional Setting

Sediments and volcanic rocks of ORS age outcrop widely in Scotland (Fig.1.1a). These attest to the former presence of a series of structurally controlled basins of varying style. Important fine grained lacustrine sediments characterise the fill to much of the Orcadian basin, but non-marine conglomerates and

FIGURE 1.1

(A)Distribution of Lower ORS sedimentary and volcanic rocks in mainland Scotland in relation to major tectonostratigraphic zones. Major faults bounding these zones are abbreviated MT - Moine Thrust; GGF - Great Glen Fault; HBFZ - Highland Boundary Fault Zone and SUF - Southern Uplands Fault.

(B)Conventional interpretation of the palaeogeography of the Midland Valley and Grampian Highlands during Lower ORS times. After Bluck (1978), Morton (1979), Armstrong and Paterson (1970), and Mykura (1983).

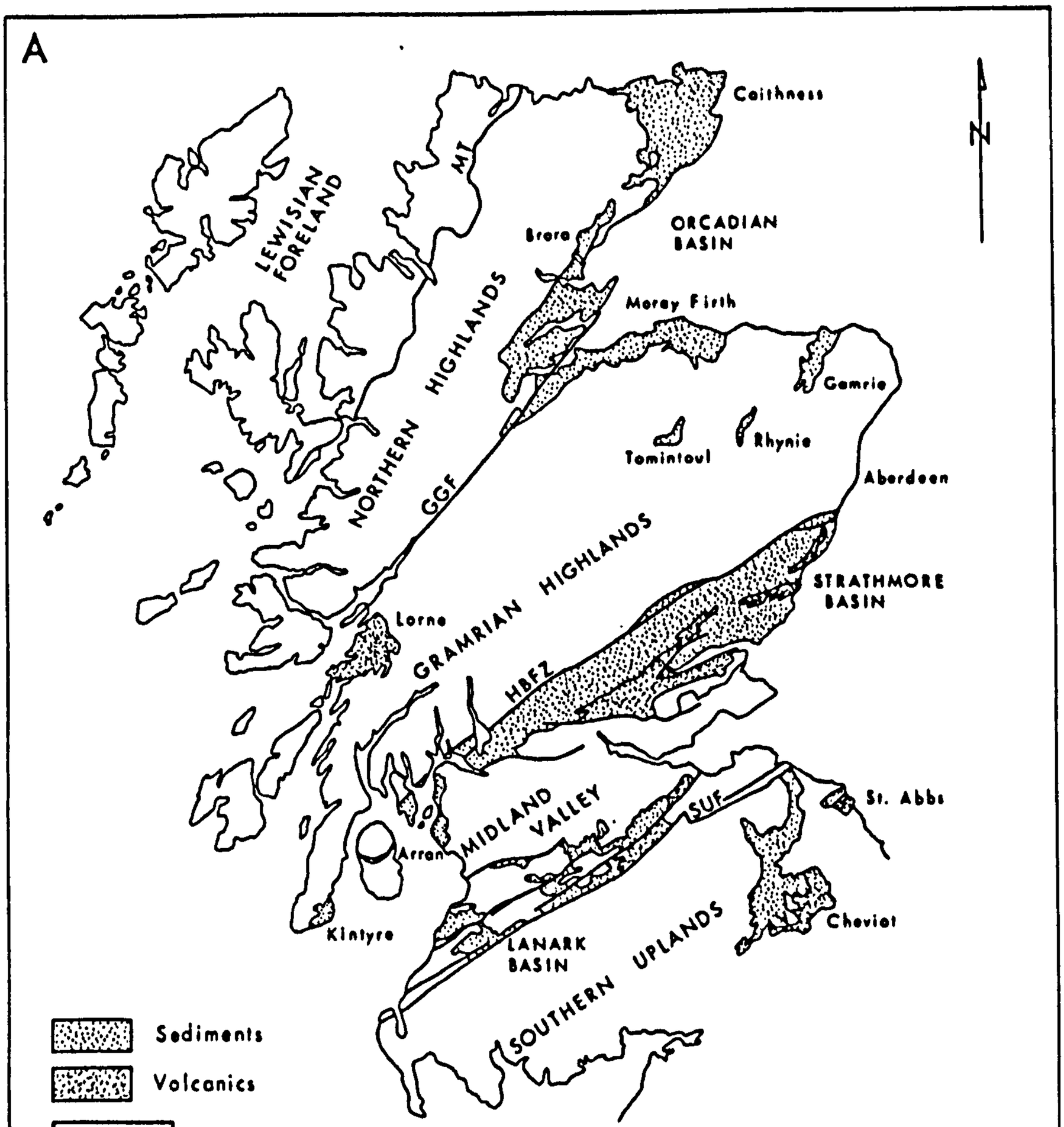
A
Caithness
N
LEWISIAN FORELAND
MT
NORTHERN HIGHLANDS
GGF
Brora
ORCADIAN BASIN
Moray Firth
Gamrie
Rhynie
Tomintoul
Aberdeen
GRAMPIAN HIGHLANDS
STRATHMORE BASIN
Lorne
HBFZ
MIDLAND VALLEY
SUF
St. Abbs
Arran
Kintyre
LANARK BASIN
SOUTHERN UPLANDS
Cheviot
Sediments
Volcanics
0
50 km.

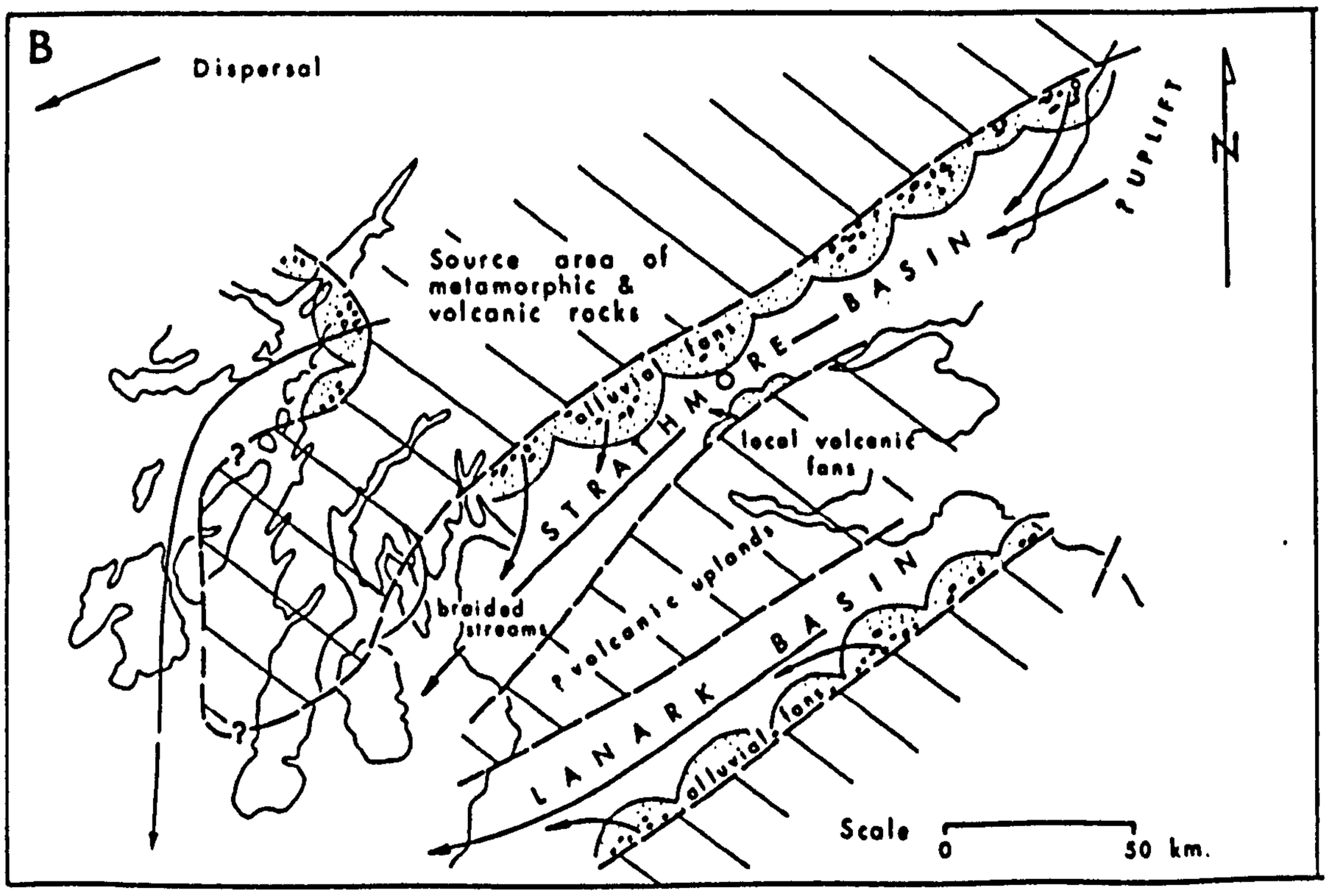
B
Dispersal
Source area of metamorphic & volcanic rocks
alluvial fans
STRATHMORE BASIN
PUPLIFT
N
local volcanic fans
volcanic uplands
braided streams
LANARK BASIN
alluvial fans
Scale
0
50 km.

sandstones dominate elsewhere. With the exception of the Lanark succession, the ORS unconformably overlies rocks which have been deformed and metamorphosed. Important unconformities also occur within the Scottish ORS, and these form the basis of a subdivision of the sequence into the Lower, Middle and Upper ORS (Murchison 1859). Whilst all three subdivisions are recognised in the Orcadian Basin, only the Lower and Upper ORS are present south of the Highland Boundary Fault where they are separated by a substantial unconformity.

The Midland Valley of Scotland includes extensive deposits of Lower ORS sedimentary and volcanic rocks. These occur in two belts which are outcrop bounded (terminology of Bluck 1978 Fig.7a) by the Southern Uplands and Highland Boundary Faults (Fig. 1.1). The northern belt is the most extensive of these outcrops and comprises a major syncline (the Strathmore Syncline) together with a complimentary, although faulted, anticline (the Sidlaw Anticline). The southern outcrop is smaller and less continuous, and is disrupted by sub-parallel NE trending faults. The two outcrop belts have been interpreted as the fill to separate elongate basins. Bluck (1978, 1983) considered that volcanic uplands associated with the Ochil-Sidlaw-Heads of Ayr volcanic axis played an important role in separating the Midland Valley Lower ORS into two discrete basins, a northerly Strathmore Basin, and a southerly Lanark Basin (Fig. 1.1b). Armstrong et al. (1985) however envisage sedimentation by braided streams in a basin which occupied the full width of the Midland Valley, with only local segmentation by volcanic uplands during deposition of the Arbuthnott Group.

The Lower ORS rocks exposed in the northern Midland Valley occupy an area of more than 4000km^2 (Fig. 1.2). They are bounded to the north by either an unconformable junction with the Highland Border Complex, or structural truncation on one of the many sub-parallel faults making up the Highland Boundary Fault Zone. To the south, they are either masked by the unconformable Upper ORS, or terminated by the Ochil Fault. The outcrop geometry is largely determined by the asymmetrical Strathmore Syncline, one of the longest continuous structures in the British Isles (Bluck

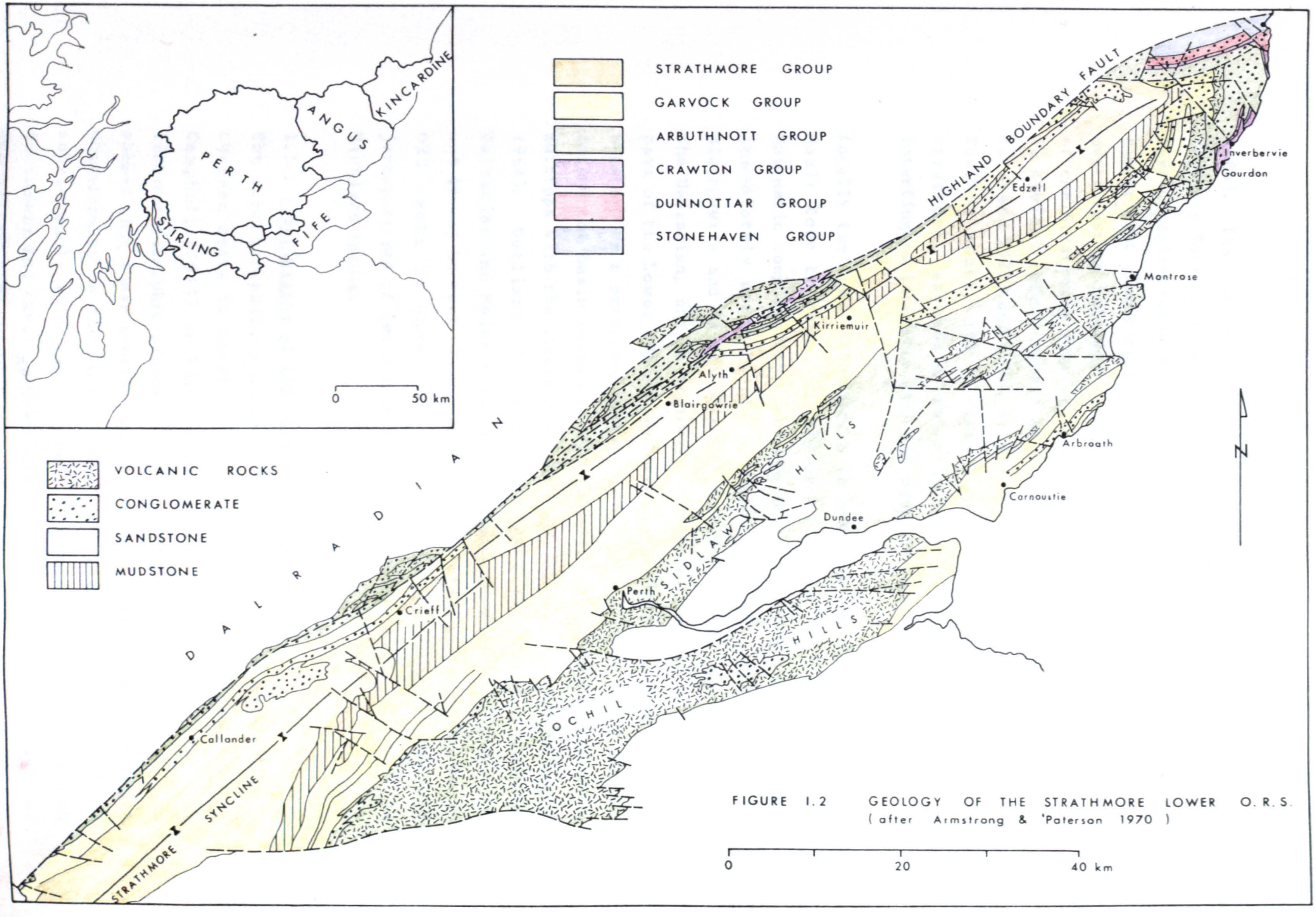

FIGURE 1.2 GEOLOGY OF THE STRATHMORE LOWER O.R.S.
(after Armstrong & Paterson 1970)

1984). Its north-western limb steepens towards the Highland Boundary Fault Zone and becomes vertical and locally overturned. Basal conglomerates and sandstones along this northwestern limb either rest unconformably on the Highland Border complex, or are overthrust by Dalradian metamorphic rocks. The southeastern limb of the Strathmore Syncline dips gently northwards. The syncline is divided into a number of axial culminations (Armstrong and Paterson 1970) and these appear to control the outcrop pattern. Further south, the Sidlaw Anticline, an open symmetrical structure, exposes a thick calc-alkaline lava pile which interfingers laterally with the conglomerates and sandstones.

Locally the Lower ORS appears to overstep the Highland Boundary Fault Zone to rest directly on Dalradian metamorphic rocks. Enigmatic conglomerates, sandstones and volcanic rocks occurring immediately north of the Highland Boundary Fault near both Blairgowrie and Crieff (Fig.1.2) rest with basal unconformity on the Dalradian, and on radiometric evidence (Thirlwall 1983a) are part of the Lower ORS succession. George (1960) regarded these outcrops as a preserved transgression over a fault which did not define the basin margin. More recently the continuity of these outcrops with the Strathmore Lower ORS has been questioned (Bluck 1984). Outliers of Lower and Middle ORS occur widely on Dalradian and Moine rocks in the Grampian Highlands (Fig.1.1), and it may be that these share a closer affinity with the Lower ORS rocks in question. This would require structural juxtaposition of two unrelated Lower ORS successions along the Highland Border.

1.1.2 Stratigraphy of the Strathmore Lower ORS

The stratigraphic subdivision of the Strathmore Lower ORS in current usage is based on a scheme originally established by Campbell (1913) in Kincardineshire. Campbell defined five lithostratigraphic groups in the Lower ORS of this district, and showed that these overlie Downtonian rocks which rest with basal unconformity on the Highland Border Complex. Allan (1928, 1940) subsequently extended Campbell`s nomenclature to Lower ORS sediments and lavas in the Blairgowrie and Crieff districts of the Highland Border. More recently, Armstrong and Paterson

(1970) modified and expanded the Kincardineshire stratigraphy to accommodate all the Strathmore Lower ORS between the east coast and Loch Lomond. Their stratigraphic framework has been adopted in many subsequent studies (Morton 1976, Wilson 1980).

Correlation within the Strathmore Lower ORS is necessarily largely lithostratigraphic. Although the terrestrial sandstones and conglomerates have locally yielded important vertebrate fossils, these tend to be stratigraphically restricted. Consequently there is no rigorous palaeontological control on correlation across the outcrop. The validity of tracing lithostratigraphic groups for over 180km along strike is therefore open to question. Many of the boundaries are likely to be diachronous and correlation is further complicated by the poor exposure, considerable structural complexity, and the likelihood of complex original stratigraphical and sedimentological interrelationships. However notwithstanding the uncertainties implicit in many of the correlations, the lithostratigraphic approach has highlighted broad regional variation in the Strathmore succession.

Armstrong and Paterson (1970) recognised six major lithostratigraphic groups (Fig.1.4). These are, in ascending sequence, the Stonehaven, Dunnottar, Crawton, Arbuthnott, Garvock and Strathmore Groups. Of these, only the latter three can be recognised throughout the Strathmore sequence. The Stonehaven, Dunnottar and Crawton Groups are restricted to Kincardineshire, where the succession appears to be anomalously thick. Campbell originally estimated the sequence to be 6630m thick. Armstrong and Paterson (1970) considered 9000m to be a more appropriate estimate. This contrasts with the much thinner Lower ORS sequences along strike to the west. Friend *et al.* (1963) establish the Lower ORS on Arran to be of the order of 1500m thick. Bluck (1984) shows that the Lower ORS rests unconformably on the Highland Border Complex. An unconformity is also seen at Aberfoyle (Curry *et al.* 1982, 1984). The significance of this basal unconformity rests on the fact that thick Lower ORS sequences can no longer be projected around the Strathmore syncline to abut against the Highland Boundary Fault at depth.

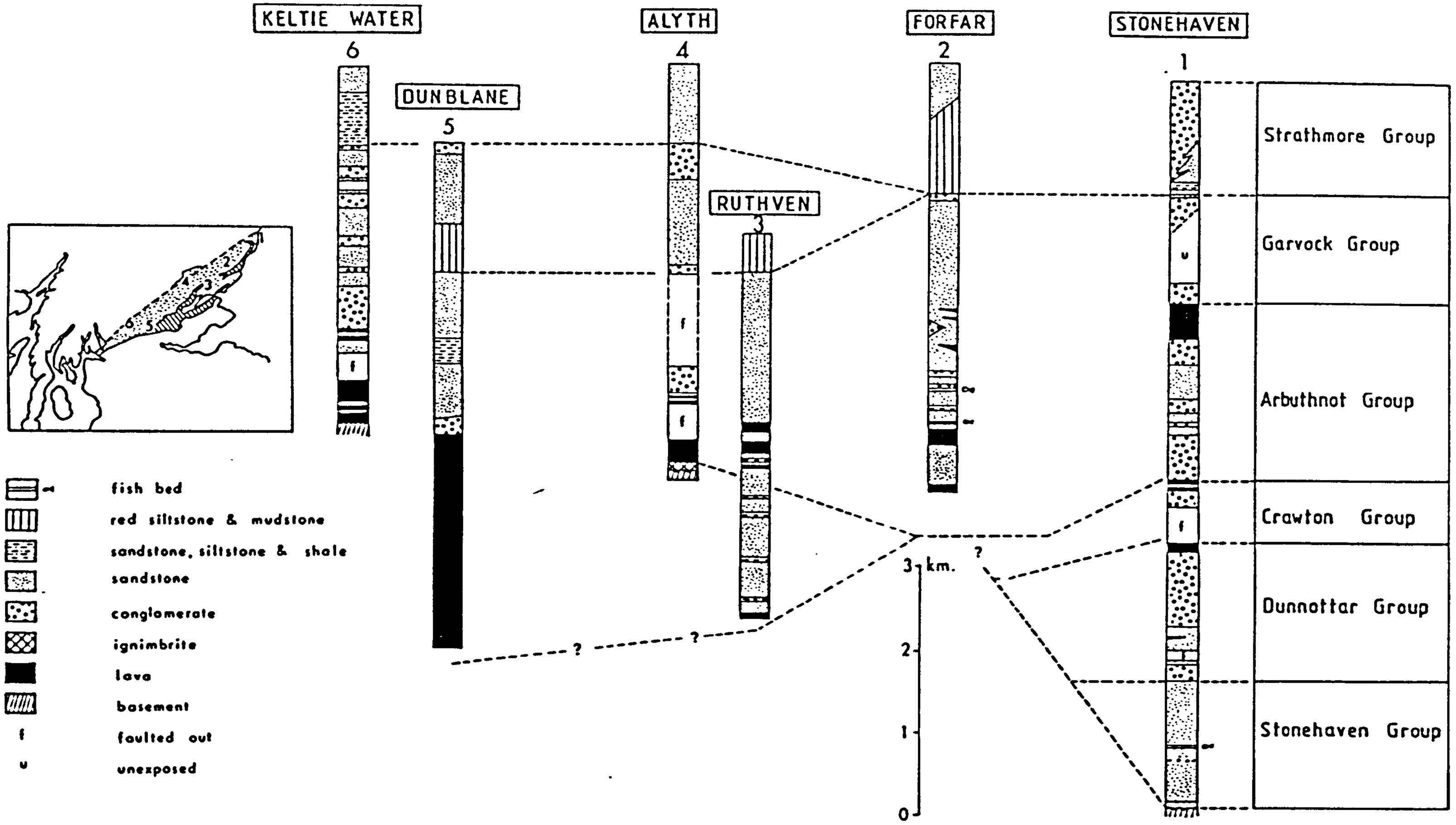

FIGURE 1.3 Comparative sections through the Lower ORS of the Strathmore region indicating correlation and progressive south-westerly overstep. Based on stratigraphic synthesis by Armstrong and Paterson (1970).

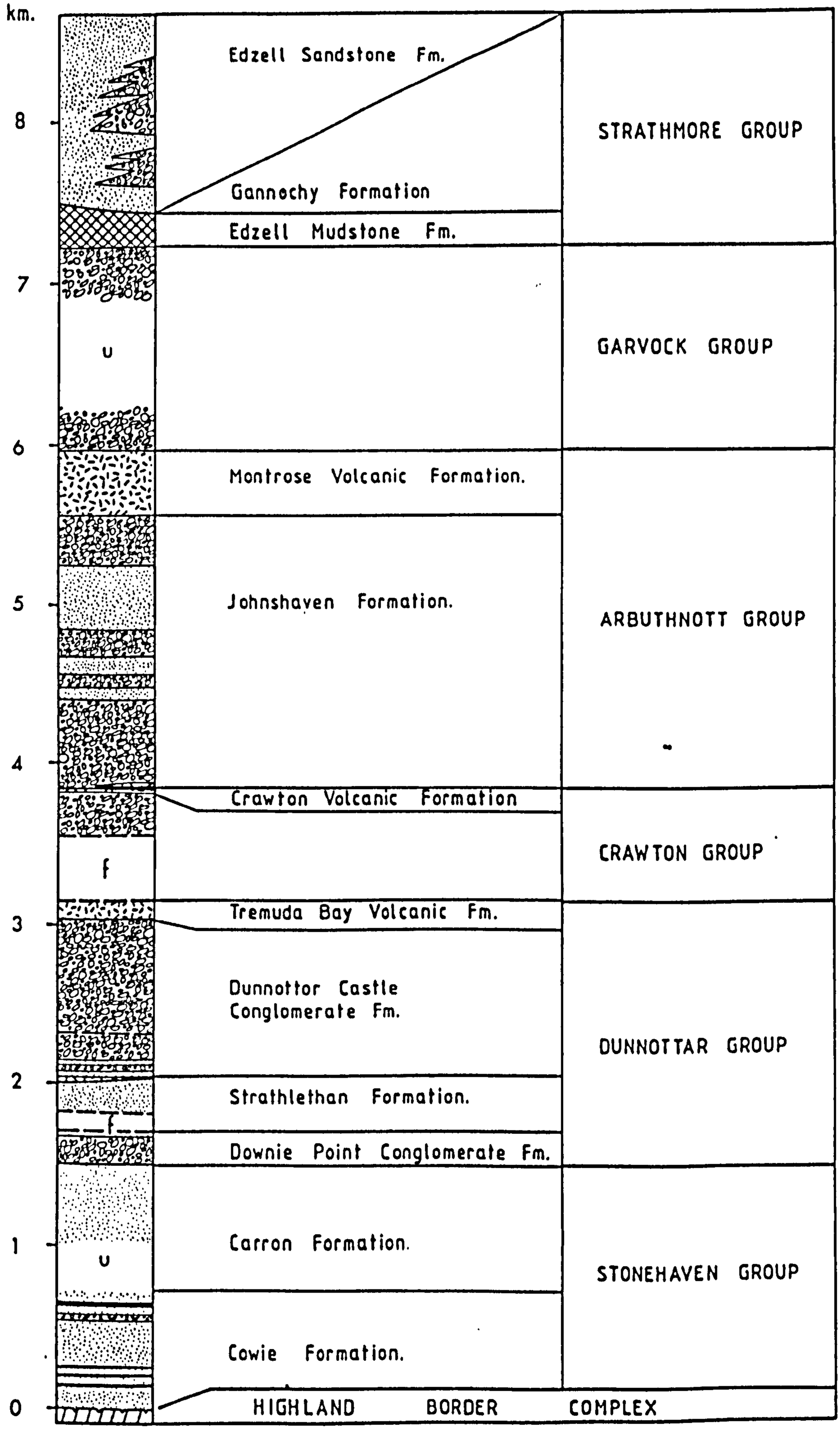

FIGURE 1.4 Informal stratigraphic nomenclature for the Lower ORS of Kincardineshire (after Armstrong and Paterson 1970). u: unexposed. f: faulted out.

The western extension of the Strathmore succession is therefore unlikely to be much in excess of 1-2km thick.

The along-strike variation in thickness has been related to a westerly overstep of successively younger lithostratigraphic groups (Fig.1.3). Bryhni (1964) explained the restricted distribution of the lower lithostratigraphic groups by invoking a lateral migration of the basin depocentre to the southwest. Paterson and Harris (1969) re-interpreted a dacitic lava flow outcropping at Glenbervie close to the top of the Crawton Group as a remnant of a previously extensive ignimbrite sheet. They correlate the Glenbervie ignimbrite with the Lintrathen porphyry at Dunkeld, where ignimbritic rocks unconformably overlie the Dalradian. Assuming the correlation to be correct, the Stonehaven, Dunnottar and Crawton Groups are therefore overstepped towards the southwest (Armstrong and Paterson 1970). However, as the Dunkeld and Glenbervie ignimbrite localities are to the north and south of the Highland Boundary Fault Zone respectively, their correlation across the fault must necessarily be subject to some uncertainty.

1.1.3 Depositional Environment of the Strathmore ORS

Studies by Wilson (1971, 1980), Morton (1976, 1979) and Bluck (1978) have emphasised the dominant role of fluvial processes in generating the range of sedimentary rocks seen in the Strathmore Lower ORS. A feature of the Strathmore ORS is the tendency for the sediments to coarsen and become increasingly dominated by conglomerates as they are traced towards the Highland Border. Friend and MacDonald (1978), Wilson (1971) and Morton (1976) demonstrate that for the region between Crieff and Kintyre, directional structures in conglomerates adjacent to the Highland Border indicate dispersal was to the south east, normal to the fault zone. These conglomerates interfinger with finer grained sediments in which cross-stratal dips record palaeoflows towards the south-west. Palaeocurrents in conglomerates almost perpendicular to those of intertongueing finer sediments are commonly recorded in basins which are both longitudinally and laterally filled (Bluck 1978).

Armstrong et al. (in Friend and Williams 1978) note an increase in the abundance and grainsize of conglomerates when the Arbuthnott and Garvock Groups are traced northeastwards along the basin axis into Kincardineshire. They argue that the bulk of the sediment dispersed to the basin during deposition of the Arbuthnott and Garvock Groups was shed from a basin margin which lay to the east of the present coastline of Angus and Kincardineshire.

The concept of deposition within a single laterally and longitudinally filled basin has however to be substantially modified in the light of a revision of the palaeocurrent data by Bluck (1984). Whilst conglomerates in the upper part of the succession vindicate earlier dispersal studies, those towards the base of the Strathmore sequence in the Highland Border region have a dispersal contrary to that previously recorded. Thus conglomerates outcropping above the basal unconformity on Highland Border Complex rocks east of Loch Lomond have a dispersal towards the north-west. These must be accommodated by an earlier basin, the axial zone of which must have been located north of the Highland Boundary Fault in the present position of the Scottish Highlands. A significant change in the geometry of the Strathmore Basin with time is implied. Indeed it may be inappropriate to consider the Strathmore succession as the fill to a single basin as it may be that two or more essentially separate red-bed basins have been vertically amalgamated.

1.1.4 Lower Old Red Sandstone of Kincardineshire

Lower ORS sediments and volcanic rocks of Kincardineshire outcrop over an area of in excess of 420km^2 (Fig.1.5). The outcrop is bounded to the south-west by the River North Esk, to the east by the North Sea, and to the north-west by the Highland Border. All six of the lithostratigraphic groups into which the Strathmore succession has been subdivided are recognised in this the thickest development of the Lower ORS in Britain. The four lower groups, the Stonehaven, Dunnottar, Crawton and Arbuthnott Groups are particularly well exposed in coastal sections which, although locally inaccessible, extend almost continuously from Stonehaven to Montrose. The following stratigraphic account is based

FIGURE 1.5 Geological Map of SE Kincardineshire. Modified after Campbell (1913) and Armstrong and Paterson (1970)

KEY

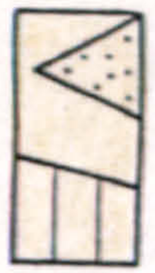

Conglomerate
Sandstone
Mudstone

STRATHMORE GROUP

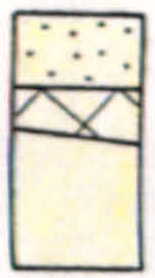

Conglomerate
Olivine basalt
Sandstone

GARVOCK GROUP

Hypersthene andesite and basalt
Conglomerate/sandstone
Hornblende and augite andesite

ARBUTHNOTT GROUP

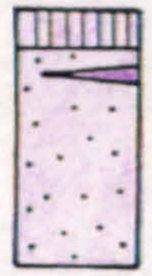

Crawton type basalt
Ignimbrite
Conglomerate

CRAWTON GROUP

Tremuda Bay basalt
Conglomerate/sandstone

DUNNOTTAR GROUP

Sandstone

STONEHAVEN GROUP

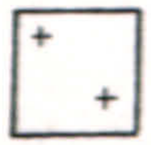

Kincardine Granite

Quartz porphyry intruding Dalradian metasediments

Highland Border Complex

FAULT

Strathmore Syncline

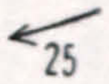

Dip arrow

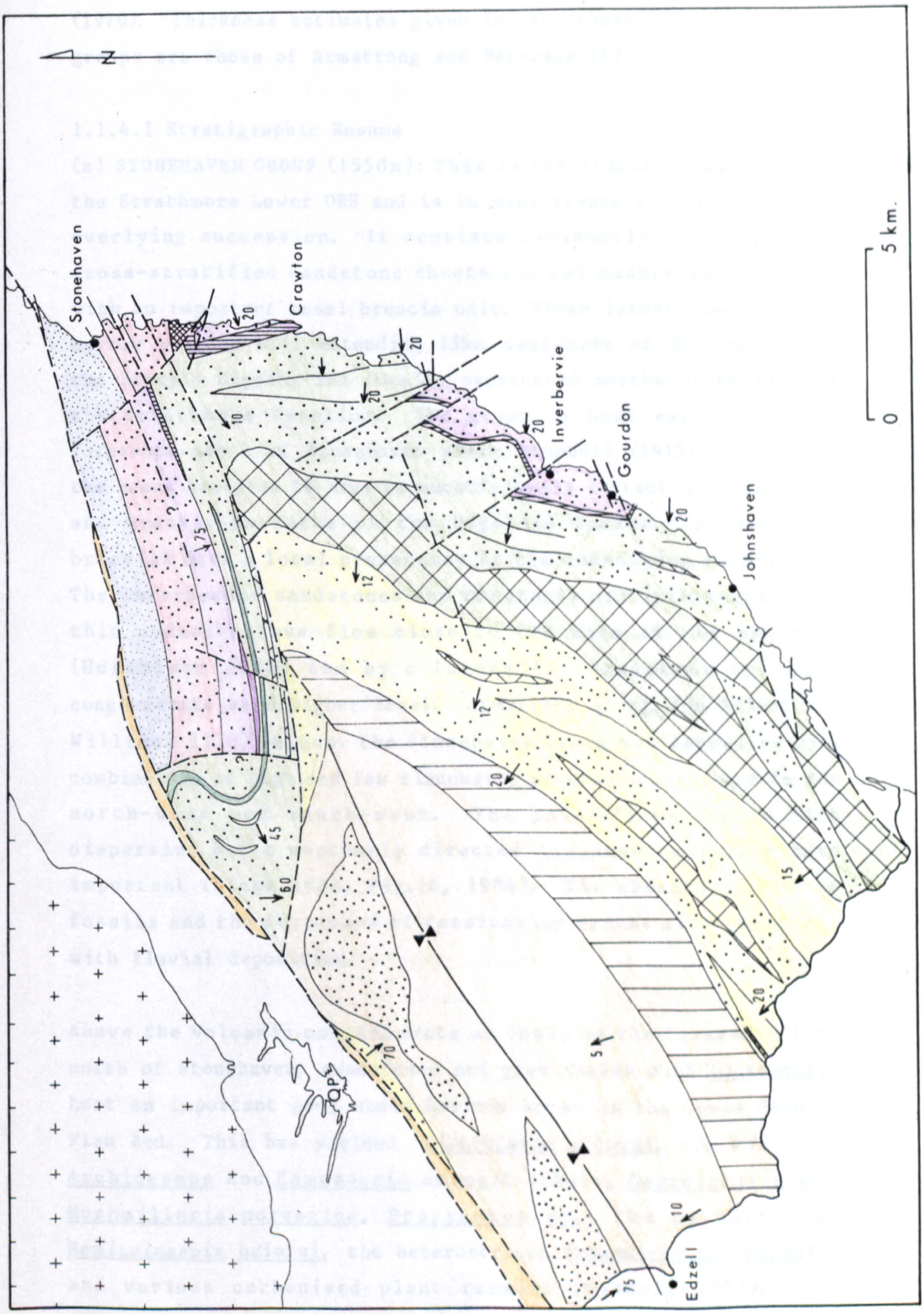
N
Stonehaven
Crawton
Inverbervie
Gourdon
Johnshaven
Edzell
OP
0
5 km.

largely on the work of Campbell (1913) and Armstrong and Paterson (1970). Thickness estimates given in parentheses for each of the groups are those of Armstrong and Paterson (1970).

1.1.4.1 Stratigraphic Resume

(a) STONEHAVEN GROUP (1550m): This is the oldest subdivision of the Strathmore Lower ORS and is in many respects atypical of the overlying succession. It consists dominantly of interbedded cross-stratified sandstone sheets and red mudstones, together with an important basal breccia unit. These lithologies occupy a narrow outcrop belt extending 13km westwards of Stonehaven, on the steeply dipping and locally overturned northwestern limb of the Strathmore Syncline. The group is best exposed on the foreshore north of Stonehaven where Campbell (1913) established the basal breccias to have an unconformable contact with Cambrian and Ordovician rocks of the Highland Border Complex. The breccias have a local provenance in the underlying rock-types. The interbedded sandstones and mudstones are interrupted by a thin andesite lava flow close to the base of the sequence (Hutchison 1928) and by a laterally persistent volcanic conglomerate at a higher level. Armstrong et al. (in Friend and Williams 1978) suggest the Stonehaven Group was deposited by a combination of high and low sinuousity rivers from sources to the north-west and south-west. The palaeoflows show a high dispersion but a northerly directed component may have been important (Bluck 1983, Fig.16, 1984). The absence of marine fossils and the abundance of dessication cracks are consistent with fluvial deposition.

Above the volcanic conglomerate at Cowie on the foreshore just north of Stonehaven, sandstones and grey shales with Dictyocaris host an important grey shale horizon known as the Cowie Harbour Fish Bed. This has yielded Dictyocaris slimoni, the myriapods Archidesmus and Kampecaris amongst others, Ceratiocaris sp., Hughmilleria norvegica, Pterygotus sp., the osteostracan Hemiteleaspis heintzi, the heterostracan Traquairaspis campbelli and various carbonised plant remains (Westoll 1977). The occurrence of Ceratiocaris is of interest. Most phyllocarids have been described from restricted shallow and near-shore marine

environments (Rolfe and Beckett 1984).

Campbell (1913) and Armstrong and Paterson (1970) differ in their definition of the top of the Stonehaven Group. Campbell (1913) excluded from his Stonehaven Beds several hundred metres of sandstones and pebbly sandstones which stratigraphically intervene between the Cowie sequence and the first of the coarse boulder conglomerates. These he assigned to the Dunnottar Group. Armstrong and Paterson (1970) subdivided the Stonehaven Group into two formations, a lower Cowie Formation and an upper Carron Formation. The latter includes all sandstones up to the appearance of coarse conglomerates at Downie Point. Armstrong and Paterson (1970) justify this subdivision on the grounds that the incoming of the coarse conglomerates marks the most significant event in the history of sedimentation, and that the redefined base to the Dunnottar Group is more readily mapped. Whilst the latter is not disputed, the Carron Formation sandstones resemble sandstones intercalated with the conglomerates at higher stratigraphic levels. They share the same south-west early dispersal as the conglomerates into which they conformably pass. They also contain many scattered pebbles of metaquartzite. If the criteria for defining the boundary between the Stonehaven and Dunnottar Groups is a significant change in the nature of sediment deposition, Campbell`s original definition is more logical in that it distinguishes sediments of very different character.

(b) DUNNOTTAR GROUP (1660m): Conglomerates and subordinate sandstones of the Dunnottar Group outcrop in continuous foreshore and cliff exposures for 2km south of Stonehaven, and for 13km west-south-westwards along the poorly exposed steeply dipping north-west limb of the Strathmore Syncline (Fig.1.5). The Dunnottar Group is almost totally devoid of fossils with the exception of a record of Parka sp. from sandstones in Strathlethan Bay (Campbell 1913), and a single acanthodian spine (Westoll 1951). The top of the Dunnottar Group is taken as the uppermost of several olivine basalt lava flows which make up the Tremuda Bay Volcanic Formation (Armstrong and Paterson 1970). These have been correlated with a single flow of similar

composition outcropping at Todhead (Campbell 1913, Armstrong and Paterson 1970).

(c) CRAWTON GROUP (>670m): The Crawton Group comprises a varied assemblage of conglomerates and sandstones which are thought to intervene between the Tremuda Volcanic Formation and a group of distinctive macroporphyritic lava flows collectively termed the Crawton Volcanic Formation (Armstrong and Paterson 1970). These olivine basalt and basic andesite lava flows form one of the few persistent marker horizons allowing correlation of sequences on both north-western and south-eastern limbs of the Strathmore Syncline. The distinctive Crawton-type lavas can be traced for 12km through heavily-faulted ground from south of Gourdon to Upper Criggie (Grid Ref. NO 833830). The Crawton Group is poorly exposed on the north-west limb of the Strathmore Syncline but includes an ignimbrite of dacitic composition at Glenbervie according to Paterson and Harris (1969). Exposures of the Crawton Group beneath the Crawton Lavas at Crawton Bay, and in cliff sections northwards to Thornyhive Bay are partly inaccessible and only expose the upper part of the group. A fuller sequence is exposed in coastal exposures between Whistleberry and Gourdon.

(d) ARBUTHNOTT GROUP (2100m): The Arbuthnott Group in Kincardineshire can be subdivided into two formations. The Lower Johnshaven Formation is largely conglomeratic and directly overlies the Crawton Volcanic Formation. It is well exposed in coastal sections between Gourdon and Johnshaven, and between Crawton and Whistleberry. It includes important northerly derived metaquartzite-bearing conglomerates, some of which are exceedingly coarse, together with volcaniclastic sandstones and thin lava flows. Sediments of the Johnshaven Formation are overlain by, and are partly equivalent to a sequence of olivine basalt and basic andesite lavas, collectively termed the Montrose Volcanic Formation. The top of the Arbuthnott Group is taken at the top of the highest lava-member. The lava sequence thins northwards and is the feather edge of a substantial lava pile to the south-south-west. Armstrong and Paterson (1970) correlate the Kincardineshire Arbuthnott Group sequence with lava dominated

sequences elsewhere. In the Ochil Hills the Arbuthnott Group consists almost entirely of extrusive rocks and associated volcanic sediments. The coarse conglomerates making up the Johnshaven Formation are replaced south-westwards in Angus by cross-stratified and thin-bedded sandstones of the Dundee Formation.

(e) GARVOCK GROUP (1525m): The term Garvock Group was used by Campbell (1913) to distinguish a dominantly conglomeratic sequence intervening between the lavas which define the top of the Arbuthnott Group, and the distinctive calcareous mudstones of the Strathmore Group. Armstrong and Paterson (1970) have since extended the outcrop of the group to include all strata at a similar level throughout the Strathmore region. In Kincardineshire, the sandstones which characterise the outcrop of the group elsewhere are largely replaced by conglomerates . Flows of basalt and andesite lava occur at several positions in the sequence, including in the Bervie Water (NO 777747) and on the Hill of Garvock (NO 740710). Close to the top of the group there is a thin but persistent zone of concretionary carbonate, locally termed the `Pittendriech Limestone`. This can be traced extensively and forms a useful marker horizon.

(f) STRATHMORE GROUP (2000m): The Strathmore Group includes the youngest of the Lower ORS sediments preserved in the Strathmore region. These occupy the axial zone of the Strathmore Syncline. The Strathmore Group consists predominantly of grey and purplish grey sandstones with conglomerates, but is characterised by the development in its lower half of bright or dull red, mottled calcareous mudstones. These are laterally very extensive and can be traced throughout much of the Strathmore Lower ORS. The base of the Strathmore Group is defined as the incoming of these distinctive mudstones. The mudstones, termed the Edzell Mudstones in Kincardineshire, reach their thickest development (1200m) on the south-east limb of the Strathmore Syncline, thinning to 200m on the north-west limb. They are partly replaced north-westwards by conglomerates of the Gannochy Formation which locally dominate the succession in the vicinity of the Highland Border. Conglomerates of the Gannochy Formation

interfinger both laterally along strike, and normal to the strike around the syncline, with the Edzell mudstones or the overlying Edzell sandstones.

1.1.4.2 Structure

The most prominant structural features in the Kincardineshire region are the Highland Boundary Fault Zone and the subparallel Strathmore Syncline. Armstrong and Paterson (1970) show an important variation in plunge along the Strathmore Syncline with segmentation of the syncline into a series of culminations and depressions. Exposure of the complete Kincardineshire succession requires an important culmination zone south of Stonehaven. Preservation of the Strathmore Group in western Kincardineshire reflects a depression of the synclinal axis between the culmination at Stonehaven and a further culmination close to Kirriemuir.

Folding associated with the development of the Strathmore Syncline is generally assumed to have been a consequence of mid-Devonian deformation (Armstrong and Paterson 1970). The extent to which the syncline was produced during this time is however uncertain (Bluck 1984). The Upper ORS is not sufficiently widely developed to constrain the geometry of pre-unconformity folding. Ramsay (1964) established the geometry and orientation of fractures traversing clasts in conglomerates adjacent to the Highland Boundary Fault Zone. These were interpreted to be the result of brittle deformation caused by sub-horizontal compression normal to the trend of the fault. This was related to south-easterly directed overthrusting. The close parallelism of the Strathmore Syncline and the Highland Boundary Fault argues for a close association between the two structures. As the clast fractures were superimposed on conglomerates which were already steeply dipping, the Strathmore Syncline would appear to have largely predated the brittle deformation. Upper ORS conglomerates in an analogous position adjacent to the Highland Boundary Fault Zone have not suffered the same degree of brittle fracturing. This is consistent with the Strathmore Syncline being an essentially mid-Devonian structure.

The Lower ORS outcrop is traversed by many faults. Their relative chronology is in many cases unclear on account of the poor inland exposure and the difficulty inherent in lithostratigraphic correlation. Large NW-SE cross faults which terminate against the Highland Boundary Fault Zone appear to be particularly common (Armstrong and Paterson 1970, Armstrong et al. 1985). These may have moved concomitantly with overthrusting. One of these faults may account for the abrupt westward termination of the Stonehaven, Dunnottar and Crawton Groups. Campbell (1913) originally explained the termination as a westward plunging anticline. Another NNW trending fault exposed at Whistleberry accounts for the juxtaposition of the Crawton and Arbuthnott Groups. Major faults parallel to the Highland Boundary Fault Zone but within the Lower ORS outcrop also appear to have been important. Apparent extreme thinning of the Arbuthnott and Garvock Groups on the north-west limb of the Strathmore Syncline south-west of Stonehaven (Fig.1.5) has been explained by the existence of a steep easterly-trending overthrust which branches from the Highland Boundary Fault (Armstrong and Paterson 1970).

1.2 AGE OF THE STRATHMORE LOWER OLD RED SANDSTONE

The absolute and relative age of the Strathmore Lower ORS is important if the succession is to be set in the wider context of Late Caledonian evolution. Much of the recent interest in the chronology of the Strathmore ORS has centred on the calc-alkaline lavas intercalated with the sediments. These chemically and isotopically resemble magmas produced at destructive continental margins (Thirlwall 1981, 1982, 1983). As such, they may constrain the termination of subduction prior to continental collision.

1.2.1 Palaeontological Constraints

Fossils only occur sporadically throughout the Strathmore sequence. Sandstones within the succession have yielded a sparse but important assemblage of fish and plants, notably in the Cowie Harbour Fish-Bed of the Stonehaven Group, and the Arbuthnott and Garvock Groups, particularly in Angus. The fish have been described by Agassiz (1835), Miller (1841), Mitchell (1860,1861), Powrie (1864), Traquair (1902) and Westoll (1945, 1951). Westoll attributed the Cowie Harbour Fish-Bed to the Downtonian on the basis that its fauna of fish and arthropods was considered to be intermediate between those in the Downton Castle Sandstone and the Psammosteus Limestone of the Welsh Borderlands. Lamont (1952) however contended that the fish-bed may be considerably older than Downtonian. Fish faunas higher in the succession in the Arbuthnott Group were described as being of Dittonian aspect, or even post-Dittonian (Westoll 1951).

Macroscopic plant fossils from the Strathmore Lower ORS have been described by Fleming (1831), Lyell (1855), Jack and Etheridge (1877), Dawson (1890), Kidston (1893), Reid and MacNair (1896), Reid et al. (1897), Hickling and Don (1915), Kidston and Lang (1924), Lang (1927, 1932) and Henderson (1932). Miospore assemblages from the upper part of the succession were reported by Richardson (1967). Assemblages from the Arbuthnott Group indicated an Upper Dittonian (Lower Siegenian) age whilst those from the Strathmore Group were considered to be Emsian. The latter effectively rule out the possibility that the Midland

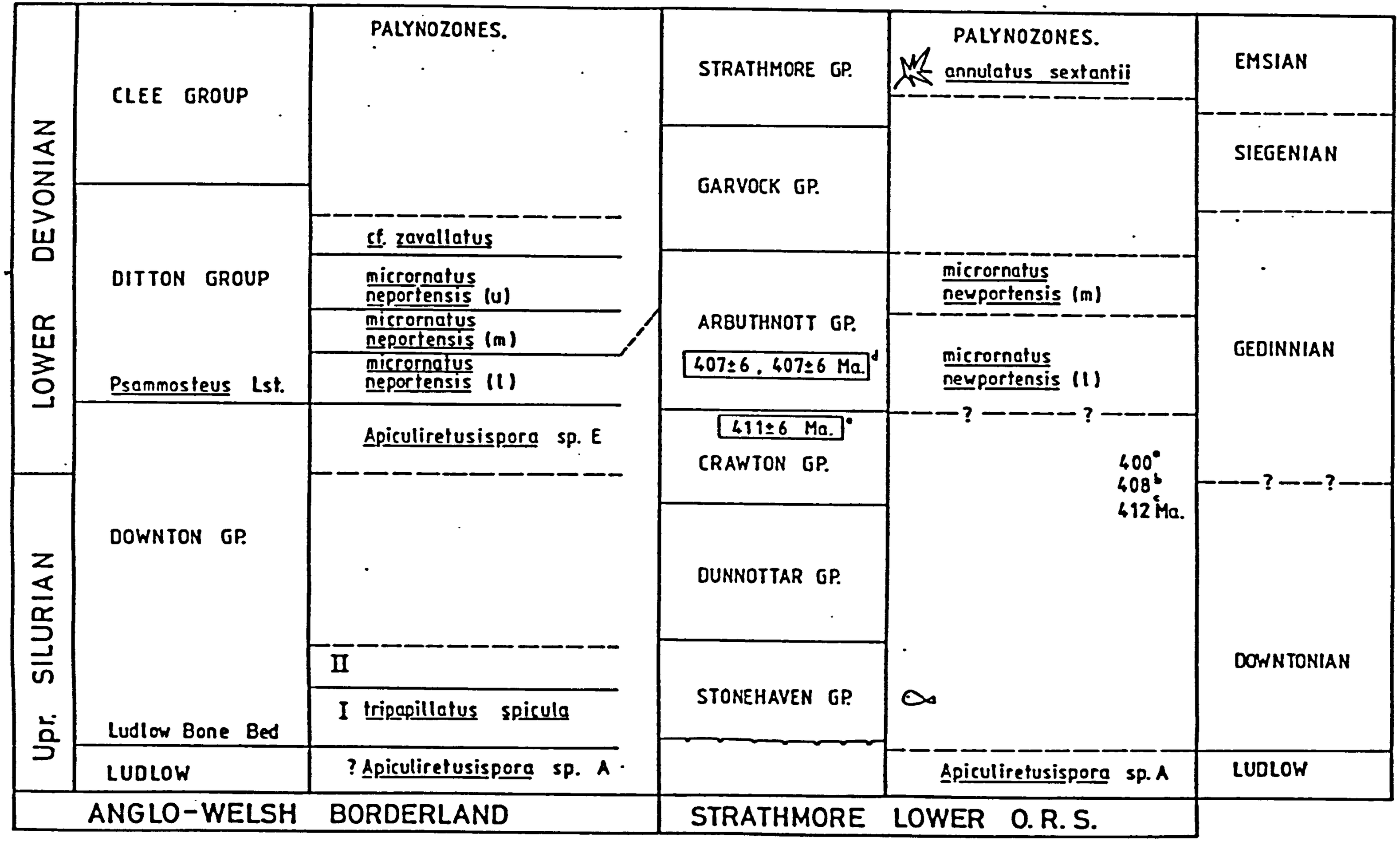

FIGURE 1.6 Age constraints and possible correlation of the Strathmore Lower ORS.
a,b,c: estimates of Siluro-Devonian boundary from Odin (1982), Harland et al. (1982) and McKerrow et al. (1984). d: Rb-Sr ages from Arbuthnott Group, Fife (Thirlwall 1983). e: Rb-Sr age for Lintrathen Porphyry (Thirlwall 1983a). Palynozones and correlation from Richardson et al. (1984).

Valley includes Middle ORS sediments comparable to those in basins north of the Highland Boundary Fault Zone (Waterston 1965).

A more recent palynological study (Richardson *et al.* 1984) confirms a Lower Devonian (Lower Gedinnian) age for the Arbuthnott Group. Samples from throughout *c* 1800m of the Arbuthnott Group sequence exposed in Angus and Fife yield miospore assemblages belonging to the lower and middle subzones of the *micrornatus-newportensis* Zone. These correspond to a Lower Gedinnian age. The Lower but not lowermost Devonian age for the Arbuthnott Group implies that the thick calc-alkaline lava pile which interfingers with the Strathmore succession at this level is also Devonian in age and not Silurian as anticipated by Thirlwall (1981).

It is however possible that the Silurian-Devonian transition does take place within the lower part of the Strathmore succession, beneath the Arbuthnott Group. The base of the *micrornatus-newportensis* Zone is located just above the *Psammosteus* limestone in stratigraphically equivalent rocks in the Welsh Borderlands. Lowermost Devonian strata therefore intervene between the base of the *micrornatus-newportensis* Zone and the Silurian-Devonian boundary. These amount to *c.* 40m in thickness in parts of the Welsh Borderlands (Richardson *et al.* 1984) but are likely to be substantially thicker in the rapidly deposited Strathmore sequence. There is no critical palaeontological evidence for the age of the sediments making up the underlying Dunnottar and Crawton Groups and this therefore does not rule out the possibility that they may in part be Silurian in age (Fig. 1.6)

1.2.2 Geochronological Constraints

Evans *et al.* (1971) determined K-Ar whole rock ages for four lava flows from the North Fife Hills. The mean of three of the determinations produced an age of 400 ± 5 Ma (recalculated using decay constants of Steiger and Jager 1977). The fourth sample was considered not to have retained its radiogenic argon. Thirlwall (1981, 1983a) suggested these were likely to be minimum

ages as K can be mobile even in lavas which are petrographically fresh. Thirlwall (1983) reports Rb-Sr mineral-whole rock age determinations for two samples from the Arbuthnott Group in Fife. Biotite and plagioclase separates from both a rhyolite boulder and an olivine-diorite intrusion are not isotopically equilibrated with their respective whole rocks. Biotite and plagioclase are completely fresh in the rhyolite boulder, but the groundmass is oxidised suggesting deuteric alteration. An age of 407 $\pm$ 6 Ma calculated from the biotite-plagioclase mineral pair is deemed to be the most reliable. The possibility that the biotite may have undergone loss of ^{87}Sr to the groundmass is taken to indicate that the age may represent a minimum. The plagioclase separate from the olivine diorite is slightly sericitised and its biotite-whole rock age at 407 $\pm$ 6 Ma is accepted as the best age for the intrusion.

Thirlwall (1983a) also presents whole rock and biotite Rb-Sr data for the Lintrathen porphyry. A two point isochron gives an age of 411 $\pm$ 6 Ma. The Lintrathen porphyry is considered by Armstrong and Paterson (1970) to belong to the uppermost Crawton Group. This age, and those for the Arbuthnott Group rocks, suggest the bulk of the Midland Valley Lower ORS volcanism is older than 405 Ma.

The absolute age of the Siluro-Devonian boundary is poorly constrained. Dates bracketing the boundary include the post-Wenlock, pre-Siegenian Gocup granite of New South Wales which has a K-Ar age of 409 $\pm$ 3 Ma (Richards *et al.* 1977), and fission track ages of 407 $\pm$ 8 (1o)Ma from bentonites in the Bringewood Formation of the Gorstian Stage in the Welsh Borderlands (Ross *et al.* 1978). Estimates for the base of the Devonian range from 400 Ma (Odin 1982) to 408 Ma (Harland *et al.* 1982) to 412 Ma (McKerrow *et al.* 1984). Only the latter two estimates satisfy the combined miospore and radiometric evidence from the Arbuthnott Group. Richardson *et al.* (1984) argue that because there is at least part of one spore zone within the Devonian below the *micrornatus*-*newportensis* Zone in both Podolia and the Anglo-Welsh Borderland, and on the basis that the average duration for a major inter-regional spore zone is estimated to be

3-4 million years, a conservative estimate for the base of the Devonian is 410 $\pm$ 6 Ma. The radiometric ages are therefore commensurate with a Lower and lowermost Devonian age for the bulk of the Strathmore Lower ORS, with the Siluro-Devonian boundary located low in the succession.

1.3 THE PRESENT STUDY

The deposition and provenance of the largely conglomeratic Dunnottar and Crawton Groups outcropping in coastal exposures in Kincardineshire are considered in the following chapters. The project as originally conceived had a wider stratigraphical brief in that it was intended to use the unusually thick sequence of Lower ORS sediments in Kincardineshire to profile progressive source unroofing. Initial work on the basal part of the sequence however revealed considerable potential at this level for constraining lateral as opposed to vertical compositional variation in the source regions which contributed sediment to the basin. This subsequently became the main theme of the research which involved sedimentological observations, particularly those pertinent to unambiguously determining palaeo-dispersal, in combination with detailed geochemical and isotopic studies on conglomerate clast populations. The research was guided by the following objectives:

1. To determine the depositional mechanism of the varied conglomerates which dominate the Dunnottar and Crawton Groups. The predominance of conglomerates is unusual in that there is no diminution in either their abundance or grainsize as the sequence is traced up to 15km normal to the conventional Highland Border source.

2. To determine the dispersal of the coarse conglomerates and to relate this to the revised north-westerly dispersal of basal conglomerates in the western Strathmore Lower ORS.

3. To account for the anomalous thickness of the Kincardineshire Lower ORS when compared with sequences along strike to the south-west.

4. To establish the petrological, geochemical and isotopic character, and the original emplacement ages, of the various granite clasts which occur with unusual abundance in conglomerates of the Dunnottar and Crawton Groups.

5. To geochemically and isotopically type metamorphic detritus occurring in the conglomerates. The determination of uplift and cooling ages in metamorphic clasts enables the early uplift history of the source to be established, allowing the viability of potential source terranes to be assessed.

6. To apply the dispersal and clast provenance data to the wider Late Silurian - Early Devonian evolution of the Midland Valley and adjacent regions. The data have implications for both the relative position of the Midland Valley and the now adjacent Grampian Highlands, and for the sub-Upper Palaeozoic basement to the Midland Valley.

CHAPTER TWO

SEDIMENTOLOGY OF THE DUNNOTTAR AND CRAWTON GROUPS

2.1 LITHOFACIES

Most sediments and sedimentary rocks show some form of basic structural organisation (Ore 1964, Campbell 1967, Bluck 1980). This is produced by the systematic assembly of depositional lithofacies to generate composite facies associations. It is the wider association and sequential development of these basic depositional lithofacies, rather than the lithofacies themselves, which are generally indicative of the depositional environment in which the sediments formed.

Figure 2.1 illustrates the basic ordering and structural hierarchy established in the largely conglomeratic sediments of the Dunnottar and Crawton Groups. Coarse-grained conglomerates comprise greater than 80% of the succession, despite the fact that the sections examined extend more than 15km from the Highland Boundary Fault. In addition, there is no obvious diminution in grain size as the succession is traced away from the Highland Boundary Fault.

Five basic lithofacies types are recognised. These combine to form a series of recurring depositional units which stack both laterally and vertically to generate composite sequences of a higher order. In addition there is an important interaction at various levels in the structural hierarchy between conglomerates and minor sandstones of non-volcanic provenance, and volcanogenic sediment independently dispersed to the basin.

A. MASSIVE OR FLAT STRATIFIED IMBRICATE CONGLOMERATES

Massive or flat stratified boulder or cobble conglomerates are the dominant lithofacies in sediments of the Dunnottar and Crawton Groups. They make up an estimated 45% of the total sequence. The conglomerates are generally clast supported, although matrix supported units do occur.

Imbrication is often spectacularly developed (Plates 2.1, 2.2, 2.3, 2.4), with strong unimodal a-b plane orientations, a-axes transverse to flow, and b-axes dipping upstream (as deduced from co-flow cross-stratification). The imbrication fabric is

Figure 2.1 Structural hierarchy recognised in conglomerates of the Dunnottar and Crawton Groups. Five basic lithofacies combine to generate two distinctive lithosomes. These have contrasting sheet-like (Lithosome 1) and channelled forms (Lithosome 2), and are distinguished on the basis of the internal relationship and directional properties of their constituent lithofacies. The two conglomerate lithosomes are also characterised by mutually exclusive textures, clast compositions and dispersal patterns. They stack to form vertical sequences which are interleaved with a third lithosome type (Lithosome 3) comprising volcanogenic sandstones and conglomerates.

C-F refers to coarse to fine lateral transitions ; C/F to coarse over fine vertical lithofacies transitions.

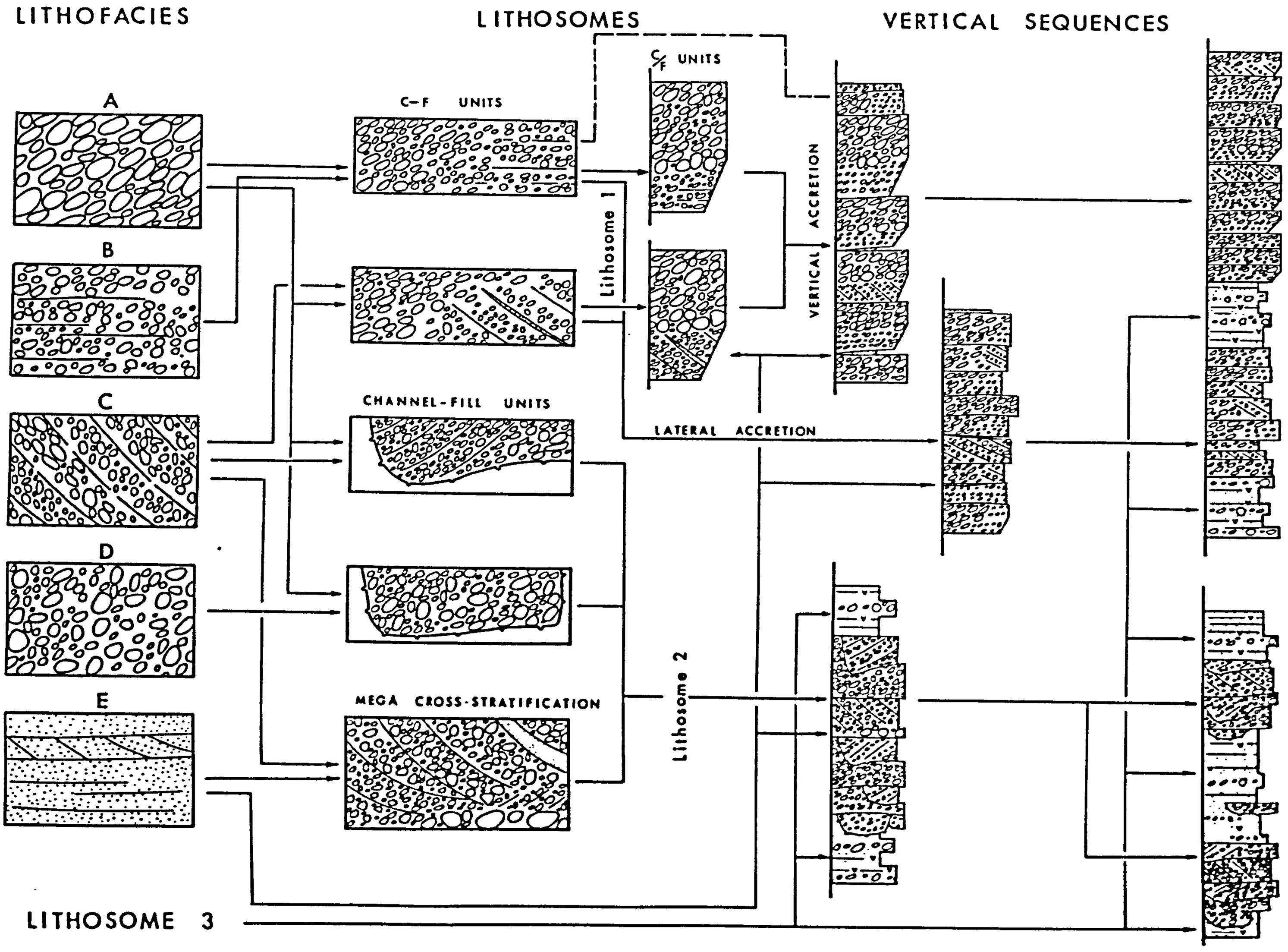
LITHOFACIES
LITHOSOMES
VERTICAL SEQUENCES
A
B
C
D
E
C–F UNITS
CHANNEL-FILL UNITS
MEGA CROSS-STRATIFICATION
C/F UNITS
Lithosome 1
Lithosome 2
LATERAL ACCRETION
VERTICAL ACCRETION
LITHOSOME 3
Lithosome 1 Association
Lithosome 2 Association

generally at a high angle to bedding with average a-b plane dips (tilt corrected) of between 30 and 45°. These are higher than recorded in recent glaciofluvial gravels (Rust 1975) and fluvial gravels (Cailleux 1945), but comparable to values recorded by Laming (1966) in breccias of alluvial origin. Much of the imbrication is of contact type, though isolate imbrication is also seen.

Many of the imbricate conglomerates are exceedingly coarse-grained, with clasts >1.0m in diameter not uncommonly encountered. Maximum clast size values (mean of the ten largest clasts in an area of $2m^2$) are frequently in excess of 40cm. Sorting is generally poor but a wide range of textures is present. Two distinct textural variants can be distinguished.

In the first instance, widespread bimodal textures are seen in conglomerates which are characterised by the ubiquitous presence of metaquartzite as an important clast component. The coarse sandstone or pebbly sandstone matrix is strongly segregated from the cobble or boulder mode which makes up the framework, with granule and pebble modes often suppressed. Open frameworks are rare in these metaquartzite bearing bimodal conglomerates. In total contrast, a range of metagreywacke bearing conglomerates in which quartzite is totally absent are very poorly sorted and frequently have open frameworks. Imbrication is less well developed in this latter variant, largely consequent on the absence of disc enrichment. Bimodal imbricate conglomerates are often strongly enriched in discoidal clasts.

Lithofacies A conglomerates occur as both extensive imbricate sheets either lateral to, or overlying texturally more mature, finer grained conglomerates of Lithofacies B or C type, or as a component in complex channel fill units. Tabular units of imbricate conglomerate can exceed 5.0m in thickness. They may be internally massive or show crude flat stratification due to internal size segregation or thin discontinuous sand lenses. Alternations of sand and pebbly sand matrix characterise some units. In others, particularly those occurring as channel fills, open frameworks may alternate with sand filled frameworks.

B. FLAT STRATIFIED TEXTURALLY MATURE CONGLOMERATE

Lithofacies B encompasses a range of pebble and cobble conglomerates often closely associated with imbricate conglomerates of Lithofacies A type. They are distinguished by their finer grain size, lack of imbrication, moderate to good sorting and generally greater overall textural maturity (Plate 2.5). On the whole they form thinner sheet-like units than accompanying Lithofacies A conglomerates and more rarely actually fill channels cutting Lithofacies A units transverse to the imbrication dip direction.

Both framework and matrix supported units occur (Plates 2.5, 2.12). The former frequently have open frameworks, whilst the latter may contain greater than 50% matrix, and grade laterally into pebbly sandstone and sandstone. Transitions from framework to matrix support can occur within the same unit over relatively short distances (5-10m). Internally the units can be massive or flat stratified, with the stratification defined by changes in grainsize or lenticular sand levels. Occasionally the stratification is of low angle type.

Lithofacies B conglomerates make up an estimated 5-10% of the succession as a whole, and are more commonly associated with bimodal quartzite bearing conglomerates of Lithofacies A type than with equivalent polymodal metagreywacke conglomerates.

C. CROSS-STRATIFIED CONGLOMERATES

Cross-stratified conglomerates of Lithofacies C are generally less common than the horizontally stratified and massive conglomerates of Lithofacies A,B and D. Cross-stratified conglomerates make up $\underline{c}$ 10% of the sequence overall. A distinction is drawn between cross-stratified conglomerates of Lithofacies C1 type which typically occur in single sets 0.5-4.0m thick, and rarer mega-cross-stratified conglomerates which have set thicknesses in excess of 4m, and which are usually co-flow with imbrication in adjacent Lithofacies A conglomerates (Lithofacies C2). Cross-strata of Lithofacies C1 type often can be shown to dip in a direction at high angle to the palaeoflow

indicated by Lithofacies A imbrication.

The cross-stratified conglomerates of C1 type form sets which can be shown to be of considerable lateral extent, bounded by either a basal erosional surface or a sub-planar scoured contact. In many cases cross-stratified units can be traced laterally into massive or imbricate conglomerates. Where a basal erosion surface can be traced beneath the two laterally contiguous units, this often downcuts beneath the cross-stratified conglomerates. Foresets are both asymptotic and angular. They generally preserve complex alternations of sandstone, pebbly sandstone, open framework, moderately sorted, pebble conglomerates, and massive cobble conglomerates, sometimes with AB planes of discoidal clasts lying parallel to the foreset boundaries. Foresets generally become coarser, and thicken, when traced downwards (Plate 2.7). Re-activation surfaces are commonly seen. The conglomerates preserved in the foresets are generally finer grained and texturally more mature than laterally equivalent Lithofacies A conglomerates.

Exceedingly thick (4-6m) mega-cross-stratification (Lithofacies C2) is seen in several sequences. These are both texturally less mature than C1 cross-stratified conglomerates, and often are coarser grained. The foresets are generally planar, with individual foresets traced out for over 30m along strike. Counterflow foresets are commonly observed, as are characteristic concentrations of very coarse boulder grade clasts (often some of the coarsest clasts seen in the sequence) along the base to the foresets. Texturally the mega-foresets are very variable, but frequently the conglomerates making up the foresets are no more mature than the associated massive or flat stratified conglomerates. Evidence for re-activation is often more commonly seen than in cross-stratified conglomerates of C1 type.

D. MASSIVE CONGLOMERATES

Lithofacies D encompasses a range of massive generally framework supported conglomerates which show neither clast imbrication nor enhanced textural maturity. Texturally, they resemble conglomerates of Lithofacies A and can in some instances be

traced laterally into imbricate conglomerates of Lithofacies A type. Often the development of massive conglomerates is accompanied by a high abundance of volcanic clasts within the conglomerate unit. Sorting is generally poor, but both bimodal and polymodal units can be distinguished. The former are generally restricted to the quartzite and metapsammite bearing conglomerates, whilst the latter typify conglomerates dominated by lithic arenite and metagreywacke clasts. Volumetrically massive conglomerates account for some 15-20% of the succession.

E. FLAT BEDDED AND CROSS-STRATIFIED SANDSTONES

Lithofacies E includes a range of medium to coarse-grained sandstones which are interstratified with the conglomerates as thin typically discontinuous beds, but also as occasionally thicker multistorey units of pebbly sandstone. The sandstones generally show a continuity with sandstones making up the matrix in adjacent conglomerates, and they are interpreted as having been deposited in close association with these units. An important distinction is made between Lithofacies E sandstones and volumetrically more important sand-dominant volcanogenic units which are also interstratified with the conglomerates. The latter however do not share the same provenance as the conglomerates in being almost exclusively derived from volcanic sources.

Lithofacies E sandstones can be either cross-stratified or parallel bedded. Cross-stratification is generally of planar type but trough sets do occur rarely. Two important associations between Lithofacies E sandstones and related conglomerates are seen. In the first instance, sandstones form large planar foresets either in co-sets with related conglomerates, or as extensive sheets beneath conglomerates of Lithofacies A or B type. These vary from 10cm to 1.0m in thickness and generally have gravel interfingers wedging out downwards along the foresets (Plate 2.10). The foresets typically have asymptotic bases and evidence for multiple re-activation. Sandstones also form thin units (normally <1.0m) which drape over underlying conglomerates, and which have scoured or channelled tops. These can be massive, flat stratified or cross-stratified internally, and can be traced

as discontinuous units for in excess of 30m (Fig.2.3), often draping different lithofacies. Foreset dips are generally at high angle to the high stage palaeoflow determined from imbrication. In contrast, foresets dips in the cross-stratified sandstones which interfinger with, or pass laterally into, cross-stratified conglomerates (Lithofacies C) show less angular divergence from the associated imbrication.

2.2 LITHOSOME STRUCTURE

Lithosomes are generated by the assembly of lithofacies during aggradation or lateral migration of a depositional system. The structure of the lithosome can be established by recognising both the relative geometry of the component lithofacies, and the relationship between these lithofacies and the directional properties of the lithosome as a whole. Recognition of structural relationships at the lithosome level is important because it is at this level that the depositional environment may be critically determined.

Three very different types of lithosome can be recognised in the conglomerates of the Dunnottar and Crawton Groups. The first is characterised by an important lateral segregation of lithofacies within tabular sheets. The second is a differentiation of lithofacies associated with channelised conglomerate bodies. These two lithosomes are the starting point for a fundamental division of the conglomerates studied into two disparate associations. A third type of lithosome includes sediments almost exclusively of volcanogenic origin.

2.2.1 Lithosome 1: Laterally Differentiated Conglomerate Sheets

2.2.1.1 Structure

Units characterised by lateral and vertical grain size and textural differentiation are widely developed in many of the Dunnottar and Crawton Group conglomerates. Units which perceptibly coarsen upwards from a sharp base are particularly common, but it is in rarer instances in which size and shape segregation can be seen laterally within a single depositional unit which are critical to an understanding of the depositional mechanism. In addition, the laterally differentiated conglomerate sheets preserve a lateral record of lithofacies which are texturally equivalent to those making up the coarsening upwards units. It is possible the latter may therefore have evolved from the former by a vertical transposition of lithofacies.

Laterally differentiated conglomerate sheets are particularly

well developed in coastal exposures of the uppermost Crawton Group at Whitehouse south of Gourdon. Large scale plane table mapping, together with detailed textural and fabric measurements across individual well exposed units demonstrate the importance of units which fine in the direction of palaeoflow. In many instances coarse-grained boulder conglomerates with very strong imbricate fabrics (Lithofacies A) can be traced laterally into finer grained texturally more mature pebble or cobble conglomerates which are generally not imbricated (Lithofacies B). In other cases transitions to massive conglomerates of Lithofacies D type, or to cross-stratified conglomerates (Lithofacies C) can be recognised. Of the laterally differentiated sheets studied four have been chosen for illustration.

Unit 1: Figure 2.2 illustrates the structure of a single down current transition from imbricate to non-imbricate boulder grade conglomerates. The unit is one of several strongly differentiated conglomerate sheets outcropping at Whitehouse, south of Gourdon. The conglomerates are of northerly derivation and are quartzite bearing, with a characteristic abundance of bimodal textures. A very coarse (M.C.S. >40cm) contact-imbricate unit has been traced laterally for 50m along the foreshore (Plates 2.1, 2.2). The imbrication persists for 30m and then the fabric breaks down. Maximum clast size shows little differentiation between the imbricate and non-imbricate portions of the unit, but the lowest values of M.C.S. determined significantly do come from the non-imbricate conglomerate. Clast shape (after Zingg 1935) is however strongly partitioned between the imbricate and non-imbricate conglomerates. Disc and blade shaped clasts dominate in the imbricate zone, whilst the breakdown in imbrication is accompanied by a concomitant increase in the abundance of sphere and rod shaped clasts. Sequential measurements of the imbricate fabric over the disc and blade enriched portion of the unit show strongly preferred orientations and unimodal dispersal to the south. Palaeoflow is constant over the 30m imbricate conglomerate with no rotation of the fabric when traced down current. The rapid transition to the non-imbricate part of the unit appears to be transverse to the

Figure 2.2 Lithofacies transition in Lithosome 1 polycyclic conglomerates, Whitehouse (NO 824704).
A. Maximum clast size (open circles) and shape enrichment (solid lines) profiles across Lithofacies A-D transition (Unit 1 described in text). Rose diagrams indicate sequential down-flow orientation of imbricate fabric (a-b plane dip + 180°). Arrows are vector means. n = number of observations.
B. Plane table map indicating location of profile shown in a. Note coarse to fine transition in overlying unit, and large scale cross-bedded Lithofacies C conglomerates dipping (as indicated by arrow) at an angle to the imbrication in Unit 1.
C. Sketch map showing location of plane table map B. Northerly derived polycyclic conglomerates overlie southerly derived first cycle Lithosome 2 conglomerates exposed around Gourdon Harbour.

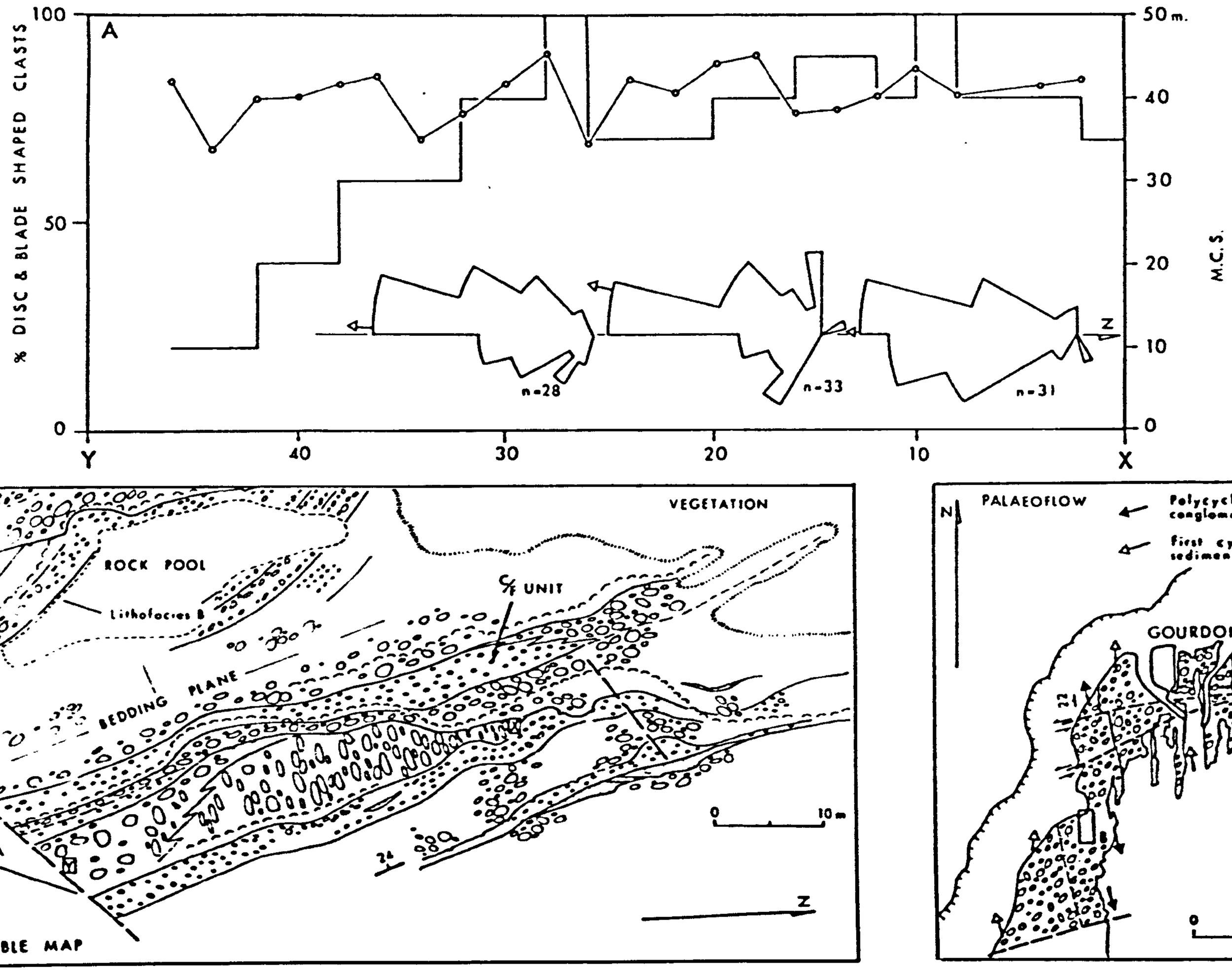
A
% DISC & BLADE SHAPED CLASTS
100
50
0
50 m.
40
30
20
10
0
M.C.S.
n=28
n=33
n=31
N
Y
40
30
20
10
X
B
VEGETATION
Palaeoflow
ROCK POOL
Lithofacies B
UNIT
BEDDING PLANE
Lithofacies A
0
10 m
Z
PLANE TABLE MAP
C
N
PALAEOFLOW
Polycyclic conglomerates.
First cycle sediments.
GOURDON
0
300 m

Figure 2.3 Plane table map of polycyclic conglomerates exposed on foreshore northeast of Whitehouse (NO 824705) showing lateral fining of maximum clast size in Unit 2 described in text. Imbrication over Unit 2 indicates a north to south palaeoflow. Imbrication measurements at `a` however indicate a dispersal towards the northwest. Imbrication in polycyclic conglomerates in the zone directly overlying the transition from southerly derived Lithosome 2 conglomerates to northerly derived Lithosome 1 conglomerates tend to show a high dispersion, with palaeoflows often opposed to those higher in the Lithosome 1 sequence.

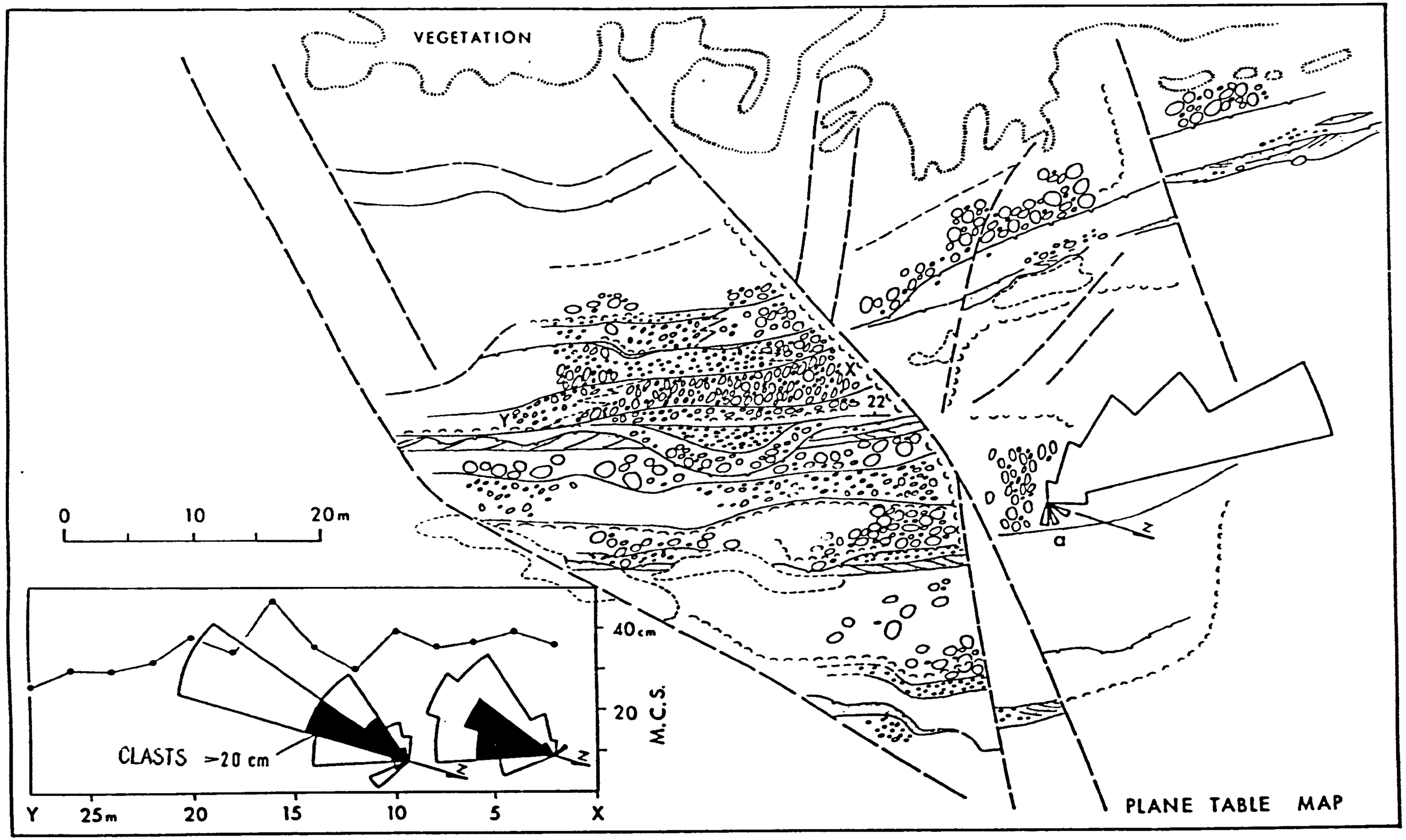
VEGETATION
X
X'
Y
Y'
22°
0
10
20m
a
N
0
40cm
20
M.C.S.
CLASTS >20 cm
N
N
Y
25m
20
15
10
5
X
PLANE TABLE MAP

palaeocurrent.

The unit can only be traced for 50m before it is terminated by a fault. It is likely however to be part of a substantially larger unit which probably fined down current. Contacts above and below the unit are sharp. The base is planar whilst the top is weakly convex, giving a lenticular geometry overall. The imbricate conglomerates are little more than one clast thick and wedge out abruptly up current. The unit never exceeds 1.0m in thickness and shows no verical differentiation. Sphere and rod enriched pebble conglomerates over- and under-lie the coarse shape-segregated conglomerate unit. These can be traced northwards into massive coarse-grained conglomerates and therefore these also form part of laterally differentiated lenticular sheets. They show strong grain size segregation with fining in the direction of palaeoflow. The finer grained pebble conglomerates are better sorted than the corresponding coarse units along strike, and some show open frameworks (Plate 2.5). They represent lateral down current transitions from Lithofacies A or D to Lithofacies B. The imbricate to non-imbricate transition shown by Unit 1 is not accompanied by an appreciable grain size decline or increase in textural maturity, and therefore is referred to a Lithofacies A-D transition.

The package of lenticular differentiated sheets associated with Unit 1 is overlain by a four metre thick unite of cross-stratified conglomerates of Lithofacies C type (Fig.2.2, Plate 2.7).These are finer grained and marginally more mature than Lithofacies A and D conglomerates in the units beneath, and show down-dip coarsening of foresets. Tilt-corrected foreset dips are shown in Figure 2.2. These are rotated to the west of the southerly palaeoflow recorded by the imbrication in Unit 1.

Unit 2: A second laterally differentiated unit is illustrated in Figure 2.3 and Plate 2.3. This is also from bimodal quartzite bearing conglomerates exposed at Whitehouse. Shape segregation is less obvious over this unit, but the maximum clast size shows a fining down current. Imbrication measurements over the 30 metres of the unit which can be traced out laterally show no

deflection when traced down flow, and again a southerly dispersal. The imbricate fabric shows greater dispersion in the upcurrent part of the unit than in the finer downcurrent region. This is a consequence of a rotation of the finer clasts relative to the accompanying coarser clasts in the upcurrent sector. Tilt corrected clast a-b plane dips average 44° upcurrent and 34° downcurrent.

Unit 2 again forms a thin broadly lenticular unit. It overlies a channel conglomerate which trends at high angle to the imbrication in Unit 2, and which downcuts into underlying massive lithofacies D conglomerates and a thin discontinuous unit of cross-bedded coarse sandstone (Lithofacies E). The bedding surface on which Unit 2 is exposed shows a complex lateral transition normal to the palaeoflow into adjacent size differentiated units. The finer tail of Unit 2 wraps around another coarse imbricate unit. Unit 2 is therefore part of a lateral amalgam of similar units which internally show textural segregation at a scale considerably smaller than that seen in Unit 1.

Unit 3: Bimodal conglomerates exposed at Todhead Lighthouse also show strong lateral facies segregation. The stratigraphical position of these conglomerates is unclear. They lie immediately below a lava flow which has been correlated by Campbell (1913) with several flows of similar composition outcropping at Tremuda Bay, the Tremuda Bay Volcanic Formation of Armstrong and Patterson (1970). These lavas are defined as marking the top of the Dunnottar Group. It is possible the conglomerates exposed at Todhead Point are therefore close to the boundary between the Dunnottar and Crawton Groups. It is also possible however that these conglomerates are considerably higher in the succession.

A well exposed lateral transition from contact imbricate to finer massive conglomerates which become matrix supported is seen in a unit exposed 8m below the Todhead lava (Figs 2.4, 2.5). Imbricate conglomerates of Lithofacies A can be traced for 20m before the unit passes laterally into finer non-imbricate conglomerate of Lithofacies D type. Fining of maximum clast size

Figure 2.4 A. Detailed log through polycyclic Lithosome 1 conglomerates and an intercalated lava flow exposed at Todhead Point (NO 870767). The section illustrates a marked change in the orientation of the imbricate fabric developed in coarse grained Lithofacies A conglomerates beneath the lava flow. As the deflection is observed in fabrics developed at high flow stage, a significant re-orientation of the main channel flow is indicated. Lava eruption onto the fan surface may have modified the drainage pattern. The imbricate conglomerates at B make up Unit 3 described in the text. A lateral MCS profile within this unit is illustrated in Figure 2.5.

B. Location of Todhead section at the base of a major fining-upwards megasequence with intercalated volcaniclastic units.

A

DISPERSAL

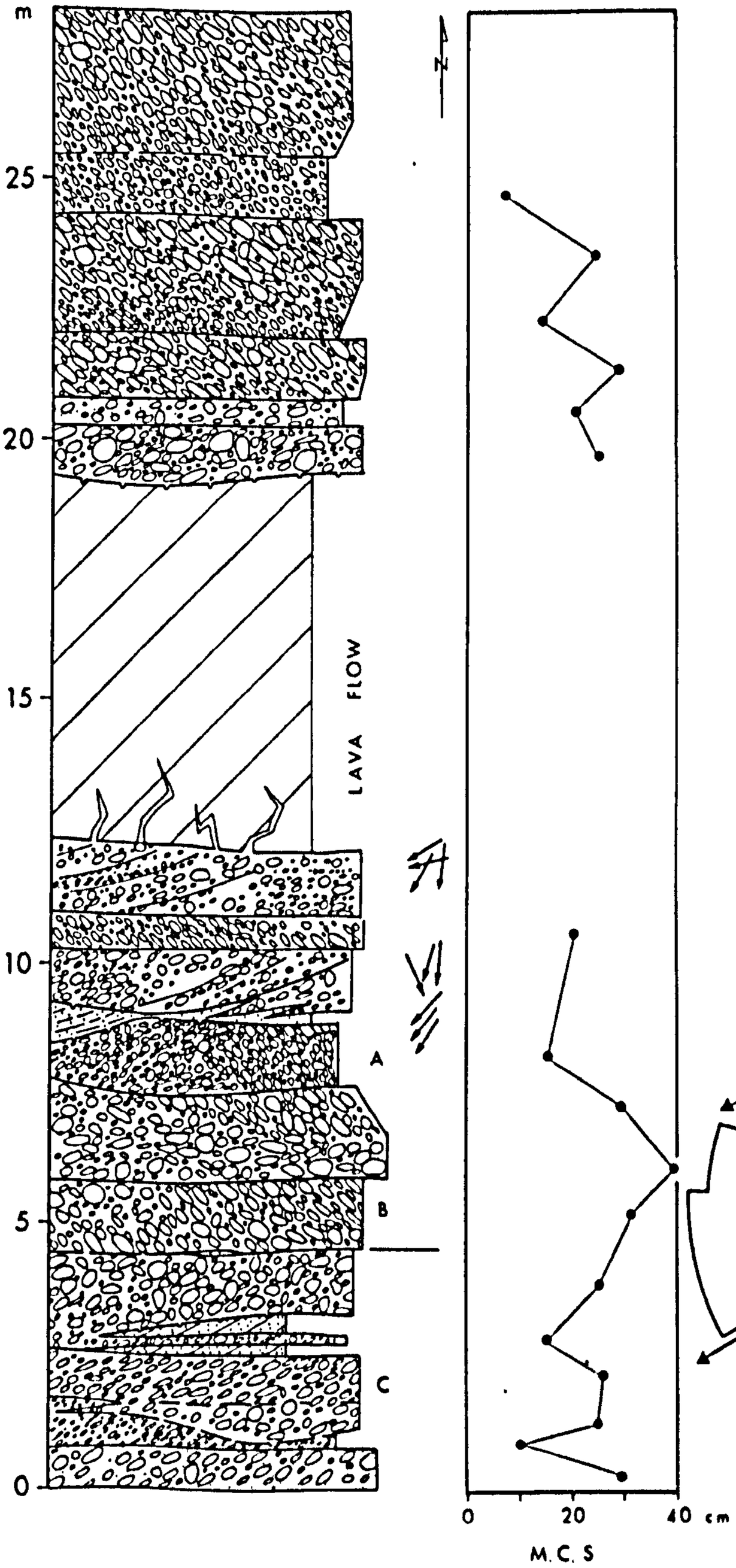

Cross bedding

TODHEAD SOUTH SECTION

B

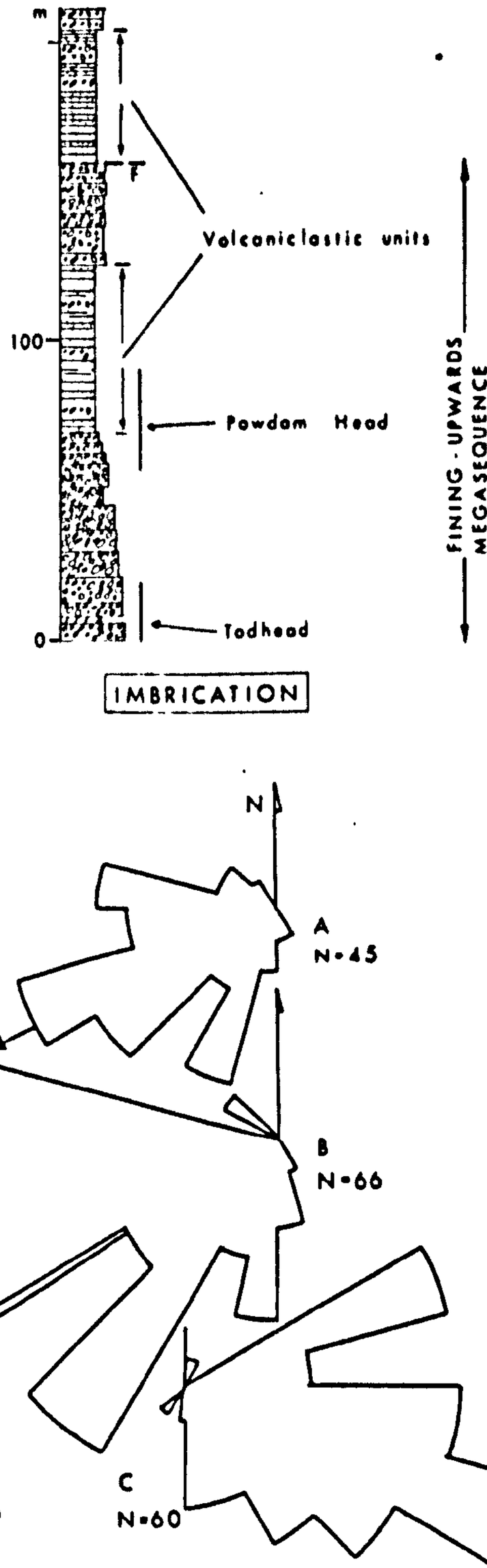

IMBRICATION

Figure 2.5 Lateral maximum clast size profile across size and shape segregated conglomerate unit at Todhead Point (NO 870767). Section measured normal to imbricate dip fabric and illustrates down flow fining interrupted by an increase in grain size directly downstream of imbricate portion of the unit. Unit 3 referred to in text.

Figure 2.6 Complex interfingering conglomerate and sandstone unit exposed at Powdam Head (NO 867763). A. Field sketch of vertical surface illustrating interfingering of conglomerate and cross-stratified sandstones. Arrows indicate tilt-corrected current indicators and gravel interfinger orientations. The gravel interfingers are at a high angle to imbrications and cross- and trough-cross-stratification measurements. B. Plan view of sketch section shown in A. C. A possible interpretation. The gravel interfingers are interpreted as lateral accretion surfaces generated by modification of a longitudinal bar during waning flow. The cross-stratified sandstone exposed in north-south section is possibly the tail of a subsequently accreted lateral bar.

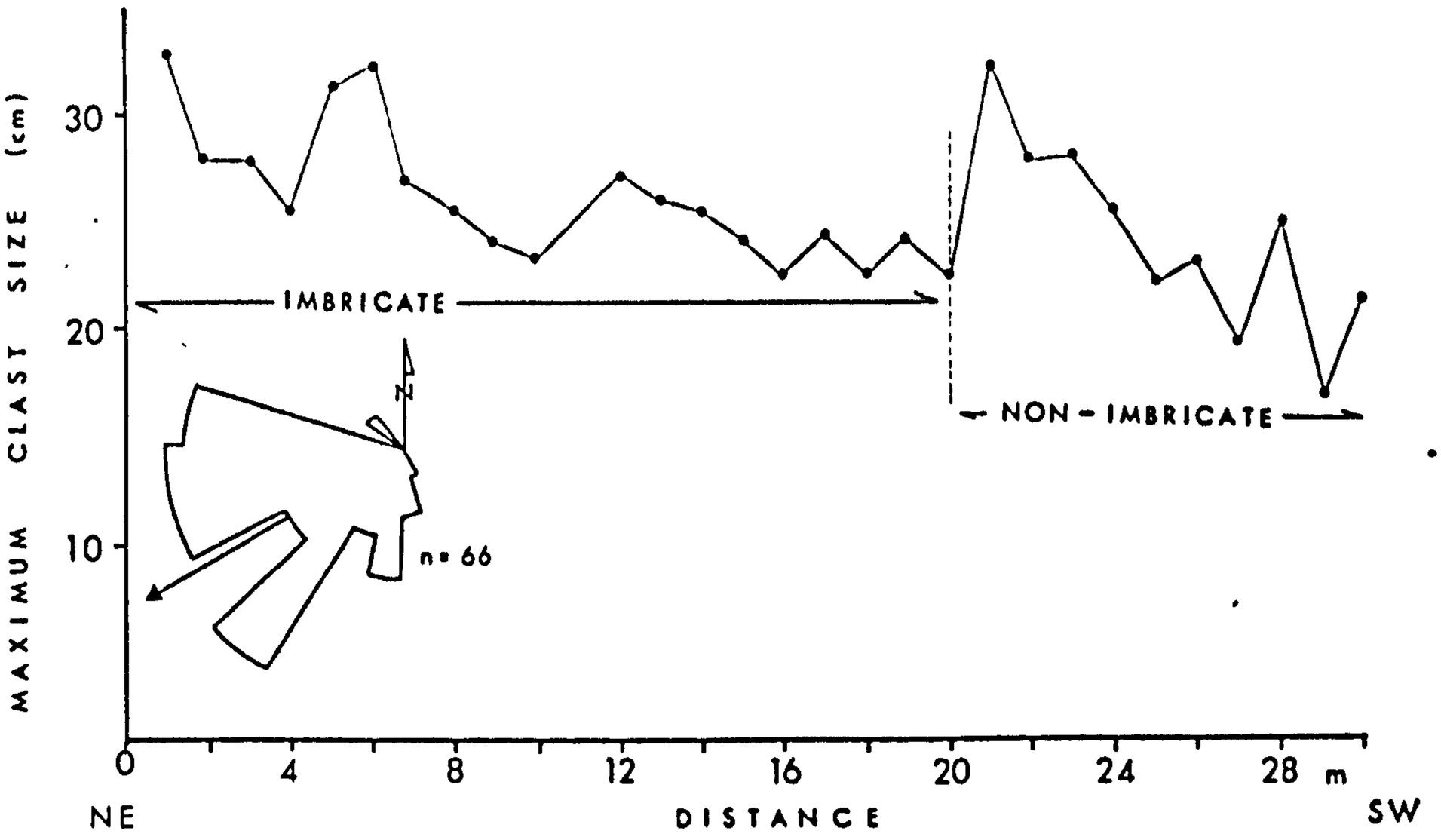
CLAST SIZE (cm)
30
20
10
IMBRICATE
NON - IMBRICATE
N
n = 66
MAXIMUM
0
4
8
12
16
20
24
28 m
NE
DISTANCE
SW

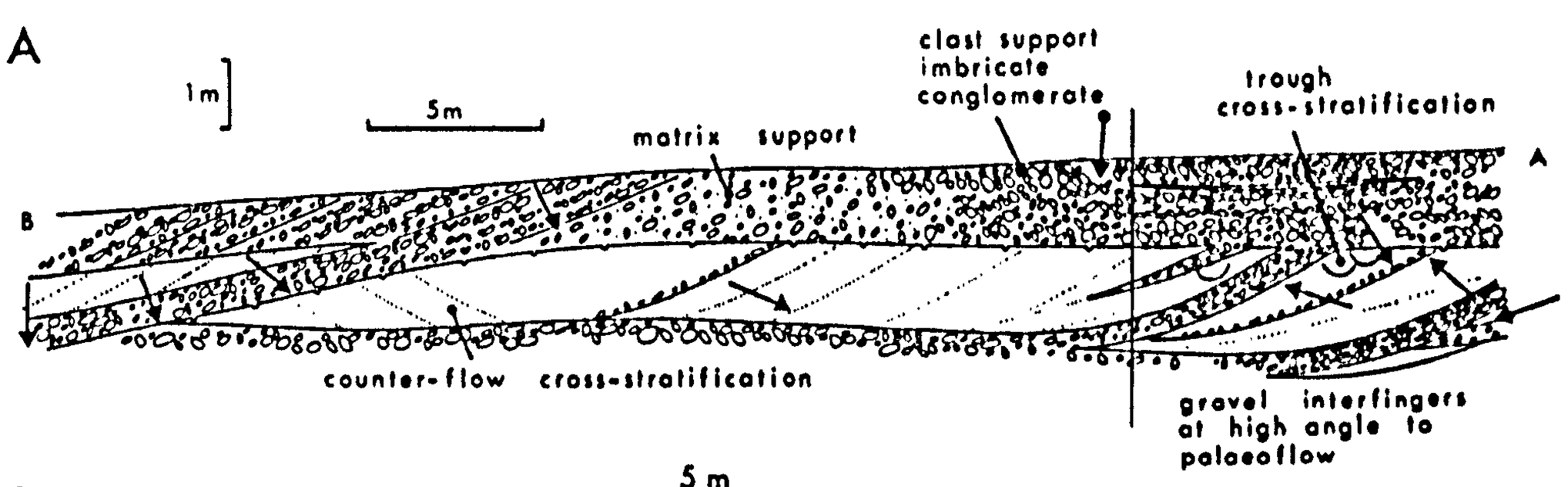
A
1m
5m
matrix support
clast support
imbricate
conglomerate
trough
cross-stratification
A
B
counter-flow cross-stratification
gravel interfingers
at high angle to
palaeoflow
B
5 m
B
A
N

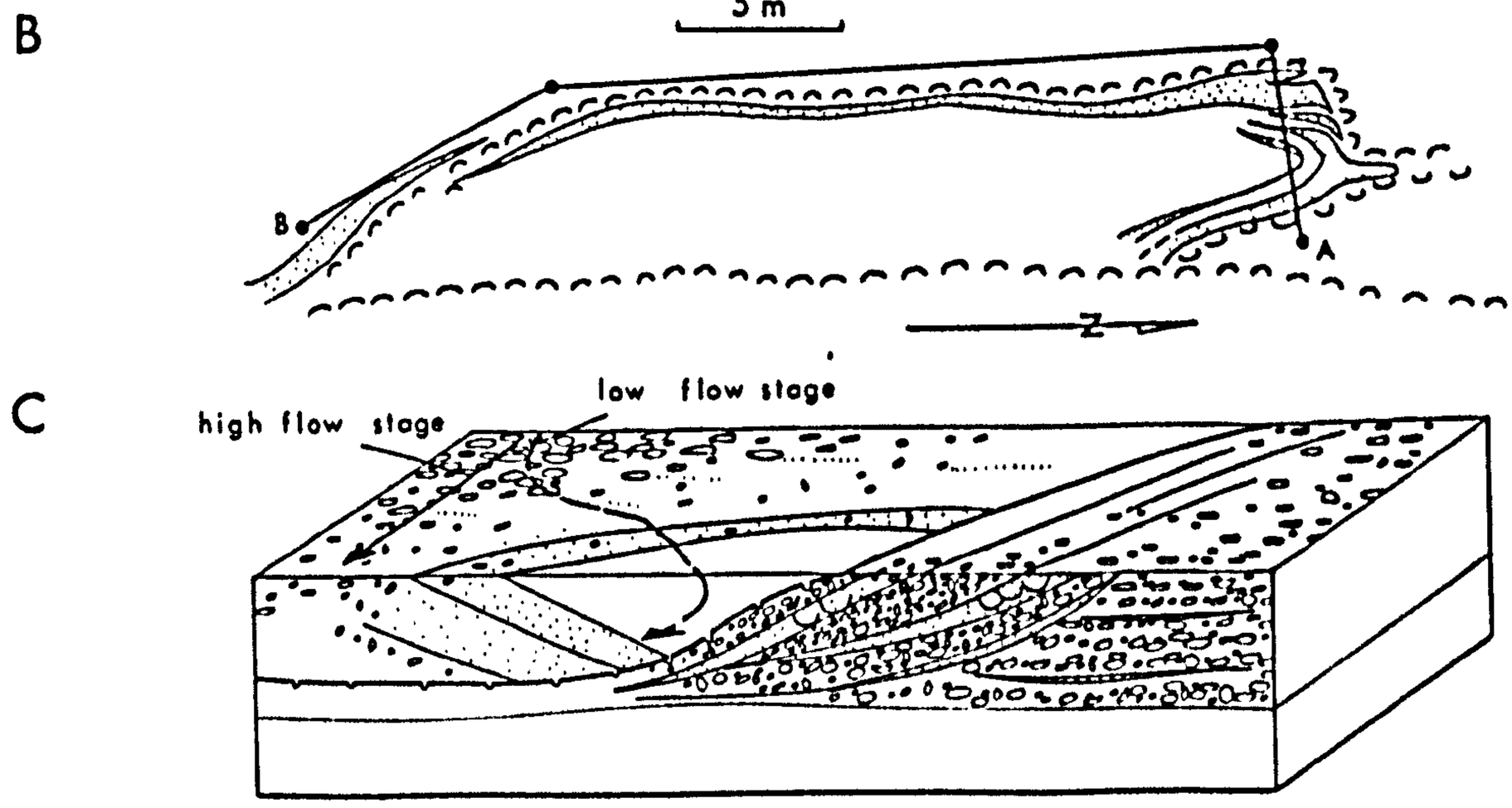
C
low flow stage
high flow stage

PLATE 2.1: Imbricate Lithofacies A conglomerates, Lithosome 1, Whitehouse (NO 824704). Part of Unit 1 (see text). Beds dip gently into plane of photograph. Palaeoflow from right to left. Note disc enrichment and textural contrast with enclosing conglomerates. Coarse unit is little more than one clast thick.

PLATE 2.2: Imbricate Lithofacies A conglomerates, Lithosome 1, Whitehouse (NO 824704). Beds dip gently to left. Palaeoflow towards observer. Coarse unit wedges out up flow. Note moderate a-axis orientation normal to flow. Viewed towards north.

PLATE 2.3: Imbricate Lithofacies A conglomerates, Lithosome 1, Whitehouse (NO 824705). Beds dip gently to left. Palaeoflow towards observer. Note strong a-axes orientation normal to flow. Hammer is 30cm long. Unit 2 (see text). Viewed towards north.

PLATE 2.4: Textural contrast between Lithofacies A and B conglomerates, Lithosome 1, Whitehouse (NO 824704). Beds dip gently into plane of photograph. Coarse Lithofacies A imbricate conglomerates, disc-enriched with palaeoflow from right to left, are overlain by sphere enriched well sorted Lithofacies B conglomerate. Note this is not part of a fining up couplet. These are separate laterally size differentiated sheets which have been vertically transposed. Hammer is 30cm.

PLATE 2.5: Detail of Lithofacies B conglomerate, Lithosome 1, Whitehouse (NO 824704). Vertical surface normal to the bedding. Note typical bimodal texture and the high degree of rounding characteristic of Lithosome 1 conglomerates. Lens cap 5cm diameter.

PLATE 2.6: Lateral accretion surface, Whitehouse (NO 824705). Beds dip gently to left as indicated by clast a axis orientation. Sandstone lense dips 10-15^{o} steeper than bedding, truncating coarse imbricate conglomerate.

PLATE 2.7 Lithofacies C cross-stratified conglomerate, Lithosome 1, Whitehouse (NO 823703). Bedding strikes parallel to hammer shaft and dips gently into plane of photograph. Cross-strata dip to left. Palaeoflow from right to left. Foreset to left of hammer coarsens downwards. Cross-strata overlain by fine pebble conglomerate. Viewed towards the west.

PLATE 2.8 Lithofacies C low angle cross-stratified conglomerate, Lithosome 1, Whitehouse (NO 823703). Moderately well sorted conglomerate foresets overlying coarse imbricate conglomerate unit (Lithofacies A). Some of foreset conglomerates are matrix supported.

PLATE 2.9 Lithofacies C conglomerates filling channel, Lithosome 2, Kings Step (NO 844729). Vertical NE-SW trending cliff-face, viewed towards north-west. Hammer is 30cm long. Unit of moderate to well-sorted pebble conglomerate 1.0m above hammer strikes directly into coarse massive Lithofacies D conglomerates. Boundary separating lithofacies is a steep channel margin striking normal to cliff face. Stratification within pebble conglomerate dips to left normal to the channel trend and abuts directly against the channel margin.

PLATE 2.10 Coarsening upwards unit, Lithosome 1, Powdam Head (NO 867763). Unit of clast supported imbricate conglomerate overlying planar cross-stratified sandstone with which the conglomerate interfingers. Hammer is 40cm. Viewed towards WNW. Flow from right to left.

PLATE 2.11 Detail of imbricate conglomerate member forming coarsening upwards unit shown in Plate 2.10. Note thin interbedded sandstone.

PLATE 2.12 Matrix support and sphere enrichment in down flow extension of coarse member shown in Plate 2.11. Flow from left to right. Note parallel lamination in conglomerate matrix.

over the imbricate portion of the unit is well developed. Clasts directly in the lee of the imbricate conglomerate are however unusually coarse-grained, resulting in a sudden jump in the M.C.S. profile. This then fines again in the direction of palaeoflow, as the unit becomes increasingly dominated by matrix supported conglomerate.

Unit 3 is dispersed from the NE. The imbricate fabric is of contact type over the first 10m but grades into isolate imbricate conglomerates. The unit overlies further coarse-grained Lithofacies A conglomerates which are dispersed from the NW. There is therefore a 90° rotation in high stage palaeoflow between the successive conglomerate units.

Unit 4: Unit 4 comprises a lower division of cross-stratified sandstone overlain by a complex upper division of conglomerate which both interfingers with the underlying sandstone and passes from imbricate (Lithofacies A) to cross-stratified conglomerate when traced out laterally (Fig. 2.6). The unit is exposed at Powdam Head, c 60m above the Todhead lava, where conglomerates which are finer grained than those which outcrop at Whitehouse or Todhead Point are exposed.

The upper conglomerate division is imbricate over its upcurrent extension, particularly towards the top of the unit (Plate 2.11). When the imbricate conglomerates are traced out downcurrent, the imbrication and clast-supported framework become less apparent, and the coarse division becomes increasingly matrix supported, particularly in its basal part (Plate 2.12). Eventually the flat stratified conglomerates are totally replaced by cross-stratified conglomerate (Lithofacies C). The conglomerates interfinger with the lower sand division which is made up of a single set of large scale cross-stratified coarse sandstone, together with minor trough cross-stratification. Back-sets and re-activation surfaces are also seen.

2.2.1.2 Interpretation

Lateral size and shape segregation of the sort illustrated by the four lithofacies transitions described above, is a feature of

gravel bars in both braided and meandering streams (Bluck 1982). Whilst bar forms show a range of morphology and internal structure, most show a differentiation into a coarser upstream portion (the bar head) and a finer downstream region (the bar tail).

Relatively unmodified bars with morphologies determined by depositional processes alone have been termed unit bars by Bluck (1974) and Smith (1974). These are units of size segregation which form the basic building blocks in the assembly of larger composite gravel bar forms in both braided and meandering streams. Bluck (1982) illustrates the development of texturally differentiated small unit bars from disorganised units with poor grain size and shape segregation. The bars evolve by concentrating coarse disc and blade shaped clasts in the bar head region. These imbricate and impede the downstream migration of the head region relative to the finer tail, allowing the bar to extend. The net effect is to produce a strong size and shape segregation along the bar. Unit bars migrate and attach themselves to larger composite bar structures to generate a range of medial and lateral bar forms (Bluck 1979). The accretion of unit bars to larger bars is followed by a process of adjustment whereby the shape and grain size segregation present on the newly attached unit bar is fused with existing size gradients and shape differentiation over the larger composite bar form. Bluck (1982) suggests a process of clast selection and rejection may be important in producing uniformity in grain size and rate of size decline downstream of the bar head.

The strong lateral shape and size segregation seen in many of the laterally differentiated conglomerates of the Dunnottar and Crawton Groups have a direct analogy in gravel bars seen in many gravelly braided streams. The imbricate disc and blade enriched conglomerates (Lithofacies A) are interpreted as having predominantly formed in the bar head region. These can be traced down current into finer grained often sphere and rod enriched conglomerates which are thought to have accumulated in the bar tail (Lithofacies B). The better sorting and occasional open frameworks seen in the finer grained conglomerates attributed to

the bar tail are commensurate with their having accumulated at lower levels on the bar, with exposure to more prolonged winnowing and reworking. The bar head is generally topographically higher than the bar tail and normally only records the flood stage, being emergent at low flow stage.

Cross-stratified conglomerates (Lithofacies C) are also found in a position analogous to the Lithofacies B conglomerates and they also are thought to have formed in the bar tail region by accretion of the bar tail platform face. This explains the generally finer grain size and more mature textures of the cross-stratified conglomerates. Cross-stratified conglomerates which are finer grained than accompanying massive or flat stratified conglomerates have been recorded in proximal braided streams by Smith (1974) and in ancient alluvium by Eynon and Walker (1974), Steel and Thompson (1983) and Rust (1984). Textural differentiation of the foresets is not as well developed as those described by Steel and Thompson (1983) and Rust (1984). Bar top sorting and the arrival of bar top gravel bedforms at the slip face (Baker 1973, Rust 1984) are both considered to contribute to the textural differentiation of conglomeratic foresets. Both the Malbaie conglomerates and the Bunter Pebble Beds considered by Rust (1984) and Steel and Thompson (1983) respectively are considerably finer grained than the conglomerates considered here and bar top sorting and gravel bedform migration are therefore likely to have been more effective. Gravel bedforms are unlikely to have developed in the bar top environment in the coarse conglomerates of the Dunnottar and Crawton Groups. The coarsening and thickening of foresets when traced downwards is consistent with an origin by avalanching. The thicker cross-stratified conglomerate units (>3.0m) may reflect migration of the bar platform into a deeper scour pool or channel.

Whereas the bar head can be traced down current directly into the bar tail in some gravel bars forming meandering streams, in braided streams the bar head often rotates to parallel the channel trend, trapping the bar tail against the accretionary bank (Bluck 1982). This may account for the trans verse orientation of the transition from imbricate to non-imbricate

conglomerate with respect to the palaeoflow noted above and in Figure 2.2 for Unit 1. It also explains the general discordance often seen between palaeoflow estimates based on imbrication in the bar head and cross-stratification in Lithofacies C conglomerates which are interpreted as having accumulated in the bar tail. The sense of rotation between palaeoflow estimates from the bar head and the bar tail can therefore be used to identify the bar accretion direction, and hence the direction of channel migration for fluvial systems in which the channel migrates by preferential attachment of bars to a single bank. Preliminary data for conglomerates from Whitehouse suggest that channels were predominantly migrating eastwards.

2.2.1.3 Implications for Coarsening Upwards Units

Whilst laterally differentiated conglomerates showing down-current lithofacies transitions are found to characterise a small proportion (10%) of the Dunnottar and Crawton Group succession, units which perceptibly coarsen upwards from a sharp base are altogether more common particularly in the Dunnottar Group (Fig. 2.7). These have the following characteristics:

1. They form tabular or sheet like units generally between 2 and 5m thick, but occasionally reaching as much as 7.0m. Some can be traced laterally for over 50m.

2. They have sharp, in some cases erosional, bases. Often distinct fine and coarse members can be recognised. These are separated by a sharp contact or rapid transition. Only in instances in which the fine member is dominated by sand can lateral interfingering between fine and coarse members be discerned. Some coarsening upwards units show a diffuse contact between fine and coarse members, and continuous grading.

3. The most frequent upward transition is from Lithofacies B to Lithofacies A or D. Cross-stratified conglomerates (Lithofacies C) or sandstones (Lithofacies E) occasionally make up the fine member. The lithofacies interface is often characterised by concentrations of large volcanic clasts which may confuse coarsening upwards trends.

Figure 2.7 Part of detailed log through a sequence of Lithosome 1 conglomerates exposed at Downie Point (NO 883853) illustrating the importance of 2-6m thick units which coarsen upwards. MQS and MVS measurements (mean of the ten largest metaquartzite and volcanic clasts within $2m^2$ respectively) complement MCS data allowing concentrations of outsized volcanic clasts to be identified. Clast compositions are based on 50 counts of clasts with MCS greater than 25cm. Clast imbrications measured at X indicate a north-easterly provenance. Arrows are tilt-corrected cross-bed dip azimuths. Note bedding is vertical over measured section and large tilt-corrections have to be applied to orientation data. For legend refer to 2.16.

m.

100

90

80

70

60

50

40

30

F

X

CLAST COMPOSITIONS

KEY

Coarsening upwards units

Outsize volcanic clasts

• M.C.S

+ M.Q.S.

× M.V.S.

metaquartzite

volcanics

others

M.C.S.

0 20 40 60

cm.

50 100

%

N

n=38

IMBRICATION

Figure 2.8

A. Two mechanisms for producing coarsening upwards cycles. The upper sequence illustrates progressive downstream migration of the head region of a gravel bar over the finer grained bar tail. The bar form develops from a diffuse gravel sheet with poor grain size and shape segregation. Coarse discoidal clasts are concentrated in the upstream bar head impeding downstream migration and allowing the bar to extend its long axes. Coarse spheres are rejected from the imbricate fabric and are concentrated in the mid-bar region or in downstream scour pools. Extension and migration of the bar downstream generates coarsening upwards cycles. The lower sequence illustrates the generation of coarsening upwards sequences by downstream accretion and growth of a bar from an immobile or fixed head region. Sediment supplied to the bar is distributed over progressively greater lengths as the bar aggrades vertically and extends laterally.

B. Terminology for lateral bars (i.e. bars found on lateral channel margins) after Bluck 1982.

A

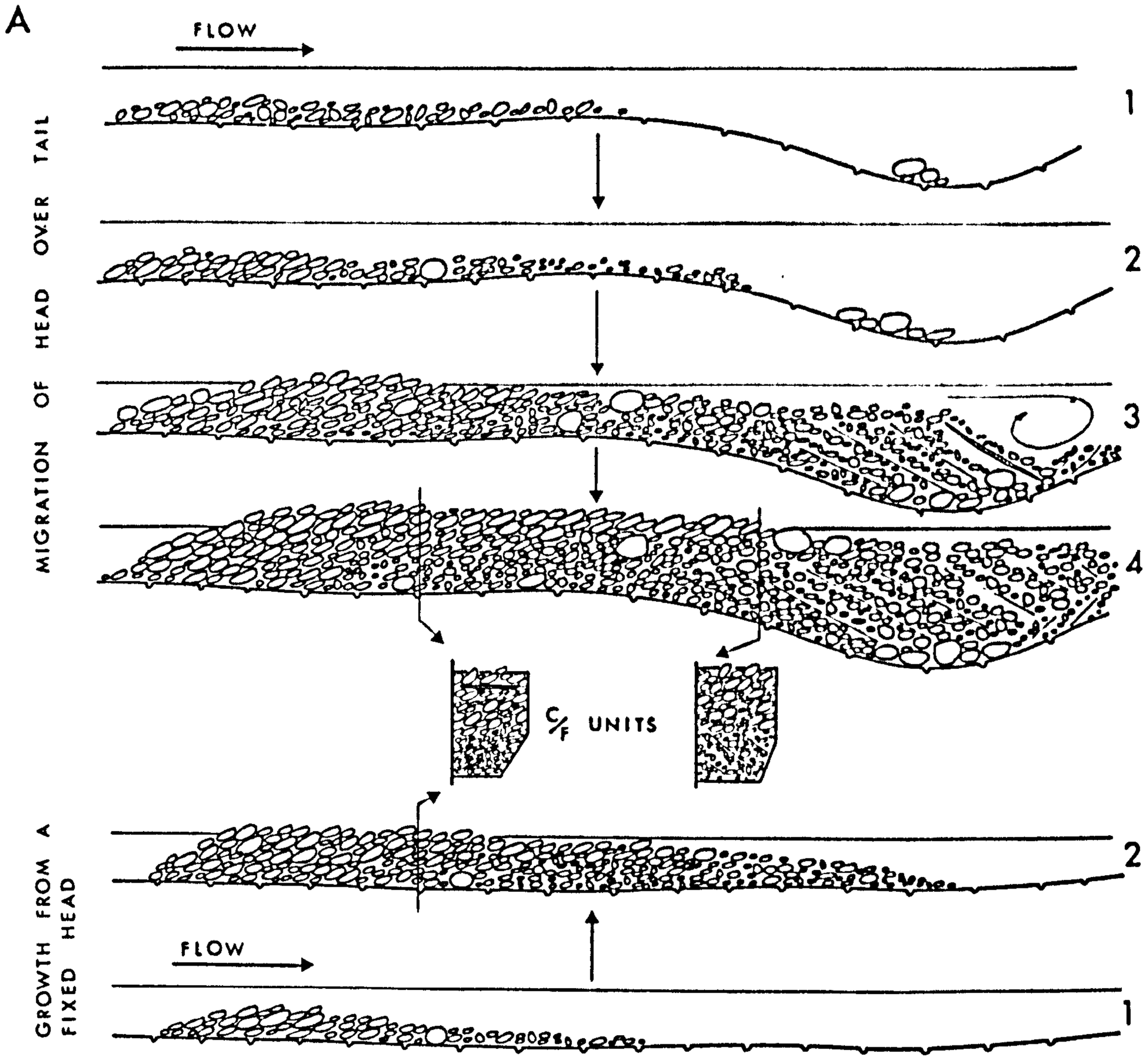
FLOW
HEAD OVER TAIL
MIGRATION OF
1
2
3
4
C/F UNITS
GROWTH FROM A
FIXED HEAD
FLOW
2
1

B

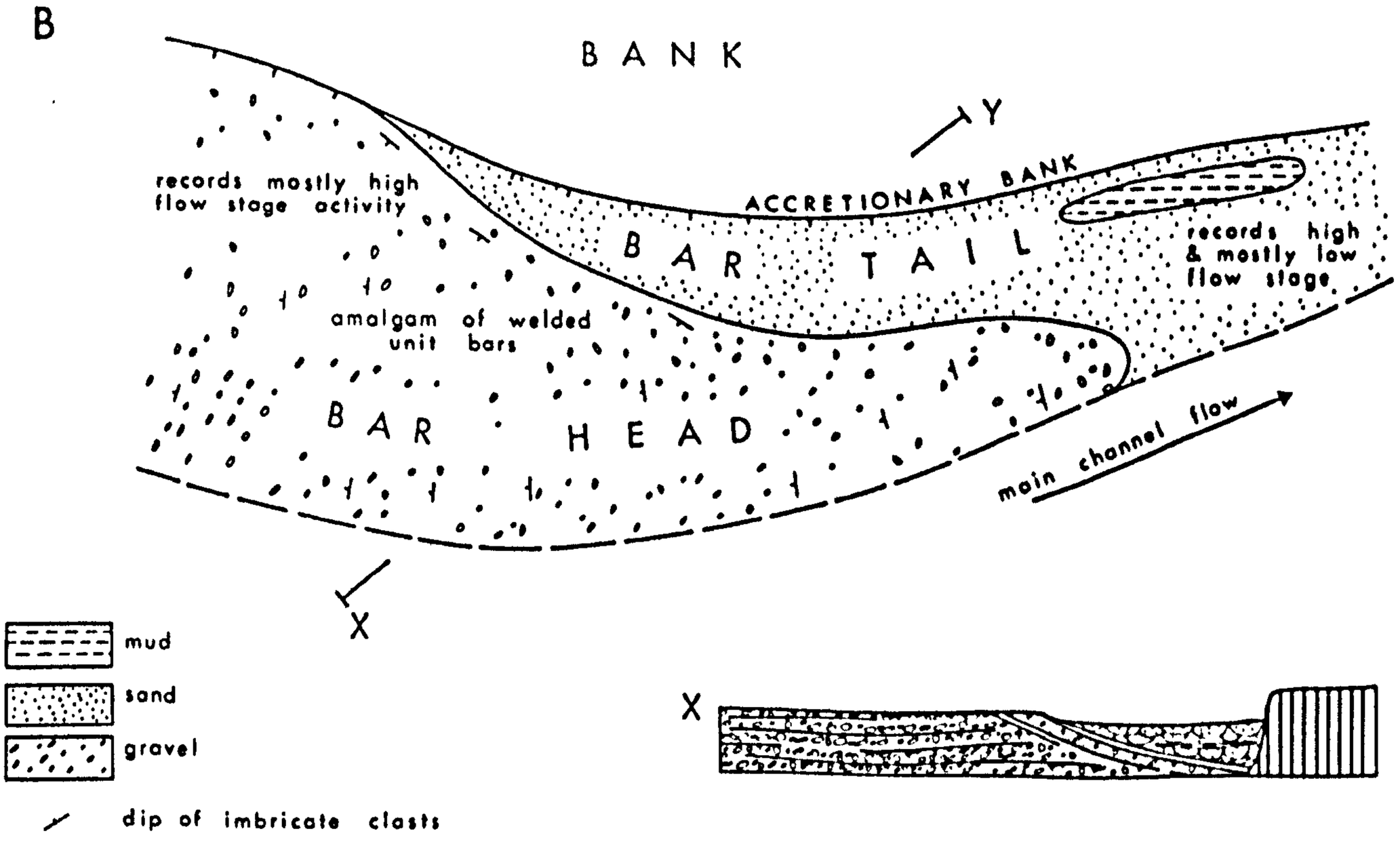
BANK
Y
ACCRETIONARY BANK
records mostly high
flow stage activity
BAR TAIL
records high
& mostly low
flow stage
amalgam of welded
unit bars
BAR HEAD
main channel flow
X
mud
sand
gravel
dip of imbricate clasts
X
Y

4. The coarse member may or may not be well imbricate. The textural maturity of the coarse member appears to be a function of the abundance of volcanic clasts it contains.

5. The inclination of the interface between coarse and fine members is generally low, but in some cases it is relatively steep, with the coarse member climbing over the fine member.

6. The coarser member is almost always thicker than the underlying fine member.

Vertical changes in grainsize have not been widely recognised in flat stratified gravel sheets in braided stream environments. Smith (1974) showed a general trend towards upward fining in exposed unit bars in the Kicking Horse river. This was attributed to accretion during waning flow. Larger composite bars however showed no systematic vertical grain size distribution. Bluck (1976) recorded coarsening upwards in medial bars produced by migration of the bar head over the bar tail. Coarsening upwards units occurring in pebbly sandstones of the Upper ORS were subsequently shown to probably reflect the operation of a similar process, with strong size segregation on small sediment bars followed by translation of the coarse head over the finer tail by downstream migration (Bluck 1980). Steel and Thompson (1983) recorded sequences in which graded and texturally complex flat stratified conglomerates were replaced vertically by coarser grained less mature, massive conglomerates. The coarsening upwards cycles were shown to be compatible with a model involving bar head migration over bar-tail gravels, but the scale of the units was thought to favour progradation at a larger scale, with possible migration of gravel sheets from upstream reaches over finer grained bars further downstream.

The laterally differentiated conglomerate sheets described in 2.2.1.1 show that shape and size segregation was a feature of sediment accumulation during deposition of a substantial part of the Dunnottar and Crawton Groups. Textural and grain size equivalents of the lithofacies making up the coarsening upwards

(CU) cycles can be recognised within single laterally preserved depositional units. The transposition of coarse over fine seen in the thick upward coarsening units therefore does not require that the two members accumulated in different reaches of a braided stream, and were subsequently juxtaposed by large scale progradation of the depositional system. Migration of the coarse grained Lithofacies A or D bar head over finer grained texturally more mature sediments of the bar tail (Lithofacies B or C) has the potential to produce the required textural and grain size transitions seen in the CU cycles. In this respect the coarse to fine lateral lithofacies transitions are a higher order of organisation than the CU cycles they produce by lithofacies transposition.

The considerable scale of the coarsening upwards units is of interest in that they approach in thickness coarsening upwards phenomena attributed by others to the operation of allocyclic processes. Thus Steel et al (1977) describe coarsening upwards sub-cycles of the order of 10-25m thick in marginal fan deposits of the Hornelen Basin. These they attribute to aggrading base-level conditions in response to episodic basin-floor subsidence.

Migration of bar head gravels over the bar tail can be seen in units transitional between strictly laterally differentiated sheets and CU cycles. In these units the coarse member-fine member interface is steep, and the coarse member climbs over the fine member. Where the bar head is made up of strongly imbricate disc enriched conglomerates it may have been relatively immobile (Bluck 1982). Physical migration of the bar head over the bar tail in such instances may not have been an effective mechanism for producing coarsening upwards units. The growth of a bar by downstream accretion from a fixed head however should also produce coarsening upwards cycles by redistributing and size segregating sediment supplied to the bar over progressively greater lengths as the bar aggrades vertically and extends laterally (Fig. 2.8). The low angle interface between coarse and fine members may reflect rapid regrading of the bar surface as unit bars are intermittently accreted and absorbed within the bar structure, or the migration, attachment and merging of larger

composite bar structures.

The concentration of large outsized volcanic clasts on the interface between coarse and fine members often serves to complicate the coarsening upward trend. The concentration of outsized clasts at the base of the coarse member is analogous to the perturbation in maximum clast size profiles along laterally fining units noted above. Bluck (1982) suggested textural modification on sediment bars may involve a process of selection and rejection, with the imbricate bar head acting as a template in controlling grain size and shape selection over the bar supraplatform. The coarse clasts of the bar head may create sufficient turbulence to allow only clasts large enough to tolerate the induced turbulence to settle downstream of the head. The strong contact imbricate fabric often developed in the head will also reject those rod and sphere shaped clasts which cannot slot into the existing fabric. The concentration of large clasts in the lee of the imbricate zone in laterally differentiated sheets, and on or close to the coarse-fine interface in CU cycles, may reflect a rejected clast population concentrated in the mid-bar region.

The high sphericities of many of the volcanic clasts, and the fact that the volcanic detritus is dispersed independently to the basin and is consequently in disequilibrium with the non-volcanic conglomerates with which it is admixed, result in a high proportion of the rejected clasts being volcanic. Where volcanic clasts dominate the coarse member, imbrication is less well developed and massive conglomerates of Lithofacies D type dominate. The extent to which volcanic clasts are admixed with the non-volcanic conglomerates therefore exerts an important control on the structure of the lithosome.

2.2.2 Lithosome 2: Channel-fill Conglomerates

Lithosome 1 is characterised by sheet-like laterally differentiated conglomerates which resemble gravel bars in modern braided and meandering streams. Aggradation of these bars and transposition of their internal lithofacies in many instances produces sequences dominated by CU cycles. In total contrast,

the structure of Lithosome 2 is critically controlled by the development and lateral migration of conglomerate filled channels. Whilst the internal structure of these channel-fills in many cases involves laterally differentiated units similar to those described making up Lithosome 1, it is the geometry and behaviour of the channels which critically control and distinguish the development of the lithosome.

2.2.2.1 Channel Form

Lithosome 2 shows a more intimate interaction with volcanogenic sediment than does Lithosome 1. Whereas Lithosome 1 is dominantly conglomeratic (c 90%), sandstones make up a more important component in sequences ascribed to stacking of Lithosome 2 (c 50%). However these sandstones, and subordinate matrix-supported conglomerates associated with them, have a volcanic provenance quite unlike the provenance of the non-volcanic framework-supported conglomerates which fill the channel structures. A conventional interpretation of the interbedded sequence of channelised conglomerates and laterally extensive coarse sandstones as channel and related flood plain deposits respectively is therefore misleading, as the two are largely generated by unrelated sets of processes (2.5.2).

The alternation of sand dominated volcanogenic sediment with channel-fill (tectonogenic) conglomerates is illustrated by a measured section (Fig. 2.9) through conglomerates and sandstones of the upper part of the Crawton Group exposed at Kings Step (Grid reference NO 844729). A recurring pattern is a vertical stacking of channel-fill conglomerates involving an upward increase in channel scale, density and interconnectivity. Fine-grained polymict conglomerates occur in thin and unconnected channel structures towards the base of these sequences. Channel depth increases in successive channels, as does the maximum clast size of the channel-fill conglomerates. Increasing channel interconnectivity produces laterally continuous amalgamated units of coarse polymict conglomerate in which it becomes increasingly difficult to recognise channel margins (Plate 2.9). Cross-strata in excess of 6m thick in some of these units attest to considerable channel depths. The channelled sequence is rapidly

Figure 2.9 Detailed log of Lithosome 2 conglomerates exposed at Kings Step (NO 845729) illustrating basic structure, dispersal and clast compositions. Vertical channel margins indicate northwest-southeast and east-west channel orientations. Cross-stratified conglomerates filling channels have cross-stratal dips at high angle to channel trends. Clast compositions are based on 50 and 100 counts for >20cm and 5-10cm size intervals respectively at each sampling site. For legend refer to Figure 2.16.

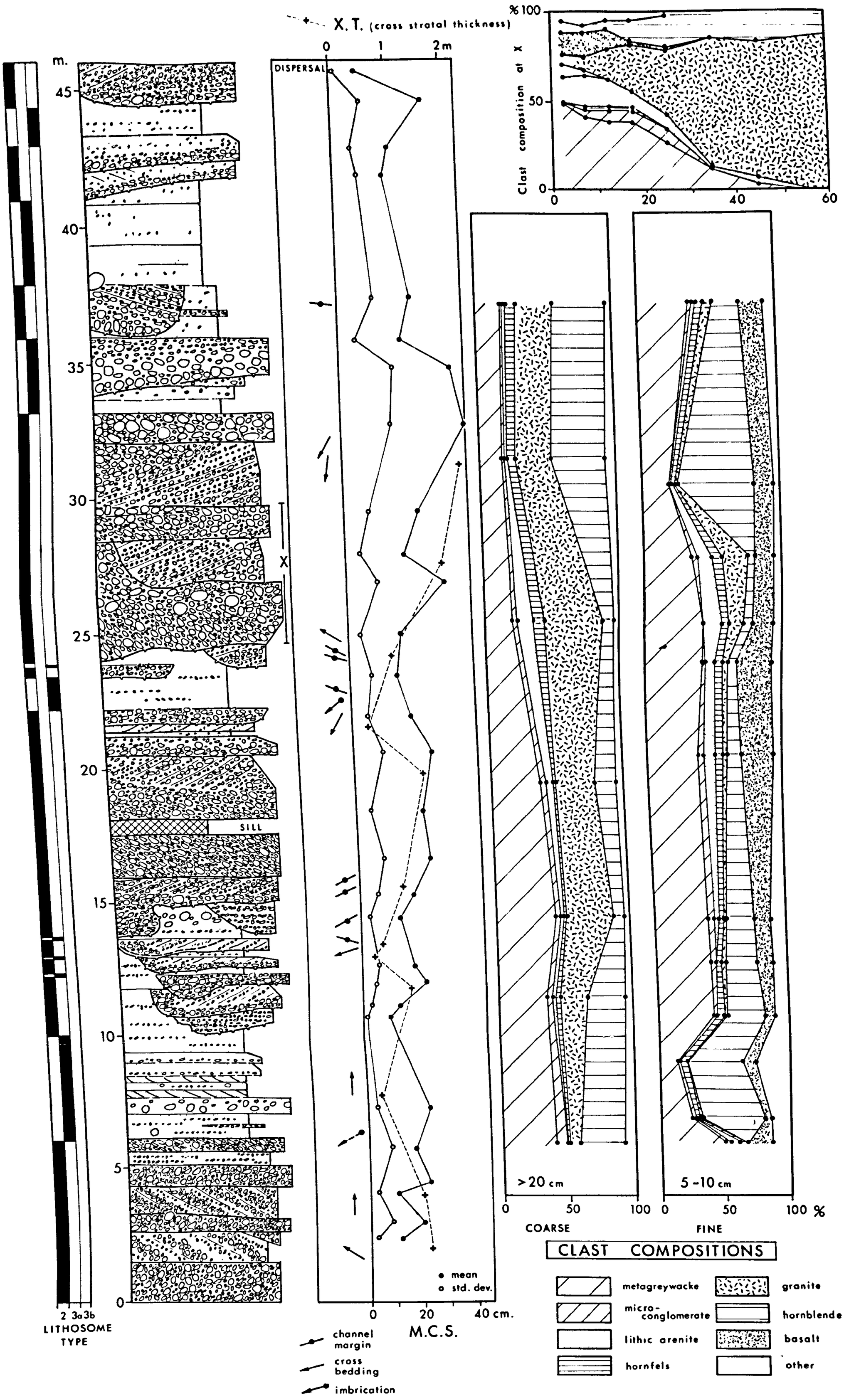
m.
45
40
35
30
25
20
15
10
5
0
X
SILL
2 3a 3b
LITHOSOME TYPE
X. T. (cross stratal thickness)
0 1 2m
DISPERSAL
0 20 40 cm.
M.C.S.
channel margin
cross bedding
imbrication
mean
std. dev.
% 100
50
0
Clast composition at X
0 20 40 60
>20 cm
5 -10 cm
0 50 100
0 50 100 %
COARSE
FINE
CLAST COMPOSITIONS
metagreywacke
micro-conglomerate
lithic arenite
hornfels
granite
hornblende andesite
basalt
other

abandoned by a return to volcanogenic sandstones and conglomerates, although occasional isolate channels may persist.

The channels tend to have rectangular cross-sections, with a distinct flat or undulose base and steep margins which sometimes are stepped. Frequently only a single margin is present, and the channel floor is at its deepest close to this margin. Where channels preserving a single margin are stacked, often successive channels preserve the same margin. Where both channel margins are preserved, the channels are generally symmetrical and have low width/depth ratios. Many of the steep channel margins show evidence for undercutting (Plate 2.16) particularly when developed directly on volcanogenic substrates, suggesting the banks were relatively cohesive. As the undercut banks are generally composed of very coarse tuffaceous sands, this suggests they must have undergone early cementation. In longitudinal section the channels have a range of open and steepsided scour hollows (Plates 2.13, 2.14). Large angular blocks of the volcanogenic sandstone which often form the bank and floor to the channels are sometimes found floating in the channel fill (Plate 2.13). Bright red mudstone intraclasts are also occasionally found concentrated close to the channel floor, as are outsized volcanic clasts.

2.2.2.2 Structure of Channel Fill

The channels show a range of internal structure. Clast supported frameworks and polymodal clast distributions are almost ubiquitous (Plates 2.17, 2.18). Open-frameworks are more commonly observed than in conglomerates of Lithosome 1. Channels in which only a single channel margin is preserved have a complex internal structure whilst channels in which both margins are seen generally have massive fills of either crudely imbricate (Lithofacies A) or massive non-imbricate poorly sorted conglomerate (Lithofacies D). The greater complexity of channels in which only a single bank is exposed suggests that channel migration is largely responsible for producing differentiation in the channel-fill. Conglomerates directly adjacent to the channel margin commonly occur as large planar foresets, dipping normal to the channel trend and abutting directly against the steep channel

PLATE 2.13 Longitudinal section through deep scour hollow along base of Lithosome 2 channel, Kings Step (NO 844728). Vertical face normal to bedding. Palaeoflow from right to left (east to west). Note undercutting of scour margin (a) and large block of tuffaceous sandstone displaced from hollow (b). Hammer is 30cm.

PLATE 2.14 Longitudinal section across open scour structure along base of Lithosome 2 channel conglomerate, Kings Step (NO 844728). Vertical face normal to bedding. Palaeoflow from right to left (east to west). Note very poor sorting and steep near vertical imbrication over scour exit. A large outsized volcanic clast occurs close to the base of the channel (a).

PLATE 2.15 Cross-section through small channel illustrating lateral lithofacies transition, Lithosome 2, Kinneff (NO 858746). Vertical rock face viewed from the south east normal to channel margin orientations. Coarse massive conglomerate unit (1.2m thick) in centre right passes laterally to southwest into planar cross-stratified sandstone with conglomerate interfingering down foresets. Foreset dip orientations are normal to channel trend.

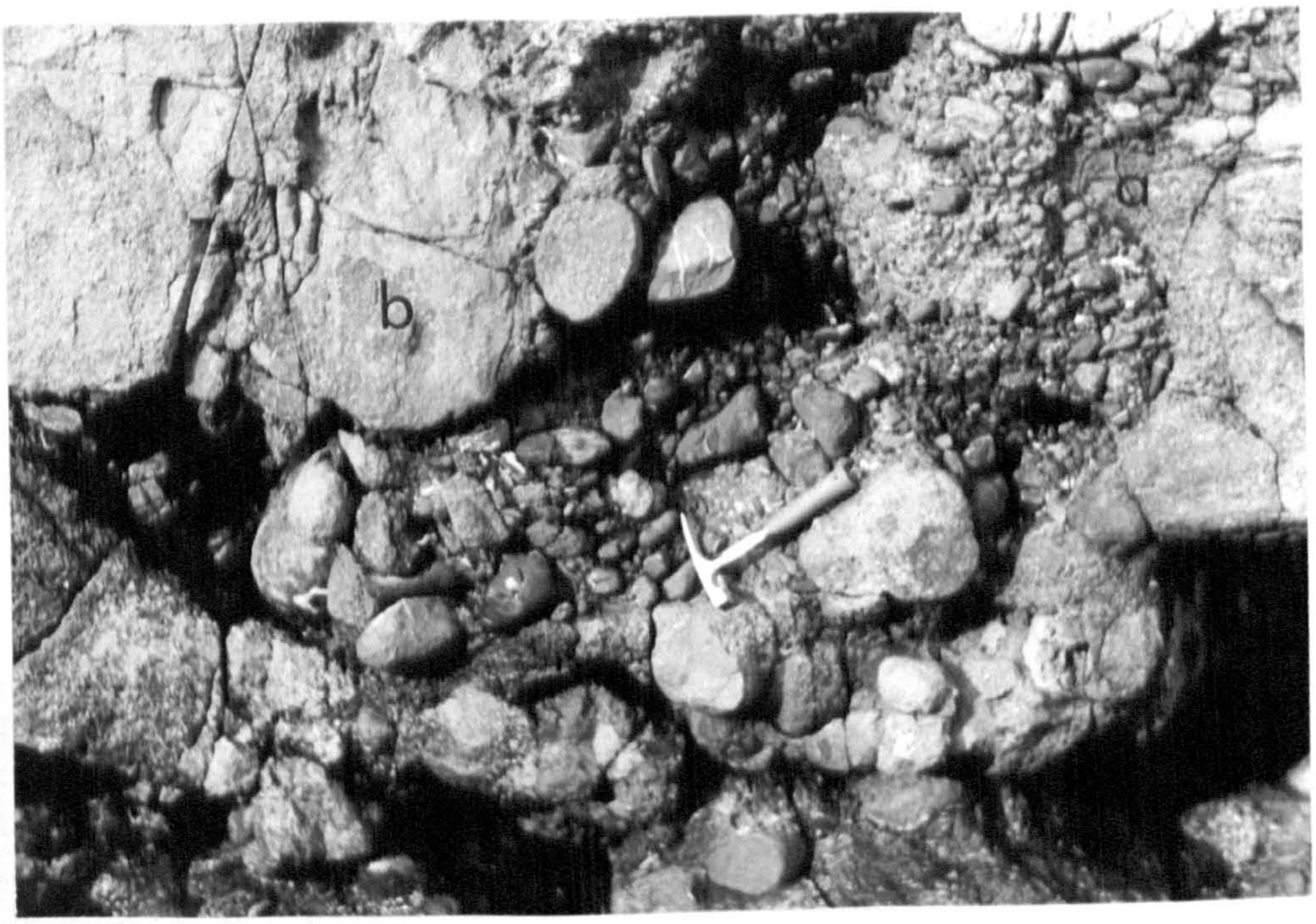
b
a

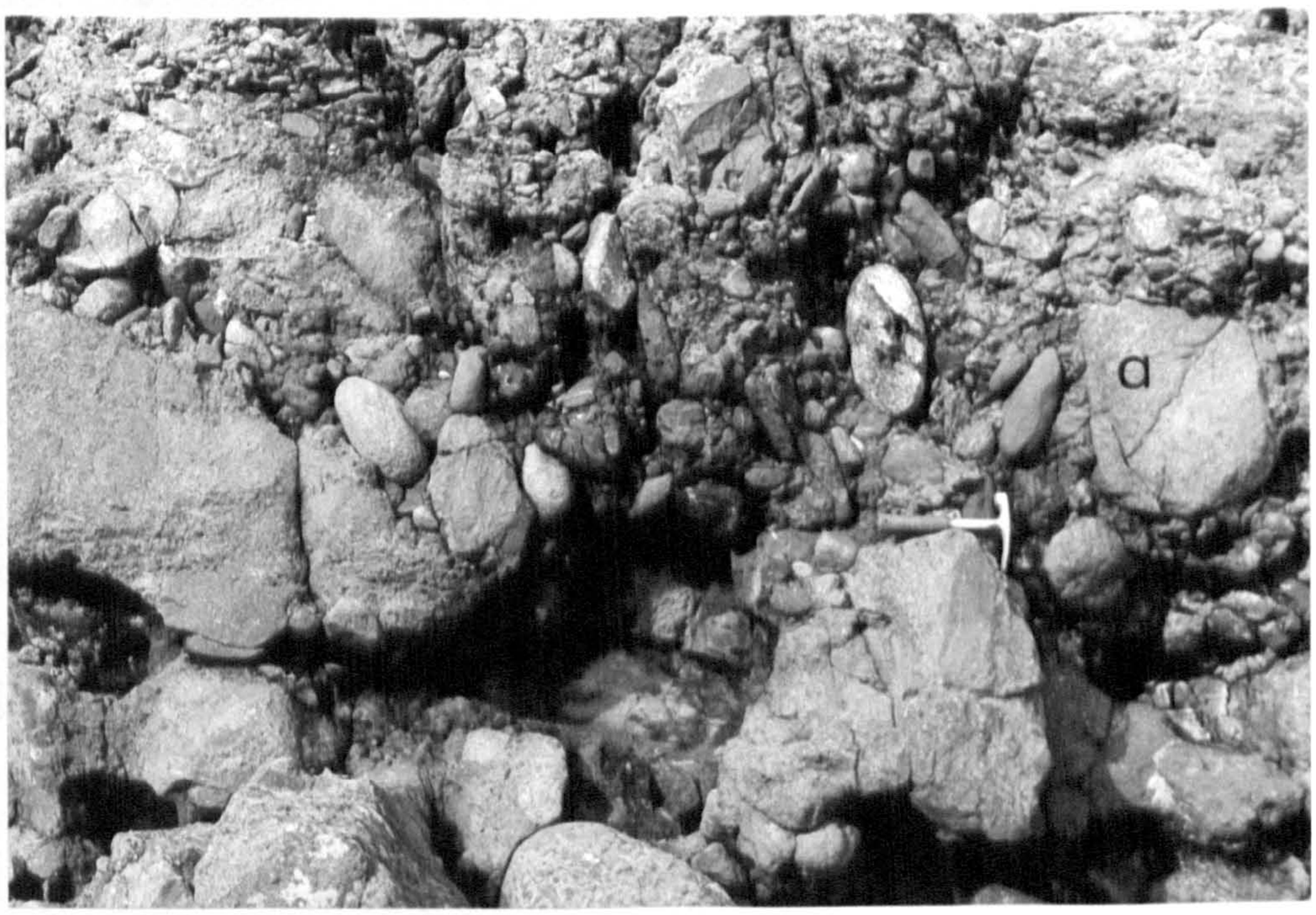
a

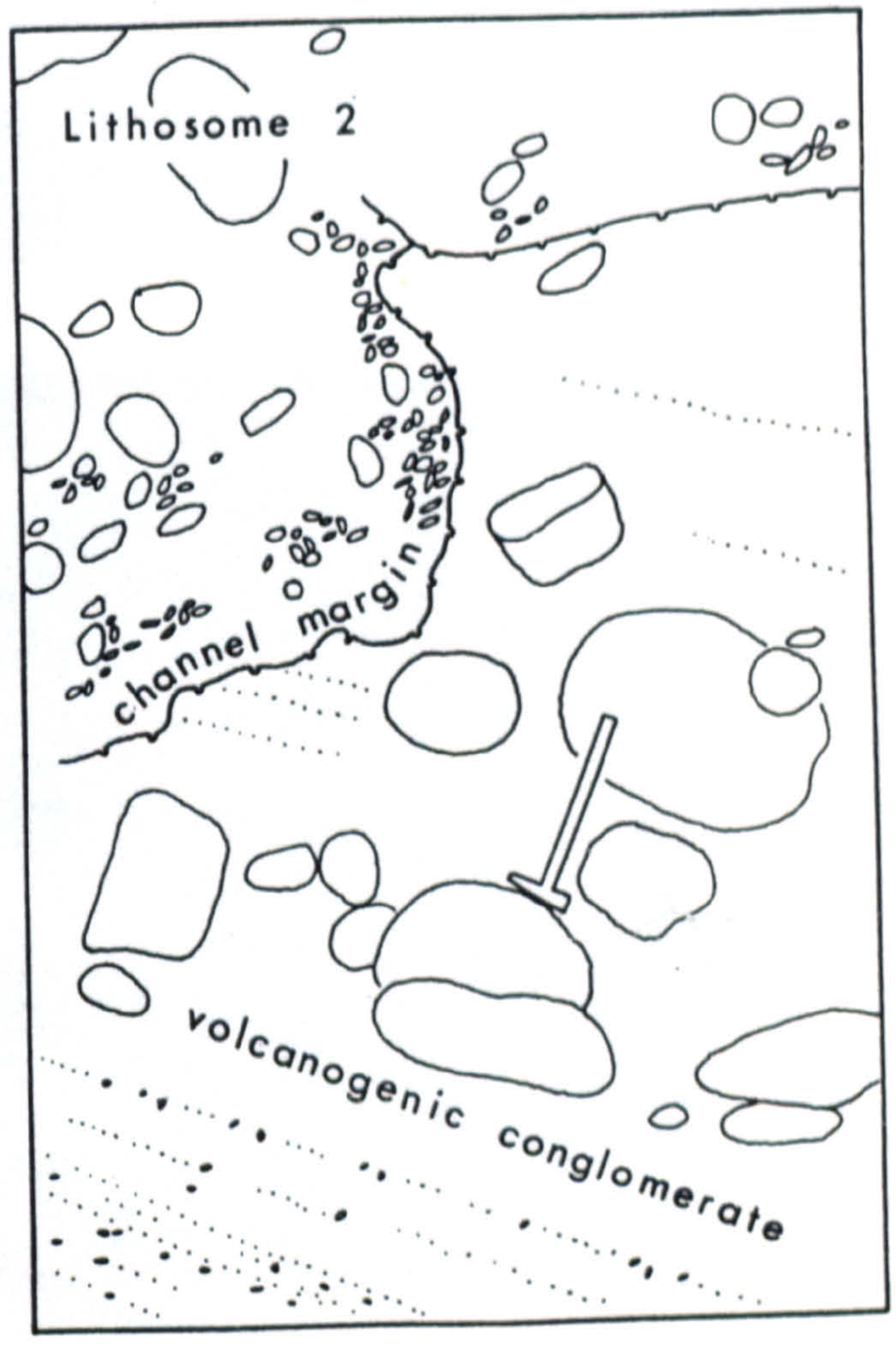

PLATE 2.16 Transition from volcanogenic unit to Lithosome 2 conglomerate, Kings Step (NO 844728). NE-SW trending vertical cliff face, viewed from SE. Steep undercut channel margin cuts coarse matrix supported volcanogenic conglomerate (Lithosome 3a) at the base of a channelled Lithosome 2 conglomerate sequence.

PLATE 2.17 Texture of Lithosome 2 conglomerates, Kings Step (NO 844728). Very poorly sorted crudely imbricate (a) Lithofacies A conglomerate composed dominantly of clasts of equigranular hornblende-biotite granite, lithic arenite and metagreywacke. Note angularity of many clasts and contrast with bimodal Lithosome 1 conglomerates. Lens cap 5cm. Vertical face with flow from right to left.

PLATE 2.18 Texture of cross-stratified conglomerates, Lithosome 2, Kings Step (NO 844728). Viewed normal to bedding with cross-bed dip parallel to base of Plate. Note crude grain-size segregation, foreset parallel orientation of disc and blade shaped clasts and open framework. Lens cap 5cm.

PLATE 2.19 Thin coarsening upward unit, Kinneff (NO 858746). Sheet of massive poorly sorted conglomerate overlying thin planar cross-stratified pebbly sandstone with which it interfingers in centre right.

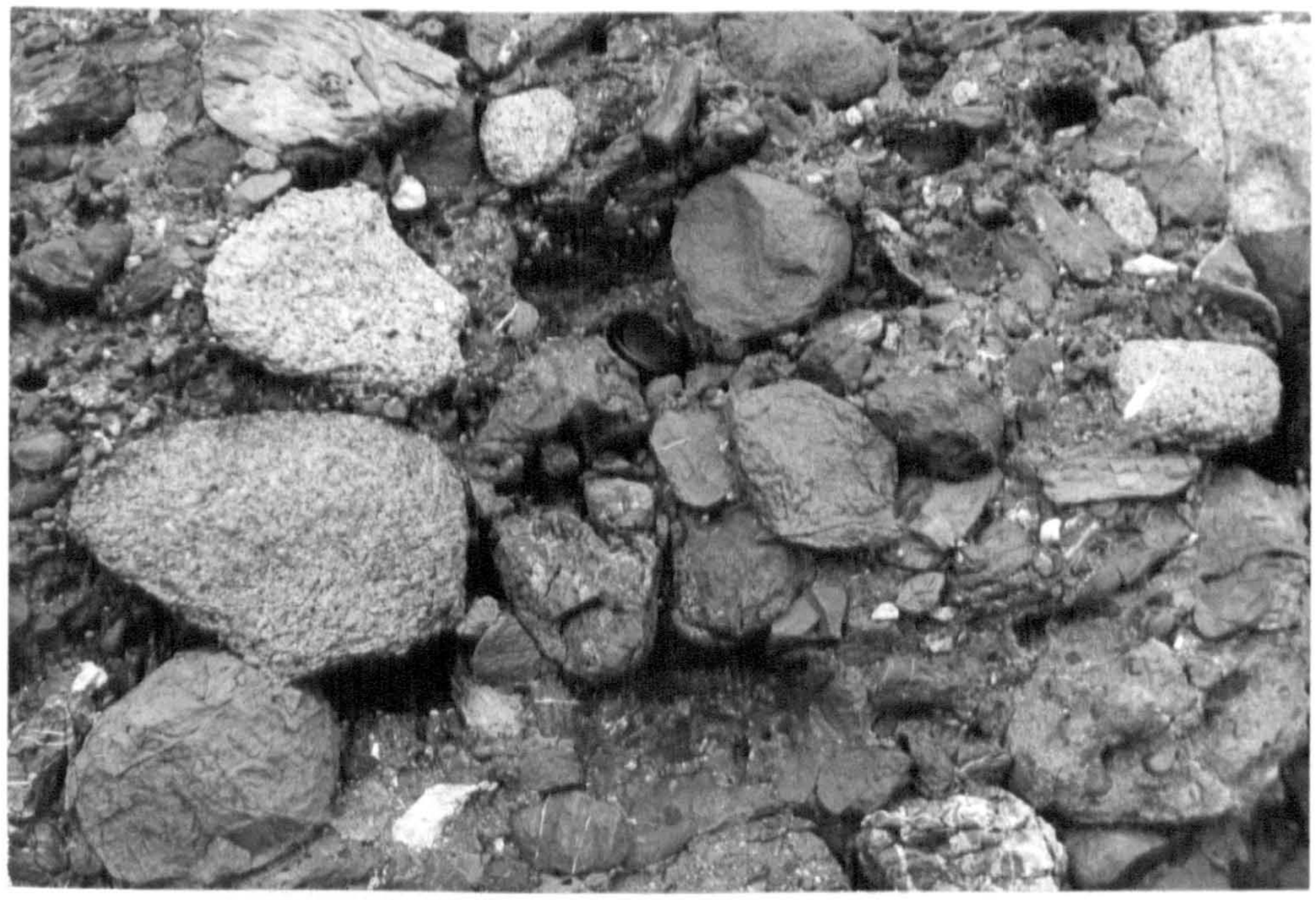

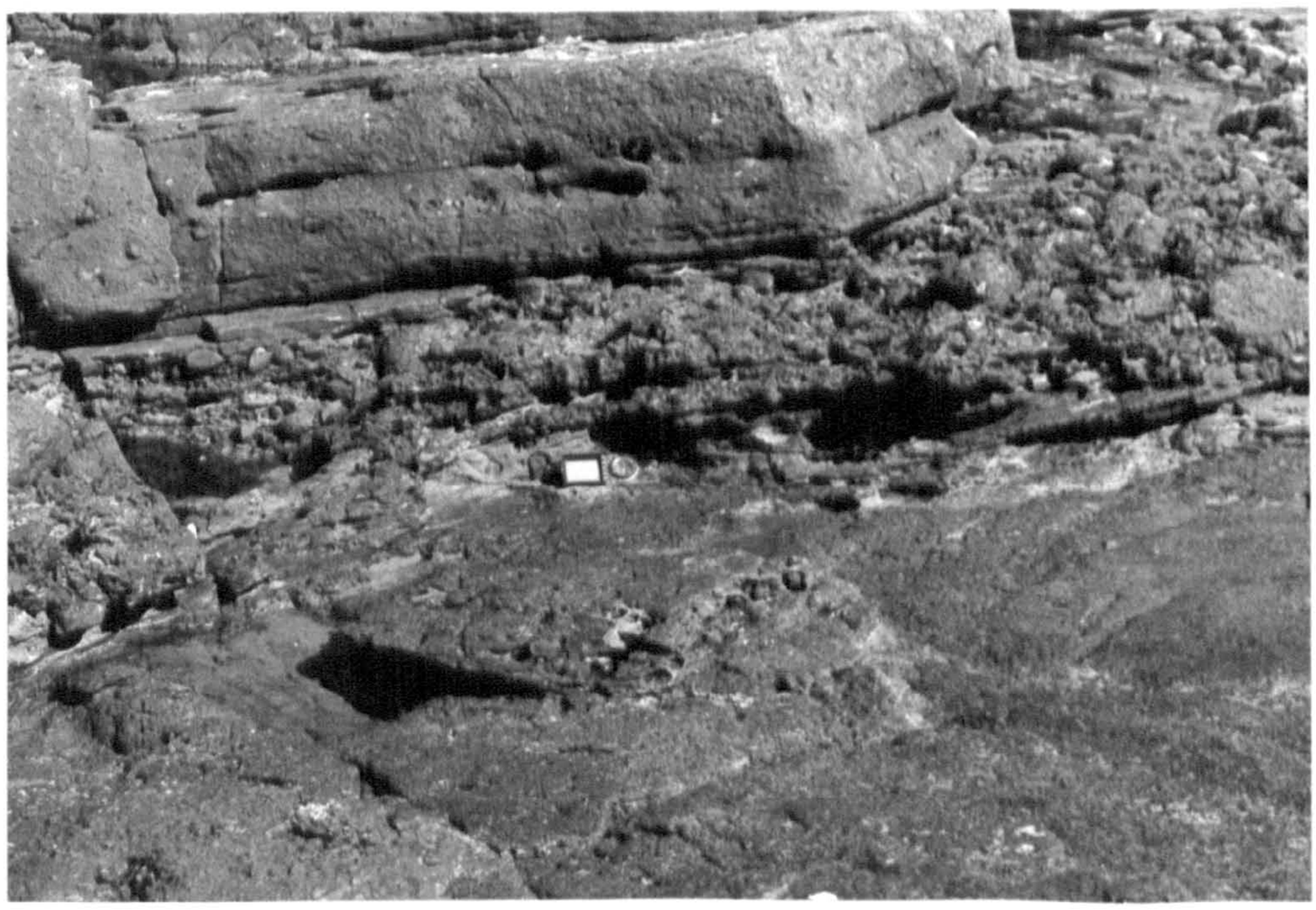

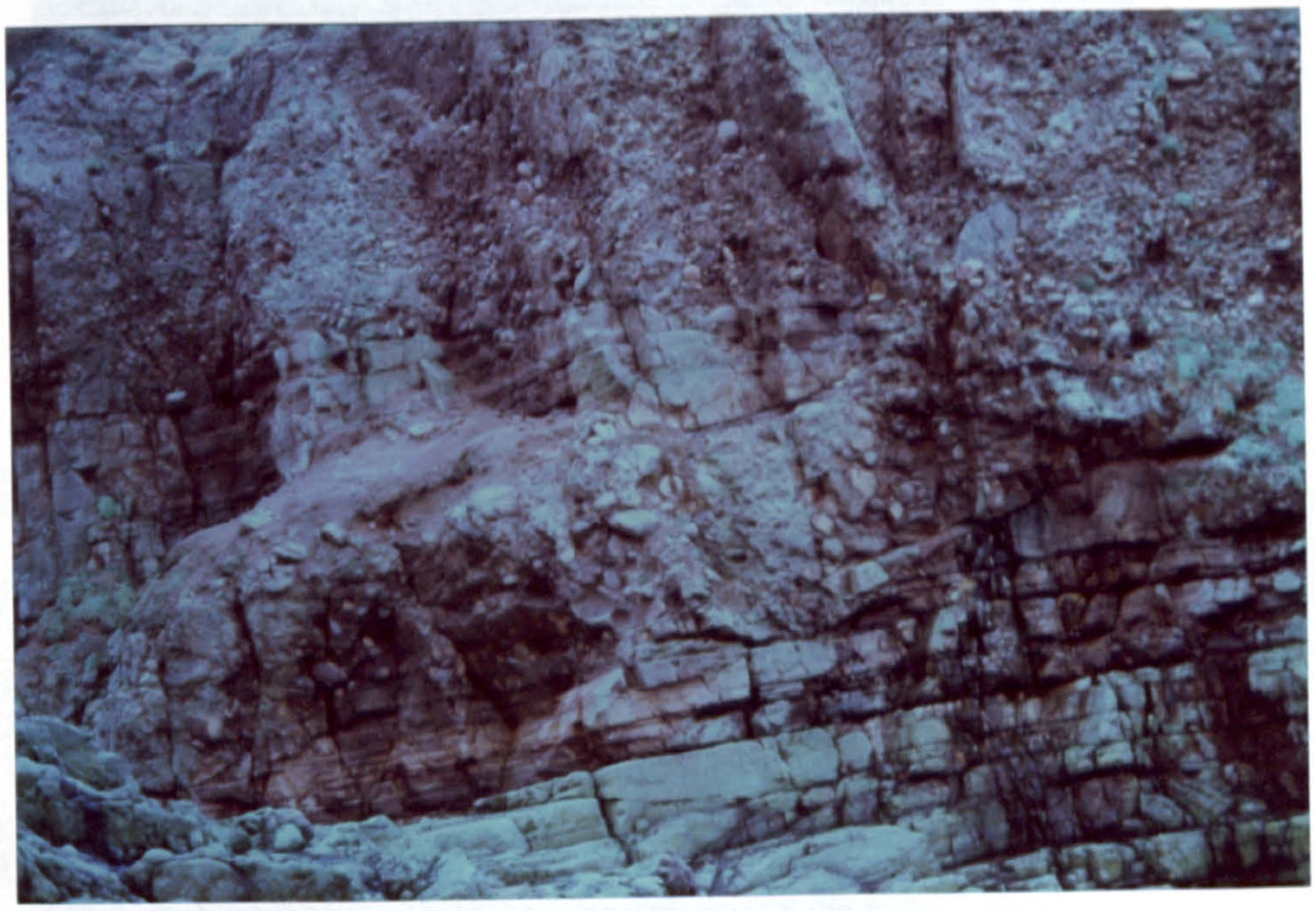

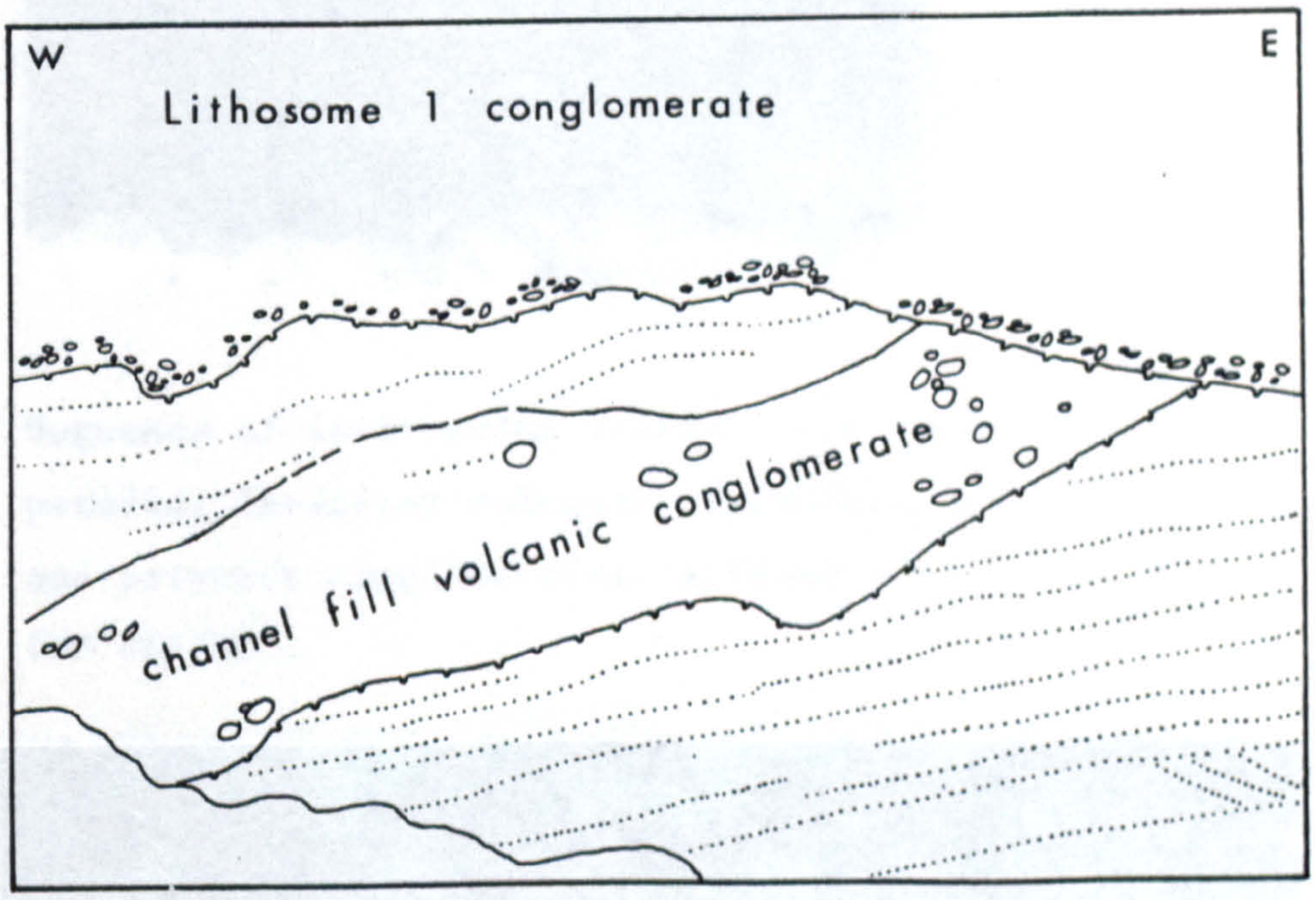

PLATE 2.20 Angular contact between northerly and north-easterly derived Lithosome 1 association conglomerates and southerly and easterly derived volcanogenic sequence at Kinneff (NO 858746). Vertical cliff face trending east-west and viewed from south. Large channel is 5m deep and filled with volcanic clasts of a single lithology.

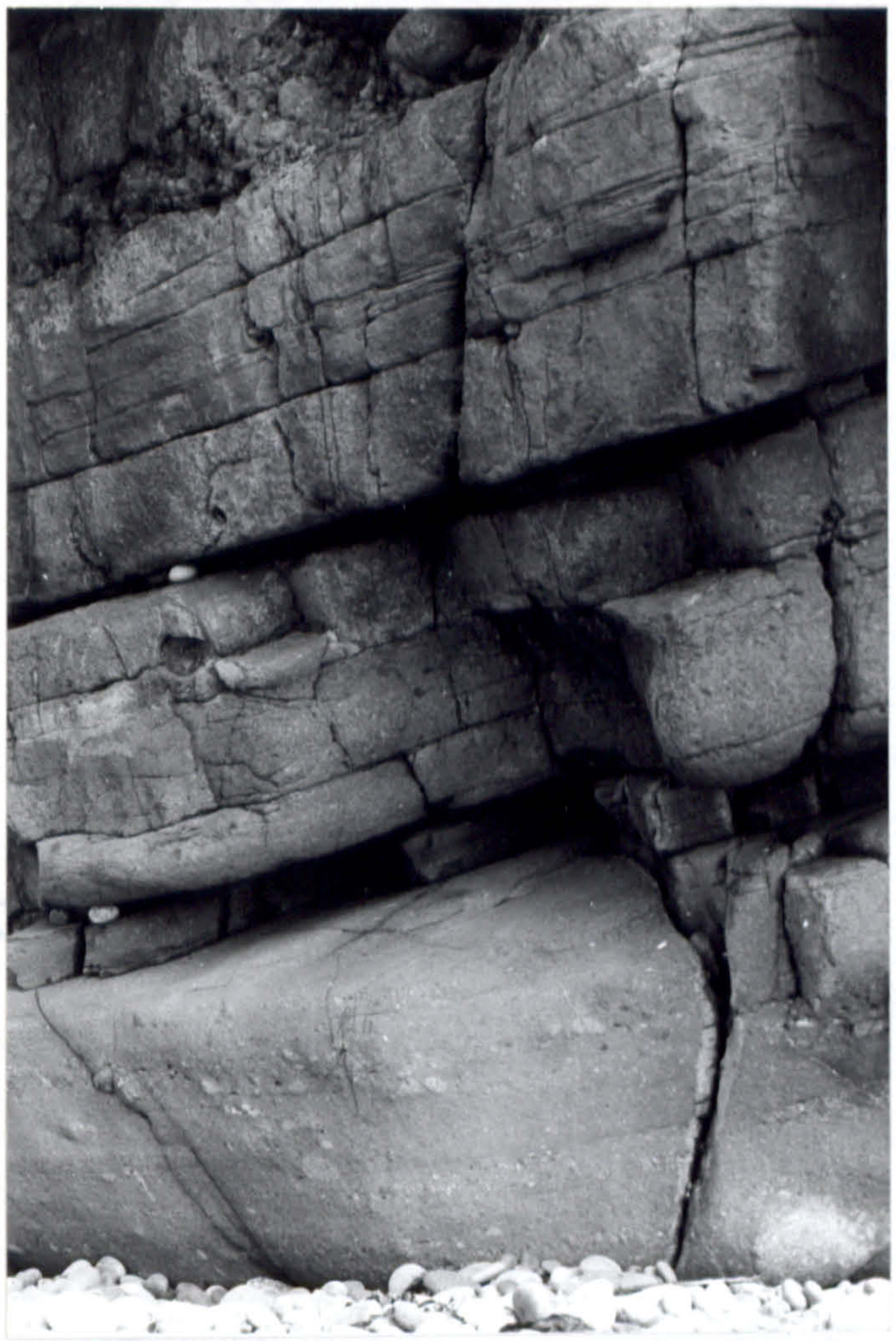

PLATE 2.21 Sequence of interbedded massive tuff breccia sheets, parallel laminated volcanic sandstones, and volcanic and polymict conglomerates. Lithosome 3, Darn Bay (NO 849738).

PLATE 2.22 Well-rounded metaquartzite clast showing percussion marks, Todhead Point (NO 871769).

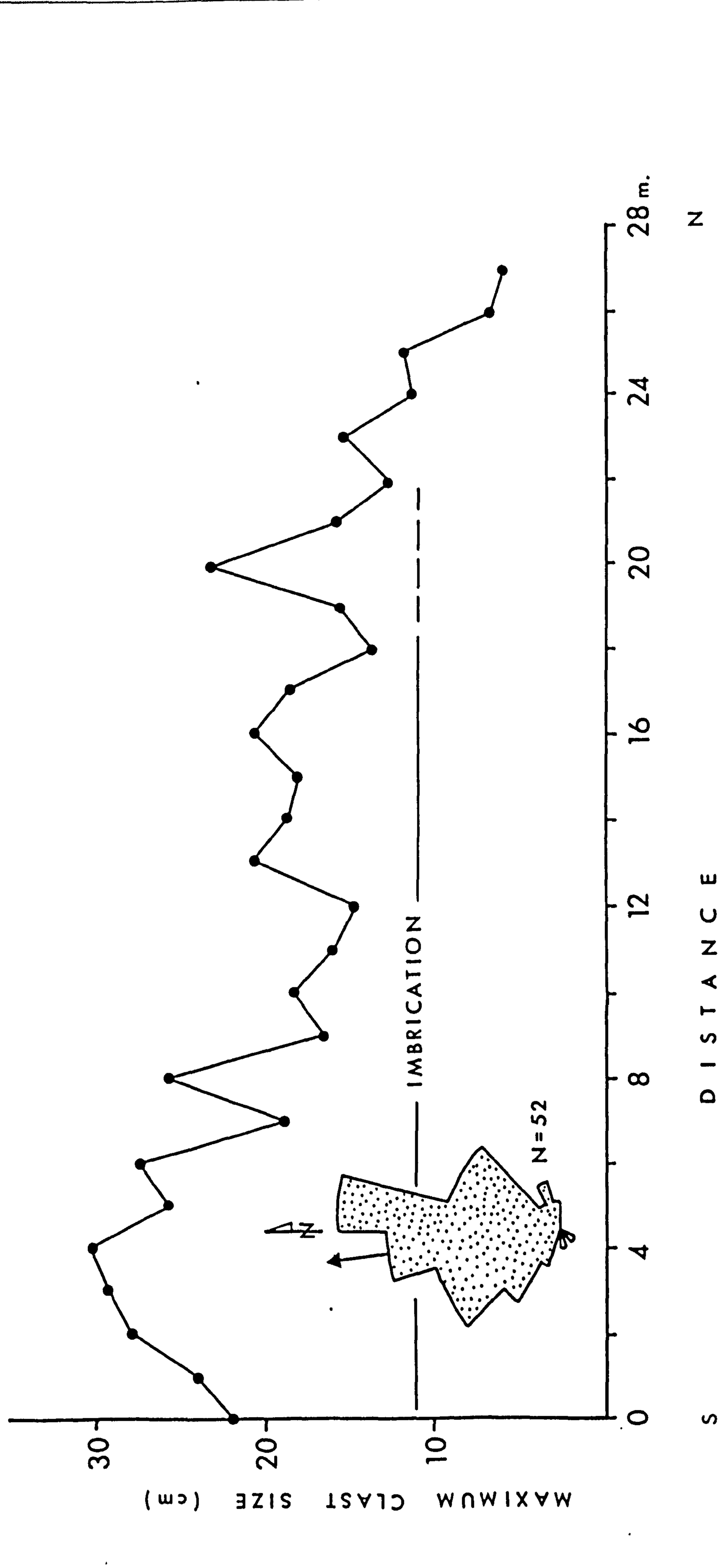

Figure 2.10 Lateral maximum clast size profile in southerly derived Lithosome 2 conglomerates exposed at Hawks Crag, north of Yellow Ark.

cut-bank (Fig. 2.9, Plates 2.8, 2.15). When the channel fill is traced away from the margin, the foresets generally diminish in thickness and are eventually replaced laterally by coarser grained texturally less mature massive or imbricate conglomerates. The imbrication dip direction in the latter is often parallel to the channel trend. The dip of the imbricate fabric in some instances is close to vertical (Plate 2.14). These units may show size segregation parallel to the channel trend (Fig. 2.10) but Lithofacies A - Lithofacies B down current transitions are less commonly seen than in conglomerates of Lithosome 1.

Sandstones only rarely occur as discrete lenses of sheets in the coarse channel fill conglomerates. Open frameworks are also common, pointing to a general deficiency in sand (Plate 2.18). This may partly reflect the cohesive structure of the channel banks, which cannot have contributed large volumes of sand to the channels during bank erosion. The polymodal often well packed textures of the conglomerates may also have inhibited effective sand infiltration. Whilst much of the sand grade material lateral to, and enclosing channel fill conglomerates of Lithosome 2 is volcanogenic in origin, non-volcanic sand and related pebble conglomerates were also deposited lateral to the channel-fill conglomerates. Thin sheet-like pebble conglomerates, interfingering with cross-stratified sands beneath, can be recognised in sand dominated units lateral to channelled units (Plate 2.19). These are interpreted as having been deposited as thin segregated gravel and sand bars during high stage discharge when channels became unconfined and deposition took place on the interchannel platform.

2.2.2.3 Interpretation

Lithosome 2 is inferred to have been generated by confined low sinuousity streams, many of which were deeply incised into blankets of volcanogenic sandstone. Sediment deposition was for the most part in channels, with thick and laterally extensive units of coarse conglomerate contructed by amalgamation and migration of these channels. Some finer sediment was distributed to the interchannel area during high discharge, but the channel

substrate was accreted largely by unrelated processes.

Large foresets dipping at high angle to the channel trends have the geometry and some of the characteristics of epsilon cross-stratification. However the fact that the large foresets abut directly against the channel margins, and that they can be traced laterally normal to the channel trends into massive often imbricate conglomerates (Lithofacies A or D), suggests they do not represent lateral accretion deposits generated by migration of the channel in the direction of foreset dip. The single steep preserved channel margins are interpreted as accretionary banks against which texturally and size differentiated lateral bars accreted. The pebble conglomerates which make up the foresets are inferred to record accretion of the bar tail against the bank to which the bar has become attached. The orientation of the foresets which dip at high angle to the channel trend can be accounted for by migration of the bar head imbricate or massive conglomerate parallel to the channel so that the tail lies between the bar head and the bank to which it accretes (Figure 2.8). Whilst lateral attachment of bars may produce cross-stratification which superficially resembles epsilon cross-stratification, the direction of implied channel migration is at 180^{o} to that were the foresets to represent true lateral accretion surfaces.

Many Lithofacies C cross-stratified conglomerates associated with the channelled lithosome show a wide divergence of dip directions relative to the channel trend. Typically the degree of divergence is greater than that seen in Lithosome 1 indicating the bar heads were probably more mobile. However, a group of exceedingly thick cross-stratified conglomerates (4-6m) also associated with Lithosome 2 show no direct relationship with channel margins, and have dip directions which are co-flow with imbrication measurements in adjacent coarse conglomerates. Counter flow gravel foresets up to 0.5m thick attest to the fact that strong flow separation must have accompanied the bed forms which generated the cross-stratification. The base to these large Lithofacies C2 foresets are characterised by very coarse outsized clasts of either andesite or granite.

The origin of these large scale cross-stratified units is unclear. They show some similarity with large gravel bars produced during catastrophic flood discharge (Bretz et al. 1956, Barker 1973). The commonly observed upstream transition into massive Lithofacies D or A conglomerates is however difficult to reconcile with deposition as the giant ripple bedforms described from catastrophic break-out flood deposits. The co-flow orientation of the cross-strata with high flow stage imbrication, together with the evidence for vigorous flow separation, suggest the structure of Lithofacies C2 units was largely determined at high flow stage, perhaps by downstream migration of a poorly differentiated gravel bar over a deep pool or channel. The very coarse boulders which are concentrated along the base of the foresets may have been trapped in a pool prior to migration of the bar platform. Almost every pool in the upper reaches of recent braided rivers in Scotland has concentrations of outsized clasts (Bluck pers.comm. 1985). The great thickness of the Lithofacies C2 foresets indicates considerable water depths and channel topography. These were probably acheived by rapid excavation of the channel downwards at high stage as the banks in many cases appear to have been relatively cohesive and would therefore have inhibited lateral flow expansion. Reactivation surfaces are common in the mega-cross-stratified conglomerates indicating that they are unlikely to have been generated during a single high discharge event.

2.2.3 Lithosome 3: Volcanogenic Sediments

Substantial units of sediment sharing a provenance largely in contemporaneous volcanic rocks comprise a third lithosome type. These units are distinguished both by their distinctive compositions, and by the dominance of sandstone over conglomerate. A range of constituent lithofacies can be identified. These include matrix- and clast-supported conglomerates, tuff breccias, agglomerates, and tuffaceous sandstones. Together these account for 15-20% of the Dunnottar and Crawton Groups. A distinction is drawn between the structure of sediments comprised almost entirely of volcanic detritus (Lithosome 3a), and those which although dominantly of volcanic provenance, do have a significant non-volcanic component (Lithosome 3b). The former include primary and reworked volcaniclastic sediments, whilst the latter are more complex mixtures of volcaniclastic, epiclastic and non-volcanic sediment.

2.2.3.1 Lithosome 3a

Volcaniclastic sediments attributed to Lithosome 3a include sheet-like tuff breccias, flat and cross-stratified volcanic sandstones, matrix-supported volcanic conglomerates and rare clast-supported conglomerates filling large channel structures. The tuff breccias occur in units 0.2-1.5m thick (Fig. 2.21). These have non-erosional bases and are laterally very extensive. Some can be traced for over 100m. Clasts are angular, rarely exceed 2-3cm and generally are of a single volcanic lithology. In thin section the tuff breccias are non-welded and composed of both lithic, and to a lesser extent, crystal fragments. The lithic fragments are typically non-vesicular and aphanitic. Rare non-volcanic grains occur including granitic and sedimentary lithologies. The absence of internal stratification or grading, the poor sorting, the planar bounding surfaces and the angular outlines of many of the fragments indicate that traction currents cannot have played an important role in the genesis of these units. Breccias dominated by fragments of single lithology have been attributed to deposition from pyroclastic ash flows (Vessell and Davies 1981). It is however difficult to reconcile such an origin with the absence of vesicular pumice fragments, shards or eutaxitic textures. The origin of the massive tuff breccia

sheets remains unclear but deposition from a fine grained debris flow is probable.

Coarse-grained tuffaceous sandstones with internal parallel lamination are often interbedded with the massive units of tuff breccia. The lamination is generally defined by strong grain size differentiation and is often bedding parallel but in some cases is of low angle type. More rarely, the tuffaceous sandstones are planar cross-stratified, with co-sets up to 1.0m thick. At Kinneff parallel laminated and cross-stratified tuffaceous sandstones occur lateral to a series of large asymmetrical channel structures which are up to 5.0m thick (Fig. 2.18, Plate 2.20). These have a single steep margin and a coarse clast-supported conglomeratic fill exclusively composed of subrounded volcanic clasts. The channel fill is ungraded and undifferentiated. Cross-stratification in tuffaceous sandstones lateral to the channels indicates dispersal at high angle to the channel trend. This suggests that some of the parallel laminated and cross-stratified tuffaceous sandstone sheets may be the product of overbank processes associated with large channels dispersing coarse volcanic sediment.

Matrix-supported cobble and boulder conglomerates are locally important in volcanogenic sequences. These tend to be laterally discontinuous and almost invariably bimodal in texture. Large subrounded volcanic clasts are often concentrated in the upper parts of these units (Fig. 2.16). The matrix is generally a coarse volcanic sandstone. These units superficially resemble subaerial volcanic debris flows or lahars (Fisher and Schminke 1984). The bimodal textures and clast rounding suggest remobilisation from pre-existing volcanogenic sediment. The possible debris flow origin is of interest in that debris flows have not been recognised in the non-volcanic conglomerate lithosomes which dominate the fill to the basin. This implies that the slope of the depositional surface during dispersal of volcanogenic sediment to the basin may have exceeded the critical threshold for the mobilisation of debris flows. Slopes otherwise appear to have been maintained below this level (2.6).

2.2.3.2 Lithosome 3b

Much of the volcanogenic lithosome comprises interbedded flat and cross-stratified pebbly sandstones and conglomerates of mixed provenance (Fig.2.16). Whilst dominantly composed of volcanic material, non-volcanic detritus may amount to 20-30% of the total. In some cases this detritus is compositionally similar to that preserved in the non-volcanic conglomerates in which the volcanogenic sequences are enclosed. In other cases the non-volcanic detritus is unique to the volcanogenic lithosome (2.7.1).

Mixed provenance conglomerates within Lithosome 3b are generally clast-supported and form lenticular sheets. These texturally range from poorly to moderately well-sorted. The volcanic clasts tend to be equant in shape and consequently imbrication is poorly developed. The conglomerates occasionally fill broad scour structures. They may be structureless or planar bedded internally. Associated coarse sandstones and pebbly sandstones are both parallel laminated and more rarely cross-stratified. Cross-strata reach as much as 1.0m in thickness and generally show a wide dispersion. Some are associated with counter-flow ripples.

Whilst detailed facies analysis has yet to be carried out on these mixed volcanogenic sediments, the association of structures suggests deposition in a rapidly aggrading braided fluvial system. Similar sediments have been described by Vessell and Davies (1981) from the medial and distal volcaniclastic facies in the Guatemala fore-arc.

2.3 STRUCTURE OF VERTICAL SEQUENCES

Each of the three lithosome types described in 2.2 individually make up vertical sequences of varying thickness. The volcanogenic sediments comprising Lithosome 3 are frequently interstratified with thick sequences of either Lithosome 1 or 2, forming two composite lithosome associations (Fig. 2.1). These lithosome associations are largely independent of one another and are only rarely seen in contact. The vertical transposition of the two disparate associations constitutes the highest level in the structural hierarchy recognised in the basin fill.

The two lithosome associations are spatially separated in outcrop (Fig. 2.11). The Lithosome 1 association occurs predominantly in the northernmost exposures of the Dunnottar and Crawton Groups. The Lithosome 2 association is restricted to the upper part of the Crawton Group exposed on the gently dipping southeasterly limb of the Strathmore Syncline between Whistleberry and Gourdon. It is overlain with angular unconformity by conglomerates of the Lithosome 1 association (Fig. 2.11).

Vertical sequences of Lithosome 1 conglomerates may be subdivided according to the relative importance of lateral as opposed to vertical accretion processes. Sequences dominated by coarsening-upwards cycles are distinguished from those in which size and shape segregation occurs laterally within single depositional units (Fig. 2.1). The latter are thought to reflect rapid accretion of lateral bars to the channel bank as the active channel migrated. Lateral accretion structures in the form of sand draped surfaces dipping normal to the imbrication fabric are occasionally seen (Plate 2.6). The coarsening upwards units are thought to record downstream migration of the coarse bar head gravels over the fine bar tail. Preservation of sequences dominated by coarsening upwards cycles suggests rapid aggradation of the depositional surface.

That sequences tend to be dominated by either vertical or lateral textural differentiation suggests that the accretion mechanism varied systematically. One possibility is that differential

subsidence may have controlled the accretion mechanism, with vertical accretion favoured in areas of higher subsidence. Lithosome 1 conglomerates dominated by lateral accretion are significantly best developed in the most southerly exposures of the Crawton Group at Whitehouse, some 15km from the Highland Boundary. Sequences closer to the Highland Boundary tend to more commonly show coarsening upwards units. Given the two dimensional nature of the coastal exposure, it is however difficult to distinguish lateral changes in depositional processes from those occuring temporally in the basin fill.

2.4 SEDIMENT PROVENANCE

The sheet-like conglomerates of Lithosome 1, and the channel-fill conglomerates of Lithosome 2, each stack vertically to produce two very distinctive vertical profiles. These two profile types are not only distinguished by the different structure of the lithosomes from which they are constructed, but also by a striking contrast in provenance, revealed in the very different clast compositions which occur in association with each.

2.4.1 Composition of Lithosome 1 Conglomerates

Conglomerates associated with Lithosome 1 are truly polymict, comprising varying proportions of metaquartzite, psammite, various granites, lavas and porphyries, and many lesser components including jasper, spilite, granophyre, amphibolite, appinite and gabbro. Compositions tend to become more diverse upwards, with sequences towards the base of the Dunnottar Group predominantly composed of a bimodal assemblage of metaquartzite and lava, together with minor spilite. The conglomerates have a complex provenance in that a substantial proportion of the clasts show evidence for derivation from pre-existing gravels, whilst other clasts appear to be of first cycle origin.

The evidence for clast recycling includes :

1. Many clasts tend to be unusually well rounded. This is particularly true of the metaquartzite clasts, which despite being amongst the most resistant of the clast types present in the conglomerates, often show the highest degree of rounding.
2. Clasts of metaquartzite occasionally show evidence for fracturing and rerounding. Reddened skins on some clasts suggest a previous weathering history prior to dispersal to the basin.
3. Rb-Sr uplift and cooling ages for psammitic clasts (Chapter 6) indicate rapid uplift some 50Ma prior to deposition of the conglomerates. No younger uplift ages have been determined from the clasts.
4. The absence of pelitic lithologies and the general enrichment in a wide range of stable clast types are compatible with a history of sediment recycling. That pelitic lithologies may have been important in the original source and in conglomerates of

earlier generation, is indicated by the abundance of detrital garnet in heavy mineral populations separated from conglomerate matrices.

5. A range of textural features suggests the conglomerates making up Lithosome 1 were selectively sourced by already size graded gravels. These include the strong shape enrichment, the widespread bimodal textures, and the generally low volume of sandstones and finer sediments preserved within the basin.

As recycling was an important element in the provenance of the largely bimodal polymict conglomerates associated with Lithosome 1, not all clasts may share the same provenance. The metaquartzites are more well rounded than the accompanying psammite clasts suggesting a different history of recycling. Had the two components shared the same provenance, the less resistant psammite clasts might be expected to show comparable if not more advanced rounding than the very durable metaquartzite clasts. Isotopic and geochemical evidence suggests the provenance of the granite clasts may be equally complex (5.6). Granite clasts in these conglomerates show a diverse compositional range. This can be resolved into two components. Two-mica granite clasts of Ordovician age are distinguished from evolved biotite granites which may be largely of late Silurian age. These latter granites are therefore probably only marginally older than the basin in which they occur as clasts. This would preclude their involvement in a long history of recycling prior to dispersal to the basin. A similar constraint applies to the various volcanic clasts which were derived from contemporaneous lava piles flanking and possibly within the basin of deposition.

2.4.2 Composition of Lithosome 2 Conglomerates

Conglomerates associated with Lithosome 2 contain no elements of the Lithosome 1 provenance. Equigranular granites, both foliated and unfoliated, together with lithic arenite and metagreywacke, generally dominate the clast assemblage. Metaquartzite and psammite clasts are notably absent. Other less abundant clast components include amygdaloidal basalt, biotite hornfels, micritic limestone, jasper, andesitic and dacitic lavas, and vein quartz.

Figure 2.11 Compositional variation in conglomerates exposed in coastal sections east of Inverbervie.
A. Summary log with distribution of clast types by size for four sites. Numbers refer to lithosome type.

KEY TO CLAST TYPES


Metagreywacke.


Microconglomerate.


Lithic arenite.


Hornfels.


Vein quartz.

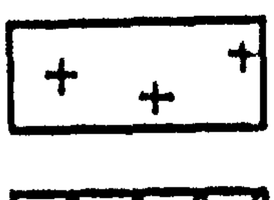
Tonalite and granodiorites.


Andesitic, dacitic and rhyolitic lavas.

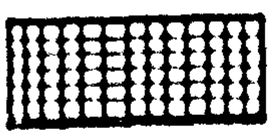
Amygdaloidal basalt.


Biotite psammite.

Metaquartzite.


Two-mica granite.

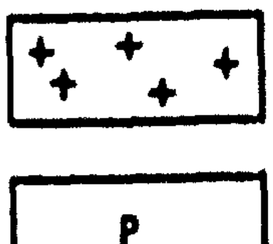
Biotite granite.

Quartz-feldspar porphyry.


Others, including spilite, jasper and limestone.

B. Location of section.

Dip

A

50 m.

0

ARBUTHNOTT GP.

CRAWTON LAVA

CRAWTON GROUP

1

2

F

% 100

50

0

20

40

60 cm

B

Crawton lava

Bervie Brow

Inverbervie

20

21

22

N

0

1 km

In contrast to the Lithosome 1 provenance, conglomerates of Lithosome 2 have angular clasts, are generally polymodal and are almost certainly of first cycle provenance. The basin in which conglomerates belonging to the Dunnottar and Crawton Groups accumulated consequently received sediment from two distinct sources, one of which included a significant polycyclic component, whereas the other was of first cycle origin.

A thick albeit faulted sequence (>300m) of interstratified Lithosome 2 conglomerates and associated volcanogenic sediments is exposed at Bervie Brow (Fig.2.11). A progressive change in the composition of the conglomerates when traced up the succession is seen. Granite clasts become more abundant towards the top of the succession. Detailed compositional profiles for maximum and modal clast size intervals across a single upward coarsening interval of Lithosome 2 conglomerates are shown in Figure 2.9. These illustrate both the strong size dependence of the conglomerate compositions, and the compositional distinction between the channel fill conglomerates and the interstratified flat bedded pebbly sandstones. Porphyritic andesite clasts are suppressed in the Lithosome 2 provenance, whilst they dominate the interstratified pebbly sandstones.

2.5 SEDIMENT DISPERSAL

Directional structures in braided stream alluvium generally have a mean orientation which broadly coincides with the mean direction of flow (Bluck 1974, 1976). Different structures may however show a considerable variability in their orientation. This is largely a function of the flow stage at which the structures are developed. Bed topography generated during high flow stage tends to become partially emergent during falling discharge, deflecting the flow. Directional structures formed during the low flow stage therefore usually have a greater inherent variability, and in many cases may be more difficult to relate directly to the mean flow direction. As a result, it is important to distinguish directional structures formed at high flow stage from those formed during falling or low flow stage, and to relate these to the larger scale progradation of the lithosome as a whole.

Directional structures found in conglomerates and related sandstones of the Dunnottar and Crawton Groups can be ranked according to their respective variability in orientation, and the flow stage at which they are inferred to have formed (Fig.2.12). Imbrication is the dominant directional structure. As imbricate fabrics are developed predominantly at high flow stage, palaeoflow estimates based on imbrication tend to have a low variability and are consequently often a more reliable indication of dispersal than accompanying cross-bedded sandstones. Bluck (1974) shows cross-stratification within lateral bars on Icelandic sandurs to have a greater dispersion than the channel orientation and related gravel imbrication. The mean dispersal directions indicated by the various structures are in this instance close to the mean flow direction. There are however cases where the mean orientation of cross-stratification may significantly deviate from the mean flow direction, for example, in alluvium generated by preferential attachment of lateral bars to one bank (Bluck 1980). Normally, repeated switching of the channel migration direction as the alluvial system aggrades vertically compensates for directional bias within a single lithosome. Bluck (1980), however, shows that sediment

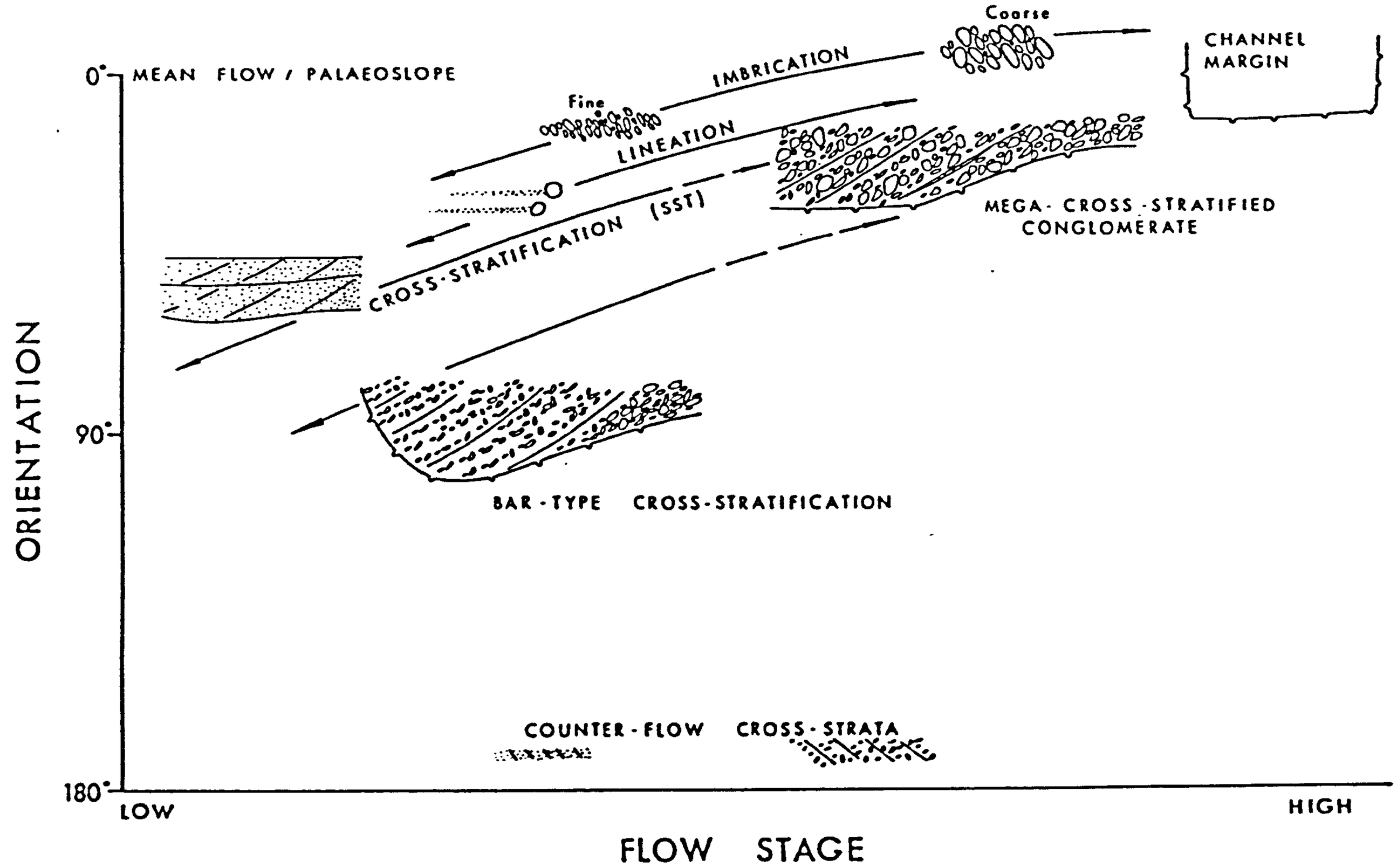

FIGURE 2.12 Possible relationship between flow stage and the maximum deviation of structures used to infer palaeodispersal from the mean flow or palaeoslope orientation.

accumulating on the extremities of sediment cones may be subject to a preservational bias in favour of lithosomes generated by channels migrating in a single direction. In these instances mean cross-stratal dip orientations, even averaged over substantial vertical sequences, may deviate significantly from the mean flow direction, and the palaeoslope. Clast imbrication, developed largely at high flow stage, is free from such effects, and is therefore both a preferable directional indicator and a useful reference to which cross-stratal dip orientations can be referred.

Imbricate clast fabrics have been measured by recording the orientation of the a-b planes of all disc and blade shaped clasts within a given area. The measurements at any one site were made within single depositional units. The four fold shape classification of Zingg (1935) was used to determine clast shape. The maximum clast diameter was recorded during imbrication measurements to monitor for size dependence of fabric orientation. Typically 30-60 clast orientations were measured at each sample locality. Rust (1975) found samples of 30-40 clasts to give consistently significant individual vector means in Recent glaciofluvial gravels.

Several types of cross-stratification can be distinguished on the basis of the relative orientation of the foresets with respect to the mean flow direction as recorded by clast imbrication. These include mega-cross-stratified conglomerates which are generally co-flow with imbrication in adjacent units, and bar-type cross-stratification associated with channel fill conglomerates, which typically are orientated normal to the flow direction. Cross-stratified conglomerates occurring in sequences of Lithosome 1 type tend to show modest rotations of the order 20-40° with respect to the imbricate fabric (dip + 180°). Planar cross-stratification developed in sandstones associated with the conglomerates usually show highly diverse dip orientations often at high angle to clast imbrication.

2.5.1 Lithosome 1 Dispersal

Conglomerates belonging to Lithosome 1 have a general northerly

provenance. Whilst imbrication often shows a consistent orientation over sequences up to several hundred metres thick, palaeocurrent data for the Dunnottar and Crawton Groups taken as a whole indicate that the Lithosome 1 dispersal is highly variable (Fig.2.13). The range in dispersal is at its largest over the most northerly outcrops, where the pattern is bimodal with southwesterly and east-northeasterly directed palaeocurrents. Lithosome 1 conglomerates exposed in sections further south have a more restricted, generally unimodal dispersal, from the north and northeast.

The variable dispersal implied by the imbrication measurements contrasts with the very narrow range found by Rust (1984) in the Malbaie conglomerates of the Gaspe Peninsula, and by Steel and Thompson (1983) in Triassic conglomerates of northern England. Rust (1984) infers that the palaeoslopes were uniform during the deposition of the Malbaie sequence and deposition on alluvial plains was favoured over deposition on alluvial fans. Steel and Thompson (1983) similarly favour deposition on a braided river-plain for the Bunter Pebble Beds. The coarse grainsize and radial dispersal of Lithosome 1 conglomerates suggest that an alluvial fan or sediment cone site for their deposition may be more appropriate.

Figure 2.14 illustrates the wide discrepancy in dispersal direction between structurally juxtaposed sequences dominated by Lithosome 1 occurring at the base of the Dunnottar Group, south of Stonehaven. The coarse conglomerates exposed at Downie Point share a southwesterly dispersal with the underlying sandstones outcropping south of Stonehaven Harbour. Polymict conglomerates exposed at Bowdun Rocks are also dispersed towards the SW. However, the intervening conglomerates outcropping in Strathlethan Bay are dispersed towards the ENE (Fig.2.13) in a direction opposite to that established for the conglomerates outcropping to the immediate north and south. The dispersal geometry requires that either the conglomerates were dispersed from the flanks of a small basin with basin margins lying to the immediate NE and SW, or that they were deposited on large isolate alluvial fans in a position proximal to a basin margin to the

Figure 2.13 Summary of dispersal data collected from coastal exposures between Stonehaven and Inverbervie.

KEY

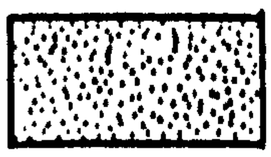
Cross-bedding in sandstones associated with Lithosome 1 conglomerates.

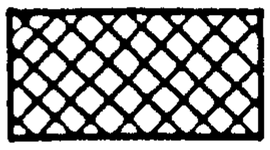
Imbrication in Lithosome 1 polycyclic conglomerates.

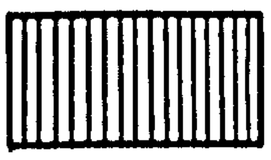
Cross-bedding in Lithosome 2 conglomerates and pebbly sandstones.

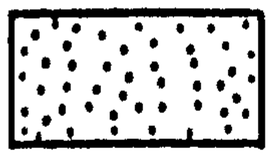
Imbrication in Lithosome 2 first cycle conglomerates.


Vector mean.

n Number of observations.

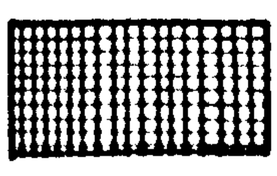
Tremuda Bay Volcanic Formation.

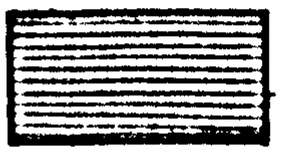
Crawton Volcanic Formation.

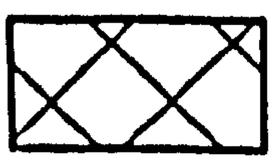
Montrose Volcanic Formation.

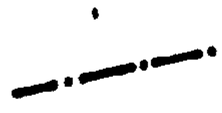
Fault.

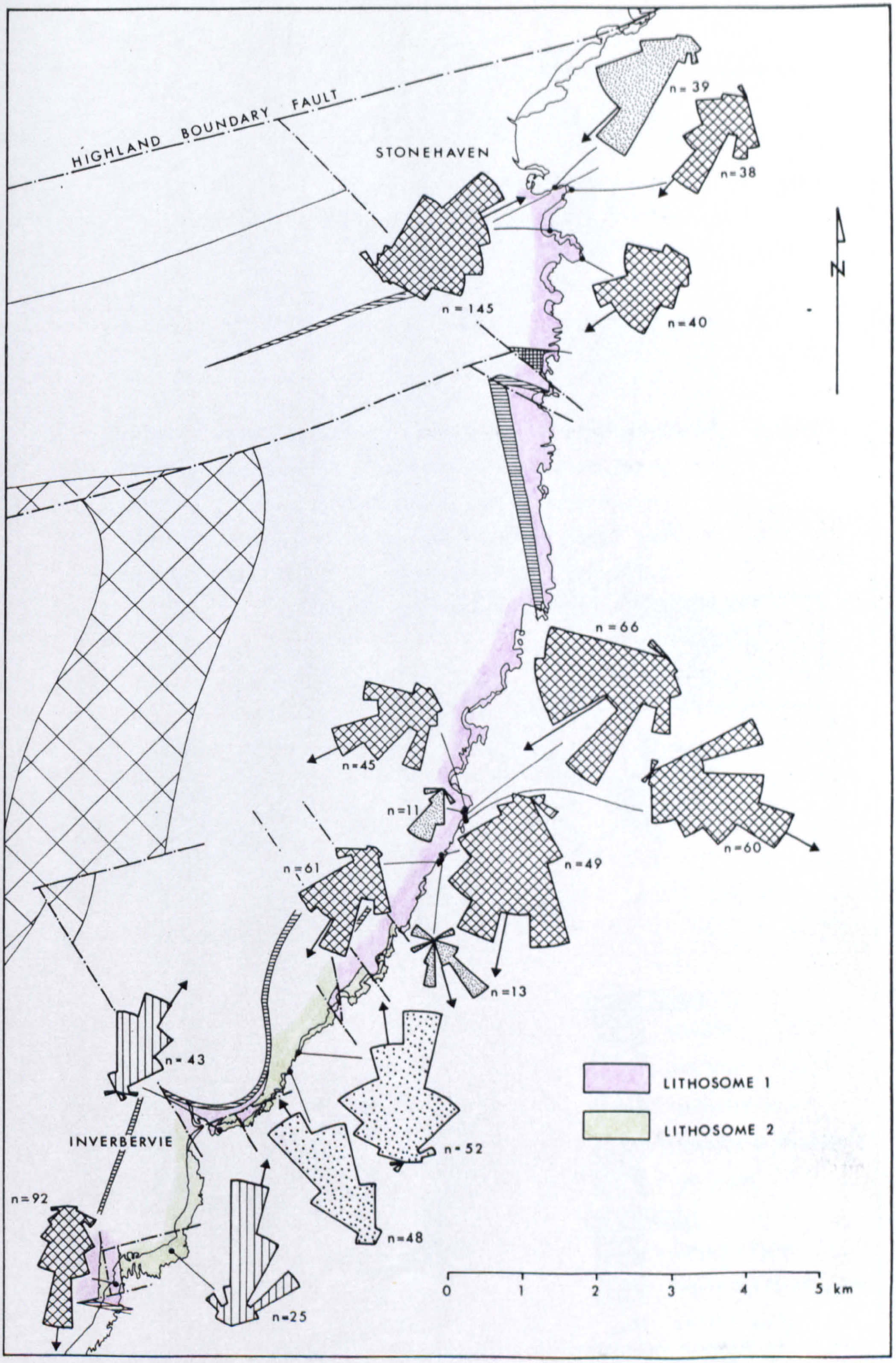
HIGHLAND BOUNDARY FAULT
STONEHAVEN
INVERBERVIE
n = 39
n = 38
n = 145
n = 40
n = 66
n = 45
n = 11
n = 60
n = 49
n = 61
n = 13
n = 43
n = 52
n = 92
n = 48
n = 25
N
LITHOSOME 1
LITHOSOME 2
0
1
2
3
4
5 km

Figure 2.14 Dispersal of conglomerates and sandstones in the basal Dunnottar Group south of Stonehaven. Clast compositional data includes data from Van Breemen and Bluck (1981). Section AB is shown in Figure 2.20. Note high dips and the large tilt corrections implicit in the orientation data.

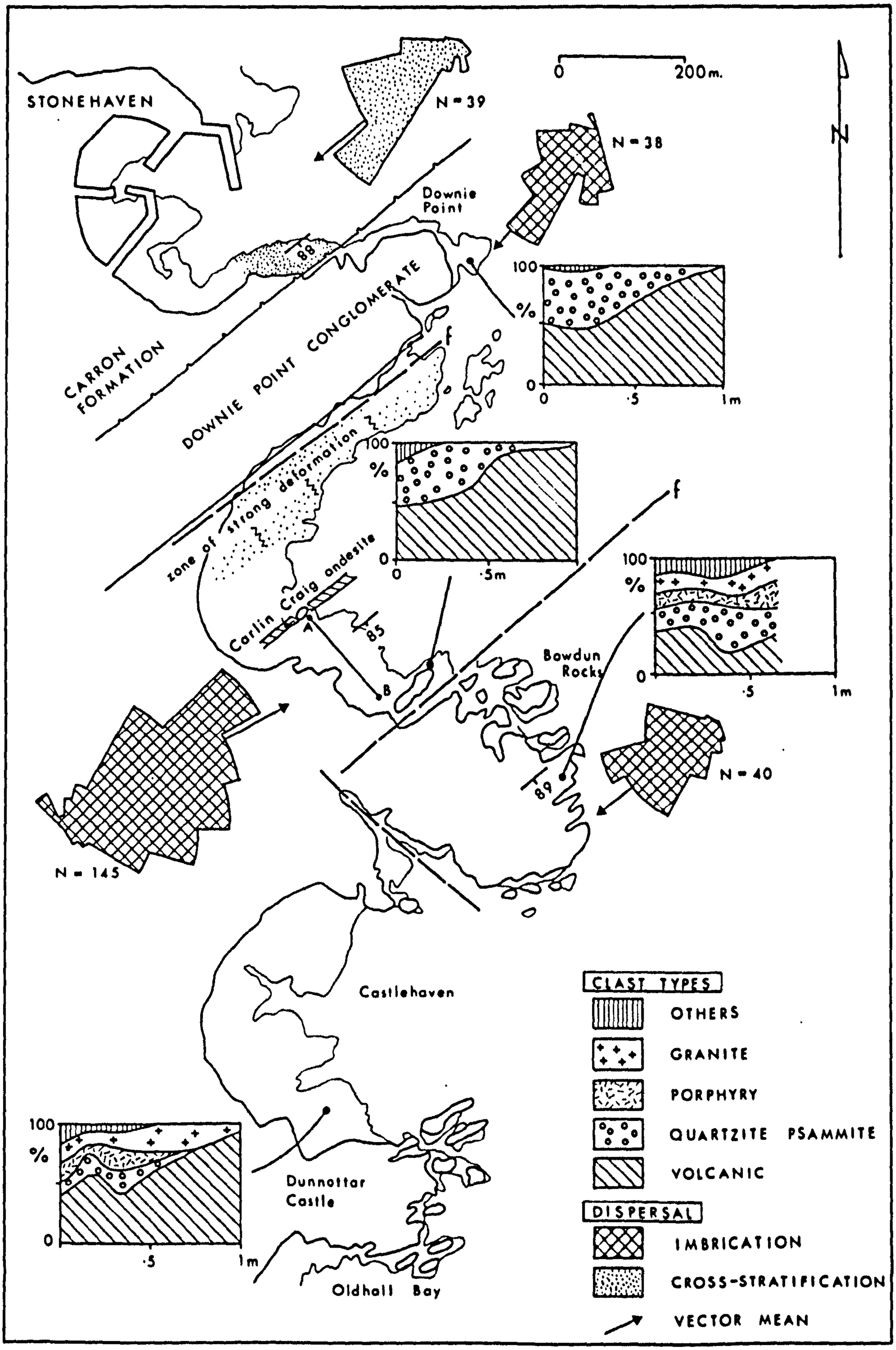
STONEHAVEN
N = 39
0
200m.
N
N = 38
Downie Point
88
CARRON FORMATION
DOWNIE POINT CONGLOMERATE
f
100
%
0
0
·5
1m
zone of strong deformation
Carlin Craig andesite
A
85
B
Bowdun Rocky
f
100
%
0
·5
1m
N = 40
89
N = 145
Castlehaven
CLAST TYPES
OTHERS
GRANITE
PORPHYRY
QUARTZITE PSAMMITE
VOLCANIC
DISPERSAL
IMBRICATION
CROSS-STRATIFICATION
VECTOR MEAN
100
%
0
·5
1m
Dunnottar Castle
Oldhall Bay

NW. The latter interpretation is favoured as the palaeocurrents swing to have an increasingly important southerly directed component when traced southwards away from the inferred basin margin. Large angular discordances in dispersal are to be expected in sediments accumulating close to the margin of basins characterised by sediment deposition on isolate lateral alluvial fans (Fig.2.15). This is because radial dispersal from the apex of an isolate fan is largely parallel to the basin margin in the zone immediately flanking the source. Where alluvial fans coalesce to form aprons, a greater proportion of the sediment will be deposited normal to the basin margin.

Accepting that deposition on isolate alluvial fans or sediment cones can account for the dispersal geometry seen in the basal part of the succession constrains the position and orientation of the basin margin from which the sediment was dispersed. The wide angular discordance close to 180^{o} implies that the basin margin probably lay a short distance to the north close to the present trace of the Highland Boundary Fault. As the Highland Boundary Fault (s.s.) is an essentially late reverse structure, (Bluck 1984) it is unlikely to have been the structure which bounded the basin. It is possible that overthrusting along the Highland Boundary Fault masks more significant older structures which may have played an important role in defining the Lower ORS basin margin during deposition of the Dunnottar Group. If the palaeocurrents record dispersal parallel to the basin margin the northern margin of the basin probably had a NE-SW trend parallel to the regional strike. The close proximity to the north-western margin of the basin implied by the dispersal data serves to distinguish the Dunnottar Group from strike equivalent Lower ORS conglomerates outcropping in the western Midland Valley. Here, Bluck (1984) established a north-westerly dispersal in conglomerates which are exposed immediately to the south of the Highland Boundary Fault. This requires that they originally filled a basin the axial portion of which must have extended north of the Highland Boundary with subsequent truncation of the succession against the Highland Boundary Fault. In contrast, the basin in which sediments of the Dunnottar Group accumulated does not appear to have been bisected by later displacements on the

Figure 2.15 A. Cartoon illustrating the potential for dispersal parallel to a basin margin on the proximal flanks of large isolate alluvial fans dispersed from point sources.

B. Hypothetical palaeocurrent orientations in three segments progressively more distant from the basin margin.

C. Coalesced lateral fans with detritus shed predominantly normal to the basin margin.

A

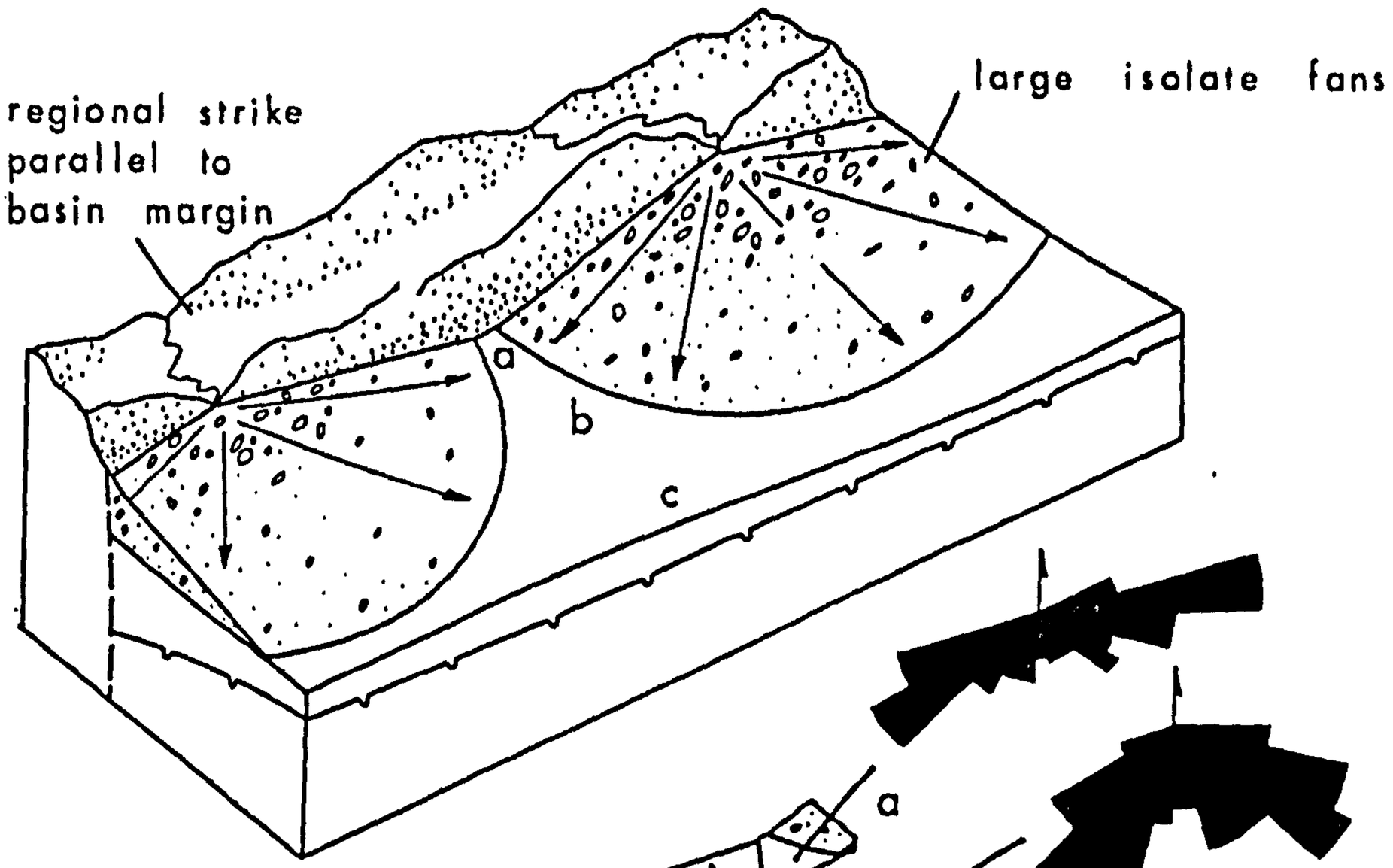
regional strike
parallel to
basin margin
large isolate fans
a
b
c

B

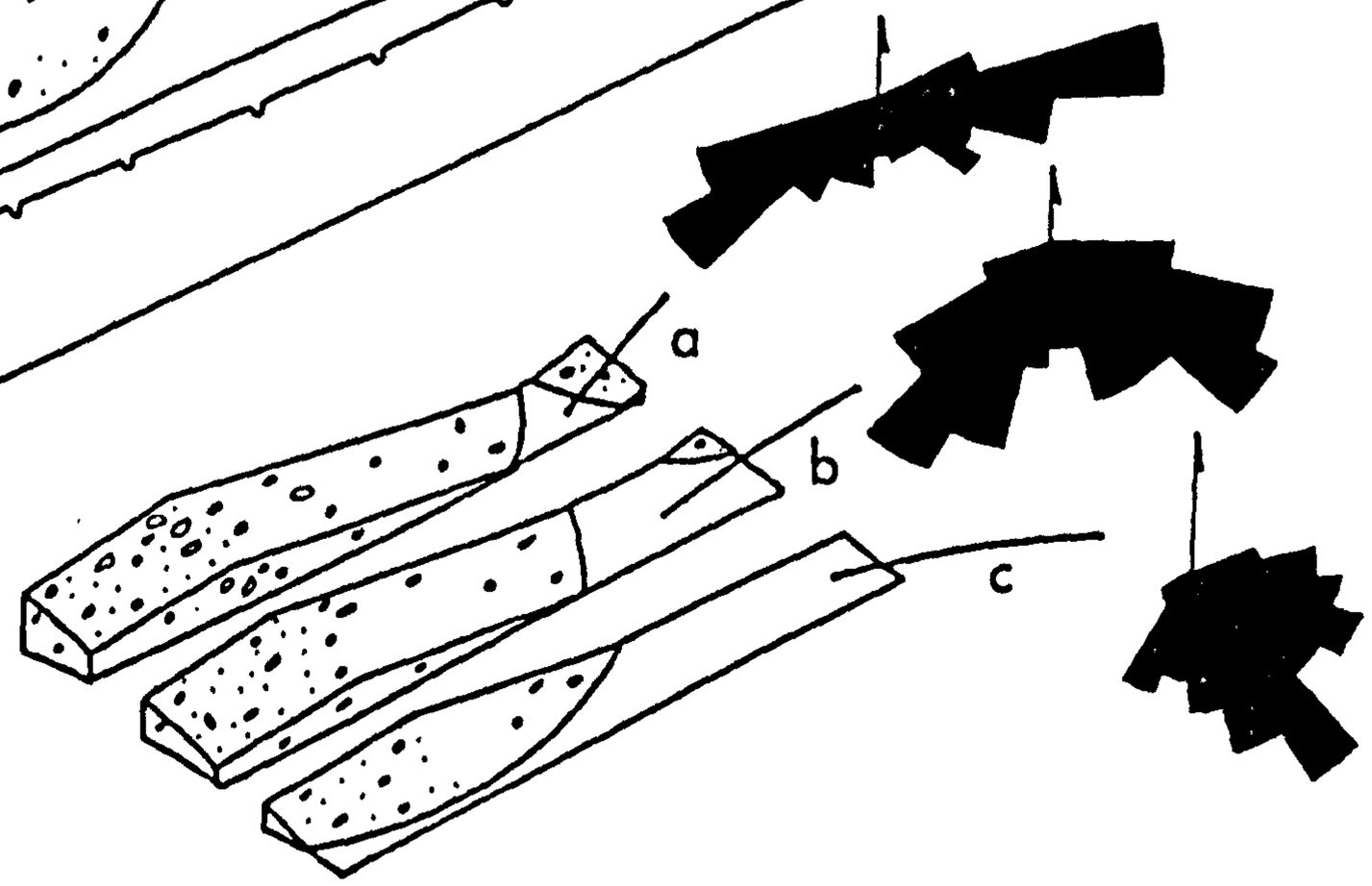
a
b
c

C

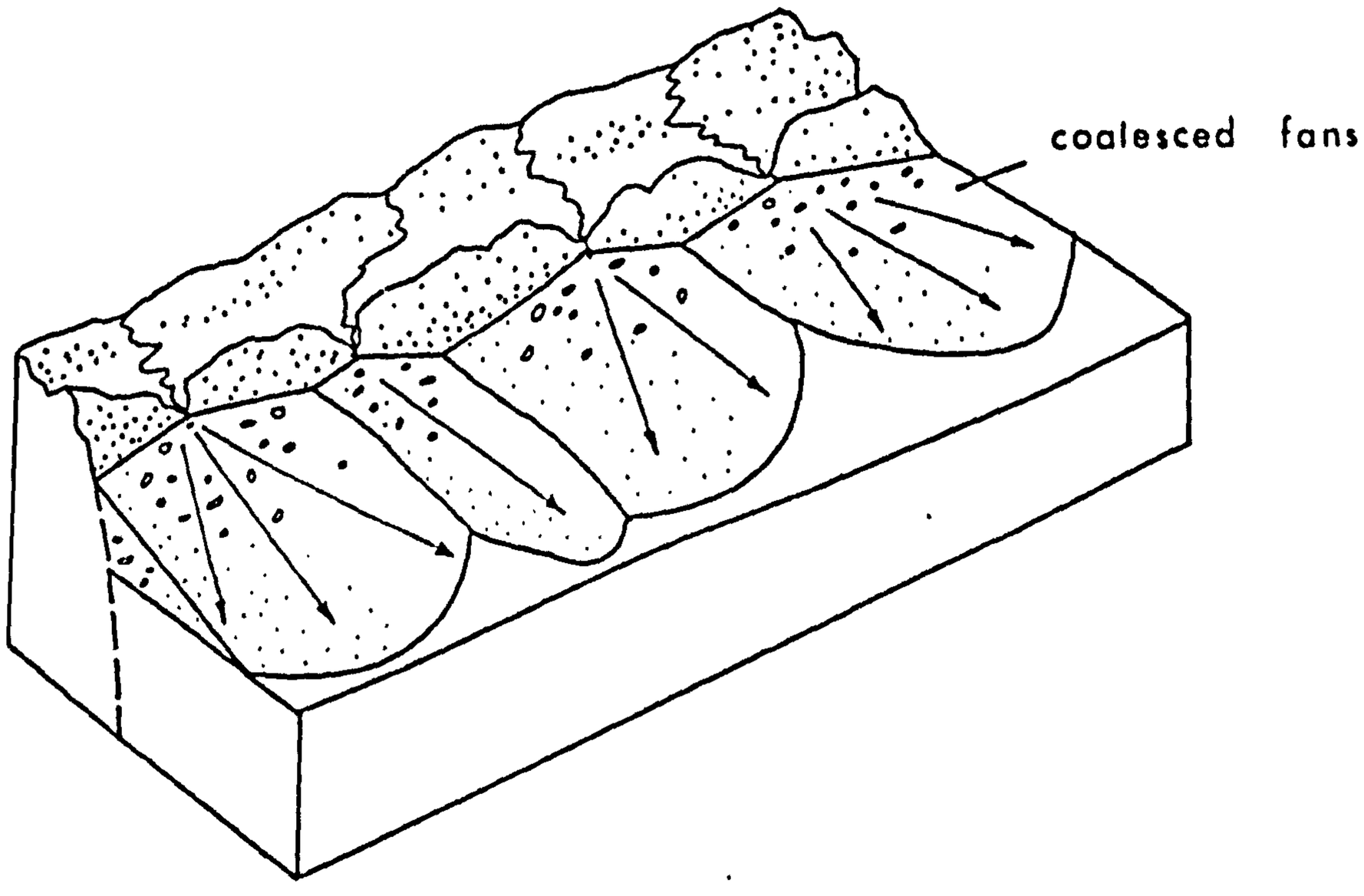
coalesced fans

Highland Boundary Fault or one of its precursors.

Compositional data for the conglomerates are included in Figure 2.14. Both the Downie Point and Carlin Crag conglomerates have similar clast compositions being dominated by andesitic and dacitic lava, and meta-quartzite. Gabbro, spilite and granophyres occur as rarer clast components. Conglomerates sharing a similar meta-quartzite and calc-alkaline lava provenance have been widely recognised in the Strathmore Lower ORS (Wilson 1971, 1980, Morton 1976, Bluck 1978). South of Strathlethan Bay, a strike fault juxtaposes conglomerates of disparate composition and dispersal. Meta-quartzite and lava bearing conglomerates are replaced southwards and higher in the succession by conglomerates which compositionally show a greater range of diversity. Granite, porphyry and psammite clasts all become important clast components in polycyclic conglomerates of Lithosome 1 type stratigraphically above this level. These polymict conglomerates compositionally have no analogue in Lower ORS sequences outside Kincardineshire. There is therefore an important vertical transition in the composition of Lithosome 1 conglomerates from those which share a provenance which can be recognised widely in the Strathmore Lower ORS, to conglomerates rich in granite detritus which have a more restricted distribution. The latter can be traced westwards as far as the North Esk where the characteristic clasts of two-mica granite occur in conglomerates assigned by Armstrong and Paterson (1970) to the Strathmore Group. These have a dispersal from the southwest or south-southwest (Bluck pers.comm. 1985).

Previous accounts have emphasised the role of vertical unroofing in producing compositional variation in conglomerates making up the thick Kincardineshire Lower ORS succession (Campbell 1913, 1929, Bluck 1978, Mykura 1983). It is possible however that lateral compositional variation in the source may have been equally if not more important. The coincidence of the sudden vertical transition to a compositionally more diverse provenance with a rotation in dispersal of close to 180^{o} can be explained by juxtaposition of sediments originally deposited on adjacent sediment cones or fans. These may have been fed to the basin by

dispersal systems draining compositionally distinct parts of the source area. Whilst the juxtaposition of the two sequences is in part structural, the extension of the diverse granite rich provenance westwards to include the North Esk section by Strathmore Group times suggests that the granite rich provenance may have migrated westwards during deposition of the Lower ORS. If this was the case, lateral compositional variation in the source may be revealed by vertical compositional variation in the basin fill.

Lithosome 1 conglomerates exposed at greater distance from the inferred northwestern basin margin appear to have been dispersed largely from the north and northeast, and less commonly from the north-west (Figs 2.2,2.3,2.4,2.16). Dispersal towards the south-east might intuitively be expected to dominate the fill of a basin bounded by a NE-SW trending margin parallel to the regional strike. Indeed dispersals normal to inferred basin margins have been recognised in the Lower ORS in the western Midland Valley and Kintyre (Friend and Macdonald 1968, Wilson 1971, Morton 1976, Bluck 1984). The suppression of south-easterly dispersals in polycyclic conglomerates of northerly provenance in the Dunnottar and Crawton Groups implies that if the basin was bounded by a NE-SW trending margin, the bulk of the sediment of northerly provenance was not dispersed normal to this margin. This point is returned to in 3.2.1.

Whilst palaeoflows determined at outcrop level in more distal Lithosome 1 conglomerates generally show a consistent orientation, occasionally successive conglomerate units show a wide divergence in the orientation of their imbricate fabrics. An angular deviation of 90° in the dispersal of superimposed coarse imbricate conglomerates at Todhead Point is shown in Fig. 2.4. The sudden rotation in fabric orientation occurs across a sharp sub-planar non-erosional surface. As the imbrication occurs in conglomerates with clasts in excess of 30cm the abrupt rotation in dispersal cannot be a falling stage effect. Bluck (1974) records deflections in sandur dispersal orientation by partial blocking of valley trends by lava flows. A lava flow succeeds the change in dispersal at Todhead Point and may have

Figure 2.16 Detailed log illustrating contrast between northerly derived polycyclic conglomerates (Lithosome 1, Powdam Head, NO 867763) and overlying volcanogenic sediments (Lithosome 3, Rouen Bay, NO 865759). The contact between the two units is a sharp sub-planar surface. Whilst the polycyclic conglomerates contain many rounded cobbles of biotite and higher grade psammite, the volcanic conglomerates in contrast include subordinate clasts of angular chlorite grade psammite. Rose diagrams indicate orientation of imbricate fabric at A and B (dip of clast ab plane + 180°). Note angular discordance between cross-bed, gravel interfinger and imbrication orientation.

m

DISPERSAL

KEY

Imbricate conglomerate

Massive conglomerate

Flat-stratified conglomerate

Matrix-supported "

Massive sandstone

Flat-stratified sandstone

Cross-stratified "

Coarse-grained tuffaceous sandstone & tuff breccia

Imbrication

Cross-stratification

Channel margin

Gravel interfinger

Channel or scour contact

Gradational contact

Sharp contact

A

B

N

>15cm

A
N=61

B
N=49

M.C.S.

0 20 40cm

contributed to the observed deflection in palaeoflow. A second instance in which marked discordance in imbricate fabrics is seen is at the base of Lithosome 1 sequences where they directly overlie conglomerates of Lithosome 2 type. Imbrication in the basal Lithosome 1 conglomerates indicates an anomalous northeasterly or northerly dispersal at Whitehouse (Fig. 2.3) and Bervie Brow (Fig. 2.11). These are rapidly succeeded by Lithosome 1 conglomerates having a more typical south or southeasterly dispersal.

2.5.2 Lithosome 2 Dispersal

Directional structures occurring in channel fill conglomerates associated with Lithosome 2 are characterised by a wide variation in orientation. In many instances cross-stratal dips show large angular deviations with respect to imbrication (fabric dip + 180°) and channel margin orientations. Clearly palaeoflow estimates based on cross-stratification alone would be erroneous. Meaningful palaeoflow determinations can only be made when the various directional structures are considered in combination such that intrinsic variation in their orientation relating to the structure of the lithosome can be accounted for.

The tilt-corrected orientation of directional structures are plotted on several sections through conglomerate sequences of Lithosome 2 type in Figures 2.9,2.17,2.18,2.19. The dispersal geometry is obviously distinct from that established for Lithosome 1 conglomerates, as might have been anticipated on the basis of the disparate clast compositions of the two lithosomes. Channel orientations, clast imbrication and cross-stratification indicate the importance of northerly and north-westerly sediment dispersal, together with less common westerly and southwesterly palaeoflows. The latter are well developed in conglomerates exposed at Kings Step (Figure 2.9) where three dimensional outcrops allow the orientation of channel margins to be accurately measured. These show a marked east-west alignment. Preferential preservation of steep southerly margins implies that the channel system was systematically migrating northwards. Cross-stratification at high angle to the channel trend is analogous to the bar-type cross-stratification of Bluck (1976).

Figure 2.17 Logged sequence through interfingering southeasterly derived Lithosome 2 conglomerates and volcanic sandstones, Little Johnshaven (NO 855743). Legend as in Figure 2.16.

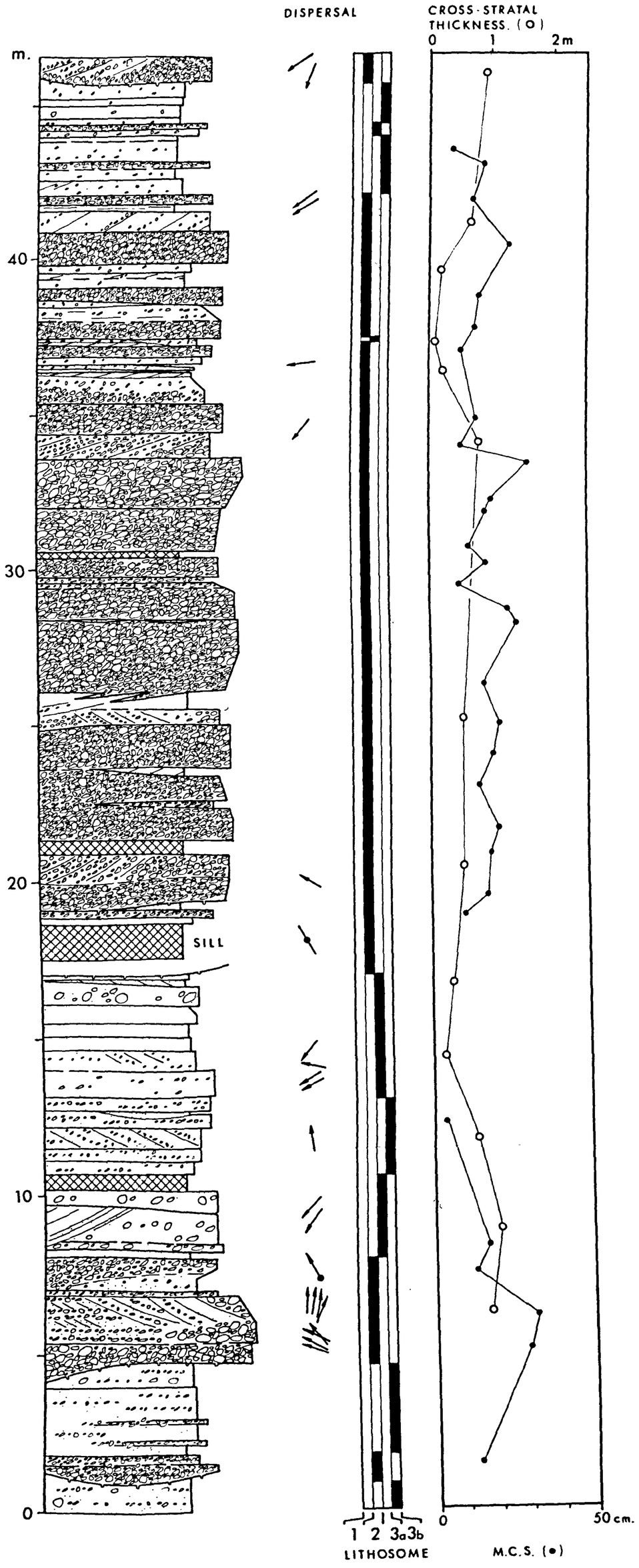
m.
40
30
20
10
0
SILL
DISPERSAL
CROSS-STRATAL
THICKNESS. (O)
0
1
2m
1 2 3a 3b
LITHOSOME
0
50 cm.
M.C.S. (•)

Figure 2.18 Vertical section through sequence exposed on the foreshore at Kinneff (NO 858746) illustrating complex interfingering of conglomerates and sandstones of disparate provenance, composition and structure. Lithosome 2 conglomerates fill NW-SE trending channels incised in volcanogenic sediment towards the base of the sequence. Cross-stratal dips show a wide dispersion from the channel trends. At 5m, a channel is plugged with coarse flat stratified volcanic sandstone. A transitional unit intervenes between the Lithosome 2 conglomerates and a sequence of volcanic sandstones and massive conglomerate filled channels. The section is capped by a sharp unconformable contact with northerly derived Lithosome 1 polycyclic conglomerates. For legend refer to Figure 2.16.

m.

30

25

20

15

10

5

0

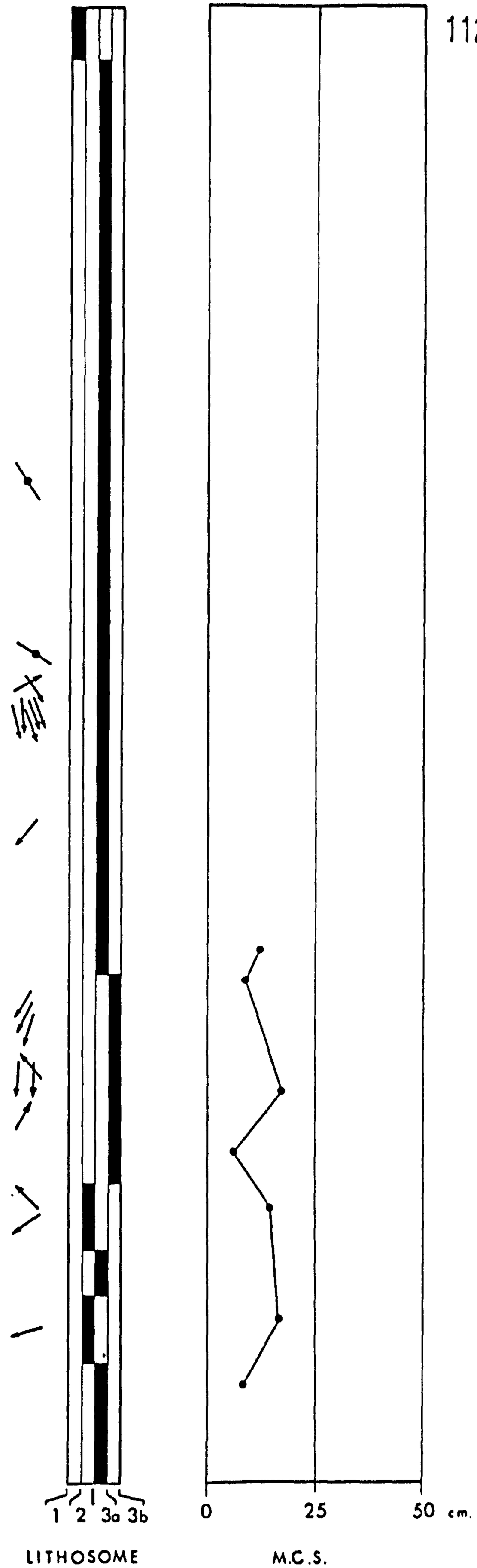

LITHOSOME

M.C.S.

Figure 2.19 Detailed log through a proximal sequence of Lithosome 2 conglomerates exposed on the foreshore east of Gourdon (NO 832708) illustrating the importance of cross-stratification (Lithofacies C) and the predominance of northerly and northwesterly orientated foreset azimuths. The cross-stratification in this case is largely co-flow with imbrication and with down-flow fining. For legend refer to Figure 2.16.

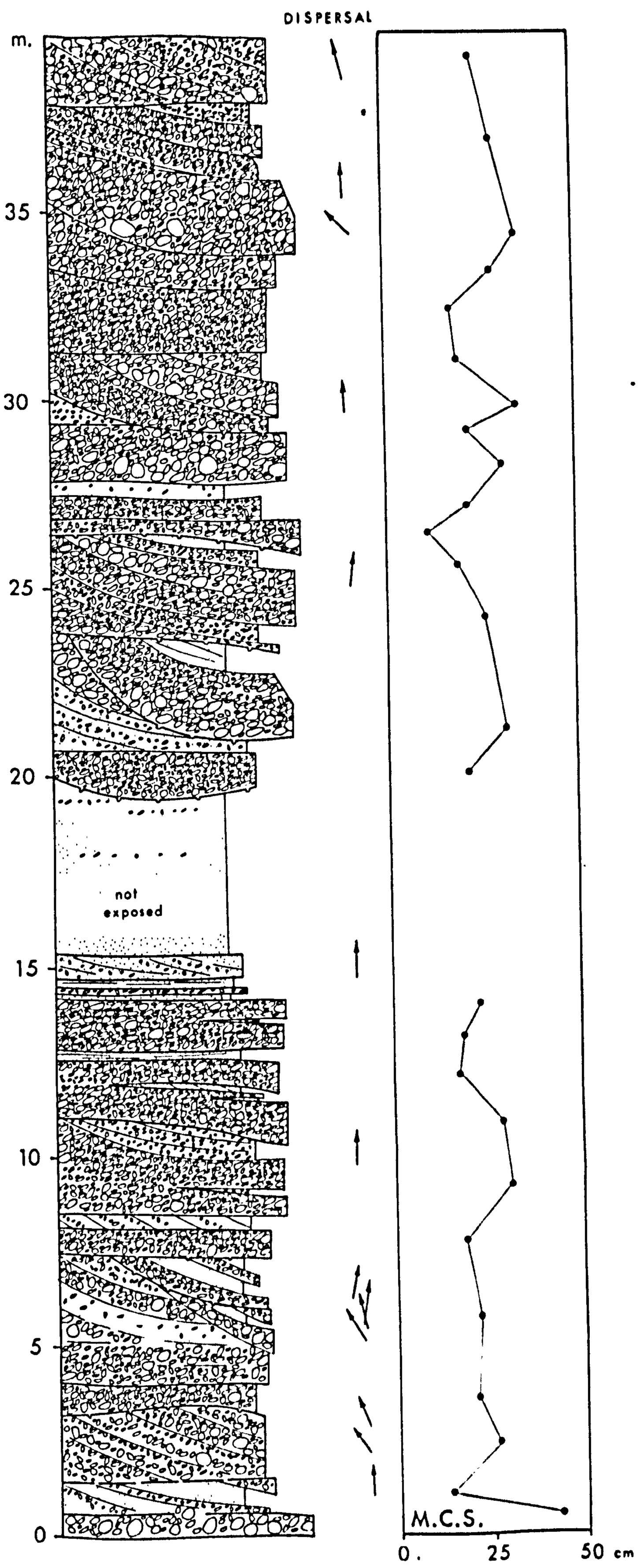
DISPERSAL
m.
35
30
25
20
not
exposed
15
10
5
0
M.C.S.
0.
25
50 cm

Figure 2.20 Measured section through part of coarsening upwards megasequence exposed south of Carlin Crag, Strathlethan Bay (NO 880847). The sequence illustrates repetitive interfingering between sandstones and conglomerates of volcanic provenance and conglomerates characterised by abundant metaquartzite detritus. Whilst palaeocurrent data for the volcanogenic units show a wide dispersion, cross-bed and imbrication measurements (indicated by rose diagrams) indicate a consistent easterly and northeasterly dispersal. Note that bedding is close to vertical and large tilt corrections have subsequently been applied to the data.

KEY

CLAST-SUPPORT CONGLOMERATE

CROSS-STRATIFIED CONGLOMERATE

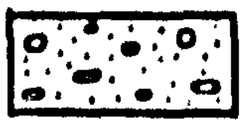

PEBBLY SANDSTONE/MATRIX-SUPPORT CONGLOMERATE

MASSIVE SANDSTONE

CROSS-STRATIFIED SANDSTONE

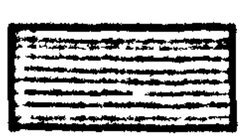

PARALLEL LAMINATED SANDSTONE

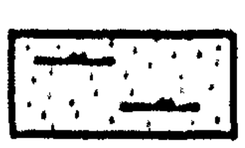

RIPPLE LAMINATED SANDSTONE

SOFT SEDIMENT DEFORMATION

RED MUDSTONE

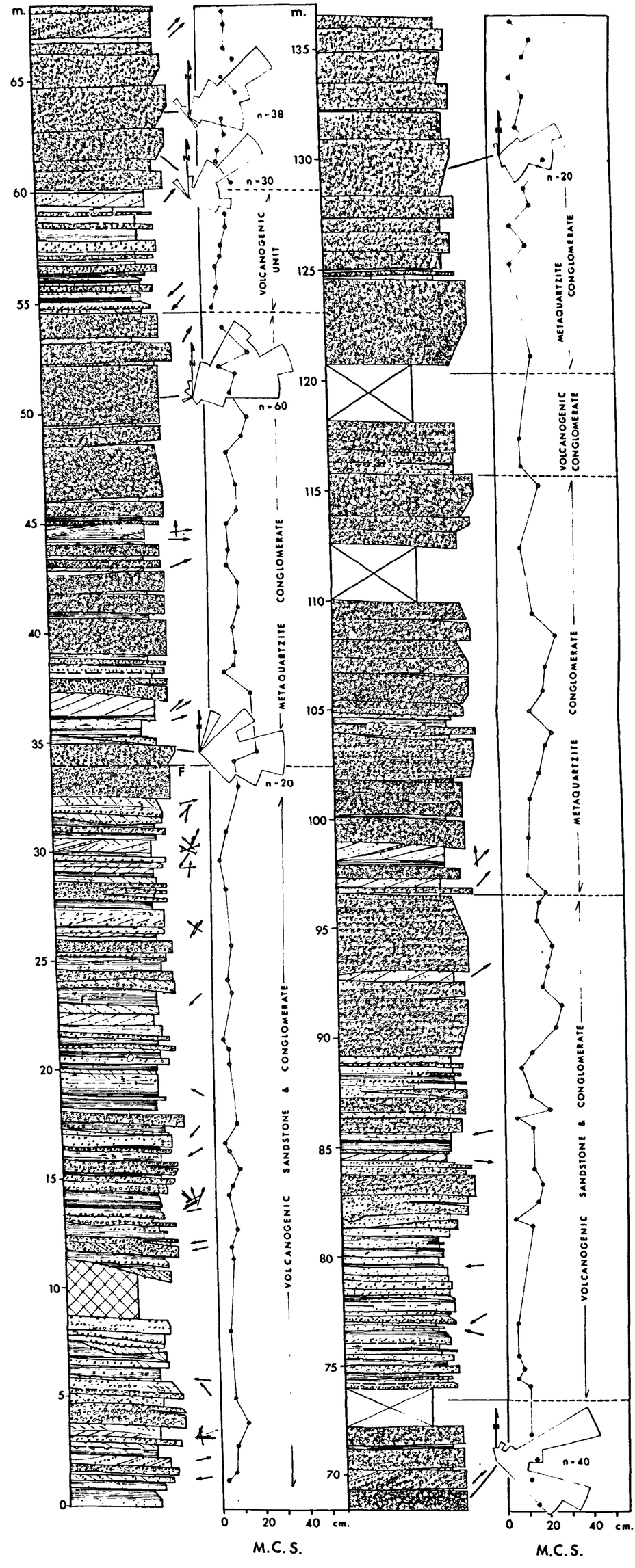
m.
65
60
55
50
45
40
35
30
25
20
15
10
5
0
n - 38
n - 30
VOLCANOGENIC UNIT
n - 60
METAQUARTZITE CONGLOMERATE
n - 20
F
VOLCANOGENIC SANDSTONE & CONGLOMERATE
0 20 40 cm.
M.C.S.
m.
135
130
125
120
115
110
105
100
95
90
85
80
75
70
n - 20
METAQUARTZITE CONGLOMERATE
VOLCANOGENIC CONGLOMERATE
METAQUARTZITE CONGLOMERATE
VOLCANOGENIC SANDSTONE & CONGLOMERATE
n - 40
0 20 40 cm.
M.C.S.
cross-stratal orientation
counter-flow cross-stratification

	LITHOSOME 1	LITHOSOME 2
GEOMETRY	Lateral and vertical differentiated sheets; channelling rare.	Abundant channels preserved; geometry in part determined by interbedded volcanigenic sediments.
STRUCTURE	Dominantly flat-stratified and massive conglomerate; rare cross-stratification up to 4m in thickness; modest rotation of cross-stratal dips relative to co-flow imbrication.	Cross-stratification common up to 6m in thickness. Commonly at high angle to co-flow imbrication.
TEXTURE	Many bimodal units; dominance of well-rounded clasts; well developed imbricate fabrics; open frameworks rare.	Typically polymodal or poorly sorted; angular clasts. Open framework common. Imbrication less well developed.
CLAST COMPOSITION	Diverse granites, porphyries, volcanics, metaquartzite, psammite; subordinate granophyre, appinite, spilite, gabbro.	Granodiorite, lithic arenite, meta-greywacke, hornfels, hornblende andesite; less abundant basalt, limestone, jasper, vein quartz.
DISPERSAL	Dominantly from N, NE.	From the S, SE, and E.

TABLE 2.1 Contrast in conglomerate lithosome structure.

Similar large angular discordances in foreset dip orientation have been recorded in Recent low sinuousity streams devoid of sand e.g. Moffat Water (Bluck 1976).

The northerly and north-westerly dispersal characterising the bulk of Lithosome 2 conglomerates is taken to indicate depositon on alluvial fans prograding from a basin margin lying to the immediate south-east. The coarse grainsize and highly angular nature of many of the component clasts emphasize that the conglomerates are proximal to their source implying that the basin margin can have lain no great distance to the south. The less common westerly directed component of the dispersal may reflect axial transport parallel to the basin margin, or interfingering between sediment dispersed from adjacent southeasterly and easterly margins of a rhombohedral type basin. The variation in Lithosome 2 dispersal is however not inconsistent with radial dispersal on alluvial fans associated with a NE-SW trending margin.

2.5.3 Lithosome 3 Dispersal

Directional structures are less obvious in the volcanogenic lithosome. Where cross-stratification is developed, the cross-stratal dips tend to show a wide range of orientations (e.g.Figure 2.20). The equant dimensions of many volcanic clasts result in clast imbrication being poorly developed. Consequently it is difficult to critically establish the palaeoflow for many of the volcanogenic units.

At least two distinct sources of volcanic detritus are however required. Volcanogenic units in each of the two lithosome associations are compositionally distinct. Those interstratified with Lithosome 1 sequences are polymict and encompass a wide range of constituent volcanic lithologies. In contrast volcanogenic sediment interstratified with southerly derived conglomerates are dominated by detritus of a single volcanic lithology, a distinctive porphyritic hornblende bearing andesite. Hornblende andesite clasts fill large NW-SE trending channels in Lithosome 3 sediments exposed at Kinneff (Fig.2.18). A south-easterly source for the detritus is probable.

2.5.4 Implications of Dispersal Data

Compositionally distinct conglomerates belonging to Lithosomes 1 and 2 have contraposed dispersals. Whereas polycyclic Lithosome 1 conglomerates share a general northerly provenance, Lithosome 2 conglomerates are derived from sources to the south and east. The dispersal data are compatible with deposition of the two lithosomes on fluvial dominated fans building out laterally from opposite margins of a small basin. The proximal character of both Lithosomes 1 and 2 (in the sense requiring that the basin margins with which they are associated were close to the present limits of the outcrop) suggest the basin in which they accumulated was relatively narrow and had a dominantly conglomeratic fill. The very different provenance of the material making up the two lithosomes requires that this basin overlay a fundamental change in crustal structure.

Referral of the two lithosomes to deposition within a single basin requires that contemporaneity in dispersal be established. In this respect, the relationship between sequences of Lithosome 1 and 2 is critical. Polycyclic conglomerates of Lithosome 1 type overlie Lithosome 2 conglomerates and related volcaniclastic sequences in several sections in the heavily faulted coastal exposures between Whistleberry and Gourdon. These outcrops probably represent a single structurally disrupted sheet of polycyclic Lithosome 1 conglomerates deposited on a rotated surface of southerly and easterly derived first cycle conglomerates. Interleaving of southerly and northerly derived conglomerates at Bervie Brow (Fig. 2.11) may represent interfingering between conglomerates dispersed from opposite margins of the basin, but the coincidence of several lithosome transitions with mappable faults suggests the repetition is largely structural. The nature of the exposure therefore makes it difficult to confidently establish lateral interfingering of synchronously dispersed conglomerate units.

Contemporaneity in dispersal appears however to be implied by the larger scale relationships. Lithosome 2 conglomerates are restricted to outcrops between Whistleberry and Gourdon,

stratigraphically below the Crawton Lava. Correlative sequences on the northern limb of the Strathmore syncline beneath the Crawton lava, exposed at Crawton, are wholly in Lithosome 1 conglomerates. A substantial part of the Crawton Group is however faulted out in Thornyhive Bay. Lithosome 2 conglomerates therefore appear to be replaced laterally northwards by conglomerates of Lithosome 1 type. Caution must however be exercised when using the Crawton lavas as a stratigraphic marker by which to correlate conglomerate units which occur stratigraphically beneath it. Discordance of units beneath the Crawton lava are seen on Bervie Brow (Fig.2.11) and it may be that the lavas of Crawton type were extruded onto a sediment surface which had already been substantially modified by differential uplift, rotation and erosion.

Exposures of the Dunnottar Group are dominated by Lithosome 1 conglomerates together with volcanogenic sediment packages of Lithosome 3 type. As the Dunnottar Group is only seen on the steeply dipping northern limb of the Strathmore syncline, it is uncertain whether northerly derived sediments were matched by correlative conglomerates of Lithosome 2 type dispersed from a contemporaneous, and unseen, basin margin to the south. The fact that northerly derived conglomerates of the Dunnottar Group contain rare clasts resembling (both in appearance and chemistry) those subsequently dispersed northwards during deposition of the Crawton Group (the `haggis` rock clasts of Campbell 1913) indicates that both sources contributed to the basin-fill at this time. Rare recycled clasts of an original southerly provenance may have been incorporated in southerly dispersed fans by either reworking of northerly dispersed fan toes, or by mixing of sediment from the two sources prior to subsidence of the basin.

2.6 ORIGIN OF CONTRASTING LITHOSOME STRUCTURE

The contraposed dispersal and distinctive composition of conglomerates belonging to Lithosomes 1 and 2 are most easily explained by envisaging deposition on lateral fans prograding from opposite margins of a small basin. As the internal structure, size and thickness of marginal fans are sensitive to the wider tectonic framework (Gloppen and Steel 1981), the contrasting structure of the alluvium is of interest. Similar contrasts in the structure of marginal fans across small tectonically active basins have been described by Hooke (1972), Gloppen and Steel (1981), and Hempton et al. (1983).

Some of the more important features distinguishing the two lithosomes are tabulated in Table 2.1. These include the presence and absence of channelling, and the relative abundance and scale of cross-stratification. Cross-stratification is relatively uncommon in sequences of Lithosome 1 type. This suggests the bed topography or channel/bar relief was generally low. Low channel/bar reliefs are a feature of braided stream alluvium in which the channels are unconfined (Rust 1978). This is compatible with the general lack of evidence for channeled erosion surfaces, and the sheet like geometry. Flow stage may also act to determine the relative abundance of cross-stratification. Bluck (1979 Fig.23) shows that alluvial bars which are constructed dominantly at low flow stage tend to be internally cross-stratified. Those formed at high flow stage tend to be dominated by flat stratified gravels and sands. The very coarse grainsize of many Lithosome 1 conglomerates require that their structure was largely determined at high flow stage and consequently this may partly explain the low abundance of cross-stratification.

Cross-stratified conglomerates are in contrast much more abundant in sequences generated by Lithosome 2. In addition channelled erosion surfaces abound. The lithosome is interpreted as having been produced by the lateral and vertical aggradation of confined low sinuousity streams. These in many cases were incised into cohesive blankets of volcanogenic sediment which would have

allowed considerable bed topography to develop as lateral flow expansion was probably inhibited. This accounts for the greater abundance and larger scale of the cross-stratal sets in Lithosome 2 (reaching 6.0m) when compared with Lithosome 1 (generally less than 4.0m). The evidence for channelling in sediments prograding from the southeasterly basin margin conflicts with the probably unconfined nature of the flows which simultaneously operated on sediment fans dispersed from the opposite side of the basin. This cannot simply be explained as the regrading of southeasterly fans in response to episodic volcanogenic blanketing. Sediment dispersed from both basin margins was periodically diluted with volcanogenic detritus. The structure of Lithosome 1 however appears to have been relatively insensitive to blanketing by volcanogenic fines and shows little variation in internal structure when traced towards contacts with the volcanogenic lithosome.

A possible analogue for the contrasting structure of the alluvium dispersed from opposite margins of the basin is illustrated by Hooke (1972). Recent fans in Death Valley show an asymmetry in structure across the basin. Large fans bounding the western margin of the basin are heavily disected, whilst fans developed along the eastern flank of the basin are small, isolate and have active segments adjacent to the fan apex. The different behaviour of fans on opposite margins of the basin is attributed to tilting of the basin floor. Gloppen and Steel (1981) and Hempton et al. (1983) illustrate a similar effect in the Devonian Hornelen and Recent Lake Hazar basins respectively. Here differential subsidence is invoked to explain the restriction of small debris flow dominated fans to one basin margin, and larger lower gradient fluvial dominated fans to the other. A similar mechanism may account for the difference in lithosome structure tabulated in Table 2.1. High subsidence rates along the northwestern margin of the basin may have allowed sediment to accumulate rapidly in this zone, whilst low subsidence rates over the southeastern part of the basin may have contributed to a tendency for channel incision and a more complex interaction with packages of volcanogenic sediment. There is however no evidence for the development of steeper gradient, smaller radius fans to

the northwest as predicted by a simple basin floor tilting model.

The very coarse grainsize of many Lithosome 1 conglomerate sheets, and the abundance of percussion marks on many clasts (Pt. 2.22), suggest deposition from high energy streams. Whilst these are commonly related to high gradients, many of the features associated with modern high gradient braided streams are apparently lacking. Longitudinal and transverse clast dams, characteristic of braided streams on alluvial fans with slopes >5% (Bluck pers.comm.1985) have not been recognised. The total absence of recognisable debris flow deposits intercalated with the fluvial lithosome confirm that gradients were likely to have been low. The development of well defined unit bars with size and shape segregation is a feature typically recorded in streams with gradients less than 1-2%. The large size of the marginal fans which dominate the fill to the basin also suggest low to moderate fan gradients. Unlike the Hornelen Basin, a basin probably of comparable size, no axial dispersal system is apparent.

A further anomaly in the structure of Lithosome 1 is the inferred scale of the original fluvial system in the context of the size of the basin. Bluck (in press) has shown a direct relationship between the rate of change of grain size on Recent unit bars and overall bar length parallel to high stage flow. If the rate of grain size decline can be measured on ancient bar deposits it is possible to compute the probable original length of the bar on which the grain size decline was esablished. Using this logic, together with the maximum distances for which single size segregated units can be traced out in outcrop, a preliminary estimate of bar scale can be made. Preserved bars in northerly derived units of the Crawton Group must have been of substantial scale, with bar lengths of the order of 100m. Whilst it is difficult to relate bar scale directly to the scale of the dispersal system (as the bar scale may relate to a single anabranch of a much larger dispersal system) it is clear that the scale of Lithosome 1 bars are anomalous in the context of a rather small laterally filled basin. One possibility is that the basin has tapped part of a larger regional dispersal system for

which it acted as a sediment sink. This may account for the evidence for low stream gradients and the absence of debris flow deposits. The high flux of sediment to the basin may have maintained a low topographic contrast between the basin and the source.

Whilst the asymmetrical lithosome structure developed across the basin may reflect differential subsidence, intrabasinal processes alone probably cannot wholly account for the difference in structure. The contrast may partly reflect the distinction between a pre-existing dispersal system captured by the basin (Lithosome 1) and a first-cycle dispersal system initiated by basin subsidence and showing a more intimate connection with basin margin fault displacements. A summary model and speculative cross-section of the basin are included in Figure 2.22.

2.7 SOME IMPLICATIONS OF THE SIMULTANEOUS DISPERSAL OF VOLCANIC AND NON-VOLCANIC SEDIMENT.

Whereas conglomerates of Lithosomes 1 and 2 share a largely non-volcanic provenance, Lithosome 3 encompasses a range of sediment types characterised by an almost exclusive volcanic provenance. This strong segregation of volcanic and non-volcanic sediment argues for a contemporaneous source for the volcanic material in extant volcanoes flanking, and possibly within, the basin. This is confirmed by the presence of lava flows and tuff breccias which interfinger with the sediments.

The dispersal of large volumes of volcanogenic sediment to basins also receiving a supply of non-volcanic sediment has a number of important implications for the resulting sediment fill. These arise largely from firstly the textural disparity between sediment liberated from volcanic and from what may be termed tectonogenic sources, and secondly, from the essentially independent and often episodic contribution of volcanogenic sediment. The interaction between volcanogenic and tectonogenic sediment is of some wider significance in that many basins can be expected to simultaneously receive sediment from both contemporaneous volcanic and tectonogenic sources. These include pull-apart and arc-related basins.

2.7.1 Source Modification

An important aspect of the overlap of volcanism and sediment dispersal is the possible modification of the source configuration by volcanic activity. This may take the form of blanketing and suppression of source rocks which might otherwise appear in the basin fill. Alternatively, volcanism may be responsible for allowing access to source lithologies not otherwise sampled by drainage systems transferring sediment to the basin of deposition. The latter appears to have been important in the case of volcanogenic units interleaved with conglomerates of the Dunnottar and Crawton Groups, and it is strikingly seen in the range of clasts entrained in thick volcanogenic breccia and tuff units intercalated with Lithosome 1 conglomerates of northerly provenance. These units locally have

an abundance of large angular clasts of chlorite-grade psammite which in all respects are almost identical to the rounded biotite and higher grade psammites occurring in the adjacent polycyclic conglomerates which enclose the volcanogenic units. Thus both groups of clasts show comparable internal grainsize, textures and detrital mineralogy, and in addition are geochemically closely related (Chapter 6).

The implication is that volcanism has allowed access to a low grade part of the source terrane which was not hitherto sampled by the polycyclic Lithosome 1 conglomerates. A possible mechanism whereby this was achieved may have involved rapid uplift of blocks on the flanks of active volcanoes in an analogous manner to similar uplifts described by Vessell and Davies (1981) on the Fuego volcano, Guatemala. Low grade greenschist facies basement may therefore have been exposed in localised block uplifts yielding first cycle sediment with angular clasts occasionally in excess of 2.0m. An important corrolary of the observed partitioning of psammite detritus between volcanic and non-volcanic units is that higher grade metamorphic zones within the metamorphic terrane which yielded the detritus must have been uplifted prior to the associated low grade zones sampled by the volcanogenic units.

2.7.2 Control of Lithosome Geometry

Volcanogenic sediment exerts an important control on the geometry of sequences generated by stacking of Lithosome 2. Channel density in alluvial sequences has been theoretically modelled in terms of variation in channel type, combined with variable rates of lateral channel migration, avulsion and vertical floodplain accretion (Leeder 1978). Such models assume the channels develop in a matrix of overbank fines. Variation in the density of channels giving rise to the crude interlayering of channellised conglomerates and flat bedded sandstones which characterise Lithosome 2 sequences cannot however be related to a simple channel-overbank model. This is because the sand dominated `flood-plain` deposits within which the conglomerate filled channels are supported are largely constructed by volcanogenic

sediment which often cannot be regarded as overbank to the channels. Rather the channel and apparent floodplain lithosomes have in many instances been constructed by independent processes. Thus the sand dominated intervals are seen as episodic additions of volcanogenic sediment which exert an important control on the geometry and density of the channels distributing non-volcanic sediment.

A transition from a conglomerate dominated to a sand dominated sequence is shown in Figure 2.21. This serves to illustrate the change in provenance associated with the change in lithosome structure. A 6m thick mega-cross-stratified conglomerate (Lithofacies 2) occurs close to the boundary between the two sequences allowing the instantaneous change in bedload composition to be examined as the boundary is approached. Clast compositions at constant grain size show a progressive increase in the percentage of volcanic clasts in successive foresets suggesting the bedload became progressively diluted by volcanogenic sediment. This indicates that an influx of volcanogenic sediment to the basin was in some cases initially accommodated by dispersal systems graded to distribute non-volcanic sediment. The textural disparity between sediment liberated from volcanogenic and tectonogenic sources however requires that the nature and geometry of their respective dispersal systems differ substantially. With continuing dominance of a volcanic sediment source the tectonogenic dispersal system is blanketed and abandoned. Occasionally channels filled with flat laminated volcanic sandstones are preserved close to the transition to volcanogenic units. These are thought to reflect plugging of existing channels as the dispersal system is transformed to distribute volcanic sediment.

As the influx of volcanic material to the basin wanes, channels dispersing tectonogenic material become re-established on volcanogenic substrates. The trend towards upward coarsening, increasing channel depths and more mobile channels reflects the regrading and growth of the previously suppressed stream dominated fans under tectonic control. The volume and temporal pattern of volcanogenic sediment addition consequently exerts an

Figure 2.21 Detailed log through transition from non-volcanic Lithosome 2 conglomerates to sand dominated volcanogenic Lithosome 3 sequence, Rich Madam (NO 845730). Arrows indicate tilt-corrected cross-stratal dip orientations (i is a visual estimate of imbricate fabric). Clast compositions have been recorded vertically up a 6m megacross-stratified conglomerate unit immediately beneath the transition to the volcanogenic sequence. Compositions were measured by counting 100 clasts with maximum clast diameters between 5 and 15cm. The progressive dilution with volcanic clasts within the same grain size interval suggests the bedload arriving at the bedform which generated the cross-stratification was systematically modified.

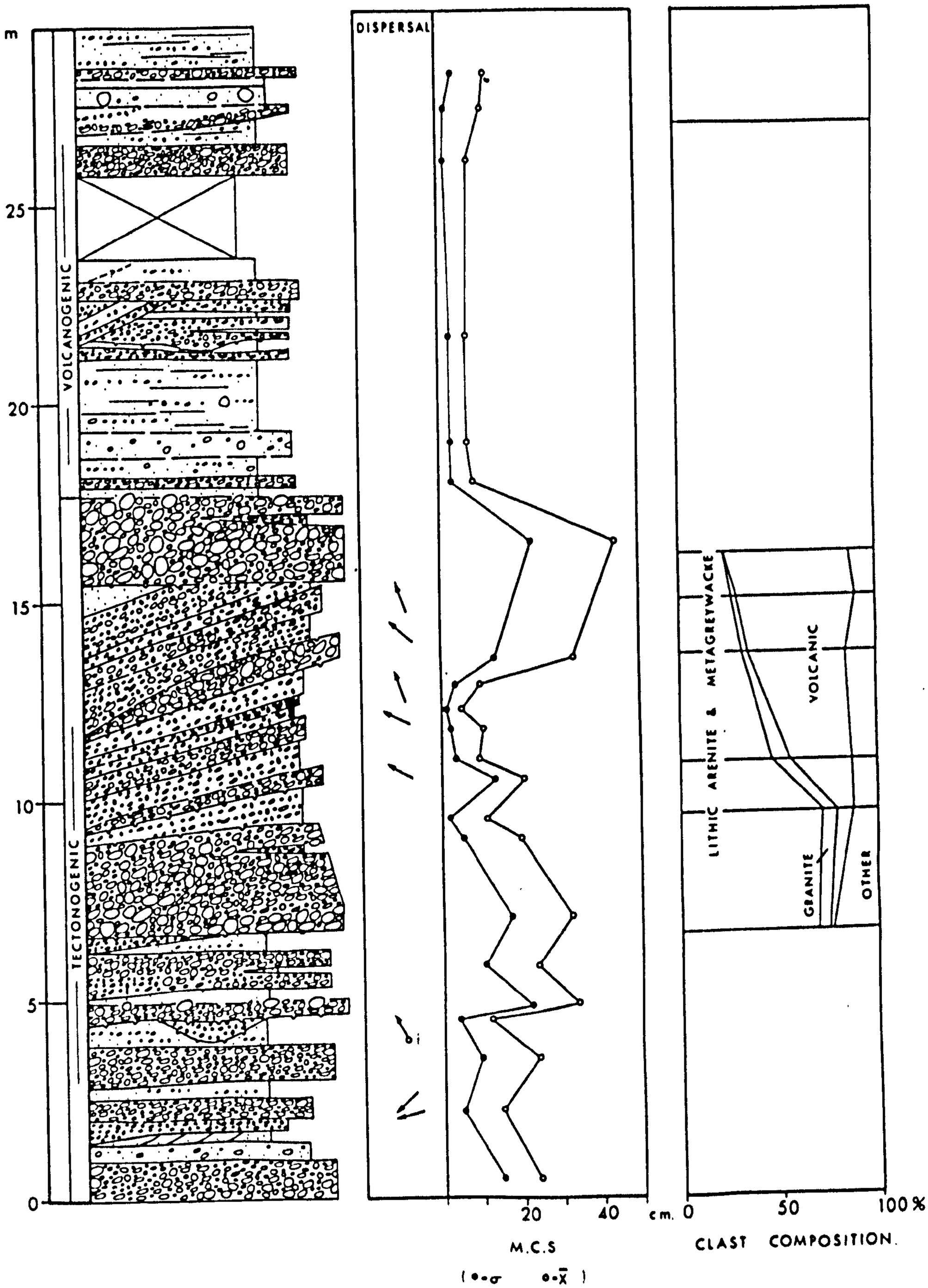
m
25
20
15
10
5
0
VOLCANOGENIC
TECTONOGENIC
DISPERSAL
20
40
cm.
M.C.S
(0-σ 0-x̄)
LITHIC ARENITE & METAGREYWACKE
VOLCANIC
GRANITE
OTHER
0
50
100 %
CLAST COMPOSITION.

important control on the vertical and lateral geometry of channel-fill conglomerates of Lithosome 2 type.

Volcanogenic sandstones and conglomerates also occur in association with northerly derived Lithosome 1 conglomerates. The interaction here is however quite different. Within coarse-grained proximal sequences volcanic material is typically admixed with material derived from non-volcanic sources. However, in more distal parts of the system, volcanic and non-volcanic material are strongly segregated into discrete units. This is illustrated by the coarsening-upwards unit shown in Figure 2.20. The lower finer grained part of the sequence is characterised by an interleaving of metaquartzite dominated and volcanic dominatd pebble conglomerates. A feature of these and other units sharing a volcanic provenance is their passive role in determining the sequential structure of the associated non-volcanic conglomerates. Thus volcanogenic units punctuating coarsening or fining upwards megasequences developed in thick Lithosome 1 successions do not unduly modify the trends developed at megasequential scale (Heward 1978). This contrasts with the fundamental control on Lithosome 2 geometry exerted by interstratified volcanogenic units. The differential response of dispersal systems distributing sediment from opposite margins of the basin to the contemporaneous dispersal of volcanogenic sediment implies a substantial change in process across the basin. This has already been discussed in 2.6.

2.7.3 Influence on Lithosome Structure

Although tectonogenic and volcanogenic sediments were dispersed separately to the basin, limited mixing between volcanogenic and non-volcanic lithosomes did occur. Given the textural characteristics of volcanogenic detritus, its incorporation into non-volcanic lithosomes can influence the structure of the resulting sediment mixture. The role of volcanic dilution in suppressing the ability of clasts to imbricate effectively has already been outlined (2.2.1.3). This in turn can determine the extent of textural differentiation on shape and size segregated sediment bars.

Volcanic clasts in units which are largely composed of non-volcanic detritus are commonly outsized. Channelling of Lithosome 2 conglomerates into blankets of volcanogenic sediment can be shown to have resulted in reworking of large volcanic clasts into the channels where they were in disequilibrium with the flow (Plate 2.16). It is common to find large outsized volcanic clasts concentrated along the base of these channels. Evidence for mixing between volcanogenic sediment and polycyclic Lithosome 1 conglomerates is largely restricted to coarse proximal conglomerates. This may reflect more efficient mixing in the areally restricted fan head. Outsized volcanic clasts, or concentrations of very coarse clasts are again characteristic of these mixed provenance conglomerates. The implied disequilibrium with the flows which generated the lithosome structure require that caution be exercised in using maximum clast size (MCS) measurements to estimate flow competence. The coarse-tail population in mixed sequences may include volcanic clasts in disequilibrium with the gravel population they are hosted by. Variation in the extent of volcanic dilution may therefore produce spurious MCS trends. By combining measurements of MCS with measurements of maximum volcanic and non-volcanic clast sizes spurious trends can be identified (Fig.2.7).

2.8 CONCLUSIONS

1. Five recurrent lithofacies can be recognised in the largely conglomeratic sediments of the Dunnottar and Crawton Groups. These form two important lithofacies associations or lithosomes. The two lithosomes were produced by aggradation or lateral migration of two distinct depositional systems. The lithosome structure can be recognised by establishing the relative geometry of the component lithofacies, and the relationship between these lithofacies and the directional properties of the lithosome as a whole. In addition, a subordinate third lithosome includes sediments almost exclusively of volcanogenic origin.

2. Lithosome 1 is characterised by sheets of massive or imbricate conglomerate which show either lateral or vertical grain size and/or shape segregation. Laterally size and shape segregated sheets generally fine in the direction of palaeoflow and have a direct analogy in gravel bars in Recent gravel bed rivers. The low abundance and relatively small scale of associated cross-stratification, together with the apparent absence of channelling, indicate deposition from unconfined flows. The lack of a discrete flood-plain lithosome, and the low directional variability of imbrication at outcrop scale suggest a braided stream depositional setting.

3. Coarsening-upwards cycles 2-7m thick make up an important component of Lithosome 1. Textural equivalents of the lithofacies transposed to generate the coarsening-upwards cycles can be recognised within single laterally differentiated sheets. The coarsening upward units are thought to record downstream migration of coarse-grained bar-head gravels over the finer grained bar tail. Where the bar-head is made up of strongly imbricate conglomerates it may have been relatively immobile, and the coarsening upwards may reflect the progressive downstream accretion and growth of a bar from a fixed head.

4. Lithosome 2 is distinguished by an abundance of channelled erosion surfaces. The structure of the channel fill is dependent on the stability of the channel. Channels which have migrated

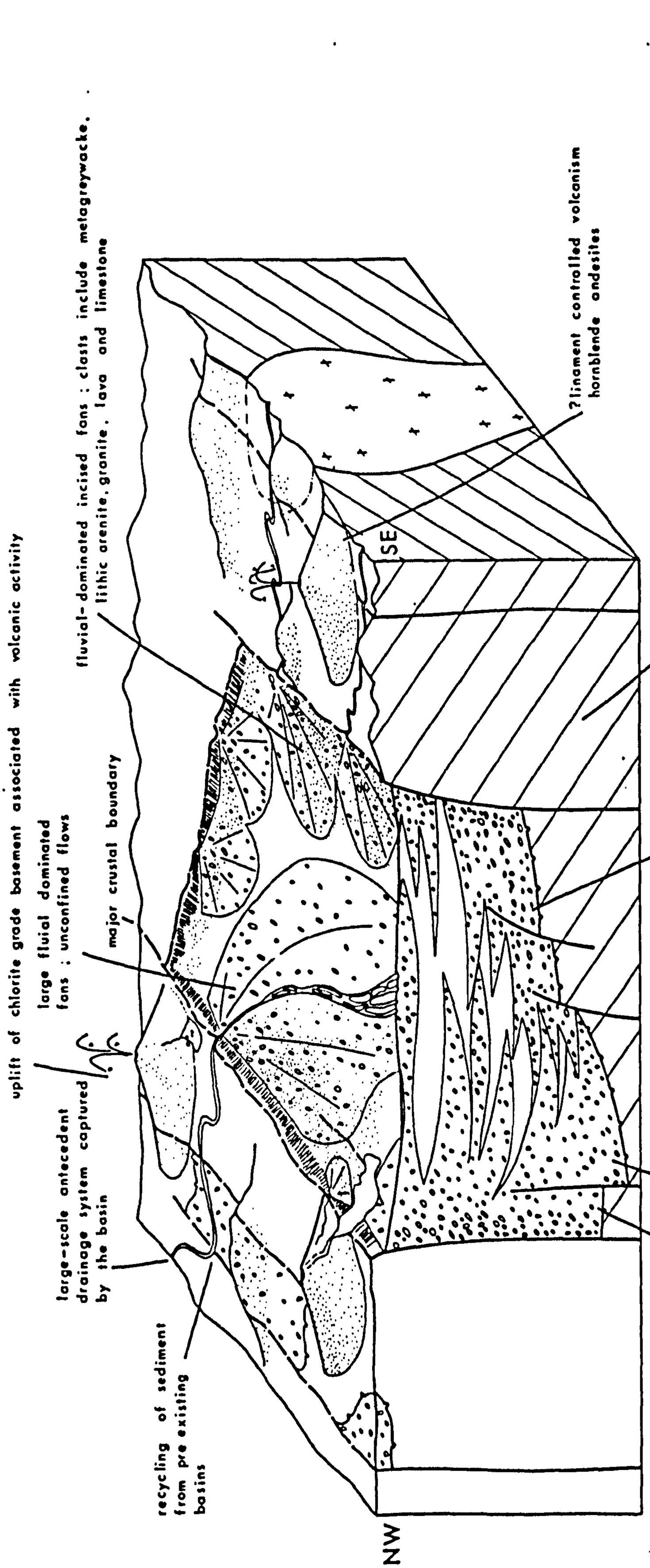

Summary Depositional Model for the Dunnottar and Crawton Groups

Figure 2.22

laterally have a more complex differentiated fill. Frequently this entails bar-type cross-stratification dipping at high angle to the channel trend and abutting directly against a steep channel margin. These are interpreted as bank attached lateral bars which are inferred to have formed in confined low sinuousity streams. Many of these were deeply incised into blankets of volcanogenic sediment. The often high angular discordance between imbrication and bar-type cross-stratification implies the bar heads were probably more mobile than those in Lithosome 1. Large scale cross-stratificaiton which is co-flow with imbrication measurements in adjacent coarse conglomerates are interpreted as having formed by downstream migration of poorly differentiated gravel bars over deep pools or channels.

5. Lithosomes 1 and 2 are compositionally distinct and they cannot share the same provenance. Lithosome 1 conglomerates include an important recycled component, whereas the sediments comprising Lithosome 2 have a first-cycle provenance. The Lithosome 1 provenance shares some affinity with recycled conglomerates elsewhere in the Midland Valley, although granite clasts are unusually enriched. The assemblage of clasts occurring in Lithosome 2 conglomerates however record a previously unrecognised element in the provenance of the Lower ORS.

6. Directional structures establish a contraposed dispersal pattern for conglomerates of Lithosomes 1 and 2. Lithosome 1 has a general northerly provenance. Large angular discordances in the dispersal of Lithosome 1 over its northernmost exposure can be explained by radial deposition from a point apex on the proximal part of isolate alluvial fans. Lithosome 2 is derived from a source to the east and south.

7. Lithosomes 1 and 2 build essentially separate thick vertical profiles. Lithosome 2 is only exposed in the upper part of the Crawton Group on the southeasterly limb of the Strathmore Syncline. A correlative section beneath the Crawton Lava on the northwestern limb of the syncline is wholly in Lithosome 1, although a substantial part of the sequence is cut out by

faulting. The difference in lithosome structure, clast provenance and dispersal geometry, developed apparently at similar stratigraphic levels, is compatible with deposition of the two lithosomes on fluvial dominated fans building out laterally from opposite margins of a small basin. The disparate clast compositions require that the basin overlies a significant change in crustal structure.

8. Accepting deposition of the two lithosomes on fans dispersed from opposite margins of a small basin requires that the different lithosome structure be explained. Analogous variations in marginal fan structure have been recognised across a number of both Recent and ancient, tectonically active basins where basin floor tilting has been proposed. A similar mechanism may have operated during the deposition of the Dunnottar and Crawton Groups. Scale considerations however suggest intrabasinal and fault margin processes may not wholly be responsible for the difference in lithosome structure. The contrast in structure may in part reflect the distinction between a larger regional dispersal system captured by the basin (accounting for Lithosome 1) and a smaller system initiated by basin subsidence and more intimately connected with basin margin processes (Lithosome 2).

9. Both Lithosomes 1 and 2 are interstratified with sediment packages sharing an almost exclusive volcanic provenance (Lithosome 3). The volcanic detritus is interpreted to have a source in extant volcanoes flanking and possibly within the basin. Episodic sediment addition to the basin from volcanogenic sources produces a number of side effects. These include modification of non-volcanic sediment sources, the control of lithosome geometry in associated non-volcanic conglomerates, and the modification of lithosome structure by progressive dilution with outsized volcanic clasts.

CHAPTER THREE

BASIN ANALYSIS

3.1 THE DUNNOTTAR AND CRAWTON GROUPS IN THE WIDER CONTEXT OF THE STRATHMORE SUCCESSION

The Strathmore Lower ORS has conventionally been thought of as the fill to a single Strathmore Basin (Bluck 1978). This may or may not have been linked with a contemporaneous Lanark Basin to the south (Armstrong *et al.* 1985, Bluck 1983). Although lateral correlation within the Strathmore sequence is difficult, the Stonehaven, Dunnottar and Crawton Groups cannot (with the possible exception of the Lintrathen porphyry) be recognised outside Kincardineshire. When the sedimentology and dispersal of the Dunnottar and Crawton Groups described in the preceding chapter are compared with the overlying Arbuthnott, Garvock and Strathmore Groups, it becomes apparent that they were deposited in radically different settings. This requires that the concept of a single Strathmore Basin be critically re-examined. Amongst the more important criteria distinguishing the earlier and later evolution of the Strathmore Lower ORS are :

1. The sediments comprising the Dunnottar and Crawton Groups accumulated in a small basin which probably was not much more than 20km wide. The Arbuthnott, Garvock and Strathmore Groups in contrast appear to have been deposited in an elongate basin which can be traced for over 180km along strike, and which may have been integrated with other Lower ORS basins (Simon and Bluck 1982).

2. The Dunnottar and Crawton Group sucessions are largely conglomeratic. Conglomerates account for 70-80% of the sediment preserved. Sandstones when they occur in any abundance are largely volcanogenic. The Arbuthnott, Garvock and Strathmore Groups are in contrast largely composed of sandstones and mudstones, with important but subordinate marginal fanglomerates along both the Highland Border and volcanic uplands to the south.

3. Coarse conglomerates of the Dunnottar and Crawton Groups were laterally dispersed to the basin from fault controlled basin margins. There is surprisingly no evidence for a substantial axial dispersal system. Bluck (1978) calculates that as much as

70% of the upper part of the Strathmore succession exposed south-west of Crieff is axially derived. The ultimate source of this axial system may have been lateral fans or an uplift in or beyond the North Sea. The axial component was deposited by very large south-westerly flowing river systems, as single cross-bed sets in excess of 10m high have been recorded (Bluck pers. comm. 1985).

4. Conglomerates of the Dunnottar and Crawton Groups dispersed from basin margins lying to the north-west and south-east are compositionally distinct. The basin simultaneously received first cycle and polycyclic detritus. The first cycle source is unique to the lower part of the Kincardineshire succession. Whilst the upper Strathmore sequence also appears to have a complex dispersal from both the north-west and south-east (Bluck 1984), it is more difficult to compositionally distinguish the two sources.

5. Sandstones within the Dunnottar and Crawton Groups, and making up the underlying Stonehaven Group, are characterised by pervasive soft sediment deformation. Armstrong et al. (1985) note that the Lower Devonian sequence exposed in the Perth and Dundee districts is poor in penecontemporaneous deformation structures which might be ascribed to seismic activity. Relative tectonic quiescence during deposition of the upper stratigraphic groups is confirmed by the abundance of pedogenic carbonate at this level.

Given that the early and later history of sediment accumulation in the Strathmore region was of markedly different character, it is possible to relate the two sequences to either the time dependent evolution of a single basin, or to the amalgamation of essentially unrelated basins. Previous workers have interpreted the Strathmore succession as the fill to a single basin, attributing the westerly overstep and thinning to the inception and growth of this basin. Bryhni (1964) suggested a lateral migration of the basin depocentre to the south-west to explain the apparent restriction of the lower lithostratigraphic groups to the north-east Midland Valley (Fig. 3.1a). Bluck (1978) proposed that the basin was initiated in the north-east and

A. Basin depocentre migration.

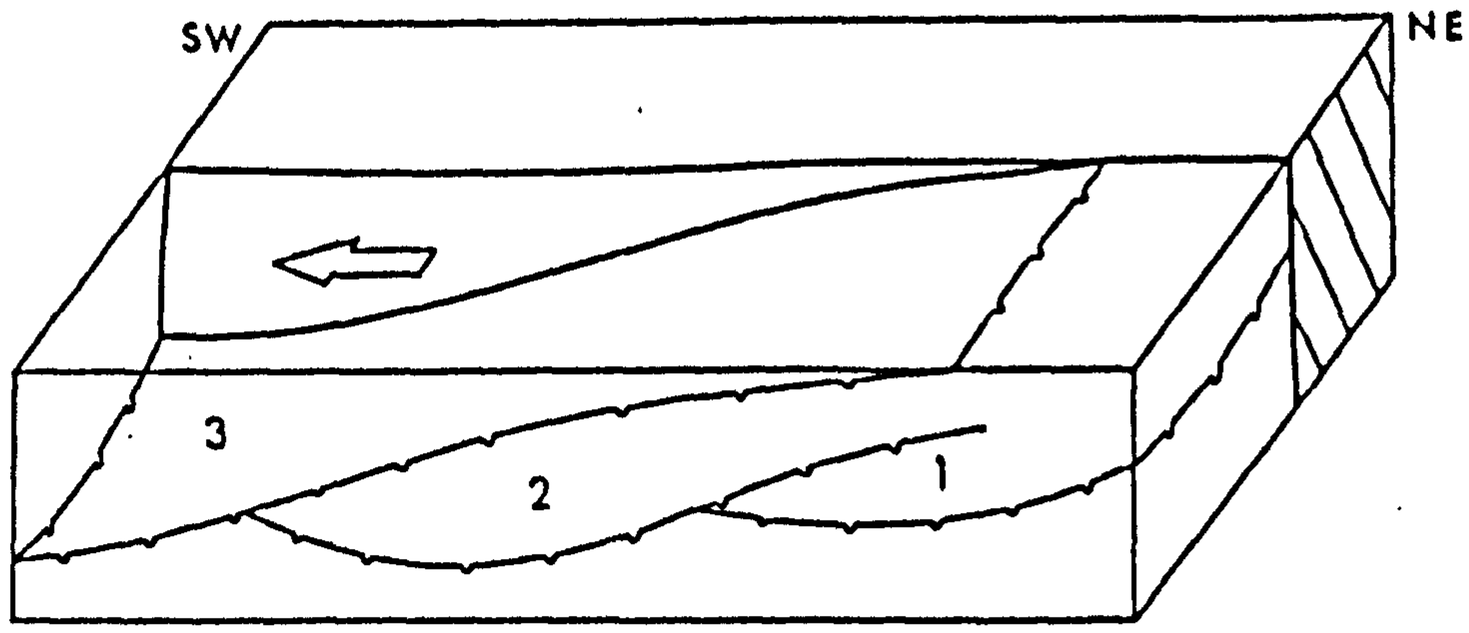

B. Propagating basin-bounding fault system.

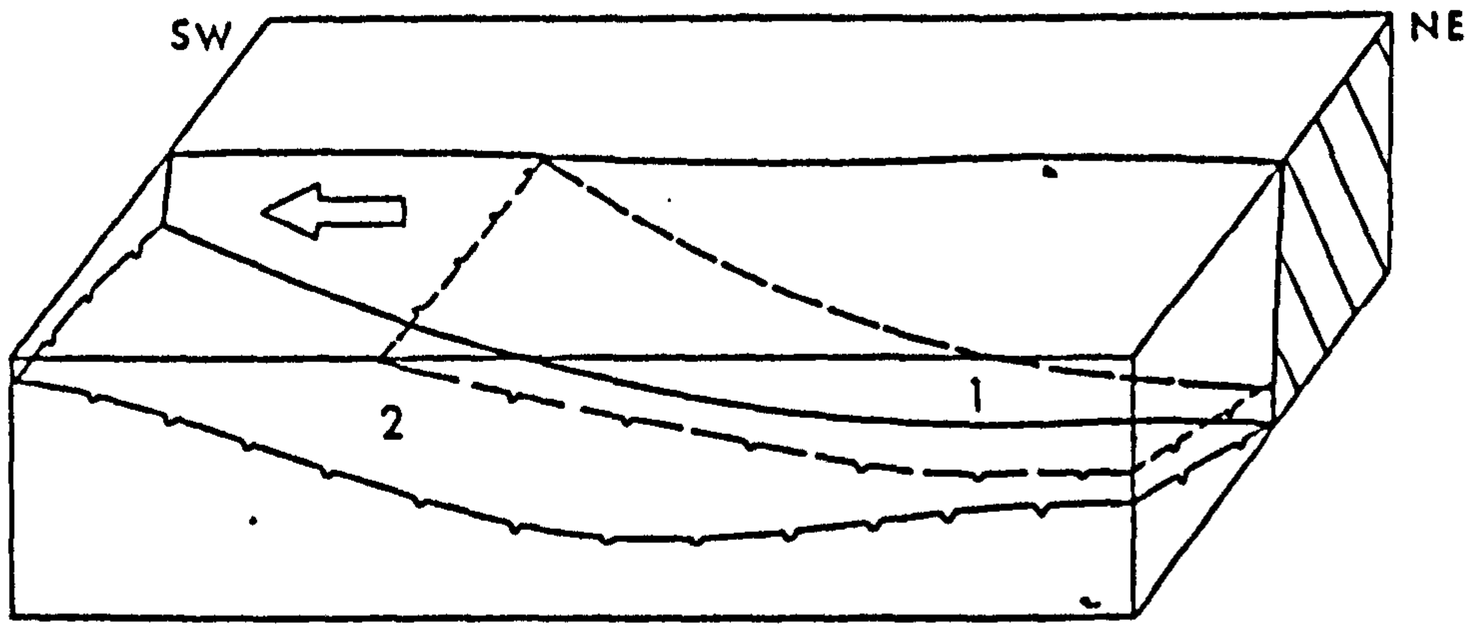

C. Basin amalgamation.

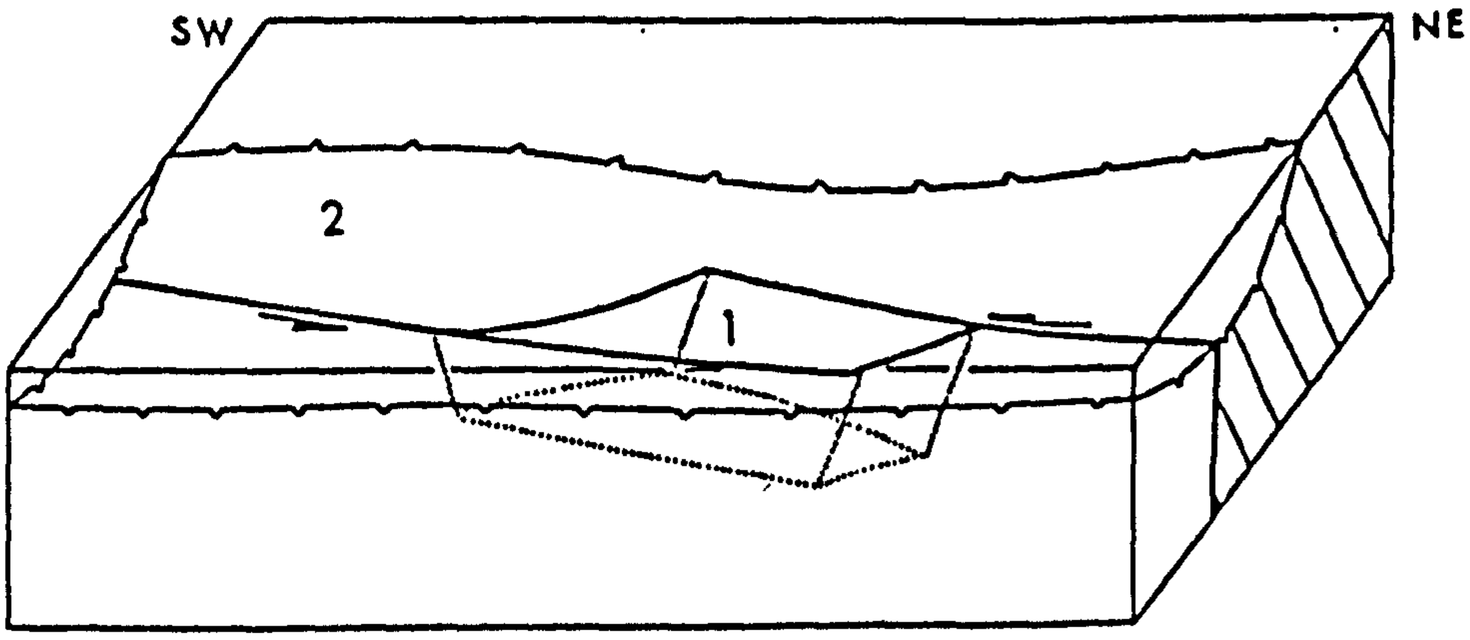

FIGURE 3.1 Cartoon illustrating contrasting models proposed to account for lateral stratigraphic and thickness variation in the Strathmore Lower ORS. (a)basin depocentre migration model after Bryhni (1964) (b)southwesterly propagating basin-bounding fault after Bluck (1978). (c)a new interpretation taking into account the different character of the lower and upper stratigraphic groups. These are seen as having accumulated in essentially separate but vertically transposed basins.

enlarged by migration of displacements on a south-westerly propagating basin bounding fault system (Fig. 3.1b).

It is difficult however to reconcile the disparity between the Dunnottar and Crawton Groups on the one hand, and the Arbuthnott, Garvock and Strathmore Groups on the other, with a continuous history of basin subsidence. The transition from a small laterally filled basin to a large longitudinally filled basin appears to have been a rapid one. The Arbuthnott Group is widely recognised along the length of the Strathmore Syncline, occurring in Kincardineshire (Campbell 1913), Tayside (Armstrong et al. 1985), the western Midland Valley and possibly even in Kintyre (Morton 1976). It overlies the Crawton Group which is in contrast areally far more restricted. All three of the upper lithostratigraphic groups appear to have a similar areal distribution and there is no evidence for a progressive south-westerly overstep at this level.

The basal unconformity of the Strathmore succession on the Highland Boundary Fault further constrains the relationship between the Lower and Upper Groups. The Stonehaven Group rests with basal unconformity on the Highland Border Complex north of Stonehaven. To the south-west conglomerates high in the succession (judging by their position beneath distinctive Strathmore Group lithologies) also rest directly on the Highland Border Complex (Curry 1982, 1984, Bluck 1984, pers. comm. 1985). In the intervening ground a great deal of the succession has therefore been lost. The unconformity beneath conglomerates stratigraphically high in the succession extends north-eastwards possibly as far as Clattering Brig (Grid Ref. NO 665783) where angular poorly sorted conglomerates rich in Highland Border Complex detritus are found in close proximity to outcrops of the Highland Border Complex itself (Bluck pers. comm. 1985). Clattering Brig is no more than 10km along strike from the westerly extension of the Stonehaven Group, south of the Highland Boundary Fault Zone. Within this distance the whole of the Stonehaven, Dunnottar and Crawton Groups and possibly part of the Arbuthnott Group have been overstepped. This is most easily explained by envisaging the lower part of the succession as the

fill to a small but tectonically active basin which subsequently was covered by the fill to a later more extensive basin reflecting more regional subsidence. The different character of the lower and upper parts of the succession can within this framework be related to contrasting tectonic controls on the development of separate basins.

The basin amalgamation model is illustrated in Figure 3.1c. A small sub-basin, here termed the Crawton Basin, is thought to have preceded the development of a much larger basin for which the name Strathmore Basin is retained in a more restricted sense than originally defined (Bluck 1978). The model accounts for the great thickness of the Kincardineshire succession in that this is attributed to the vertical amalgamation of basins in this area. More modest thicknesses elsewhere in the Strathmore Lower ORS may reflect the absence of an early sub-basin.

3.2 TECTONIC SETTING OF THE CRAWTON BASIN.

3.2.1 Evidence for a strike-slip setting.

The Crawton Basin is characterised by a predominantly conglomeratic fill dispersed laterally to the basin from fault controlled margins to the north-west and south-east. Hempton *et al.* (1983) note that basins occurring in strike slip settings have a number of distinctive characteristics. These include (1) great stratigraphic thickness relative to the size of the basin (2) high rates of sedimentation (3) asymmetry of sediment thickness and facies patterns (4) organisation of the facies into marginal fault-bounded fanglomerates and axial flood basin and lacustrine deposits and (5) textural cycles that reflect tectonic activity.

The Crawton Basin satisfies many of these criteria. The basin fill is in excess of 2.5km thick despite the basins probable small overall size. The dominance of conglomerates and the evidence for moderate gradients suggest high sedimentation rates. The contrasting lithosome structure of sediments prograding from opposite margins of the basin suggests an asymmetry in facies development and possible variation in subsidence rates across the basin. Similar facies variations have been described from basins of pull-apart type where greater vertical displacement on one of the master faults induces rotation or tilting of the basin floor. The Crawton Basin however does not show internal differentiation into marginal fanglomerates and axial flood basin or lacustrine deposits. Textural cycles, both coarsening and fining upwards megasequences, may relate to tectonic activity.

Whilst fulfilling many of the criteria normally thought to typify basins of pull-apart type, these taken alone are ambiguous, and are open to alternative interpretation. A number of other features however concur with a strike-slip setting for the Crawton Basin, and these when considered together with the criteria above allow greater confidence in a pull-apart interpretation. Pull-apart basins are defined as basins produced by extension at a discontinuity or step along a through-going strike-slip fault (Mann *et al.* 1983).

Perhaps the single most important attribute of the Crawton basin is the totally distinct provenance of the conglomerates dispersed from opposite margins of the basin. This requires that the basin nucleated on a major crustal lineament which separated disparate crustal segments. Either the basin formed over an old fracture zone along which two distinct crustal terranes were juxtaposed at some earlier time, or it developed as a direct consequence of the lateral translation of the two terranes.

A pull-apart origin is also favoured by regional tectonic considerations. Soper and Hutton (1984) and Watson (1984) argue for a widespread episode of sinistral transpression during the late Silurian - early Devonian. Sinistral displacements on faults of the Loch Tay Fault Set which traverse the Grampian and SW Highlands can be shown to overlap with the emplacement of c. 400 Ma granites. Smith (1961) demonstrates that minor intrusions cut some of these sinistral fractures. Other faults and shear zones appear to have been instrumental in channelling magmas to the surface (Watson 1984). Hutton (1982) emphasised the important role of regional sinistral transpression in controlling the emplacement mechanism of granite plutons in Donegal, NW Ireland. Non-axial planar cleavage occurs widely in the paratectonic Caledonides and has been explained as a consequence of late Silurian sinistral transpression (Cameron 1981, Soper and Hutton 1984, Murphy 1985). A strong early Devonian sinistral component has also been recognised in north central Newfoundland (Dewey and Shackleton 1984). The widespread record of regional sinistral transpression provides a logical framework for interpreting the structural control on the Crawton Basin.

A pull-apart setting may explain some features of the sediment fill. The dispersal of polycyclic conglomerates along the inferred northern margin of the basin can be resolved into northeasterly and southwesterly components. Polycyclic conglomerates furthest from this margin are largely derived from the north and northeast and there is a general paucity of southeasterly dispersed flows. Assuming the basin to have been

bounded by a NE-SW trending northern margin parallel to the regional strike, sediment transport normal to this margin is notably suppressed. Hooke (1972) documented preferential deposition on a single flank of recent alluvial fans along the eastern margin of Death Valley. This was attributed to dextral displacement of the fan relative to its source area. It is possible the anomalous southerly and southeasterly dispersal of polycyclic conglomerates within the Crawton Basin may record an analogous process. Sinistral translation of fan drainage basins along a NE-SW trending fault should produce preferential accretion on the southwesterly flanks of marginal fans, resulting in an inherent bias in the palaeocurrent data.

Sinistral translation of the source relative to the basin may also explain the compositional distinction between Lithosome 1 conglomerates at the base of the Dunnottar Group and those higher in the sucession. Conglomerates having a compositional affinity with Lower ORS conglomerates elsewhere in the Midland Valley are replaced vertically by a provenance unique to Kincardineshire. These latter conglomerates extend southwestwards to the North Esk close to Edzell where they occur in the Strathmore Group. The vertical and lateral change in conglomerate composition is commensurate with the lateral translation of a differentiated source terrane by strike slip. Thus vertical compositional variation in the Lithosome 1 basin fill may ultimately reflect vertical transposition of lateral source variation.

The absence of well developed marginal and axial depositional systems in the Dunnottar and Crawton Groups distinguishes the Crawton Basin from many described pull-apart basins. Lacustrine sediments tend to be the most voluminous deposits in strike-slip basins (Hempton and Dunne 1984). Recent pull-apart basins are often characterised by a large topographic contrast between the basin floor and flanking uplands, indicating subsidence generally outpaces sediment supply. Exceptions do however occur, particularly in instances in which the drainage system dispersing sediment to the basin is antecedent. Hempton and Dunne (1984) demonstrate that the longitudinal or axial mode of basin fill is

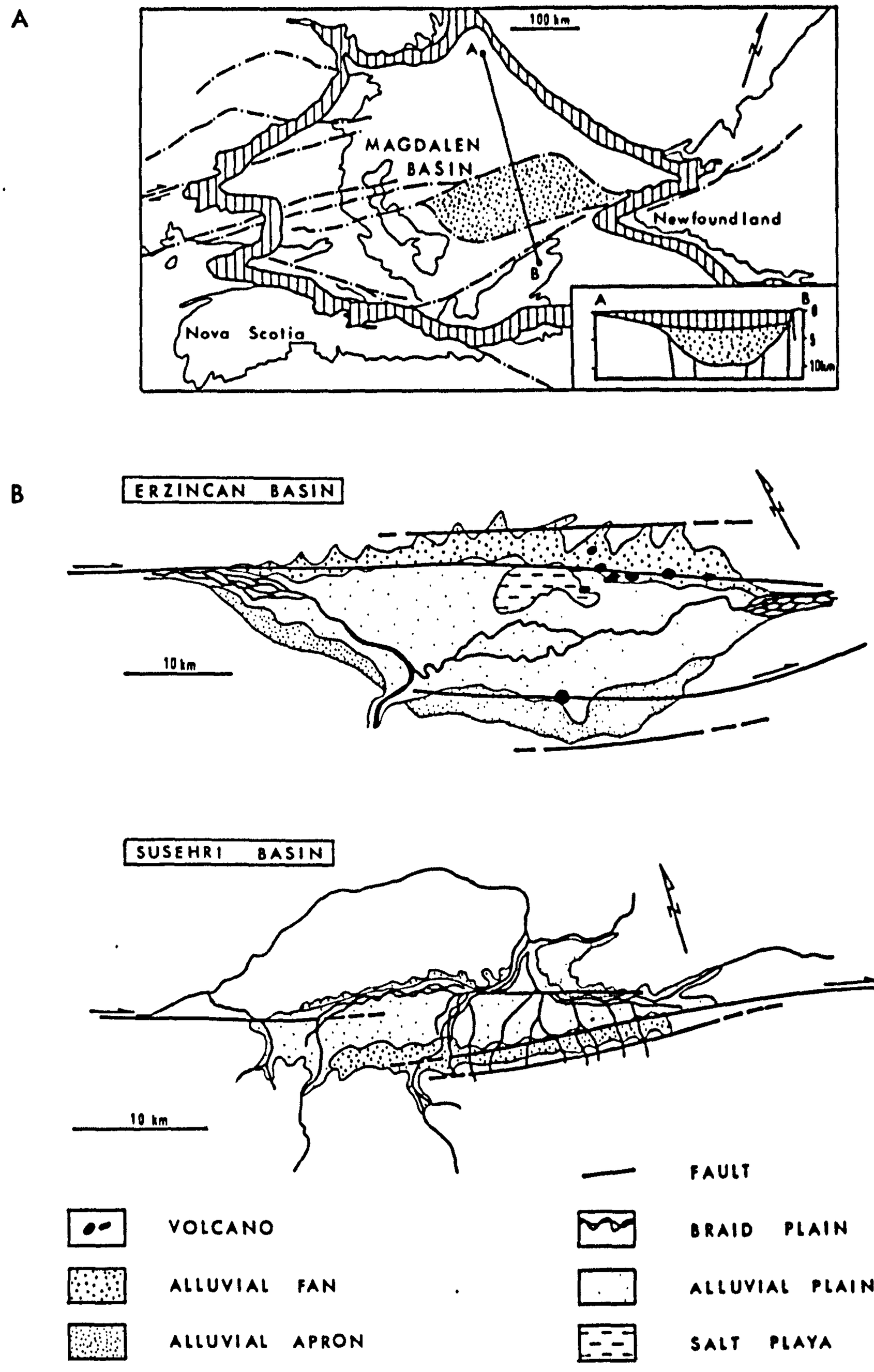

Figure 3.2 Structure and depositional characteristics of selected pull-apart basins. From Hempton and Dunne (1984) and Bradley (1982).

not always dominant in pull-apart basins along the North Anatolian Fault where the drainage is largely antecedent (Fig. 3.2). These basins contain no lacustrine deposits in contrast to the internally drained Lake Hazar Basin on the East Anatolian Fault. The contrast between internally drained basins and those integrated with an external drainage system therefore appears to be an important one. The possibility that the Crawton Basin captured a regional dispersal system has already been considered. If this were the case, this may account for the lack of well defined marginal and axial dispersal systems.

The association with contemporaneous calc-alkaline volcanic activity is an important feature of the Strathmore Lower ORS. Because of the high rates of sedimentation, volcanoes are only found in a small percentage of pull-apart basins. Pull-apart basins are however sites of localised crustal stretching and lithospheric extension, and consequently are often associated with high heat flows. Occasionally volcanoes are actually found within pull-apart basins e.g. Erzincan Basin on the North Anatolian Fault Zone (Aydin and Nur 1982, Hempton and Dunne 1984). More commonly, it is the large transform and transcurrent faults associated with pull-apart basins which are the sites of persistent volcanism. Detritus derived from volcanoes situated on these `leaky` transcurrent faults may find its way into pull-apart basins along strike. Gill (1982) notes that leaky transcurrent faults are one of the few settings outside of island and continental arc regimes where orogenic andesites may occur. Lower ORS volcanic rocks in the Midland Valley have generally been ascribed to the operation of a volcanic arc which persisted into the Lowermost Devonian (Thirlwall 1981). This is however difficult to reconcile with evidence for the cessation of subduction in the Silurian (Watson 1984). It is possible that lineament controlled volcanism is a more realistic mechanism to account for the voluminous Lower Devonian volcanic rocks.

3.2.2 Subsidence History of the Strathmore Lower ORS

The contrast between the Crawton and overlying Strathmore Basins is analogous to the subsidence history of several large pull-

apart basins which show a two stage subsidence history (Mann et al. 1983). McKenzie (1978) has shown that the development of many extensional basins can be modelled in terms of an initial phase of stretching followed by an episode of gradually declining thermal subsidence. The rapid subsidence associated with stretching reflects an isostatic response to net density changes accompanying crustal thinning, heating and thermal expansion. The second stage relates to cooling and contraction of the crust and is amplified by sediment loading. Several authors have extended McKenzie's model to include basins of pull-apart origin. Sclater et al. (1980) applied the McKenzie model to the subsidence history of pull-apart basins in the Carpathian region. Bradley (1982) showed the model to satisfactorily account for the late Palaeozoic evolution of basins in the northern Appalachians. The Carboniferous Magdalen Basin opened as a pull-apart in the Gulf of St. Lawrence between overlapping dextral faults. About 7km of clastic sediments, evaporites and volcanics were deposited in a small fault controlled basin during the stretching phase. Later Carboniferous clastic deposition was in contrast not fault controlled and the pull-apart basin was subsequently buried by an enlarged basin which onlapped onto pre-Carboniferous basement (Fig. 3.2a).

A similar history of stretching followed by more widespread thermal subsidence may account for the inferred geometry of Lower ORS basins in the Midland Valley. The Crawton Basin shares many of the features normally assigned to basins developed in a pull-apart setting. In addition, subsidence of the basin overlaps with established sinistral transpression. The extensive overlying Strathmore Basin is less obviously controlled by marginal faulting and in the Highland Border region overlaps onto the Highland Border Complex. It therefore bears some resemblence to those basins generated by thermal subsidence following crustal extension. The coincidence of the transition from a small laterally filled extensional basin to a large axial filled basin significantly coincides with the acme of Lower ORS volcanism in the Midland Valley. This might be anticipated in a dual pull-apart - thermal subsidence model as the period of maximum crustal extension would immediately precede the transfer

to a thermal subsidence mechanism.

The poor biostratigraphic control precludes the construction of detailed subsidence curves for the Strathmore Lower ORS. Some rough calculations (Fig. 3.3) can however be made on the basis of the time scale of Harland *et al.* (1982) and the lithostratigraphic thicknesses of Armstrong and Paterson (1970). Richardson *et al.* (1984) establish a Lower but not Lowermost Gedinnian age for the basal part of the Arbuthnott Group. The only control on the age of the lower part of the sequence is a probable Downtonian or Pridoli age for the Cowie Harbour Fish Bed in the Stonehaven Group. The Dunnottar and Crawton Groups are therefore bracketed by rocks of Pridoli and Lower Gedinnian age. Harland *et al.* (1982) establish absolute ages of 414 and 408 Ma for the base and top of the Pridoli respectively. Richardson *et al.* (1984) suggest an age of 410 Ma for the base of the Devonian (*i.e.* top Pridoli). Thirlwall (1983a) shows the lower part of the Arbuthnott Group in Fife to be 407 ± 6 Ma. A granite clast dated at 412 ± 2 Ma from the top of the Crawton Group (6.) further constrains the maximum age of the sequence. Similar clasts occur throughout the Dunnottar Group suggesting the sequence is no more than 412 Ma. A conservative estimate for the duration of the sedimentation in the period between the Cowie Harbour Fish Bed and the Arbuthnott Group is therefore *c.* 5 Ma. Armstrong and Paterson (1970) show that approximately 3.5km of sedimentary and minor volcanic rocks intervene between the two stratigraphic levels. This is equivalent to a subsidence rate of 0.7mm per year.

The upper part of the Strathmore sequence in Kincardineshire includes the Arbuthnott, Garvock and Strathmore Groups. These have a cumulative thickness of 4-5km (Armstrong and Paterson 1970), although they are probably substantially thinner in the western Midland Valley where along the Highland Border they are unconformable on the Highland Border Complex. There is evidence that the upper part of the succession accumulated over a substantially greater time interval and probably encompasses the equivalent of at least two Devonian stages. The Arbuthnott Group appears on palynological evidence to be almost entirely of Lower

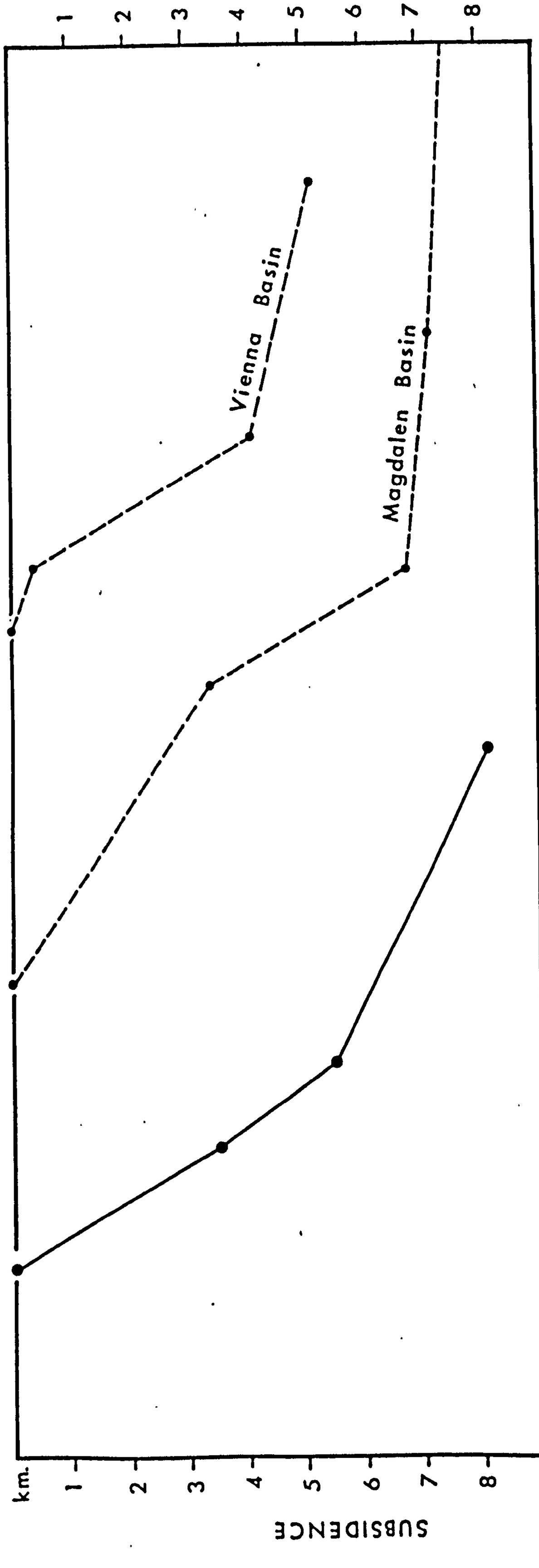

FIGURE 3.3 Subsidence curve for the Strathmore Lower ORS in Kincardineshire showing probable two stage subsidence history. Based on macrofossil (Westoll 1977) and miospore data (Richardson 1967, Richardson et al. 1984), geochronological constraints (Thirlwall 1983, 1983a) and Paterson (1970). Should the upper part of the sequence be in fact thinner than estimated by Armstrong and Paterson, the two stage subsidence history will be emphasised not obscured. Time scale used is that of Harland et al. (1982). Subsidence curves for the Magdalen (Bradley 1982) and Vienna basins (Scaleter et al. 1980) are included at the same scale for comparison.

Gedinnian age (Richardson et al. 1984). This implies rapid subsidence, as the Gedinnian stage has a duration of c. 7 Ma (Harland et al. 1982). Up to 2km of sediment and volcanic rock therefore accumulated within c. 3.5 Ma. This translates to a subsidence rate of c. 0.6mm per year.

The deposition of the Garvock and Strathmore Groups is bracketed by a Lower Gedinnian age for the underlying Arbuthnott Group, and a possible Emsian age for the Strathmore Group. Plant fossils for the latter suggest a late Siegenian age (Westoll 1977) but miospores indicate that Lower to Middle Emsian equivalents may be present near the top of the group (Richardson pers. comm. in Westoll 1977). The Upper Gedinnian, Siegenian and Lower Emsian stages are therefore all probably represented in the Garvock and Strathmore Groups. These groups reach a cumulative thickness of 3.0-3.5km according to Armstrong and Paterson (1970) and must have a duration of c. 15 Ma years. This converts to a subsidence rate of c. 0.2mm per year, substantially less than that indicated during the earlier phase of subsidence. There is therefore some evidence for an appreciable slowing of the subsidence rate with time in accordance with theoretical models for extensional basins.

A possible subsidence curve for the Kincardineshire ORS is shown in Figure 3.3 and serves to illustrate the probable two-stage subsidence history. The rates and pattern of subsidence are closely comparable to those in other basins having a pull-apart origin (e.g. Vienna Basin, Sclater et al. 1980, Magdalen Basin, Bradley 1982). The apparent decay in subsidence rate is matched by a concomitant fining of the sediment fill upwards. The Dunnottar and Crawton Groups are dominated by coarse conglomerates, whilst conglomerates are only found as subordinate isolate marginal fans in the Strathmore Group. The upward fining of the Strathmore Lower ORS contrasts with many molasse sequences which demonstrably coarsen upwards. Contemporary Lower ORS sediments in Wales and the Welsh Borderlands also form a progressively upward coarsening sequence (Dineley and Williams in Friend and Williams 1978). Should the Welsh and Scottish Lower ORS have been linked in a single dispersal system, as is

suggested by Simon and Bluck (1982), it is necessary to account for the contrasting basin fill trends. One possibility is that the initial development of deep rapidly subsiding basins in Scotland may have starved areas further south of coarse detritus. The reduction in subsidence and transfer to a large depositional basin may have subsequently allowed more efficient transfer of coarser detritus southwards.

3.3 A FRAMEWORK FOR SEDIMENT PROVENANCE STUDIES

Evidence has been presented establishing a probable transpressional setting for the development of early Lower ORS basins. The Crawton Basin received compositionally distinct detritus from either margin. The provenance of this detritus is critically important in that it allows constraints to be placed on both the nature of the crustal transition which the basin must overlie, and the affinity of the two source terranes which lay adjacent to the basin during the late Silurian and Lowermost Devonian.

Granite clasts abound in conglomerates of both northerly and southerly derivation allowing the provenance to be considered in some detail (Chapters 5 and 6). Granite clasts are of particular significance in that rigorous geochemical and geochronological studies can establish both the character and temporal pattern of magmatism within the source. In addition many granites can be shown to be chemically and isotopically sensitive to bulk crustal character. Clasts can therefore be used to image the continental crust through which the source plutons have been emplaced. This is particularly relevant in clastic sequences which overlie major crustal breaks or which are far removed from their source. Granite clasts derived from sources within juxtaposed terranes will show contrasting crustal signatures reflecting emplacement or sourcing within different crustal segments.

Granites show a wide range of variety in terms of their appearance, constituent mineralogy and chemistry. This variety makes them attractive for uniquely discriminating the provenance of conglomerates. Granite clasts can be linked with potential sources on a number of levels. Matching clasts with individual plutons is only realistic in late orogenic or intra-plate settings where granites intrude cratonised host-rocks. Stabilisation precludes further regional uplift which might otherwise either remove the <u>in situ</u> pluton, or at least reveal deeper levels within the intrusion which are less easily correlated with clasts derived from fractionated upper levels.

Orogenic belts and continental arcs are major sites of voluminous granitic magmatism. The association of these environments with thickened continental crust implies that many granite plutons are unlikely to survive *in situ* the high rates of uplift attendant on return of the crust to normal thickness. Adjacent sedimentary basins may retain in their fill the only record of these materials. Obviously matching of clasts with *in situ* plutons is unlikely to be successful with sequences of this type. Broader concepts of source discrimination are required. Fortunately, granites show temporal and spatial coherence in terms of their chemistry and isotope signatures such that wider grouping is possible. The level of grouping varies from local consanguinous units to large scale chemical provinces reflecting regional uniformity in source materials and/or crustal assimilant. Thus super-units (Cobbing and Pitcher 1972) and segments (Atherton 1979) have been recognised in the Peruvian Coastal Batholith, magma sequences (Bateman and Dodge 1970) in the Sierra Nevada, suites (White and Chappell 1983) in the Lachlan Fold Belt, and chemical provinces along the length of the Caledonian-Appalachian Belt (Halliday and Stephens 1984). This concept of wider coherent grouping of granite magmas associated with specific crustal segments is particularly useful in assigning a provenance to granite bearing conglomerates.

At its broadest level, a fundamental coherence amongst granite magmas according to geotectonic environment is emerging. Granite clasts can therefore potentially yield important evidence for both the tectonic setting of the source terrane and the basin in which the clasts occur. Peacock`s (1931) alkali-lime index has been used to discriminate active and passive margins on the basis of the common association of volcanic arc magmatism and granites of calc-alkaline affinity. Passive margins and within plate settings tend to be associated with alkaline and peralkaline magmas. Petro *et al.* (1979) developed a broader range of major element discriminants for active and passive margins based on an empirical study of Mesozoic and Tertiary granites. Pearce *et al.* (1984) subdivide granites into four groups using major element discrimination diagrams, again empirically derived.

While it may be possible to demonstrate a link between granite clasts and crustal segments showing similar temporal and chemical magmatic histories in some cases the granites preserved as clasts may be a unique sample of crustal material not conserved during orogenic contraction. Given the likelihood of large vertical and lateral displacements during plate convergence it is to be expected that cratonised orogens retain an incomplete record of the orogenic process. Conglomerates may go some way towards redressing this preservational bias in allowing the presence of previously unrecognised geotectonic elements to be established. By way of an example, Longman et al. (1979) and Bluck (1983) have demonstrated the existence of an Ordovician arc terrane within the Midland Valley on the basis of isotopic and geochemical constraints imposed by granitic detritus in a conglomeratic fore-arc sequence south of Girvan.

CHAPTER FOUR

CHEMISTRY AND GEOCHRONOLOGY OF SOUTHERLY DERIVED GRANITE CLASTS - IMPLICATIONS FOR MIDLAND VALLEY EVOLUTION

4.1 FIELD RELATIONS

Granite clasts are an important component in southerly derived conglomerates. They are especially enriched in the coarser size fractions, and their abundance increases towards the top of the Crawton Group (Fig. 4.1). Three important granite types are easily distinguished in the field. G1 is a strongly foliated biotite tonalite (Plate 4.1); G2 an equigranular biotite granodiorite and G3 a biotite - hornblende granodiorite. In addition, a rare fourth granite type, a medium to fine-grained biotite-garnet bearing granite is present. G2 and G3 are grey in colour when fresh, whilst G1 can be divided into a coarser white or grey facies and a finer, generally more biotite rich pink or red type.

G3 is the commonest of the granite clasts (Fig. 4.1b) and must dominate the granite bedrock in the source. G2 is marginally more abundant than G1. Both G2 and G3 occur as exceedingly large clasts, often greater than 1.0m in diameter. G1 clasts are rarely >50cm in diameter, probably reflecting the role of their strong foliation in reducing the size of the blocks initially weathered from bedrock in the source.

All the granite clasts are rounded to well-rounded (Pettijohn 1973) and have high sphericities. The accompanying lithic arenite and metagreywacke clasts are however very angular to angular and obviously are of first cycle derivation. This is clearly an instance of textural disequilibrium resulting from the poor sensitivity of granite clasts to rounding during transport. Angular granite blocks are only rarely produced by normal weathering processes , and the introduction of rounded to well-rounded granite clasts to transporting systems from weathering zones in the source appears to be the norm. Rounding of granite clasts is therefore a poor indication of proximity to source. As the granites can be shown to intrude the greywackes (4.6.1) they too are of first cycle derivation. As many Lower ORS red bed sequences are demonstrably of second- or multi-cyclic provenance this is of some significance. The study of first-cycle sediment

FIGURE 4.1 Compositional variation in granite clasts of southerly provenance. A:relative abundance of granite clasts by size and position in sequence. Log illustrates a vertical sequence through conglomerates and sandstones comprising the upper part of the Crawton Group exposed in coastal outcrops east and northeast of Inverbervie. Numbers refer to lithosome type. Granite clasts become more abundant upwards. B:Phi diagrams illustrating relative abundance of four granite types in southerly and easterly derived Lithosome 2 conglomerates at Kings Step (X on section). Granite types are G1: foliated biotite tonalites, G2: equigranular biotite granodiorite, G3: equigranular hornblende-biotite granodiorite and G4: equigranular biotite granite.

A. CLAST COMPOSITIONS

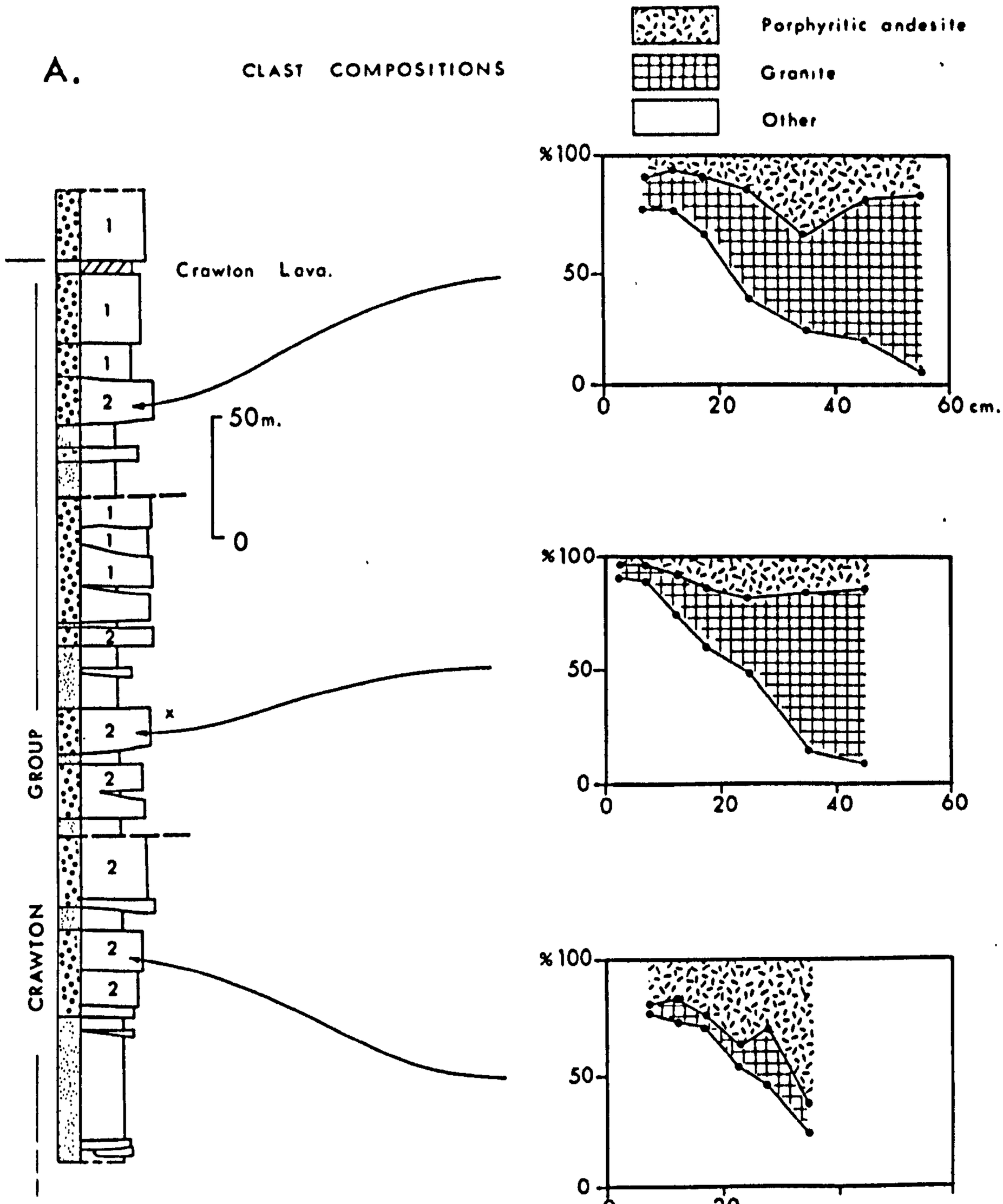

B.

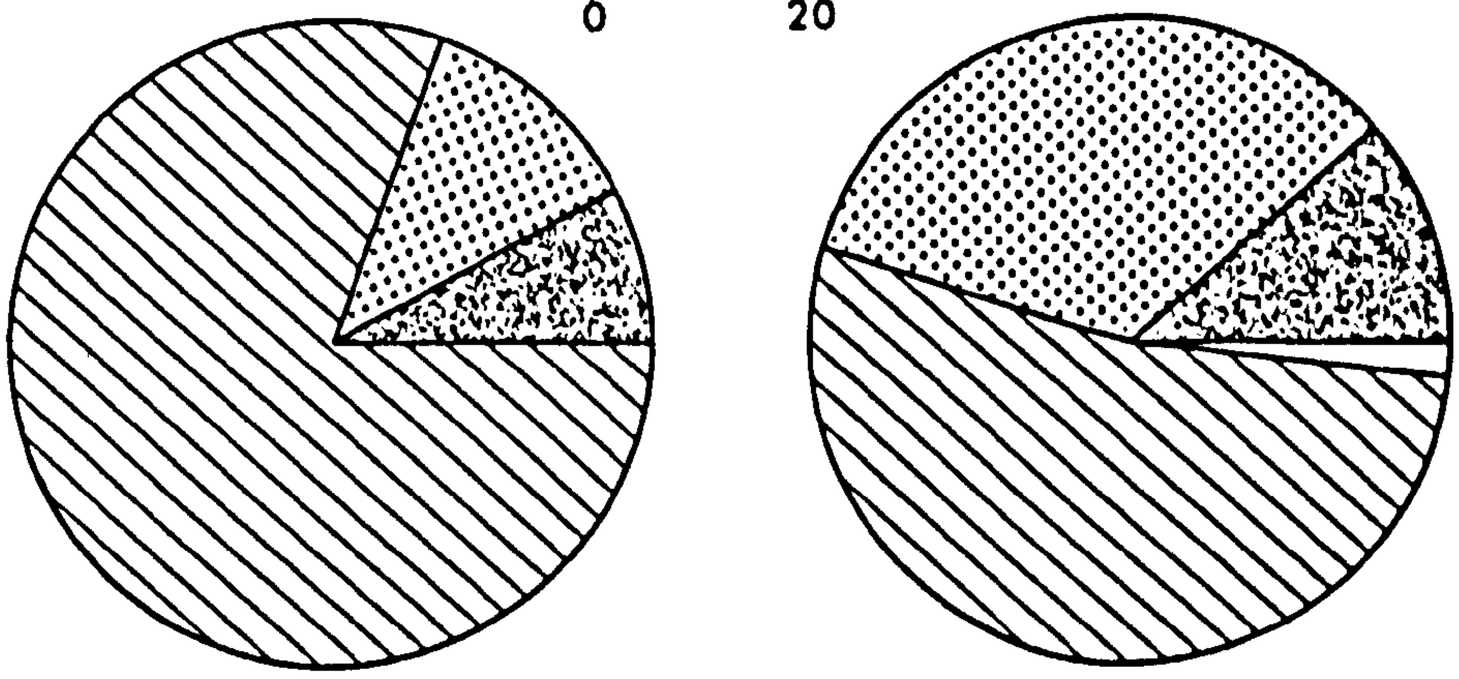

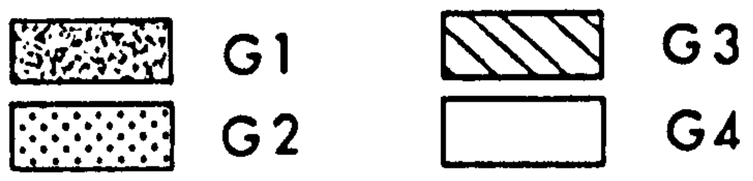

provenance allows greater confidence in the interpretation of the relationship of bedrock-types in the source drainage area. In addition, first-cycle deposits are likely to be less biased towards more resistant clast lithologies, and therefore the range of clast types will most closely approximate the variety of lithologies in the source.

Both G1 and G3 show a rather narrow range of textures in hand specimen. G2 is texturally quite variable ranging from coarse- to medium-grained, and occasionally cut by thin pegmatitic veins. The more evolved G2 samples tend to be the finer grained. All granite clasts are equigranular in hand specimen with no obvious phenocryst phases. This is in notable contrast to the northerly derived granite clasts in which large K-feldspar phenocrysts characterise several suites.

Enclaves are particularly common in clasts of G3 and to a lesser extent G2. These include angular metasedimentary xenoliths, often banded and rich in biotite, and also rounded hornblende-rich autoliths or cognate xenoliths, presumably derived from residues after partial melting. G1 contains rare sheared basic clots which are likely also to be restite. It is possible that some of the autoliths represent xenoliths of lava as the indications are that the granites, G3 in particular, were emplaced at very high level. Xenoliths of metasedimentary origin can be quite large (>15cm). Plate 4.2 shows a clast which preserves the contact relationships between a fine-grained biotite granite and a biotite hornfels. Xenoliths can be seen spalling away from the granite - hornfels contact. The granite adjacent to the contact has a chemistry compatible with an evolved high-K suite of G3 type. The fact that it is more evolved than the other clasts of G3 type and is free of amphibole suggests the clast does not represent the marginal relationships between G3 and its hornfels country rocks. Rather the biotite hornfels may represent a large stoped block which has fallen into a more evolved part of the magma.

Porphyritic volcanic clasts (VA) also occur abundantly in the conglomerates. They can be shown to have an independent

PLATE 4.1 Foliated biotite tonalite clast of G1 type in southeasterly derived Lithosome 2 conglomerate, Kings Step. Lens cap 5cm.

PLATE 4.2 Contact between equigranular biotite granite and hornfelsed sediment. Clast in southerly derived conglomerates at Gourdon. Lens cap 5cm.

dispersal to the basin of deposition largely reflecting contemporaneous episodic vulcanism (Chapter 2). Texturally they resemble the granites of G3 type, particularly in those clasts which are rich in phenocrysts. Phenocrysts include euhedral hornblende and biotite, and large 5-8mm plagioclases. These are either randomly orientated or show flow alignment and banding. Some clasts preserved rubbly contacts and welded breccias. The clasts are dominantly acid andesites and dacites and are purple or red in colour indicating extensive hydrothermal alteration. Rounding is variable from subangular to rounded. The larger clasts tend to show the highest rounding and invariably have high sphericities. Grain size distributions are strictly bimodal with modes in the cobble and coarse sand fractions, with the latter often dominant and comprising largely detrital feldspar grains. The cobble fraction is typically very poorly sorted with outsized clasts in the coarse tail population often exceeding 1.5m maximum diameter.

4.2 SAMPLING

Sixty three granite clasts were sampled from southerly derived conglomerates of the Crawton Group exposed in coastal outcrops between Gourdon and Kinneff. Sample localities included coarse conglomerates exposed north and south of Whitehouse and flat foreshore exposures east of Gourdon and northeast of the confluence of the Bervie Water with the sea. Cliff exposures east of Bervie Brow at Kings Step and Yellow Ark were extensively sampled. Good cliff exposures close to Kinneff also provided samples. A full list of sample numbers, clast types, localities and grid references is given in Appendix 1. Sample localities are shown in Figure 4.2.

The sixty three granite clasts included eleven clasts of G1, twenty clasts of G2 and thirty one clasts of G3. A single clast of G4 was sampled. Every effort was made to sample the full range of lithologies present although some of the more basic clasts are probably under-represented on account of the difficulty of finding unaltered samples. Whilst xenolithic clasts were usually avoided, some clasts containing xenoliths were also sampled (see Appendix 1) to examine the effects of bulk contamination on the magma chemistry.

In addition, a range of porphyritic acid andesite and dacite clasts were collected from the localities mentioned above. Twenty three clasts in all were sampled representing the freshest material available at outcrop. The andesites were amongst the most seriously weathered clast types and the sample is therefore possibly quite strongly biased. The principal objective in sampling the volcanic clasts was to explore possible links between these clasts and the granite clasts to which they bear a superficial resemblance.

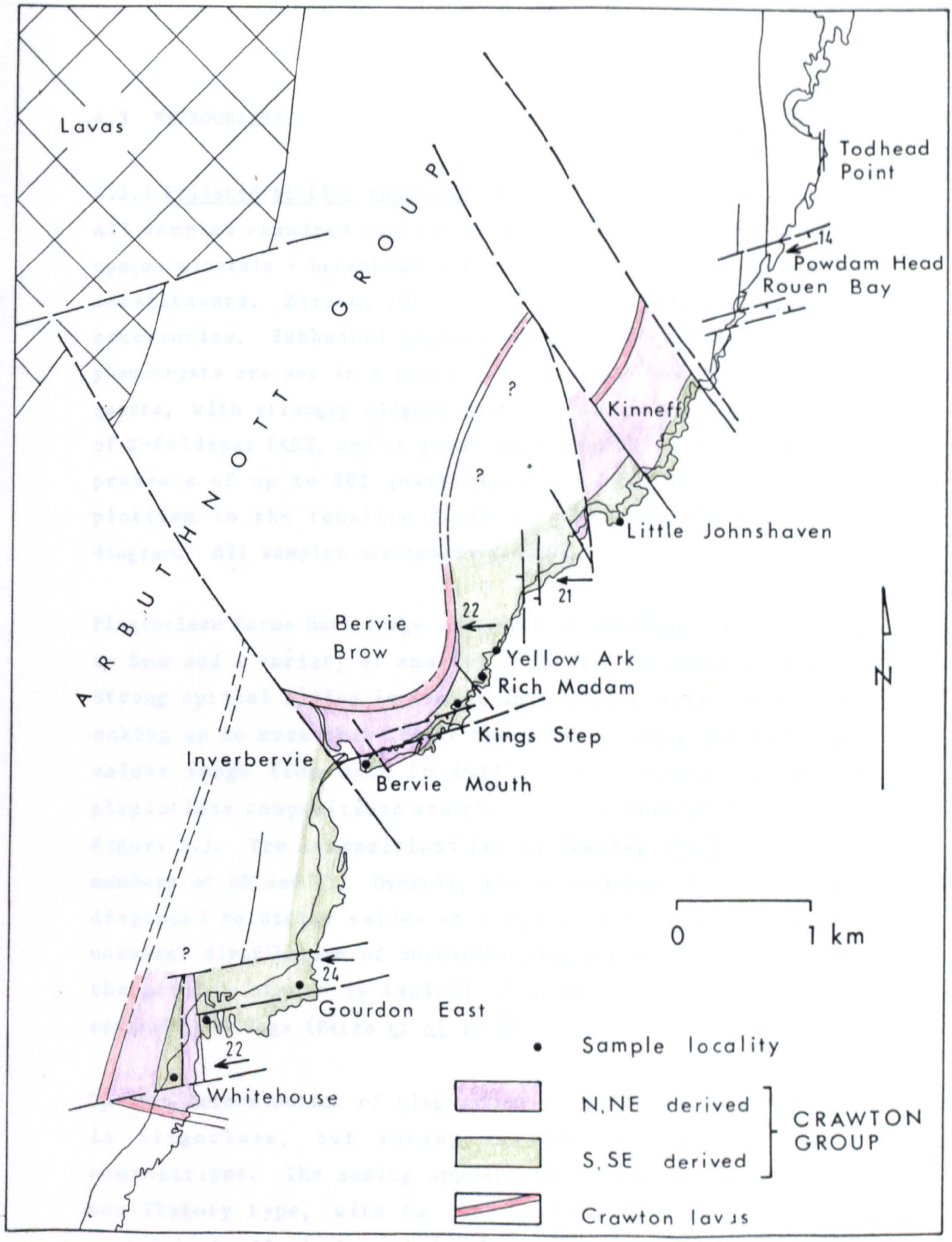

Figure 4.2 Sampling localities for southerly derived granite clasts

4.3 PETROGRAPHY

4.3.1 Foliated biotite tonalites (G1)

All samples examined contain plagioclase + quartz + biotite + opaque minerals + hornblende ± K-feldspar ± chlorite as the major constituents. Zircon, rutile, epidote and garnet are common accessories. Subhedral to euhedral optically zoned plagioclase phenocrysts are set in a matrix of granulated and recrystallised quartz, with strongly aligned biotite clots. The low abundance of K-feldspar (<5%, and in some cases totally lacking), and the presence of up to 30% quartz result in the G1 type samples plotting in the tonalite field of Streickesen's (1976) QAP diagram. All samples are coarse-grained.

Plagioclase forms both large subhedral to euhedral phenocrysts up to 8mm and a variety of smaller subhedral to anhedral grains. Strong optical zoning is almost ubiquitous, with cores often making up no more than 10% of the total volume. Normative An values range from An26 to An32 for G1 clasts. Normative plagioclase compositions are plotted in a histogram format in Figure 4.3. The compositions for G1 overlap the An rich end-members of G2 and G3. Overall, the An contents of G1 clasts are displaced to higher values at comparable silica levels. The unimodal distribution of normative plagioclase compositions for the granite clasts is typical of granites in compressional tectonic settings (Petro et al. 1979).

Optical determination of plagioclase compositions suggests much is oligoclase, but zoning results in highly variable compositions. The zoning appears to be mostly of normal or oscillatory type, with Ca rich cores weakly to moderately sericitised. Plagioclase obviously did not remain in equilibrium during crystallisation. Lamellar twinning is well developed, particularly in the large phenocrysts where it is commonly restricted to the cores. The large elongate crystals show a weak to moderate grain alignment fabric parallel to the biotite foliation. Some phenocrysts have curved lamellar twin planes indicating ductile deformation. On the whole, however, the

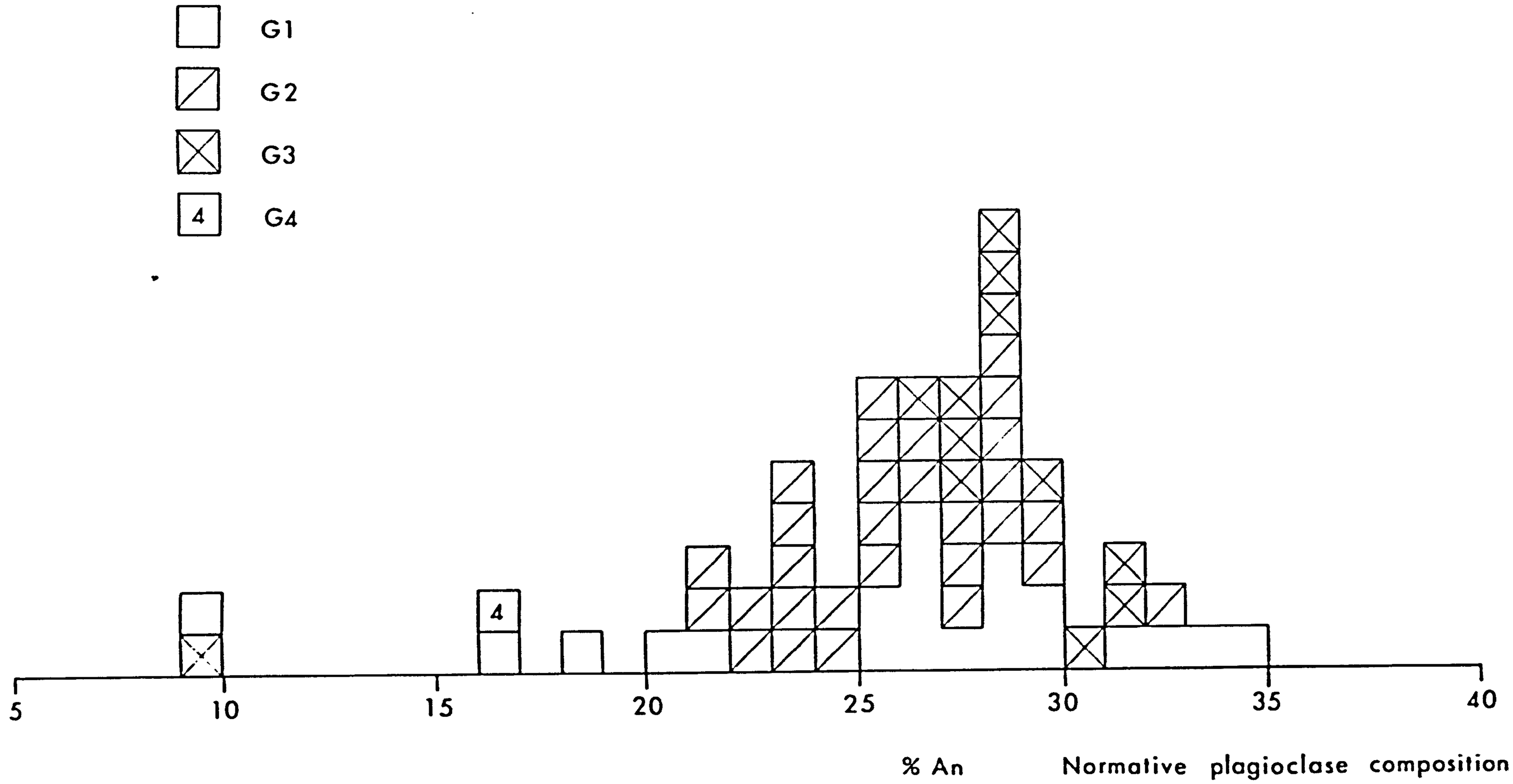

FIGURE 4.3 Histogram of normative (CIPW) feldspar compositions for southerly-derived granite clasts.

plagioclase phenocrysts have escaped the high strain shown by the recrystallised quartz and deformed biotites. Inclusions within plagioclase are rare but include zircon, apatite and corroded biotite. Myrmekitic intergrowths of plagioclase and quartz occur but are also rare.

K-feldspar is absent in several samples. In others it occurs in proportions less than 5%, as equant grains of microcline and anhedral orthoclase, sometimes mantling plagioclase.

Quartz occurs up to 30% as irregular recrystallised masses of variable grain size. Grain boundaries are typically sutured and the morphology varies from fine granulated masses surrounding plagioclase phenocrysts to coarse mosaics. Oblique extinction is common.

The mafic component is dominated by biotite with minor amounts of relict amphibole, together making up 10-15% of the total. The biotites are olive-green to green-brown in colour and occur both as large corroded masses up to 3mm and finer grained felted aggregates occurring in discontinuous crenulate lenses up to 15mm long (Plate 4.3). The net effect is to impart a strong biotite foliation in hand specimen. Biotites within the crenulate lenses are strongly deformed and partially recrystallised. Pale green euhedral amphibole occurs rarely and is more often replaced by alteration products, chiefly carbonate, opaque minerals and microcrystalline quartz. The euhedral outlines are commonly well preserved and attest to the presence of amphibole prior to alteration. The relict amphiboles commonly occur intergrown with biotite within the mafic lenses and are also deformed.

Chlorite occurs as a minor alteration product partially replacing biotite. Other minor or accessory phases include zircon, which occurs as both euhedral and anhedral pale yellow grains, apatite, epidote and rutile. Garnet also occurs as inclusion free subhedral grains.

4.3.2 Equigranular biotite granodiorite : G2

Clasts of G2 granite show the widest range of compositional and textural variation. G2 clasts are easily distinguished from clasts of G1 in having equigranular textures, and lacking grain alignment fabrics (Plate 4.4). K-feldspar is also more abundant, reaching 15%, in the more evolved end-members of the suite (e.g. 4238). The bulk of the samples plot in the granodiorite field of Streickeisen`s (1976) QAP diagram. The lack of granophyric textures, and the dominance of biotite over hornblende in the mafic component distinguish clasts of G2 from those of G3 type.

All samples contain varying proportions of plagioclase + quartz + K-feldspar + biotite + hornblende + opaque minerals ± chlorite. Accessories include zircon and apatite. Textures are dominantly granular and non-porphyritic. Grain size varies from coarse in the less evolved end-members to medium grained in the evolved end-members of the suite.

Plagioclase forms subhedral to euhedral prisms up to 6mm in the coarser grained lithologies. These are randomly orientated. Whilst optical zoning is present in many grains, zoning of plagioclase is not as well developed in G2 clasts as it is in clasts of G1. Normative plagioclase compositions (Fig.4.3) show a wide range, with lower An contents from more evolved rock types. Optical determinations indicate the bulk of the plagioclase is of oligoclase composition, but more Ca-rich compositions may be present in zoned cores. These tend to be more strongly sericitised. Inclusions within plagioclase include rare quartz and zircon grains.

K-feldspar occurs both as 1-2mm orthoclase grains and more commonly as irregular interstitial masses, surrounding plagioclase. It is most abundant in more evolved lithologies. Quartz also occurs as large irregular interstitial masses and occasionally as discreet grains. It typically makes up 20-25% of the total by volume.

The mafic component is characteristically strongly

glomeroporphyritic with aggregates of biotite and less abundant hornblende. Biotites are corroded irregular grains, light to dark brown in colour, and of irregular grain size. They can be up to 4mm. The euhedral habit common in clasts of G3 type is significantly absent. Inclusions within biotite include corroded quartz, plagioclase and amphibole grains, and opaques and accessory zircon. Biotites are generally free of chloritisation, but some minor chlorite replacement of biotite is observed. Amphibole makes up to approximately 20% of the mafic component. It occurs as euhedral prisms in association with biotite. Corroded biotite grains core some of the amphibole grains. The amphibole is variably preserved. In fresh samples it can be seen to be a pale green hornblende. In slightly altered samples, the hornblende is often replaced by alteration products but retains its distinctive prismatic habit. Significantly, there is no evidence for hornblende replacing pyroxene.

4.3.3 Equigranular hornblende-biotite granodiorite: G3

Clasts of G3 type are distinguished from the biotite granodiorites (G2) by the greater abundance of amphibole and by the euhedral habit of both the amphibole and biotite. K-feldspar also forms an important interstitial phase, often occurring as granophyric intergrowths with quartz. Texturally, the G3 clasts are relatively homogeneous, showing little variation in grain size.

The mineral assemblage is plagioclase + quartz + K-feldspar + hornblende + biotite + opaque phases. Accessories include abundant apatite and less common rounded zircons. Textures are granular and non-porphyritic, and generally holocrystalline (see below).

Plagioclase forms subhedral to euhedral prisms up to 5mm. These are randomly orientated. Many are strongly zoned and weakly to moderately sericitised. Normative plagioclase compositions range from An_{26} to An_{32} (Figure 4.3). Both albite-law and pericline twinning are well developed. Inclusions within plagioclase are rare but include occasional corroded biotite grains. K-feldspar forms an important interstitial phase accounting for up to 15% of the total volume. It occurs typically as orthoclase forming granophyric intergrowths with quartz. Plagioclase and mafic crystals often float in a matrix of granophyre (Plate 4.6).

Mafic crystals account for c. 25% of the total with amphibole and biotite having comparable abundances. Both biotite and amphibole have characteristic euhedral forms and tend to occurr as glomeroporphyritic aggregates. The amphibole is a pale to olive green pleochroic hornblende, occurring as crystals of varying size but reaching a maximum of 3mm. The larger grains often have relict cores of corroded biotite. Biotite crystals reach 3-4mm and have a randomly orientated prismatic habit. They exhibit a straw to rust brown pleochroism and in some instances show partial alteration to opaque phases.

Quartz occurs as both irregular interstitial masses and as intergrowths with K-feldspar. The quartz has none of the strain

features seen in quartz in clasts of G1 type. More rarely, prismatic quartz crystals are preserved growing into irregular interstitial spaces filled with either microcrystalline quartz or what resembles a devitrified glass (Plates 4.7, 4.8). This suggests parts of the plutons from which the clasts were derived were very rapidly quenched.

4.3.4 Biotite garnet granite: G4

The single clast of G4 sampled (4279) is an equigranular grey biotite granite characterised by the presence of garnet as an important phase (Plate 4.10). G4 is finer grained than the bulk of the accompanying southerly derived granite clasts and is both unfoliated and unstrained. The mineral assemblage includes plagioclase + quartz + perthite + biotite + garnet with accessory opaques, apatite and zircon.

Plagioclase forms subhedral to euhedral fresh prismatic crystals which are randomly orientated. Typically these are strongly zoned with weak sericitisation restricted to more calcic cores. Twinned cores are frequently rimmed by thin irregular untwinned rims, or more rarely, by myrmekite. K-feldspar occurs as discreet generally equant grains of coarse perthite which average 1mm in size. Quartz is randomly distributed as irregular grains with an interstitial form, and straight extinction. Biotite is the sole mafic constituent (making up 10% of the total) and is characterised by the presence of dark radiation damage haloes surrounding small inclusions. The biotites occur as anhedral grains with ragged outlines and no preferred orientation. They show straw-brown to olive-brown pleochroism. The garnets occur as scattered isolate subhedral grains, many of which are corroded, and are generally less than 0.5mm. Many occur in association with biotite.

4.3.5 Porphyritic andesites and dacites: Vs

Volcanic clasts which accompany the southerly derived granites are notable in that they are dominated by a single volcanic lithology, a distinctive strongly porphyritic lava type. Phenocrysts typically make up between 10 and 40% of the total and include relict euhedral amphibole, variable altered biotite,

plagioclase, and less commonly, resorbed quartz. The phenocrysts are generally less than 5mm and are either randomly distributed or show a weak flow foliation (Plate 4.11). They are set in a fine grained oxidised matrix. Texturally, particularly in those clasts with high phenocryst-matrix contents, the volcanic clasts begin to resemble the hornblende-biotite granodiorite clasts (G3). Unfortunately, the clasts show evidence for substantial low temperature alteration with mafic phenocryst phases variably replaced by carbonate and haematite.

PLATE 4.3 Deformed biotites and granulated grain boundaries in G1 foliated tonalite clast (4278). Magnification x30. Cross polarised light.

PLATE 4.4 Equigranular texture and random orientation of anhedral biotites in G2 biotite granodiorite (4282). Magnification x30. Cross polarised light.

PLATE 4.5 Optically zoned plagioclase and deformed biotites in G1 foliated tonalite (4385). Magnification x30. Cross polarised light.

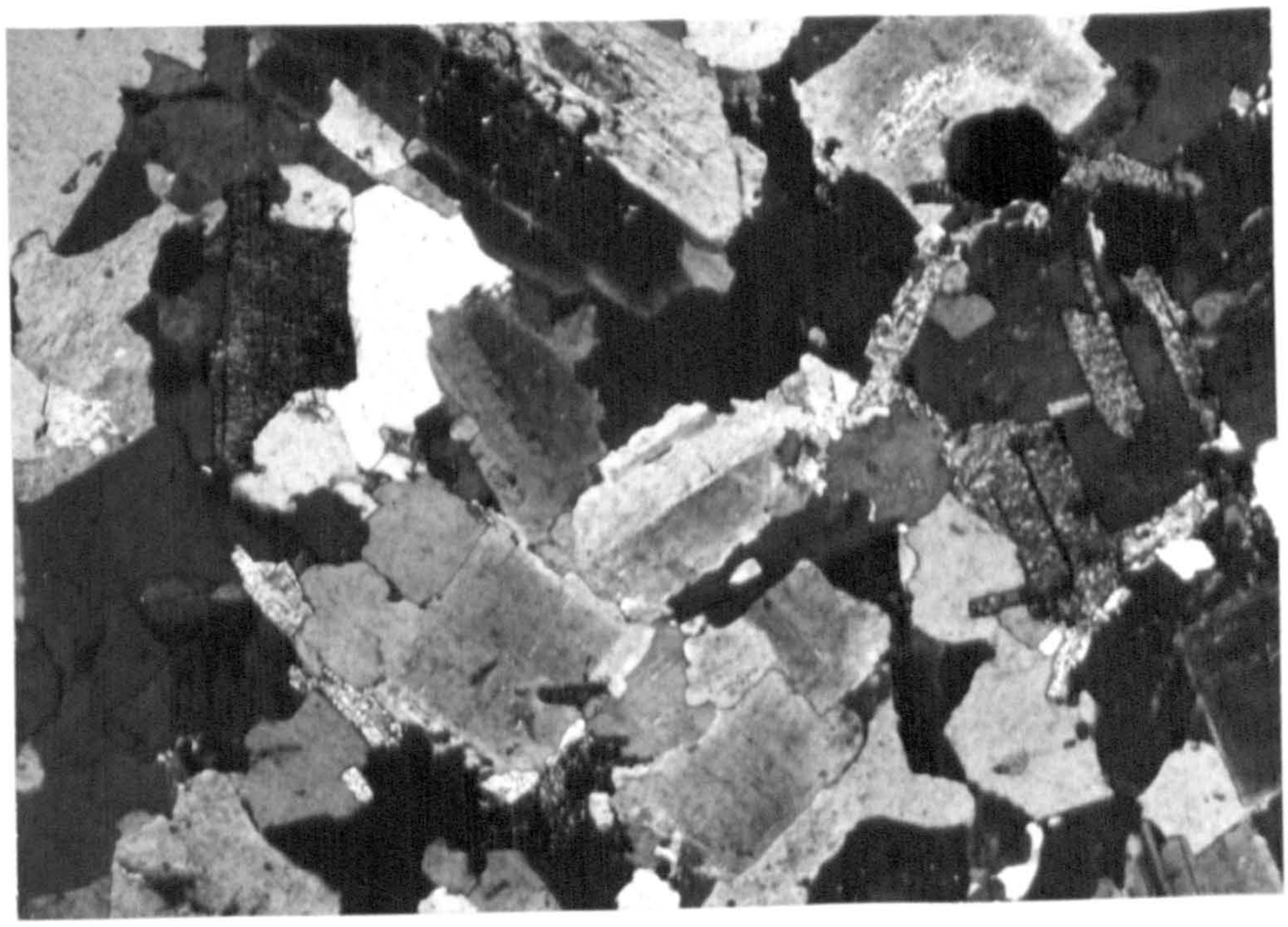

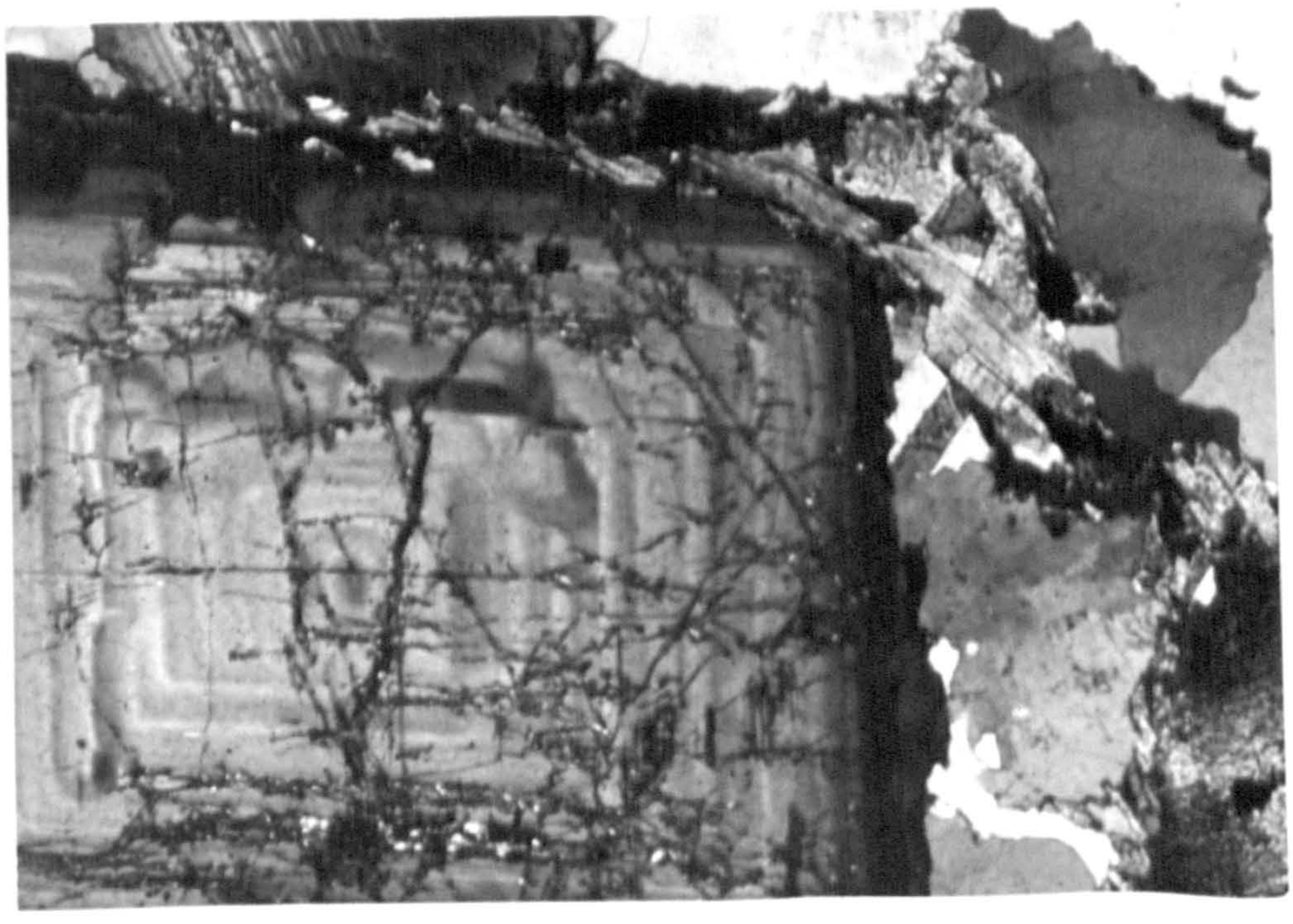

Plate 4.6 Granophyric quartz and K-feldspar enclosing euhedral amphibole and biotite in clast of G3 type granodiorite (4329). Magnification X30. Cross polarised light.

Plate 4.7 Euhedral quartz crystal terminations projecting into interstitial microcrystalline quartz and possible devitrified glass. Clast 4462 (G3). Magnification X75. Plane polarised light.

Plate 4.8 As above with crossed polarised light.

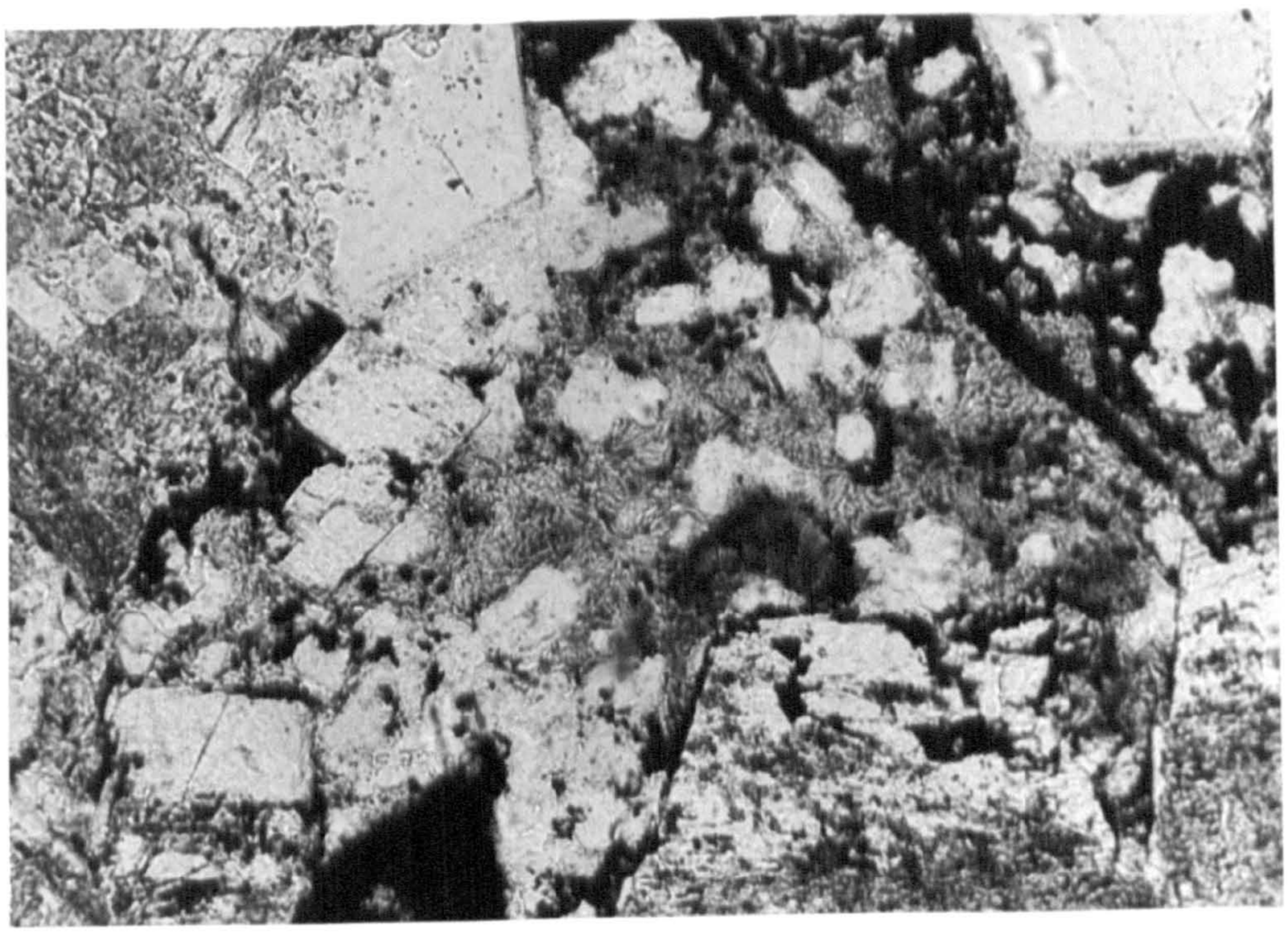

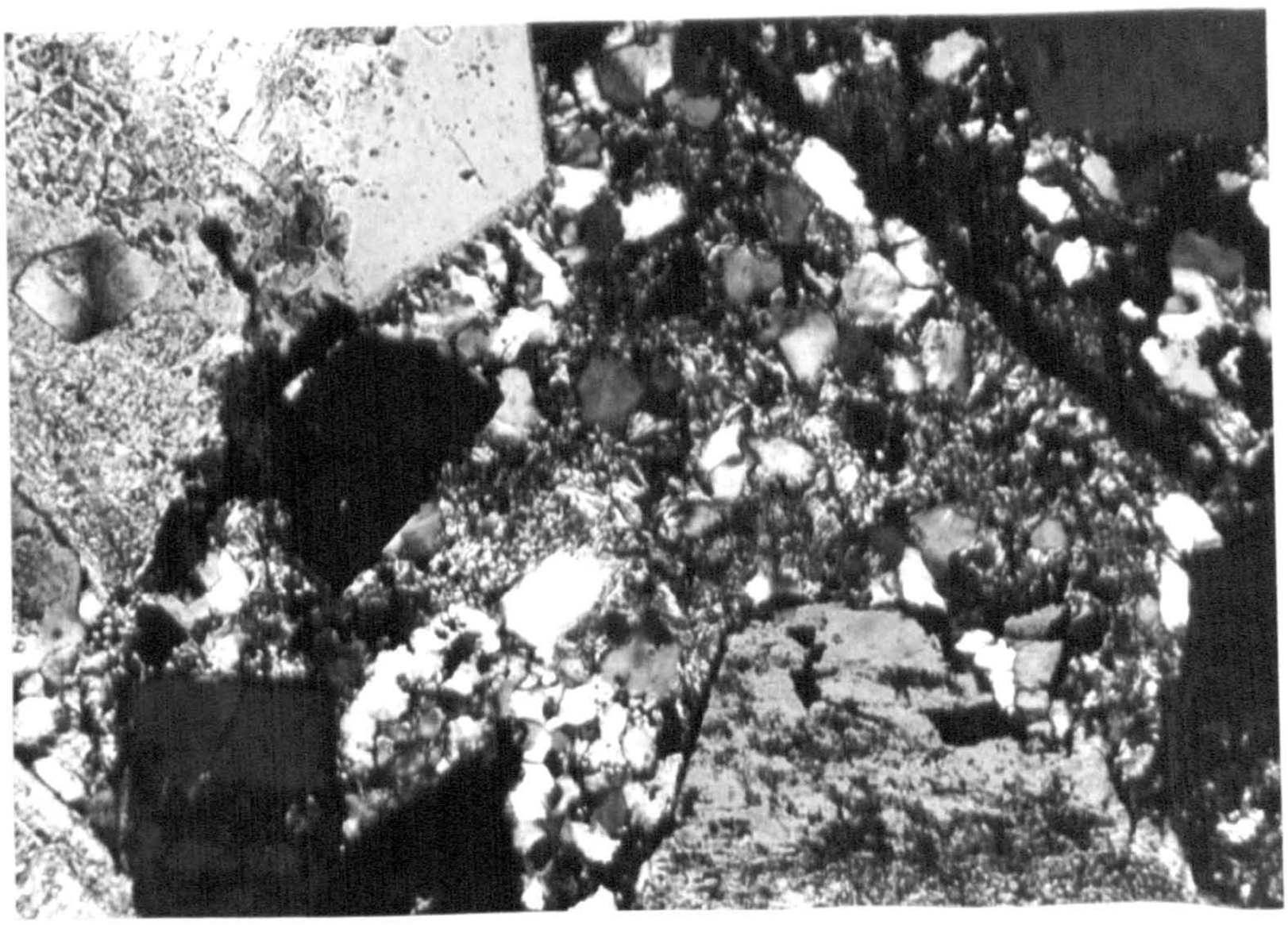

Plate 4.9 Contact between equigranular biotite granite and biotite hornfels. Clast 4335. Magnification X30. Cross polarised light.

Plate 4.10 Biotite-garnet granite of G4 type (clast 4279). Magnification X30. Plane polarised light.

Plate 4.11 Typical southerly derived porphyritic volcanic clast with plagioclase, corroded biotite and euhedral relict amphibole phenocrysts (clast 4231). Magnification X30. Plane polarised light.

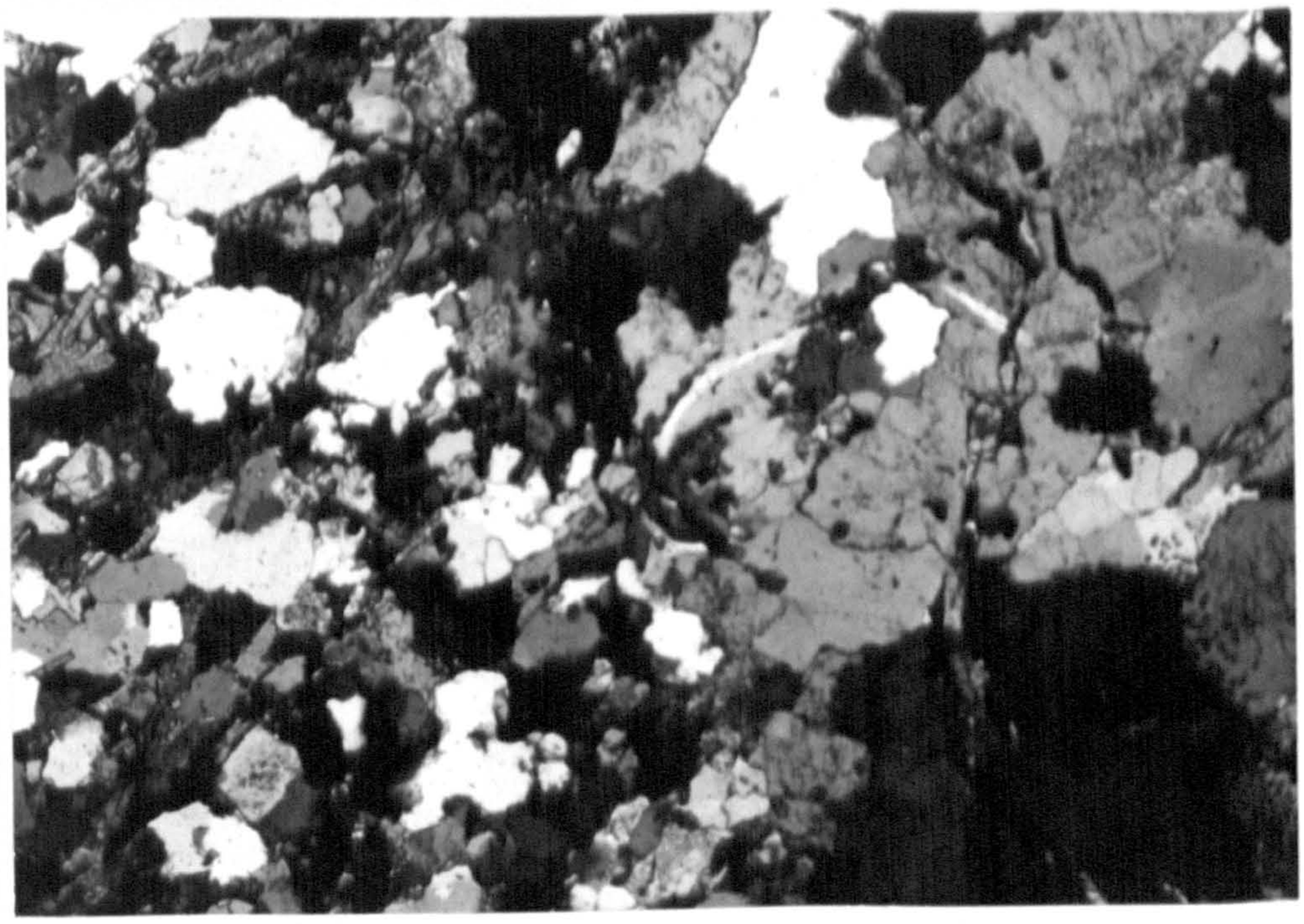

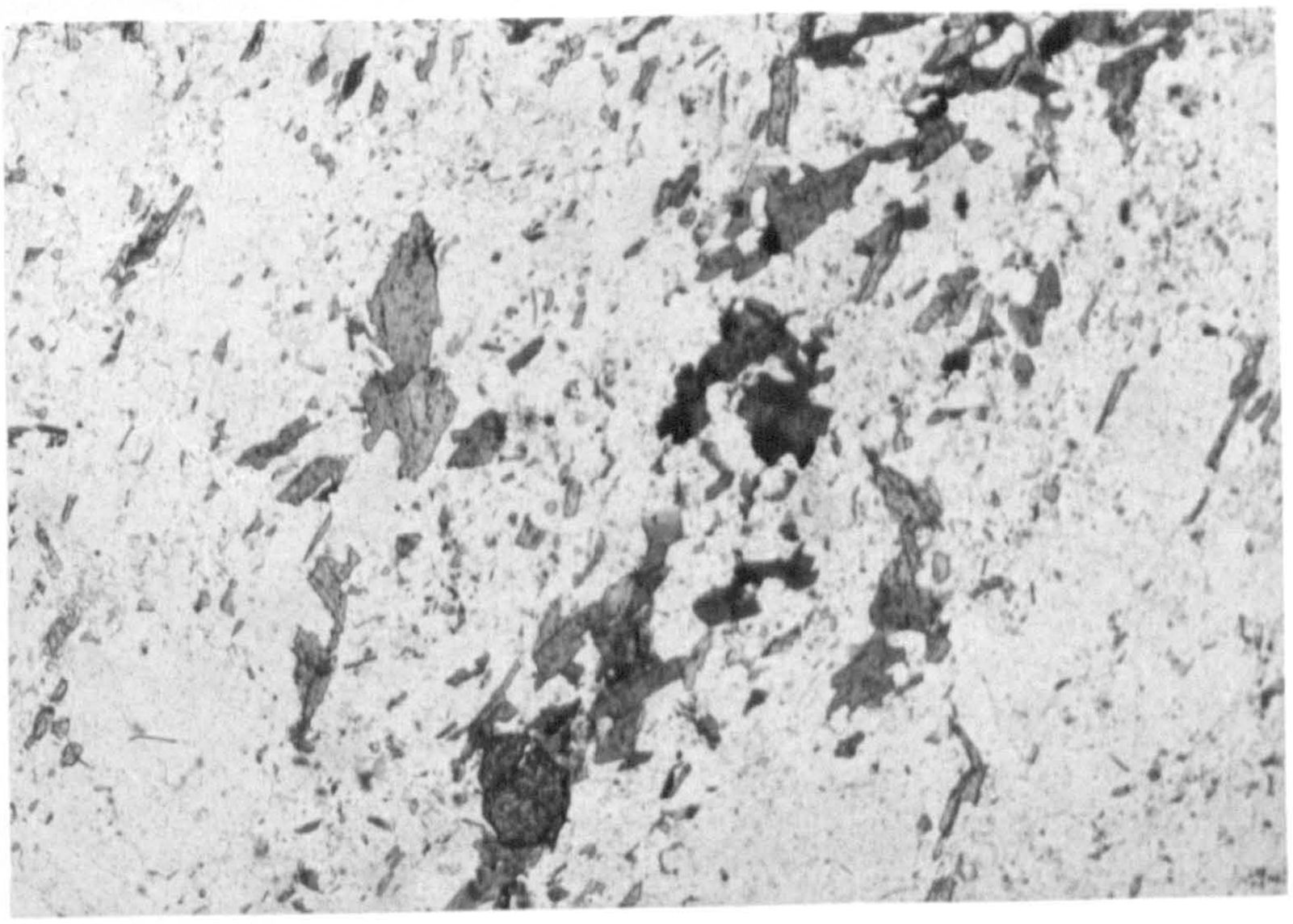

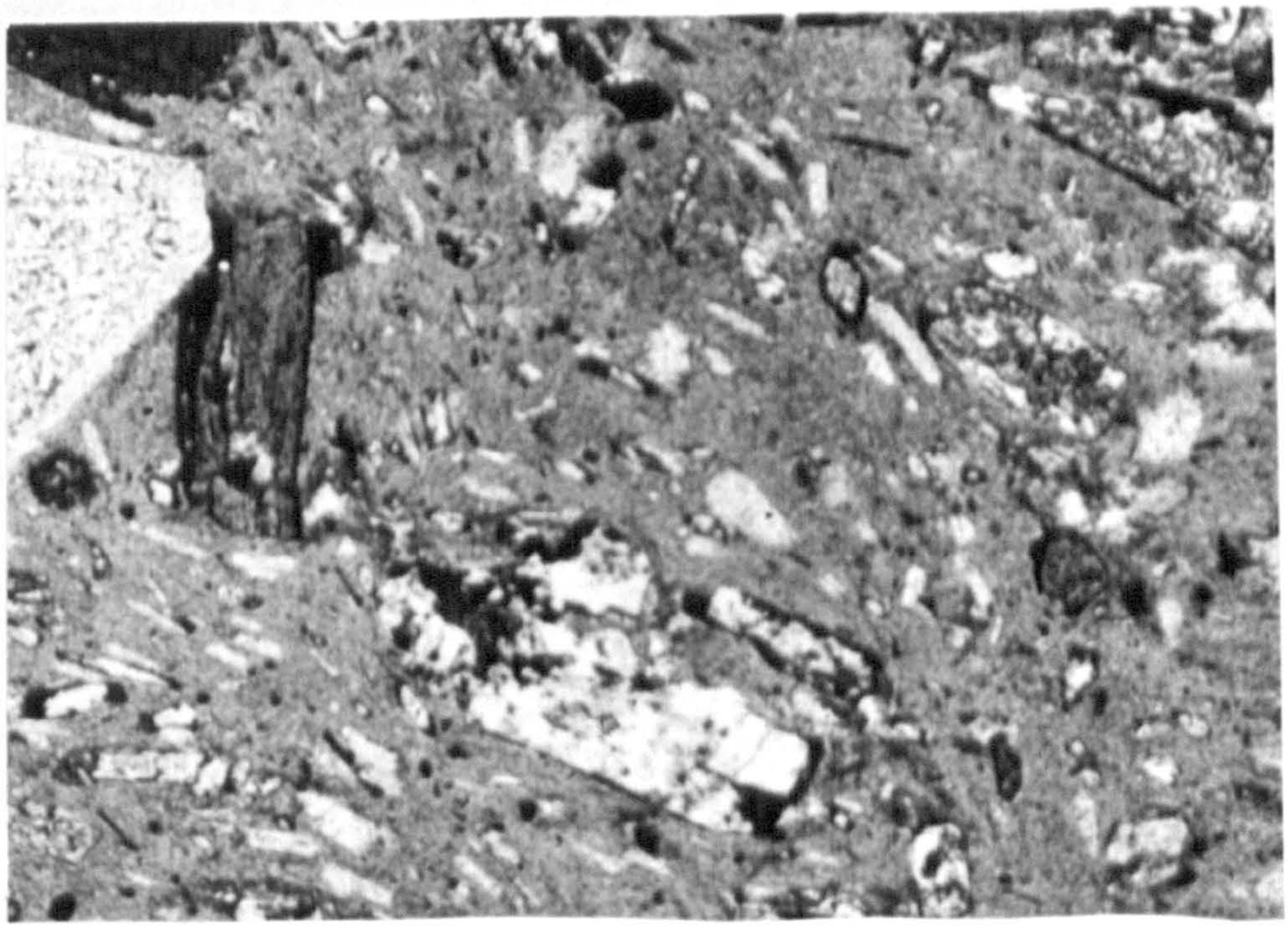

4.4 GRANITE CLAST GEOCHEMISTRY

Sixty three granite clasts of southerly derivation have been analysed for ten major and sixteen trace elements. Full details of sample preparation methods, analytical procedure and precision are given in Appendix 2. Analyses and CIPW norms are presented in Table 4.1.

In the following discussion of the data, emphasis is placed on using the clast geochemistry to rigorously establish the relationship within and between the clast types. It is particularly important to be able to determine whether or not certain groups of clasts are likely to be comagmatic and derived from the same intrusion. In addition, an understanding of the extent and effect of high level fractionation and contamination on the magma chemistry is an important prerequisite to regional comparison. High level fractionation tends to homogenise the chemistry of magmas such that subtle chemical variation inherited from regionally diverse source regions is masked.

4.4.1 Major element geochemistry

4.4.1.1 K_2O and Na_2O

K_2O has been widely used to classify calc-alkaline magmas (Peccerilo and Taylor 1976) and to monitor regional compositional variation in magma chemistry associated with destructive margins. Although less confidence can be placed in K-h relationships than was originally anticipated (Arculus and Johnson 1978) magmas which have passed through thick continental crust do show K-enrichment, and gradients in K_2O at constant SiO_2 transverse to active continental margins have been widely recognised.

K_2O is plotted against SiO_2 in Fig. 4.4. Fields for low, normal and high K calc-alkaline magmas after Peccerilo and Taylor (1976) are superimposed. The three granite suites, G1, G2, and G3 are well discriminated, falling in the low, normal and high K fields respectively. Three samples, 4312, 4313, and 4321 plot to values intermediate between suites G2 and G3 on this and other element-element plots although similar in appearance and petrography to

Table 4.1 Major and trace element geochemistry of southerly derived granite and volcanic clasts.

Key to groups

1: Foliated biotite tonalite

2: Equigranular biotite granodiorite

3: Equigranular hornblende-biotite granodiorite

4: Biotite-garnet granite

Vs: Biotite-hornblende-andesite and dacite

SAMPLE	4237	4278	4286	4366	4369	4371	4382	4383	4392
GROUP	1	1	1	1	1	1	1	1	1
MAJORS									
SiO_2	66.25	67.30	66.45	66.71	65.61	66.45	67.78	68.38	68.39
Al_2O_3	16.26	16.04	16.62	16.84	17.01	17.02	16.16	16.23	16.71
TiO_2	0.38	0.43	0.40	0.40	0.46	0.42	0.40	0.38	0.37
MnO	0.08	0.07	0.04	0.06	0.07	0.06	0.07	0.05	0.07
$(Fe_2O_3)^t$	2.96	3.03	2.89	2.91	3.30	2.99	2.93	2.75	2.77
MgO	1.87	1.83	2.00	2.09	2.53	2.21	2.12	1.81	1.95
CaO	3.88	3.17	3.97	3.83	3.84	3.62	3.32	3.23	3.27
Na_2O	5.18	4.79	4.97	4.83	4.81	4.80	4.87	5.04	4.71
K_2O	1.10	1.42	1.00	1.02	0.94	0.78	1.11	1.20	1.08
P_2O_5	0.11	0.10	0.10	0.10	0.10	0.10	0.10	0.09	0.08
LOI	1.49	1.24	1.30	1.29	1.50	1.68	1.53	1.15	1.25
FeO	nd	nd	nd	nd	1.47	1.65	nd	nd	nd
Fe_2O_3	nd	nd	nd	nd	1.66	1.15	nd	nd	nd
TOTAL	99.56	99.42	99.74	100.08	100.00	99.94	100.39	100.31	100.65
TRACES									
Cr	36	28	43	37	55	44	38	24	43
Co	6	7	4	5	7	8	5	3	7
Ni	13	11	16	13	24	20	16	9	15
Cu	1	3	0	1	1	0	0	0	3
Zn	38	44	38	30	31	32	26	30	26
Ga	18	16	17	19	19	19	17	18	17
Rb	33	34	38	29	40	20	30	57	28
Sr	477	449	493	531	481	479	461	478	468
Y	8	7	8	10	8	11	9	9	6
Zr	95	81	95	100	94	96	96	94	98
Ba	275	309	291	324	213	240	325	293	312
La	3	7	9	12	9	9	9	12	9
Ce	21	29	11	21	21	23	25	23	21
Pb	10	7	8	4	5	9	8	8	5
Th	0	0	0	0	1	4	4	5	0
U	1	0	1	1	3	2	1	2	1
CIPW NORMS									
Or	6.50	8.39	5.91	6.03	5.56	4.61	6.56	7.09	6.38
Ab	43.82	40.52	42.04	40.86	40.69	40.61	41.20	42.64	39.84
An	17.87	15.07	19.04	18.35	18.40	17.31	15.82	15.44	15.70
Q	19.91	23.93	21.70	22.86	21.39	23.94	23.90	24.33	26.38

SAMPLE	4395	4398	4230	4232	4254	4282	4311	4314	4321A
GROUP	1	1	2	2	2	2	2	2	2
MAJORS									
SiO_2	66.98	67.67	65.62	64.56	66.79	64.98	66.20	66.08	64.99
Al_2O_3	16.32	16.34	16.09	15.90	16.41	15.41	16.23	16.01	15.86
TiO_2	0.43	0.40	0.47	0.47	0.52	0.47	0.49	0.46	0.49
MnO	0.06	0.06	0.05	0.08	0.09	0.06	0.07	0.05	0.07
$(Fe_2O_3)^t$	3.09	2.79	3.48	3.50	4.02	3.37	3.69	3.25	3.75
MgO	2.06	1.94	1.85	1.92	2.21	1.73	2.17	2.07	1.77
CaO	3.38	3.37	3.89	4.62	2.46	4.33	3.90	3.29	4.70
Na_2O	4.68	4.91	5.08	4.57	3.79	4.33	4.90	4.71	4.77
K_2O	1.18	1.12	1.78	1.63	2.00	1.77	1.65	1.74	1.81
P_2O_5	0.10	0.09	0.13	0.12	0.10	0.12	0.12	0.12	0.13
LOI	1.64	1.62	1.53	2.68	1.36	2.41	1.54	1.74	2.33
FeO	1.28	0.95	0.90	nd	nd	nd	nd	0.77	0.70
Fe_2O_3	1.67	1.73	2.48	nd	nd	nd	nd	2.39	2.97
TOTAL	99.78	100.20	99.87	100.05	99.75	98.98	100.96	99.43	100.59
TRACES									
Cr	39	70	37	36	48	52	59	53	77
Co	8	3	7	6	4	6	4	7	3
Ni	13	16	12	12	18	17	18	15	15
Cu	3	5	5	4	2	3	5	42	3
Zn	37	31	43	43	33	38	43	43	43
Ga	20	19	16	15	21	17	15	19	17
Rb	32	42	96	69	63	91	94	73	80
Sr	478	474	497	403	366	414	446	449	451
Y	9	7	12	13	14	11	11	8	11
Zr	101	92	105	111	135	99	112	122	114
Ba	322	328	344	340	373	346	350	359	349
La	12	8	17	18	18	16	16	15	10
Ce	22	17	32	32	38	34	28	27	33
Pb	9	8	8	14	10	11	9	11	12
Th	4	5	4	6	4	3	0	4	2
U	2	1	2	2	1	1	0	1	2
CIPW NORMS									
Or	6.97	6.62	10.52	9.63	11.82	10.46	9.75	10.28	10.70
Ab	39.59	41.54	42.97	38.66	32.06	36.63	41.45	39.84	40.35
An	16.12	16.13	15.84	18.06	11.55	17.39	17.42	15.54	16.52
Q	24.35	24.19	18.11	19.20	27.66	21.28	19.33	21.32	18.19

SAMPLE	4328	4363	4373	4374	4375	4376	4377	4378	4384
GROUP	2	2	2	2	2	2	2	2	2
MAJORS									
SiO_2	67.12	70.05	70.43	66.66	66.95	67.54	68.57	67.07	70.32
Al_2O_3	16.03	15.79	16.01	15.48	15.80	15.96	15.71	15.78	15.68
TiO_2	0.44	0.30	0.26	0.44	0.47	0.45	0.43	0.47	0.28
MnO	0.06	0.05	0.04	0.06	0.05	0.06	0.06	0.07	0.03
$(Fe_2O_3)^t$	3.41	2.10	1.56	3.20	3.45	3.29	3.01	3.45	1.88
MgO	1.93	1.47	1.11	1.93	2.10	1.92	2.05	1.95	1.30
CaO	2.48	2.20	1.74	4.04	3.21	2.76	2.71	2.90	2.04
Na_2O	4.90	4.69	4.81	4.27	4.55	4.34	4.41	4.52	5.07
K_2O	2.16	2.02	2.33	1.63	1.92	1.94	2.10	1.98	2.19
P_2O_5	0.11	0.08	0.08	0.11	0.12	0.10	0.10	0.11	0.08
LOI	1.56	1.20	1.10	2.06	1.69	1.64	1.22	1.55	1.12
FeO	1.34	0.81	0.79	0.67	0.71	1.20	1.24	0.95	nd
Fe_2O_3	1.92	1.20	0.68	2.45	2.66	1.96	1.63	2.39	nd
TOTAL	100.05	99.86	99.38	99.80	100.23	99.87	100.23	99.74	99.99
TRACES									
Cr	38	22	14	34	48	38	89	40	25
Co	7	2	0	6	6	4	5	5	1
Ni	14	6	0	7	10	13	14	16	1
Cu	2	4	0	5	3	12	0	5	3
Zn	38	24	14	37	35	26	33	41	20
Ga	18	18	16	18	19	18	21	19	17
Rb	59	62	58	75	108	79	70	89	72
Sr	470	513	440	436	480	433	432	427	504
Y	11	9	6	14	10	12	10	12	8
Zr	105	102	107	113	112	112	112	113	102
Ba	592	501	583	382	401	432	442	404	527
La	21	13	9	29	17	17	21	17	11
Ce	32	27	25	59	31	35	39	40	20
Pb	8	10	17	13	8	9	9	11	14
Th	5	2	3	9	1	5	3	4	3
U	2	2	2	1	2	1	1	2	3
CIPW NORMS									
Or	12.77	11.94	13.77	9.63	11.35	11.47	12.41	11.70	12.94
Ab	41.45	39.68	40.69	36.12	38.49	36.71	37.31	38.24	42.89
An	11.59	10.39	8.11	18.26	15.14	13.04	12.80	13.67	9.60
Q	21.49	27.78	27.98	23.69	22.49	25.45	25.47	23.22	25.85

SAMPLE	4386	4391	4393	4397	4242	4243	4275	4280	4281
GROUP	2	2	2	2	3a	3a	3a	3a	3a
MAJORS									
SiO_2	68.49	66.40	67.15	63.70	63.32	63.12	67.77	63.17	63.01
Al_2O_3	15.35	15.90	15.61	15.03	14.58	15.69	14.36	15.06	14.96
TiO_2	0.36	0.48	0.42	0.55	0.62	0.63	0.49	0.60	0.64
MnO	0.06	0.06	0.07	0.07	0.08	0.10	0.08	0.07	0.07
$(Fe_2O_3)^t$	2.88	3.45	3.24	3.76	4.37	3.78	3.75	4.22	4.47
MgO	1.72	2.05	1.91	1.91	3.53	3.31	3.11	3.20	3.63
CaO	3.12	3.46	2.86	5.49	3.43	3.88	1.11	3.25	3.47
Na_2O	4.68	4.81	4.68	3.96	4.38	4.23	4.64	4.05	3.67
K_2O	1.84	1.67	2.05	1.79	3.30	3.19	3.25	3.36	3.21
P_2O_5	0.10	0	0.11	0.11	0.25	0.26	0.20	0.23	0.26
LOI	1.94	2.29	1.72	3.98	2.01	2.96	1.73	2.40	2.66
FeO	nd	0.94	nd	0.63	nd	nd	0.62	nd	nd
Fe_2O_3	nd	2.46	nd	3.06	nd	nd	3.06	nd	nd
TOTAL	100.54	100.46	99.82	100.28	99.87	101.15	100.42	99.61	100.05
TRACES									
Cr	29	47	44	43	117	116	92	107	116
Co	2	5	7	4	13	14	5	14	14
Ni	9	13	15	10	55	48	41	47	50
Cu	147	3	4	6	9	77	17	8	10
Zn	21	36	39	29	55	73	52	61	58
Ga	17	19	18	16	18	17	17	17	18
Rb	98	77	84	106	81	81	97	104	85
Sr	432	445	424	287	502	567	299	532	515
Y	11	11	12	20	14	10	13	13	12
Zr	103	111	108	148	157	166	133	142	149
Ba	366	385	460	393	574	616	471	625	674
La	16	16	19	21	34	35	17	32	31
Ce	34	31	35	42	66	70	66	58	61
Pb	10	10	11	13	14	23	18	17	16
Th	5	3	3	5	10	11	16	9	10
U	2	2	3	3	2	3	3	3	2
CIPW NORMS									
Or	10.87	9.87	12.12	10.58	19.50	18.85	19.21	19.86	18.97
Ab	39.59	40.69	39.59	33.50	37.05	35.78	39.25	34.26	31.05
An	14.83	16.45	13.47	17.95	10.38	14.40	4.20	12.99	14.87
Q	24.43	20.90	22.49	20.33	13.17	13.49	20.82	14.85	16.17

SAMPLE	4285	4315	4316	4322	4325	4329	4335	4350	4364
GROUP	3a	3a	3a	3a	3a	3a	3a	3a	3a
MAJORS									
SiO_2	63.10	63.87	66.44	62.39	63.63	63.94	68.67	64.06	64.68
Al_2O_3	15.13	15.06	15.46	14.64	15.35	15.05	14.46	15.10	15.07
TiO_2	0.61	0.60	0.48	0.63	0.59	0.65	0.64	0.56	0.57
MnO	0.08	0.07	0.05	0.07	0.05	0.09	0.04	0.06	0.11
$(Fe_2O_3)^t$	4.45	4.15	3.36	4.46	4.00	4.54	3.86	3.91	3.95
MgO	3.61	3.82	2.45	3.99	2.95	3.71	1.93	2.53	3.28
CaO	3.37	3.73	2.86	3.83	3.69	3.11	0.75	3.27	2.65
Na_2O	4.54	4.36	4.79	4.23	4.29	3.79	3.76	4.27	4.24
K_2O	3.02	3.01	3.05	2.98	2.86	3.27	4.42	2.77	2.92
P_2O_5	0.26	0.25	0.18	0.27	0.22	0.27	0.08	0.20	0.22
LOI	1.74	1.66	1.88	2.43	2.00	1.58	1.36	1.98	1.79
FeO	1.53	1.39	0.78	1.34	1.12	nd	2.62	0.87	0.89
Fe_2O_3	2.75	2.60	2.49	2.97	2.75	nd	0.95	2.94	2.96
TOTAL	99.74	100.42	100.91	99.77	99.50	100.00	99.68	98.61	99.38
TRACES									
Cr	107	118	84	125	101	119	71	90	101
Co	14	11	9	14	15	10	7	6	9
Ni	54	52	28	54	54	61	25	42	43
Cu	10	10	14	13	2	10	0	6	15
Zn	65	65	56	62	27	56	21	73	64
Ga	19	16	17	17	16	17	15	19	18
Rb	77	78	77	76	67	89	106	66	87
Sr	569	562	516	537	508	559	149	520	495
Y	16	16	10	15	15	15	21	13	13
Zr	155	162	140	153	142	153	162	145	159
Ba	556	540	611	532	502	674	465	511	587
La	27	37		34	34	26	23	27	36
Ce	66	74	53	71	68	72	37	68	67
Pb	15	16	20	11	8	15	15	13	15
Th	10	12	7	11	11	12	8	10	10
U	3	3	2	3	2	3	2	3	3
CIPW NORMS									
Or	17.85	17.79	18.03	17.61	16.90	19.33	26.12	16.37	17.26
Ab	38.41	36.88	40.52	35.78	36.29	32.06	31.81	36.12	35.87
An	11.99	12.63	11.68	12.16	14.18	13.67	3.20	13.86	11.71
Q	12.67	13.78	16.99	12.84	15.54	16.69	24.62	17.55	17.81

SAMPLE	4365	4368	4370	4379	4380	4381	4385	4386A	4388
GROUP	3a	3a	3a	3a	3a	3a	3a	3a	3a
MAJORS									
SiO_2	63.18	67.13	65.10	65.27	64.40	63.89	66.82	64.74	62.45
Al_2O_3	15.53	14.85	15.58	14.81	14.56	15.28	15.25	15.34	14.98
TiO_2	0.59	0.51	0.57	0.56	0.59	0.60	0.49	0.57	0.65
MnO	0.10	0.08	0.10	0.10	0.08	0.09	0.07	0.07	0.11
$(Fe_2O_3)^t$	4.25	3.41	4.08	3.98	4.15	4.18	3.56	3.96	4.75
MgO	3.38	2.47	2.22	3.17	3.55	3.14	2.40	3.03	4.05
CaO	3.16	2.35	3.10	2.70	3.08	2.92	2.61	2.58	3.23
Na_2O	4.27	4.20	4.16	4.60	3.94	4.31	4.14	4.48	4.66
K_2O	2.99	3.69	2.93	3.16	3.25	3.25	3.05	3.10	2.62
P_2O_5	0.24	0.18	0.18	0.23	0.24	0.24	0.16	0.22	0.26
LOI	2.13	1.81	2.05	2.08	2.33	2.02	1.45	1.85	2.36
FeO	1.04	0.70	0.77	1.20	nd	1.24	0.78	1.05	1.27
Fe_2O_3	3.12	2.63	3.22	2.65	nd	2.80	2.69	2.79	3.34
TOTAL	99.73	100.60	99.98	100.53	100.17	99.78	99.91	99.82	99.98
TRACES									
Cr	109	109	91	101	107	118	65	105	134
Co	11	6	12	11	13	12	9	10	15
Ni	49	37	42	46	49	53	25	44	57
Cu	17	9	9	8	11	13	7	9	10
Zn	58	41	48	46	55	48	37	55	61
Ga	19	18	20	18	19	19	20	19	20
Rb	86	105	75	80	89	86	63	93	72
Sr	579	481	566	505	514	536	505	529	506
Y	14	12	13	14	15	14	12	16	17
Zr	144	144	150	165	167	166	148	163	162
Ba	630	602	546	644	620	733	568	651	529
La	31	32	28	35	31	33	28	33	34
Ce	63	59	58	70	66	71	52	66	72
Pb	12	18	19	13	17	20	11	16	9
Th	9	10	11	11	12	12	10	13	10
U	1	1	1	4	4	4	2	4	5
CIPW NORMS									
Or	17.67	21.81	17.32	18.68	19.21	19.21	18.03	18.32	15.48
Ab	36.12	35.53	35.19	38.92	33.33	36.46	35.02	37.90	39.42
An	14.11	10.48	14.20	10.43	12.45	12.75	11.90	11.36	12.22
Q	14.58	19.44	19.11	16.87	16.95	15.00	21.34	16.30	12.21

SAMPLE	4389	4390	4394	4396	4462	4312	4313	4321	4279
GROUP	3a	3a	3a	3a	3a	3b	3b	3b	4
MAJORS									
SiO_2	64.29	64.97	65.53	63.45	65.09	65.11	66.19	64.51	72.07
Al_2O_3	14.88	15.41	15.16	15.28	15.17	15.50	15.57	15.80	14.36
TiO_2	0.58	0.55	0.55	0.61	0.60	0.50	0.45	0.52	0.16
MnO	0.08	0.08	0.07	0.08	0.10	0.06	0.04	0.06	0.06
$(Fe_2O_3)^t$	4.02	3.87	3.86	4.21	4.21	3.71	3.36	3.89	2.63
MgO	3.39	2.29	2.82	3.56	3.49	2.20	2.10	2.29	0.43
CaO	2.61	2.85	2.88	2.73	3.25	3.07	2.89	3.40	1.39
Na_2O	4.46	4.20	4.51	4.55	4.06	4.53	4.65	4.32	3.88
K_2O	2.99	3.29	3.05	3.12	3.22	2.60	2.43	2.29	3.53
P_2O_5	0.22	0.19	0.18	0.23	0.22	0.19	0.16	0.20	0.08
LOI	2.37	2.13	1.81	1.79	nd	1.73	1.34	1.80	0.44
FeO	nd	nd	1.09	1.15	nd	1.01	nd	0.89	1.67
Fe_2O_3	nd	nd	2.65	2.93	nd	2.59	nd	2.90	0.77
TOTAL	99.89	99.83	100.30	99.48	99.19	99.69	99.18	98.98	98.84
TRACES									
Cr	110	90	88	126	109	69	54	65	12
Co	13	9	10	10	13	5	5	9	2
Ni	44	43	43	55	48	32	25	34	0
Cu	6	19	11	8	7	4	1	7	2
Zn	51	56	44	49	49	48	36	48	32
Ga	17	17	19	19	20	16	17	18	15
Rb	77	87	89	80	98	64	53	55	121
Sr	475	508	504	553	590	559	537	621	138
Y	15	13	14	15	17	10	11	11	12
Zr	158	143	151	171	164	153	141	156	152
Ba	548	682	609	688	585	538	498	522	414
La	32	30	28	39	31	29	33	28	19
Ce	71	58	62	69	73	58	52	45	40
Pb	10	15	15	14	17	12	8	14	21
Th	13	6	11	13	11	7	7	7	5
U	1	2	1	4	4	2	2	1	3
CIPW NORMS									
Or	17.67	19.44	18.03	18.44	19.03	15.37	14.36	13.53	20.86
Ab	37.73	35.53	38.15	38.49	34.35	38.32	39.34	36.55	32.82
An	11.51	12.90	12.12	12.04	13.66	13.99	13.29	15.56	6.37
Q	15.77	17.89	16.90	13.38	16.66	19.04	20.00	19.38	31.71

SAMPLE	4401	4400	4477	4482	4485	4480	4399	4403
GROUP	Vs	Vs	Vs	Vs	Vs	Vs	Vs	Vs
MAJORS								
SiO_2	65.74	61.08	63.12	67.95	65.35	61.68	60.23	60.96
Al_2O_3	15.26	15.65	13.76	15.20	15.91	16.44	16.84	17.23
TiO_2	0.63	0.67	0.68	0.54	0.65	0.68	0.67	0.65
MnO	0.09	0.10	0.09	0.05	0.06	0.07	0.15	0.07
$Fe_2O_3{}^t$	4.17	5.08	4.34	3.73	4.85	5.19	5.35	4.92
MgO	1.22	2.45	1.67	1.69	1.61	2.71	3.54	1.67
CaO	2.24	3.01	4.17	1.53	1.11	2.14	1.28	2.88
Na_2O	4.79	6.29	4.57	4.34	5.29	5.63	6.51	6.09
K_2O	4.02	2.81	3.26	3.84	4.39	3.74	3.33	3.49
P_2O_5	0.23	0.24	0.28	0.18	0.23	0.23	0.22	0.21
LOI	1.99	3.23	3.96	1.53	0.91	2.33	2.41	2.65
FeO	nd	nd	nd	nd	nd	nd	nd	nd
Fe_2O_3	nd	nd	nd	nd	nd	nd	nd	nd
TOTAL	100.38	100.61	99.90	100.58	100.36	100.84	100.53	100.82
TRACES								
Cr	116	124	138	71	144	128	98	107
Co	3	7	9	5	4	9	9	7
Ni	35	35	65	34	49	57	41	36
Cu	14	11	50	10	12	8	15	11
Zn	20	43	38	35	26	46	56	24
Ga	16	13	9	17	10	12	15	15
Rb	112	51	65	101	97	78	65	79
Sr	434	372	438	529	571	442	365	426
Y	13	22	18	13	25	15	19	16
Zr	182	171	168	164	171	184	179	178
Ba	1447	911	1009	939	1359	698	1054	928
La	41	49	52	37	47	49	47	40
Ce	76	91	93	72	169	90	111	89
Pb	37	26	22	22	31	24	46	31
Th	15	8	7	7	12	9	10	12
U	3	3	1	2	3	3	3	2

Table 4.1 (cont.) Andesitic and dacitic clasts of southerly provenance.

SAMPLE	4402	4464	4465	4458	4231	4284	4288	4461
GROUP	Vs	Vs	Vs	Vs	Vs	Vs	Vs	Vs
MAJORS								
SiO_2	66.02	55.92	58.66	57.85	61.38	60.71	62.62	65.23
Al_2O_3	15.43	15.31	15.82	16.20	15.99	15.49	14.77	15.24
TiO_2	0.64	0.68	0.64	0.69	0.68	0.62	0.67	0.60
MnO	0.18	0.06	0.07	0.11	0.06	0.06	0.05	0.07
$Fe_2O_3{}^t$	4.86	6.03	5.26	4.93	4.69	4.56	5.06	4.54
MgO	1.23	3.08	3.08	1.29	1.78	1.24	1.84	2.20
CaO	1.12	5.58	3.89	5.39	2.63	3.41	2.48	1.77
Na_2O	5.74	6.21	7.08	5.84	5.91	5.38	5.16	5.21
K_2O	3.78	2.70	2.08	3.74	3.46	3.44	3.76	3.27
P_2O_5	0.21	0.24	0.21	0.24	0.26	0.23	0.26	0.18
LOI	1.24	4.64	4.02	4.21	2.74	3.32	2.61	2.20
FeO	nd	nd	nd	nd	nd	nd	nd	nd
Fe_2O_3	nd	nd	nd	nd	nd	nd	nd	nd
TOTAL	100.45	100.45	100.81	100.49	99.58	98.46	99.28	100.51
TRACES								
Cr	105	131	124	121	130	145	125	117
Co	6	9	9	3	9	5	13	9
Ni	30	49	45	43	51	36	59	53
Cu	18	9	5	10	24	30	36	27
Zn	21	36	40	28	34	31	50	21
Ga	12	12	12	15	12	12	12	14
Rb	79	63	50	84	83	70	60	81
Sr	356	393	269	409	380	322	405	419
Y	15	18	14	19	16	17	19	12
Zr	172	182	165	184	180	162	156	161
Ba	1206	925	639	1192	965	931	1032	1259
La	39	53	42	47	51	38	41	40
Ce	91	112	71	89	92	85	101	66
Pb	38	31	28	31	35	32	37	31
Th	11	9	9	8	10	11	9	6
U	2	2	4	2	2	5	2	3

Table 4.1 (cont.) Andesitic and dacitic clasts of southerly provenance.

SAMPLE	4289	4318	4327	4330	4331	4332	4283
GROUP	Vs	Vs	Vs	Vs	Vs	Vs	Vs
MAJORS							
SiO_2	65.13	58.63	54.00	62.62	60.13	59.82	58.64
Al_2O_3	15.44	15.27	13.50	15.34	15.31	15.56	16.37
TiO_2	0.60	0.69	0.72	0.59	0.63	0.76	0.70
MnO	0.05	0.06	0.11	0.08	0.06	0.06	0.04
Fe_2O_3	3.81	4.99	5.21	4.17	4.95	5.92	5.04
MgO	2.55	0.51	2.54	1.74	3.56	2.82	0.60
CaO	2.70	5.50	8.69	3.61	3.06	4.06	4.71
Na_2O	5.01	5.05	4.96	5.86	5.68	4.29	5.88
K_2O	3.26	4.41	3.19	3.38	3.05	3.32	4.22
P_2O_5	0.23	0.27	0.44	0.27	0.27	0.41	0.27
LOI	1.26	4.14	6.95	3.09	3.41	2.43	3.70
FeO	nd	nd	nd	nd	nd	nd	nd
Fe_2O_3	nd	nd	nd	nd	nd	nd	nd
TOTAL	100.04	99.52	100.31	100.75	100.11	99.45	100.17
TRACES							
Cr	145	107	182	103	115	220	135
Co	11	3	8	6	11	11	6
Ni	49	32	73	45	37	95	37
Cu	8	15	5	23	16	5	11
Zn	48	16	39	32	49	43	14
Ga	17	13	13	13	12	19	13
Rb	82	95	70	77	68	86	95
Sr	529	352	454	401	310	709	322
Y	16	20	18	27	17	16	16
Zr	157	153	193	154	174	213	173
Ba	664	1293	795	885	793	1123	1279
La	40	40	74	40	42	55	49
Ce	71	94	155	231	84	109	100
Pb	26	34	29	19	24	27	33
Th	8	10	10	12	9	13	10
U	4	3	2	4	2	3	2

Table 4.1 (cont.) Andesitic and dacitic clasts of southerly provenance.

FIGURE 4.4a Plot of K_2O vs SiO_2 with fields of Peccerilo and Taylor (1976). Fields are: HKA-high K andesite; A-andesite; LKA-low K andesite; HKD-high K dacite; D-dacite; LKD-low K dacite; R-rhyolite; LKR-low K rhyolite. Symbols used distinguish granite clast suites. These are: open triangles - foliated tonalites (G1); open circles - equigranular biotite granites (G2); filled circle - contaminated G2 clast; ruled open circles - G2 clast with high LOI; open squares - equigranular hornblende biotite granodiorite (G3); filled squares - contaminated G3 clasts; half-filled squares - subset of G3 granite clasts; open diamond - biotite-garnet granite (G4).

FIGURE 4.4b Total alkalis ($Na_2O + K_2O$) vs SiO_2 plot with fields of Kuno (1966). Fields are: A-alkali; HA-high alumina; T-tholeiitic. Symbols as in Figure 4.4a.

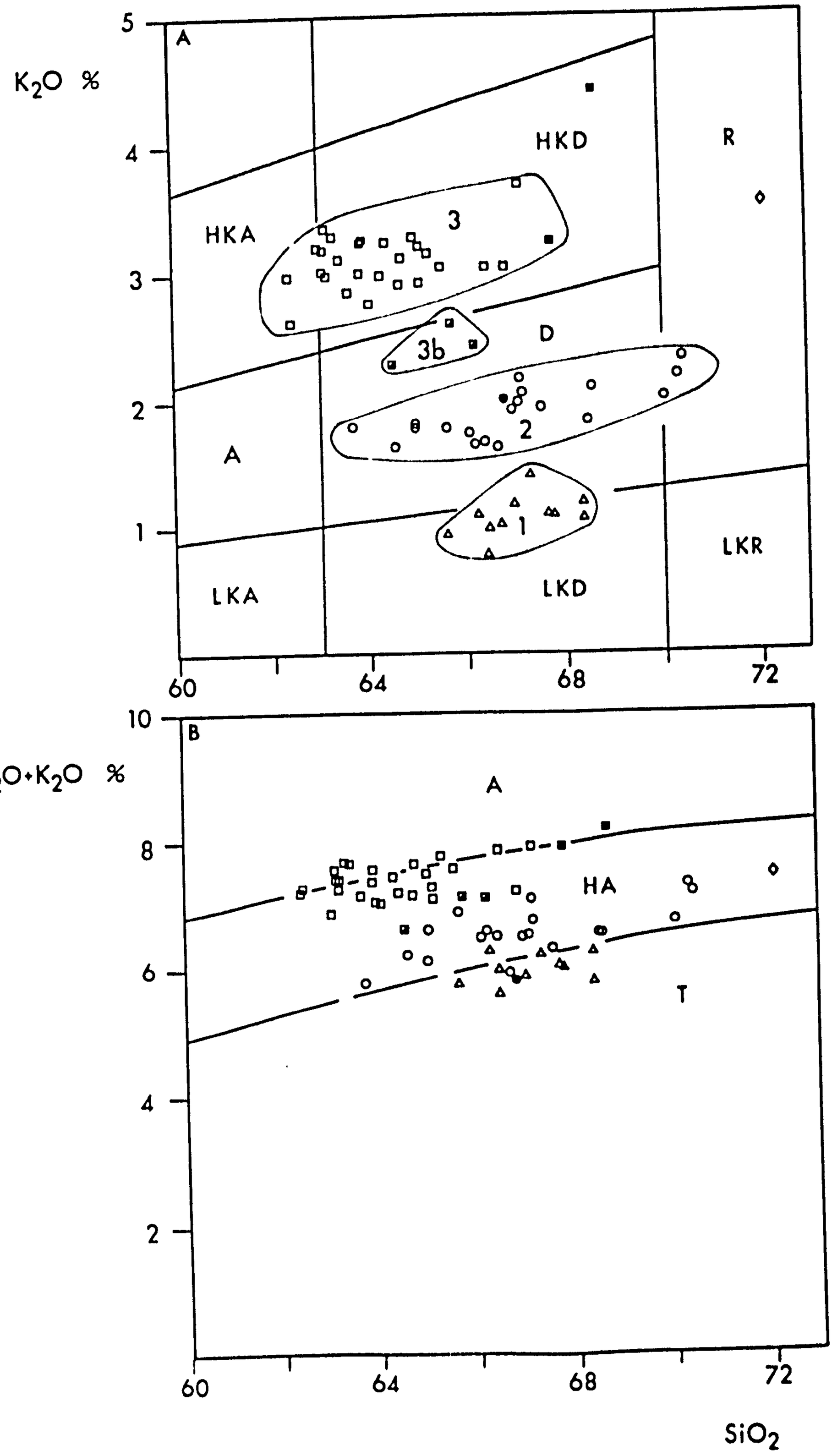
K_2O %
5
4
3
2
1
A
HKD
R
HKA
3
3b
D
2
A
1
LKR
LKA
LKD
60
64
68
72
Na_2O+K_2O %
10
8
6
4
2
B
A
HA
T
60
64
68
72
SiO_2

G3. They are subsequently treated as a sub-set of suite G3 and referred to as G3-B. Clast 4279 (G4) plots off the trend of the three granite suites recognised and is clearly unrelated. Its age and isotopic signature also distinguish it (Section 4.5).

The three suites show a positive correlation of K_2O with SiO_2. G3 shows the greatest scatter which probably reflects inhomogeneity introduced by assimilation. Metasedimentary xenoliths are common in G3 clasts although only rarely seen in G1 and G2. At constant SiO_2, a remarkable range in K_2O is apparent, far in excess of that for late Caledonian granitoids, which largely plot in the high K field of Peccerilo and Taylor (1976). The distribution of K_2O with SiO_2 rules out high level differentiation as the mechanism whereby the between suite chemical variation was generated. Fractionation processes may however have been largely responsible for producing the within-suite variation.

Na_2O is plotted against K_2O in Figure 4.5 and total alkalis against SiO_2 in Figure 4.4b. The southerly derived granites show Na enrichment at constant K_2O when compared to I-type granites of the Lachlan fold belt, Australia (White and Chappell 1983). Na-enrichment has been widely recognised in late Caledonian granites. Hall (1967) demonstrated enhanced levels of Na in Caledonian over Variscan granites which he attributed to higher pH_2O. Halliday and Stephens (1984) showed Na enrichment to be a feature of all late Caledonian granites of Britain and Ireland both north and south of the Iapetus suture, irrespective of whether they are of I or S-type affinity. They suggest the high Na content and low K_2O/Na_2O might reflect a regional feature of the crust in Britain and Ireland, possibly inherited through recycling of K-depleted granulite facies basement. The recognition of Na-enrichment in granitoids from the Midland Valley completes a record of Na-enriched magmatism in all tectonic zones of the Caledonides in Britain and Ireland irrespective of crustal structure. Given the diverse character of the various crustal segments involved in late Caledonian magmatism it is difficult to reconcile Na-enrichment with a low K/Na province of crustal origin.

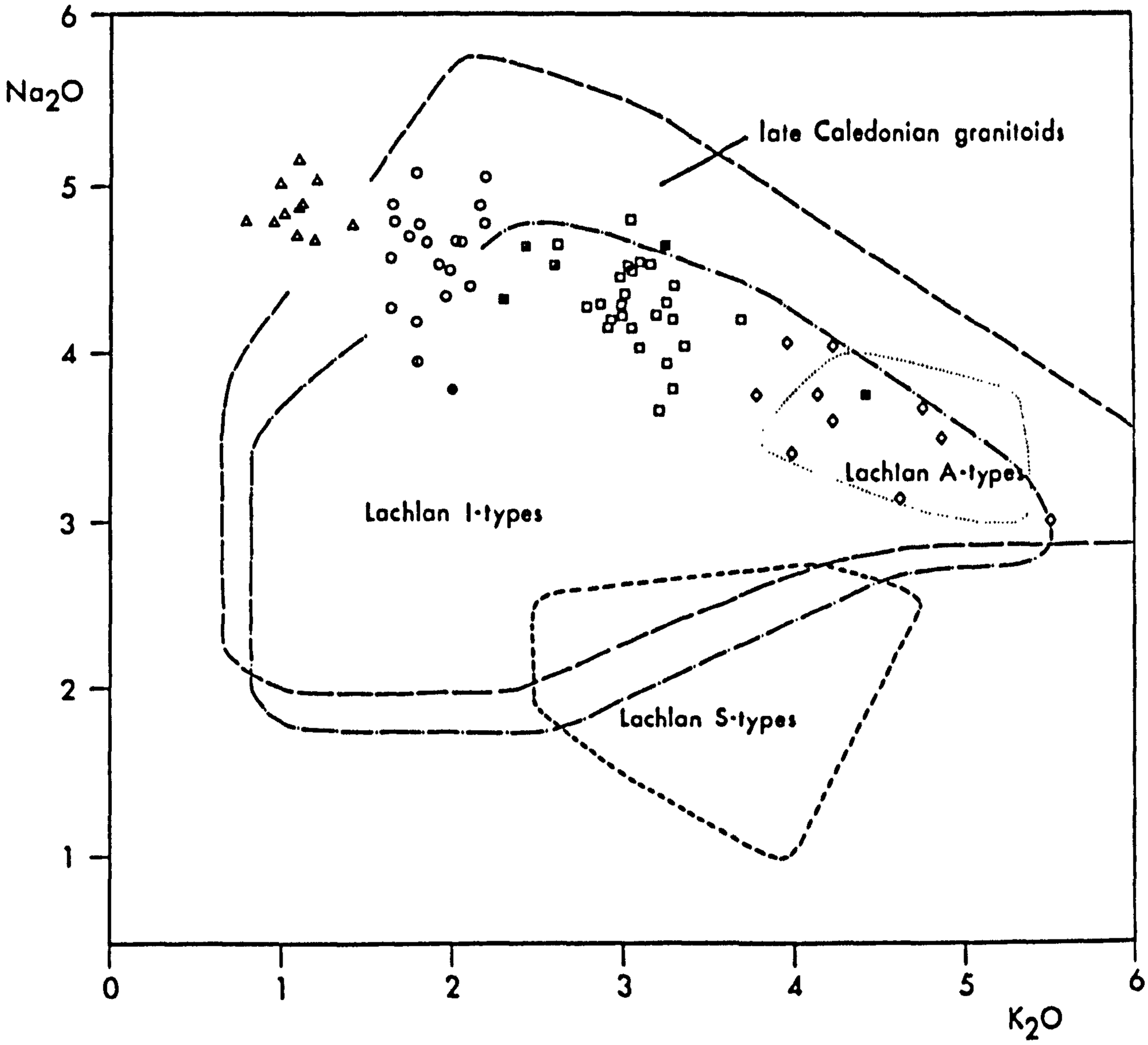

FIGURE 4.5 Na_2O vs K_2O plot of southerly-derived granite clast data (G1, G2 and G3) with fields for Lachlan I, S and A-type granites (White and Chappell 1983) and Late Caledonian granites (Stephens and Halliday 1984) superimposed. Symbols for G1, G2 and G3 as in Figure 4.4a. Open diamonds are northerly derived two-mica granite clasts.

There is a consistently high level of Na_2O across a range of K_2O for the southerly derived clasts (Fig.4.5). There is a tendency for Na_2O to decrease slightly with increasing K_2O. Also plotted are compositional fields for Lachlan I-, S- and A-type granitoids (White and Chappell 1983), late Caledonian granites (Stephens and Halliday 1984) and a suite of northerly derived two mica S-type granite clasts (Chapter 5). The latter, although in all other respects satisfying the S-type definition of White and Chappell (1983), plot in the A-type Lachlan field emphasising the ubiquity of Na-enrichment in both I and S type granitoids. G1 significantly plots outside the Caledonian granite field and is unusually low in K_2O.

Figure 4.4b shows the relationship between total alkalis and silica. G3 plots on the boundary of the alkali and high alumina fields of Kuno (1966). G2 plots in the high alumina field and G1 towards more tholeiitic compositions. G1 is noticeably depleted in alkalis relative to the bulk of other Caledonian granites.

Peacock (1931) showed the silica level at which the abundance of total alkalis becomes equal to the abundance of CaO in a volcanic rock series to have a tectonic significance. The critical level of silica at which curves for total alkalis and CaO compositions intersect was termed the alkali-lime index. This index was used to classify volcanic rock series into four genetic groups. Peacock (1931) termed these groups alkalic (<51), alkali-calcic (51-56% SiO_2), calc-alkaline (51-61) and calcic (>61% SiO_2). The calc-alkaline and alkalic groups have become synonymous with magmatism in destructive and extensional tectonic settings respectively.

Figure 4.6 plots total alkali and CaO curves for each of the granite clast suites. CaO for suites G1 and G2 largely overlap, but the field for G3 is significantly displaced towards lower SiO_2. The range of silica in the three granite suites does not permit a graphical determination of the alkali-lime index. However, back projection of the trends using least squares regression of the CaO and total alkalis data for each of the

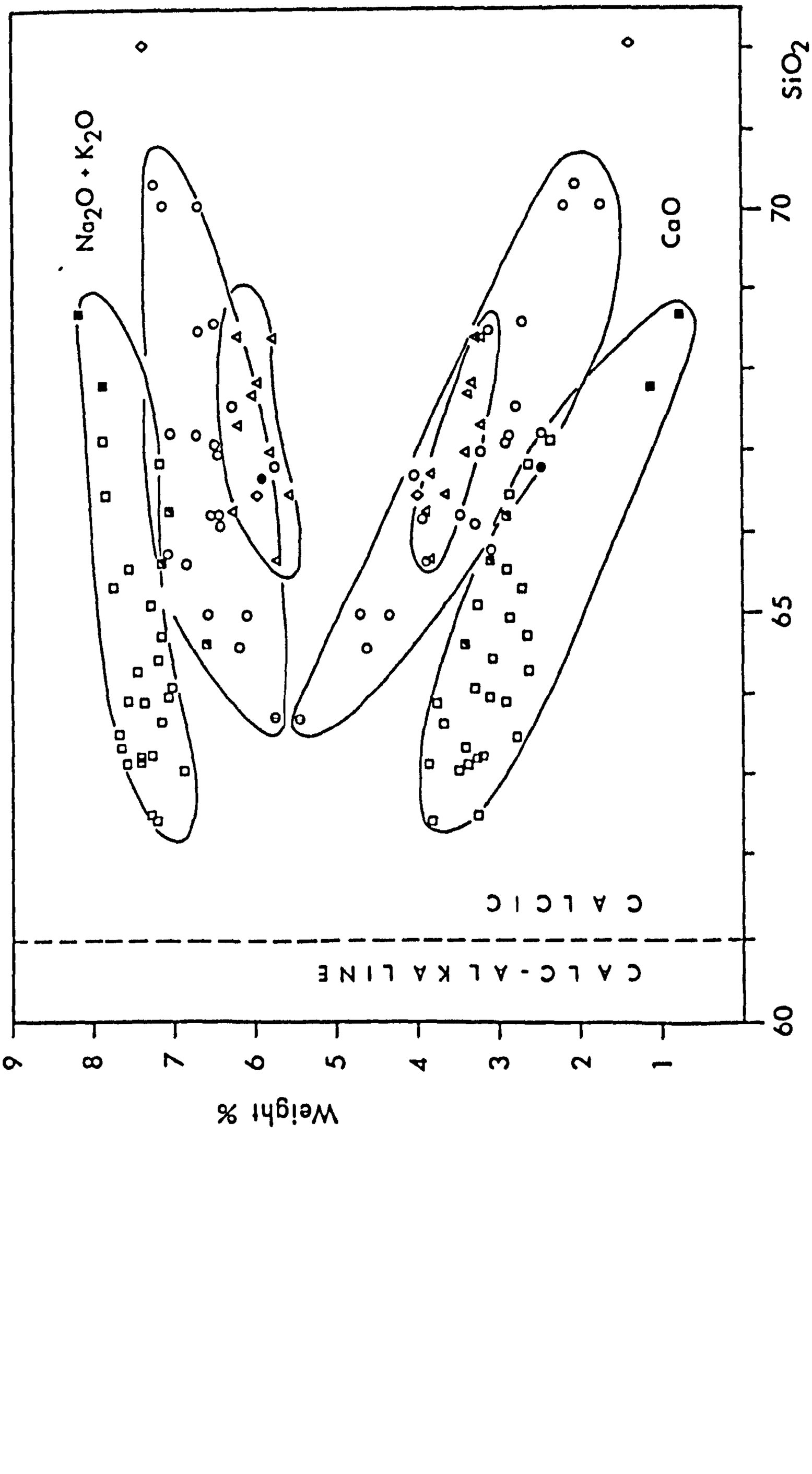

FIGURE 4.6 Total alkalis and CaO vs SiO_2 plot with fields for calc-alkaline and calcic magmas after Peacock (1931). Symbols as in Figure 4.4a. Data for G1 and G3 back-project to intersect in calc-alkaline field. G2 clasts project to intersect close to boundary between the calc-alkaline and calcic fields, if altered sample (high LOI) 4397 is ignored.

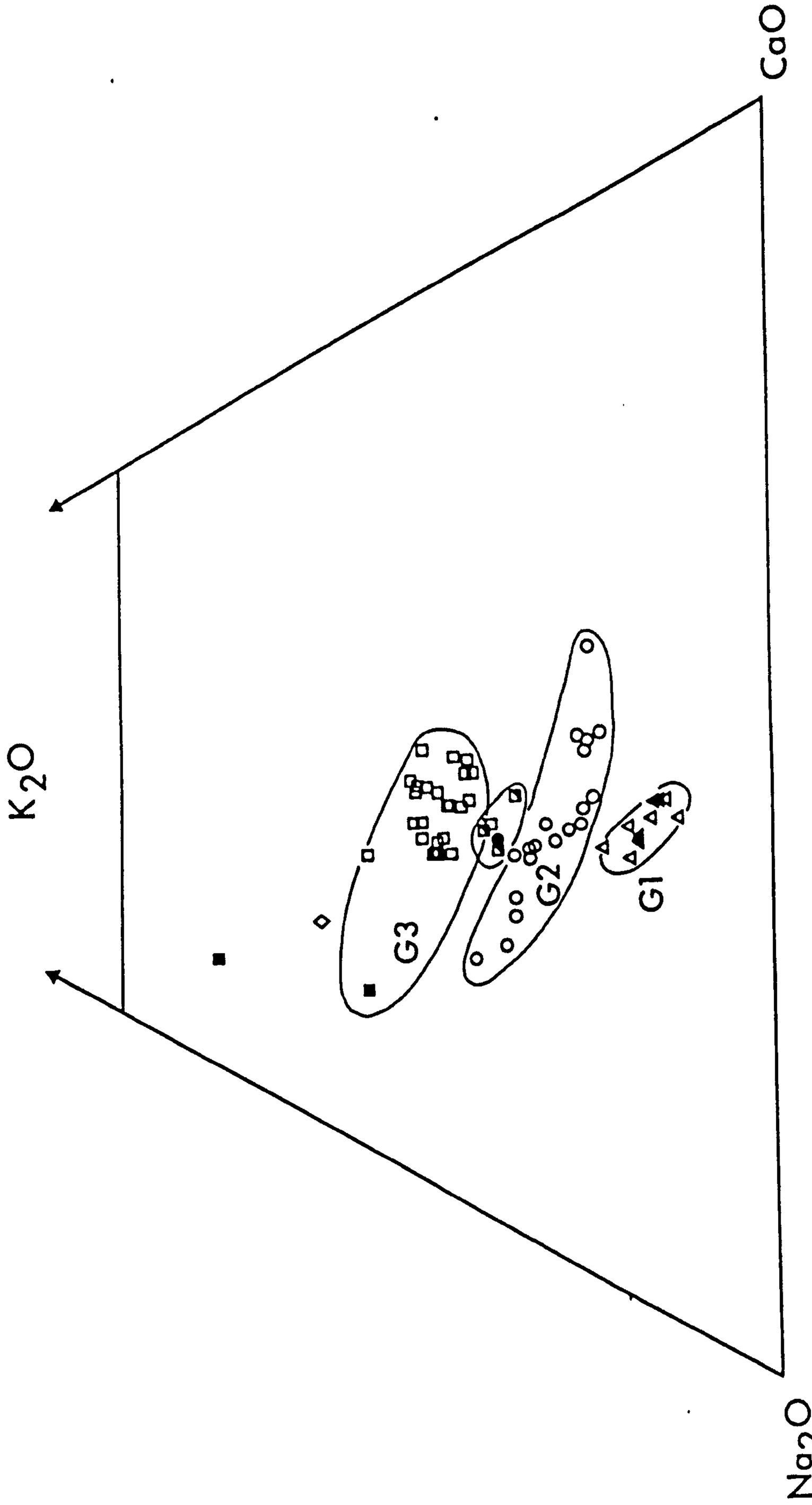

FIGURE 4.7 Na_2O-K_2O-CaO triangular plot with symbols as in Figure 4.4a.

suites establishes all three suites have alkali-lime indexes characteristic of calc-alkaline magma series. Whilst this suggests a connection with destructive margin processes, and subduction in particular, two points are worth considering. Firstly, there are instances of calc-alkaline style magmatism which cannot be linked with active subduction, for example, the Taos volcanic field (Lipman and Mehnert 1979). Secondly, Zhou (1985) has shown termination of subduction by collision is not coincident with cessation of calc-alkaline magmatism in modern collision zones. The presence of magmas of calc-alkaline affinity cannot be therefore invoked to infer the operation of contemporaneous subduction, although this may often be the case.

A K_2O-Na_2O-CaO ternary diagram (Fig.4.7) emphasises the clear chemical separation of the three main groups and the internal coherency associated with each suite. G1, although strongly depleted in K_2O relative to the other granite clasts, is not depleted in Na_2O, and if anything, is slightly more sodic. Whatever the process involved in generating the between-suite separation, the alkalis are clearly uncoupled. Figure 4.7 also highlights the poor spread of data for clasts of G3 type, with a bias towards the least evolved clasts. The significance of this feature is returned to in 4.6.4.

4.4.1.2 A/CNK

The ratio mol. $Al_2O_3/(CaO + Na_2O + K_2O)$, or A/CNK, provides a measure of the alkali-alumina balance in magmas. Peraluminous magmas are defined as having molar proportions of Al_2O_3 in excess of the summed molar proportions of Na_2O, K_2O, and CaO (A/CNK >1.0). There appears to be no single origin for the development of peraluminous compositions. A number of mechanisms have been proposed. These include fractional crystallisation of amphibole (Cawthorn and O`Hara 1976), crustal anatexis (White and Chappell 1977), assimilation (Halliday et al. 1981) and vapour phase transfer of alkalis (Luth et al. 1964). Halliday et al. (1981) review and apply isotopic constraints to several instances of peraluminous magma development. They highlight coupling of $(^{87}Sr/^{86}Sr)_i$, $\delta^{18}O$ and the major element budget during the development of peraluminous compositions, suggesting assimilation

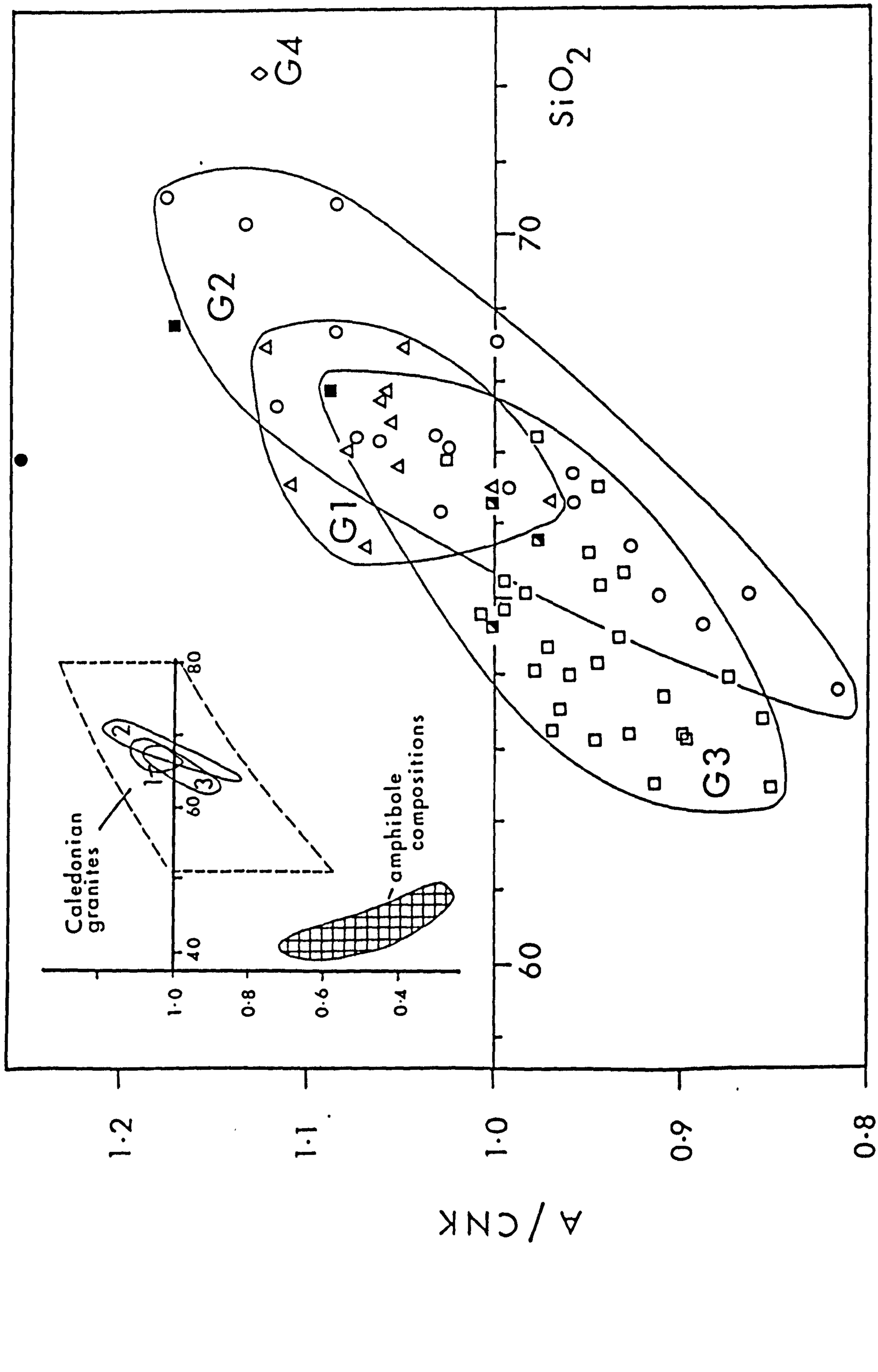

FIGURE 4.8 A/CNK (mol $Al_2O_3/(CaO + Na_2O + K_2O)$) vs SiO_2 plot for granite clasts of southerly derivation. Symbols as in Fig. 4.4a. Inset shows clast fields compared to Caledonian granite array and amphibole compositions.

or crustal fusion to be the only viable processes.

A/CNK ratios for southerly derived granites are plotted against SiO_2 (Fig.4.8). G2 shows an exceptionally wide compositional range equal to the combined range of G1 and G3. The G2 array spans both metaluminous and peraluminous fields with a trajectory somewhat steeper than the collective late Caledonian array shown in Figure 4.8. G1 and G3 plot with more restricted distributions. G1, with the exception of 4369, plots entirely in the peraluminous field with A/CNK >1.0. Significantly, garnet is an important accessory phase. Garnet commonly occurs in strongly corundum normative silicic rocks with an origin attributed to the melting of pelitic material deep in the crust (Green 1977). Isotopic evidence (4.5) precludes such an origin for G1.G3 is largely confined to the metaluminous field with A/CNK less than or marginally greater than 1.0.

Several samples plot with A/CNK >1.10, the delimiting value for S-type granites according to the definition of Chappell and White (1974). In every other respect however they are atypical of S-types. Two samples, 4335 and 4254, which plot to high values of A/CNK are obviously contaminated in containing abundant xenoliths of biotite hornfels. They plot in a position intermediate between the suites to which they belong and the field for the greywackes which the granites intrude. The single clast of G4, 4279, has an A/CNK ratio of 1.127 and shares some S type characteristics.

The inset in Figure 4.8 shows the fields for the clasts relative to the field for natural and synthetic amphibole compositions. The granite trends back-project to intersect the amphibole field in the region of synthetic amphiboles generated at lower temperatures. As G3 samples which plot with more metaluminous compositions have higher $(^{87}Sr/^{86}Sr)_i$ the development of peraluminous compositions in this instance cannot simply be related solely to increasing crustal involvement (4.5). A model involving varying degrees of amphibole fractionation better satisfies the data for suites G1 and G3. In addition isotopic constraints for clasts of G2 type suggest the wide compositional

variation within this suite may reflect a process of crustal assimilation (4.5.4).

4.4.1.3 FeO,Fe_2O_3,MgO

Total iron as Fe_2O_3 $(Fe_2O_3)^t$ and MgO have similar distributions when plotted against SiO_2 or DI (Fig. 4.9a,b). Fields for each of the granite suites broadly overlap with good negative correlations for both individual suites and the data taken as a whole. G1 and G3 tend to form linear arrays on both plots whilst G2 clasts fall on a curvilinear trace, steepening with increasing silica. The different behaviour of G2 is highlighted on a MgO vs $(Fe_2O_3)^t$ plot (Fig. 4.10a). G2 and G3 clasts fall on coherent linear arrays with high positive correlations, but the G2 array is significantly steeper than that for G3. This may reflect either differences in the proportions and/or chemistry of fractionating phases, or possibly restite effects reflecting differing source compositions.

The behaviour of $(Fe_2O_3)^t$ with respect to total alkalis and MgO is best demonstrated on a ternary AFM plot (Fig. 4.10b). The data plot in a position typical of other orogenic granitoids in the calc-alkaline field of Kuno (1968). Note the lack of iron enrichment typical of calc-alkaline magmas. Fields for c 400Ma Caledonian granites (Stephens and Halliday 1984) and Ordovician granite clasts (Longman 1980) are included for comparison.

FeO has been determined for thirty eight representative samples. FeO determinations were by titration against standard dichromate solution. Oxidation ratios $(Fe_2O_3/(FeO + Fe_2O_3))$ are higher than might be anticipated in tonalites and granodiorites of this type. Oxidation ratios for 532 I-type granites from the Lachlan fold-belt average 0.33 (White and Chappell 1983). Oxidation ratios for G1, G2 and G3 clasts average 0.54, 0.70 and 0.71 respectively. These are comparable to values of 0.60 for Lower ORS lavas of the eastern Sidlaw hills (Gandy 1975) and 0.67 for ORS lavas of the northern Lorne Plateau (Groome and Hall 1974). Enhanced oxidation ratios almost certainly in part reflect low temperature hydrothermal or deuteric alteration. Wilshire (1959) has shown that although FeO/Fe_2O_3 ratios are increased in

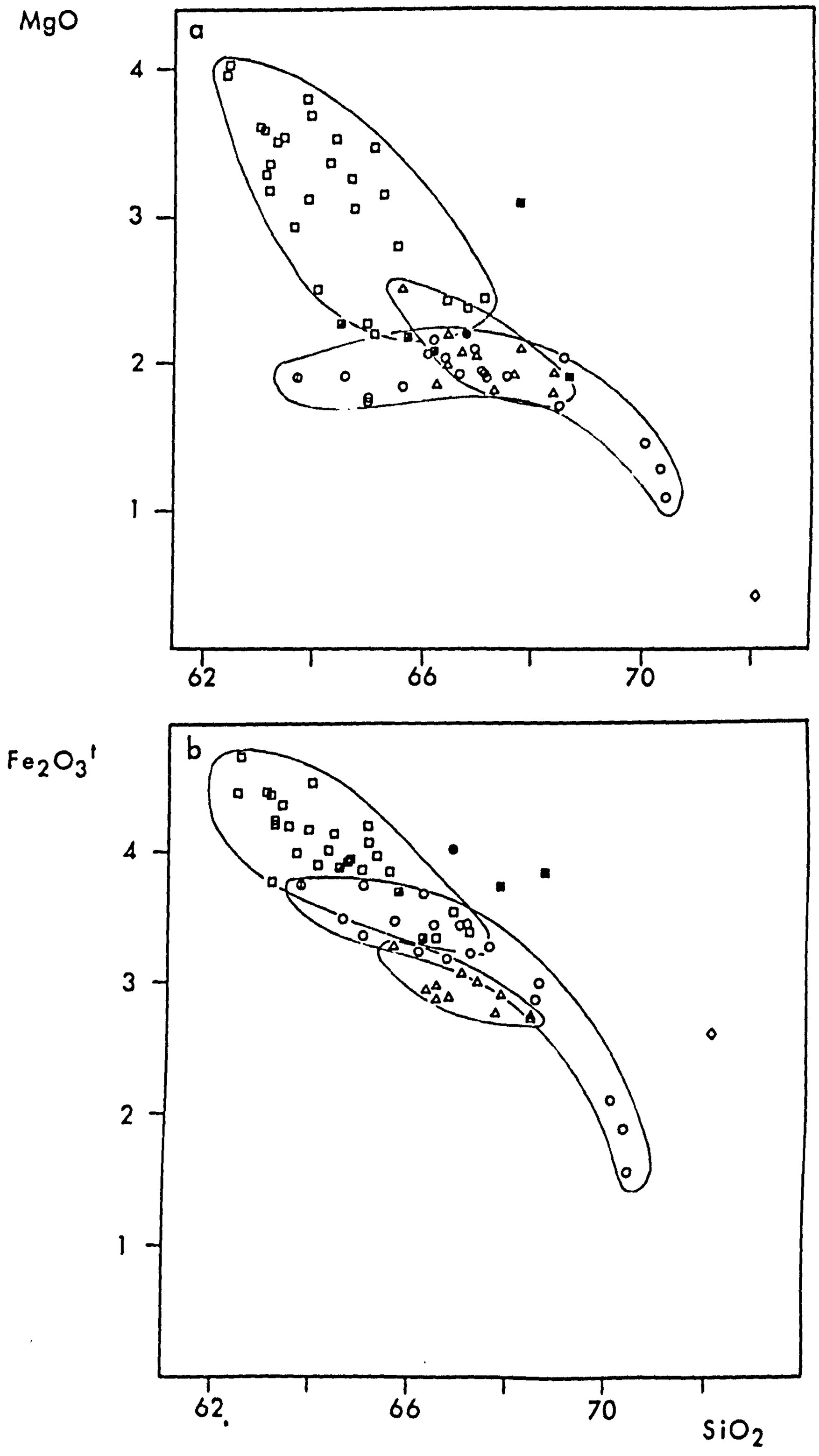

FIGURE 4.9 (a)MgO vs SiO_2 plot for granite clasts of southerly derivation with clast suites outlined. Symbols as in Fig. 4.4a.
(b)$Fe_2O_3{}^t$ (total iron as Fe_2O_3) vs SiO_2.

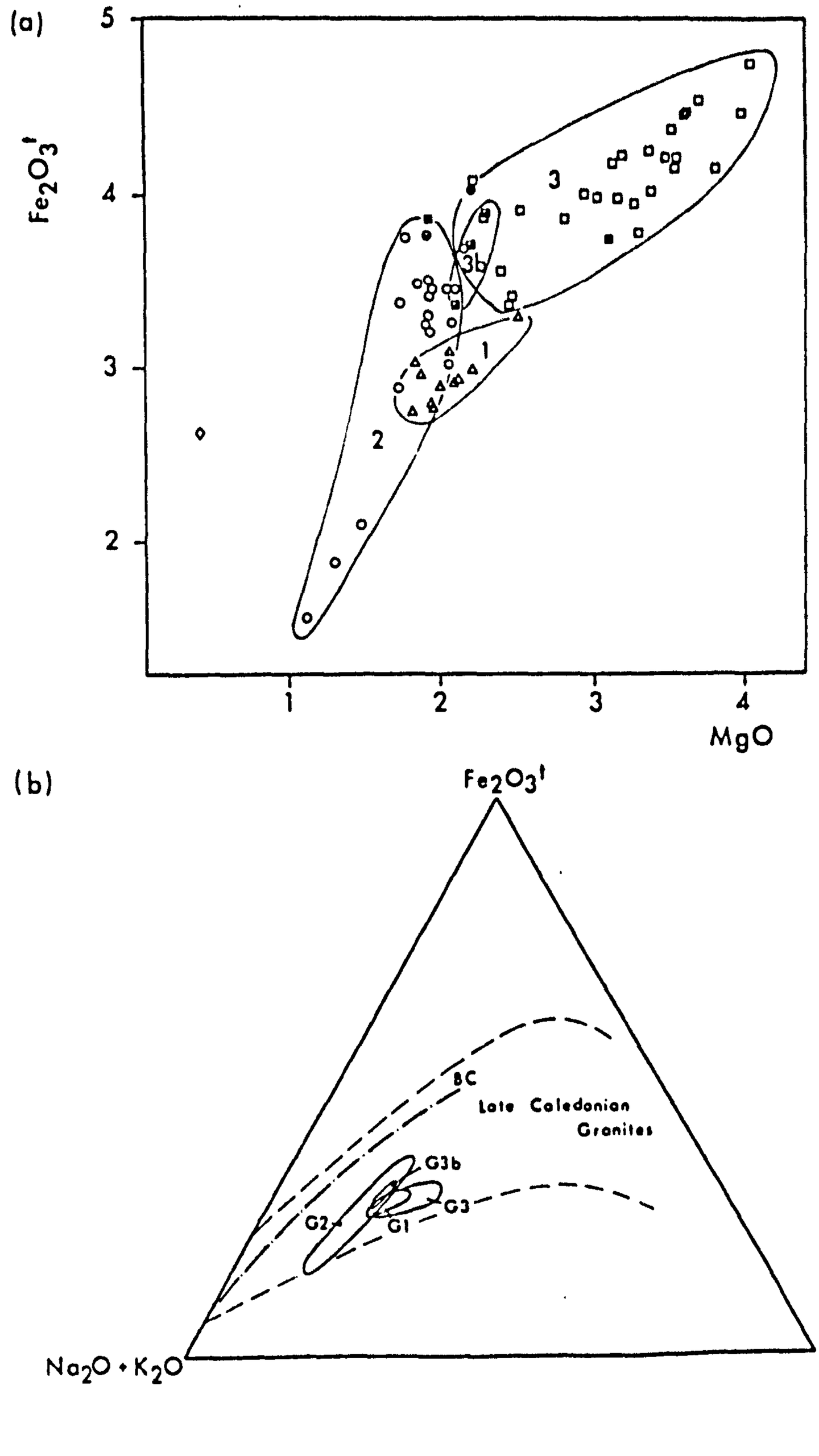

FIGURE 4.10 (a)$Fe_2O_3^t$(total iron as Fe_2O_3) vs MgO. Symbols as in Fig. 4.4a.
(b)AFM plot showing fields for each of the southerly derived granite clast suites together with field for Late Caledonian granite compositions (Stephens and Halliday 1984), and trend of granite clasts in the Benan conglomerate (BC), from Longman (1980).

basaltic rocks undergoing deuteric alteration, the total iron is relatively constant. McKinstry (1966) reached a similar conclusion for a variety of rock types including granites. The high correlation of total iron as Fe_2O_3 against SiO_2 for the granite clasts also suggests low temperature alteration has not modified magmatic iron contents. Alteration would be expected to introduce scatter about magmatic trends.

Oxidation ratios are plotted against LOI in Figure 4.11. A positive correlation for G2 clasts is evident, with increasing oxidation of Fe associated with higher LOI values. Thirlwall (1981) used LOI as an index of alteration in Lower ORS volcanic rocks. A similar correlation between LOI and extent of alteration on the basis of thin-section inspection is recognised here for the granite clasts. Clasts with LOI <2.5% are thought to be relatively free of alteration effects having normal volatile contents with respect to in-situ saturated plutons. Most clasts belonging to G1 and G2 have LOI below 2% whilst G3 clasts fall dominantly in the range 1.5 to 2.5% reflecting their high amphibole content.

Mild hydrothermal alteration might be anticipated for a number of reasons. Firstly, amphibole appears to have been an important liquidus phase indicating the magmas may have been water saturated or at least water rich. These water rich magmas were emplaced into a thick lithic arenite and metagreywacke pile, at least part of which underwent lower greenschist metamorphism. Granite emplacement depths, at least for G3, were very shallow at subvolcanic level, allowing possible interaction with meteoric water systems. Cu is notably enhanced in some samples e.g. 4314, 4386 suggesting limited porphyry-copper style rock-fluid interaction may have taken place. Secondly, low temperature alteration may have occurred during late Silurian unroofing, weathering and production of granite-clast gravels. Sampling from conglomerates presupposes at least one phase of subaerial weathering before final preservation. Lastly the effects of burial diagenesis must be considered. The conglomerates which host the granite clasts were buried to several kilometres after deposition. Sandstones from the conglomerate matrices show

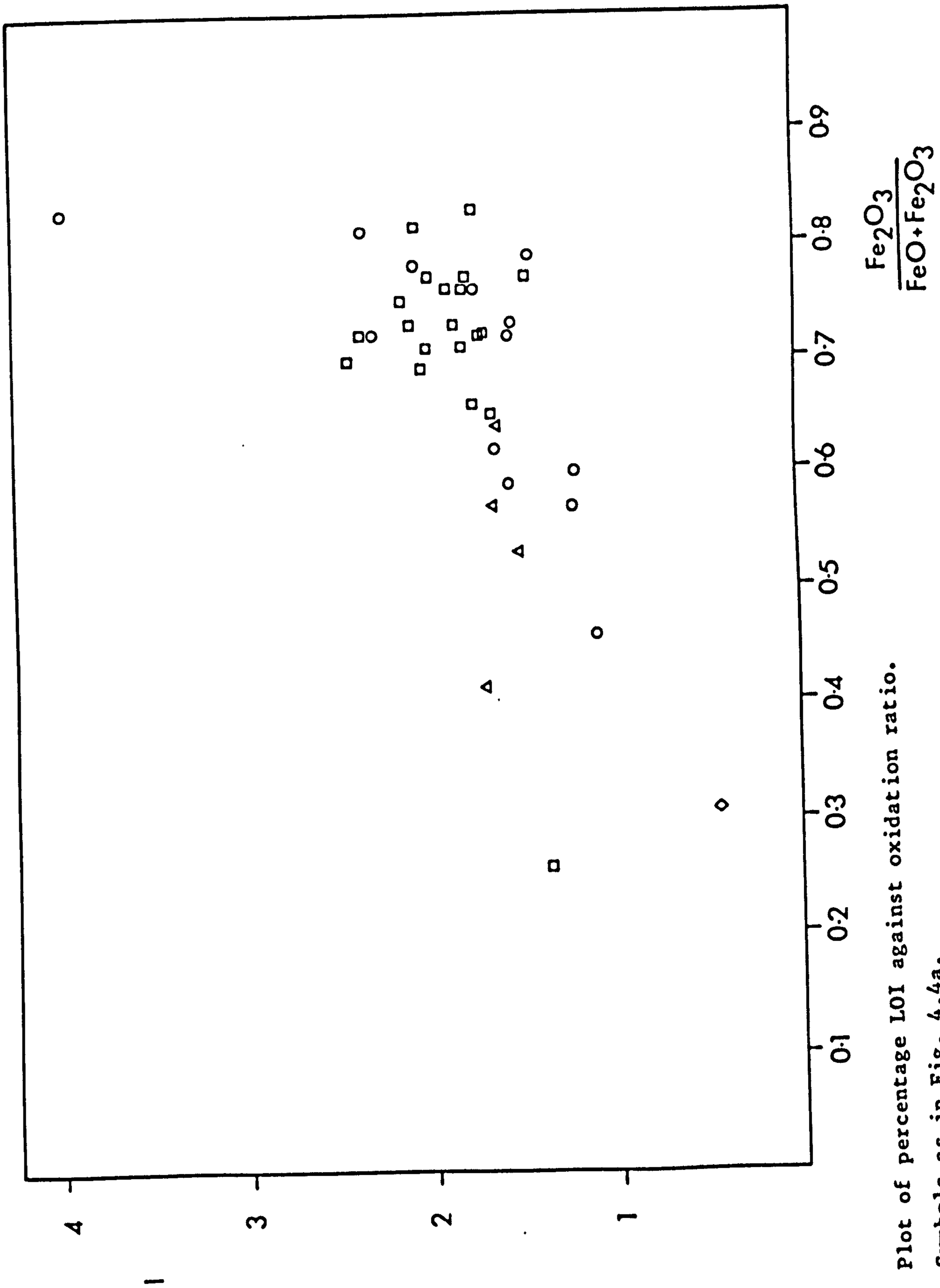

FIGURE 4.11 Plot of percentage LOI against oxidation ratio. Symbols as in Fig. 4.4a.

evidence of aggressive carbonate cementation and it is possible that smaller or fractured clasts have exchanged with formation waters. Many of these secondary effects are avoided by sampling from only the centre of large unfractured clasts which show no evidence for case hardening.

4.4.1.4 P_2O_5, TiO_2

The abundance of P_2O_5 and TiO_2 in granitic magmas is critically controlled by fractionation of apatite and ilmenite and/or biotite. The distribution of TiO_2 with SiO_2 and DI is similar in many respects to that of $(Fe_2O_3)^t$ and MgO against SiO_2 (Fig.4.12a). The three suites show sub-parallel negative trends, broadly linear for G3 clasts, but falling on a well defined curvilinear trend for clasts of G2 type, ignoring clasts 4397 and 4254. 4397 has the highest LOI value of all clasts analysed (LOI >3.5%) and has clearly suffered deuteric alteration. 4254 is contaminated with abundant hornfels xenoliths. The two strongly contaminated clasts, 4254 (G2) and 4335 (G3), are displaced towards more enriched TiO_2 compositions. Lithic arenites and metagreywackes into which G2 and G3 were emplaced have TiO_2 contents between 0.65 and 1.20%. The contaminated clasts are therefore thought to plot on mixing lines between the uncontaminated granite trend and the metagreywacke compositions. 4279, the sole representative of G4, plots on the projected extension of the granite array at higher silica content.

P_2O_5 decreases in all three suites with increasing DI and SiO_2 (Fig. 4.12b), suggesting apatite fractionation occurred over the range of compositions sampled. P_2O_5 is similar to K_2O in that it highlights the compositional gap between each of the suites. Clasts from each of the suites plot along distinct linear and curvilinear trends of different orientation. The G3 suite of clasts is significantly enriched in P_2O_5 over the clasts of other suites and plots with a steeper array projecting to intersect the SiO_2 axis at 73%. The coherent distribution within the suites and the significant separation between them require each suite to represent a series of possibly comagmatic rock types derived from a distinct and separate batch of magma.

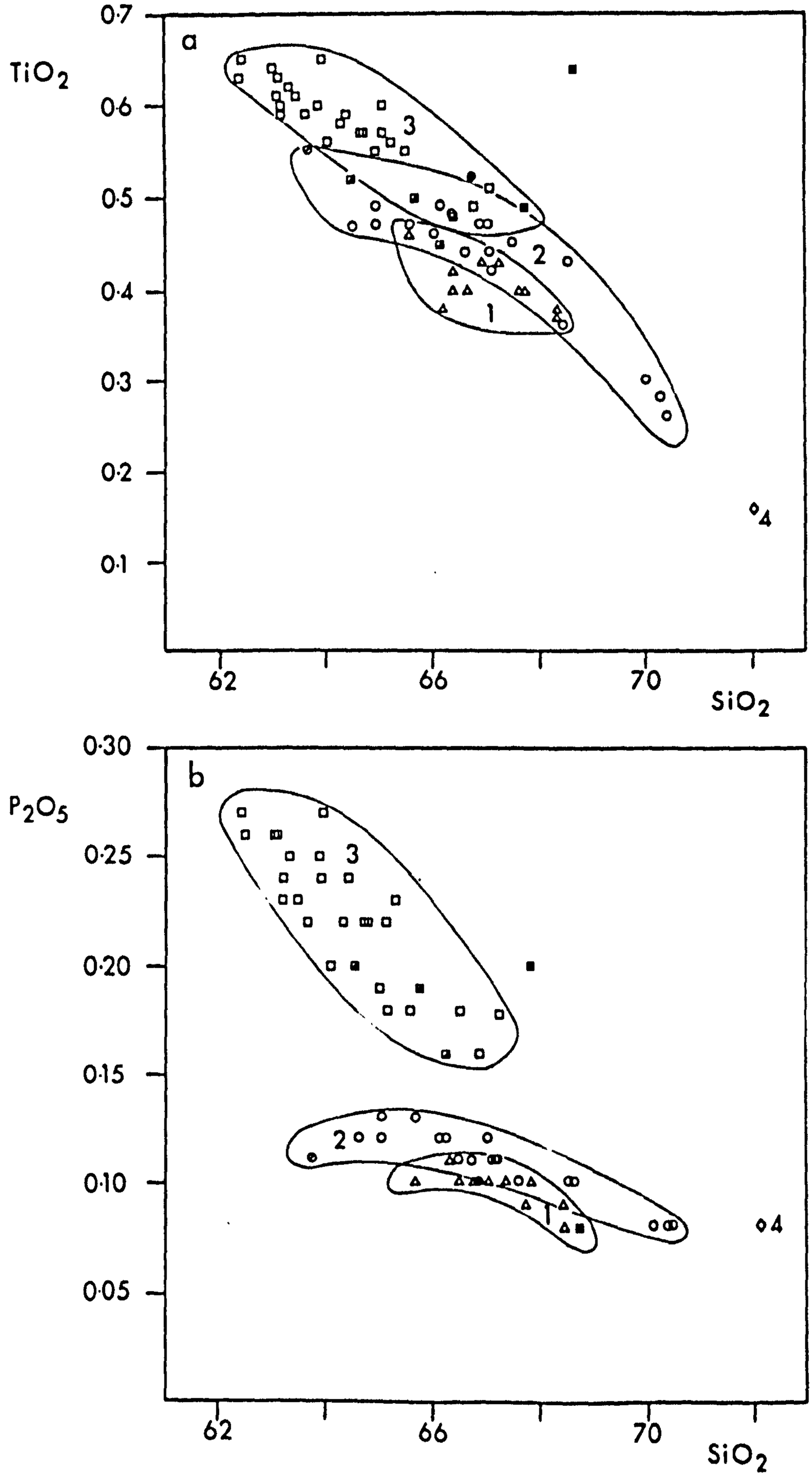

FIGURE 4.12 (a)TiO_2 vs SiO_2 plot for granite clasts of southerly provenance. Symbols as in Figure 4.4a.
(b)P_2O_5 vs SiO_2 plot.

4.4.2 Normative Mineralogy

CIPW norms have been calculated for all analyses using a nominal oxidation ratio of 0.35. The oxidation state of iron can have an important influence on normative values in that increased oxidation leads to higher normative magnetite at the expense of diopside, hypersthene and olivine in the norm (Cox et al. 1979). As An, Ab, Or and Q dominate the normative mineralogy of granite rocks any uncertainty in the estimated oxidation ratio will not significantly influence the normative results. A more serious problem in applying CIPW norms to rocks of granitic composition was raised by Barth (1959). Barth noted that rocks rich in biotite or hornblende often do not produce meaningful CIPW norms in that substantial amounts of potassium in biotite may be assigned to Or. The result is a shift towards the Or apex in Ab-Or-Q projections. Barth (1959) introduced a new normative calculation, the mesonorm, to counter these difficulties in mesozonal rocks. Mesonorm projections have been widely used to interpret rocks of granitic composition (e.g. Brown et al. 1981). Larsen and Sorensen (1960) point out some difficulties with `mesonorm` calculations including the ambiguous nature of the hornblende component. CIPW norms are therefore used here to explore An-Ab-Or-Q relationships.

Two aspects of the normative mineralogy are considered. Firstly, the relationship between normative corundum and diopside with increasing silica, and secondly, relations in the `granite system` An-Ab-Or-Q-(H_2O) following Winkler (1979).

Figure 4.13 demonstrates a continuous trend from diopside-normative to corundum-normative compositions with increasing silica. Such trends are common in many intrusive and extrusive calc-alkaline suites. Cawthorn et al. (1976) showed amphibole compositions to lie on back projections of the calc-alkaline trend and proposed amphibole fractionation as the most plausible model to explain corundum-normative magmas. The three suites G1, G2 and G3 plot in separate fields of Figure 4.13. G2 shows an exceptional range spanning both diopside- and corundum-normative compositions. G3 plots largely in the diopside-normative field and G1 in the corundum-normative field. As the G1 granites which

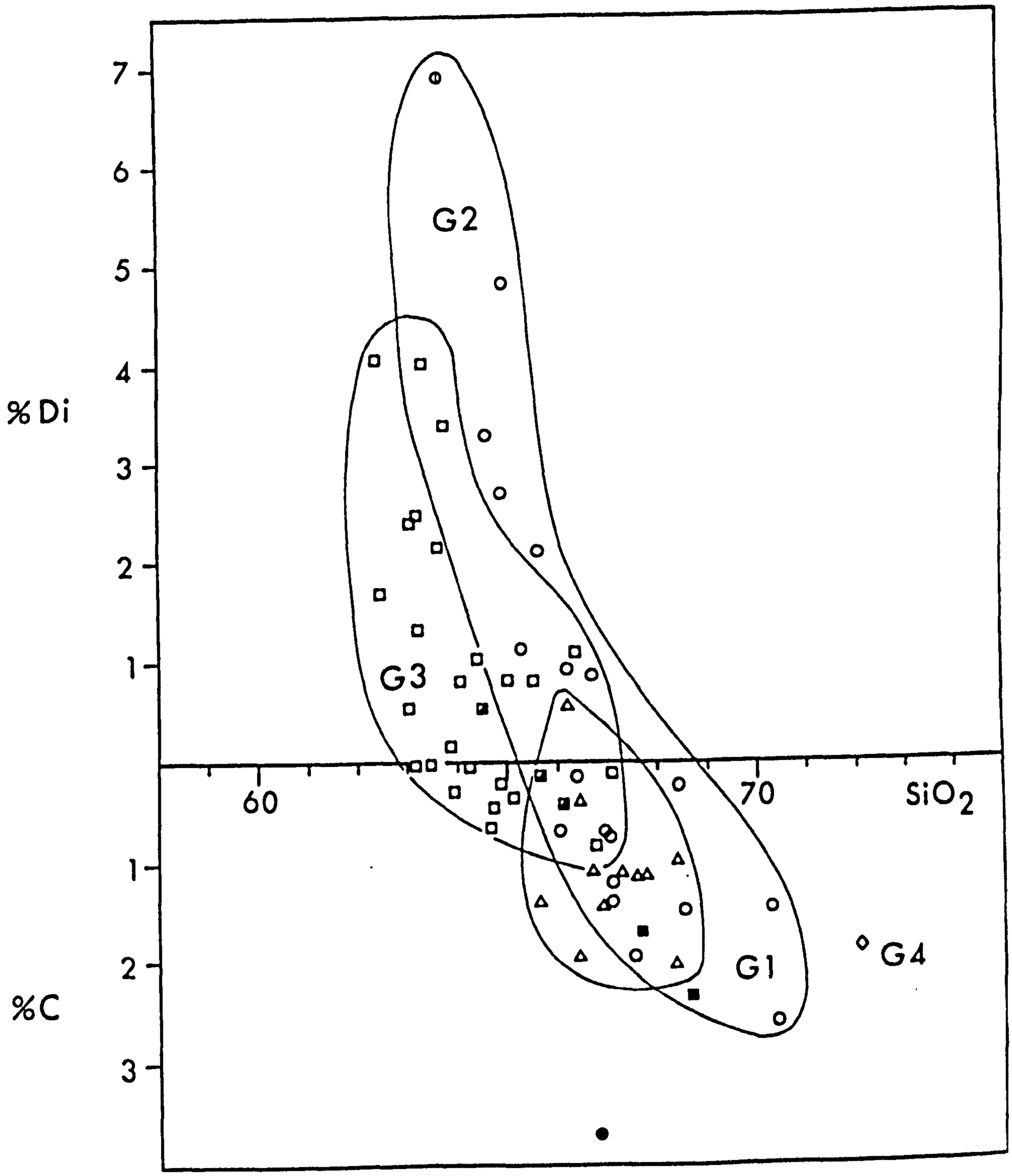

FIGURE 4.13 Plot of normative (CIPW) diopside and corundum vs SiO_2. Corundum normative granite clasts are peraluminous. Symbols as in Figure 4.4a.

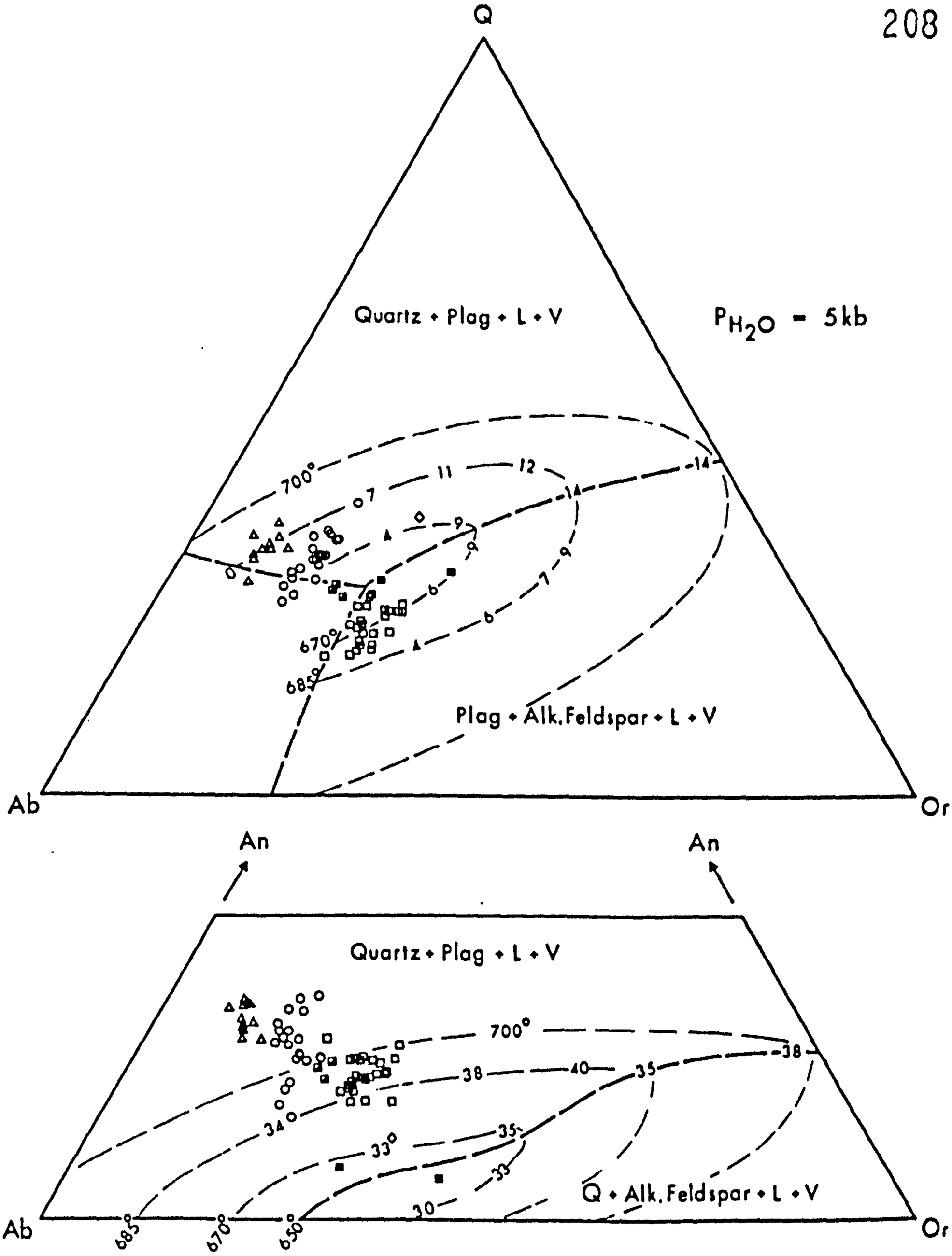

FIGURE 4.14 Normative (CIPW) data plotted in the system Q-Ab-Or-An-H_2O. Data projected from the fourth component onto the Q-Ab-Or and An-Ab-Or ternary faces of a Q-Ab-Or-An tetrahedron. Cotectic surfaces and lines, and the position of the tertiary minimum are for P_{H2O} = P_{total} = 5kb, and are taken from Winkler (1979). Dashed lines are isothermal contours on cotectic surfaces, annotated for the fourth component. Symbols as for Figure 4.4a.

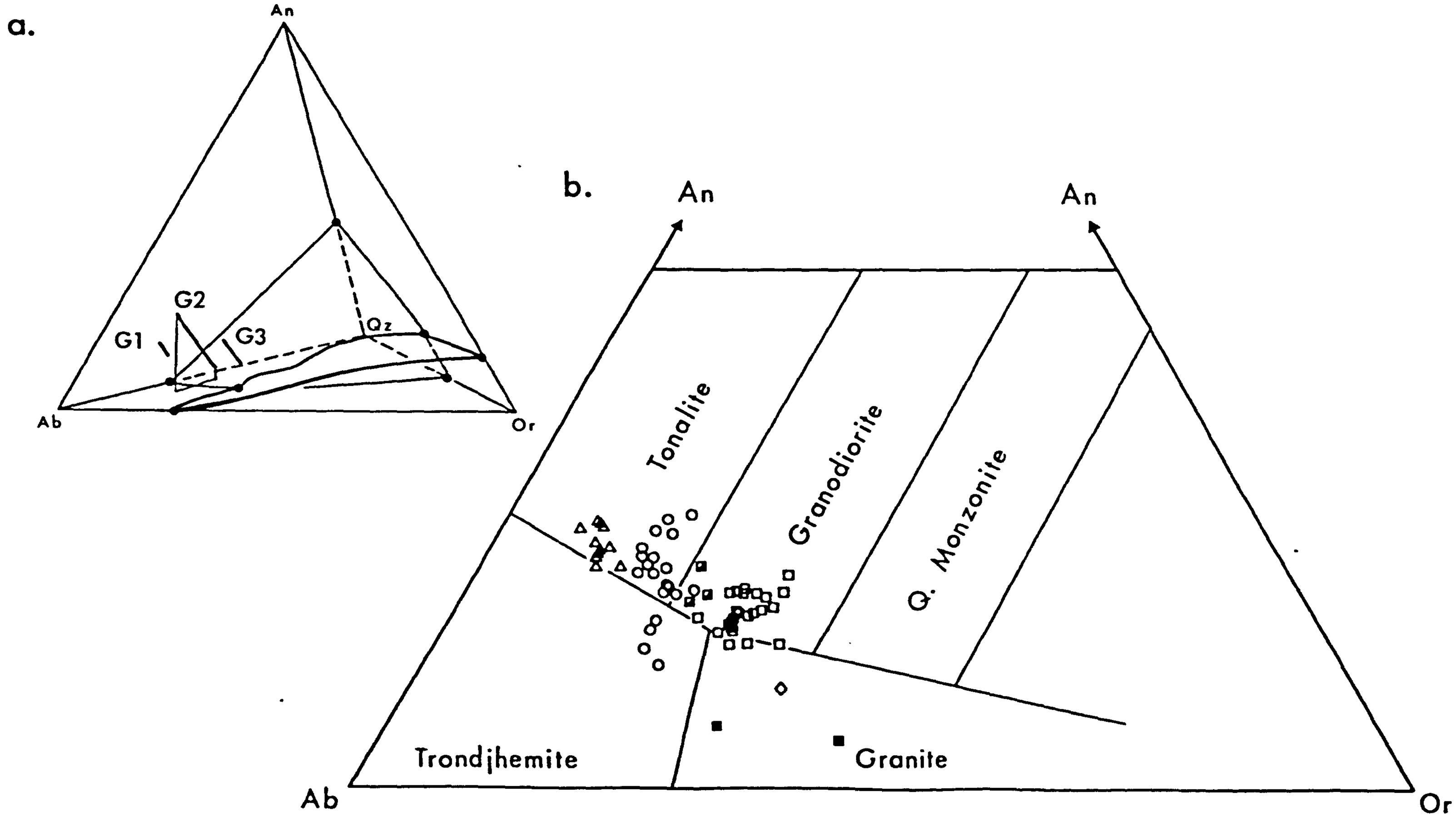

FIGURE 4.15 (a)Q-Ab-Or-An tetrahedron showing position of cotectic surfaces and lines at P_{H2O} = P_{total} = 5kb (after Winkler 1979), together with summary trends for clast suites. (b)clast data plotted on An-Ab-Or triangular plot on which classification grid of O`Connor (1965) is superimposed. Symbols as in Figure 4.4a.

plot with corundum-normative compositions also have the lowest $^{87}Sr/^{86}Sr_i$ (Section 4.5) an origin for the development of corundum-normative magmas by mixing with an aluminous metasedimentary melt component, as developed by Stephens and Halliday (1979) for Southern Uplands granites, is improbable for G1. Given the importance of amphibole as a likely liquidus phase in the petrogenesis of the granite clasts, amphibole fractionation is considered to have governed the development of corundum-normative compositions. The extreme variation in G2 is however accompanied by a modest increase in initial ratio with increasing SiO_2 suggesting the evolved peraluminous compositions may reflect an increasing meta-sediment contribution to the alumina budget.

Normative data are plotted in the system Q-Ab-Or-An-H_2O in Figure 4.14. The data are projected from the fourth component onto Q-Ab-Or and An-Ab-Or ternary faces of a Q-Ab-Or-An tetrahedron. A perspective view of the system Q-Ab-Or-An-H_2O is shown in Figure 4.15 showing the relevant cotectic surfaces at pH_2O = 5Kb, and summary trends for the clast data. The position of the cotectic surfaces and lines, and the ternary minimum follow Winkler (1979) and Winkler et al. (1975, 1978) and assume $P_{H2O} = P_{total}$ = 5kb. This is the pressure at which the geometry of the system is best understood (Brown et al. 1981). The ternary data have been plotted by summing the apex components to 100%.

A number of conclusions can be drawn from the data displayed on these plots.

1. The plots suggest clearly different but sub-parallel fields for each of the granite clast types G1, G2 and G3. Each suite defines its own curve, originating in the plagioclase field, at a high angle to the quartz saturation field. This suggests separate equilibrium fusion events may be the underlying mechanism whereby suite diversity is established (Presnall and Bateman 1973, Atherton et al. 1979).
2. Trends for individual suites mimic the general trend for Sierra Nevada granitoids (Bateman et al. 1963, Presnall and Bateman 1973, Noyes et al. 1983) trending away from the An apex towards the Ab-Or-Q base and the Or-Q sideline. This trend is

best developed for G2. The scatter in the data for G3 reflects heterogeneity introduced by the considerable crustal assimilation indicated by the abundant xenoliths in clasts of this type.

3. Trends for each of the clast suites are displaced towards the Or apex in the order G1, G2 to G3.

4. All the data plot in the plagioclase primary phase field, much of it some distance from the cotectic surfaces.

5. The data for G3 plot close to the ternary eutectic. K-feldspar does not form a phenocryst phase in these granites and the eutectic compositions indicated by the quenched granophyric matrices must have been arrived at via the quartz saturation surface.

4.4.3 Trace Element Geochemistry

Granite systems are less amenable to rigorous trace-element modelling than their basaltic counterparts. The rheology of granite magmas is such that a complete separation of mineral and melt phases is not easily achieved, and as a result, processes of crystal fractionation are less efficient. Granite magmas are best visualised as complex crystal-liquid mushes rather than true liquids and in addition, they may contain a residual or restite component inherited from a source melting event. Trace element variation within a related suite of granites may therefore reflect a wide range of possible processes including partial melting, the entrainment of restite, differentiation, crustal contamination and magma mixing. As no single process may dominate the chemical diversity so produced, unravelling the petrogenetic history is often difficult and not without controversy (Tarney and Saunders 1979).

Trace element modelling requires that elements obey Henry's Law for the phases under consideration. Whilst some elements may be present in trace amounts in granitic rocks they may be concentrated as essential structural components in minor mineral phases. Zr and P are often present in trace amounts in granites but their concentrations are strongly determined by the behaviour of the accessory minerals, zircon and apatite respectively.

A further difficulty in the application of trace elements to granite petrogenesis is the poorly constrained nature of mineral-melt distribution coefficients for intermediate and acid magmas. These coefficients are strongly dependent on the temperature and composition of the mineral and melt under study (McIntire 1963). Thus the behaviour of a given element in terms of its distribution between melt and residual or crystallising phases may radically alter during the progressive evolution of a magma. Mineral-melt distribution coefficients used below are from the compilations of Pearce and Norry (1979) for Ti, Zr and Y, Hanson (1978), Arth (1976) and McCarthy (1976) for Ba, Rb and Sr.

Notwithstanding the above limitations, trace elements may be usefully used both to refine petrogenetic models for the evolution of acid magmas and to `image` their source materials. The following account concentrates on the broader features of the trace element distributions both within and between the three granite suites with a view towards assessing likely fractionating phases and establishing the relationship between the suites and their respective sources. More detailed interpretation requires mineral chemistry and REE data, as yet unavailable for the granite clasts.

4.4.3.1 Large Ion Lithophile Elements. Ba, Rb, Sr.

The LIL elements, Ba, Rb, and Sr, are useful petrogenetic tracers in granite systems in that their abundance is sensitive to the behaviour of the major silicate minerals and not the less significant accessory phases (McCarthy and Hasty 1976). Progressive Rb-enrichment paralleled by a depletion in Ba and Sr is commonplace in granitic rock suites and has widely been interpreted as the result of fractional crystallisation. McCarthy and Robb (1978) showed Ba to initially increase in systems dominated by plagioclase fractionation with subsequent depletion associated with a change in the cumulus mineralogy with the incoming of K-feldspar as a cumulus phase. Cumulus-melt relationships are however often merged in granitic systems by crystallisation of trapped interstitial liquid reflecting the inability of viscous and crystal-charged mushes to completely separate cumulus and melt phases.

	Ba	Rb	Sr	Ce	
BIOTITE	6.36	3.26	0.12	-	(1)
	9.70	2.24	-	-	(2)
	10.0	3.0	0.4	-	(3)
	-	-	-	0.32	(4)
K-FELDSPAR	6.12	0.659	3.87	-	(1)
	6.12	0.34	3.87	-	(2)
	6.0	0.80	3.60	-	(3)
	-	-	-	0.04	(4)
PLAGIOCLASE	0.308	0.041	4.40	-	(1)
	0.36	0.048	2.84	-	(2)
	0.40	0.04	3.35	-	(3)
	-	-	-	0.30	(4)
HORNBLENDE	0.054	0.0077	0.094	-	(1)
	0.044	0.0140	0.22	-	(1)
	-	-	-	1.50	(4)
GARNET	0.017	0.0085	0.015	-	(1)
ORTHOPYROXENE	0.0029	0.0027	0.0085	-	(1)
CLINOPYROXENE	0.131	0.032	0.516	-	(1)

	Ti	Zr	Y	
PLAGIOCLASE	0.05	0.03	0.06	(5)
BIOTITE + ZIRCON	2.50	2.00	2.00	(5)
HORNBLENDE	3.00	1.40	2.50	(5)
MAGNETITE	9.00	0.20	0.50	(5)
ORTHOPYROXENE	0.25	0.08	0.45	(5)
CLINOPYROXENE	0.40	0.25	1.50	(5)
APATITE	0.10	0.10	40	(5)

1: HANSON (1978)

2: ARTH (1976)

3: MCCARTHY (1976)

4: COX *et al.* (1979)

5: PEARCE AND NORRY (1979)

TABLE 4.2 Mineral-melt distribution coefficients for intermediate and acid magmas.

Sr-Rb, Sr-Ba and Rb-Ba logarithmic projections of the southerly derived granite clast data are shown in Figure 4.16a-c and serve to illustrate the distribution of the LIL elements between the three granite suites recognised. In addition to the granite data, eleven whole-rock analyses of porphyritic andesite and dacite clasts, also of southerly derivation, are included. These have been selected on the basis of being the least altered of the volcanic clasts sampled, with LOI values of less than 3% and SiO_2 greater than 60%. Theoretical fractionation vectors for the change of composition of a melt as a result of fractional crystallisation of various phenocryst phases are also plotted. These have been calculated assuming a Rayleigh-type fractionation model using mineral-melt distribution coefficients given in Table 4.2. These are taken from compilations by Hanson (1978), Arth (1976) and McCarthy (1976).

Figure 4.16 highlights large ranges in both Rb and Ba and a remarkable consistency in Sr between the three granite suites. The Sr content of G2 is slightly depleted relative to G3 but both show a comparable range in Rb. G1 has notably low concentration of Rb as might be expected in a low-K tonalite of this type. Samples which show obvious metasediment contamination in containing abundant xenoliths (4254) or which are close to granite-country rock margins (4335) plot to lower Sr values. Greywackes which are thought to host the plutons have low Sr contents, significantly lower than Southern Uplands greywackes (Tindle and Pearce 1984). Assimilation of material of this type would lower the bulk Sr content of the magma. Assimilation alone however cannot explain the slightly lower Sr content of G2 samples with respect to G3 in that metasediment xenoliths are abundant in G3 clasts implying emplacement by stoping and the potential for considerable contamination. This is confirmed by the isotopic data (section 4.5).

Sample 4279 (G4) also plots with depleted Sr relative to other granite clasts emphasising its very different character. It is clearly unrelated to G1, G2 or G3.

FIGURE 4.16 Large ion lithophile element covariation. Vectors indicate the change in melt composition as a result of fractional crystallisation of the named phenocryst phases. Constructed using mineral-melt distribution coefficients given in Table 4.2. Symbols as in Figure 4.4a, except solid triangles which are the least altered of the southerly derived porphyritic andesite clasts. Abbreviations are: Bi-biotite; AMB-amphibole; PLAG-plagioclase; OPX-orthopyroxene; Gt-garnet; CP-clinopyroxene; K-SPAR-K-feldspar. Letters refer to different estimates of the distribution coefficients (Table 4.2). The percentage of fractional crystallisation of the original melt to produce corresponding changes in Rb, Sr and Ba abundances is indicated along the vectors. (a)Sr vs Rb plot (b)Sr vs Ba plot (c)Ba vs Rb plot (d)Sr and Rb(ppm) vs SiO_2 (%).

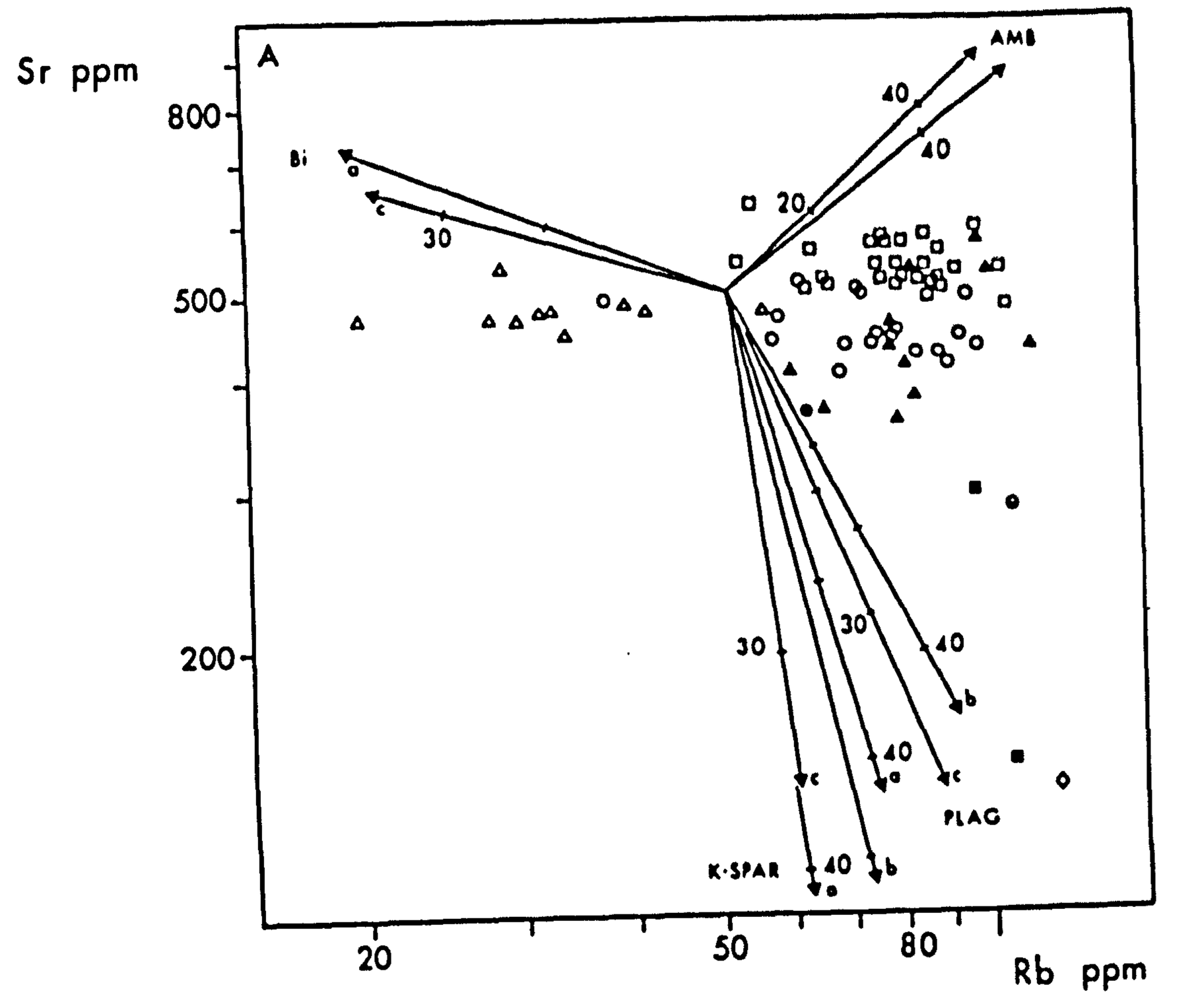
A
Sr ppm
800
500
200
20
50
80
Rb ppm
AMB
40
40
Bi
c
30
20
30
40
b
30
40
c
a
c
PLAG
K-SPAR
40
b
a

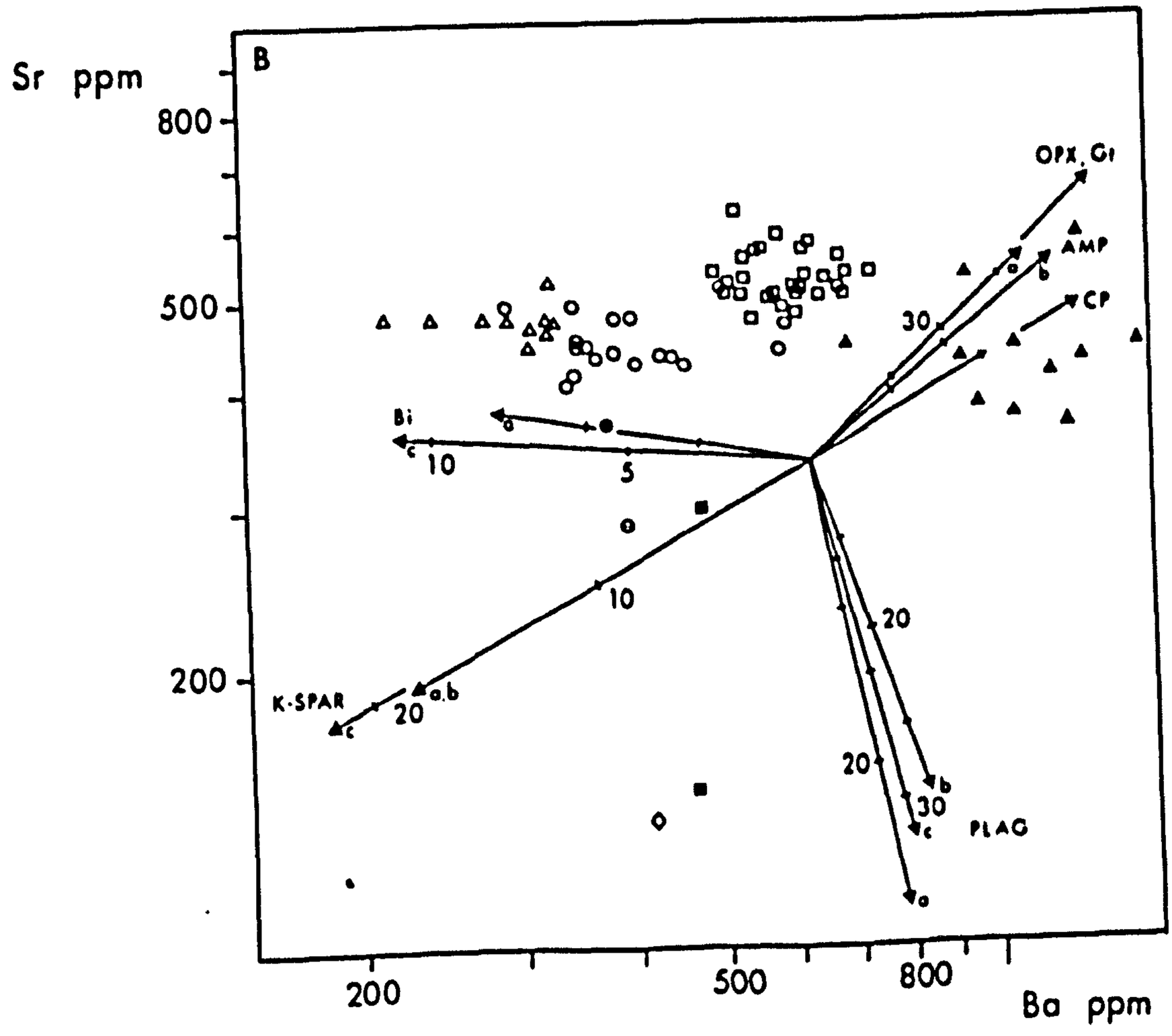
B
Sr ppm
800
500
200
200
500
800
Ba ppm
OPX, Cl
AMP
CP
30
Bi
c
10
5
10
K-SPAR
20
a,b
c
20
20
b
30
c
a
PLAG

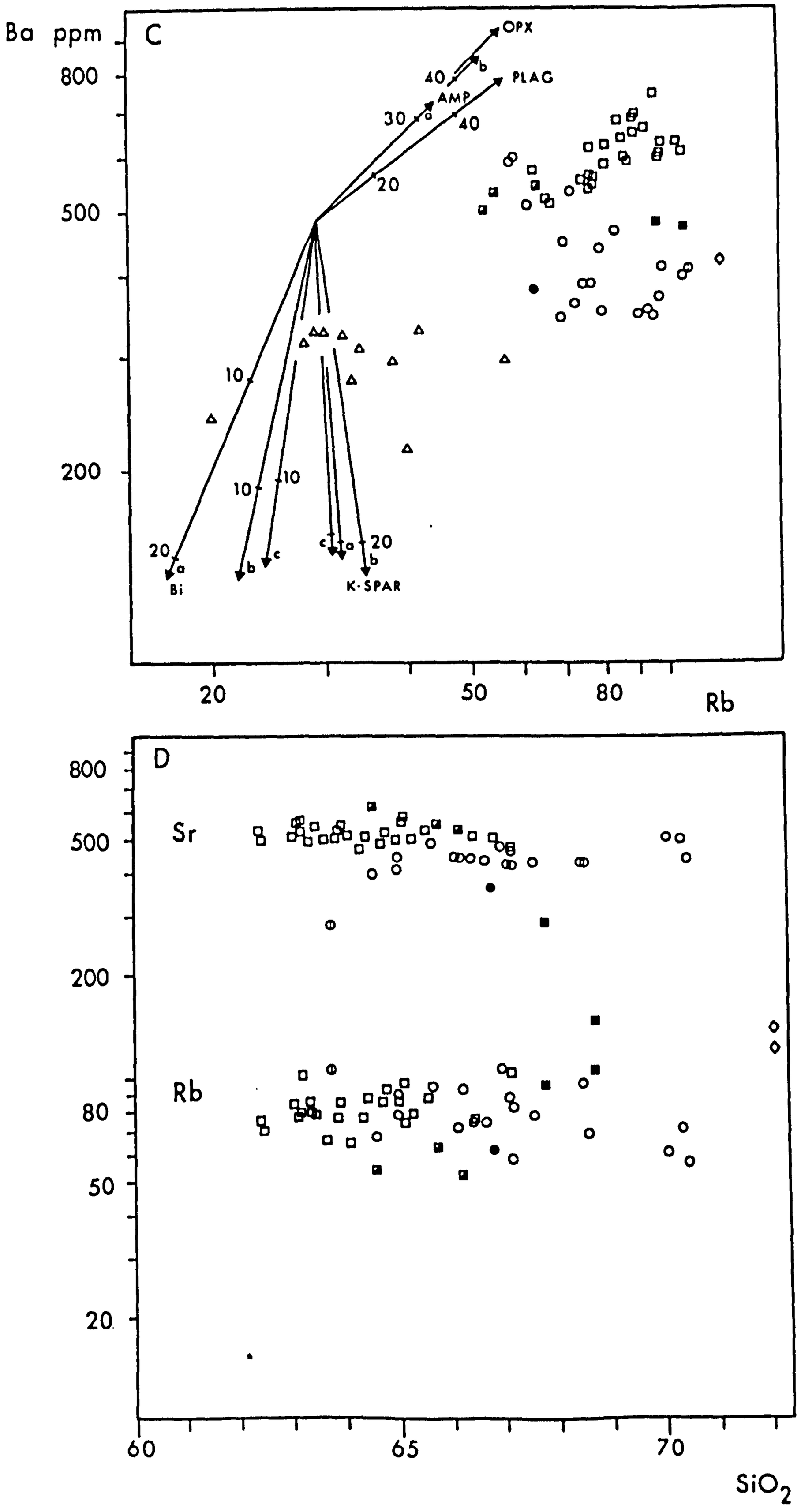
Ba ppm
C
800
500
200
OPX
PLAG
AMP
40
b
30
a
40
20
10
10
10
20
a
b
c
c
a
20
b
Bi
K-SPAR
20
50
80
Rb
D
800
500
200
80
50
20
Sr
Rb
60
65
70
SiO2

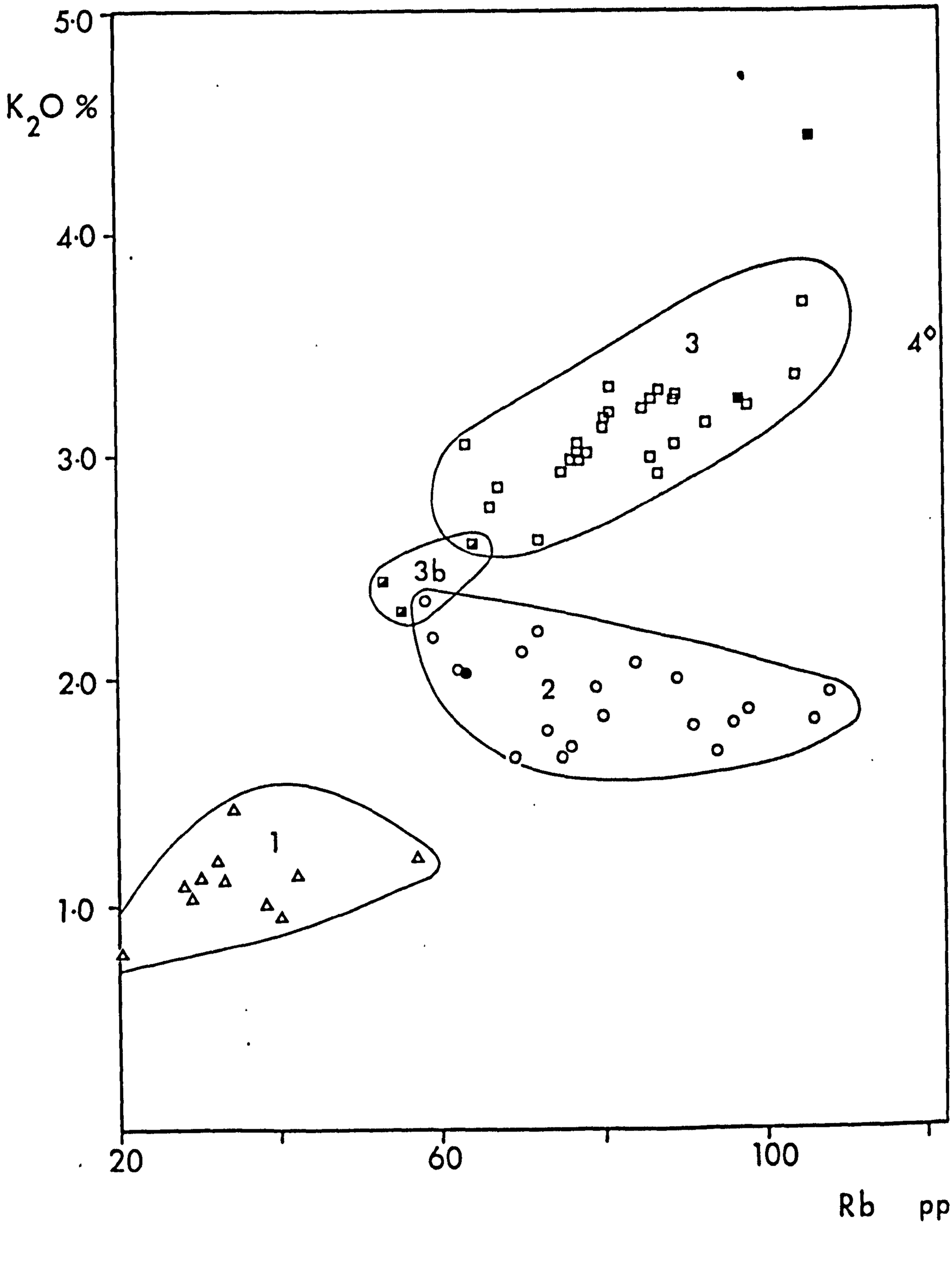

Figure 4.17 K_2O vs Rb plot for granite clasts of southerly provenance. The G3 hornblende biotite granodiorites, and to a lesser extent the foliated tonalite clasts (G1), have normal positive correlations. Data for the biotite granites assigned to G2 however show an anomalous negative trend. It is possible that this is the result of grouping together clasts which although showing a general geochemical coherence, are not truly comagmatic. Symbols as in 4.4a.

The lack of a significant decrease in Sr abundance with increasing Rb, DI and SiO_2 (Fig. 4.16d) precludes the involvement of plagioclase or K-feldspar fractionation alone in generating the within-suite compositional variation. Rb/Sr ratios are constant for G1 and G3 and marginally decrease with fractionation for G2. K/Rb ratios for G2 and G3 show scattered, though positive, trends when plotted against SiO_2 or DI. Calculated fractionation vectors for K-feldspar and plagioclase intersect LIL data trends at high angle on logarithmic projections. If fractional crystallisation is considered to account for the chemical variation, mafic rather than felsic mineral phases must dominate the fractionation scheme. This is borne out by the petrography of G3 granite clasts in particular. Euhedral amphibole and biotite are ubiquitous suggesting both were important liquidus phases. The presence of hornblende as a liquidus or near liquidus phase has important implications for the water content of the magmas. Piwinskii and Wyllie (1970), Eggler and Burnham (1973) and Stern (1975) all show amphibole to be the dominant liquidus phase in saturated calc-alkaline magmas. The implications of water saturation or at least high water contents are returned to in Section 4.6.4.

Both Sr and Ba are enriched over comparable Lachlan granitoids (White and Chappell 1983) and Palaeozoic granites of southern Newfoundland (Elias and Strong 1982). Halliday and Stephens (1984) showed enhanced Sr contents to characterise all $\underline{c}$ 400Ma late Caledonian granites north of the Iapetus suture with the exception of a group of low Sr intrusives which can be shown to have undergone extensive low pressure fractionation. Thirlwall (1981, 1982) demonstrated similar spatially variable Sr enrichment in related ORS volcanic rocks. As granites of similar age in eastern Canada and the Appalachians do not show elevated Sr and Ba Halliday and Stephens (1984) conclude that granites of Britain and Ireland owe their unique chemical fingerprint to spatially restricted processes operating within the confines of a high-K, high-Sr chemical province. Significantly, the development of high Sr magmas may also be temporally restricted. Ordovician granites preserved as clasts within fore-arc conglomerates overlying the Ballantrae ophiolite do not show

anomalous Sr contents (Longman 1980). These clasts however are silicic, with SiO_2 commonly 70%, indicating the suite to be evolved and to have probably suffered feldspar fractionation and subsequent Sr depletion. Similarly, the older Caledonian granites (Pankhurst and Pidgeon 1976, Pidgeon and Johnson 1974) and the c 460Ma granites of NE Scotland (Pankhurst 1974) also have modest Sr contents. The lower Sr abundances in these granites however reflect their origin as anatectic crustal melts. It is therefore not possible to establish whether the high-K, Sr magma source that was widely available during c 400Ma late Caledonian magmatism existed prior to this, as a comparable source was not tapped during earlier largely anatectic melting episodes.

Halliday and Stephens (1984) consider several mechanisms whereby Sr enriched magmas may be generated. These include low degree partial melts from mantle sources in which plagioclase is not a stable phase, melting of a feldspathic source and fusion of granulite facies basement. The lack of significant europium anomalies (Pankhurst 1979) and the refractory nature of granulite facies crust make the latter two mechanisms unlikely. They conclude derivation from a feldspar free source which had not had an upper crustal history to best satisfy the data. On the basis of common high Ni diorites and volcanic rocks (Thirlwall 1981) a mantle component is likely. Stephens and Halliday (1984) suggest the mantle component may have been introduced to a lower crustal magma source region by a process of hydrous fluid transfer.

4.4.3.2.High field strength elements : Zr, Y, Nb

High field strength elements (i.e. those with high charge/radius ratios) are not easily transported in aqueous fluids and tend to remain unaffected by low temperature alteration. They have therefore been used to fingerprint altered and spilitised basic rocks with respect to their original tectonic environment (Pearce and Cann 1973, Floyd and Winchester 1975, 1978). Pearce and Norry (1979) have developed a petrogenetic framework for the interpretation of Zr, Nb, Y and TiO_2 covariation in volcanic rocks of basic, intermediate and acid compositions. They use data from experimental runs, coexisting phases in ultrabasic

rocks and phenocryst-matrix pairs in volcanic rocks to compile relevant mineral-liquid distribution coefficients. McCourt (1981) qualitatively applied HFS modelling using Pearce and Norry`s framework to rocks of granitic composition. The interpretation of such data in granite systems is hampered by the overriding control of zircon, apatite and Fe-Ti oxides on the respective distributions of Zr, Y and TiO_2. It may therefore be difficult to isolate the role of major silicate phases in generating HFSE chemical variation against a background of accessory mineral fractionation.

In the absence of, or with subdued accessory phase fractionation, Y, Zr and Ce should all increase progressively in successive differentiates if plagioclase dominates the fractionation series. Y and Zr should decrease and Ce increase in series strongly influenced by hornblende fractionation (Lambert and Holland 1974).

Y-Zr and TiO_2-Zr logarithmic projections for the granite clast data (Fig. 4.18) show steep arrays with granites from each of the three suites plotting in distinct fields. Zr concentrations are relatively constant within each of the suites but there is a significant between-suite variation with increasing Zr content in the order G1<G2<G3. Zr variation with DI and SiO_2 content shows uniform Zr contents with supposed fractionation for G1, whilst G2 and G3 show poorly defined negative correlations. These may reflect minor zircon fractionation.

Y concentrations fall with increasing DI and SiO_2. The relationship is best defined for G2, which shows a decrease from 20 to 6 ppm with increasing fractionation. Y is strongly partitioned into apatite (K_d = 40). Linear trends for P_2O_5 vs SiO_2 suggest apatite fractionation took place in all three suites. Y depletion in more evolved samples undoubtedly partly reflects removal of apatite. Theoretical fractionation vectors, constructed using distribution coefficients arrived at by Pearce and Norry (1979) for intermediate and acid compositions, are also plotted in Figure 4.18a. They are consistent with amphibole fractionation accompanying removal of apatite but note that

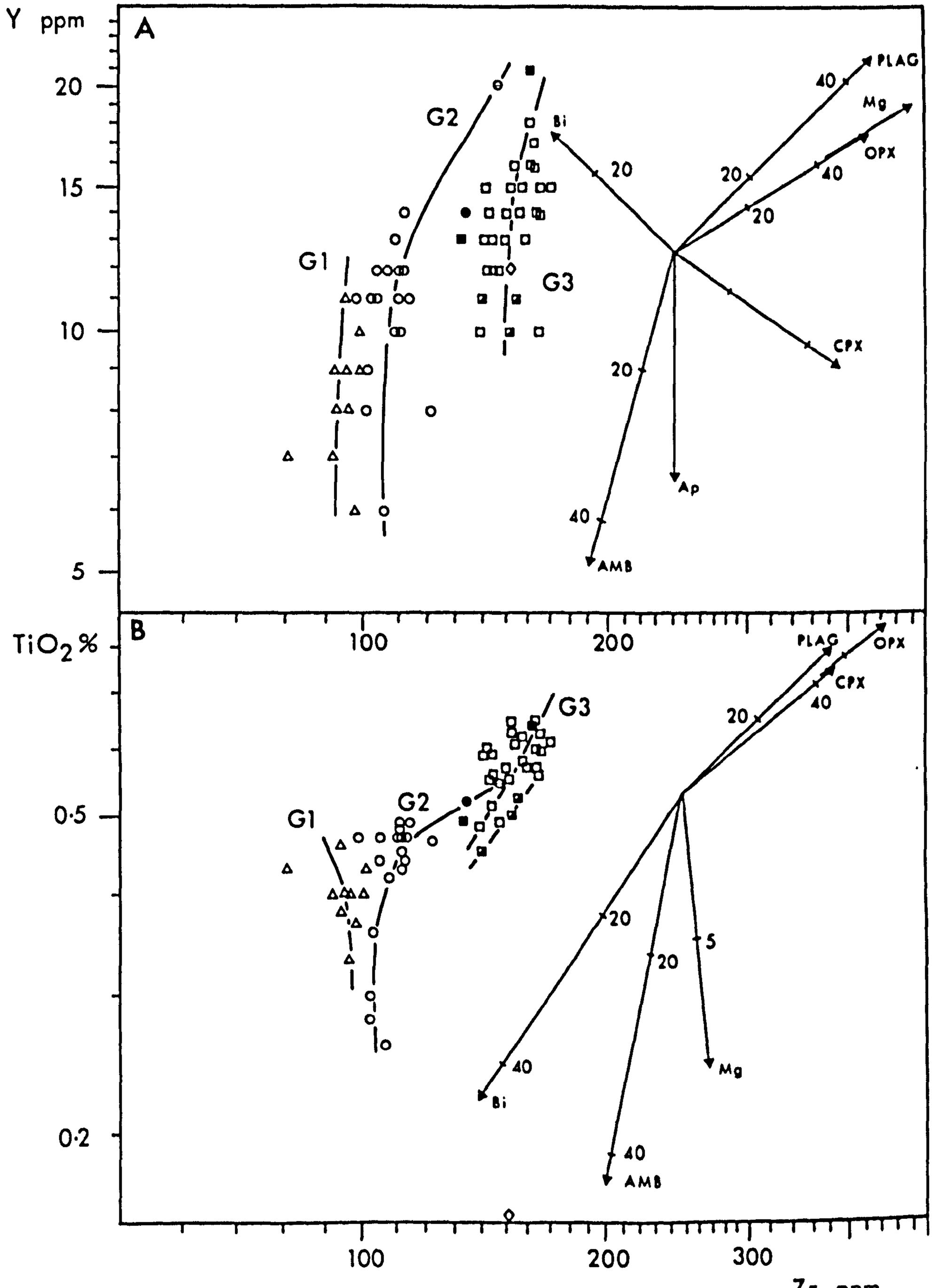

FIGURE 4.18 High field strength element covariation in granite clasts of southerly provenance. Vectors for percentage fractional crystallisation constructed using mineral-melt distribution coefficients of Pearce and Norry (1979) given in Table 4.2. Symbols as in Fig. 4.4a. Abbreviations used are: Bi, biotite PLAG, plagioclase; Mg, magnetite; OPX, orthopyroxene CPX, clinopyroxene; AMB, amphibole; Ap, apatite.

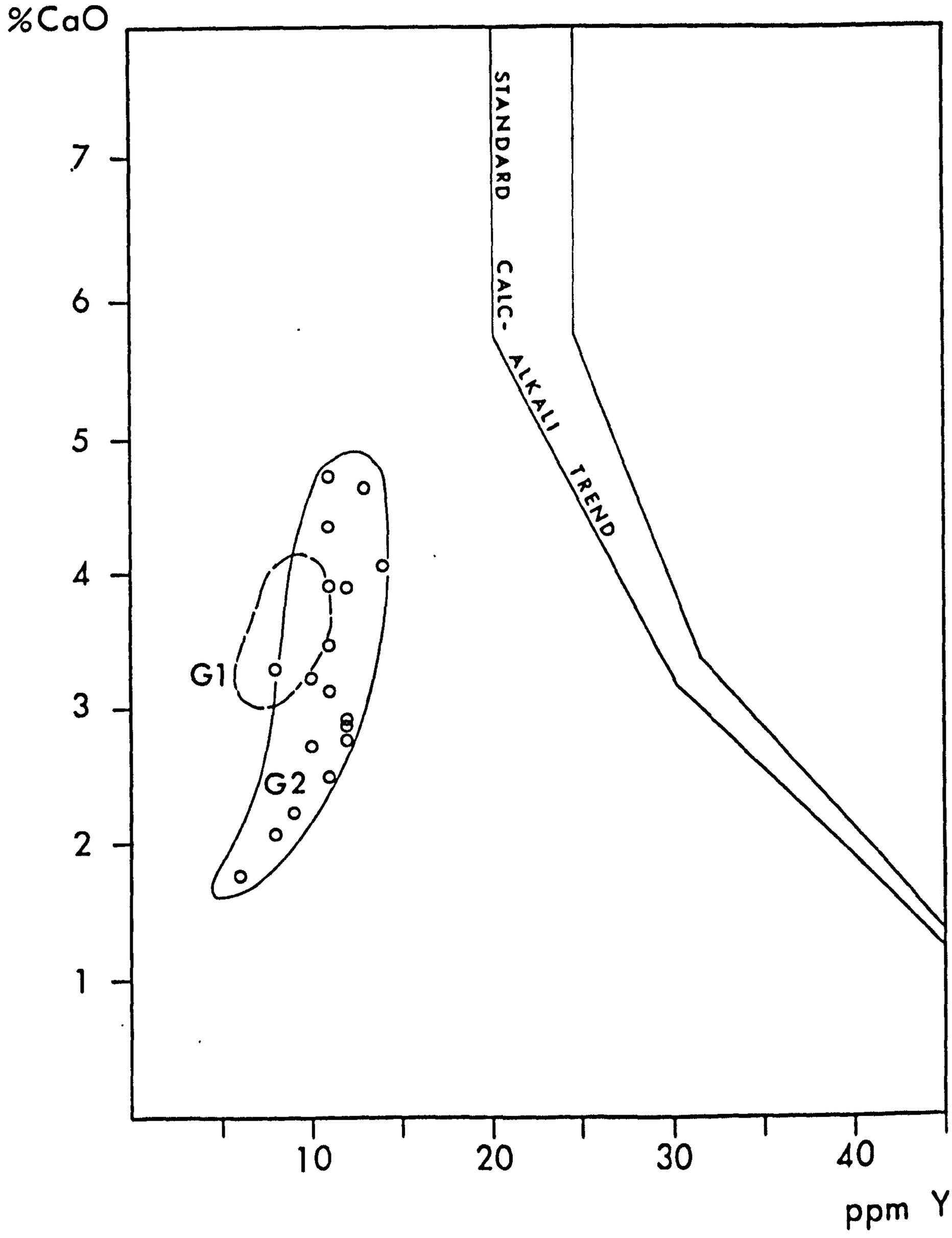

Figure 4.19 CaO vs Y plot with standard calc-alkali trend from Lambert and Holland (1974). Clasts assigned to G2 show a J-type trend.

plagioclase fractionation would drive the residual melt composition in a direction opposite to that observed.

TiO_2 also shows a good negative correlation with increasing SiO_2. This is most likely to reflect extraction of Fe-Ti oxides and/or biotite. TiO_2-Zr covariation can be modelled in terms of varying proportions of biotite, amphibole and magnetite (Fig.4.18b). Again notice plagioclase fractionation produces trends contrary to those observed.

Lambert and Holland (1974) use the close affinity of Y and CaO to distinguish J-type or hornblende series from L-type or pyroxenitic series with respect to a standard calc-alkaline trend on an CaO-Y covariation plot. The standard calc-alkaline trend is plotted along with the granite clast data for G2 in Figure 4.19. The clasts have a J-type distribution similar to other calc-alkaline suites characterised by Y depletion at low CaO. J-trends are most easily explained as hornblende, calcic-garnet and/or to some extent apatite fractionation. L-trends would result from kaesutite or plagioclase and clinopyroxene fractionation at high CaO, or K-silicate fractionation at low CaO (Lambert and Holland 1974).

The results of qualitative HFSE modelling, although necessarily limited by uncertainties in the effects of minor phase fractionation, do concur with the LIL modelling in suggesting hornblende and biotite to be important fractionating phases in producing the within-suite variation. Feldspar fractionation probably was sufficient to buffer Sr enrichment, but clearly did not dominate the fractionation scheme.

4.4.3.3.Ni, Cr

Ni and Cr are particularly intriguing trace elements in Caledonian magma petrogenesis. Ni contents in many Lower ORS basalts and andesites (Thirlwall 1981), and in the least evolved dioritic plutonic rocks like Kilmelford (Halliday and Stephens 1984) are high enough to require the magmas to represent liquids of mantle derivation, relatively uncontaminated by continental crust and free from the effects of mafic fractionation.

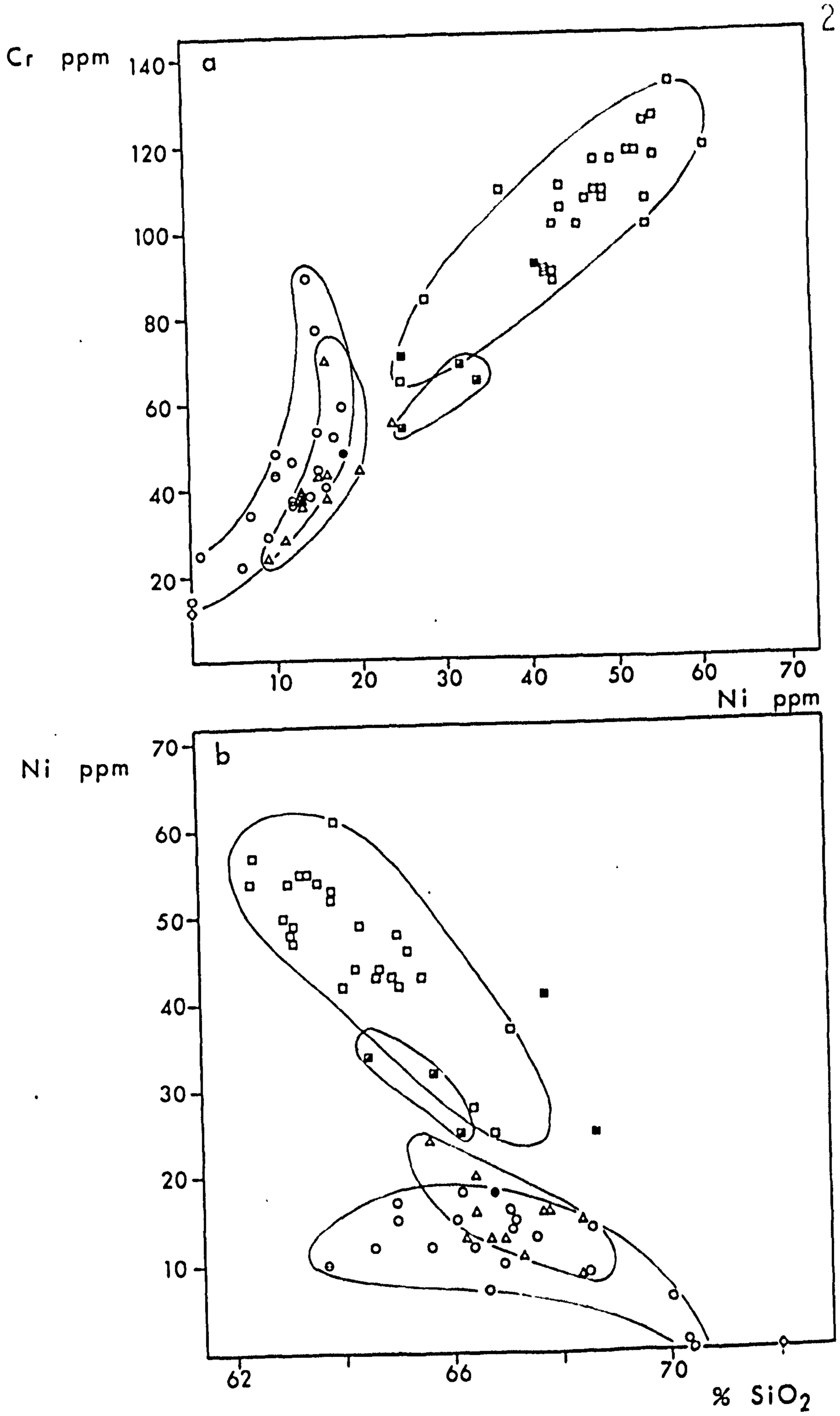

FIGURE 4.20 (a)Plot of Cr vs Ni (ppm) for granite clasts of southerly provenance. Symbols as in Fig. 4.4a.
(b)Plot of Ni (ppm) vs SiO_2 (%).

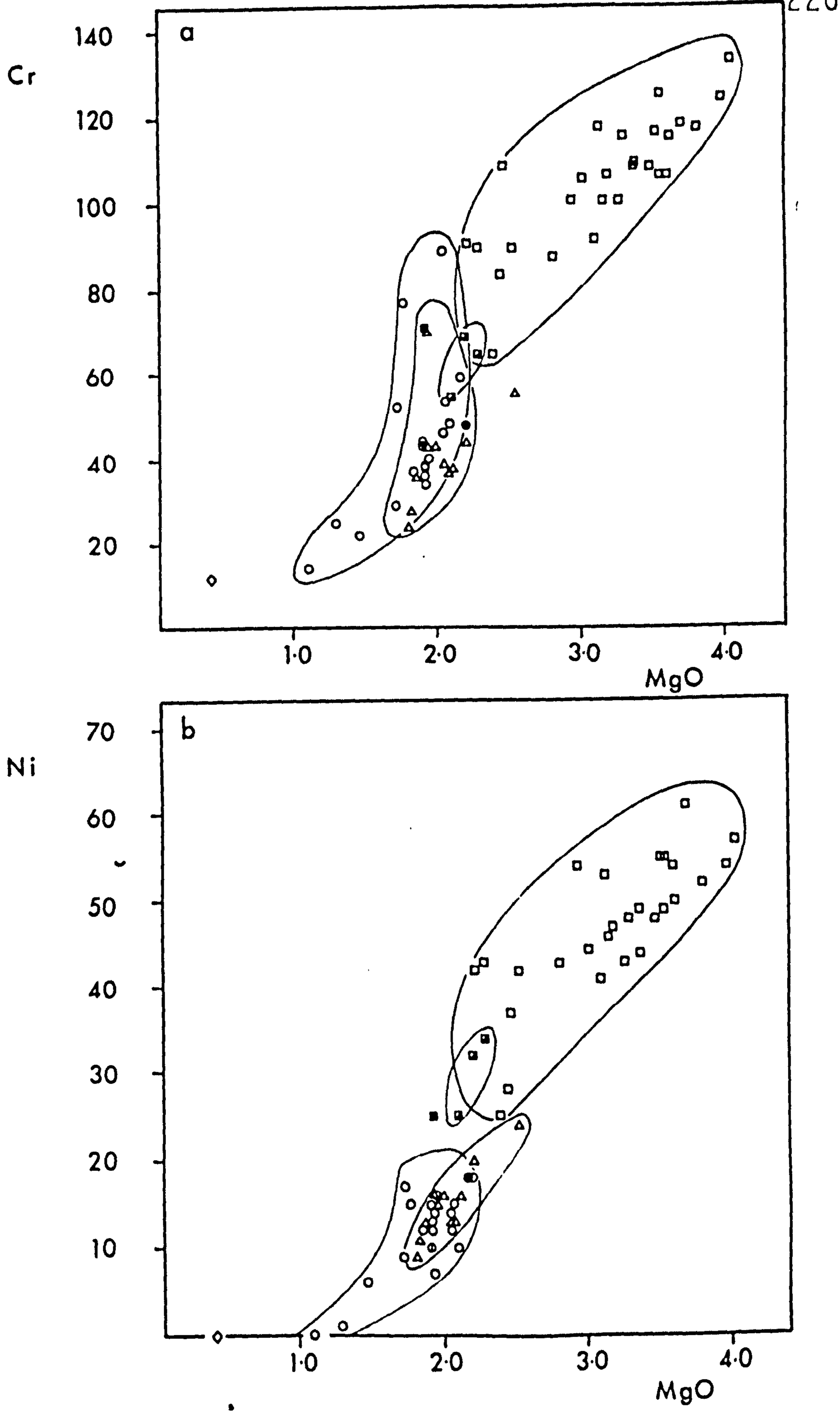

FIGURE 4.21 Plots of Ni and Cr (ppm) vs MgO (%).

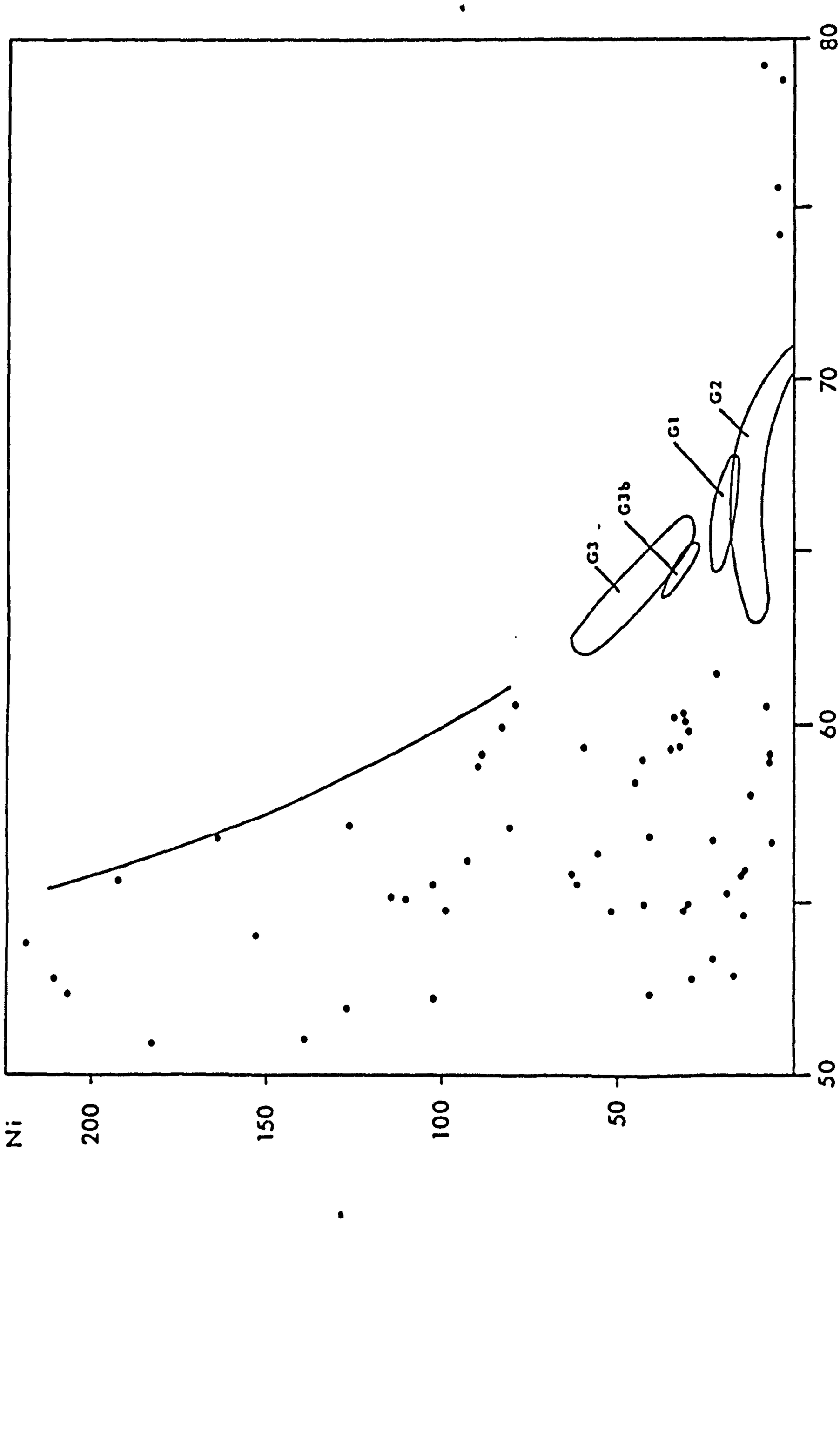

FIGURE 4.22 Comparison of Ni abundances in each of the granite suites of southerly proven ORS volcanic rocks of Fife. Data from Thirlwall (1983).

Ni versus Cr and Ni versus SiO_2 are plotted in Figure 4.20 a and b. The discrimination between clasts of G1 and G2, and G3 is strong. The Ni versus Cr plot shows good correlations between the two trace elements in each of the three suites. Ni concentrations in G3 are high compared to G1 and G2. G3 clasts fall on a linear trend in contrast to the curvilinear trend for G2. The frequency with which linear trends for G3 and curved trends for G2 are observed on element-element plots suggests a fundamental difference in the underlying cause of within-suite variation within each of the groups. The good correlation of Ni and Cr, and their correlation with MgO (Fig 4.21 a,b) suggests their distribution is governed by the behaviour of mafic phases rather than incompatible complex ions (Ringwood 1955) or sulphides. The lower concentrations of Ni in G1 and G2 with respect to G3 is compatible with these groups having undergone strong mafic fractionation. Figure 4.23 shows the relationship of the granite clasts with Ni concentrations from the Lower ORS lavas of Fife (data from Thirlwall 1983). The field for G3 clasts plots on the extension of the inferred primitive liquid compositions for the lavas. G1 and G2 have comparable Ni contents to lavas which are thought to have undergone high level fractionation.

4.4.3.4 La, Ce

Ce discriminates between the three main groups of granite clasts, with Ce abundances highest for clasts of G3 type, and decreasing in the order G3>G2>G1. Ce concentrations decrease with increasing fractionation for G2, and to a lesser extent for G3 suggesting feldspar separation alone cannot produce the chemical variation. Feldspar dominated fractionation would be expected to progressively enrich the residual magma in Ce. G3 is also enriched in La relative to the clasts of G1 and G2 type in the order G3>G2>G1, but there are no clear trends of La abundance with SiO_2 and DI. Similarly La/Y ratios fail to produce coherent trends when plotted aginst SiO_2, with the exception of clasts of G2 type which do show an increase of La/Y in more evolved clasts, suggesting a steepening of chondrite normalised light rare earth pattern.

The use of MgO as the abscissa does not appreciably increase the coherence for La or Ce. Ce shows a positive correlation with MgO for G3, but trends for G2 and G1 are poorly defined. Ce mineral-melt distribution coefficients are given in Table 4.2. Ce is strongly partitioned into amphibole in acid liquids (K_d = 1.5), and also into apatite (K_d = 35). The depletion in Ce with decreasing MgO in G3 therefore is likely to reflect a combination of apatite and amphibole removal, the former required by the high P_2O_5 contents and steep trend of G3 clasts on the P_2O_5 versus SiO_2 variation diagram shown in Figure 4.12b. Ce contents in G2, and to a lesser extent G1 do not correlate with MgO, with large variations in Ce content at constant MgO. This suggests a fundamentally different mechanism for generating the within-suite variation in G2 and G3.

The characteristic enrichment of trace element abundances in the order G3>G2>G1 is not restricted to La and Ce alone. Co, Cr, Ni, Cu, Zr, Zn, Ba, Pb and Th all show a similar pattern of depletion in G2 and G1 at constant silica and DI.

4.4.4 Major and Trace Element Chemistry of Associated Volcanic Clasts

A total of twenty three of the freshest available andesitic and dacitic clasts have been analysed. Full major and trace element analyses are presented in Tables 4.1. A subset of eleven clasts were chosen as being the least altered in having LOI values of less than 3%, and these are thought to be representative of magmatic compositions. As the sample is subject to much bias, and as the clasts are all porphyritic with the volume of phenocrysts varying from 10 to 40%, only the general features of the chemistry are briefly outlined below.

Figure 4.23 summarises the relevant major element variation plots, with compositional fields for the southerly derived granites superimposed. Figure 4.23a shows the K_2O-SiO_2 relationships with fields for high, normal and low-K suites plotted after Peccerilo and Taylor (1976). The volcanic clasts clearly fall in the high-K field, displaced to slightly higher

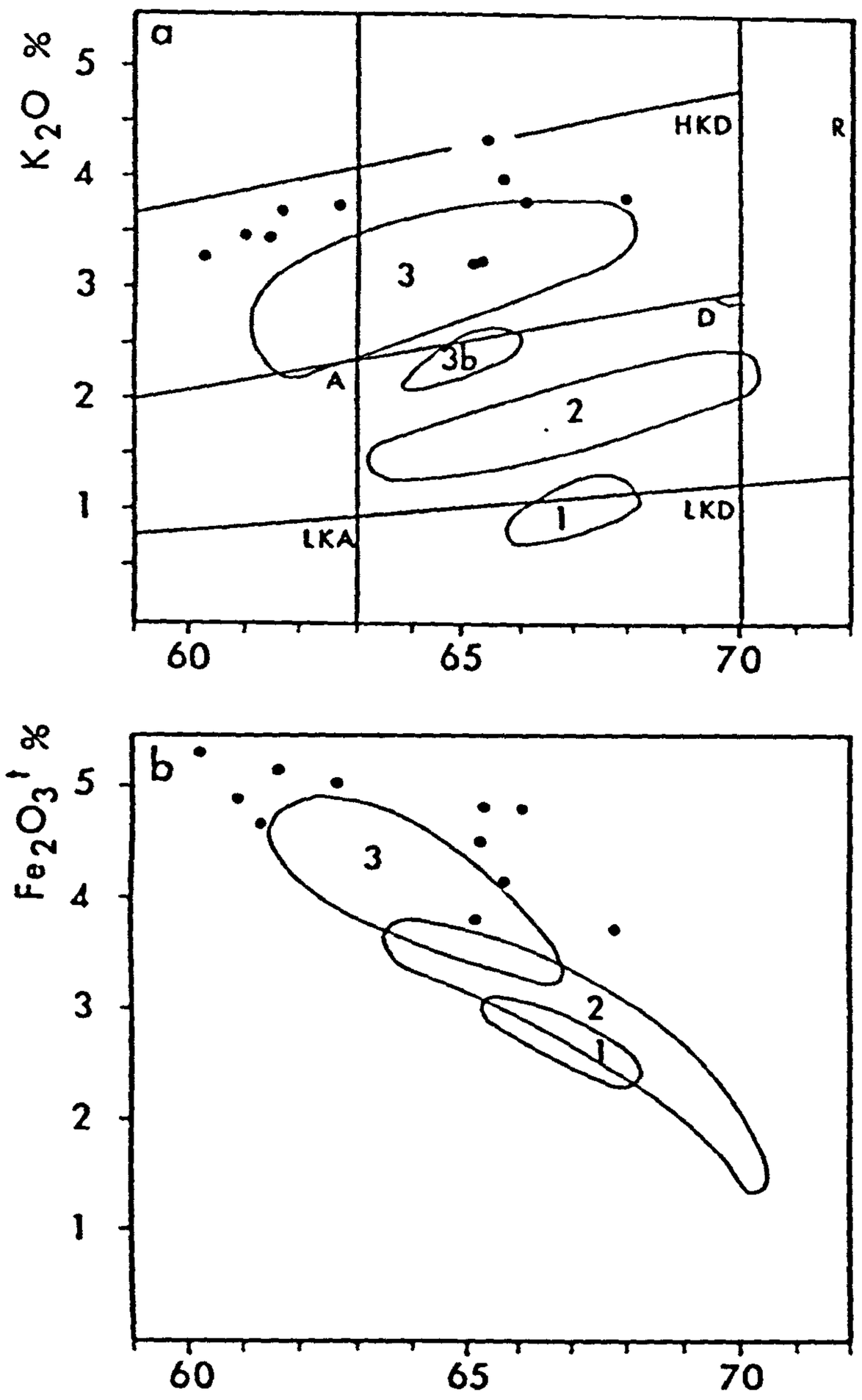

FIGURE 4.23 Comparative major element chemistry of southerly derived volcanic and granite clasts. Least altered volcanic clasts (LOI <3.0%) shown by filled circle symbol. Fields for each of the granite clast suites outlined. (a)K_2O vs SiO_2 plot with fields for orogenic magmas after Pecerillo and Taylor (1976). Abbreviations given in Figure 4.4a. (b)total iron as Fe_2O_3 vs SiO_2 plot. (c)TiO_2 vs SiO_2 plot.

K_2O contents than the corresponding G3 clasts with which they bear a superficial resemblance. High K_2O lavas are a feature of Lower ORS volcanic rocks in the Midland Valley and elsewhere (Thirlwall 1981).

$Fe_2O_3{}^t$ and TiO_2 versus SiO_2 are also plotted in Figure 4.23. Both decrease with increasing silica, but show scattered trends. The scatter is interpreted as primarily reflecting the very variable phenocryst matrix ratios in these rocks, and also low temperature alteration of mafic phenocrysts, in particular amphibole. Relative to the G3 granite suite, the volcanic clasts are marginally enriched in K_2O, $Fe_2O_3{}^t$ and TiO_2, and depleted in MgO. Na_2O is strongly enriched but this may be a metasomatic feature. Of the three granite suites, the acid andesite and dacitic clasts most closely resemble granites of G3 type and the two magmas must have had similar petrogenetic histories.

Trace element variation diagrams against silica show wide scatter, again interpreted as the result of variable phenocryst-matrix ratios and limited mobility of more mobile elements during alteration. Ni and Cr abundances are comparable with those in G3, but Ba is considerably enriched.

4.5 GEOCHRONOLOGY AND STRONTIUM ISOTOPE GEOCHEMISTRY

4.5.1 Introduction

A subset of twelve samples was selected from the 63 analysed granite clasts of southerly derivation. These formed the basis of a detailed Rb-Sr geochronological study using separated mineral phases and whole rocks. The samples were selected such that the four granite types (G1,G2,G3,and G4) were all represented. Clasts selected for isotope work were amongst the largest and freshest of the clasts available at outcrop initially sampled. A further ten clasts were chosen for Rb-Sr whole rock analysis alone, with the dual purpose of establishing whether samples from suites which can be shown chemically to be comagmatic fall on coherent whole rock isochrons, and to provide a comprehensive picture of the isotopic variation present within and between the comagmatic groups.

4.5.2 Analytical Data

Tables 4.3, 4.4, 4.5 and 4.6 summarise the Rb-Sr mineral and whole rock analytical data for the granite clasts. In addition, four analyses of feldspar phenocryst separates from the porphyritic andesites are included in Table 4.6. Mineral ages have been calculated on the basis of mineral - whole rock pairs. ϵ Sr values for whole rocks have been calculated using bulk earth parameters of 0.0839 for the $^{87}Rb/^{86}Sr$ ratio and a $^{87}Sr/^{86}Sr$ ratio of 0.7045. Errors quoted on $^{87}Sr/^{86}Sr$ and mineral ages are 2σ internal experimental errors.

Mineral - whole rock isochrons for individual clasts have been determined using the procedure of York (1969). Blanket errors of 0.5% and 0.01% are used on the $^{87}Rb/^{86}Sr$ and $^{87}Sr/^{86}Sr$ ratios respectively. These values reflect the reproducibility of duplicate analyses and therefore encompass external as well as internal errors. They are therefore thought to be more realistic than within-run errors. External sources of error include weighing inaccuracies, sample heterogeneity and contamination effects during dissolution and ion-exchange. Within-run analytical precision was considerably better than the blanket errors quoted above. Target precisions (1σ) for $^{87}Rb/^{85}Rb$ and

SAMPLE		Rb	Sr	Rb/Sr	$^{87}Rb/^{86}Sr$	$^{87}Sr/^{86}Sr$	$(^{87}Sr/^{86}Sr)_{420}$	ε Sr
4237	G1							
4237	WR	30.62	475.26	0.0644	0.18639	0.70572 ±3	0.70460 ± 3	8.6
4237	F1	8.14	552.95	0.0147	0.04257	0.70488 ±3		
4237	B1	268.56	11.10	24.222	73.0762	1.14445 ±11		
4237	B2	268.62	11.48	23.398	70.4399	1.12159 ±9		
4237	B3	260.80	12.07	21.607	64.86787	1.09495 ±6		
4382	WR	26.56	464.09	0.0572	0.16558	0.70558 ±3	0.70459 ±3	8.4
4383	WR	55.28	479.35	0.1153	0.33362	0.70659 ±3	0.70459 ±4	8.5
4278	G1							
4278	WR	32.73	461.59	0.0709	0.20511	0.70565 ±4	0.70442 ±4	6.0
4278	F1	15.91	591.98	0.0269	0.07776	0.70497 ±6		
4278	F2	5.34	438.97	0.0122	0.03520	0.70464 ±4		
4278	B	256.89	17.78	14.446	42.8346	0.96138 ±4		
4366	G1							
4366	WR	27.33	518.23	0.0527	0.15253	0.70537 ±3	0.70446 ±3	6.5
4366	F1	5.91	474.88	0.0125	0.03603	0.70478 ±4		
4366	B1	201.75	16.55	12.193	36.0057	0.91861 ±8		
4366	B2	205.23	16.16	12.697	37.5292	0.92806 ±7		
4392	WR	25.82	482.48	0.0535	0.15479	0.70542 ±5	0.70449 ±5	7.0

Table 4.3 Rb-Sr isotopic data for G1 clasts.

SAMPLE	Rb	Sr	Rb/Sr	$^{87}Rb/^{86}Sr$	$^{87}Sr/^{86}Sr$	$(^{87}Sr/^{86}Sr)_{420}$	ε Sr
4286 G1							
4286 WR	36.14	487.95	0.0741	0.21424	0.70575 ±4	0.70447 ±4	6.7
4286 F1	8.54	528.95	0.0161	0.04667	0.70478 ±4		
4286 F2	6.80	495.53	0.0137	0.03972	0.70465 ±4		
4286 B1	333.75	26.81	12.449	36.77427	0.92308 ±6		
4311 G2							
4311 WR	99.31	456.86	0.2174	0.62903	0.70864 ±4	0.70488 ±5	12.5
4311 F1	15.05	514.79	0.0292	0.08457	0.70558 ±6		
4311 B1	696.62	31.88	21.848	65.6137	1.09566 ±6		
4311 B2	689.34	31.45	21.921	65.8783	1.103046 ±4		
4282 G2							
4282 WR	92.87	432.11	0.2094	0.62193	0.70884 ±4	0.70512	15.9
4282 F1	68.76	417.20	0.1648	0.47687	0.70787 ±4		
4282 B1	661.08	50.17	13.1779	39.0073	0.94343 ±9		
4282 B2	685.22	50.36	13.6064	40.2724	0.94259 ±7		
4314 G2							
4314 WR	70.92	443.59	0.1599	0.46255	0.70785 ±4	0.70508 ±5	15.4
4314 B1	541.12	44.04	12.287	36.3003	0.92314 ±4		
4321a WR	80.50	451.75	0.1782	0.51563	0.70818 ±4	0.70510 ±5	15.6
4232 WR	67.96	407.49	0.1668	0.48257	0.70792 ±7	0.70503 ±8	14.7
4393 WR	83.27	424.24	0.1963	0.56800	0.70877 ±3	0.70537 ±5	19.5
4378 WR	88.01	430.42	0.2045	0.59164	0.70875 ±4	0.70521 ±5	17.2

Table 4.4 Rb-Sr Isotopic data for 4286 and G2 clasts.

SAMPLE		Rb	Sr	Rb/Sr	$^{87}Rb/^{86}Sr$	$^{87}Sr/^{86}Sr$	$(^{87}Sr/^{86}Sr)_{420}$	C Sr
4242	G3							
4242	WR	80.09	523.46	0.1530	0.44272	0.70803 ±4	0.70538 ±5	19.7
4242	K	176.90	215.25	0.8218	2.38057	0.71941 ±5		
4242	B1	211.69	36.42	5.8125	16.97750	0.80471 ±4		
4242	B2	200.95	37.49	5.3600	15.6482	0.79873 ±4		
4242	H	26.76	87.92	0.3044	0.88105	0.71086 ±4		
4329	G3							
4329	WR	84.22	577.35	0.1459	0.42207	0.70814 ±6	0.70561 ±6	23.0
4329	H	17.37	79.07	0.2197	0.63588	0.70951 ±6		
4329	K	280.71	258.37	1.0864	3.14854	0.72399 ±4		
4329	B1	246.26	25.31	9.7297	28.6991	0.86876 ±4		
4462	G3							
4462	WR	95.57	576.60	0.1657	0.47951	0.70813 ±5	0.70526 ±6	17.9
4462	P	22.90	961.32	0.0238	0.06894	0.70582 ±5		
4462	K	152.48	393.14	0.3878	1.12271	0.71222 ±4		
4462	B	612.60	27.42	22.341	67.1490	1.10647 ±12		
4462	H	48.50	73.68	0.6582	1.90658	0.71728 ±5		
4281	WR	85.66	526.65	0.1626	0.47061	0.70820 ±4	0.70538 ±5	19.7
4280	WR	101.97	534.76	0.1907	0.55177	0.70863 ±3	0.70532 ±4	18.9
4243	WR	79.54	571.54	0.1392	0.40270	0.70779 ±4	0.70538 ±5	19.6
4322	WR	74.33	547.04	0.1359	0.39315	0.70779 ±5	0.70544 ±5	20.5

Table 4.5 Rb-Sr Isotopic data for G3 clasts.

SAMPLE		Rb	Sr	Rb/Sr	$^{87}Rb/^{86}Sr$	$^{87}Sr/^{86}Sr$	$(^{87}Sr/^{86}Sr)_{420}$	ϵ Sr
4328	G2							
4328	WR	56.91	474.17	0.1200	0.34727	0.70760 ±4	0.70553	21.7
4328	K	130.77	450.17	0.2905	0.84074	0.71050 ±5		
4328	B	310.58	15.52	20.015	59.9162	1.06175 ±4		
4279	G4							
4279	WR	122.49	140.47	0.8720	2.5262	0.72053 ±4	0.70469*	10.2
4279	F	174.26	118.54	1.470	4.26305	0.73119 ±5		
4279	B	802.11	5.06	158.5	640.599	4.7572 ±7		

*t = 440Ma

							$(^{87}Sr/^{86}Sr)_{416}$	ϵ Sr
4288	P	13.81	959.67	0.0144	0.04162	0.70629 ±5	0.70604 ±5	29.0
4289	P	12.67	1447.78	0.0087	0.02532	0.70548 ±4	0.70533 ±4	18.9
4331	P	10.44	614.71	0.01698	0.04912	0.70661 ±4	0.70632 ±4	32.9
4351	P	21.27	640.54	0.0321	0.09608	0.70656 ±7	0.70599 ±7	28.2

Table 4.6 Rb-Sr Isotopic data for clasts 4328 and 4279, and 4 feldspar separates from volcanic andesite clasts.

SAMPLE	SEPARATES	N	AGE $\pm 2\sigma$ (Ma)	$(^{87}Sr/^{86}Sr)_i \pm 2\sigma$	MSWD
4366	WR, P1, B1, B2	4	417.7 ± 1.1	0.70451 ± 5	0.56
4237	WR, P1, B1, B2, B3	5	420.3 ± 1.9	0.70461 ± 5	2.41
4278	WR, P1, P2, B1	4	421 ± 1.4	0.70445 ± 3	0.42
4286	WR, P1, P2, B1	4	417.4 ±1.3	0.70446 ± 3	0.41
4311	WR, P, B1, B2	4	420.8 ± 3	0.70497 ± 10	4.17
4282	WR, P, B1, B2	4	433.4 ± 0.8	0.70496 ± 3	0.28
4328	WR, K, B	3	417.3 ± 0.8	0.70552 ± 2	0.14
4314	WR,B	2	421.8 ± 2.1	0.70507 ± 7	
4329	WR, H, K, B	4	400.9 ± 3.1	0.70583 ± 9	3.08
4242	WR, P, B1, B2	4	414.6 ± 3.0	0.70539 ± 13	3.78
4462	WR, P, K, B	4	420.0 ± 3.3	0.70538 ± 7	2.63
4279	WR, K, B	3	443.1 ± 3.5	0.70448 ± 21	2.76

COMPOSITE ISOCHRONS

GROUP	DATA	N	AGE(Ma)	$(^{87}Sr/^{86}Sr)_i \pm 2\sigma$	MSWD
G1	WHOLE ROCKS	7	447.4 ± 35.9	0.70444 ± 11	1.21
G1	WHOLE ROCKS/FELDSPARS	13	430.8 ± 16.8	0.70449 ± 4	1.17
G1	WHOLE ROCKS/FELDSPARS/BIOTITES	20	419.3 ± 0.9	0.70451 ± 2	1.33
G3	WHOLE ROCKS/FELDSPARS	9	414.8 ± 2.5	0.70541 ± 3	1.09
G3	WHOLE ROCKS/FELDSPARS/BIOTITES	13	416.0 ± 1.5	0.70540 ± 4	1.78

Table 4.7 Isochron regression parameters. WR - whole rock, P - plagioclase, H - hornblende, K - K-feldspar and B - biotite.

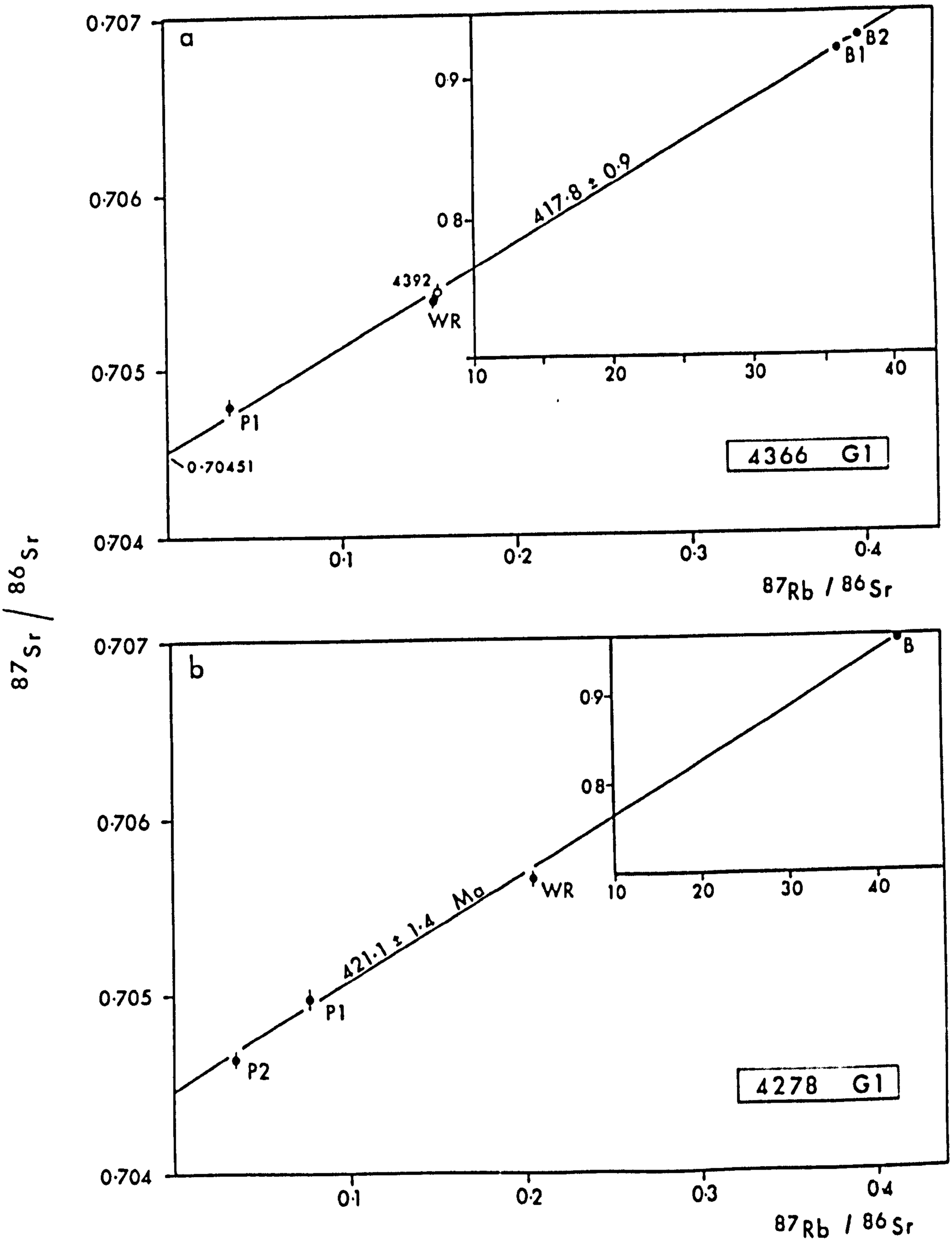

FIGURE 4.24 Rb-Sr isochron diagrams for samples 4366 and 4278, two G1-type granite clasts of southerly provenance. Biotite data shown on compressed axes.

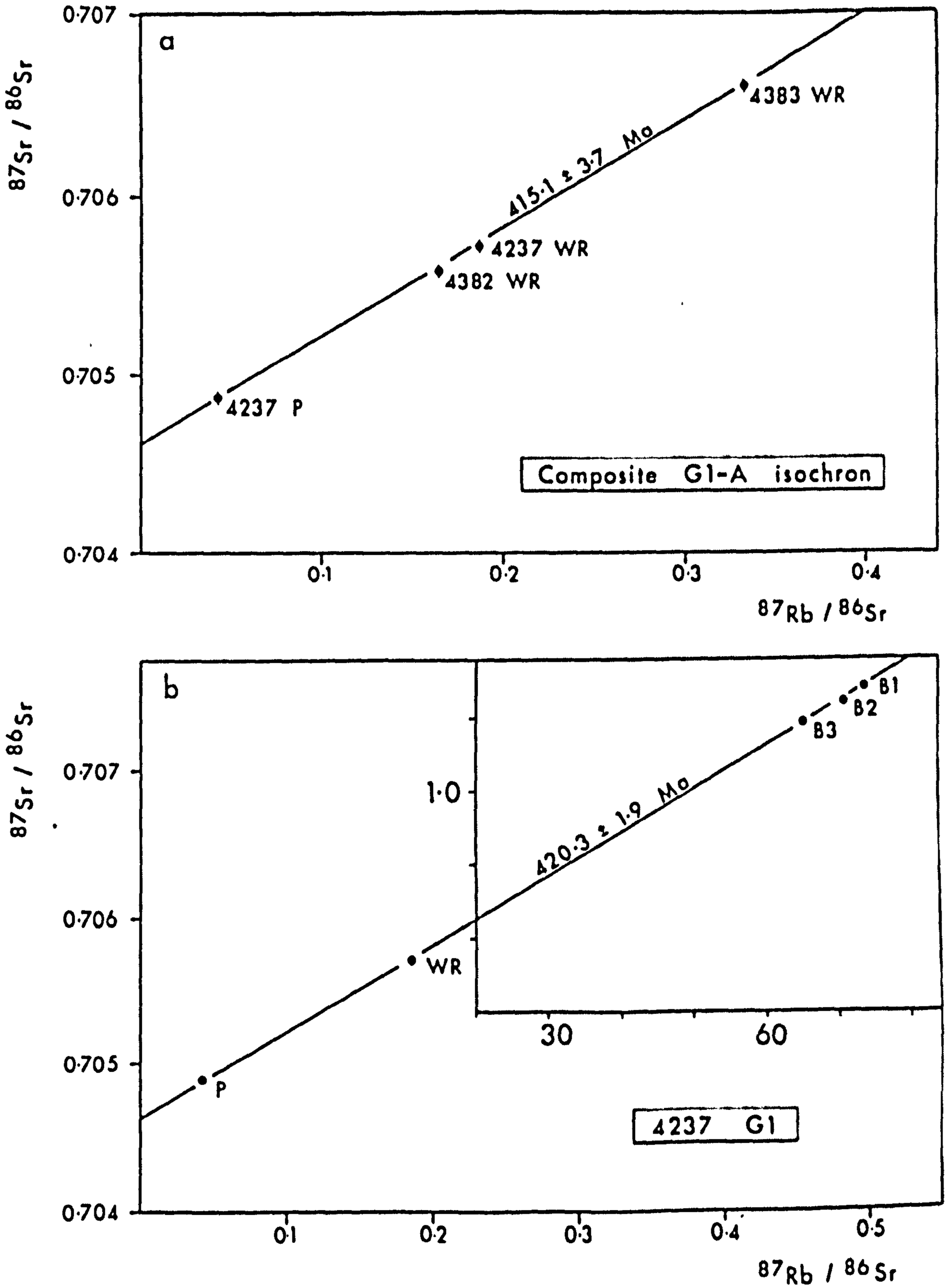

FIGURE 4.25 Rb-Sr isochron diagrams for (a) three whole rocks and a plagioclase separate from grey foliated granite clast sub-type G_{1A} and (b) sample 4237, a southerly derived granite clast of G1 type. Replicate biotite points shown on compressed axes.

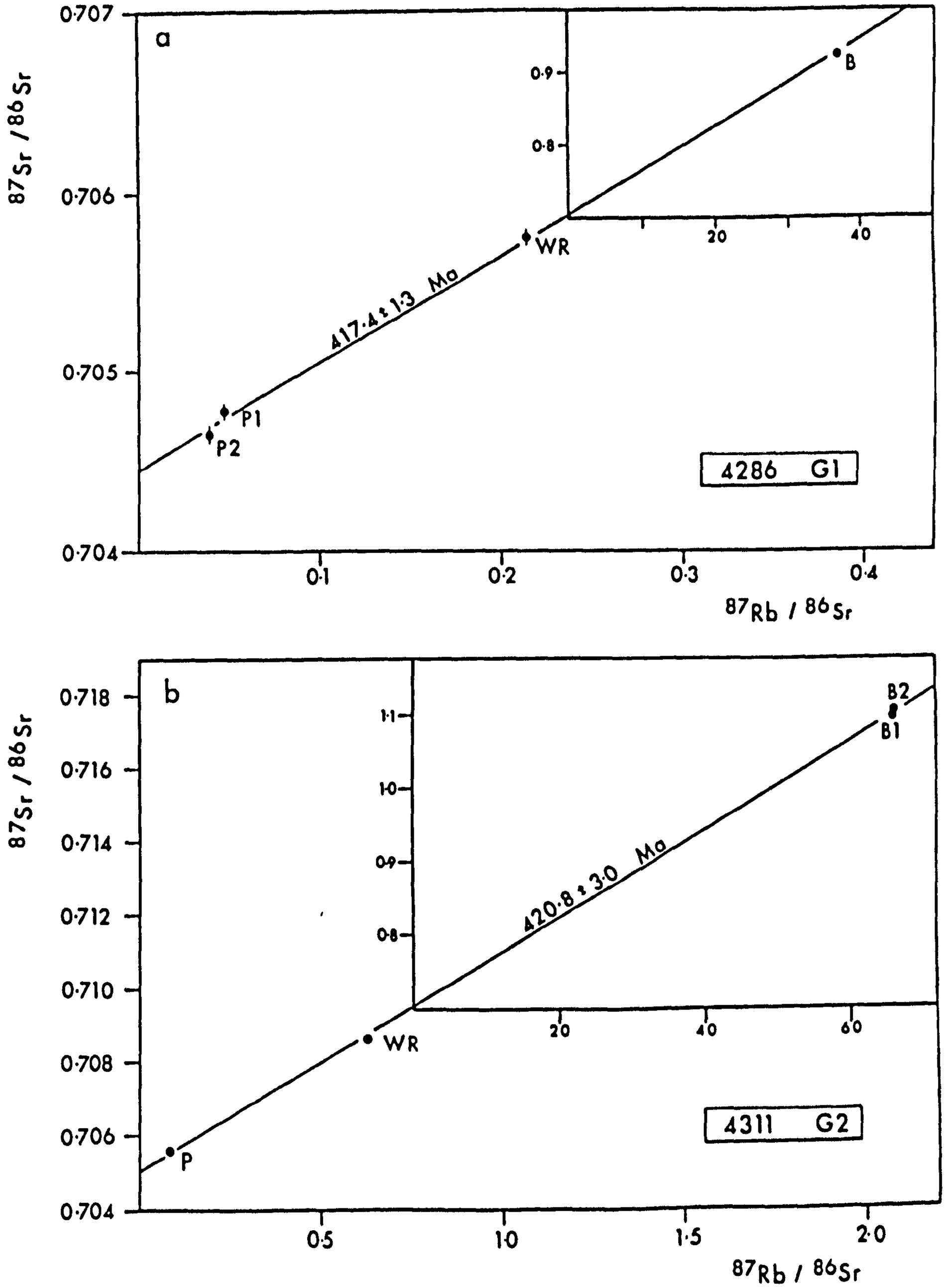

FIGURE 4.26 Rb-Sr isochron diagrams for samples 4286 and 4311. Biotite points shown on compressed axes.

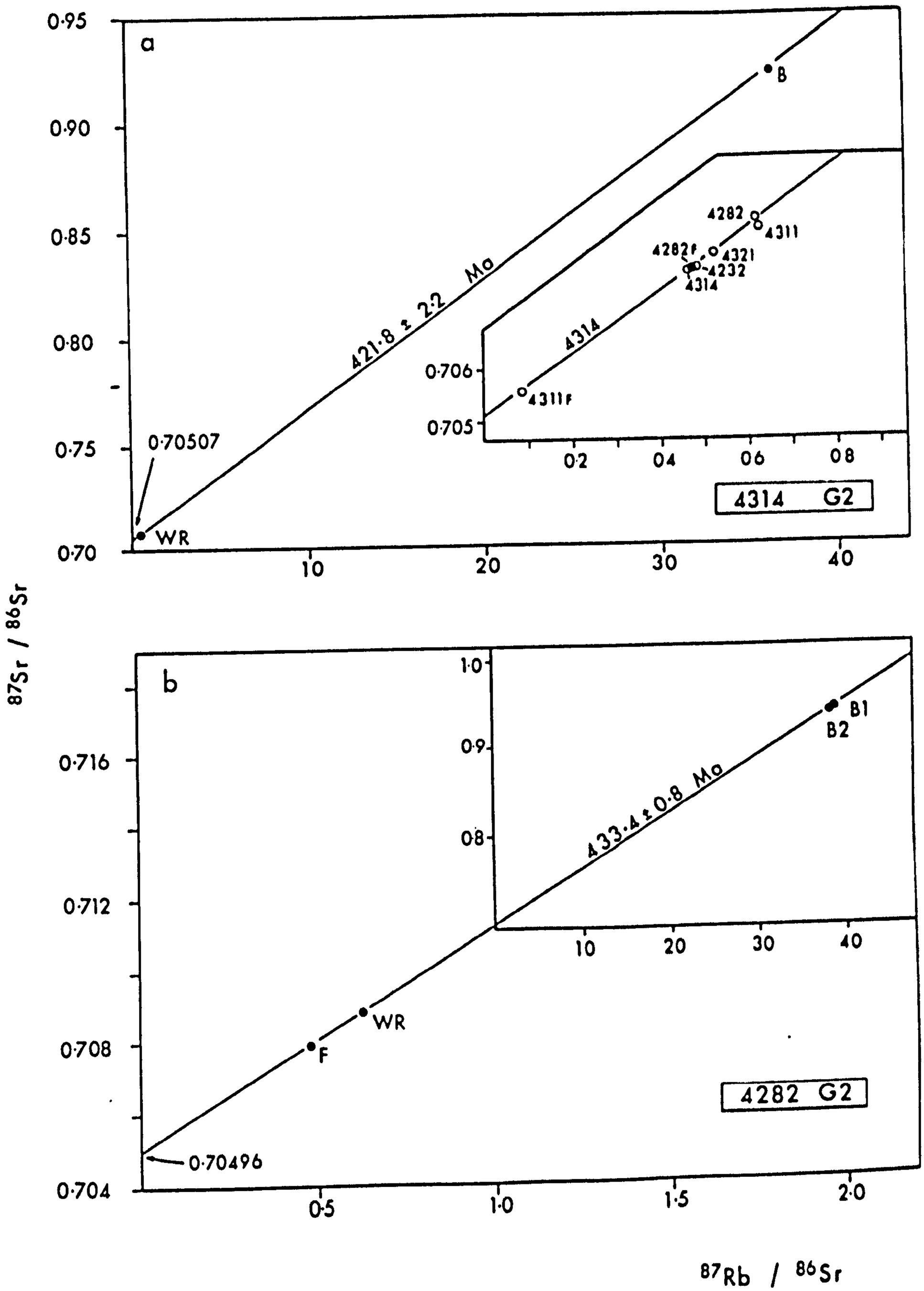

FIGURE 4.27 Rb-Sr isochron diagrams for granite clasts of G2 type. (a) sample 4314. Inset shows whole rock and feldspar data for other less evolved G2 clasts relative to the isochron for 4314. (b) sample 4282, replicate biotite points shown on compressed axes.

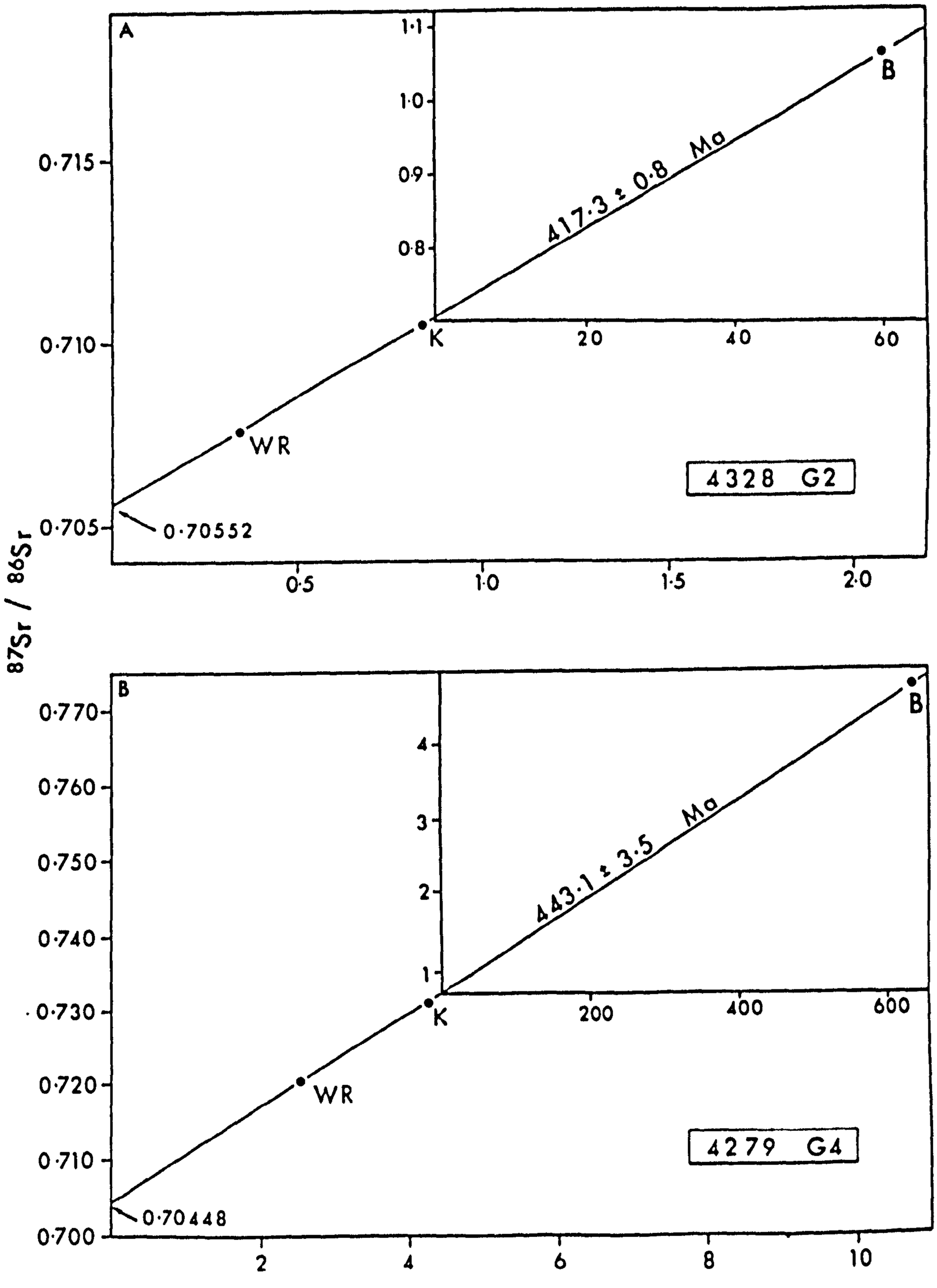

FIGURE 4.28 Rb-Sr isochron plots for (a) 4328, an evolved granite clast of G2 type, and (b) 4279, a biotite-garnet granite of G4 type. Biotite points shown on compressed axes in their true positions relative to the regression lines.

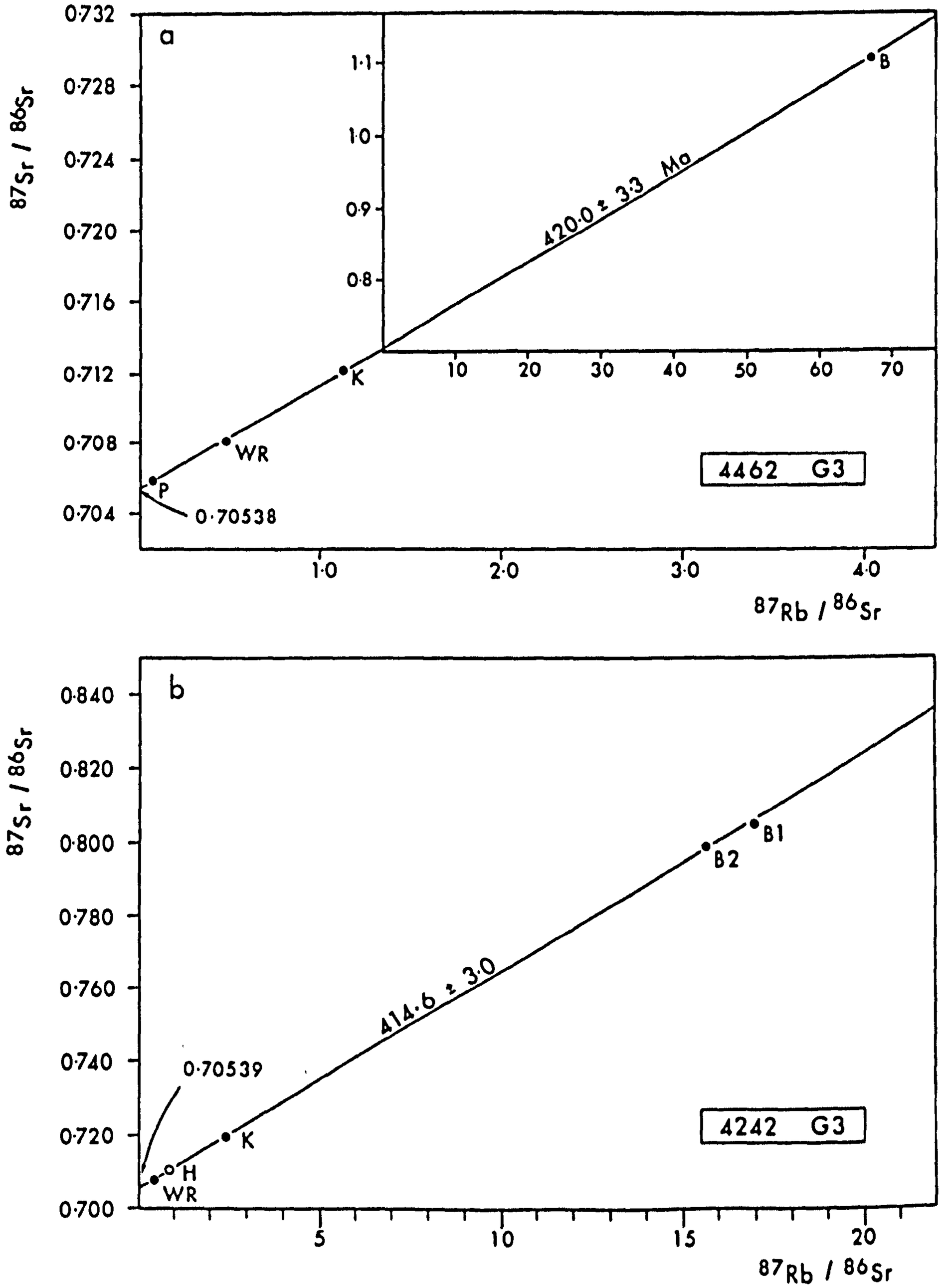

FIGURE 4.29 Rb-Sr isochron plots for two G3 clasts of southerly provenance, 4462 and 4242.

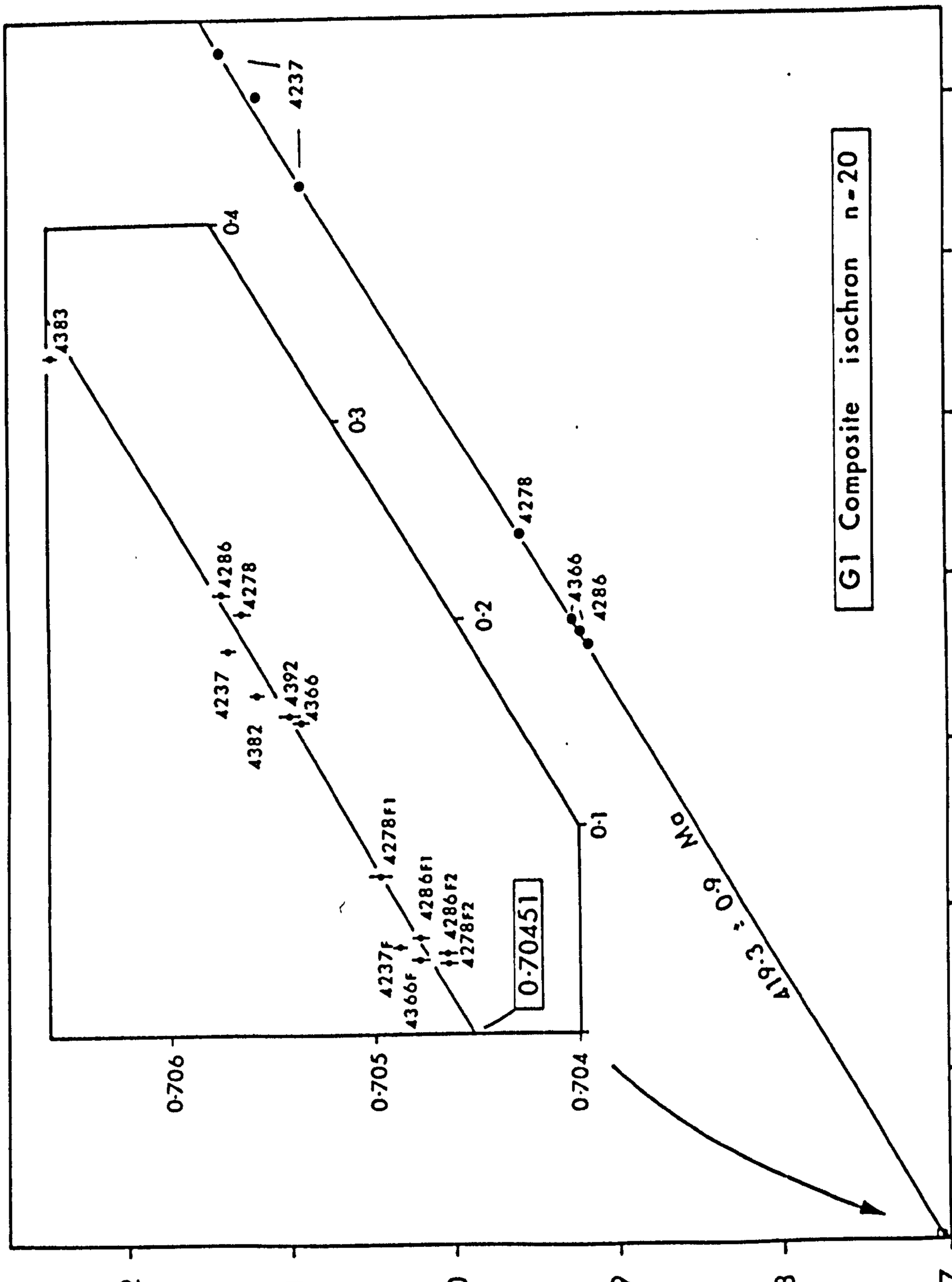

FIGURE 4.30 Twenty point Rb-Sr isochron plot combining all whole rock and mineral data for foliated tonalite clasts of G1 type.

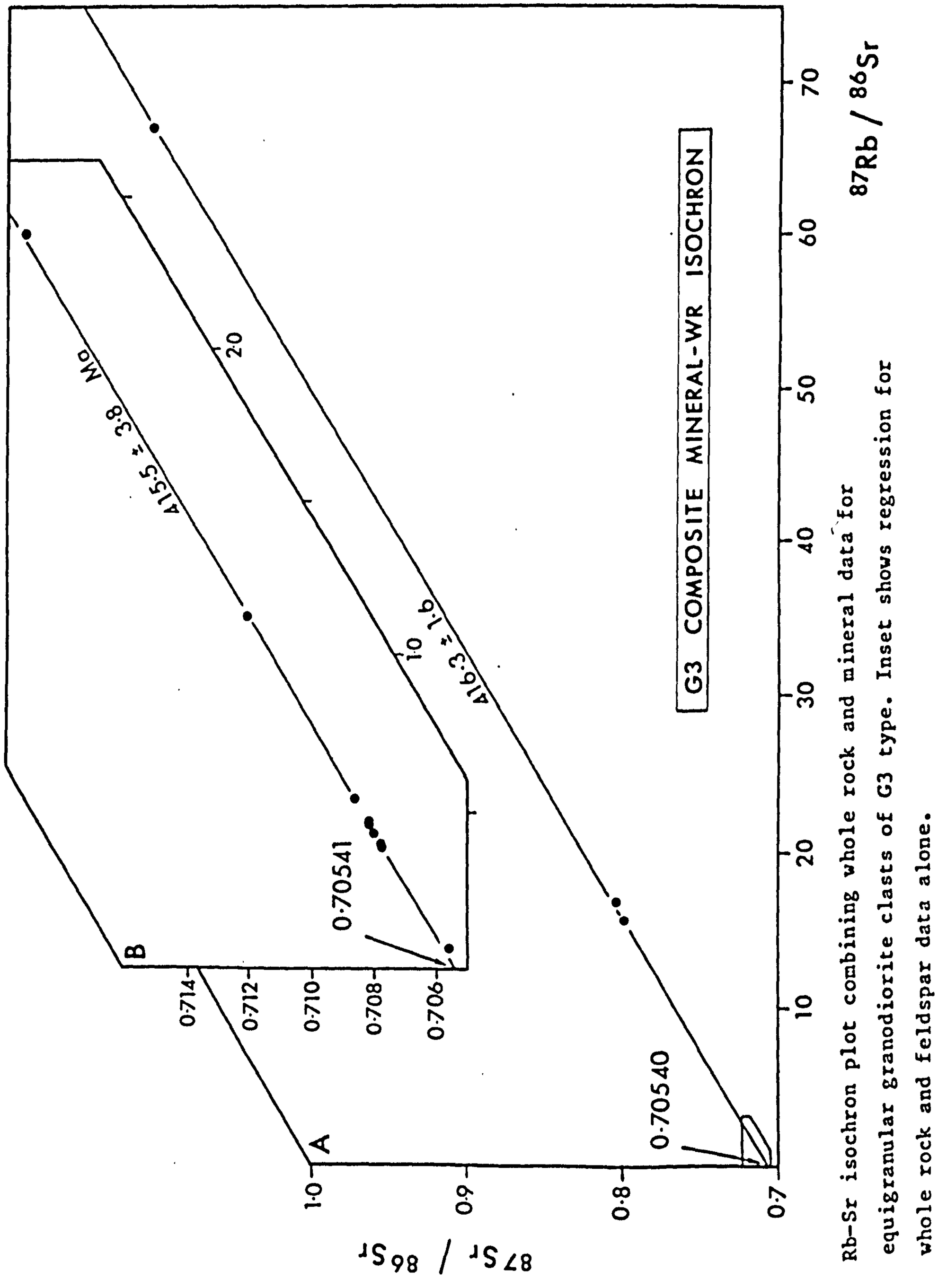

FIGURE 4.31 Rb–Sr isochron plot combining whole rock and mineral data for equigranular granodiorite clasts of G3 type. Inset shows regression for whole rock and feldspar data alone.

$^{87}Sr/^{86}Sr$ were 0.0001 and 0.00002 respectively. These were achieved in most cases. Lower levels of precision were acceptable for biotite analyses.

Table 4.7 summarises the regression parameters for the data from each of the clasts, and also details of composite isochrons for each of the granite types. Figures 4.24 to 4.31 present the data in the form of standard isochron diagrams with insets with compressed axes to show the radiogenic biotite points which plot far removed from the y-intercept. Replicate biotite analyses have been treated as separate points during York regression.

4.5.3 Results

(a) Foliated Tonalite Clasts (G1)

The four clasts of G1 type studied all yield acceptable mineral-whole rock isochrons. The ages determined from these isochrons are consistent and overlap within experimental error. The analysed clasts include both pink (G1B) and grey (G1A) subtypes. Both 4278 and 4366 are pink medium-grained biotite rich foliated tonalites. 4278 yields a four point biotite-whole rock-plagioclase isochron of 421.1 $\pm$ 1.4 Ma (MSWD = 0.42). The two plagioclase analyses represent different density separates. The initial ratio determined from the y-intercept is 0.70445 $\pm$ 3. Clast 4366 has a biotite(2)-whole rock- plagioclase isochron age of 417.8 $\pm$ 1.11 (MSWD = 0.56) and an initial ratio of 0.70451 $\pm$ 5. A whole rock analysis of a related clast, 4392, of similar chemistry and appearance, falls directly on this isochron, and the combined isochron yields a similar age.

Clasts 4237 and 4286 were chosen as being representative of the grey foliated tonalite sub-type. 4237 is coarse-grained whilst 4286 is slightly finer grained facies. Clasts 4237 yields a biotite(3)-whole rock-plagioclase isochron age of 420.3 $\pm$ 1.9 Ma (MSWD = 2.41) and an initial ratio of 0.70461 $\pm$ 5. The three biotite points are replicate analyses of the same biotite separate. The poor reproducibility reflects sample heterogeneity, which accounts for distribution of the analyses along the isochron. They are treated as separate points in the isochron regression. Two additional whole rock samples, 4382 and

4283, have a similar appearance and chemistry to 4237. These plot directly on the isochron resulting in a seven point regression giving an age of 420.3 ± 1.5 Ma. If the biotites are ignored, a composite whole rock-plagioclase isochron for the coarse grained grey tonalite G1A sub-type yields an age of 415.1 ± 3.7. This is important in that it demonstrates that the ages obtained from the largely biotite controlled isochrons can be reproduced by composite whole rock and whole rock-feldspar isochrons from groups of clasts that can be shown chemically to be clearly comagmatic. The ages determined therefore are unlikely to reflect alteration processes in biotite alone. If the ages reflect some form of secondary exchange, the feldspars and whole rocks must also have been isotopically re-equilibrated. A biotite-whole rock-plagioclase(2) isochron obtained from clast 4286 produces an age of 417.4 ± 1.3 (MSWD = 0.41) and an initial ratio of 0.70446 ± 3. This is significantly lower than the initial ratio from 4237 but comparable with 4278 and 4366.

A twenty point composite isochron for mineral and whole rock data from clasts of G1 type is plotted in Figure 4.30. York regression of this data yields an age of 419.3 ± 0.9 (MSWD = 1.33) and an initial intercept of 0.70451 ± 2. The low value for MSWD suggests phases from different clasts were originally isotopically equilibrated. This confirms the clasts are likely to have been originally comagmatic. The narrow range of whole rock Rb/Sr ratios precludes the calculation of a meaningful whole rock age. Seven G1 whole rocks give a regression age of 447.4 ± 35.9 Ma (MSWD = 1.21)

(b) Equigranular biotite granodiorite clasts (G2)

Four clasts of G2 type have been studied. Clasts of G2 type are characterised by greater heterogeneity in their isotopic signature and age relations.

Mineral and whole rock data for clast 4311 are plotted on an isochron diagram in Figure 4.26. A four-point biotite(2)-whole rock-plagioclase isochron gives an age of 420.8 ± 3.0 and an initial ratio of 0.70497 ± 10. The MSWD value of 4.17 is higher than would be expected given the experimental errors. This is

due to the two biotite replicates showing a slight scatter about the isochron. The age is very similar to ages determined from clasts of G1 type, but the initial ratio is significantly greater. Only biotite and whole rock analyses are available for 4314. These give a mica-whole rock age of 421.8 ± 2.1 Ma and initial ratio of 0.70507 ± 7. The errors are based on within-run experimental errors for $^{87}Sr/^{86}Sr$ and a blanket error of 0.5% for $^{87}Rb/^{86}Sr$.

A biotite(2)-whole rock-feldspar isochron for 4282 gives an age of 433.4 ± 0.8 Ma (MSWD = 0.28) with an intercept of 0.70496 ± 3. This is significantly older than the ages determined from other clasts of G2 type e.g. 4311 and 4314, but the initial ratio is similar.

4328 is an example of one of the more evolved clasts of G2 type. A three point isochron age of 417.3 ± 0.8 (MSWD = 0.14) compares well with ages determined for 4311 and 4314. The initial ratio is however higher. Initial ratios for other G2 whole rock samples at 420 Ma are 0.70510, 0.70503, 0.70537 and 0.70521. Clasts assigned to G2 are therefore isotopically heterogeneous with more evolved granite types showing enhanced initial ratios. Whole rocks of G2 type do not define an isochron when $^{87}Sr/^{86}Sr$ is plotted against $^{87}Rb/^{86}Sr$.

(c) Equigranular biotite-hornblende granodiorite clasts (G3)

Three clasts of G3 were studied. 4462 and 4282 give acceptable mineral-whole rock isochrons albeit with some scatter in the latter. 4239 does not give satisfactory results.

4462 shows evidence for large degrees of undercooling. A biotite-K-feldspar-whole rock-plagioclase isochron gives an age of 420.0 ± 3.3 (MSWD = 2.63) with an initial ratio of 0.70538 ± 7. 4242 has a mineral-whole rock isochron age of 414.0 ± 3.4 Ma (MSWD = 5.09). The high MSWD indicates scatter greater than the external errors. If the hornblende analysis is omitted from the regression, a four point isochron (biotite(2)-K-feldspar-whole rock) indicates an age of 414.6 ± 3.0 Ma. Hornblende analyses

for 4462 and 4329 also both plot off their respective isochrons to higher values of $^{87}Sr/^{86}Sr$. This is interpreted as resulting from isotopic exchange during low temperature alteration. The omission of hornblende reduces the MSWD to 3.78. This is still higher than should be expected, and is caused by poor reproducibility of the two biotite replicate analyses. The Sr content of the biotite and its Rb/Sr ratio are low when compared with 4462, and the slightly lower age, significant at the external error level, is thought to reflect slight resetting of the Rb/Sr systematics in the biotite as a result of low temperature alteration. A similar, if more pronounced effect is seen in 4329. A biotite-K-feldspar-hornblende-whole rock age of 400.9 $\pm$ 3.1 Ma (MSWD = 3.08) is evidently too young to fit the stratigraphic constraints on the age of the sediments which host the clast. The Crawton Group is probably in excess of 405Ma and may even be 410Ma old (see discussion in Chapter 1). Whilst resetting of biotite may partially explain the high initial ratio (0.70583 $\pm$ 9) derived from this isochron, recalculating the initial ratio from the whole rock at 416Ma still indicates anomalously high initial $^{87}Sr/^{86}Sr$ with respect to other clasts of G3 type. 4329 was sampled as being representative of a series of G3 clasts which have abundant metasedimentary xenoliths. The enhanced initial ratio is therefore thought to reflect crustal contamination with radiogenic metasediment. Clast 4462 provides the most reliable estimate of the age of G3 clasts, on account of the high Rb/Sr ratio of its unaltered biotite (hand picked) and the low MSWD of its mineral-whole rock isochron.

A composite G3 mineral-whole rock isochron is shown in Figure 4.31. Data for 4329 are ignored on the basis of likely contamination and alteration effects. Four additional whole rock analyses are included. A nine point plagioclase-whole rock-K-feldspar regression gives an age of 415.5 $\pm$ 3.8Ma (MSWD = 1.23) and an initial ratio of 0.70541 $\pm$ 4. This age is independent of biotite which fundamentally controls the individual mineral-whole-rock isochrons. Inclusion of three G3 biotite points (omitting 4329 B1) produces a composite isochron age of 416.3 $\pm$ 1.6 (MSWD = 1.93) and initial ratio 0.70540 $\pm$ 3.

(d) Biotite-garnet granite (G4)

A single sample of G4, 4279 has been analysed. A three point biotite-K-feldspar-whole rock isochron produces an age of 443.1 ± 3.5 Ma with an initial ratio of 0.70448 ± 21 (MSWD = 2.76). The Rb/Sr ratio of the biotite is very high, higher than any of the other biotites analysed. The age is also markedly different, and this, combined with the geochemical evidence suggesting no relationship between G4 and the other granite types argues for a separate origin for G4.

4.5.4 Discussion

4.5.4.1 Significance of the mineral-whole rock ages

The ten analysed clasts of the granites G1, G2 and G3 (with the exception of 4329, see above) produce good mineral-whole rock isochrons. These indicate a narrow range of closure ages with a mean of 420.4 Ma and a standard deviation of 5.1. This result is somewhat surprising considering both the range of chemical variation between each of the granite types (for instance the variation in K_2O from low- to high-K fields (Fig. 4.4)), and also the fact that both strongly foliated and unstrained equigranular granitoids have been sampled. This latter point is considered further in 4.6.3.

The ages indicated by the isochrons are interpreted as dating the emplacement of the granites as opposed to secondary equilibration processes or open-system behaviour. The evidence for this interpretation is based on the following points.

(a) The Rb-Sr systematics cannot reflect cooling, following uplift, of plutons intruded at depth at some earlier time. There is good evidence to suggest high levels of emplacement (Section 4.6.3).

(b) The narrow range of ages determined suggest a unique event. Alteration processes might be expected to produce a random scatter of ages less than the true emplacement age reflecting partial resetting. Biotites in northerly derived muscovite-biotite granite clasts show this type of behaviour, with re-set ages scattered from the emplacement age at 455-460Ma to as low as 420Ma. Van Breemen and Bluck (1981) interpret these random biotite ages as the result of chloritisation during the Devonian weathering. Goldich and Gast (1966) record a similar scatter of weathered biotite ages up to 75% less than the corresponding Rb-Sr ages for fresh biotites, in a study of the Morton Gneiss, Minnesota.

(c) The low Rb/Sr ratios of the whole rocks result in small spreads on $^{87}Sr/^{86}Sr$ vs $^{87}Rb/^{86}Sr$ plots. However composite whole rock and whole rock-feldspar isochrons from clasts which can be shown chemically to be comagmatic do reproduce the ages determined by mineral isochrons using biotite. With the exception of 4329, the biotite ages are therefore unlikely to

reflect alteration-related resetting. This is confirmed by the low values of MSWD for many of the isochrons indicating biotite last equilibrated with the other mineral phases. If some process of low temperature alteration is thought to account for the mineral isochron ages, it must have been capable of re-equilibrating large volumes of granite such that whole rock isochrons from comagmatic clasts no longer record older ages. As this is improbable, the Rb-Sr systematics are thought to reflect closure on cooling of granitoid magmas emplaced to high crustal levels. The mineral-whole rock isochrons can therefore be used to date this emplacement.

(d) The Silurian emplacement ages indicated by the isochrons are compatible with other geological evidence. The granites show many features in common with other late Silurian granites intruding adjacent crustal blocks, and appear to share the same chemical province. The granite clasts thus are enriched in Na_2O and Sr and have low Rb/Sr and $(^{87}Sr/^{86}Sr)_i$ ratios. In addition, clasts of G3 type are closely related to clasts of porphyritic andesite, which can be shown to be derived from contemporaneous lava piles erupted close to and within the basin of deposition.

(e) The granites intrude a thick pile of lithic arenites and metagreywacke. Clasts of these lithologies also make up an important component of the southerly derived conglomerates. The provenance, chemistry and affinity of these clasts are considered in Chapter 6. One possibility is that they are derived from a proximal Highland Border Complex equivalent. This is strengthened by the occurrence of limestone clasts containing fragmentary brachiopod and crinoidal debris of Ordovician age in the southerly derived conglomerates (Curry pers. comm. 1985). A Silurian age for the granites intruding the lithic arenite and metagreywacke pile is reasonable, should an Ordovician age for the sequence or their correlation with lithic arenites occurring within the largely Ordovician Highland Border Complex, be substantiated.

Whilst the evidence outlined above is strongly in favour of a Silurian emplacement age for the granites sampled by the clasts, there must necessarily be a degree of uncertainty, particularly with the strongly foliated clasts. Andre and Deutsch (1985) show

very low grade metamorphic resetting of magmatic Sr isotopes is possible. They record Sr isotopic homogenisation and loss of radiogenic Sr from biotite and K-feldspar at temperatures estimated to be less than 250°C. It is possible similar effects are present in the clast data but the combination of factors outlined above suggest this is probably unlikely. The data for the foliated tonalite clasts must however be treated with caution as mineral-whole rock equilibration may have taken place when the granite was deformed. At best the age for G1 is therefore a minimum age. U-Pb work is under way on representative clasts from each of the suites to clarify the age relationships.

Accepting a Silurian age for the bulk of the granite magmas sampled by the conglomerates raises a number of interesting possibilities. Firstly, only a single late Caledonian granite, the Distinkhorn tonalite of Devonian age is known to outcrop within the Midland Valley (Pidgeon and Aftalion 1978). Although schematic cross sections purporting to show the regional deep geology of the Caledonian orogeny across northern Britain at the close of the Silurian have included granite plutons emplaced into the Midland Valley block (e.g. Simpson et al. 1979, Brown and Hennessy 1978), there has until now been no conclusive proof that Silurian granite magmatism actually occurred in this zone. The data from the clasts confirm widespread magmatism in the period 435-390 Ma in all zones of the Caledonides.

Secondly, the Silurian granites sampled by the conglomerates are especially intriguing when considered in the wider context of Midland Valley magmatism. Longman et al. (1979), Longman (1980) and Bluck (1983) show granite clasts, occurring within a fore-arc setting in conglomerates developed on top of the foundered Ballantrae Ophiolite, to have a provenance in a plutonic-arc complex sited some way to the north but still within the confines of the Midland Valley. Internal whole rock-feldspar Rb-Sr isochrons from the granite clasts show a long history of magmatism within the source. The distribution of ages cluster into two groups at c 550Ma and c 470Ma. The latter group of ages, duplicated by U-Pb and Pb-Pb zircon geochronology, are particularly reliable. An interesting feature of the younger

clasts is the fact that they record emplacement ages which are very close to the estimated absolute age of the sediments in which they occur as clasts (Bluck 1983). The youngest reliable age, from a clast sampled from the Tormitchell conglomerate, yields an age of 451 ± 8 Ma and an initial ratio of 0.7062 ± 8 (Longman et al. 1982). There is then a substantial gap in the record of Midland Valley igneous activity until the voluminous outpouring of basalts and andesites in the Lower ORS. Thirlwall (1983) has dated a rhyolite block and an olivine diorite intrusion consanguineous with the lava pile at 406.5 ± 5.6 and 407.3 ± 5.6 respectively. These dates, from lithologies which do show signs of hydrothermal alteration should however be treated with caution.

Against this background of both earlier and later magmatic events, the southerly derived granites fill a gap in what can now be seen as a long history of continuous magmatism extending over an interval of greater than 150 Ma. In addition the record of end-Silurian magmatism preserved in the southerly derived conglomerates of the Crawton Basin provides an insight into a significant change in the nature of the magmatic evolution as effusive rocks begin to dominate the preserved record of igneous activity at the expense of plutonic rocks. The implication of the apparent transfer to eruption at the surface is considered further in 4.6.4.

4.5.4.2 Strontium isotope geochemistry

Initial $^{87}Sr/^{86}Sr$ ratios have been calculated for all the clasts for which isotopic data is available. These include the twelve clasts used for whole rock-mineral age determinations, along with ten additional granite clasts and four fresh phenocryst separates from the associated volcanic clasts. All initial ratios are normalised to an age of 420Ma. Although the volcanic clasts are probably younger than this, their very low Rb/Sr plagioclase ratios mean their calculated initial ratios are relatively insensitive to the age correction.

Initial $(^{87}Sr/^{86}Sr)_{420}$ ratios are plotted against SiO_2 and $10^3/Sr$ in Figure 4.32a,b. The initial ratios of granite clasts from

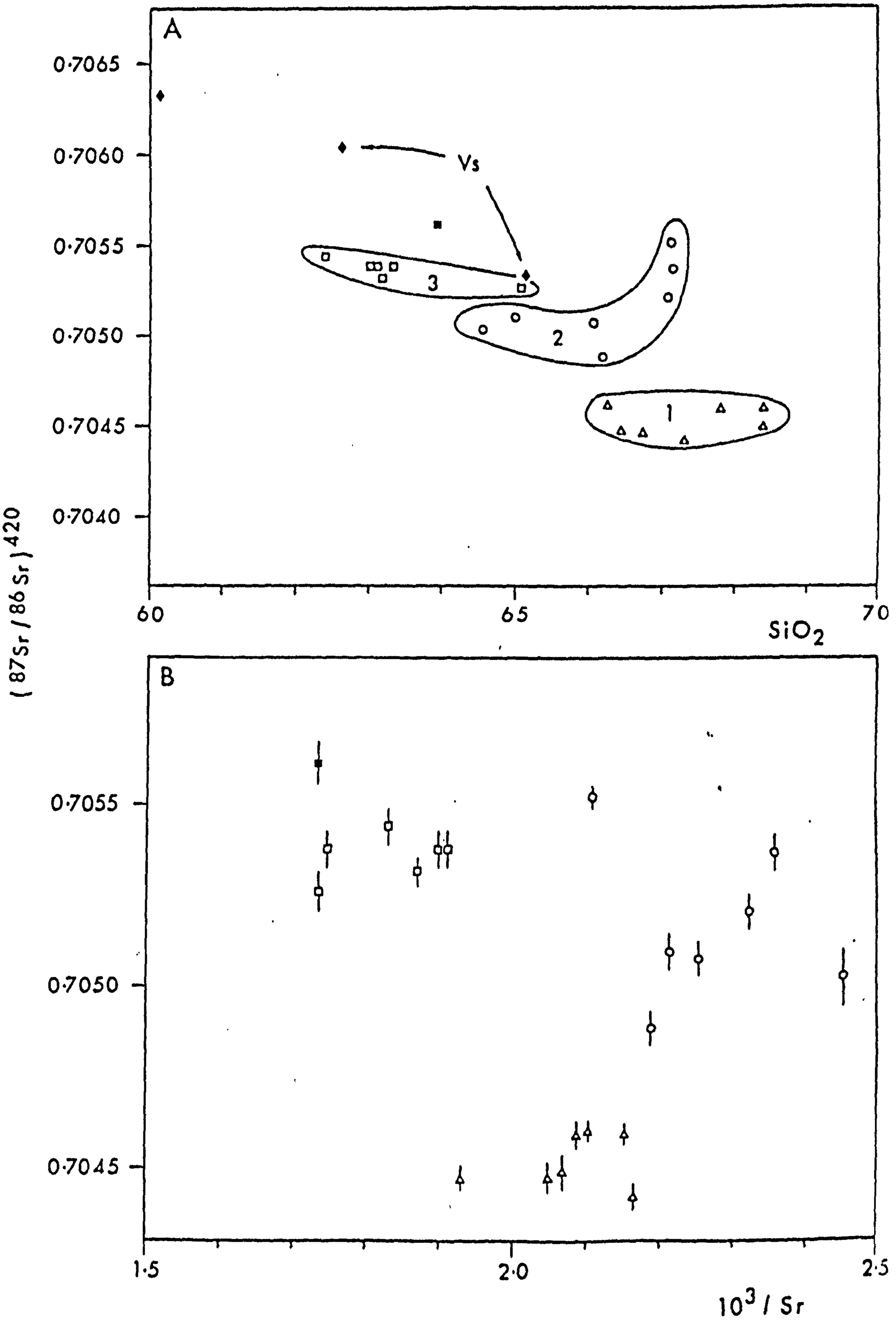

FIGURE 4.32 Plots of initial $^{87}Sr/^{86}Sr$ (calculated at 420 Ma) vs (a)SiO_2 and (b)$10^3/Sr$. Symbols as in Figure 4.4a except filled square - altered G3 clast (4329), filled diamonds - feldspar separates from southerly derived porphyritic andesites (Vs). 2σ errors indicated in (b) by vertical lines.

each of the granite suites show a coherence on both plots. Each of the suites is clearly distinguished by its range of initial ratios. These are highest for granites of G3 type, ranging from 0.70526 to 0.70561, and progressively decrease to 0.70487 - 0.70537 for G2 and 0.70442 - 0.70461 for G1. The between-suite variation in initial ratio confirms the conclusion based on the clast geochemistry that the three suites cannot be related solely by high-level fractionation processes. The initial ratios are all low and would normally be considered to indicate a subcrustal source region. However, low initial ratios carry no implication other than derivation from a source with low Rb/Sr ratios, or in which the time integrated decay of ^{87}Rb has been insufficient to promote enhanced $^{87}Sr/^{86}Sr$ ratios. Potential sources therefore include the mantle, young igneous rocks or volcanogenic sediment, a crustal underplate or old crustal rocks with low Rb/Sr ratios (Leake 1978, Pankhurst 1979).

Turning to the isotopic variation within each of the suites a range of behaviour can be seen. G2 shows the widest range of initial ratios with a tendency for the more evolved end-members to have higher ratios. Hence, the more evolved end-members of G2 have $(^{87}Sr/^{86}Sr)_{420}$ comparable to G3. Fig. 4.32b shows no correlation between initial ratio and $10^3/Sr$ content for samples of G2. This suggests the isotopic variation is not related to simple two component mixing (Faure 1977). As clasts of G2 contain hornfelsed metasediment xenoliths, although not in the same abundance as encountered in G3, it is possible that the isotopic variation reflects some form of contamination by relatively radiogenic Sr, which preferentially affected the more evolved compositions. This suggests the clasts of G2 may have been derived from a pluton which had a similar history of composite intrusion to those described by Halliday et al. (1980) from the Southern Uplands. Clasts of G2 type show a complete range from metaluminous to strongly peraluminous compositions with increasing SiO_2 and DI. This is compatible with the more evolved members containing a greater aluminous metasediment component. This may have been incorporated in the melt by assimilation during ascent or by mixing with a melt derived by anatexis of crustal metasediment.

Whilst the ages for three of the four G2 clasts for which Rb-Sr data are available are broadly concordant, 4282 appears to be slightly older. This is unlikely to reflect erroneous isotopic data for the biotite separate as this was re-analysed and gave similar results. Clasts of G2 type are treated as a coherent group on the grounds that they produce linear arrays on several variation digrams e.g. K_2O vs SiO_2 (Fig. 4.4a). This does not imply that all the clasts are necessarily comagmatic, but they must share similar petrogenetic histories. The slightly older age for 4282 may reflect a history of composite emplacement for the pluton(s) from which clasts assigned to G2 are derived.

Isotopic variation within G3 is more restricted. The single contaminated clast, 4329, plots away from the trend defined by the remaining six clasts towards slightly less radiogenic compositions. This trend towards lower initial ratios with more evolved compositions is the opposite to that seen in G2. Again, there is no obvious trend with $10^3/Sr$ indicating simple two component mixing is unlikely. As the marginal zones of granite plutons are more susceptible to contamination, and as the marginal lithologies are likely to be the most basic in plutons showing normal zoning, the simplest interpretation of the weak trend towards less radiogenic compositions is preferential contamination of less evolved marginal rock-types.

Initial ratios determined for clasts of G1 type show a slight heterogeneity with clustering of ratios into two groups. The coarse-grained grey-white tonalites (G1A) have initial ratios of 0.70446 - 0.70460, whilst the grey-pink and pink tonalites are slightly less radiogenic with initial ratios ranging from 0.70442 - 0.70451. A composite isochron for all the whole rock and mineral data for G1 clasts using blanket errors produces an initial ratio of 0.70451 $\pm$ 2 with a MSWD value for the isochron of 1.33. This suggests the difference between the more and less radiogenic compositions is small enough not to be significant. It is possible that there was slight loss of ^{87}Sr during `reddening` of the pink foliated tonalites.

Clasts of G1 type have the lowest initial ratios of any of the clasts analysed. This produces a crude decrease in $(^{87}Sr/^{86}Sr)_{420}$ with increasing silica for all the data plotted on Figure 4.32a. Whilst this in part reflects non-random sampling, for example none of the most basic and most acid end-members of G2 type clasts have been analysed, the more evolved suites G1 and G2 do have lower initial ratios than the more primitive hornblende rich G3 suite.

Pankhurst (1979) describes a similar anomaly from the Foyers granite complex. Here the most evolved rock types are also the most primitive isotopically with a uniform $^{87}Sr/^{86}Sr$ ratio at 415Ma of $\underline{c}$ 0.7045. Halliday et al (1981) show the trend towards low initial ratios of the evolved granite to be paralleled by the development of metaluminous major element compositions. They attribute the coupling of alumina balance and $^{87}Sr/^{86}Sr$ to a process of aluminous metasediment assimilation.

Figure 4.33 summarises the relationship between $(^{87}Sr/^{86}Sr)_i$ and the alumina balance for the Foyers and Strontian granites, and clasts from the three suites. Only G2 shows variation compatible with the metasediment mixing model of Halliday et al (1981). The highly peraluminous character of G1 and its low initial ratios show that the alumina balance and initial ratios are uncoupled, suggesting a fundamentally different model for the development of the aluminous compositions. What is required is a process of radically increasing the alumina content without enhancing the initial ratio. This is most easily achieved by evoking large degrees of amphibole fractionation, a process which is known to potentially produce strong alumina enrichment (Cawthorn $\underline{et\ al}$. 1976).

Three analyses of fresh feldspar phenocryst separates from the acid andesite and dacite clasts with SiO_2 > 60% are also plotted in Figure 4.32a. These show a decrease in initial ratio with increasingly more evolved compositions. As the volcanic clasts are prone to hydrothermal alteration it is not known to what extent this trend reflects low temperature secondary equilibration, preferentially affecting the more basic clasts. A

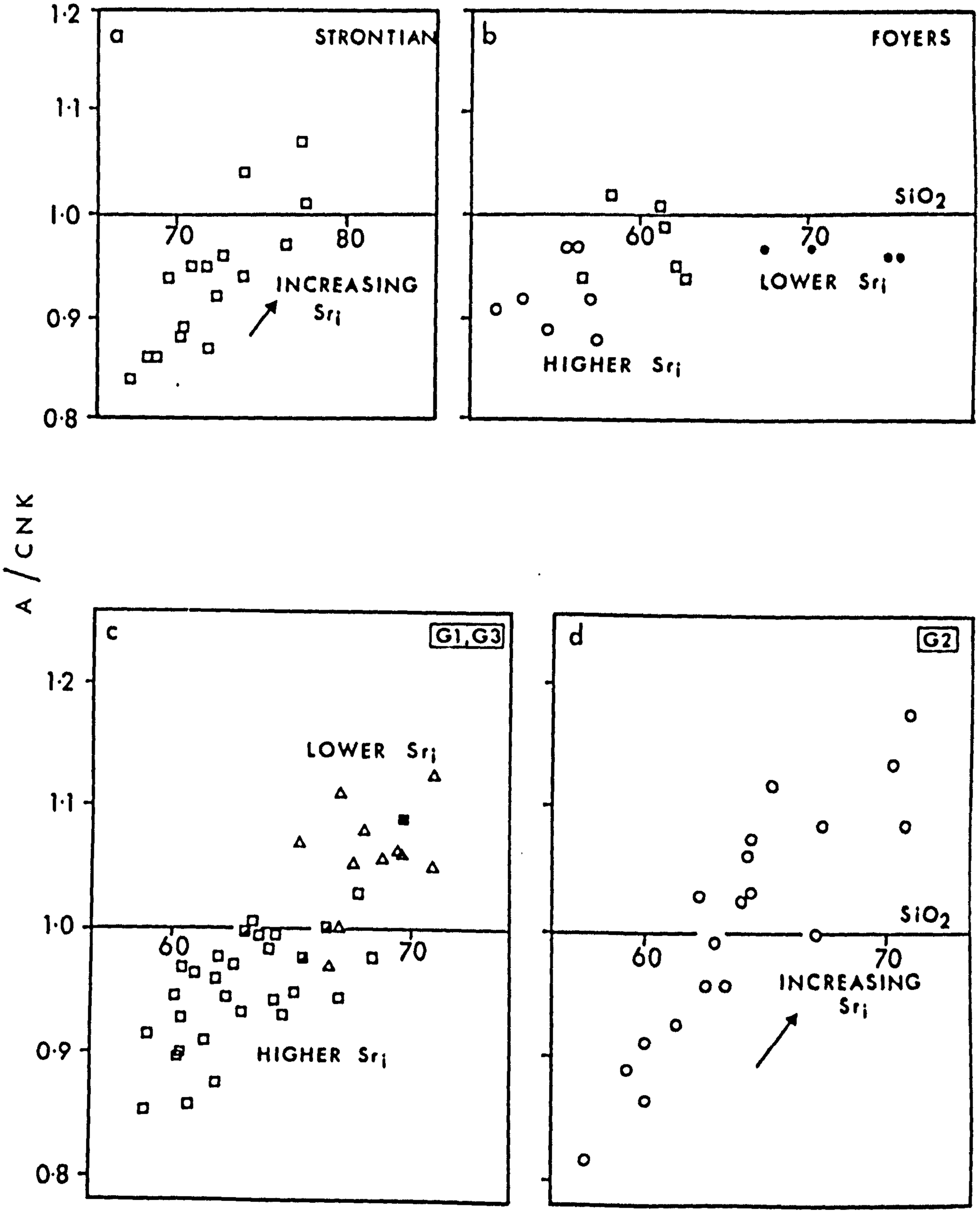

FIGURE 4.33 Relationship between A/CNK (mol $Al_2O_3/(CaO + Na_2O + K_2O)$), SiO_2 and initial $^{87}Sr/^{86}Sr$ (Sr_i) a,b. A/CNK vs SiO_2 plots for Strontian and Foyers granites, from Halliday et al. 1981. c,d. A/CNK vs SiO_2 plots for G1 and G3, and for G2 clasts. G2 shows coupling of A/CNK and Sr_i. G1 clasts are peraluminous despite having lower Sr_i than the less evolved G3 clasts.

combined stable isotope study is required to fully understand what the ratios represent in terms of primary magmatic or secondary alteration related signatures. It is significant however that the most evolved dacite clast, which is probably the least altered, has an initial ratio comparable to clasts of G3 granite, and falls on the G3 trend on Figure 4.32a.

Figure 4.34 shows the distribution of initial $^{87}Sr/^{86}Sr$ with age for granites intruding the Midland Valley and Scottish Highlands. The Scottish Highland data are taken from a compilation by Aftalion et al.(1984) of recent high precision analyses, and from Halliday (1984). The Midland Valley data are from Longman (1980). Average analyses for G1, G2, G3 and G4 are also plotted.

A number of conclusions can be drawn on the basis of this plot. Firstly, there is a clear distinction between granite magmas associated with the two crustal blocks over much of the preserved record. This was emphasised by Van Breemen and Bluck (1981) with respect to c 470Ma magmatism across the Highlands and Midland Valley. They interpret the higher $^{87}Sr/^{86}Sr$ ratios of Ordovician granites in the Highlands as reflecting isotopic zonation normal to an active arc-trench system overlying a northwesterly dipping Benioff Zone. Given the probable lateral separation of the Midland Valley and Highland terranes during the Ordovician (Bluck 1984) it is dangerous to assume that isotopic trends now seen normal to the Caledonian strike reflect original lateral variation, as these may have been generated by juxtaposing terranes with unrelated magmatic histories. Thus whilst the isotopic character of the two blocks is consistent with a model involving isotopic zonation normal to an Ordovician trench system to the south, it may be also satisfactorily explained by regarding the Midland Valley as an arc terrane accreted against a plutonic-metamorphic terrane not directly associated with subduction.

An anomalous feature of pre 435Ma magmatism in the Highlands, in terms of an arc setting, is the connection with crustal shortening, thickening and subsequent uplift. The evidence for crustal shortening in Andean tectonics is relatively minor, and

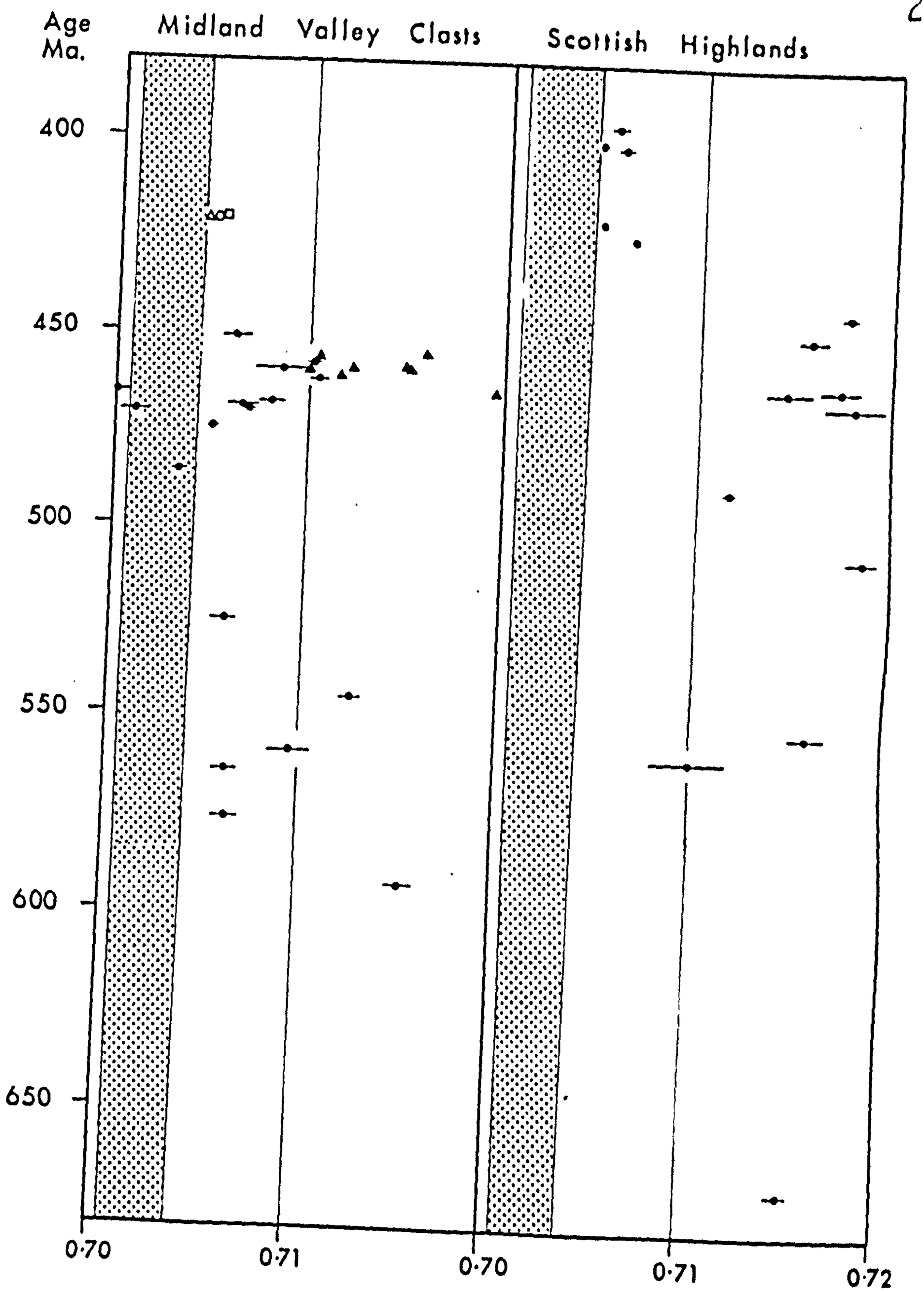

FIGURE 4.34 Comparative Sr isotopic evolution of granite magmas from the Midland Valley and Scottish Highlands. Midland Valley data based on clast analyses by Longman (1980), Van Breemen and Bluck (1981) and the present study. Scottish Highlands data from compilation of high precision analyses by Aftalion et al. (1984). Stipple indicates composition of magmas dominated by a contemporary mantle component. Horizontal lines are 2σ error bars. Filled triangle symbols are northerly derived two-mica granite clasts from the Dunnottar and Crawton Groups. Open triangle, circle and square symbols are average G1, G2 and G3 initial $^{87}Sr/^{86}Sr$ respectively.

it is not considered to have contributed greatly to crustal thickening (Cobbing and Pitcher 1983). The isotopic distinction between the Highlands and Midland Valley magmas up to c 435Ma may therefore reflect a difference in the mechanism whereby crustal thickening was achieved. Whilst the Highlands underwent orogenic contraction, the Midland Valley possibly had a history more comparable with Andean evolution, with crustal thickening achieved by underplating (Cobbing and Pitcher 1983). Partial support for this hypothesis comes from the lower crustal granulite data presented by Halliday et al.(in press). Lower crustal granulite xenoliths occur in Carboniferous volcanics of the Midland Valley. Nd-Sm T_{dm} ages for these xenoliths suggest the basic granulite material beneath the Midland Valley is very young, and this is consistent with a model involving underplating.

A second feature of Figure 4.34 is the apparent convergence in initial Sr isotopic signatures for granites intruding both Highland and Midland Valley terranes in the period following c 435Ma. This suggests both terranes were unified in a single magmatic province at this time, and subsequent displacement between the terranes was insufficient to disrupt the continuity of this chemical and isotopic province (Halliday et al. 1984). The granites occuring in the Midland Valley at c 420 ± 5 Ma are not paralleled by time-equivalent magmatism in the Grampian Highlands terrane sandwiched between the Great Glen and Highland Boundary Faults. Here, granites emplaced in the period 440 - 415 Ma are rare, although there was abundant calc-alkaline plutonism at this time north of the Great Glen Fault (Van Breemen and Bluck 1981). In terms of magmatic activity, the Midland Valley is therefore more closely affiliated with the Northern rather than the Grampian Highlands terrane during the Silurian. Magmatism in the Grampian terrane seems to have been inhibited during this period, possibly by convergence of major strike-slip faults in this zone.

Sr isotopic data from northerly derived peraluminous granites occurring as clasts in the Midland Valley Lower ORS are included in Figure 4.34 (data from Van Breemen and Bluck 1981 and Chapter

5). In age and isotopic signature these have a `Highland` signature and the simplest interpretation is that they have indeed been derived from the Grampian Highlands terrane during the late Silurian. This requires a late Silurian docking of the Midland Valley and Grampian terranes. This is in keeping with the convergence of magmatic character with time shown in Fig.4.34. See Bluck (1984) however for an alternative hypothesis.

4.6 DISCUSSION

4.6.1 Chemical Constraints on the Physical Relationship of Granite Types

There are a number of constraints imposed by the chemical and isotopic data presented above on the physical relationship of the distinct granite types which have been recognised. There are two fundamental problems which need to be addressed. Firstly, what is the relationship between clasts of G1, G2 and G3 in terms of whether they may be derived from separate, or a single zoned pluton; and secondly, what can be inferred about the intrusive relationships of granite and country rock.

(a) Separate or zoned plutons ?

Evidence has been developed above to show that the granite clasts from different suites cannot be related by high level differentiation processes. Several variation diagrams indicate wide separation of trends for each of the suites at constant SiO_2 (e.g. K_2O vs SiO_2, P_2O_5 vs SiO_2). Others show different orientations for trends from different suites (e.g. MgO vs $Fe_2O_3{}^t$). Furthermore Or-Ab-An-Q-(H_2O) relations suggest each suite represents a distinct fusion event. The implication is that each granite suite was formed as a distinct fusion event and that the magma batches so produced underwent very different deep and shallow level differentiation. The granite clasts are therefore unlikely to be derived from a single pluton, and several separate plutons must be envisaged in the sediment source region. This is in spite of the fact that wide compositional variation in single plutons of zoned or composite type is well known. Zoned plutons are common in Cordilleran settings and can show a variety of both continuous and discontinuous compositional variation in both normal (i.e. basic margins to acid core) and reverse sense. The origin of zoned plutons is complex and has been attributed to a number of processes including in-situ fractional crystallisation at high-level, pulsed intrusion of magmas from deeper level magma chambers and progressive magma mixing. In many cases however the trends produced on Harker variation diagrams are linear or curvilinear over wide ranges of compositions e.g. Foyers (Marston 1971, Pankhurst 1979), Loch

Doon (Tindle and Pearce 1981). Others involve bundles of overlapping trends representing several magma pulses e.g. Etive (Clayburn et al. 1983). The wide separation of trends for each of the clast suites, importantly seen at constant silica, cannot be reconciled with the chemical variation seen in the bulk of zoned intrusions. The evidence is therefore in favour of clasts of each suite being derived from separate plutons.

(b) Granite-country-rock relations

Establishing the relationship between igneous and non-igneous clasts in conglomerates is important for a full understanding of the nature of the provenance and for identifying the relative chronology of events in the sediment source area. Granite clasts dispersed to the Crawton Basin are accompanied by large volumes of lithic arenite and metagreywacke detritus. Intrusive relations between the granites and greywackes can be established on a number of grounds.

1. Granite clasts of G2 and G3 type are often rich in metasediment xenoliths. These are frequently angular and invariably recrystallised to granular biotite hornfels. Both texturally and chemically (4335x) the least reworked of these xenoliths closely resemble the clasts of greywacke.

2. Hornfels clasts accompany the clasts of lithic and arenite and metagreywacke. These clasts show a complete gradation with the lithic arenite clasts. They are interpreted as having been derived from a narrow thermal aureole surrounding the granites (see 4.6.3) in which sediment adjacent to the granite was progressively hornfelsed.

3. Granite clasts which are contaminated by metasedimentary and hornfelsed xenoliths do not plot on the trends defined by uncontaminated clasts of the same suite on variation diagrams. Instead, they plot on apparent mixing lines between the field for the sedimentary and metasedimentary clast compositions and their respective suites.

4.6.2 Foliated and Undeformed Granite Clasts

The strong foliation of G1 clasts and the apparent lack of deformation in G2 and G3 clasts requires some explanation. Granite foliations do not necessarily imply transposition of regional deformation fabrics affecting granite and country rocks alike. Holder (1979) demonstrates pulsed deformation associated with successive intrusive phases in a zoned post-tectonic pluton. The rheology and viscosity of fractionating acid magmas are subject to fractionation-dependent variation controlled by residual concentration of volatiles. Volatiles significantly lower the viscosity of a melt and this may allow more evolved magma batches to balloon through and auto-deform earlier formed more basic carapaces. Strong foliations reflecting intrusion related deformation are widely recognised in the marginal zones of many plutons. Stephens and Halliday (1979) record marked foliation and protoclastic textures in marginal granodiorites of the Criffell pluton. Roddick and Hutchinson (1974) noted similar marginal foliations in the Coast Plutonic Complex, British Columbia.

A number of features suggest that G1 clasts have not been foliated by processes of auto-deformation. Firstly, the marginal granites should be more basic than the more evolved granites which deform them, assuming normal zoning. This is not the case with G1 clasts which are amongst the more evolved granite clasts sampled. Secondly, there is no obvious undeformed granite related by high level differentiation to G1 which might have supplied the stress. Thirdly, G1 clasts are notably free of metasediment xenoliths, a fact not easily reconciled with a position marginal to the pluton required by the auto-deformation model. Xenoliths are very abundant in G3 and moderately so in G2 suggesting stoping was an important mechanism in their emplacement to high crustal levels. In containing abundant xenoliths they are unlikely to have intruded and deformed G1.

Given that auto-deformation by multiple intrusion is not a viable explanation for the development of foliated and unfoliated clasts, other mechanisms must be considered. Obviously the chronolgy of emplacement is critical. Two possible scenarios can

be envisaged on the basis of the relative age of foliated and unfoliated clasts.

Firstly, if the foliated clasts prove to be older than the unfoliated clasts, an intervening period of regional deformation might be anticipated. An analogy would be the distinction between `older` and `younger` Caledonian granites. The former precede major orogenic deformation and invariably are strongly foliated. Attempting to relate foliated and unfoliated granite clasts to regional deformation in conglomerate source regions is complicated by the possibility that the unfoliated granite clasts are derived from plutons which escaped a period of deformation due to excessive ductility contrast between pluton and host country-rocks. Differential ductility between pluton and surrounding country-rocks may be such that tectonic contraction is totally accomodated by more ductile country rocks. It is therefore important to establish the nature of the country-rock succession into which plutons represented by the granite clasts were intruded. In this case, intrusive relationships can be established between G2 and G3 and accompanying lithic arenite and metagreywacke clasts (Section 4.6.1). The clasts, on account of their coarse grainsize (pebbles up to 10cm) and large inferred bed thickness are considered to be part of a proximal greywacke pile with a high greywacke to shale ratio. Ductility contrasts between the granites and host succession are therefore thought to be minimal and consequently the age of unfoliated clasts are a reliable lower age bracket of any deformation in the conglomerate source region.

As xenoliths are not seen in G1 clasts it is uncertain whether they too are sourced from a granite pluton intruding the lithic arenite and metagreywacke pile. Deformation of the metagreywackes is mild in comparison with the strong cataclastic foliation developed in G1.

Should the emplacement ages of foliated and unfoliated granite clasts prove to be the same an alternative explanation is required. Hutton (1982) presented an elegant model to account for a variety of foliated and unfoliated granites of similar

emplacement age (c 400Ma) intruding the Dalradian Supergroup, Donegal, Ireland. Strongly foliated (Main Donegal Granite) and unfoliated granites (Thorr pluton) occur in close association and can be related to the heterogeneous stress distribution associated with the prevailing oblique slip tectonic framework. The stress environment in oblique slip mobile belts can vary from compression associated with local displacement gradients on discreet shear zones, to broad extensional areas between such shear zones or transcurrent faults. Unfoliated granites can therefore be emplaced in the extensional field between shear zones whilst foliated granites have a more intimate connection with the localised shear zones themselves. Hutton (1982) proposes the strongly foliated Main Donegal Granite formed as the result of magma injection into an incipient and developing dilational opening on a major sinistral shear zone. Foliated and unfoliated granites of the same age may therefore be characteristic of granite magmatism in oblique slip mobile zones. A corollary of this is that granite clasts sourced in such terranes may be both foliated and unfoliated, but show the same emplacement ages.

The simultaneous closure of the southerly derived foliated and unfoliated clasts to isotopic exchange indicates that the clasts may have been derived from a composite batholith similar in style to Donegal. Whilst the emplacement age of the strongly foliated clasts must remain in doubt, should the Sr isotopes have been re-equilibrated by deformation at c 420 Ma, it is still necessary to account for the strong foliation occurring in some clasts but not in others. The occurrence of a single clast of unfoliated biotite granite of Late Ordovician age suggests regional deformation cannot have occurred post 440 Ma. Silurian magmatism in association with regional oblique slip tectonics is compatible with the data as they stand.

4.6.3 Depth of Emplacement

Granites emplaced at different crustal levels display a variety of emplacement styles controlled by the temperature and rheity of their host rocks (Buddington 1959). A number of criteria are available to distinguish granites emplaced at different crustal

levels (Hughes 1982), some of which are applicable to granites occurring as clasts in conglomerates. Granite textures and contact relationships are particularly important. Several features suggest shallow levels of emplacement for the plutons which yielded the granite clasts to the southerly derived conglomerates. Evidence for high-level emplacement of G3 is particularly strong.

1. Primary granophyric texture is an almost ubiquitous matrix component in G3 clasts suggesting the crystal nucleation rate was low relative to the growth rate. Swanson (1977) showed crystal growth rates in synthetic granite and granodiorite compositions to commonly increase with increased undercooling ($T = T_{(liquidus)} - T_{(growth)}$), with large single crystals giving way to a coarse open array of dendritic to skeletal crystals. Large degrees of undercooling are only likely to be achieved at shallow crustal levels. Bussell (1983) described granophyric intrusions from the Peruvian Coastal Batholith where water under-saturated granitic magma is interpreted as having been emplaced at pressures of approx. 0.5 Kb. Dunham (1965) records high level granophyres and felsites from Rhum which appear to have originated from similar liquid compositions but differ in the extent of undercooling. Again differences in undercooling are related to level of emplacement. The occurrence of granophyric matrix textures in clasts of G3 granite therefore argue for the high level emplacement of a crystal charged melt that was subsequently rapidly quenched. Quenching produced rapid crystal growth outstripping the ability of new crystals to nucleate, resulting in the intergrowth of alkali-feldspar and quartz in ternary minimum proportions.

2. A single specimen (YA 4462) shows small patches of possible interstitial glass in lieu of the usual granophyric matrix. Extremely rapid quenching is indicated. The development of matrix quench textures is therefore quite variable. In other cases microgranite replaces matrix granophyre. Variable quench textures reflect different degrees of undercooling. Kirkpatrick (1976) showed the degree of undercooling to vary with respect to proximity to marginal cooling surfaces and the extent of

crystallisation.

3. There is no evidence for the formation of drusy or miarolitic cavities suggesting intrusion depths were sufficient to inhibit subterranean vesiculation.

4. Angular metasedimentary xenoliths are common in G2 and G3 and suggest emplacement largely by stoping of brittle host-rocks. Stoping is common in high level magmas emplaced above the brittle-ductile transition.

5. The granites intrude a thick pile of lithic arenites and metagreywackes. Large stoped blocks of greywacke are recrystallised at biotite hornfels facies. Biotite hornfels clasts, and clasts gradational between biotite hornfels and lithic arenite, accompany granite and lithic arenite clasts in the southerly derived conglomerates. They are interpreted as the product of thermal metamorphic reworking of lithic arenite in the contact aureole adjacent to the granite plutons. The proportion of hornfelsed to unhornfelsed lithologies and granite clasts is shown in Figure 4.35. The hornfelsed clasts make up only a small proportion of the total volume of lithic arenite and metagreywacke clasts suggesting the zones of contact metamorphism surrounding the granites were relatively narrow. In addition, petrographic inspection has failed to identify Al_2O_5 polymorphs in the hornfelsed lithologies suggesting pressures and temperatures in the aureole rocks were insufficient for their development. This is compatible with their emplacement at high crustal levels.

6. Andesite clasts, found in volcanogenic conglomerates interspersed with the granite-lithic arenite metagreywacke units, and mixed with these non-volcanic units in all proportions, show a textural and chemical similarity with clasts of G3 granite. The volcanic clasts are strikingly porphyritic with euhedral hornblende, biotite and plagioclase phenocrysts. The volume of phenocrysts varies considerably and in those clasts with high phenocryst/matrix ratios, a close resemblance with G3 clasts is discernable. There appears to be a textural continuity between

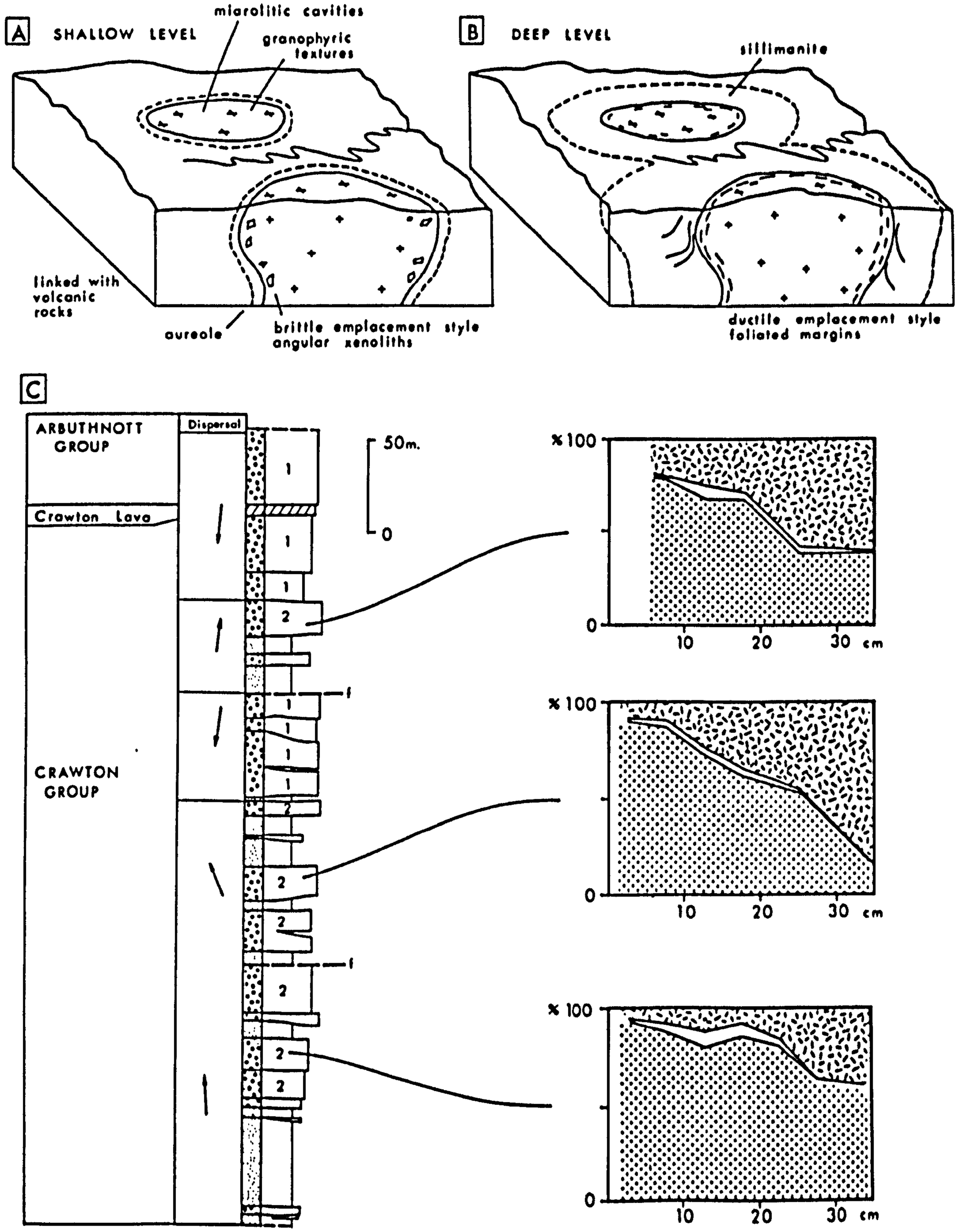

FIGURE 4.35 Constraints on the original emplacement levels of the plutons which supplied the clasts. A,B: criteria allowing granites emplaced at shallow and deep level to be distinguished. C: section through upper part of Crawton Group exposed at Bervie Brow with summary dispersal orientations and relative abundance of granite, country-rock and hornfels clasts. 1,2 refer to Lithosomes 1 and 2 respectively.

granite and volcanic clasts. Chemically, the volcanic clasts also share a certain similarity with G3 granite clasts (4.4.4). The andesites plot in the high-K field of Peccerilo and Taylor (1976) and have similar Rb/Sr ratios.

Sedimentological analysis shows the volcanic clasts to have a contemporaneous volcanic provenance, with vulcanism within the source, and possibly within the basin itself, overlapping subsidence and basin filling. Age constraints on the granite clasts (4.5) suggest they may predate the basin by up to 10Ma, and therefore the volcanic and G3 granite clasts are unlikely to be consanguineous. However their close textural and geochemical affinity (although somewhat masked by the greater low temperature alteration of the volcanic clasts) implies that they may belong to the same suite (sensu Bayly 1968). Geochemical studies carried out on the Peruvian Coastal Batholith have shown that groups of chemically related rocks (the `superunits` of Pitcher and Berger 1972) do not necessarily imply consanguinity in the sense originally proposed. Isotopic age constraints show similar rock associations to be separated by considerable lengths of time, and they therefore cannot be related to a single fusion event. There clearly must be repeated access to the same source materials and the operation of similar lines of petrogenetic descent during long term magmatic evolution.

The similarity of G3 and the andesite clasts is thought to reflect a coincidence of source and petrogenetic processes for separate batches of magma rising to different levels in the crust. G3 rose to sub-volcanic levels and was rapidly quenched, whilst the andesite magma was erupted at the surface. The association of G3 with related volcanic rocks lends support to high level emplacement of G3.

7. Isotopic evidence presented in 4.5 establishes that the granites were emplaced no more than 10Ma prior to their unroofing and dispersal as clasts to the basin of deposition. This constrains the depth to which the granites were originally emplaced in that they were exposed through unroofing relatively quickly.

4.6.4 Relationship between Volcanic and Intrusive Rocks

The relationship between volcanic and intrusive clasts of southerly derivation has been outlined in 4.6.3. The andesites are thought to belong to the same suite as the high-K hornblende-biotite G3 granite clasts, but consanguinity is unlikely on the basis of probable time separation. This is compatible with recent studies in the Andes where broad similarities evident between volcanic and intrusive rocks cannot be substantiated in terms of direct linkage between volcanic and plutonic components (Thorpe and Francis 1979). Rather plutonic and volcanic activity within a given province appears to be divorced in time with separate magma batches either `freezing` before they reach the surface to form plutons, or rising to breach the surface as extrusive rocks. Magma water content may be instrumental in determining whether a magma reaches the surface or whether it crystallises as a plutonic rock at depth (Harris et al. 1970). Interaction with meteoric water may also induce a magma to `freeze` at depth, inhibiting any tendency to rise to higher crustal levels (Pitcher 1978).

The relationship between volcanic and intrusive clasts takes on an added significance when viewed within the wider context of what is known of Midland Valley magmatism. Bluck (1983) drew attention to a vertical change in the composition of igneous clasts in conglomerates sourced from the Midland Valley in the time interval Llanvirn to late Silurian/Lower Devonian. Basic extrusive and intrusive clasts abound in Ordovician conglomerates along with abundant granite and diorite clasts and subordinate acid effusive rocks. With decreasing stratigraphic age there is an upwards transition to increasing proportions of acid and intermediate plutonic and volcanic clasts. A complete transition to basic, intermediate and acid effusive clasts is seen in late Silurian/Lower Devonian conglomerates where the contemporaneous lava source is also preserved. This progressive vertical change was likened to time dependent changes in plutonic and volcanic regimes operating in continental margin settings described by Pitcher (1978) and Bussell (1983).

Seen in this context, the southerly derived conglomerates provide

an insight into a major change in the magmatic history of the northern Midland Valley. Prior to c 415Ma the magmatism appears to have been exclusively plutonic. The oldest available date, from a single clast of G4, extends the history of plutonism back to in excess of 440Ma. The bulk of the intrusive rocks appear to have been emplaced at 420 ± 5 Ma. The single Ordovician granite significantly is garnet bearing, strongly peraluminous and has the most radiogenic Pb signature of any Caledonian granite in Scotland. At c 415Ma the character of magmatism in the northern Midland Valley abruptly changed as plutonism gave way to dominantly effusive processes. Magmas which prior to 415Ma appear to have been unable to penetrate to the surface were suddenly able to do so. The southerly derived conglomerates record this initial transfer to magma eruption which was subsequently to build a substantial volcanic pile (up to 2.4km thick, Francis et al. 1970) during the Lower ORS Arbuthnott Group. There are a number of reasons why a transfer to subaerial eruption may have taken place.

1. Bussell (1983) relates sequences of Andean tectonic magmatic activity to variation in seafloor spreading rates. Basic volcanism is thought to accompany dilation associated with low spreading rates and secondary spreading tectonics, whilst more rapid spreading may result in compression, crustal thickening and attendant crustal fusion to produce voluminous granitoid plutons. A model involving a sudden slowing of sea-floor spreading rate to explain the late Silurian plutonic to volcanic transition presupposes continuing subduction along the northern margin of the Iapetus ocean at this time. It is by no means certain that this is the case.

2. Cann (1970) pointed out some implications of the negative slope on pressure-temperature plots of the melting curve for granites saturated with water vapour (Fig. 4.36a). The shape of the wet melting curve is such that the distance a liquid can rise, and the depth at which it must recross the melting curve, depend on the ratio of water vapour pressure to total pressure at which the granite melted originally. Hornblende is thought to be an important liquidus component in the southerly derived granite

(a)

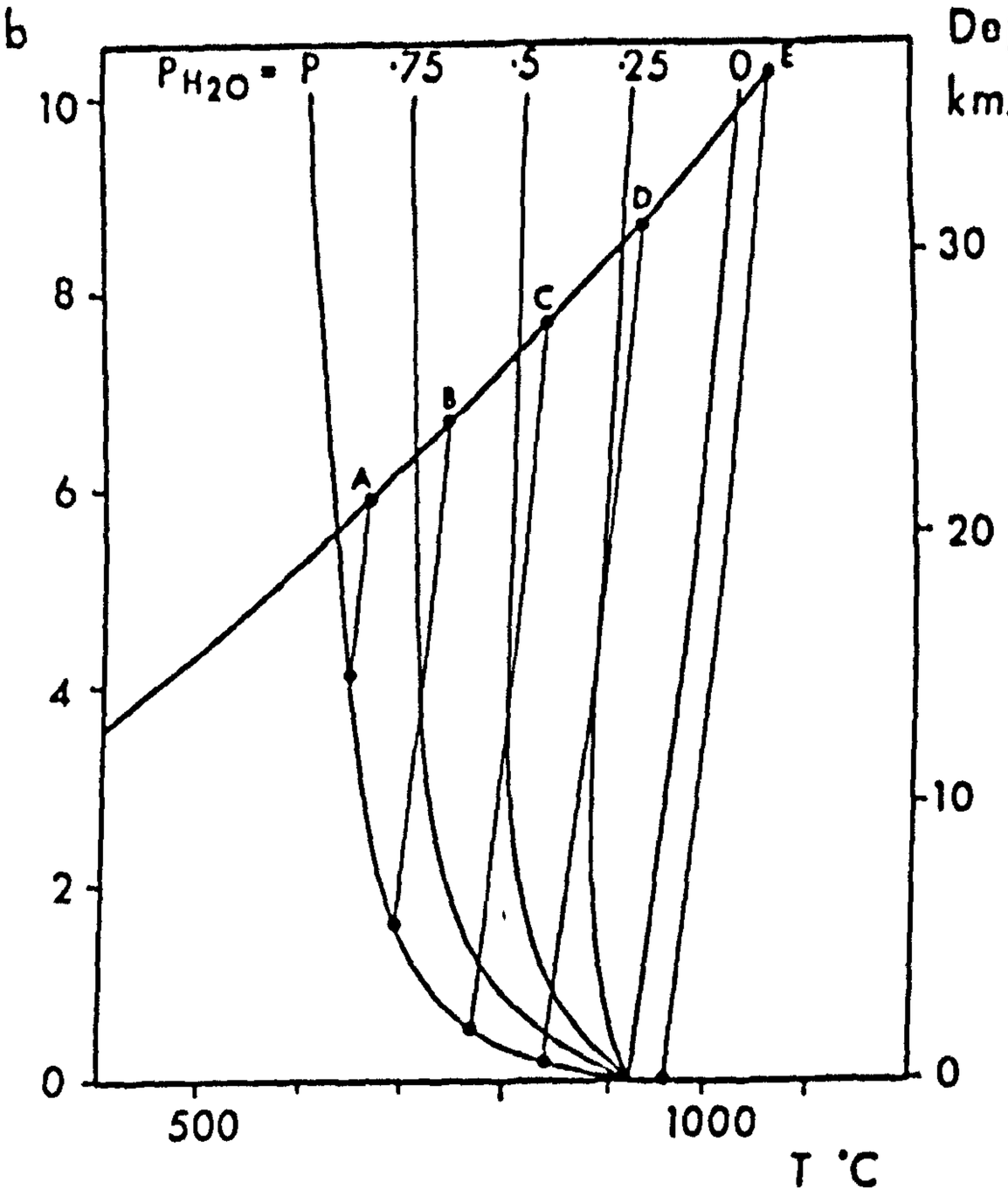

(b)

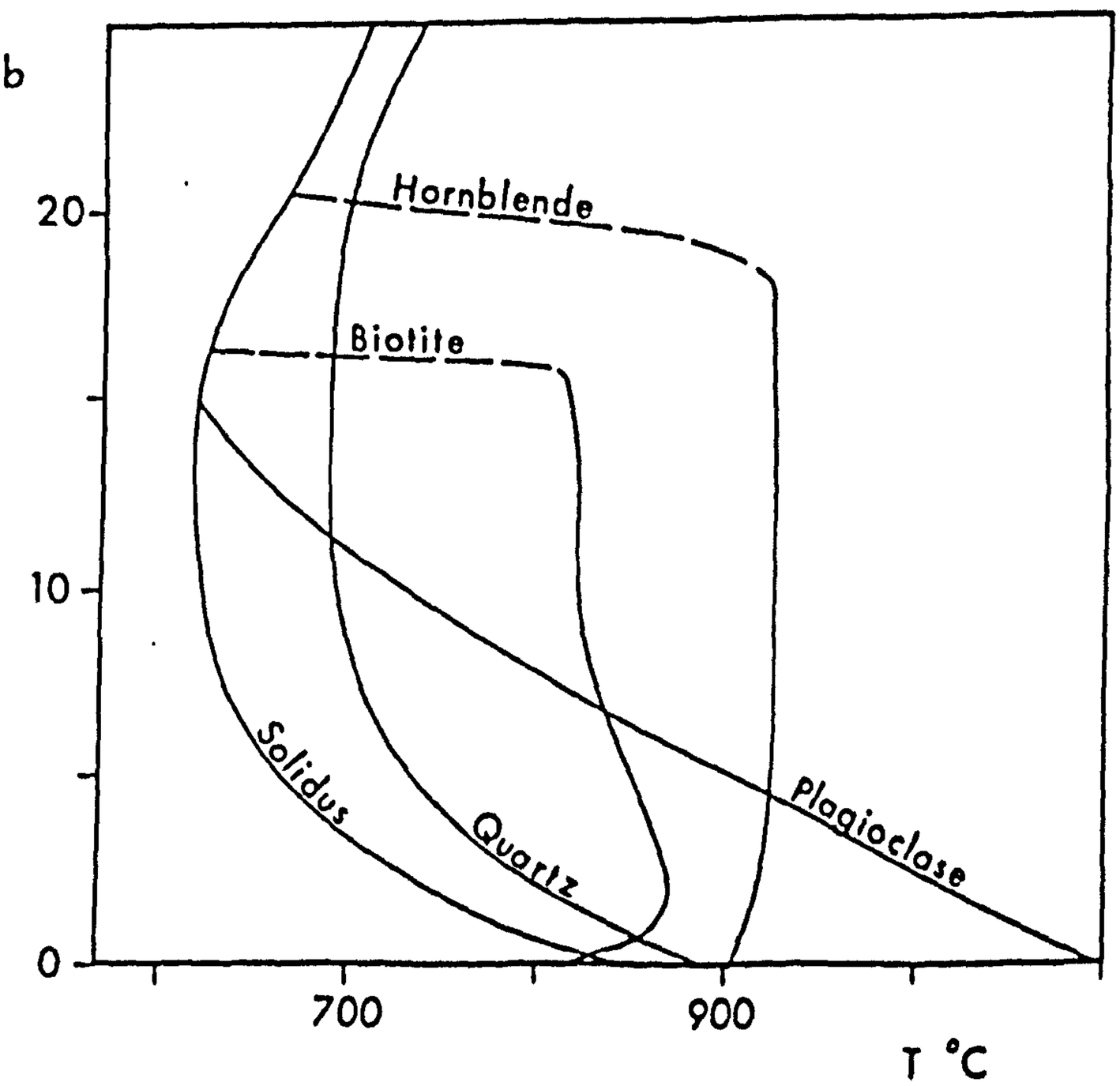

FIGURE 4.36 (a)Schematic pressure-temperature diagram showing melting curves for granite at various ratios of water vapour pressure to total pressure. ABCDE represents geotherm. Tielines are adiabats followed by rising granite magma. After Cann (1970).

(b)Water pressure-temperature plot showing the upper stability limit of phases in tonalitic rocks. Based on Piwinskii (1973a,b) and Lambert and Wyllie (1974).

clasts. A number of studies have shown hornblende to be the dominant liquidus phase in water saturated calc-alkaline magmas (Piwinskii and Wyllie 1970, Eggler and Burnham 1973, Stern 1975). It is therefore likely that the granites had high water contents and this would mitigate against eruption of the magmas at surface. It did not however stop the granites rising to high crustal levels (Wyllie et al. 1976). Shallow emplacement may have been facilitated by buffering or reductions of water contents by hornblende fractionation.

Turning to the lava-pile formed after the transition to surface eruption the evidence is overwhelmingly in favour of water undersaturated magmas. Gandy (1975) in a study of the petrology of Lower ORS lavas of the eastern Sidlaw Hills, finds no evidence for hydrous minerals, apart from infrequent occurrences of biotite, in porphyritic lavas with combinations of olivine, plagioclase, clinopyroxene, orthopyroxene, K-feldspar and opaques as phenocrysts. Similarly, Thirlwall (1982) finds hornblende to be absent, and biotite restricted to infrequent rhyolites and minor acid intrusions, in Lower ORS lavas of the Fife district.

There is good evidence therefore to suggest magma water content played an important role in determining the transition to magma eruption at surface. Thorpe and Francis (1979) appealed to a similar control of intrusive and extrusive rocks in the Andes. The change from plutonic to volcanic magmatism may then reflect a time dependent change in the water content of the magmas. This may be the result of either an exhaustion of the available water supply in the source regions or a migration of the source region to less hydrous materials.

3. Pitcher (1978) attributes high level `freezing` of magmas to interaction with meteoric water. Should the sediment pile into which magmas are emplaced undergo uplift and unroofing, less hydrous rocks with reduced permeability, reflecting deeper crustal histories, are brought closer to the surface. The zone of meteoric water circulation may be therefore progressively displaced towards the surface, allowing magmas to reach shallower crustal levels before `freezing`. Earlier intrusions may have a

similar effect reducing the effectiveness of meteoric circulation. Such a mechanism could conceivably account for a vertical transition from plutonic to extrusive magmatism.

4. An alternative explanation for the apparent temporal separation of volcanic and plutonic rocks in the northern Midland Valley invokes differential preservation. Volcanic rocks erupted at the surface, particularly in regimes associated with regional uplift and large topographic expressions, are likely to have rather low preservation potentials. Thorpe and Francis (1979) point out that Peruvian volcanic rocks exposed at the surface are mostly less than 20Ma old, whereas the Coastal Batholith granitoids show evidence of a much longer history (>70Ma). What is more, much of the recent volcanic rock budget has been lost through erosion and it is by no means certain that the remaining recent volcanic rocks will be preserved when the arc segment is eventually cratonised. Francis (1982) considers the problem of actually preserving in-situ volcanic rocks in the rock-record. Volcanoes associated with subsidence hinge lines can explain several instances of the preservation of thick volcanic piles in the geological past, including the Lower ORS Ochil-Sidlaw volcanic rocks. The emphasis in preserving volcanic rocks is on subsidence, and this subsidence must occur directly after eruption to avoid the extremely high erosion rates seen on the flanks of modern active volcanoes (Davies et al. 1978).

The sudden appearance of volcanic rocks intercalated with alluvium in the Lower ORS may thus be interpreted as reflecting a change in the tectonics of preservation, and not a shift in magmatic processes as outlined above. Regional uplift, associated with return of the crust to normal thickness would preclude preservation of volcanic rocks prior to c 415Ma. Uplift gave way to local tectonically controlled subsidence in the late Silurian allowing volcanic rocks to be conserved. Such a model assumes plutonic rocks were intruded beneath the cover of Lower ORS lavas, and that the granite clasts had contemporaneous volcanic equivalents. These do not appear to have been sampled by the conglomerates.

In summary, given the evidence for higher water contents in the plutonic rocks, and the temporal separation of plutonic and volcanic rocks in more recent continental margin settings, a change in the character of the magmatism is inferred. The effects of preservational bias are thought to be secondary and serve to highlight this change. No single factor is likely to be responsible for this transition to magma eruption but magma water contents and the geometry of meteoric water circulation were probably important.

4.6.5 Origin of Coherent Chemical Variation within Granite Clast Suites

The coherent variation of element relationships requires some comment. Linear or curvilinear relationships are frequently observed for element abundances plotted against SiO_2 or DI. Linear trends tend to characterise the clasts of G3 type, whilst clasts of G2 type show more complex curvilinear trends.

(a) G1

G1 clasts show a remarkably small range of variation, in spite of the fact that the clasts which have been analysed were sampled from southerly derived conglomerates which are widely separated both spatially and vertically in the sequence. This suggests that the foliated granite which produced the detritus must have been reasonably homogeneous. Sub-linear trends on variation diagrams over the small range of compositions available are typical of trends normally expected from acid magmas undergoing limited differentiation i.e. mild increase in K_2O, decreases in MgO, $Fe_2O_3{}^t$, TiO_2 and Ni with SiO_2. The greatest variation is seen in the LIL elements, with the data plotting on a flat trend on the Rb-Sr plot shown in Figure 5.16a, indicating uncoupling of Rb and Sr variation, and considerable variation in Rb content. Initial Sr isotopic compositions show no coherent variation with silica, and are low precluding any significant involvement of crustal contamination in the petrogenesis. The chemical and isotopic data are consistent with the pluton which supplied the clasts of G1 type only undergoing modest high level differentiation without crustal assimilation. If the `depleted` nature of the pluton as a whole is to be ascribed to fractional

crystallisation it must have occurred at deep level. The pluton was emplaced as a homogeneous crystal charged magma which solidifed without significant high level in-situ fractionation.

(b) G2

Clasts of G2 show the widest range in chemical and isotopic compositions of any of the suites. Silica varies from $\leq$ 64 to 71% and over this range there is a variety of elemental behaviour. Trends tend to be curvi-linear, with a distinct inflexion at 68% SiO_2. K_2O increases whilst MgO, $Fe_2O_3{}^t$, TiO_2, Y and Ni decrease. Whilst the trends for $Fe_2O_3{}^t$ and TiO_2 have a gentle negative slope between 64 and 68% SiO_2, those for MgO and Ni are remarkably flat showing no decrease over this range. This is emphasised on the plot of Ni vs MgO in Figure 4.21b. The flat pattern of MgO and Ni in the less evolved rock types precludes mafic mineral fractionation as a viable mechanism for producing the variation between 64 and 68% SiO_2. The negative correlation of Y and SiO_2 rules out substantial feldspar fractionation over the whole range of compositions. This is at variance with the behaviour of Y in the northerly derived granite clasts in which it is progressively enriched, indicating feldspar fractionation was fundamental to the petrogenesis of these granites.

More evolved G2 compositions show an increase in their initial $^{87}Sr/^{86}Sr$ ratios, and in K_2O/Rb (Fig.4.17). This is most easily reconciled with an increasing radiogenic peraluminous component, derived from either magma mixing or crustal assimilation (4.5.4.2). The origin of the complex internal variation in clasts of G2 type therefore probably involves a combination of both hybrid mixing of magma and crustal material, and in-situ fractionation. The evidence for both crustal contamination and strong (amphibole) fractionation in the evolved rock types suggests a process of combined assimilation - crystal fractionation (ACF) may have operated, with assimilation of cold crustal material triggering fractionation so as to maintain the thermal budget of the magma. Crustal assimilation may explain the more scattered pattern of the peraluminous rock-types of G2 on plots of A/CNK vs SiO_2 (Fig. 4.33d.). Whilst the metaluminous low SiO_2 end-members show low scatter with A/CNK <1.0, the

scatter of the data increases markedly with A/CNK >1.0. This may reflect progressive assimilation of a heterogeneous crustal alumina component which is poorly mixed with the magma.

(c) G3

Clasts of G3-type tend to form linear or sub-linear arrays. Again trends typical of magma differentiation elsewhere are seen, with a mild increase in K_2O, and decreasing CaO, MgO, $Fe_2O_3{}^t$, TiO_2, and Ni. A notable feature of the trends for G3 clasts are their often greater scatter. This is attributed to the clasts being derived from a magma which was compositionally heterogeneous. This chemical and isotopic heterogeneity is thought to result from crustal contamination. Samples which plot furthest from the trend are those that visibly contain angular xenoliths. Other clasts displaced from the trends may also have been adjacent to xenoliths, but these may not have been sampled in the clast. This highlights a difficulty in the interpretation of chemical data from granite clasts in a conglomerate. One can only be certain of the physical relationships of the granite sample over the volume of the clast itself. There is therefore uncertainty over any larger scale relations. For example, the granite which formed the clast may have been adjacent to a contact, large xenolith or raft, but no evidence to suggest such a proximity may be preserved in the clast itself.

The linear correlation of Ni and Cr, and between Ni and Cr, and MgO suggests that the magmatic variation, on which contamination effects are superimposed, largely reflects fractionation of the mafic phases, hornblende and biotite. Their euhedral form, and occurrence as inclusions in plagioclase, suggest both were important liquidus phases and were partially separated from the magma. The steep P_2O_5 vs SiO_2 array confirms that apatite was also crystallising throughout the differentiation of the magma.

The distribution of samples is strongly skewed towards more basic lithologies with relatively few evolved G3 types. This is unlikely to reflect sampling bias as it is the more basic clasts which are usually under-represented on account of their greater susceptibility to weathering. The predominance of basic types

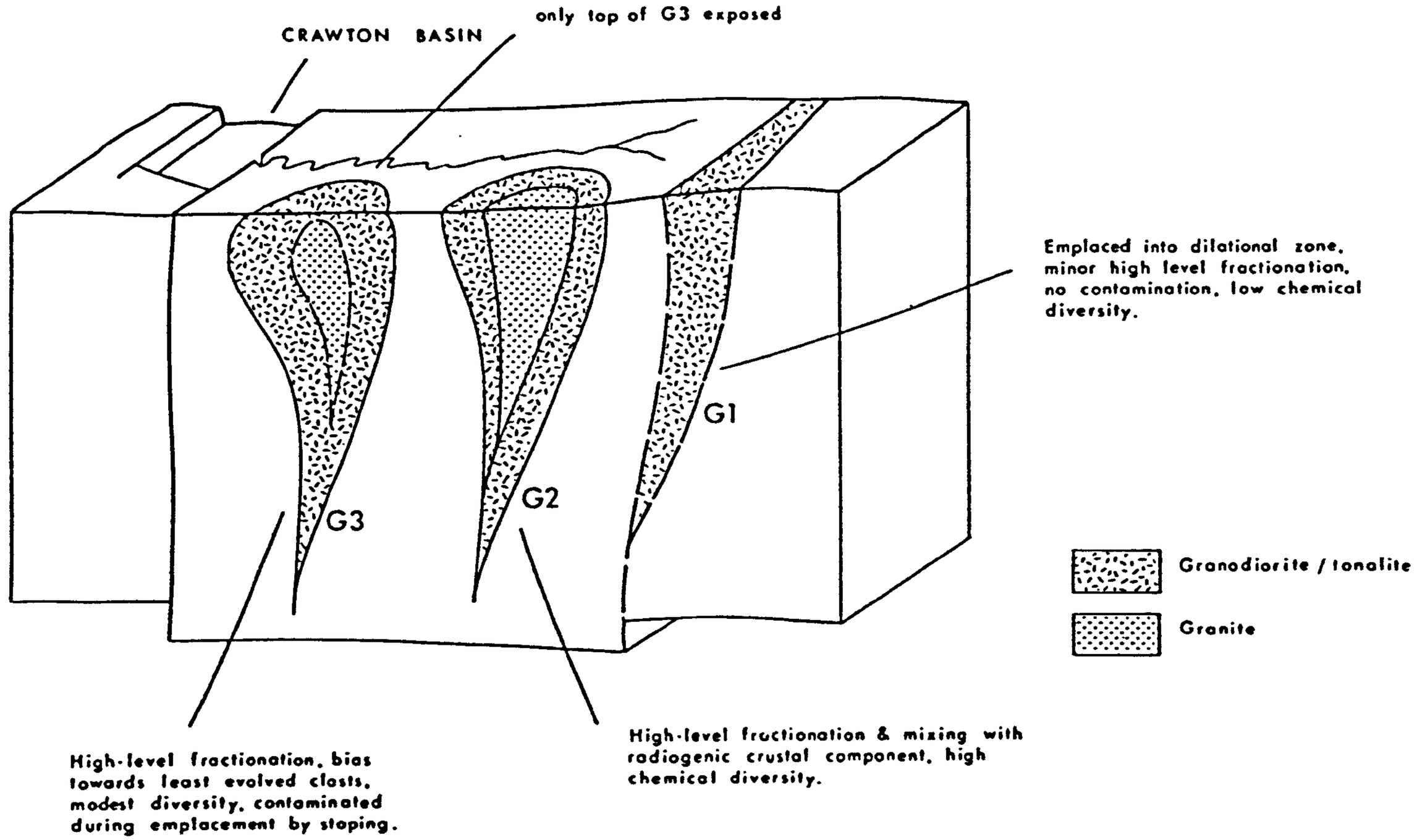

FIGURE 4.37 Model accounting for variation in chemical and isotopic diversity within each of the granite clast suites. The diversity is determined not only by the inherent variability in the original magma, but also by the level of exposure of the pluton which sourced the detritus.

might reflect a real bias towards basic rock-types in the pluton which supplied the clasts, indicating limited differentiation. However, a more realistic assumption is that the clasts are derived from the top of an intrusion in which erosion has yet to reveal a substantial more-evolved component within the core of the pluton. Support for this is the occurrence of possible glass in the interstices of 4462 suggesting very high emplacement levels, and undercooling which can only be achieved very close to the surface. An implication of this model is that much of the pluton may have been left intact within the source terrane, as erosion of the source was terminated at the top of the Crawton Group by overstep of younger northerly derived sediments and contemporary volcanic rocks. It may still be possible therefore to image this pluton geophysically, assuming it has not been removed any great distance laterally by subsequent strike-slip off-set.

Figure 4.37 presents a summary model of the variation seen within each of the suites in which the chemical diversity present in each of the clast suites is related to both the magma petrogenesis and emplacement mechanism, and the level of unroofing. G1 is derived from a uniform magma emplaced passively into dilational opening without in-situ fractionation. G2 shows the effects of both magma mixing and fractionation, and had been unroofed to the extent that a wide range of composition was available at the surface. The narrower range of chemical variation in G3, the evidence for extreme undercooling and the bias towards basic lithologies suggest the pluton from which the clasts were derived was only partially unroofed. The enhanced $(^{87}Sr/^{86}Sr)_{420}$ may reflect crustal contamination as a result of assimilation during emplacement by stoping.

4.6.6 Origin of the Diverse Magma Compositions

A striking feature of the geochemistry of the southerly derived clasts is the wide diversity of magma compositions which exists between each of the clast suites. This diversity cannot have arisen through high level fractional crystallisation or assimilation alone. Significantly, the diversity in composition between the suites is minimal for a range of elements, but

extreme in others. Between-suite variation is best developed in K_2O, and to a lesser extent also in Ni, Cr and P_2O_5. Other elements e.g. TiO_2, Na_2O broadly overlap or show only slight separation. Any explanation for the development of the between-suite diversity must account for this apparent uncoupling of `incompatible` element behaviour.

Wide variations in magma composition at constant silica resulting in separate but subparallel trends are not without precedent. Many instances of restricted provinces showing distinct magmatic lineages have been described in the literature. Foden and Varne (1980), for example, show wide compositional variations in K_2O content at constant silica in adjacent active volcanoes from the Sunda Arc. They appeal to mineralogical and chemical source heterogeneity to explain the data. Varne (1985) proposes that the heterogeneity is produced by introducing continental lithosphere to the arc via arc-continent collision. The K-rich material appearing in the arc volcanoes is considered to be derived from ancient subcontinental mantle involved in the collision zone.

Appleton (1972) demonstrates a similar variation in K_2O from a single volcano, Roccamonfina, in the potassic Roman province. A high-K suite of lavas was found to be also enriched in P, Ba, Ce, Rb, Sr, Th and Zr relative to a low-K suite. Both suites show a sub-parallel evolution indicating that broadly similar high level histories are superimposed on an earlier high- or intermediate-pressure differentiation event.

K_2O variation at constant SiO_2 is not only associated with continental or subcontinental lithosphere. Meijer and Reagan (1983) demonstrated offset K_2O-SiO_2 trends from volcanoes of the Mariana island arc. Here there is no involvement of continental crust, and the volcanoes overlie a Benioff Zone at constant depth. Isotopic evidence suggests a homogeneous source region and the variation is thought to arise from variable degrees of partial melting.

Turning to the granite clasts, there are a number of mechanisms

which may have controlled the development of the between-suite magma diversity. These may be divided into shallow and deep level processes. High level processes leading to magma diversification include vapour phase transfer, crustal contamination, magma mixing and fractional crystallisation. Those at deeper level include partial melting and source heterogeneity.

Vapour phase transfer can be ruled out as Zr is enriched with K_2O. Zr is unlikely to be transported in a vapour phase. K_2O is also uncoupled from Na_2O.Crustal contamination is a more likely mechanism in that the most enriched suite (G3) shows abundant evidence for assimilation of crustal material, and has enhanced initial $^{87}Sr/^{86}Sr$. There are however a number of problems. The metagreywackes which the granites intrude, and which form the most likely contaminant, are substantially more radiogenic than Southern Uplands greywacke. This limits the amount of material the granites can have assimilated without enhancing their initial $^{87}Sr/^{86}Sr$ ratios beyond that which is observed. A three fold increase in K_2O is accompanied by an increase in the initial ratio of only 0.001. The high Sr content of the granites with respect to the greywacke assimilant would make the Sr initial ratios rather robust features of the magmas but this is countered by the low K_2O contents of the lithic arenites and metagreywacke clasts. In addition, these clasts have low P_2O_5 abundances which make it difficult to explain the enhanced P_2O_5 contents in magmas which should be more contaminated. Samples which do show obvious effects of crustal contamination appear to plot on mixing lines between their respective suites and the metagreywacke country rock compositions, but in several instances these contamination vectors do not coincide with offsets between the suites.

Variable contamination of a mantle derived magma by a melt of crustal origin potentially could explain enrichments in K, Ba, and Sr but is less likely to account for high Ni and Cr. In addition, the variation of A/CNK and normative corundum with silica indicates that the more peraluminous compositions which might be expected to have larger sediment melt components are in

fact the least enriched. Incorporation of sediment-derived melts is therefore an improbable mechanism.

High level fractionation has contributed to the within-suite variation. But can fractionation processes, perhaps at deeper level, explain the between suite variation ? The origin of the low K_2O G1 magmas is fundamental to this question. Barker and Arth (1976) evoke an important role for amphibole in the genesis of high-Al_2O_3 tonalites and trondhjemites. Amphibole controlled fractionation has been inferred in the gabbro-diorite-tonalite-trondhjemite suite of SW Finland by Hietanen (1943), who suggested that the tonalitic and trondhjemitic magmas arose by fractional crystallisation of hornblende and biotite from a gabbro parental magma. Arth et al. (1978) modelled the petrology of the suite chemically and arrived at a similar conclusion. Many low K intermediate and acid rocks however have no relation with more basic magmas and various models involving partial melting of mantle sources have been evoked. Suitable mantle sources include eclogite (Arth and Hanson 1972, 1975), amphibolite (Arth and Barker 1976) and mantle rich in phlogopite (Hietanen 1975) which will retain K.

A possible model for the origin of the diverse magma suites might involve either fractionation of amphibole or partial melting of an amphibole-rich mantle source. An early, high pressure, amphibole fractionation event might strip the magmas of Ni, Cr and K_2O, resulting in the K_2O depleted G1 suite. Magmas of G3 type must have escaped such a process. This model explains a number of features of the granite clasts, notably the high Ni content of the high K_2O suite (G3) and the development of peraluminous compositions in the low K_2O suites. Isotopic variation between the suites requires that shallow level assimilation and fractional crystallisation overprint the early deep level differentiation. As the granites form part of a regional late Caledonian event characterised by anomalously high K_2O, Sr and Ba, the problem is not so much one of accounting for unusual enrichment of these elements in G3 but explaining the depletion in G1 against a background of high K magmatism. A high-K mantle or continental lithosphere source was regionally

widely available (Halliday et al. in press). G1 has the lowest concentrations of K_2O of all late Caledonian granites in the silica range 65-70%.

Melting of tonalitic compositions has been investigated experimentally by Lambert and Wyllie (1974). Experimental phase relations found for melting of natural tonalites in the presence of excess water are shown in Figure 4.36b. Hornblende is the liquidus phase for pressures greater than 2 to 3 Kb and is encountered to pressures of the order of 18-20 Kb, the high pressure stability limit (see also Eggler 1972, Allen et al. 1972). If G1 was produced by a deep level fractionation event involving amphibole, the fractionation must have occurred at depths of less than 60km.

Models involving different degrees of partial melting of amphibolitic and eclogitic source materials are difficult to distinguish from a deep-level fractional crystallisation model (cf. Arth et al. 1978). As the latter event would have taken place at depth the resulting cumulates will not necessarily be found at surface level. The wide range of compositions which distinguish the suites G1, G2 and G3 would require a large degree of fractional crystallisation to account for the diversity. Should deep-level differentiation of separate magma batches explain this diversity a particularly effective mechanism of segregating cumulate from melt is required. A possible clue to this mechanism is the fact that clasts of the low K suite are strongly foliated.

Hutton (1982) proposed that the range of intensive styles seen in c 400 Ma granites of Donegal can be related to granite intrusion within a framework of regional sinistral transpression. Soper and Hutton (1984) show sinistral transpression to have widely affected both the ortho- and paratectonic Caledonides during the late Silurian. Sinistral transpression therefore was synchronous with the intrusion of a voluminous phase of c 400 Ma late Caledonian granite magmas. Watson (1984) drew attention to the coincidence between the onset of magmatism amd a fundamental change in the regional tectonic framework, from horizontal

shortening and thrusting to dominantly oblique-slip tectonics. A possible analogue for coupled magmatism and oblique-slip tectonics in the Caledonides is described by Gabrielse (1985). Climactic episodes of granite emplacement along the eastern margin of the Intermontane belt, British Columbia, can be correlated with transitions from dominantly compressive to dominantly transcurrent and related tensional strain.

Leake (1978) first drew attention to the possible role of deep reaching faults in the generation and channeling of Caledonian magmas to the surface. The strongly foliated G1 clasts appear to be broadly of the same age as clasts which are unfoliated (G2, G3). This suggests magmatism in the source terrane may be analogous to that established in Donegal by Hutton (1982). The foliated low K_2O G1 clasts may therefore be derived from a pluton which was intimately associated with shearing and localised compression. The large degrees of deep-level fractionation of amphibole required to explain the low K_2O chemistry, and strongly peraluminous compositions, may be a direct consequence of this close association with a possible shear zone. Filter pressing (Propach 1976) is likely to be a particularly effective mechanism in separating liquid and crystal phases in transcurrent shear zone environments. A longstanding problem with filter pressing generated by tectonic overpressure has been to account for the dilation that is required to accompany the compression, in order that room may created for the filtrate. Transcurrent shear zones are characterised by heterogeneous stress distributions involving both local extension and compression, and they are therefore particularly attractive sites for filter differentiation.

A hypothetical model accounting for the diverse magma compositions is outlined in Figure 4.38. G3 is shown intruding the extensional field between adjacent transcurrent faults. It escaped deep level differentiation and is compostionally similar to other c 400 Ma Caledonian granites. The emplacement of G1 is inferred to have been controlled by a deep reaching shear zone which channeled the magma into a dilational zone at high level. The magma was strongly differentiated at deep level by possible filter pressing with extraction of amphibole, and possibly

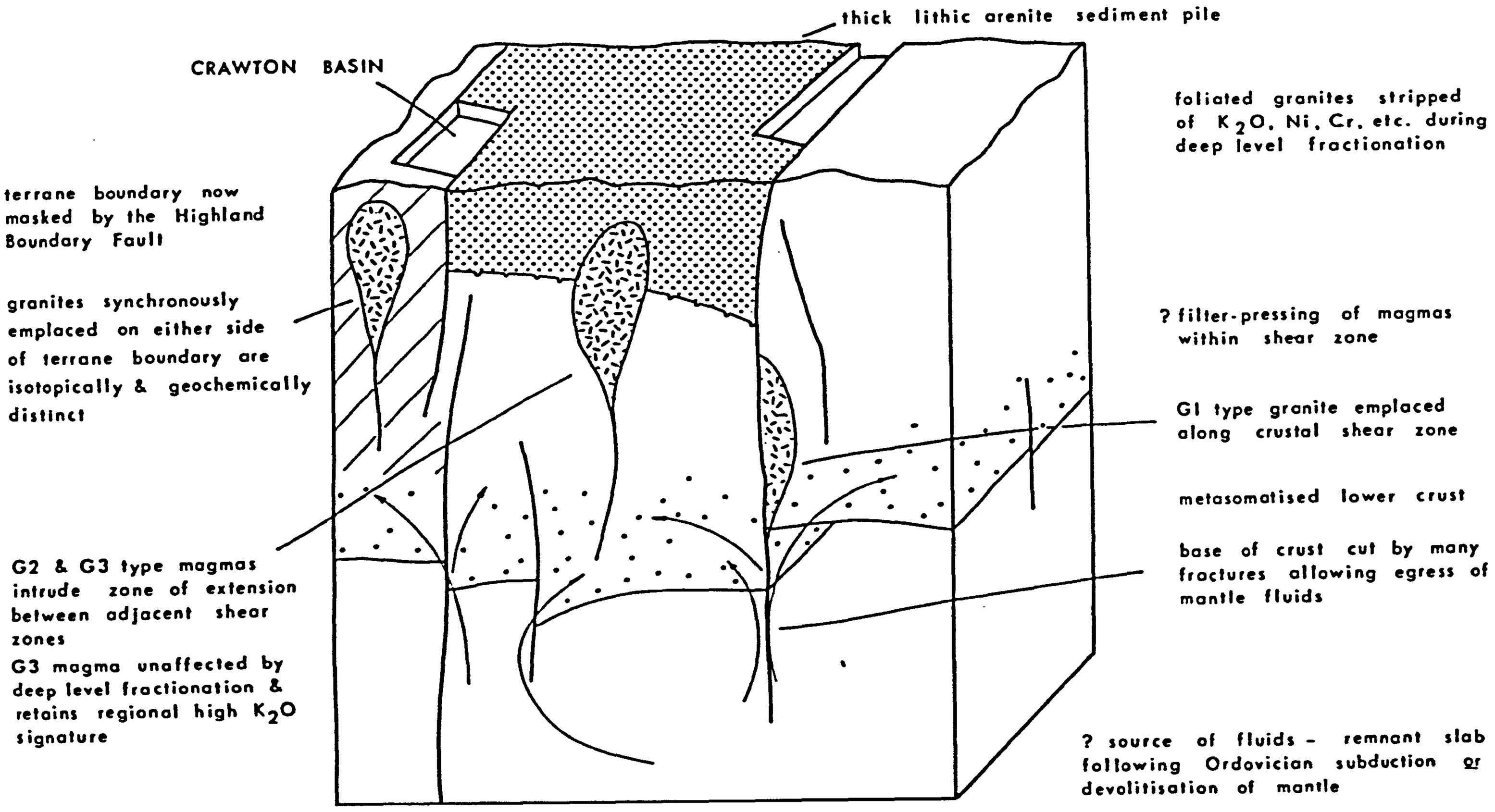

Figure 4.38 : Cartoon illustrating possible role of oblique slip tectonics in determining magma chemistry.

biotite, driving the magma towards peraluminous compositions. Dilation to accomodate the pluton was followed by compression to deform it. Magmas of G2 type are chemically and isotopically intermediate between G1 and G3 and show the greatest range in within suite diversity. They are interpreted to have a complex history of both deep level differentiation and mixing with a metasedimentary component.

4.7 CONCLUSIONS

1. Granite clasts preserved in southerly derived conglomerates of the Crawton Group are a unique sample of granites which can no longer be found in outcrop. The clasts were derived from a source terrane which during the late Silurian - early Devonian occupied the east central Midland Valley.

2. The granite clasts can be subdivided into four distinctive suites (G1-G4) on the basis of their field appearance and petrography. Clasts of equigranular biotite-hornblende granodiorite (G3) dominate the granite component in the conglomerates. Foliated tonalites (G1) and biotite granodiorites (G2) are also important clast lithologies. A fine-grained biotite garnet granite (G4) is only rarely encountered.

3. The conglomerates which host the granite clasts are demonstrably of first cycle origin and are proximal to the source from which they received detritus. Consequently source relationships can be identified with some confidence. Major and trace element chemistry for the granite clasts allows constraints to be placed on the relationship between each of the different clast types.

4. Compositional variation between the granite clasts can be resolved into two components. Amongst clasts assigned to the same suite, chemical variation is generally continuous and produces linear or sublinear trends on variation diagrams. Internal variation of this type is overprinted by a compositional separation of each of the suites.

5. K_2O shows the largest range of between-suite compositional variation. The granite clasts span the full spectrum of compositions from low to high K magmas. This distinguishes them from the high potassic late Caledonian granites which show a more restricted range of K_2O at constant silica. The clasts however show Na enrichment comparable to that seen in other Caledonian granites.

6. The alkali-lime index and AFM trends for the clasts reveal the calc-alkaline nature of the granites which supplied the detritus. Calc-alkaline magmas are generally found in destructive margin settings.

7. The foliated tonalites (G1) are strongly peraluminous and contain accessory garnet. Clasts of G3 type are metaluminous whereas the G2 clasts show a wide compositional variation from metaluminous to peraluminous compositions. G4 is strongly peraluminous.

8. Qualitative trace element modelling suggests feldspar fractionation cannot have played an important role in determining the chemical variation amongst clasts of the same suite. Amphibole may have been the dominant fractionating phase but assimilation and possible magma mixing may also have been important in generating the range of compositions seen in any single clast suite. The extent to which plutons are unroofed in the source will also determine the range of clast compositions occuring in the conglomerates.

9. Rb-Sr mineral isochrons establish that the bulk of the granite clasts are of Silurian age. The exception is the biotite-garnet granite (G4) which is of late Ordovician age. Clasts of G1, G2 and G3 produce a narrow range of ages (420 $\pm$ 5 Ma) despite their wide range in chemical composition. Strongly foliated G1 clasts have ages which are indistinguishable from those obtained from undeformed clasts of G2 and G3 type.

10. The Silurian ages for granite clasts derived from plutons located within the Midland Valley are of some significance in that they establish that granites of calc-alkaline affinity were emplaced in the Midland Valley at a time when magmatism was suppressed in the Grampian Highlands. In this respect, the Midland Valley is more closely affiliated with the Northern Highlands. In the wider context of Lower Palaeozoic magmatism in the Midland Valley, the clasts occurring in the Crawton Basin fill a gap in the record of what can now be seen as a long history of continuous magmatism extending over an interval of

greater than 150 Ma.

11. Initial $^{87}Sr/^{86}Sr$ ratios for the clasts are generally low. They are highest in granites of G3 type and decrease in the order G3>G2>G1. Clasts of G2 type show the greatest internal variation, with the more evolved members of the suite showing a tendency to have higher $(^{87}Sr/^{86}Sr)_i$ and more peraluminous compositions. This is compatible with the more evolved endmembers containing an aluminous metasedimentary component. However, the peraluminous chemistry of G1 clasts cannot be reconciled with a model involving crustal assimilation as the initial $^{87}Sr/^{86}Sr$ ratios of this suite are the lowest of any measured in clasts of southerly derivation. Alumina enrichment by amphibole fractionation may explain the uncoupling of A/CNK and $(^{87}Sr/^{86}Sr)_i$ in clasts of G1 type.

12. The major and trace element chemistry, normative mineralogy and Sr isotopic variation are inconsistent with the granite clasts being related by high level differentiation processes. Whilst high level differentiation may largely account for the compositional variation within each of the clast suites, the compositional separation of the suites at constant silica cannot be explained by such a mechanism. The four suites must represent separate magma batches and the clasts were probably therefore derived from separate plutons in the source terrane.

13. Granites from which clasts of G2 and G3 type were derived were emplaced into a thick sequence of lithic arenites and metagreywackes. Intrusive-country rock relations can be established on the basis of xenoliths occurring in the granites, and clasts of biotite hornfels which are chemically similar to the lithic arenites.

14. The granite clasts were derived from plutons which were emplaced at high level.

15. Biotite-hornblende andesite clasts occur abundantly in the conglomerate sequences of southerly derivation which host the granite clasts. Texturally, chemically and to some extent

isotopically, they are very similar to granites of G3 type. The close association between granites and lavas is an important one in that the southerly derived clasts record an important transition in the character of Midland Valley magmatism from dominantly intrusive to dominantly effusive. Amphibole is an important phase in many Ordovician and Silurian granite clasts sourced from the Midland Valley. Lower ORS lavas are significantly largely devoid of hydrous minerals. Magma water contents were therefore probably important in determining the transition to magma eruption.

16. The similar age of foliated and unfoliated clasts can be explained by invoking granite emplacement in association with regional oblique-slip tectonics. The foliated clasts may have a provenance in granites which were associated with local compression along deep reaching shear zones, whilst the unfoliated clasts may have been derived from magmas emplaced in the extensional field between adjacent shear zones. Support for this interpretation comes from the fact that regional oblique slip tectonics is known to have been operative during the emplacement of the granites, and similar variations in deformation style and emplacement mechanism have been described from the Donegal Granite.

17. The role of magmatism within a framework of oblique slip tectonics may have implications for the variable chemistry of the clasts. The depletion in K_2O and a range of major and trace elements evident in G1 with respect to G3 suggest deep level differentiation may have been important, with fractionation of hornblende and possibly biotite producing the low K compositional trend of the G1 magma at high level. Channeling of the G1 magma to the surface along a deep reaching shear zone may have allowed effective filter pressing to occur producing a magma which was strongly peraluminous. The role for oblique-slip tectonics in the petrogenesis and emplacement of the plutons which source the granite clasts is an extension of the pull-apart origin inferred for the Crawton Basin itself to depth.

CHAPTER FIVE

CHEMISTRY AND GEOCHRONOLOGY OF NORTHERLY DERIVED GRANITE CLASTS - IMPLICATIONS FOR LARGE SCALE STRIKE-SLIP DISPLACEMENTS IN THE SCOTTISH CALEDONIDES

5.1 INTRODUCTION

Granite clasts also occur as an important component in northerly derived conglomerates of the Dunnottar and Crawton Groups. The wide variety of clast lithologies in these conglomerates is matched by an equally diverse suite of granite clasts. These clasts assume particular significance in any attempt to unravel the history of terrane displacement across the Highland Boundary. The close association of the Dalradian, a polymetamorphic terrane known to have undergone rapid uplift following the Grampian Orogeny, and the Lower ORS of the Midland Valley with its abundant metamorphic detritus, encouraged early workers to interpret the Lower ORS as a `molasse` type deposit analogous to the thick siliclastic deposits formed in foreland depressions adjacent to orogenic mountain belts (Campbell 1913, 1929, Allan 1928, 1929, 1940, Friend et al. 1963).

Bluck (1984), however, highlights a number of difficulties with this traditional view including the absence of metamorphic clasts of certain Dalradian type in rocks of the Midland Valley older than the uppermost Upper ORS, and the comparatively small volume of metamorphic material in a provenance that is dominated by contemporaneous volcanic material. Watson (1984) also showed the volume of metamorphic detritus that can be accomodated in sedimentary basins south of the Highland Boundary is small compared to the estimated volume of material that can be calculated to have overlain the now unroofed Dalradian. On the basis of this evidence, the Lower ORS is unlikely to have formed in a `first-cycle` molasse setting, but this does not rule out the possibility that Dalradian detritus did find its way into the Midland Valley Lower ORS basins. The polycyclic nature of the northerly derived conglomerates requires a source not in an uplifting metamorphic basement but in the recycling and handing on of sedimentary detritus from pre-existing basins in the source. These precursor basins may have had a more direct link with processes of orogenic uplift.

A crucial question in any discussion of the provenance of the Lower ORS is the relative position of the Midland Valley terrane

with respect to other terranes from which it might have received sediment during the late Silurian - early Devonian. Evidence presented by Bluck (1984) for Ordovician separation between the Midland Valley and the now adjacent Grampian Highlands terrane is convincing. The largely Ordovician shale and lava dominated Highland Border Complex cannot have lain adjacent to the Dalradian in its present position during the Ordovician as the lithologies preserved at this time (black shales, limestones) are inconsistent with a position adjacent to a terrane undergoing rapid uplift. Accepting a substantial Ordovician separation, the terranes must have been juxtaposed by the uppermost Devonian at the latest, as first-cycle material of local Dalradian provenance appears in the Upper ORS of the Firth of Clyde basin. Bluck (1984) takes this first occurrence of unequivocal first-cycle sediment of Dalradian provenance as indicating a late Devonian docking of terranes which until this time were widely separated.

Whilst the presence of certain Dalradian clasts appearing for the first time in the Upper ORS is not disputed, the nature of the clasts in Lower ORS rocks needs to be examined in some detail in order to see if a Dalradian provenance earlier than Upper ORS is possible.Granite clasts occurring in northerly derived conglomerates of the Crawton Basin have some bearing on this problem. The granite and other clast types occurring in these conglomerates are intriguing because of all the Lower ORS sediments in the northern Midland Valley, they represent the only conglomerates which can be ascribed to an unquestionable northerly provenance. This is because the northerly derived conglomerates of the Crawton Basin interfinger laterally across the basin with conglomerates of southerly derivation. These southerly derived conglomerates have a first-cycle provenance and contain no elements of the northerly provenance. There is no possibility therefore that the polycyclic northerly derived conglomerates have an original southerly derivation from within the Midland Valley and have been returned southwards during recycling.

Returning of material originally derived from a sediment source within the Midland Valley has been proposed as a viable means of

explaining the complex provenance of sediments of Lower ORS age in the western Midland Valley (Bluck 1969, Wilson 1970, Morton 1976, Bluck 1984,Fig.11). Here conglomerates are also dispersed towards both the SE and the NW but the provenance contrast between opposing dispersal directions is minimal and it is difficult to ascertain with confidence the role of recycling and returning of detritus, and hence the ultimate provenance of the sediment.

The almost total absence of granite clasts in the Lower ORS west of Crieff compounds the problem of unravelling the sediment provenance in this area. Granite clasts occur abundantly in conglomerates of the Dunnottar and Crawton Groups. These offer greater scope in discriminating sediment sources in that they show a wider diversity of appearance, chemistry and isotopic signature than do metamorphic clasts. This is particularly true in recycled conglomerates where chemically inert metaquartzites and psammites rapidly dominate the metamorphic component, but where diverse granite suites may persist through the process of recycling. An additional factor favouring the use of granite as opposed to other clast lithologies in testing models of sediment provenance is that the range of possible source regions is reasonably well constrained in terms of geochemical and chronological studies on in-situ granites. This allows a more rigorous approach to assessing the likelihood that a given terrane has supplied a sedimentary sequence with detritus.

Geochemical and isotopic constraints are applied to northerly derived granite clasts occurring in the Dunnottar and Crawton Groups in the following chapter with the aim of testing the validity of a late Devonian docking of the Midland Valley and now adjacent Grampian Highlands terrane, and to characterise the magmatic history of the terrane which was adjacent to the Midland Valley during the late Silurian, be it the Grampian Highlands or a completely exotic terrane.

5.2 PREVIOUS WORK

Van Breemen and Bluck (1981) first realised the importance of the northerly derived granite clasts in the Dunnottar Group. Clasts of two-mica granite from conglomerates exposed north of Dunnottar Castle yield muscovite Rb-Sr mineral - whole rock ages of $\leq$ 460 Ma. Van Breemen and Bluck interpreted these ages as confirming the existence of a widespread subduction related suite of Ordovician granites, occurring south of the Great Glen Fault. Initial $^{87}Sr/^{86}Sr$ ratios were shown to be intermediate between Ordovician granites of the Midland Valley described by Longman et al. (1979), and similar two-mica granites occurring intruding the Dalradian sequence of the Banff and Aberdeenshire areas to the north. The trend towards increasing $^{87}Sr/^{86}Sr$ northwards was related to increasing crustal involvement above a northwesterly dipping Benioff Zone. The contrast between the Ordovician and late Silurian style granite magmatism was attributed to subduction of comparatively younger, thinner, hotter and more buoyant oceanic crust during the late Silurian - early Devonian episode.

Two points concerning their model are worth considering further. Firstly Van Breemen and Bluck (1981) drew attention to an anomaly between the composition of granites occurring as clasts in the conglomerates and those exposed to the north of the Highland boundary in the supposed sediment source. Granites, making up to 25% of the clast assemblages and considered to be `invariably primary muscovite bearing`, cannot be matched with voluminous granites to the north which are largely Siluro-Devonian in age. The nearest plutons of $\leq$ 460 Ma age which might have produced the detritus are some 60km to the north in Banff (Pankhurst 1974). As transport of clasts >1.0m is unlikely over this distance, a more proximal source is required. Van Breemen and Bluck (1981) invoke emplacement of Ordovician plutons high into the Dalradian cover to the north into metamorphic rocks largely at greenschist facies. Subsequent erosion is assumed to have removed these plutons.

The assumption that the granite clasts are invariably primary

muscovite bearing has not been substantiated by more detailed study. Although locally, two-mica clasts are abundant, they are often subordinate and even rare compared to a range of biotite K-feldspar granite types. Furthermore, granites of two-mica type are in fact not restricted to Banff but occur considerably closer to the Highland boundary. The metasediments and amphibolites of the Aberdeen Formation surrounding Aberdeen are veined and injected by foliated biotite-muscovite granite which `may occur in such abundance that they form the dominant rock type within large areas of exposure (IGS 1982)`. These bodies of granite often have gradational contacts with their country rocks and tend to occur as sheet-like or lensoid units up to 10m thick. Larger masses occur on the coast at Cove Bay, just 10km from the Highland Boundary Fault. In addition the two-mica Aberdeen granite may also be related to the granites occurring in the vein complexes. The occurrence of clasts of psammitic metasediment cut by veins of two-mica granite in the northerly derived conglomerates of the Crawton Basin suggests much of the two-mica granite detritus may be derived from a vein-complex rather than a homogeneous pluton. This is substantiated by the heterogeneous chemical and isotopic signature of the clasts.

Given the presence of granites other than two-mica granites as clasts in the conglomerates, and the presence of two-mica granite in the adjacent Grampian terrane, the discrepancy in granite clast composition noted by Van Breemen and Bluck (1981) is not as significant as it appeared initially. This is reinforced by recent geochronological and palynological data (Thirlwall 1983, Richardson 1984) which suggests a late Silurian age for part of the Lower ORS of the Midland Valley. Much of the Lower ORS sedimentation may therefore predate the intrusion of many of the large volume `permissive` plutons emplaced in the Grampian Highlands terrane. They would therefore not be available to produce sediment dispersed to the Crawton Basin.

A second aspect of the Van Breemen and Bluck (1981) model worth some comment is the reliance on processes of subduction to produce both Ordovician and late Silurian granite suites. Stratigraphic and palaeogeographical evidence suggests that the

Iapetus ocean was effectively closed by the end of the Silurian and it is difficult to envisage a direct role for subduction in the formation of many of the large volume late Caledonian granites (Watson 1984). The fact that both widespread large-volume granite magmatism and late Silurian sinistral transpression (Soper and Hutton 1984) occur both to the north and south of the supposed Iapetus suture (Phillips et al. 1976), suggests that both Laurentian and Cadomian plates were united by similar magmatic and tectonic processes at this time. This is consistent with there being no separation across the suture. Thirlwall (1981) circumvents the problem of minimal post-Ordovician separation between Scotland and England by envisaging E-W closure of the Scottish-American and the European or Baltic plates with WNW subduction beneath the Scottish Highlands and Shetland, from a trench situated in the present North Sea. This model however, is critically dependent on the restored position of the Great Glen Fault and its extrapolation through Shetland and fails to account for largely NW-SE compositional variation in late Silurian granites.

The case for Ordovician subduction related magmatism was reviewed in Section 4.5.4.2 Whilst a good case for subduction related magmatism can be made for granites occurring as clasts in a fore-arc setting in the south-west Midland Valley (Longman et al. 1979, Bluck 1983) the relationship of these clasts to both the northerly derived two-mica granites occurring in the Crawton Basin, and two-mica granites exposed in-situ in the Banff and Aberdeenshire areas, is less certain. This is because it is difficult to both spatially relate the granites which occur in terranes known to be widely separated from each other at the time, and to relate the two-mica granites directly to subduction. The two-mica granites are chemically and isotopically compatible with a crustal origin, and were intruded during a time of maximum post-orogenic uplift. They are therefore closely associated with processes of orogenic contraction and crustal thickening and in this respect are unlike many Andean style granite magmas which are associated with crustal thickening which appears to be unconnected with bulk crustal contraction (Cobbing and Pitcher 1983).

Granites of two-mica type with broad S-type characteristics (Chappell and White 1974) are not obviously spatially related to subduction of oceanic lithosphere (Beckinsale 1979). Instead, occurrences of S-type granites around the world are linked with continent-continent and arc-continent collision events. Such collisions occur when marginal basins or oceans are closed and as closure requires subduction it is common to find peraluminous crustally derived granite magmatism overprinting older subduction related magmas in destructive margin settings. Miller and Bradfish (1980) in a review of an inner Cordilleran belt of muscovite-bearing plutons conclude that a simple subduction-zone model for their origin is untenable. Significantly, these Cordilleran muscovite-bearing intrusions are commonly located in areas of extreme polyphase deformation and regional metamorphism reaching upper amphibolite facies.

In conclusion, it is uncertain to what extent $\underline{c}$ 460 Ma granite magmatism in the Highlands and Midland Valley can be integrated in a single model involving across-arc spatial variation in chemical and isotopic parameters. An alternative interpretation might involve juxtaposition of an unrelated plutonic-arc terrane with a metamorphic-plutonic terrane which did not necessarily have a direct connection with subduction. The crucial difference between the two terranes may have been the mechanism whereby crustal thickening was achieved (4.5.4.2). Clasts occurring in the Ordovician conglomerates of SW Scotland are therefore probably the sole plutonic representatives of subduction related magmatism that can be related to active subduction along the northern margin of the Iapetus Ocean.

5.3 FIELD RELATIONS AND COMPOSITIONAL DIVERSITY.

5.3.1 Abundance of Granite Clasts

The unusual abundance of granite clasts in northerly derived conglomerates of the Dunnottar and Crawton Groups has already been discussed (5.1). These high concentrations of granitic detritus persist into the overlying stratigraphic groups above the Crawton Basin but the granite clasts diminish in abundance when these units are traced laterally to the south-west. Granite clasts are relatively uncommon in conglomerates of the Strathmore and Garvock Groups exposed in the North Esk close to Edzell, where two-mica granite clasts dominate the subdued granite component. Further to the west again, granites do not contribute substantially to a provenance which is largely in volcanic and metamorphic rocks (Morton 1979, Wilson 1980, Bluck 1984).

The increasing importance of granite clasts in proximal conglomerates along the Highland Border when traced to the north-east is paralleled by a similar spatial distribution of plutons in the adjacent Grampian Highlands terrane. The largest concentration of granite in the Highlands is seen in the associated Monadliath, Cairngorm, Lochnagar and Mount Battock intrusions of NE Scotland. Plutons in the SW Highlands are rare.

Regional variation in the distribution of late Caledonian granites have been shown to possibly relate to anomalous transverse structures in the lower crust and upper mantle (Watson 1984). It is also possible that the transcurrent fault regime which is thought to have operated during the emplacement of the late granites may have exerted an important control. A striking feature of the geometry of late Caledonian faults is the oblique convergence of the Highland Boundary and Great Glen Fault sets. Soper and Hutton (1984) interpret the Great Glen Fault, and the multitude of fractures sub-parallel to it as a Reidel shear set to the Highland Boundary Fault which is seen as having a major component of sinistral shear. If however the two fault sets are seen as part of a diverging primary fault system, the lack of granites in the SW Highlands may reflect convergence of

displacement gradients in this area, whilst the abundance of granites to the north-east may have been the result of extension between the diverging primary faults, which would have been accompanied by ductile spreading and crustal thinning.

Whatever the mechanism which produced the uneven distribution of late Caledonian granites in the Grampian Highlands terrane, it may be significant that the distribution is mirrored by the abundance of granite clasts in the northerly derived conglomerates of the Lower ORS south of the Highland Boundary Fault. Whether this is coincidental or whether it reflects a provenance for the Midland Valley Lower ORS in the now adjacent terrane hinges on establishing the chemical and isotopic signature of the granites occurring as clasts. Should these be compatible with granites occurring in the Grampian Highlands, there may be no need to invoke an alternative source region for granitic detritus contributed to Lower ORS sediments.

5.3.2. Diversity of Granite and Related Clast Types

Granite clasts occur in northerly derived conglomerates throughout the Dunnottar and Crawton Groups, and are only lacking in the basal Downie Point and Carlin Crag sections of the Dunnottar Group. These granite-deficient conglomerates share many of the characteristics of Lower ORS conglomerates of the western Midland Valley. Their replacement vertically by granite-enriched conglomerates is interpreted as reflecting the later migration of a granite rich source region by oblique-slip translation of the source terrane to the south-west. The model is discussed in detail in Chapter 3.

The granite clasts of northerly derivation show a greater range of diversity than those occurring in conglomerates dispersed to the basin from the south. They have been assigned to ten groups or suites on the basis of their texture, mineralogy and appearance. These encompass the bulk of the compositional variation seen, although rare clasts cannot be assigned to any of the groups identified. The high diversity is compatible with a complex history of sediment recycling and mixing and an areally extensive provenance.The assemblage of granite and related rock

types include:

(a) Two-mica Granite (G_1)

A range of two-mica granites are present as clasts. These are typically grey-white or grey in colour when fresh although a range of pink granites occurs both in the Dunnottar Group and in the North Esk. Both unfoliated and foliated equigranular types occur ranging texturally from fine-grained microgranites to coarse granites and pegmatites. Two-mica granites occur with particular abundance in the Dunnottar Group exposed at Castlehaven Bay (NO 881840) north of Dunnottar Castle, and close to the top of the Crawton Group at Crawton (NO 880796). In thin-section the clasts are all homogeneous with no obvious phenocryst phases. All contain both biotite and muscovite in approximately equal proportions.

Muscovite occurs typically as corroded anhedral crystals both intergrown with biotite and as isolate grains. Biotite tends to be finer grained than the accompanying muscovite, orange-brown in colour and characterised by radiation damage. Minor secondary chlorite is associated with alteration of biotite. Sodic plagioclase is the dominant feldspar occurring together with subordinate K-feldspar. The plagioclase is both zoned and unzoned with more calcic cores mildly sericitised. Myrmekitic textures are well developed in many clasts. The foliated two-mica granites have strongly aligned micas which are commonly kinked, curved plagioclase twinning and granulaton of quartz. Garnet is an important accessory mineral in many clasts.

(b) Porphyritic K-feldspar Biotite Granite (G_2)

Biotite granite clasts with a distinctive porphyritic texture are distinguished from biotite granite clasts which are equigranular. The porphyritic granite clasts are characterised by megacrystic K-feldspar (typically 10-20mm) set in a matrix of variable texture containing equigranular quartz, feldspar and biotite. Many clasts contain abundant basic clots which may represent residues after partial melting. These `contaminated` clasts (G_{2A}) are distinguished from porphyritic granite clasts in which basic clots are absent (G_{2B}). Clasts of G_2 type are generally grey or grey-white in hand specimen with randomly orientated

yellow-brown K-feldspar megacrysts. In thin section, coarse perthite phenocrysts, together with finer grained sodic plagioclase and biotite phenocrysts, float in a matrix of microgranitic granular quartz, feldspar and biotite which becomes granophyric in some clasts (e.g. 2177). In other clasts (e.g. 2215), the contrast between phenocryst phases and matrix is less well defined with the matrix comprised of medium-grained equigranular quartz, feldspar and biotite mosaics. The perthitic megacrysts are often mantled by granophyric intergrowths of K-feldspar and quartz. Many have euhedral to subhedral outlines. Rarer sodic plagioclase phenocrysts are strongly zoned and are euhedral to subhedral in outline. They tend to form glomerophytic clusters. Weak to moderate sericitisation characterises the more calcic cores of zoned plagioclase crystals in many samples. Quartz occasionally forms larger phenocrysts but generally occurs as equant granular crystals in the microgranitic matrix or as intergrowths with K-feldspar. Biotite occurs as anhedral crystals and shows greyish yellow to brownish green pleochroism. The basic clots which characterise the contaminated G_{2A} subtype are composed of medium grained equigranular sub- to euhedral green amphibole and plagioclase. Zircon, sphene, apatite and rutile, together with rare allanite occur as accessory phases.

(c) Granophyres (G_3)

Clasts of granophyre are distinguished in the field by their medium grained equigranular textures and their pale orange or pink colour in hand specimen. In thin section there is a gradation from lithologies dominated by coarse perthitic feldspar with interstitial granophyric intergrowths (2109) to clasts almost totally composed of K-feldspar and quartz granophyre with relict perthitic feldspar and quartz crystals (2160). Mafics comprise <5% of the total by volume and are strongly altered.

(d) Quartz-feldspar porphyry (G_4)

Campbell (1928) first drew attention to the unusual volume of porphyry in the conglomerates of the Lower ORS of the Stonehaven district. He equated the distinctive quartz-feldspar porphyries occurring as clasts with very similar porphyries which cut the

Peterhead Granite at Buchan Ness. In hand specimen variable proportions of quartz and feldspar phenocrysts float in a very fine red brown or grey-brown matrix. The fine matrix imparts an extremely brittle fracture to the clasts. In thin-section, the quartz phenocrysts are characteristically very strongly resorbed and many have a skeletal habit. The feldspars show a dusty alteration. Sodic plagioclase and K-feldspar phenocrysts generally retain euhedral or subhedral outlines, but also occur as ragged corroded crystals. Rare mafic phenocrysts are strongly altered. The matrix is composed of microcrystalline granular quartz with subordinate feldspar, opaques and minor epidote. Grain size within the matrix is variable, becoming cryptocrystalline around phenocrysts with euhedral outlines. The feldspar phenocrysts occasionally form glomeroporphyritic clusters and rarely preserve granophyric style intergrowths with quartz.

(e) Coarse-grained allanite bearing biotite-feldspar granite (G_5)
Although a rare clast component in the conglomerates of northerly derivation these granite clasts are particularly distinctive in the field. They are comprised of very coarse grained (c 10mm) K-feldspar with minor interstitial quartz and mafics. In thin section, the K-feldspar is a coarse perthite which occurs as randomly orientated subhedral crystals. Plagioclase is also present as strongly zoned subhedral to anhedral crystals. Altered biotite and quartz occur with an interstitial habit, but the presence of euhedral zoned allanite (up to 2mm) is perhaps the most distinctive feature of this particular granite suite.

(f) Grey equigranular granite (G_6)
Grey medium-grained granite clasts, texturally similar in appearance to the two-mica granites (G_1) but without muscovite, are occasionally found in the polycyclic conglomerates of the Dunnottar Group. In thin section they are unfoliated granodiorites or granites composed dominantly of equant sodic plagioclase, much of it strongly zoned, together with subordinate K-feldspar (orthoclase), quartz, green biotite, opaques and accessory sphene. Both biotite and quartz occur with an interstitial habit, the latter forming fine granular masses.

(g) Red equigranular biotite granite (G_7)

Granite clasts belonging to this group are particularly abundant towards the base of the Dunnottar Group and they represent the first granite detritus contributed in any abundance to the Crawton Basin. Together with the two-mica granite clasts (G_1) and porphyritic biotite granite clasts (G_2), these three groups dominate the northerly derived granite contribution. The red equigranular granite clasts are coarse-grained (feldspars are typically 5-10mm), with a very low colour index. Red K-feldspars are obvious in hand specimen together with translucent quartz and minor mafics, generally altered biotite. In some cases the granite is composed solely of feldspar and quartz with accessory quantities of opaques. In thin section, the mineralogy is dominated by coarse perthitic K-feldspar and quartz, with subordinated finer grained sodic plagoclase. Occasional myrmekite is developed in association with the latter.

(h) Equigranular hornblende granodiorites (G_8)

Although the bulk of the granite clasts of northerly derivation are highly evolved with colour indexes and mafic contents <10%, rare clasts of more basic plutonic rocks do occur. These include a distinctive hornblende rich granodiorite, together with clasts of appinitic affinity.

(i) Recycled biotite-hornblende granodiorites (G_9)

Occasionally clasts which resemble granites found in conglomerates associated with the southern margin of the basin are found in the polycyclic conglomerates of northerly derivation. Lithic arenite and metagreywacke clasts of southerly provenance also appear in the conglomerates of northerly derivation. They are interpreted as having originally been derived from a source to the south but subsequently were reworked and mixed with material of northerly provenance and returned southwards. Limited mixing of the two provenances must have occurred either prior to the basin formed or actually during basin filling (Fig. 6.1).

(j) Miscellaneous hypabyssal porphyries (G_{10})
A variety of acid porphyries can be distinguished. These are distinct from the quartz-feldspar porphyries (G4) and encompass a wide range of textures.

5.3.3 Relative Abundance of Granite Clast Types.
The diversity of granite types occurring in the northerly-derived sequences is often not appreciated at a single locality, where the range of granite lithologies has a marked tendency to be more restricted. This makes the relative volumes of each of the groups defined above difficult to estimate over the succession as a whole. The biotite-muscovite granites G_1, and biotite granites G_2 and G_7, are dominant, making up $\underline{c}$ 70% of the granite contribution to the coarse fraction. The ratio of G_1 to other types is probably close to unity and two-mica granites therefore by no means dominate the provenance.

The inequable distribution of granite types in the conglomerates, and the enrichment of a single clast type over sequences tens of metres thick suggest the multicyclic conglomerates cannot simply be modelled in terms of derivation from a well mixed pre-existing conglomerate in the source. A good example of the vertical segregation of granite clast types can be observed in sections exposed between Strathlethan Bay and Dunnottar Castle. A sequence some 100 metres thick at Bowdun Rocks shows a strong enrichment in red equigranular granite clasts (G_7) towards the base, but increasing numbers of porphyritic biotite granite clasts (G_2) are encountered when traced up the succession. Further south, the granite provenance is swamped by two-mica granite clasts in Castlehaven Bay. It was from this section just north of Dunnottar Castle that Van Breemen and Bluck (1981) established a $\underline{c}$ 460 Ma age for the two-mica granite clasts.

Isotopic data presented in 5.6 however also suggest an important contribution from late Silurian granites. As these were emplaced just shortly prior to their unroofing and dispersal as clasts to the basin of deposition in which they are found, this precludes their having been involved in an early history of recycling. In this respect, a substantial component of the granite clast

contribution may have been derived and incorporated with a mixed recycled granite-metamorphic provenance in a similar manner to the independent source envisaged for the volcanic clasts. Local variation in the composition of the granite detritus is therefore thought to reflect variable degrees of mixing between first cycle sediment shed from young high level granite plutons and well mixed recycled two-mica granite-psammite-quartzite gravels which were preserved in temporary basins within the source. As the granite clasts are invariably well-rounded (4.1) making them relatively insensitive to transport distance, granites of recycled and first cycle provenance cannot be distinguished texturally. A consequence of both the probable recycled history of the two-mica granite clasts and the young ages of the biotite granites which therefore are unlikely to have been recycled is that it is difficult to relate the abundance of granite clast types seen in the conglomerates with their original abundance in the source area. It is conceivable that the relative abundance of two-mica granite clasts has been considerably biased by a longer history of transport and redeposition which the younger granite clasts are unlikely to have been through.

5.3.4 Sampling

Sampling followed the same procedure as outline in 4.2 with the emphasis on only collecting the largest (>40 cm) unfractured clasts, from which the exterior weathered skin was removed. Given the wide diversity of granite types and the limited number of samples for which chemical analyses could be produced in the time available, only the commonest clast types were sampled in any detail. Thus ten clasts of two-mica granite (G_1), eighteen clasts of porphyritic biotite granite (G_2) and ten clasts of equigranular red biotite granite (G_7) were sampled. Together, these groups comprise $\leq$ 70% of the total granitic detritus. Other clasts sampled include four clasts of granophyre (G_3); six clasts of quartz feldspar porphyry (G_4); a single clast of G_5, the coarse-grained allanite bearing granite; three clasts of grey equigranular biotite granite (G_6); two clasts of a distinctive hornblende granite (G_8); three varied clasts of porphyry (G_{10}); and finally two granite clasts which resemble the clasts of southerly provenance described in Chapter 4. In addition, 3

clasts which are not easily assigned to the above groups were collected and analysed. They are representative of a range of rarer granite clast types which volumetrically are unimportant, often occurring as single isolate clasts with no obvious correlatives in terms of clasts sharing a similar texture and appearance. 2118 is a strongly foliated gneissose biotite granite, 2171 a fine-grained red biotite granite and 2470, a biotite K-feldspar granite with distinctive large yellow quartz phenocrysts.

Ten clasts of volcanic rock, ranging from andesite to rhyolite in composition were selected as being representative of the volcanic clasts which both accompany the polymict conglomerates and which are interbedded with these conglomerates as exclusively volcanic units. These were analysed to test for possible equivalence between the volcanic and granitic rocks in the source terrane. A total of 72 volcanic and granitic clasts sampled from northerly-derived conglomerates were subsequently analysed for major and trace elements.

Sample localities and grid references are included in Appendix 1. Coastal exposures at Downie Point (NO 884854), Strathlethan Bay (NO 880848), Bowdun Rocks (NO 885845), Castlehaven Bay (NO 881840), Old Hall Bay (NO 882837), Crawton (NO 880796), Whistleberry (NO 863753) and Whitehouse (NO 824705) provided the bulk of the samples.

Full major and trace element analyses are presented, together with selected CIPW Norms, in Table 5.2. Table 5.1 summarises the various clast groupings and assigns a symbol to each of the clast types. These symbols are used in all subsequent variation diagrams and plots. The volcanic clasts (V_N) are plotted on these diagrams for comparative purposes using a square symbol.

GROUP	CLASSIFICATION	SAMPLES	SYMBOL
G_1	TWO-MICA GRANITE	3134,3142,3152,3156,3158,3220,3301, 3305,3306,3307	◇
G_2 A	PORPHYRITIC K-FELDSPAR BIOTITE GRANITE	2177,2455,2475,2475-A,2454-2,2473, 2180,2215	○
B		3422,3244,3137,3309,4272BR,2130, 3424,3423	◒
C		3304,2467	⊘
G_3	GRANOPHYRE	2109,2160,2162,2181	◆
G_4	QUARTZ-FELDSPAR PORPHYRY	3132,3138,3144,3185,3199,3200	▽
G_5	BIOTITE-ALLANITE GRANITE	3219	◈
G_6	GREY EQUIGRANULAR BIOTITE GRANITES	3155,3159,2112	▲
G_7	RED EQUIGRANULAR BIOTITE GRANITE	2450,2457,2451,2178,3436,2445,2474, 2449,2129,2179■.	◪
G_8	HORNBLENDE GRANODIORITE	3435,3421	●
G_9	RECYCLED GRANODIORITE	2476,2468	△
G_{10}	OTHER PORPHYRIES	3187,3193,3194	⊠
V_N	NORTHERLY DERIVED ANDESITIC AND DACITIC CLASTS	2183,2208,2101,2210,2469,2466, 2471,2102,2472,2106	□
OTHERS	FOLIATED BIOTITE GRANITE	2118	⊖
	FINEGRAINED RED BIOTITE GRANITE	2171	▼
	K-FELDSPAR BIOTITE GRANITE	2470	▲

TABLE 5.1 Classification of northerly derived granite, porphyry and volcanic clasts with symbols used to distinguish groups on subsequent plots.

SAMPLE	3134	3142	3152	3156	3158	3220	3301	3305
GROUP	G_1	G_1	G_1	G_1	G_1	G_1	G_1	G_1
MAJORS								
SiO_2	74.06	74.44	74.35	73.19	72.22	73.62	74.33	73.98
Al_2O_3	14.83	14.11	14.13	14.03	13.78	14.02	14.35	13.99
TiO_2	0.11	0.11	0.15	0.25	0.23	0.15	0.09	0.20
MnO	0.06	0.05	0.09	0.06	0.06	0.05	0.06	0.06
$(Fe_2O_3)^t$	1.75	1.69	2.32	2.24	2.20	1.85	1.55	2.18
MgO	0.17	0.21	0.30	0.35	0.47	0.03	0.02	0.10
CaO	1.54	1.41	1.23	1.16	1.97	1.17	0.73	0.99
Na_2O	3.75	4.07	3.60	3.14	3.41	3.68	3.76	4.05
K_2O	3.78	3.96	4.24	4.62	3.98	4.75	4.13	4.22
P_2O_5	0.06	0.06	0.14	0.15	0.09	0.08	0.13	0.08
LOI	nd	0.48	nd	0.85	1.35	0.29	1.41	0.68
FeO	nd	nd	0.88	nd	nd	nd	nd	nd
Fe_2O_3	nd	nd	1.29	nd	nd	nd	nd	nd
TOTAL	100.11	100.59	100.40	100.04	99.76	99.69	100.56	100.53
TRACES								
Nb	8	12	nd	25	9	nd	nd	nd
Cr	0	5	0	5	37	10	21	46
Co	3	0	1	0	0	0	0	0
Ni	0	2	0	6	0	2	0	2
Cu	4	7	2	22	24	10	4	3
Zn	32	34	28	42	37	35	31	53
Ga	18	18	18	19	18	17	18	21
Rb	213	140	136	165	113	206	145	202
Sr	95	202	166	142	265	95	95	117
Y	21	13	20	17	13	16	18	12
Zr	103	74	99	162	152	102	65	177
Ba	457	584	536	725	770	405	308	655
La	31	10	21	39	30	28	12	40
Ce	58	34	44	81	63	58	25	88
Pb	26	23	19	21	16	24	28	22
Th	15	6	8	15	12	13	3	20
U	4	3	2	2	4	3	2	3

TABLE 5.2. MAJOR AND TRACE ELEMENT ANALYSES OF NORTHERLY DERIVED PLUTONIC AND VOLCANIC CLASTS.

SAMPLE	3306	3307	2177	2180	2215	2454-2	2455
GROUP	G_1	G_1	G_{2A}	G_{2A}	G_{2A}	G_{2A}	G_{2A}
MAJORS							
SiO_2	74.98	72.82	67.82	73.41	74.71	71.45	70.27
Al_2O_3	14.03	14.01	14.52	13.77	13.21	13.99	14.23
TiO_2	0.11	0.26	0.60	0.29	0.25	0.44	0.51
MnO	0.05	0.04	0.10	0.07	0.04	0.07	0.08
$(Fe_2O_3)^t$	0.95	2.10	4.20	2.50	2.38	3.26	3.77
MgO	0.00	0.07	1.19	0.28	0.23	1.09	1.16
CaO	0.38	0.75	1.69	1.18	1.18	1.35	1.54
Na_2O	3.02	3.50	3.59	3.62	3.72	3.24	3.31
K_2O	5.50	4.86	4.59	5.12	4.59	4.35	4.55
P_2O_5	0.16	0.18	0.10	0.09	0.06	0.07	0.09
LOI	0.83	1.00	1.12	0.62	0.75	1.20	0.93
FeO	nd	nd	nd	nd	1.12	2.76	2.27
Fe_2O_3	nd	nd	nd	nd	1.13	0.19	1.24
TOTAL	100.01	99.59	99.52	100.95	100.99	100.2	100.18
TRACES							
Nb	nd	nd	nd	nd	nd	nd	nd
Cr	0	17	34	22	20	19	54
Co	0	0	10	4	0	0	2
Ni	2	3	11	3	0	3	3
Cu	3	31	8	6	0	9	3
Zn	16	48	82	46	40	55	64
Ga	17	19	22	20	19	21	19
Rb	146	189	122	213	183	136	144
Sr	168	125	158	96	83	124	127
Y	15	15	35	38	44	44	43
Zr	64	169	348	271	239	324	333
Ba	701	369	947	721	501	716	780
La	8	39	83	48	57	71	73
Ce	22	80	153	102	116	143	130
Pb	23	24	20	26	22	22	25
Th	2	19	14	21	20	14	16
U	2	3	4	3	4	4	4

TABLE 5.2 (cont.)

SAMPLE	2473	2495A	2475	2130	3137	3244	3309	3422
GROUP	G_{2A}	G_{2A}	G_{2A}	G_{2B}	G_{2B}	G_{2B}	G_{2B}	G_{2B}
MAJORS								
SiO_2	73.49	71.32	73.57	73.74	69.84	68.88	70.15	68.63
Al_2O_3	13.63	14.21	13.53	13.42	14.26	13.69	14.51	14.63
TiO_2	0.33	0.45	0.32	0.31	0.36	0.58	0.34	0.65
MnO	0.08	0.07	0.06	0.06	0.07	0.05	0.08	0.11
$(Fe_2O_3)^t$	2.81	3.45	2.67	2.54	2.56	4.12	2.52	4.66
MgO	0.83	1.08	0.68	0.48	1.00	0.79	0.89	1.58
CaO	1.04	1.33	1.05	1.27	1.88	1.51	2.25	1.61
Na_2O	3.41	3.43	3.38	3.51	4.09	3.77	4.25	3.12
K_2O	4.65	4.67	4.83	4.74	4.13	4.00	4.07	3.86
P_2O_5	0.06	0.07	0.05	0.08	0.14	0.14	0.14	0.15
LOI	0.63	1.42	0.77	nd	1.08	1.06	0.88	1.51
FeO	nd	nd	1.89	nd	nd	nd	nd	2.82
Fe_2O_3	nd	nd	0.57	nd	nd	nd	nd	1.52
TOTAL	100.90	101.50	100.7	100.15	99.41	98.59	100.08	100.19
TRACES								
Nb	nd	nd	nd	29	23	nd	nd	nd
Cr	20	5	42	11	22	14	30	22
Co	1	0	1	1	3	2	4	3
Ni	4	1	1	3	18	4	14	2
Cu	36	3	2	64	8	6	0	29
Zn	48	52	58	54	37	62	37	50
Ga	20	21	22	18	18	21	17	19
Rb	160	159	135	165	115	132	123	137
Sr	87	79	120	97	407	151	419	206
Y	48	51	42	39	16	46	15	33
Zr	241	272	292	217	154	297	164	275
Ba	462	464	727	384	590	551	615	644
La	70	64	73	45	33	66	26	37
Ce	132	124	139	112	66	135	62	82
Pb	23	21	20	23	23	22	23	14
Th	17	12	12	19	17	14	nd	7
U	3	2	2	5	3	1	5	3

TABLE 5.2 (cont.)

SAMPLE	3423	3424	4272BR	2467	3304
GROUP	G_{2B}	G_{2B}	G_{2B}	G_{2C}	G_{2C}
MAJORS					
SiO_2	75.71	75.32	73.44	70.14	70.09
Al_2O_3	13.22	13.17	13.31	14.85	15.07
TiO_2	0.18	0.18	0.28	0.41	0.39
MnO	0.05	0.06	0.07	0.11	0.07
$(Fe_2O_3)^t$	1.73	1.75	2.37	2.65	2.56
MgO	0.49	0.57	0.74	1.51	1.20
CaO	0.67	0.64	0.90	2.02	1.82
Na_2O	3.51	3.38	3.08	4.37	4.60
K_2O	4.85	4.90	4.59	2.97	2.99
P_2O_5	0.02	0.02	0.05	0.11	0.13
LOI	0.70	0.54	0.66	1.13	0.83
FeO	0.86	0.96	1.30	nd	nd
Fe_2O_3	0.77	0.68	0.92	nd	nd
TOTAL	101.03	100.42	99.34	100.27	99.75
TRACES					
Nb	nd	nd	nd	nd	nd
Cr	4	0	15	37	43
Co	0	0	0	6	5
Ni	0	0	0	17	18
Cu	14	14	11	7	25
Zn	58	56	48	31	47
Ga	22	23	20	19	18
Rb	160	170	171	70	88
Sr	43	38	74	424	443
Y	46	52	47	15	13
Zr	167	193	224	141	159
Ba	147	149	382	421	476
La	55	57	62	16	27
Ce	108	114	117	33	48
Pb	22	22	22	16	17
Th	16	11	19	11	11
U	4	2	4	3	2

TABLE 5.2 (cont.)

SAMPLE	2109	2160	2162	2181
GROUP	G_3	G_3	G_3	G_3
MAJORS				
SiO_2	73.80	73.92	74.90	73.81
Al_2O_3	12.69	12.64	12.77	12.50
TiO_2	0.23	0.19	0.19	0.23
MnO	0.03	0.04	0.05	0.08
$(Fe_2O_3)^t$	2.19	2.73	2.35	2.26
MgO	0.14	0.04	0.08	0.08
CaO	0.95	0.74	0.79	0.91
Na_2O	4.11	3.90	3.89	4.14
K_2O	5.02	5.37	5.11	5.09
P_2O_5	0.02	0.02	0.01	0.03
LOI	nd	0.67	0.53	0.65
FeO	nd	nd	nd	nd
Fe_2O_3	nd	nd	nd	nd
TOTAL	99.18	100.26	100.14	99.78
TRACES				
Nb	45	45	47	42
Cr	22	2	0	1
Co	3	1	3	4
Ni	4	4	1	5
Cu	17	37	69	151
Zn	38	21	49	45
Ga	22	25	23	23
Rb	219	248	224	226
Sr	32	27	26	32
Y	67	68	57	68
Zr	274	327	288	323
Ba	95	61	61	63
La	77	75	67	71
Ce	156	166	147	162
Pb	8	10	7	9
Th	29	29	28	26
U	4	5	5	3

TABLE 5.2 (cont.)

SAMPLE	3132	3138	3144	3185	3199	3200
GROUP	G_4	G_4	G_4	G_4	G_4	G_4
MAJORS						
SiO_2	76.84	76.10	76.28	76.99	74.96	77.22
Al_2O_3	12.12	12.23	12.22	11.62	12.76	12.09
TiO_2	0.12	0.13	0.14	0.11	0.16	0.12
MnO	0.04	0.03	0.07	0.04	0.05	0.06
$(Fe_2O_3)^t$	1.89	1.97	1.95	1.96	2.10	1.88
MgO	0.02	-	0.10	-	0.11	-
CaO	1.08	0.88	0.90	0.98	0.90	0.79
Na_2O	3.33	3.20	3.70	3.53	3.51	3.13
K_2O	5.17	5.08	5.14	4.89	5.12	5.10
P_2O_5	0.02	0.01	0.01	0.03	0.01	0.01
LOI	0.48	0.77	nd	0.44	0.41	nd
FeO	nd	nd	nd	nd	nd	nd
Fe_2O_3	nd	nd	nd	nd	nd	nd
TOTAL	101.11	100.40	100.51	100.59	100.09	100.40
TRACES						
Nb	32	nd	29	nd	nd	nd
Cr	11	8	11	0	0	26
Co	4	0	0	0	0	0
Ni	1	0	2	0	3	0
Cu	11	2	9	51	11	8
Zn	70	63	64	60	73	69
Ga	21	22	21	21	22	22
Rb	155	163	162	151	171	164
Sr	48	53	48	42	66	51
Y	44	52	46	50	52	57
Zr	196	227	219	194	258	209
Ba	638	758	665	699	717	721
La	40	62	44	53	62	58
Ce	102	134	111	111	142	117
Pb	21	18	27	24	24	22
Th	14	15	17	18	21	18
U	4	4	4	3	4	4

TABLE 5.2 (cont.)

SAMPLE	3219	2112	3155	3159	2129	2178	2445	2449
GROUP	G_5	G_6	G_6	G_6	G_7	G_7	G_7	G_7
MAJORS								
SiO_2	71.53	68.65	68.18	71.23	74.43	76.35	76.91	78.50
Al_2O_3	13.68	15.88	15.26	15.41	12.64	12.12	11.05	11.63
TiO_2	0.29	0.36	0.41	0.14	0.15	0.13	0.13	0.15
MnO	0.07	0.07	0.07	0.05	0.04	0.04	0.11	0.04
$(Fe_2O_3)^t$	3.12	2.89	3.05	1.70	2.07	1.14	1.54	1.47
MgO	0.25	1.40	1.51	0.52	0.05	0.44	0.39	0.33
CaO	1.12	2.90	2.75	2.58	1.09	0.53	0.65	0.59
Na_2O	3.74	5.34	4.69	4.41	3.89	2.98	2.94	3.30
K_2O	5.54	1.48	2.56	2.23	4.97	4.58	4.09	4.26
P_2O_5	0.05	0.09	0.14	0.04	0.04	0.02	0.01	0.01
LOI	1.07	1.01	1.53	1.39	1.15	0.64	1.23	0.72
FeO	nd	nd	nd	nd	nd	0.46	0.17	nd
Fe_2O_3	nd	nd	nd	nd	nd	0.62	1.35	nd
TOTAL	100.46	100.07	100.15	99.70	100.52	98.91	99.03	101.00
TRACES								
Nb	32	8	12	3	29	30	nd	nd
Cr	0	38	34	7	8	11	38	1
Co	1	3	6	0	1	1	0	0
Ni	3	9	19	0	0	0	0	0
Cu	51	11	9	15	96	45	1	54
Zn	63	46	34	29	43	34	30	59
Ga	23	21	19	18	19	20	17	18
Rb	121	32	65	54	184	175	162	227
Sr	98	506	476	702	59	31	33	33
Y	43	10	14	4	37	48	50	42
Zr	513	92	150	80	167	124	157	197
Ba	1622	271	553	740	291	179	226	187
La	114	10	19	0	32	36	48	65
Ce	45	24	47	14	92	88	125	125
Pb	16	8	13	16	21	20	20	21
Th	15	4	10	1	20	16	15	16
U	2	2	2	3	2	3	3	4

TABLE 5.2 (cont.)

SAMPLE	2450	2451	2457	2474	3436	2179	3421	3435
GROUP	G_7	G_7	G_7	G_7	G_7	G_{7B}	G_8	G_8
MAJORS								
SiO_2	73.87	75.29	74.25	78.02	76.92	76.67	65.71	64.31
Al_2O_3	13.58	12.92	13.39	11.99	12.31	12.03	15.69	15.44
TiO_2	0.26	0.15	0.23	0.13	0.15	0.13	0.35	0.28
MnO	0.05	0.04	0.06	0.03	0.03	0.06	0.11	0.13
$(Fe_2O_3)^t$	2.10	1.45	2.05	1.32	1.59	2.07	4.70	5.44
MgO	0.65	0.46	0.56	0.45	0.62	0.04	3.19	3.67
CaO	0.90	0.59	0.71	0.35	0.38	0.78	3.69	4.62
Na_2O	3.43	3.26	3.29	3.39	3.40	2.90	2.60	2.36
K_2O	4.85	5.07	5.12	4.68	4.71	5.33	2.85	2.59
P_2O_5	0.05	0.01	0.03	0.01	0.00	0.02	0.09	0.07
LOI	0.51	0.63	0.85	0.50	0.88	0.30	2.22	1.58
FeO	0.99	nd	1.01	nd	0.28	nd	2.63	nd
Fe_2O_3	1.00	nd	0.93	nd	1.28	nd	2.23	nd
TOTAL	100.14	99.82	100.43	100.87	100.96	100.33	101.36	100.49
TRACES								
Nb	nd	nd	nd	nd	nd	25	nd	nd
Cr	4	5	2	20	7	3	38	49
Co	0	0	0	0	0	0	8	16
Ni	0	0	1	0	0	3	10	9
Cu	37	17	1	39	45	6	17	20
Zn	42	29	43	43	40	72	40	35
Ga	21	19	20	18	22	22	17	13
Rb	169	173	172	187	169	147	101	108
Sr	78	46	62	26	30	38	181	158
Y	47	40	43	51	52	57	15	12
Zr	229	165	218	143	216	205	124	97
Ba	323	254	411	180	381	530	528	486
La	56	51	71	52	52	52	14	23
Ce	113	91	140	109	123	118	42	34
Pb	25	22	24	20	21	33	14	9
Th	16	13	19	20	16	16	7	8
U	2	2	3	4	5	3	2	3

TABLE 5.2 (cont.)

SAMPLE	2468	2476	3187	3193	3194	2118	2171	2470	2101
GROUP	G_9	G_9	G_{10}	G_{10}	G_{10}			V_N	
MAJORS									
SiO_2	66.92	66.93	74.73	76.35	73.59	65.22	73.13	71.65	63.67
Al_2O_3	15.44	16.40	13.51	12.57	14.19	16.10	11.87	14.41	17.79
TiO_2	0.59	0.49	0.07	0.07	0.02	0.74	0.30	0.35	0.58
MnO	0.09	0.09	0.06	0.08	0.08	0.08	0.09	0.05	0.11
$(Fe_2O_3)^t$	3.36	3.50	1.54	1.96	1.83	4.85	3.37	2.23	4.03
MgO	1.95	2.30	0.08	0.01	0.00	1.70	0.49	1.33	1.60
CaO	2.31	3.45	0.84	0.82	0.93	1.67	2.16	1.53	2.78
Na_2O	4.84	4.56	4.34	4.10	4.97	4.88	3.17	3.74	5.87
K_2O	2.97	1.44	4.62	4.54	3.88	4.72	3.67	3.69	3.22
P_2O_5	0.19	0.09	0.03	0.03	0.05	0.10	0.08	0.09	0.17
LOI	2.25	1.42	0.70	0.77	0.75	nd	1.59	0.90	1.20
FeO	nd	1.45	nd	nd	nd	nd	nd	nd	nd
Fe_2O_3	nd	1.89	nd	nd	nd	nd	nd	nd	nd
TOTAL	100.91	100.51	100.52	101.30	100.29	100.06	99.92	99.97	101.02
TRACES									
Nb	nd	nd	15	26	nd	nd	nd	nd	nd
Cr	28	40	1	4	2	50	8	45	63
Co	4	5	0	0	0	4	0	0	14
Ni	6	16	0	4	0	19	1	11	30
Cu	4	3	25	18	6	11	5	43	14
Zn	63	38	23	28	18	62	64	14	40
Ga	19	21	16	17	23	19	19	18	18
Rb	69	36	122	142	151	129	122	92	72
Sr	591	472	200	22	23	165	112	374	581
Y	11	10	9	28	13	16	38	11	10
Zr	167	114	69	139	49	192	389	153	150
Ba	763	307	770	147	81	1180	701	636	704
La	40	19	11	26	4	49	42	35	38
Ce	70	34	37	67	33	75	99	65	54
Pb	12	5	30	18	10	33	12	12	21
Th	8	5	21	18	5	12	15	14	10
U	3	2	6	3	3	3	2	3	3

TABLE 5.2 (cont.)

SAMPLE	2102	2106	2183	2208	2210	2466	2469	2471	2472
GROUP	V_N	V_N	V_N	V_N	V_N	V_N	V_N	V_N	V_N
MAJORS									
SiO_2	65.40	70.34	62.29	63.06	63.12	69.16	63.99	68.29	69.48
Al_2O_3	16.32	14.00	16.36	16.67	15.07	14.10	15.97	13.86	15.23
TiO_2	0.56	0.10	0.91	1.05	0.67	0.53	0.76	0.65	0.33
MnO	0.11	0.08	0.12	0.11	0.14	0.07	0.12	0.09	0.08
$(Fe_2O_3)^t$	3.80	1.56	5.18	4.90	4.69	3.36	4.05	4.11	2.44
MgO	0.73	1.63	2.58	2.48	3.79	0.57	2.68	0.86	1.09
CaO	1.63	1.36	3.37	3.32	2.17	2.93	2.73	3.08	1.33
Na_2O	4.98	4.76	4.43	4.56	4.21	3.84	4.70	3.49	4.16
K_2O	4.29	4.26	3.09	3.10	3.77	3.69	2.37	3.32	4.84
P_2O_5	0.19	0.05	0.20	0.23	0.22	0.13	0.17	0.16	0.06
LOI	1.28	nd	1.54	1.16	1.69	1.01	2.43	2.08	1.23
FeO	nd	nd	nd	nd	nd	0.20	nd	nd	nd
Fe_2O_3	nd	nd	nd	nd	nd	3.14	nd	nd	nd
TOTAL	99.29	98.14	100.07	100.64	99.54	99.37	99.97	99.99	100.27
TRACES									
Nb	nd	21	nd	nd	nd	nd	nd	nd	nd
Cr	89	4	38	52	224	24	57	47	nd
Co	10	0	18	16	27	0	12	3	nd
Ni	37	7	22	29	98	7	18	19	5
Cu	46	98	17	15	24	3	34	2	5
Zn	30	29	64	64	79	13	75	21	19
Ga	14	12	21	22	21	14	18	17	14
Rb	98	97	89	92	92	109	65	101	128
Sr	395	205	418	399	523	287	329	376	156
Y	16	13	21	22	18	20	18	17	19
Zr	202	61	221	241	212	227	260	230	149
Ba	1135	812	626	582	893	810	690	825	nd
La	36	9	31	26	47	44	44	40	nd
Ce	103	69	70	71	100	77	74	69	nd
Pb	24	18	23	16	23	22	16	17	17
Th	14	8	11	8	16	13	13	13	11
U	2	2	3	5	4	4	5	5	3

TABLE 5.2 (cont.)

5.4 MAJOR ELEMENT GEOCHEMISTRY OF NORTHERLY DERIVED GRANITE CLASTS

5.4.1 Alkali Enrichment

K_2O is plotted against SiO_2 in Figure 5.1 for the granite and volcanic clast data. Fields for high-, normal- and low-K calc-alkaline magmas are superimposed following Peccerillo and Taylor (1976). The bulk of the clasts plot in the high-K field and show comparable K-enrichment to c 400 Ma late Caledonian granites (Halliday and Stephens 1984). The c 460 Ma two-mica granite clasts (G_1) show comparable K-enrichment to the bulk of the various biotite granite clasts. Those samples which do not show a high-K signature include the grey equigranular biotite granite clasts of G_6 type, and 2476, a clast assigned to G_9 on the basis of its strong resemblance to the southerly derived G2 biotite granodiorite (Chapter 4). The low potassium content is compatible with this interpretation. The hornblende granodiorites 3421 and 3435 (G_8) plot in the high-K field and may be rare basic counterparts to the evolved biotite granites.

Figure 5.1 serves to illustrate the highly evolved character of the bulk of the granite clasts, a feature which is emphasised when the chemistry of granites of northerly and southerly derivation are compared. In the conglomerates of northerly provenance clasts of granodioritic composition e.g. G_8 are exceedingly rare and the bulk of clasts are strictly true granites with SiO_2 >70%. Granite clasts with SiO_2 >70% are uncommon in southerly derived conglomerates. The accompanying volcanic clasts are also plotted in Figure 5.1. These share the high-K fingerprint of the granites and are dominantly acid-andesites and dacites. Occasional flow banded rhyolites e.g. 2106 are encountered.

The combined data for the granite and volcanic clasts produce a broad trend towards increasing K_2O with increasing SiO_2. In detail however, the distribution for clasts from individual groups is more complex. The volcanic clasts (V_N) and uncontaminated porphyritic biotite granites (G_{2B}) show normal trends with increasing abundances of K_2O in progressively more

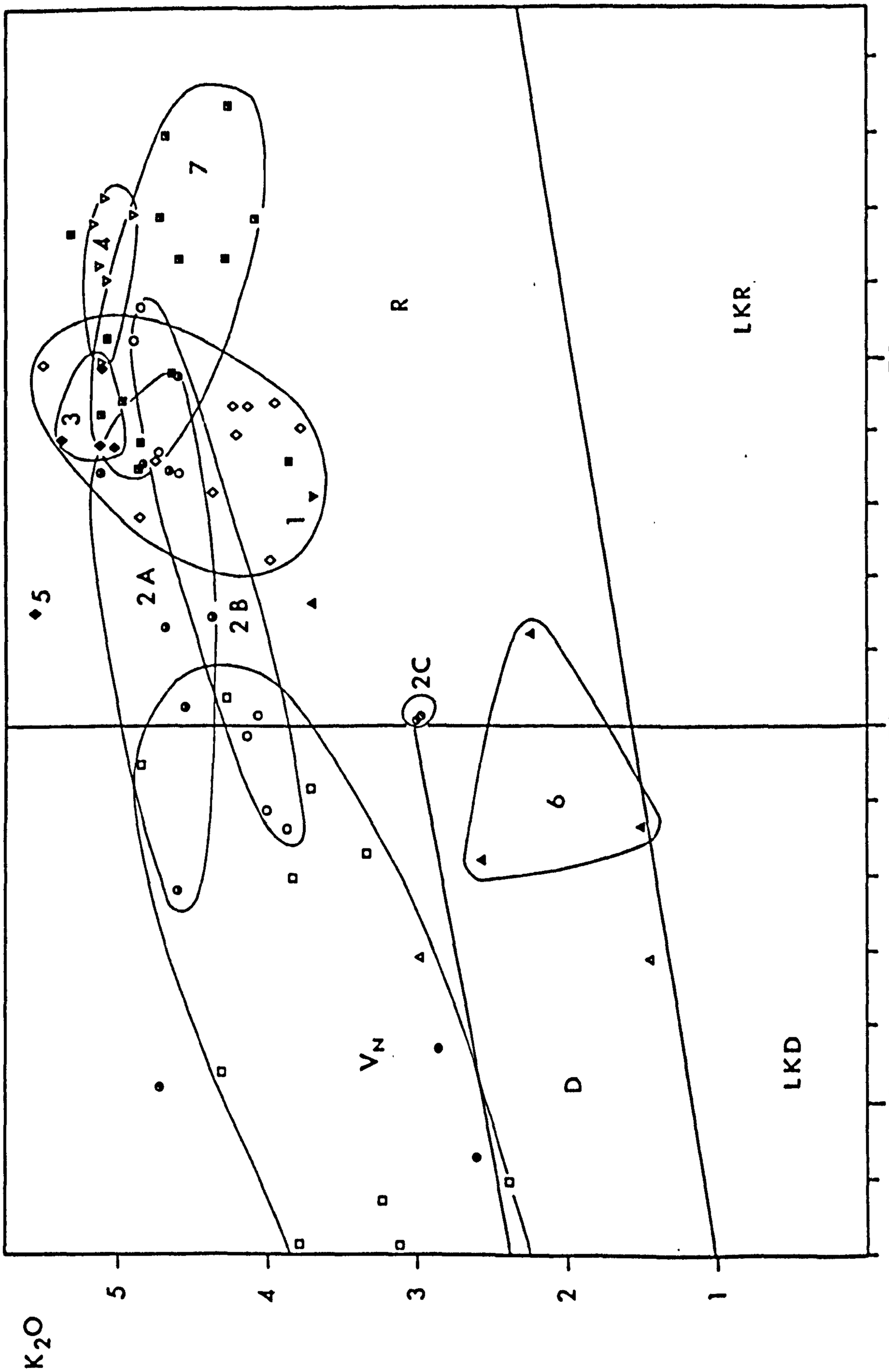

FIGURE 5.1 K_2O vs SiO_2 plot for granite, porphyry and volcanic clasts of northerly provenance. Fields from Pecerillo and Taylor (1976). Symbols as in Table 5.1. Numbers indicate various clast suites.

evolved rocks. The granophyres and quartz-porphyry clasts however have very narrow ranges of chemical composition indicating they were derived from relatively homogeneous source rock types. This is perhaps to be expected in magmas which must have been emplaced to high level with consequent large degrees of undercooling.

The equigranular red biotite granites (G_7) are the most highly evolved of any of the clasts sampled, with SiO_2 reaching 78%. They produce a clear trend towards decreasing K_2O with increasing SiO_2 suggesting fractionation of K-rich phases. The two-mica granite clasts (G_1) are characterised on this and other variation diagrams by the absence of any clear trends. The homogeneity of two-mica granite compositions, with a relatively small range in SiO_2 and erratic K_2O abundance is typical of two-mica granites recorded elsewhere, e.g. the Manaslu leucogranite of Central Nepal (Le Fort 1981). Table 5.3 compares the averaged composition of the G_1 two-mica granite clasts with other two-mica granite occurrences and with an average of 1148 two-mica granites and leucogranites from Le Fort (1981). The range of both SiO_2 and K_2O in the granite clasts is in good agreement with the data from elsewhere.

Figure 5.1 also emphasise the separation of porphyritic biotite granite clasts which contain basic clots (possible restite) from those that do not. The contaminated samples (G_{2A}), containing small clots of dark autolithic amphibole-feldspar material, plot with higher K_2O abundance at constant silica than the samples free of ?restite contamination, but both trends converge at high silica.

Na_2O is plotted against SiO_2 in Figure 5.2a. The volcanic clasts, G_6 and G_9 all show strong Na-enrichment, whilst the remaining granites have Na contents comparable to other Caledonian granites. Significantly, the two-mica granites (G_1) show similar Na_2O concentrations to the biotite granites, and in this respect are not analogous to `S-type` granites of the Lachlan fold belt. White and Chappell (1983) show `S-type` granites to have lower Na_2O contents than contemporaneous `I-

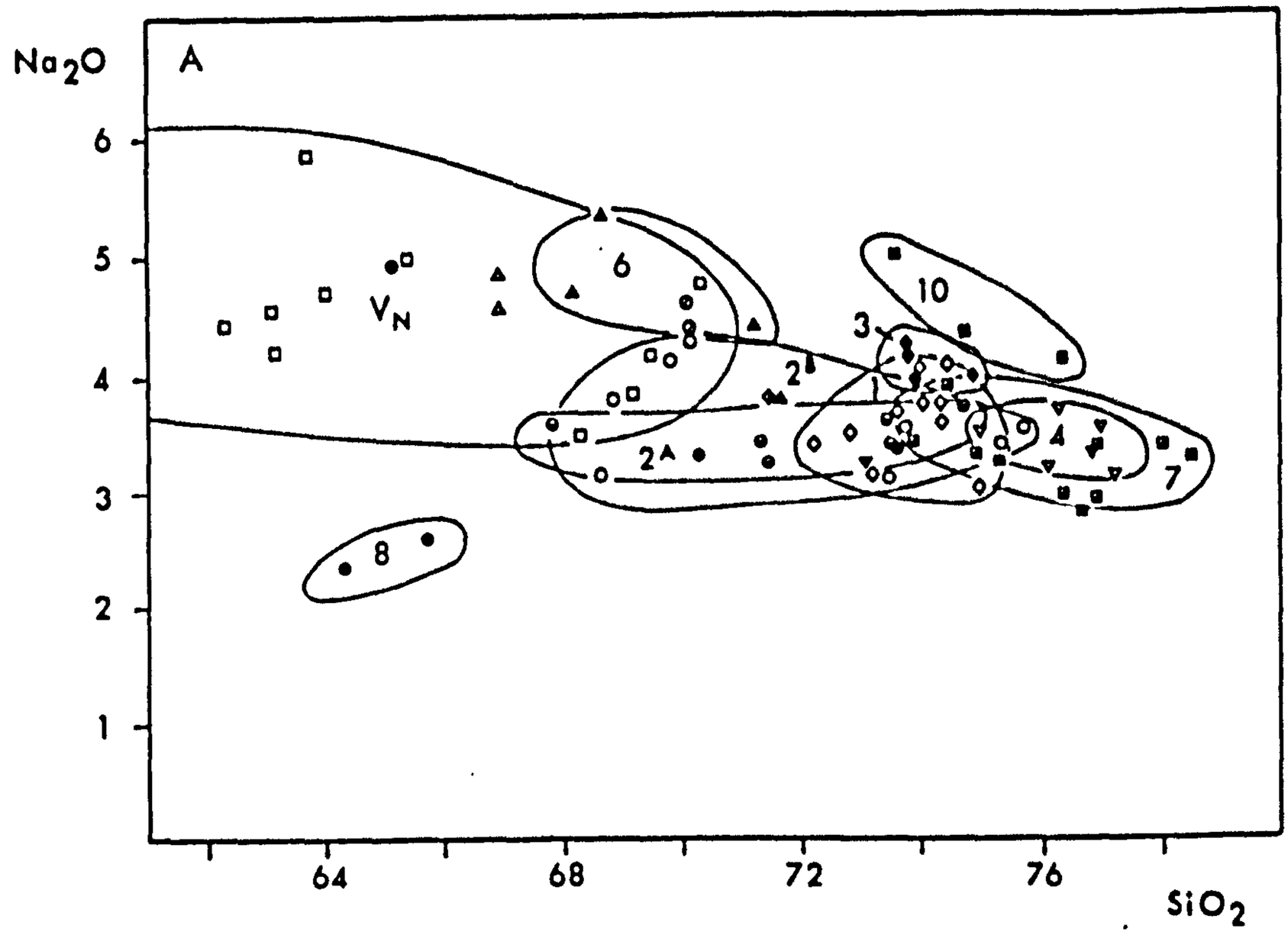

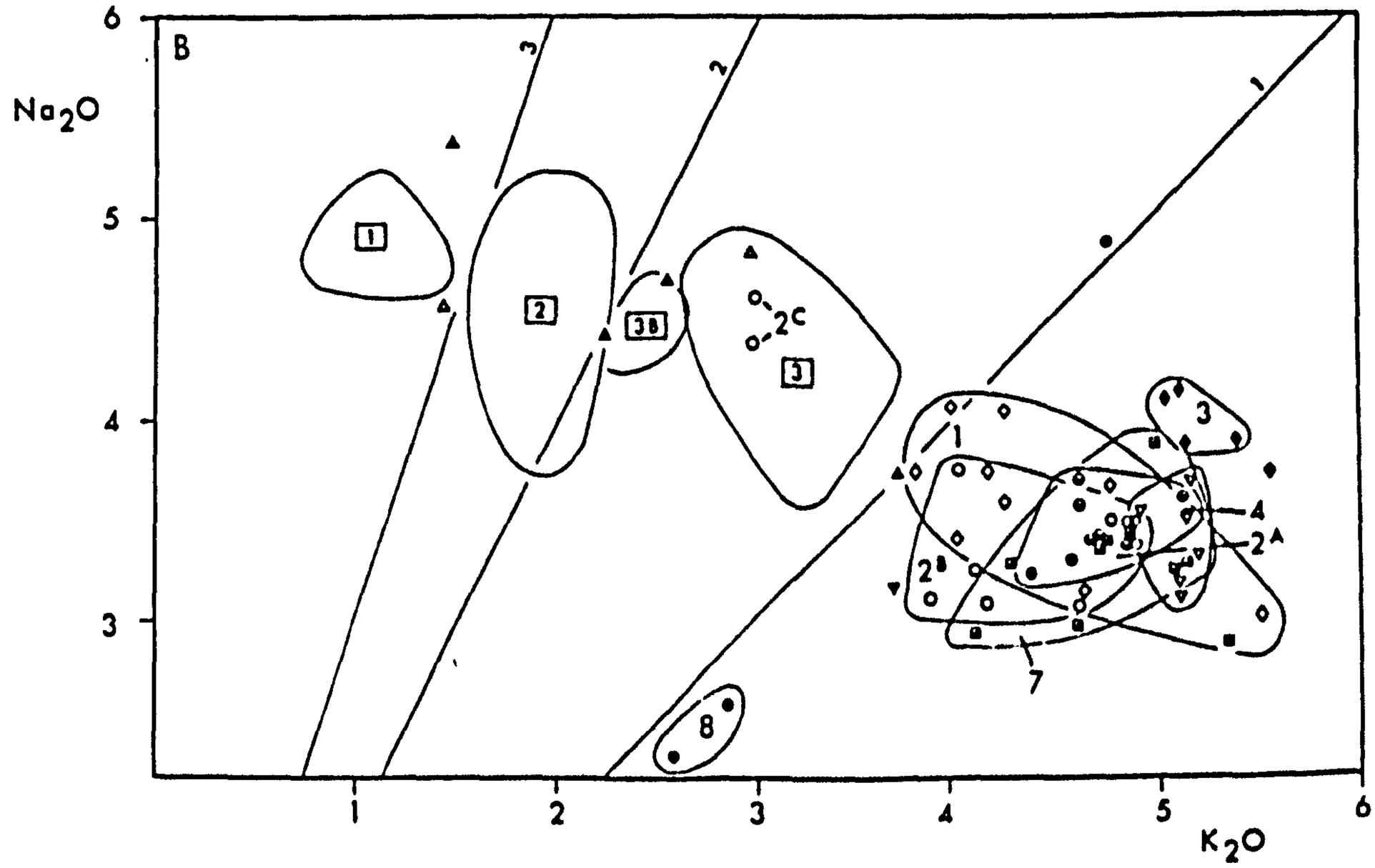

FIGURE 5.2 (A)Na_2O vs SiO_2 plot for granite, porphyry and volcanic clasts of northerly provenance.
(B)Na_2O vs K_2O plot for granite and porphyry clasts of northerly provenance. Summary fields for G1, G2 and G3 type granite clasts of southerly provenance included for comparison. For key to symbols used refer to Table 5.1.

	TWO-MICA GRANITE CLASTS		MANASLU GRANITE		GUF TWO-MICA GRANITES		HINGSTON DOWN LEUCOGRANITE	MUSCOVITE GRANITE	LACHLAN S-TYPE GRANITE
			1	2					
	X	σ	CORE	ARM	X	σ			
SiO_2	73.80	0.84	74.04	73.94	72.53	1.80	73.22	74.66	69.08
Al_2O_3	14.13	0.28	14.67	14.76	14.77	0.72	14.67	15.55	14.30
$(Fe_2O_3)^t$	1.88	0.42	0.84	0.81	1.41	0.65	0.82	0.64	4.32
MnO	0.06	0.01	0.02	0.02	0.03	0.02	0.01	0.07	0.06
MgO	0.17	0.16	0.18	0.13	0.34	0.31	0.23	0.02	1.82
CaO	1.13	0.45	0.50	0.46	0.69	0.38	0.45	0.42	2.49
Na_2O	3.60	0.34	4.06	4.14	3.27	0.50	3.85	4.29	2.20
K_2O	4.40	0.53	4.50	4.48	4.89	0.58	4.75	3.08	3.63
TiO_2	0.17	0.06	0.07	0.07	0.20	0.12	0.06	0.03	0.55
P_2O_5	0.11	0.04	0.14	0.13	nd		0.18	0.15	0.13
LOI	(0.86)		0.79	0.72	1.47	0.44	1.19	(0.76)	nd
TOTAL	100.31		99.81	99.66	99.60		99.43	99.65	98.58
n	10		36	23	1148		1	1	316

TABLE 5.3 Average chemical composition of northerly derived two-mica granite clasts (n=10) and comparison with other two-mica granites and leucogranites. Manaslu leucogranite from Le Fort (1981). GUF is average of 1148 two-mica granites and leucogranites, also from Le Fort (1981). Hingston Down leucogranite is from Hall (1973). The muscovite granite is the one experimented on by Huang and Wyllie (1973). Average S-type Lachlan granite from White and Chappell (1983).

type` granites and they attribute this feature to removal of sodium during weathering of feldspar to clay in the formation of the sedimentary source rocks they propose are required by the chemical and isotopic character of `S-type` granites. As potassium is incorporated into clays during chemical weathering to produce sedimentary rocks, $K_2O$ is not significantly depleted. Table 5.3 however shows $Na_2O$ abundances in other two-mica `S-type` granites and leucogranites to be broadly comparable with those determined for the two-mica granite clasts, and the Lachlan granites to be anomalously depleted relative to these.

There is evidence to suggest the sedimentary reservoir associated with Caledonian evolution in Northern Britain is abnormally enriched in Na_2O and that this may have been significant in determining the composition of crustally derived magmas. Scottish Dalradian pelites have an average K_2O/Na_2O ratio of 1.66 (Atherton and Brotherton 1982) compared with estimated averages for post-Archaean shales of 3.08 (Taylor and McLennan 1985), 2.53 (Clarke 1924) and 3.09 (Krauskopf 1967). Halliday and Stephens (1984) propose the low K/Na to possibly have been inherited from sediment recycling of K-depleted granulite facies Lewisian crust.

Figure 5.2b shows Na_2O plotted against K_2O and serves to emphasise the different compositions of the northerly and southerly derived clasts. The bulk of the data for the northerly-derived clasts plot with Na_2O/K_2O <1.0. With the exception of the two-mica granites, no clear compositional trends are defined. G_1 shows a poorly defined decrease in Na_2O with increasing K_2O. Le Fort (1981) found variation in the Na_2O/K_2O ratio to be the only significant coherent compositional variation in the Manaslu leucogranite, and he attributed it to non-homogenised `minimum anatectic melt` compositions. Source rocks of differing An content will produce `minimum melt` compositions that will vary in the Ab and Or content according to the Ab/An ratio of the source (Winkler 1979).

The two hornblende granodiorites (G_8) also plot with Na_2O/K_2O <1.0 and are clearly compositionally very different to granodiorites of comparable silica content derived from the south. Compositional fields for the southerly derived granites are also plotted in Figure 5.2b and all plot with Na_2O/K_2O >1.0. The clasts which are thought to be returned southwards from and original source to the south plot in or close to the fields for the granite suites from which they are thought to have been derived. The equigranular biotite granites of G_6 type also plot with compositions comparable to the southerly derived suites and it is possible that they too are originally of southerly derivation.

5.4.2 Alkali-alumina Balance

In Fig. 5.3a, Al_2O_3 is plotted against SiO_2. The two-mica granite clasts plot with higher alumina contents at comparable silica levels. Their peraluminous character is confirmed by plotting mol. $Al_2O_3/(Na_2O + CaO + K_2O)$ against SiO_2 (Figure 5.3b). Clasts of G_1 type plot with A/CNK ratios in excess of 1.0, in the field for peraluminous compositions. Halliday et al. (1981) present A/CNK data for c 460 Ma two-mica granites from the northeastern Grampian region (Strichen, Longmanhill, Aberchirder, Kemnay and Aberdeen). These have very comparable compositional ranges to the data presented here for the two-mica granite clasts. There is no obvious correlation between the initial $^{87}Sr/^{86}Sr$ ratios and the alkali-alumina balance for the four clasts for which isotopic data are available.

Clasts of granite other than the two-mica granites show a range of both metaluminous and peraluminous compositions. A striking feature of the data is the absence of a strong correlation between the development of peraluminous compositions and differentiation. In this respect the northerly derived clasts differ from those derived from the south, which show good correlations of A/CNK with SiO_2 reflecting both contamination and probable amphibole fractionation. Both the porphyritic (G_2) and equigranular red granite clasts (G_7) span both peraluminous and metaluminous compositions and show scattered trends. The metaluminous compositions are developed despite the highly

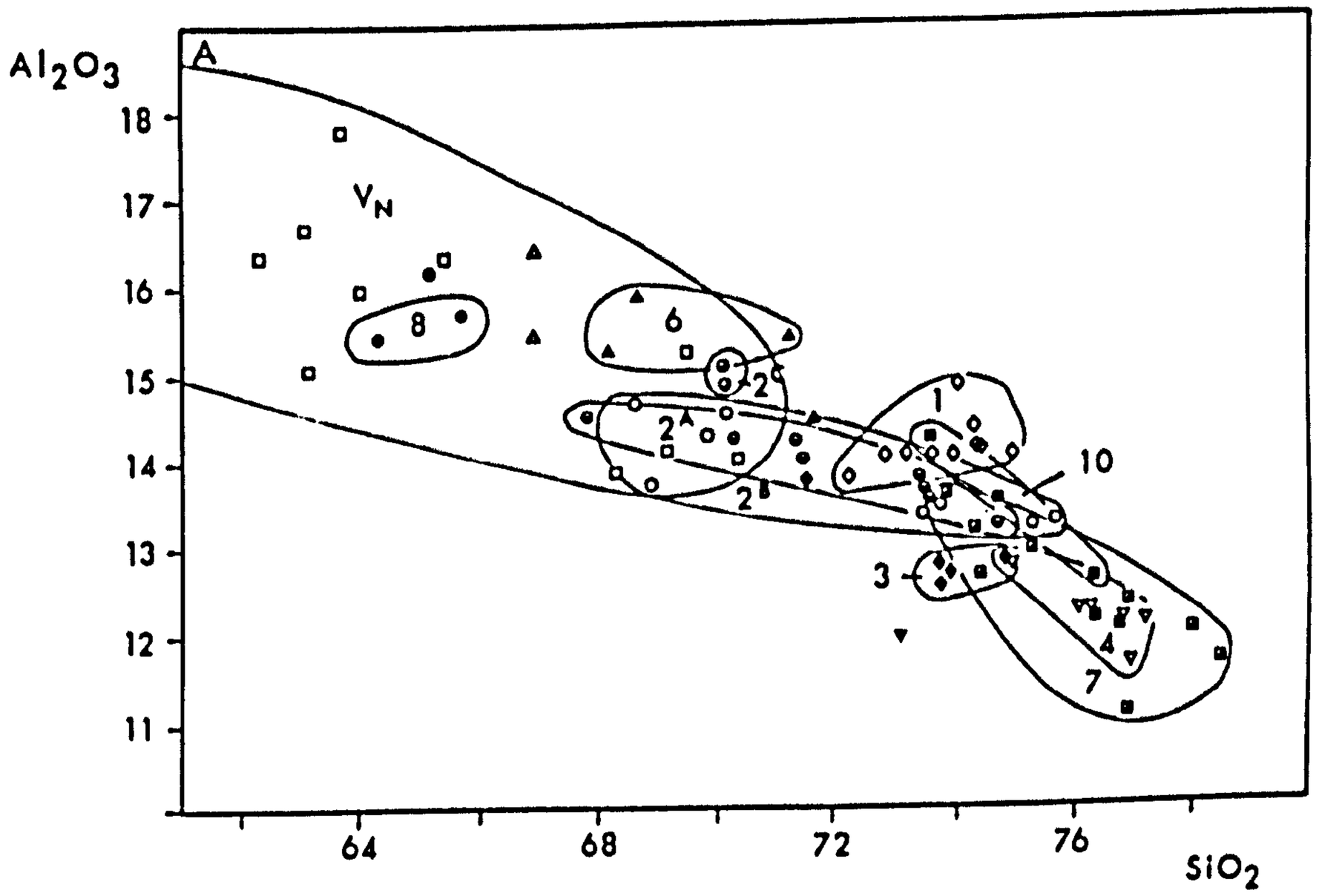

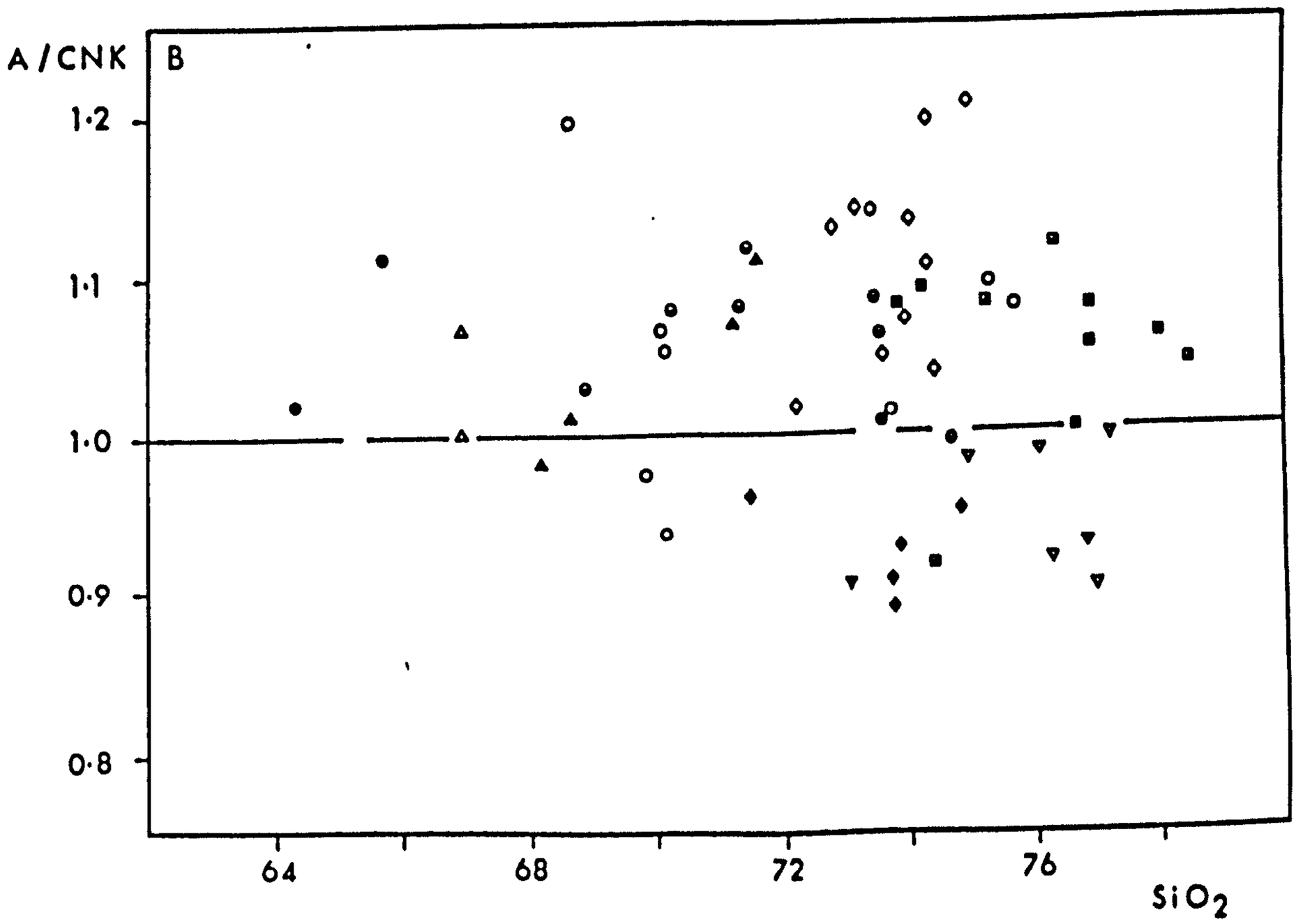

FIGURE 5.3 Alumina balance in clasts of granite and porphyry of northerly derivation.
(A)Al_2O_3 vs SiO_2 plot
(B)A/CNK (mol.Al_2O_3/(Na_2O + CaO + K_2O)) vs SiO_2.
For key to symbols used refer to Table 5.1.

evolved nature of the granites and the evidence for strong fractionation. Both the granophyres and the quartz-feldspar porphyries plot exclusively in the metaluminous field, again despite evidence for strong fractionation.

The lack of a coherent relationship between A/CNK and SiO_2 suggests uncoupling of alkali and alumina budgets during differentiation. As these granites are highly evolved, water may have been important in determining late stage alkali enrichment. For example vapour phase transfer of alkalis from a metaluminous granitic liquid might cause the liquid to become peraluminous (Luth 1964). Similarly, mass tranfer of alkalis in vapour phases, facilitated by the presence of aqueous chloride solutions (Burnham 1979), may preferentially enrich parts of the pluton in alkalis resulting in the A/CNK ratio showing no correlation with DI or SiO_2.

5.4.3 FeO, Fe_2O_3, MgO

Figure 5.4 emphasise the poor correlation of MgO with $(Fe_2O_3)^t$ (total iron as Fe_2O_3). Both show moderate negative correlations with SiO_2. This lack of correlation reflects the relatively minor role of mafic phase crystal fractionation in generating the chemical variation in these highly evolved granites. Mafic phases rarely make up greater than 10% of the total volume in granite clasts with silica greater than 70%, and in some of the highly fractionated clasts the mafic component may be less than 1%. Fractionation of iron in opaque phases and in the high Fe/Mg biotites expected in such acid liquids would compound the uncoupled behaviour of MgO and $(Fe_2O_3)^t$.

A notable feature of Figure 5.4 is the intersection of the broad positive trend defined by the data as a whole with the $(Fe_2O_3)^t$ axis at 2.0%. Many of the groups are strongly depleted in MgO, particularly the granophyres, porphyries and the two-mica granites. The strong depletion in MgO relative to $(Fe_2O_3)^t$ must reflect extraction of high $MgO/(Fe_2O_3)^t$ mafic phases during the earlier intermediate history of the magma in the case of G_2 and G_7, whereas the low MgO contents of the two-mica granite clasts reflect their origin as anatectic minimum melts. Table 5.3

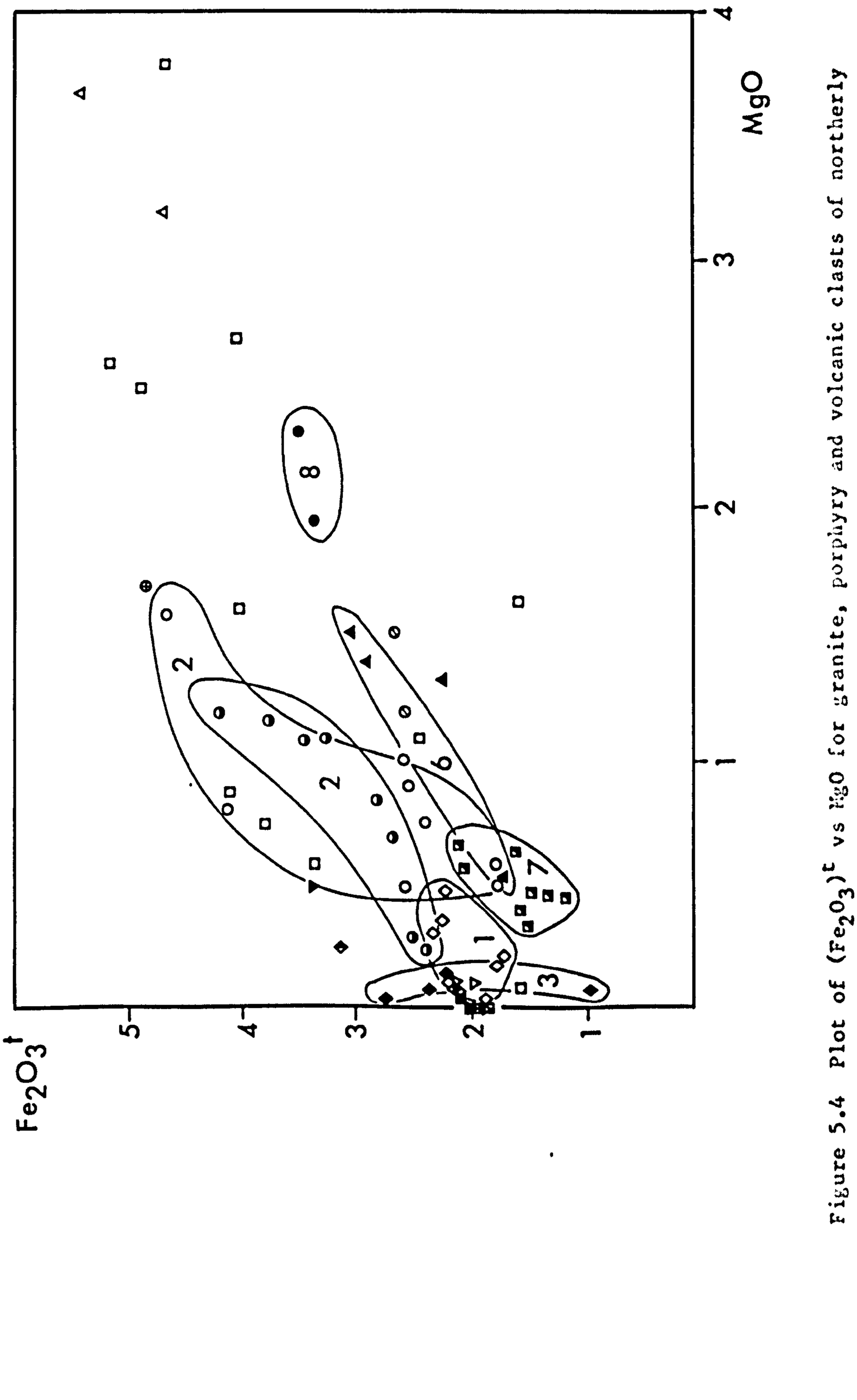

Figure 5.4 Plot of $(Fe_2O_3)^t$ vs MgO for granite, porphyry and volcanic clasts of northerly provenance. Symbols and clast types are as shown in Table 5.1.

compares the MgO and Fe_2O_3 contents of the two mica granite clasts with other two-mica granites and leucogranites. Whilst MgO contents are very comparable $(Fe_2O_3)^t$ appears to be significantly enriched over other anatectic melt compositions at comparable silica levels.

FeO has been determined for a representative selection of the granite clasts. Results are tabulated in Table 5.1. Oxidation ratios are close to normal averaging 0.34 for the biotite granites (G_2 and G_7), compared with average values of 0.35 for I-type granites of the Lachlan fold belt. This contrasts with the higher oxidation ratios of southerly derived granite clasts occurring in conglomerates which intertongue with those of northerly derivation. This suggests that the enhanced oxidation ratios in granites of southerly provenance do not reflect bulk hydrothermal alteration or burial diagensis of the conglomerate pile itself, but must be related to interaction of the granite magmas as they were intruded to high level.

5.4.4 $\underline{P_2O_5}$, $\underline{TiO_2}$

Figure 5.5a and b summarise the TiO_2 and P_2O_5 characteristics of each of the granite and volcanic clast groups of northerly derivation in the form of Harker diagrams. Both plots show general decreases in element abundances with increasing SiO_2. Trends are broadly linear for TiO_2, but P_2O_5 is enriched in the two-mica granites over other granite clasts at comparable silica contents.

The discrimination of the two-mica granite clasts (G_1) from other clasts on the P_2O_5 versus SiO_2 plot is significant because apart from MgO, there is a remarkable similarity between the chemistry of the two-mica granites and the unrelated biotite granites. The poor discrimination between these two fundamental groups of isotopically distinct magmas probably reflects the role of strong fractionation in the biotite granites, in homogenising the fingerprint of their distinct source materials and petrogenesis. Differentiation by fractional crystallisation tends to drive magma compositions progressively towards minimum melt proportions and it is therefore hardly surprising that the biotite granites,

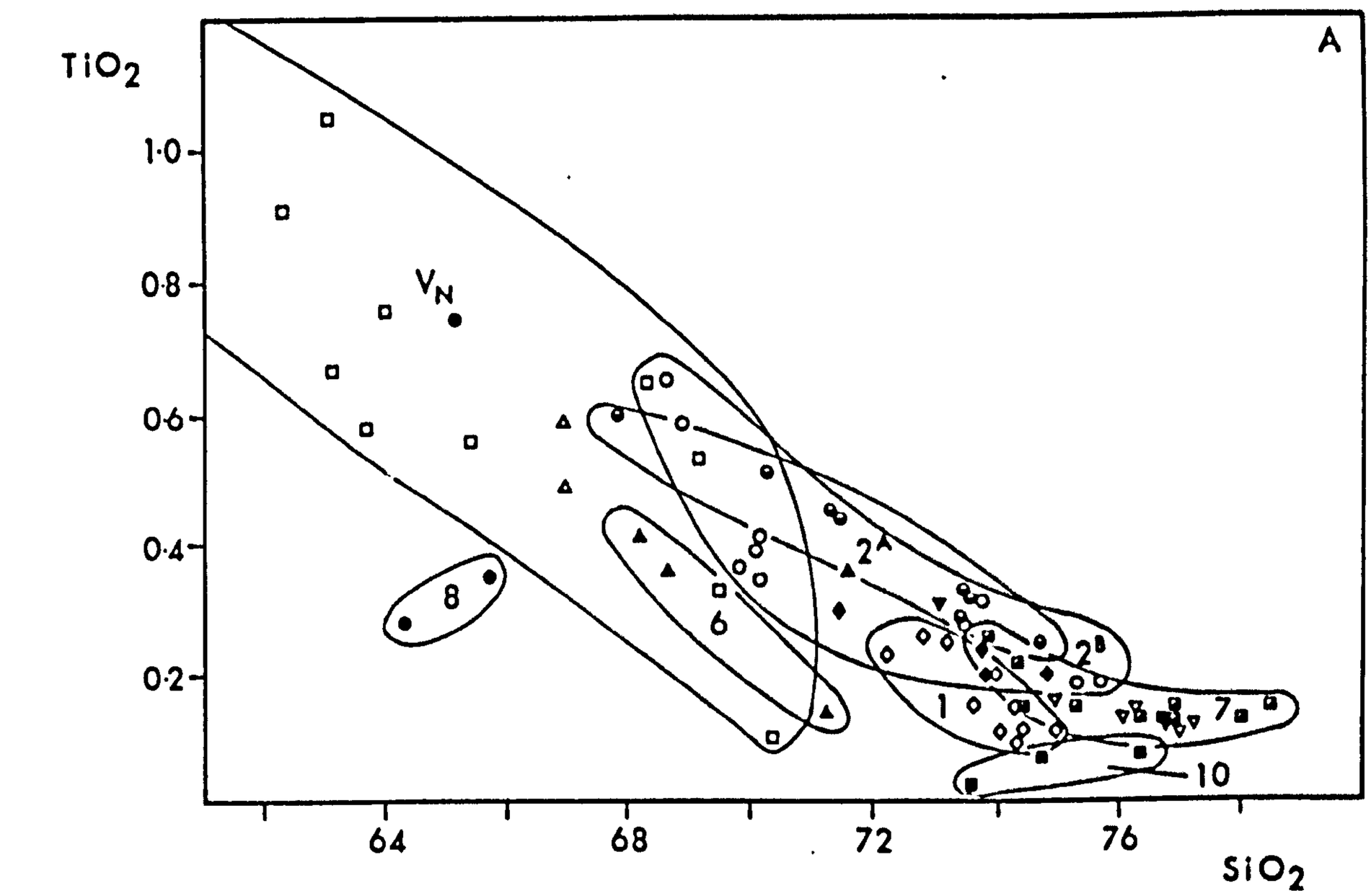

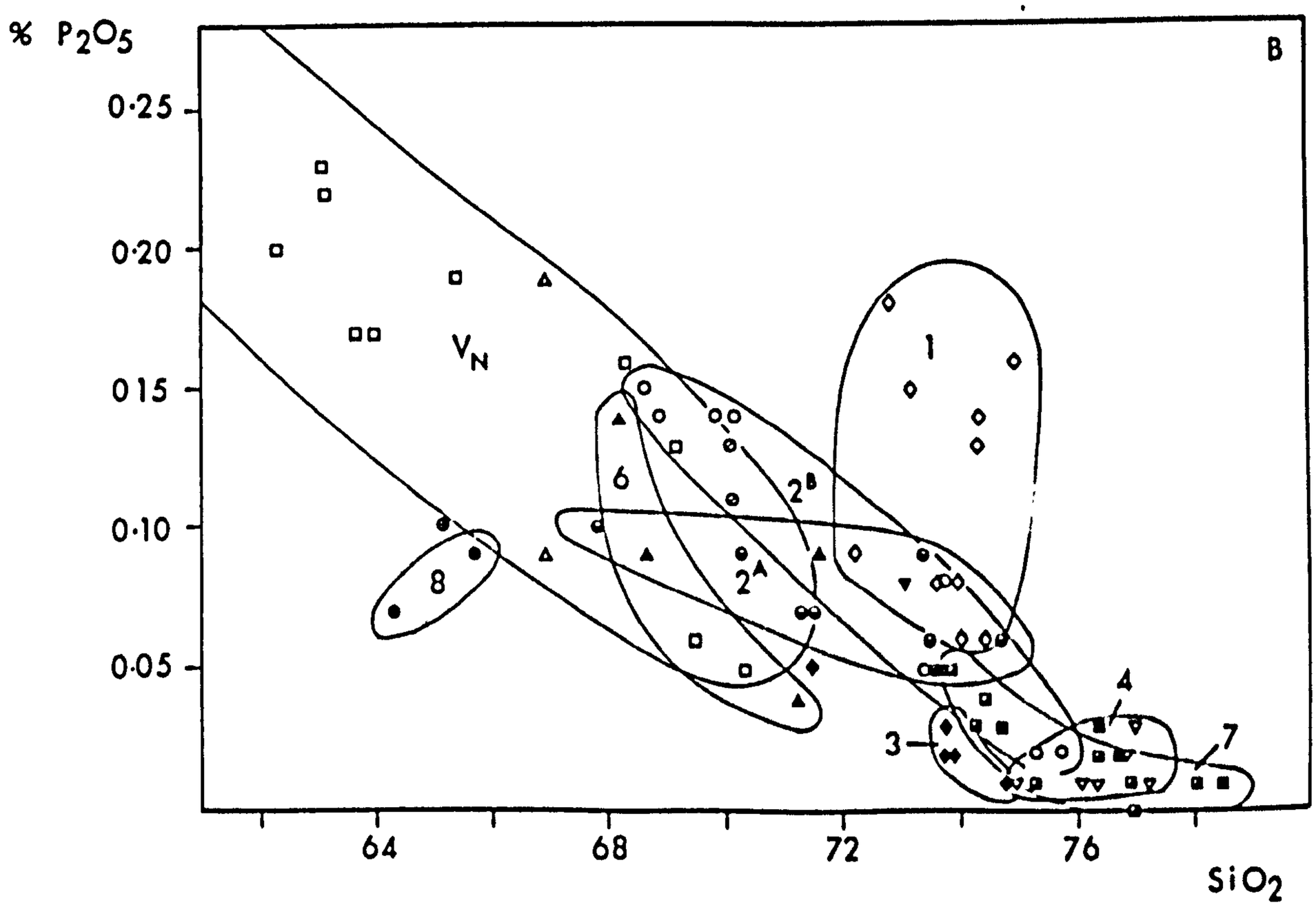

FIGURE 5.5 (A)Plot of TiO_2 vs SiO_2
(B)Plot of P_2O_5 vs SiO_2.
For symbols used refer to Table 5.1.

which can be shown to have undergone large degrees of feldspar and biotite dominated fractionation, come to resemble the two-mica granites which are regarded as the product of anatectic melting. P_2O_5 abundances in the clasts of two-mica granite reach 0.18%. This is close to the solubility limit of P_2O_5 in felsic magmas. Watson and Capobianco (1981) experimentally determined a value of 0.14% for the P_2O_5 solubility limit. Felsic magmas produced by crustal fusion cannot contain more P_2O_5 than this value, unless residual apatite crystals are entrained in the melt. If the metamorphic clasts which accompany the two-mica granite clasts in the northerly derived conglomerates are considered to be possible candidates for crustal melting, the generally low P_2O_5 in many clasts (<0.05%) suggests the high P_2O_5 contents of some of the two-mica granites can only be acheived by small degrees of melting.

Ignoring the two-mica granite clasts , P_2O_5 shows a general decrease with increasing fractionation. The contaminated megacrystic K-feldspar granite clasts (G_{2A}) show a depletion relative to the uncontaminated clasts with trends for the two groups diverging towards less evolved compositions. The chemical variation within G_{2A} is compatible with the restite model of Chappell (1984), with linear chemical variation reflecting variable degrees of unmixing of restite and melt, with the composition of the restite lying on the back projection of the data array towards more basic compositions. There is no evidence for a restite component in G_{2B} or G_7 and it is umlikely that such a model can explain the chemical variation here, particularly in the light of evidence for strong fractionation in these groups.

The TiO_2 vs SiO_2 plot (Fig. 5.5a) does not distinguish between the two-mica granites and other granite clasts. The contaminated and uncontaminated G_2 samples are also not discriminated. The two clasts of hornblende-biotite granodiorite (G_8) are unusually depleted in TiO_2, reflecting the dominance of hornblende as the mafic phase. The evolved granites, particularly the equigranular red granites, also have very low TiO_2 abundances, reflecting their low biotite contents. The trend towards decreasing K_2O with increasing SiO_2 (Fig.5.1) is most easily explained by

combined biotite and K-feldspar fractionation.

The volcanic clasts on both TiO_2 and P_2O_5 variation diagrams, plot on the extension of the biotite granite array towards more basic compositions. This is compatible with both the various biotite granite and volcanic magmas having similar petrogenetic histories, with less evolved andesitic to rhyolitic magmas, relatively free of the effects of high-level feldspar fractionation, being erupted at the surface, whilst strong fractionation of these liquids in high level magma chambers produced very highly evolved granites at shallow crustal levels. The almost total lack of metasedimentary xenoliths in the granite clasts, and the absence of foliated clasts indicates emplacement by stoping or forceful `ballooning` is unlikely. Instead, emplacement by passive piston faulting in cauldron or ring complexes is a more satisfactory mechanism. It is in such shallow level volcano-plutonic complexes that the link between volcanic and plutonic rocks is likely to be at its most intimate.

5.5 TRACE ELEMENT GEOCHEMISTRY

5.5.1 Large Ion Lithophile Modelling

Ba, Sr and Rb/Sr show a wide range in clasts of northerly derivation, and in this respect are distinct from the granite clasts of southerly derivation which have restricted Sr contents and only modest variation in Rb/Sr ratios. Rb shows a general increase with increasing SiO_2 and DI, whilst Sr and Ba both show progressive depletion in more evolved clasts. The LIL and Ce data are presented as a series of logarithimic plots in Figures 5.6 and 5.7, together with modelled fractionation vectors for the extraction of a single phase. These modelled trends assume simple Rayleigh Law fractionation and use the mineral-melt distribution coefficients tabulated in Table 4.2.

An added complication in the interpretation of the northerly derived LIL data is the extremely felsic nature of the melts which reach 78% SiO_2. Partition coefficients in such felsic melts are particularly sensitive to the physical and chemical properties of the melt itself, and may consequently show a large range. Watson (1976) showed that increased polymerisation of progressively more silicic melts can cause the solubility of Rb in the melt to increase and the solubility of Sr and Ba to decrease. Partition coefficients for Sr and Ba are therefore likely to increase during fractionation whilst those for Rb will decrease.

Evidence for high partition coefficients comes from phenocryst-matrix element distributions in silicic rhyolites and ignimbrites. Coefficients determined from sanidine (Leeman and Phelps 1981) and sodic plagioclase (Vernieres et al. 1977) in such rock-types are considerably higher than those determined from other less felsic and intermediate rocks presented by Arth (1976) and used here.For example, Leeman and Phelps (1981) determined K_D^{Ba} and K_D^{Sr} values of 22 $\pm$ 5 and 28 $\pm$ 7 respectively between sanidine and co-existing glass in high SiO_2 (77-78%) rhyolite lavas from the Yellowstone Volcanic Field. They point out however that these values should not be used outside the Yellowstone Volcanic Field without due consideration of magma

composition, although their coefficients have been used to interpret LIL element distributions in granitic rocks elsewhere (e.g. Whalen 1983). A conservative approach is adopted here using the established coefficients compiled in Table 4.2, recognising the possibility that these may be too low and therefore the degree of fractionation indicated by the modelled melt trends may be an overestimate. This does not however detract from a qualitative assessment of the role of fractional crystallisation, and the likely phases involved.

Rb and Sr have a largely linear distribution when plotted on a log-log plot (Fig. 5.6a). Linear distributions on logarithmic variation diagrams typify trends produced by fractional crystallisation. A displacement to the left of the main trend defined by the bulk of the data at high Sr contents suggests a secondary trend in the less evolved clasts characterised by a positive correlation of Rb and Sr. The main trend involves a strong depletion in Sr accompanied by a modest increase in Rb. This trend is parallel to modelled vectors for removal of K-feldspar, particularly at low Sr contents. At intermediate Sr concentrations, plagioclase may have been more important. The Sr-Rb plot does not however discriminate plagioclase and K-feldspar fractionation on account of the similarity of the distribution coefficients for Rb and Sr in these phases. Biotite does not appear to have been an important fractionating phase, but amphibole may have had a significant role in the early evolution of the magmas. This is supported by the presence of hornblende in the least evolved rock-types.

The colinearity of clasts of granite and porphyry from each of the different groups suggests the granites and related rocks from which the clasts were derived may have been consanguineous and derived from a single parental magma. The porphyries and granophyres are notably colinear with the clasts of granite although showing the greatest depletion in Sr. It is possible therefore that they represent the most highly evolved phases of the granite magmas to which they are related by feldspar fractionation.

FIGURE 5.6 Rb vs Sr and Ce vs Rb plots for granite, porphyry and volcanic clasts of northerly derivation. For symbols refer to Table 5.1. Vectors indicate modelled change in melt composition given fractional crystallisation of various mineral phases. These have been constructed using mineral-melt distribution coefficients given in Table 4.2. Abbreviations are B:biotite, K:K-feldspar, P:plagioclase, AMP or A:amphibole. The percentage of fractional crystallisation of the original melt to produce corresponding changes in Rb, Sr, and Ce abundances is marked along the vectors.

FIGURE 5.7 (overleaf) Ba vs Rb and Ba vs Sr plots for granite, porphyry and volcanic clast data.

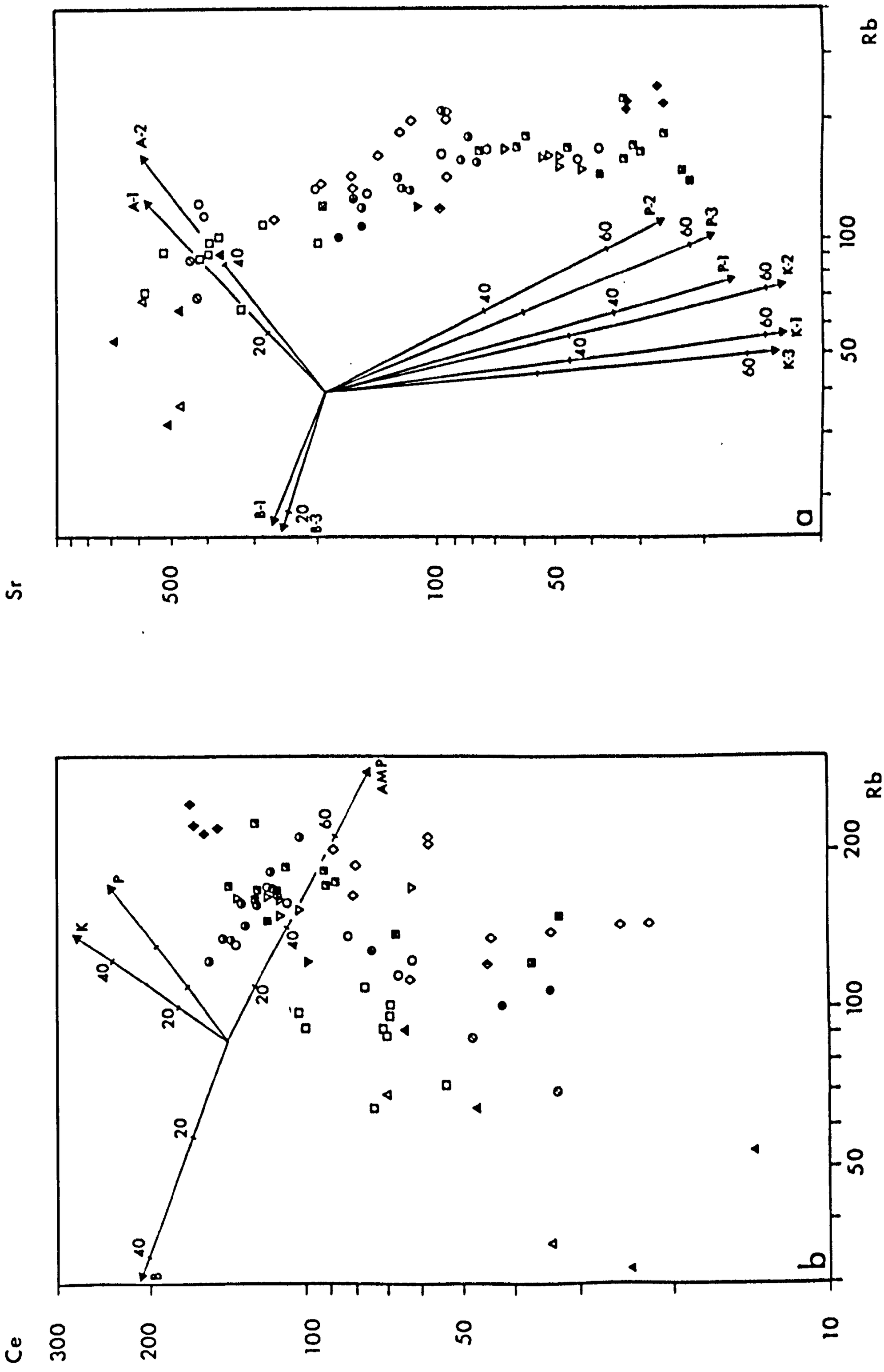
Rb
Sr
500
100
50
A-1
A-2
20
40
60
80
P-1
P-2
P-3
K-1
K-2
K-3
B-1
B-3
a
Rb
Ce
300
200
100
50
10
AMP
K
P
B
b

FIGURE 5.6

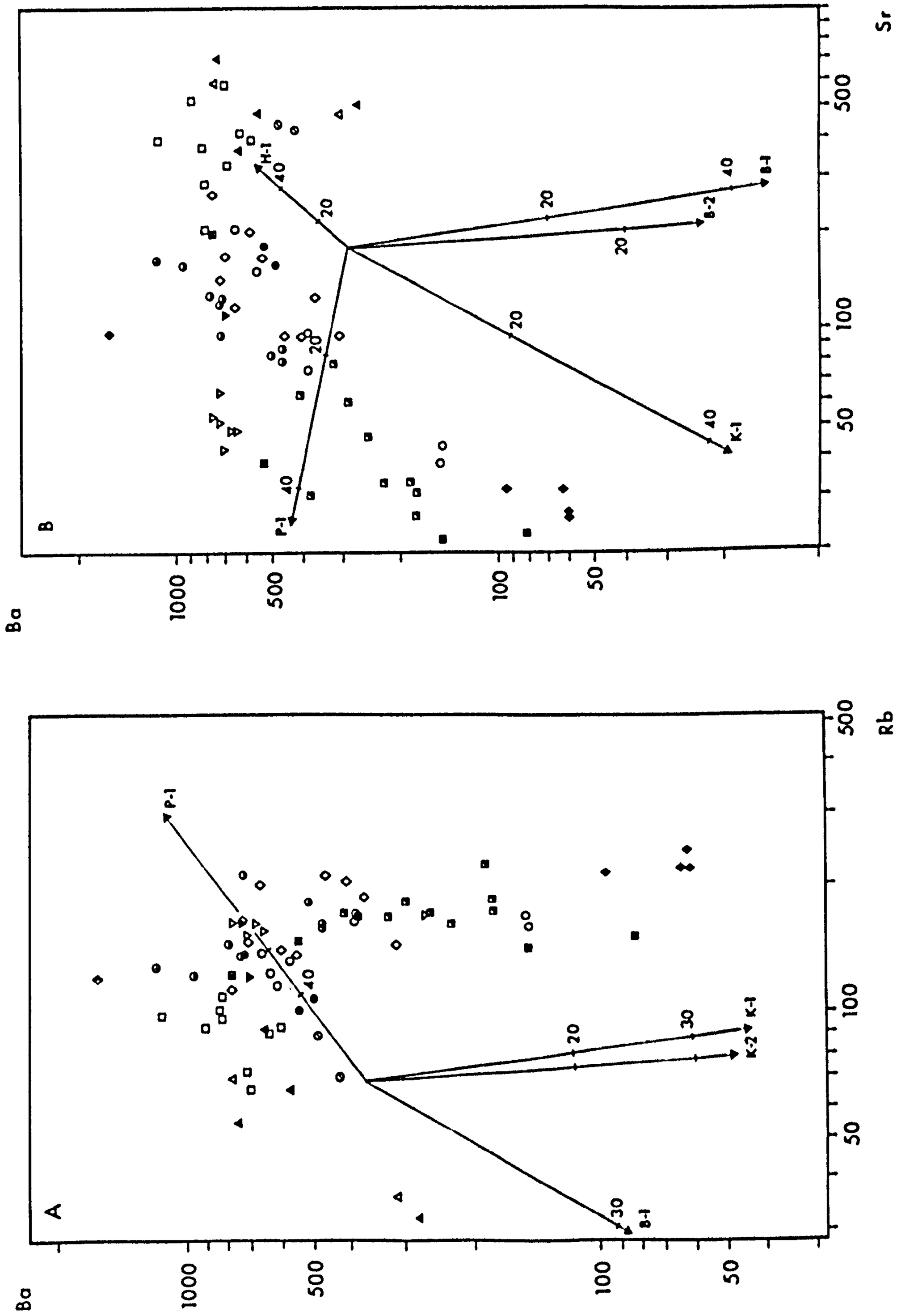
Sr
500
100
50
Ba
1000
500
100
50
B
H-1
40
20
20
B-1
40
20
B-2
20
40
K-1
40
P-1
Rb
500
100
50
Ba
1000
500
100
50
A
P-1
40
20
30
K-1
K-2
30
B-1

FIGURE 5.7

The steep trend of the data, combined with the abundance of K-feldspar as a phenocryst phase, argues strongly for K-feldspar fractionation as being important during the late stage differentiation of the magmas. Tindle and Pearce (1981) ascribe strong Sr depletion in aplitic and microgranitic phases of the Loch Doon Pluton to being unrelated to separation of mineral phases. They favour control of the chemical variation by alkali-rich fluids released during the later stages of in-situ crystal fractionation. This interpretation is based on the increase of alkali-feldspar abundance and its interstitial habit in progessively more evolved rocks. K-feldspar does not form a significant interstitial component in the granite, granophyre or quartz porphyry clasts and the LIL variation is therefore thought to primarily reflect fractionation as opposed to vapour phase processes.

The two-mica granite clasts (G_1) also plot close to the linear trend defined by the other clasts. Rb/Sr ratios in the two-mica granites are variable and show a coherent trend coincident with that of the other clasts. As these clasts of two-mica granite are clearly unrelated to the non-muscovite bearing granite types, the apparent linearity of the data as a whole cannot be used as evidence for consanguinity between groups of clasts on the basis of a single plot. The variation within the two-mica granite suite may reflect several processes including variable degrees of partial melting, source heterogeneity and fractional crystallisation. Beckinsale (1979) describes coherent variation in Rb and Sr abundances in S-type granites from the SE Asian tin belt, which he ascribes to extensive fractionation of plagioclase. It is possible that a similar mechanism operated in the case of the northerly derived two-mica granites. The data trend parallel to modelled fractionation vectors for extraction of plagioclase, with 20-30% fractionation required to produce the range of compositions seen. Fractional crystallisation, or indeed partial melting, cannot however explain the correlation of Rb/Sr with $(^{87}Sr/^{86}Sr)_i^{460}$. Two-mica granite clasts with high Rb/Sr ratios have high initial ratios suggesting source heterogeneity may have been important in controlling chemical variation within the magmas. As the two-mica granite clasts were

derived from anatectic magmas which in part were associated with vein complexes, it is likely the magmas were poorly mixed and retained an impression of their heterogeneous metasediment source regions. This is thought to be the dominant factor in controlling the variation of Na/K and Rb/Sr seen in the two-mica granite suite.

Figure 5.6b shows the relationship between Ce and Rb for the northerly derived granite and volcanic clasts. Whereas the data show considerably greater scatter than the Rb-Sr plot, the more evolved clasts do plot with enriched Ce and Rb abundances relative to the less evolved clasts, confirming the role of feldspar fractionation. The mineral-melt distribution coefficients are such that Ce should be enriched in magma series dominated by feldspar removal. Again the relative roles of K-feldspar and plagioclase in determining the melt compostiion cannot be isolated as both have similar partition coefficients for Rb and Ce. An interesting feature of the Ce-Rb data is the different trends shown by the contaminated (G_{2A}) and uncontaminated (G_{2B}) K-feldspar megacrystic granites. The contaminated clasts plot with a linear trend parallel to the vector for liquid compositions controlled by removal of amphibole. This largely reflects the variable extent of restitic hornblende separation which critically controls the chemistry of the suite. In contrast the uncontaminated megacrystic granite clasts show a trend at right angles to the contaminated clasts towards increased Ce and Rb abundances. This is commensurate with K-feldspar fractionation of the order of 40-50%.

The greater scatter evident on the Ce-Rb plot may reflect the role of minor phases in modifying REE abundances. Rb, Sr and Ba are concentrated in the major silicate mineral phases and consequently are relatively insensitive to minor phase fractionation. Ce however, a LREE, can be strongly fractionated by crystallisation of a range of accessory minerals which have very high partition coefficients for REE. These include apatite, sphene, zircon, allanite and xenotime. Miller and Mittlefehldt (1982) suggest depletion in LREE in felsic magmas results from fractionation of monzonite. The scatter on the Ce-Rb plot is

therefore thought to reflect more complex behaviour of Ce resulting from minor phase fractionation in addition to removal of feldspar.

The behaviour of Ba is important because it behaves as an imcompatible element until K-feldspar begins to crystallise, when it is then rapidly depleted from the residual melt phase. Ba-Sr and Ba-Rb plots (Fig. 5.7a,b) can therefore be used to distinguish the relative roles of plagioclase and K-feldspar fractionation in a qualitative fashion. The Ba-Rb plot clearly shows two distinct trends, an early trend towards increasing Ba and Rb abundances followed by a steep trend towards rapid dpeletion in Ba, coupled with a modest increase in Rb. The granophyres are the most strongly depleted in Ba with the more evolved biotite granites also showing strong depletions. The linear trend towards Ba depletion can be seen to be parallel to the modelled melt vectors for the incremental extraction of K-feldspar, whilst the broad trend towards Ba enrichment in the less evolved rocks can be modelled by varying proportions of plagioclase and amphibole fractionation. The two-mica granites do show a clear trend, confirming that source effects are more important than fractionation in determining their chemistry.

When Ba is plotted against Sr (Fig. 5.7b), the importance of K-feldspar over plagioclase fractionation in determining the composition of the highly evolved end-members is obvious. The granophyres and biotite granites (G_2 and G_7) again lie close to modelled trends for K-feldspar fractionation. An important feature of the Ba-Sr and Ba-Rb plots is the high Ba content of the quartz-feldspar porphyries which do not plot in a position suggestive of their evolved compositions. This indicates the Q-F porphyry clasts are unlikely to have been derived from quenched magmas related to the biotite granite magmas by crystallisation of feldspar. They must have been derived from a separate batch of chemically distinct magma. This demonstrates the need to examine LIL element behaviour on several projections before the relationship between groups of distinct clast-types can be assessed. Whilst the Q-F porphyries plot in a position compatible with derivation from the biotite granites by feldspar

fractionation on the Rb-Sr plot (Fig. 5.6a) this is not the case on Ba-Sr and Ba-Rb projections. The granophyre clasts do however plot on the extension towards greater degrees of K-feldspar fractionation of the biotite granite data (G_2 and G_7) on all Rb-Sr-Ba-Ce projections. This suggests they may indeed be related to the granite clasts.

5.5.2 High Field Strength Elements

Yttrium is a useful tracer of petrogenetic processes and is particularly sensitive to feldspar dominated fractionation during which it behaves as an incompatible element. Anomalous enrichments in Y are seen in a number of the northerly derived clast types. Similar yttrium and REE enriched granites occur in the Grampian Highlands terrane where they form part of the distinctive Cairngorm suite (Stephens and Halliday 1984). The enrichments in these plutons (e.g. Cairngorm) pose a fundamental question regarding the mechanism whereby the elevated REE, Y and U abundances and depletions in Sr are acheived. Brown and Locke (1979) and Brown et al.(1981) favour derivation of the magmas from a distinct source region which was characterised by refractory feldspar residua in the melt zone. Halliday and Stephens (1984) however argue that the chemical features of these granites which distinguish them from other late Caledonian granites of the same age can also be explained by evoking large degrees of low pressure fractionation of zircon, plagioclase and minor biotite, thereby revoking the necessity for several distinct source regions.

Y is plotted against Zr and CaO against Y in Figure 5.8. The rationale is as developed in Section 4.4.3.2. Strong yttrium enrichment is evident in the granophyres, quartz-porphyries, equigranular red granites and the more evolved megacrystic biotite granites. The volcanic clasts, grey biotite granites (G_6) and hornblende granites (G_8) show relatively depleted yttrium signatures. The low Y abundance in the least evolved rock types suggests the enrichment takes place during the transition to more evolved compositions. As the related volcanic rocks show no tendency towards higher Ytrrium concentrations in the more evolved clasts, it is probable that the yttrium

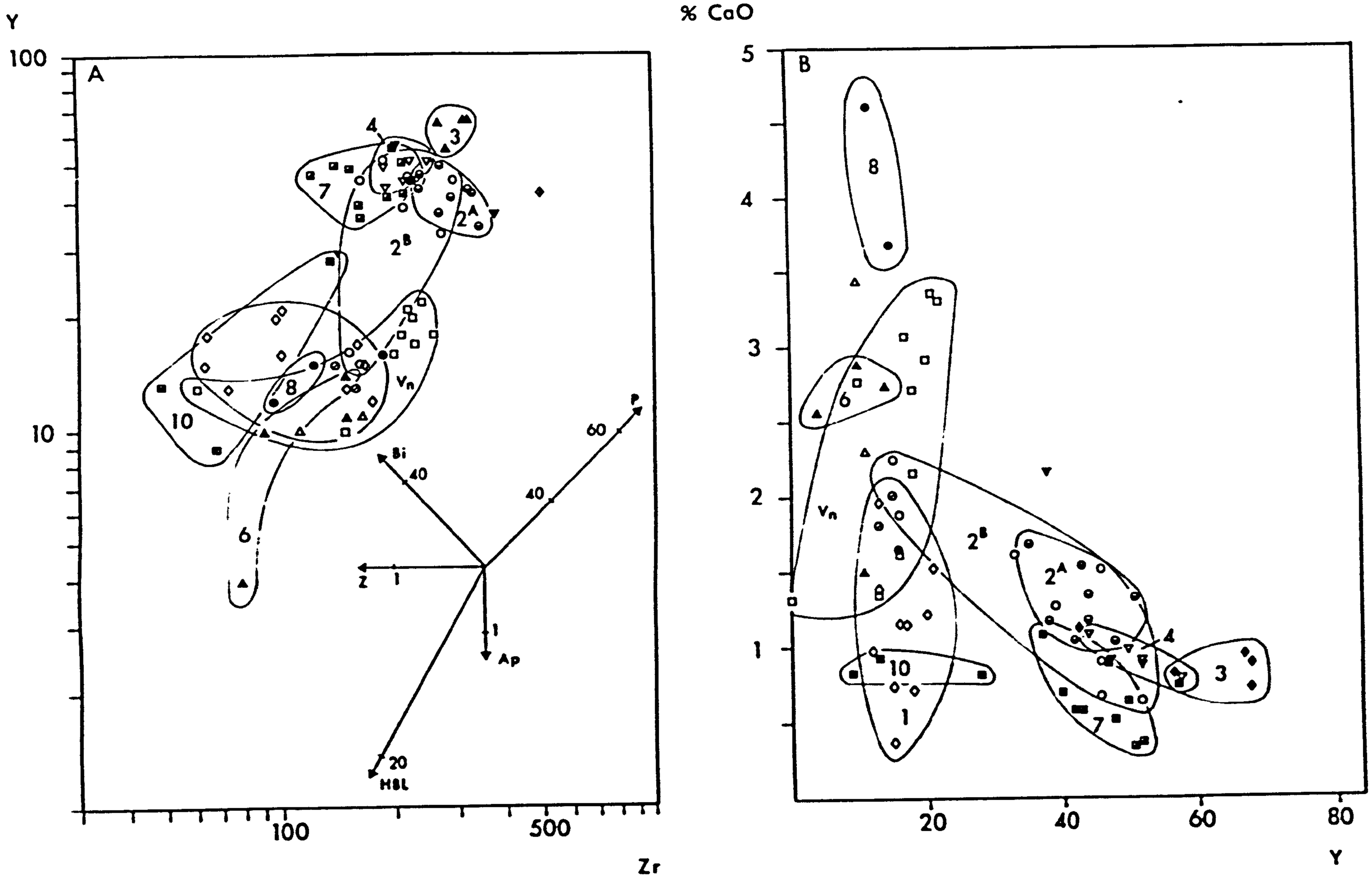

FIGURE 5.8 (A)Y vs Zr (ppm) plot for granite, porphyry and volcanic (Vn) clasts of northerly provenance. Vectors for fractional crystallisation constructed using mineral-melt distribution coefficients given in Table 4.2. (B)CaO (wt%) vs Y (ppm) plot. Symbols as in Table 5.1.

enrichment in the granites relates to a history of fractionation in high level magma chambers at low pressure. The magmas wich were erupted to form the subaerial volcanic rocks possibly came from deeper magma chambers which did not undergo extensive fractionation. This is supported by Ni concentrations up to 98ppm in the lava clasts suggesting relatively primitive liquids. The two-mica granite clasts do not show anomalous Y concentrations and clearly have not undergone significant feldspar fractionation. The various porphyry clasts (G_{10}) also show a depletion in Y and clearly are unrelated to the quartz-feldspar porphyry clasts. This implies a complex provenance for the clasts of porphyry within the northerly derived conglomerates.

Vectors for modelled melt compositions assuming extraction of a single phase by Rayleigh Law fractionation are shown in Figure 5.8a. These have been constructed using mineral-melt partition coefficients for acid magmas presented by Pearce and Norry (1979). The distribution of the data is consistent with feldspar fractionation, although the extent of enrichment requires very large degrees of cumulate-melt separation. This may reflect inappropriate values for the plagioclase-melt partition-coefficients in such felsic magmas and the important role of K-feldspar as a fractionate phase for which Y and Zr distribution coefficients are unavailable.

Nb concentrations have been determined for a selection of representative clasts. Nb shows a very similar distribution to Y between the various clast groups with strong enrichment (>40ppm) in the evolved granophyres, and modest enrichment in the equigranular red granites and porphyritic biotite granites. The imcompatible behaviour of Nb confirms a relatively minor role for biotite + zircon or amphibole in generating the chemical variation. The bulk distribution coefficient for assemblages including these phases in substantial quantity can exceed unity as the individual mineral distribution coefficients increase with increasing acidity of the melt (Pearce and Norry 1979).

5.6 GEOCHRONOLOGICAL CONSTRAINTS

5.6.1 Two-mica Granite Clasts

Van Breemen and Bluck (1981) established an age of c 460 Ma for clasts of two-mica granite sampled from the Dunnottar Group north of Dunnottar Castle. Two-mica granites occur widely throughout the Dunnottar and overlying Crawton Groups and persist to higher stratigraphic levels. Four samples of two-mica granite, from the top of the Crawton Group exposed at Crawton, and from northerly derived conglomerates at Whistleberry, have been dated using the Rb/Sr mineral- whole rock technique. The samples were selected as being representative of the two-mica granite provenance approx. 1 km stratigraphically above the sequence sampled by Van Breemen and Bluck, and can therefore be used to test the persistence of the two-mica granite source and its internal isotopic and chronological continuity.

Samples 3134 and 3152 are medium-grained equigranular muscovite-biotite clasts, 3158 is a coarse-granied strongly foliated two-mica type and 3220, a fine-grained granite with moderate foliation. Foliated and unfoliated granites were chosen to explore the possibility of significant age separation.

Table 5.4 summarises the results of isotope dilution and mass spectrometry. Biotite, muscovite and feldspar were separated using convential mineral separation techniques as outlined in Appendix 2. Muscovite and feldspar separates were fresh, but some biotites showed minor chloritisation. Care was taken to minimise chlorite contamination.

The results of York regression of the mineral and whole rock data are presented in Table 5.4. Blanket errors of 0.5 and 0.01% are used for $^{87}Rb/^{86}Sr$ and $^{87}Sr/^{86}Sr$ respectively. Mineral ages presented in Table 5.4 are mineral-whole rock two-point isochrons, except for 3158 where the whole rock sample is suspect and the feldspar is used in preference to constrain the less radiogenic end of the mineral isochrons. Errors in the case of the mineral isochrons are internal experimental errors.

SAMPLE	Rb	Sr	Rb/Sr	$^{87}Rb/^{86}Sr$	$^{87}Sr/^{86}Sr$	ε Sr	$Sr_{i(460)}$	Min.-age
3134								
3134 WR	188.7	83.8	2.252	6.54837	0.75835 ±4	163.2	0.7154 ±4	
3134 F	340.5	146.7	2.321	6.74861	0.76008 ±5			
3134 B	859.0	16.0	53.621	172.1749	1.83014 ±8			
3134 M	617.0	28.7	21.520	64.8879	1.13853 ±4			
3220								
3220 WR	218.5	91.4	2.390	6.95146	0.76051 ±4	156.3	0.7149 ±4	
3220 B	905.3	14.7	61.766	201.9503	2.03728 ±7			
3220 M	599.7	14.0	42.817	134.6393	1.59532 ±11			
3152								
3152 WR	155.9	158.0	0.986	2.85932	0.72796 ±5	74.9	0.7092 ±2	
3152 F	309.3	322.9	0.959	2.78006	0.73089 ±4			
3152 B	582.9	28.2	20.683	62.0734	1.08891 ±6			428.0 ±2.2
3152 M	379.7	25.4	14.928	44.4298	1.00102 ±5			461.1 ±2.5
3158								
3158 WR	105.3	119.8	0.879	2.54713	0.71783 ±4			
3158 F	169.0	431.2	0.392	1.13507	0.71750 ±4			
3158 B	314.5	26.9	11.703	34.6085	0.93377 ±4			453.0 ±2.4
3158 M	274.8	103.5	2.655	7.72363	0.76143 ±4			468.0 ±3.0

Table 5.4a. Rb-Sr mineral and whole rock analytical data for northerly derived two-mica granite clasts. WR: whole rock, F: feldspar, K: k-feldspar B: biotite and M: muscovite. Rb and Sr concentrations in ppm.

SAMPLE	Rb	Sr	Rb/Sr	$^{87}Rb/^{86}Sr$	$^{87}Sr/^{86}Sr$	ϵ Sr	$Sr_{i(413)}$
3309							
3309 WR	122.2	409.5	0.298	0.86376	0.71101 ±3	27.3	0.70593 ±6
3309 K	251.9	440.8	0.571	1.65482	0.71584 ±4		
3309 B1	616.4	20.4	30.222	92.0395	1.24529 ±5		
3309 B2	614.9	21.5	28.533	86.6468	1.21439 ±8		
3304							
3304 WR	84.6	414.4	0.204	0.59113	0.70991 ±10	34.5	0.70643 ±11
3304 P	30.3	934.4	0.032	0.09373	0.70663 ±4		
3304 K	239.8	314.5	0.762	2.20832	0.71837 ±5		
3304 B2	304.0	22.6	13.466	39.8143	0.93152 ±		
3137 WR	113.5	401.9	0.282	0.81734	0.71075 ±3	27.5	0.70594 ±6
QF-P							
3132 WR	155.6	42.4	3.671	10.6983	0.78108 ±5		
3138 WR	162.1	46.4	3.495	10.1804	0.77718 ±8		
3185 WR	145.4	37.8	3.842	11.2004	0.78444 ±6		
3200 WR	155.2	48.9	3.176	9.24686	0.77095 ±5		
3200 F	187.3	63.5	2.948	8.57880	0.76674 ±6		

Table 5.4b. Rb-Sr mineral and whole rock analytical data for three biotite granite clasts and four clasts of quartz feldspar porphyry (QF-P).

SAMPLE	SEPARATES	NO.OF POINTS	AGE (Ma)	INITIAL RATIO	MSWD
TWO-MICA GRANITES					
3134	WR,F,B,M	4	455.6 ± 2.0	0.7160 ± 3	1.26
3158	F,B,M	3	459.3 ± 7.3	0.7101 ± 3	14.96
3220	WR,B,M	3	459.3 ± 0.3	0.71503 ± 6	0.04
BIOTITE GRANITES					
3304	WR,P,K,B	4	396.3 ± 10.0	0.70614 ± 12	41.92
3309	WR,F,B1,B2	4	412.0 ± 1.7	0.70602 ± 7	1.70
QUARTZ-FELDSPAR PORPHYRIES					
QF-P	4 WR`s,F	5	475.3 ± 7.2	0.7085 ± 10	0.40

Table 5.4c. Regression parameters.

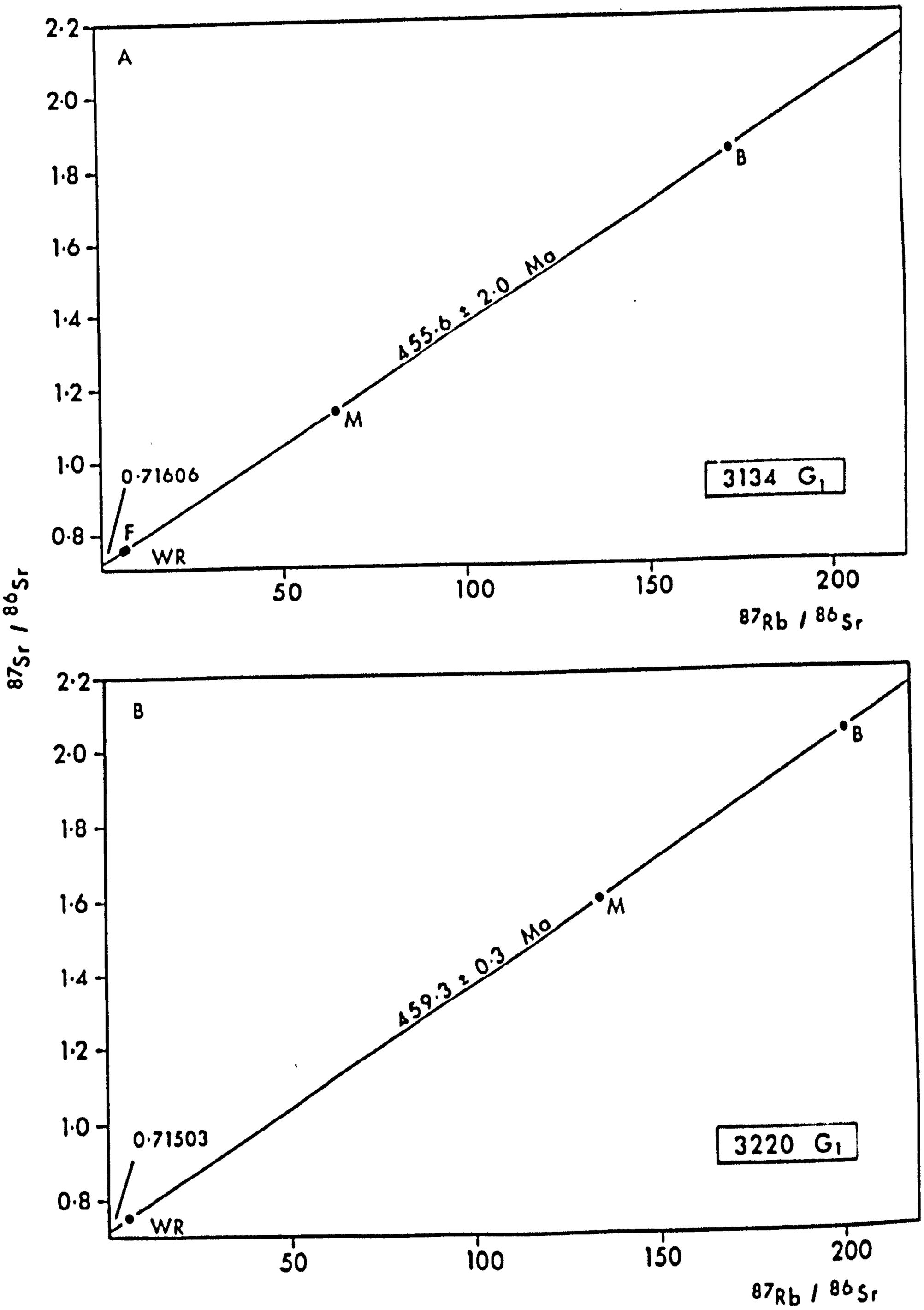

FIGURE 5.9 Isochron plots for northerly derived two-mica granite clasts (3134,3220) from the Crawton Group at Crawton. Abbreviations are B:biotite, M:muscovite, F:feldspar, WR:whole rock.

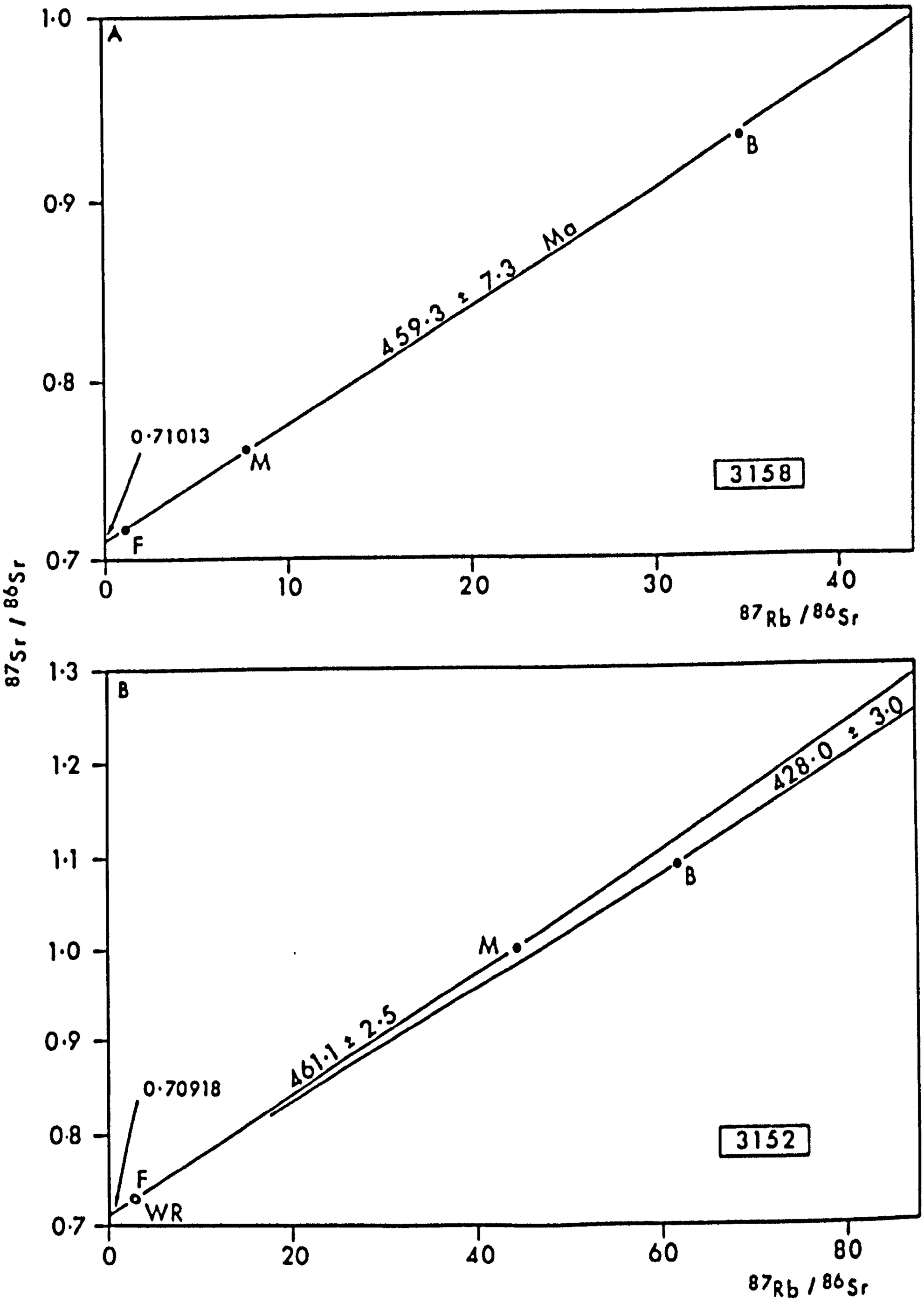

FIGURE 5.10 Isochron plots for northerly derived two-mica granite clasts (3158,3152) from the Crawton Group at Crawton. Abbreviations are B:biotite, M:muscovite, F:feldspar, WR:whole rock.

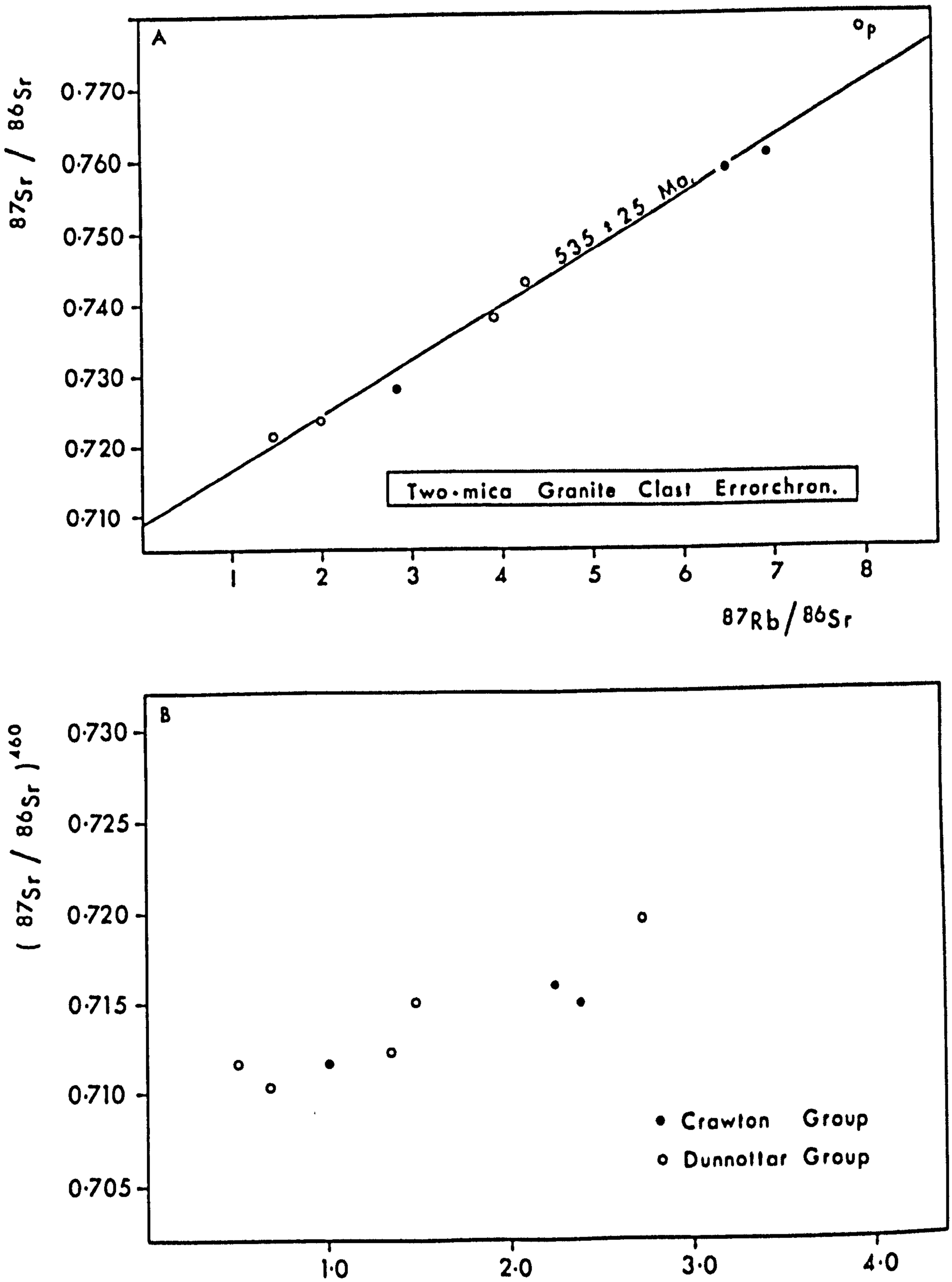

FIGURE 5.11 Sr isotopic composition of two-mica granite clasts from the Dunnottar (data from Van Breemen and Bluck 1981) and Crawton Groups (this study). A:whole rock errorchron for eight whole rock samples ignoring pegmatitic sample (P). B:linear correlation between $(^{87}Sr/^{86}Sr)^{460}$ and Rb/Sr.

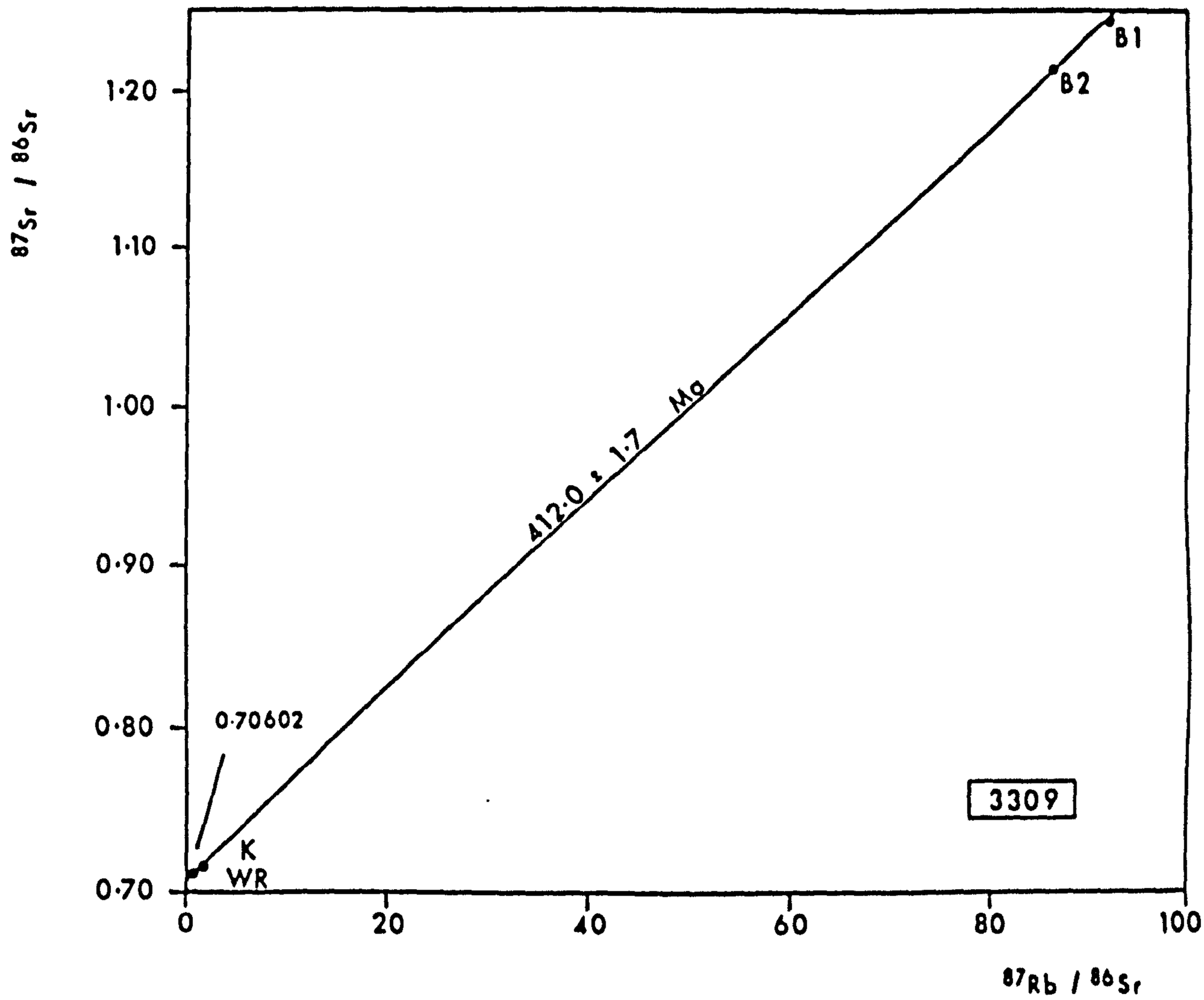

FIGURE 5.12 Isochron plot for northerly derived porphyritic biotite granite (3309) from the Crawton Group. Abbreviations are WR:whole rock, K:K-feldspar, B1,B2: replicate biotite separates.

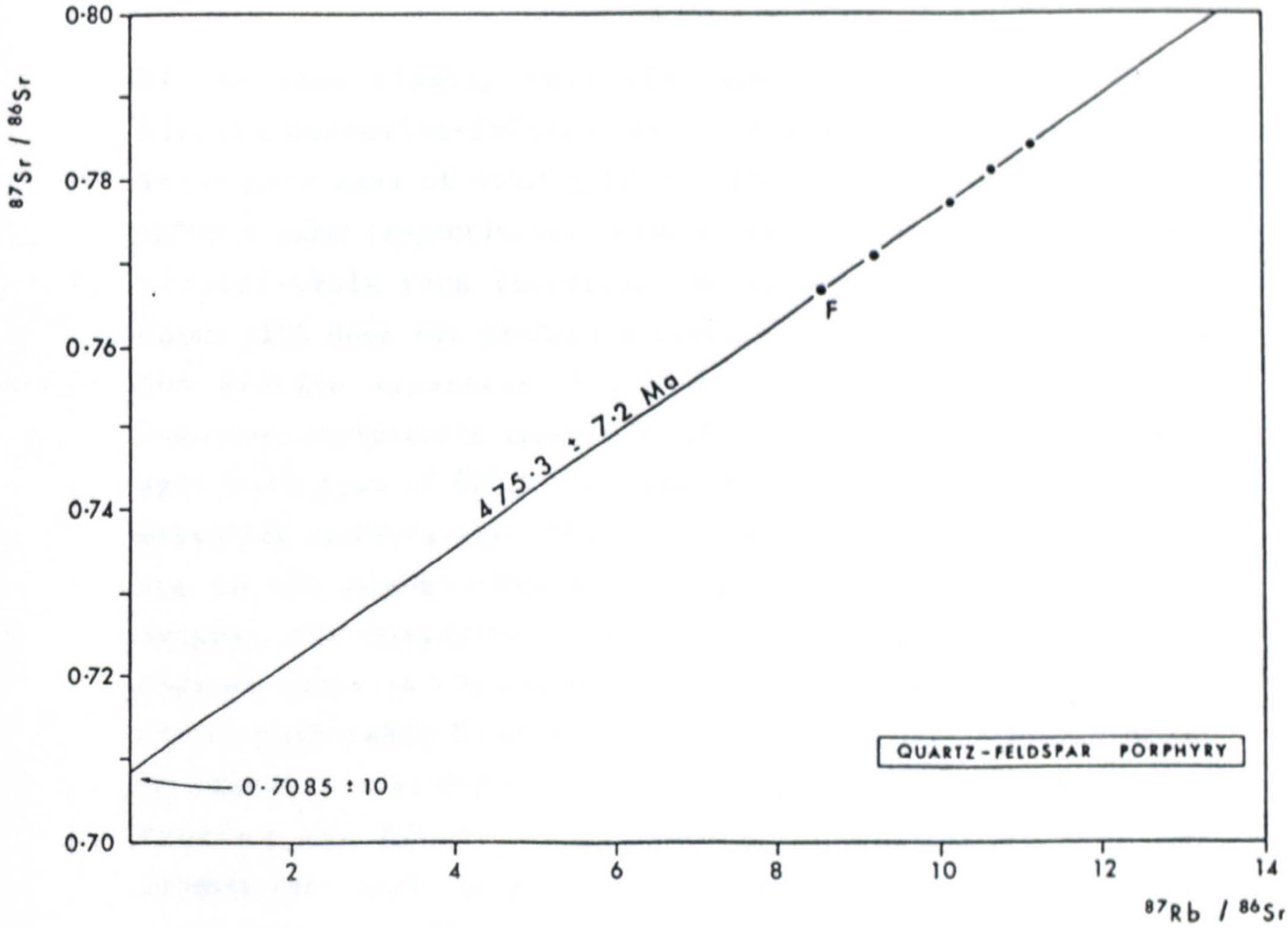

FIGURE 5.13 Isochron plot for four quartz-feldspar porphyry clasts of northerly derivation and a single feldspar separate.

PLATE 5.1 Quartz-feldspar porphyry clast, Todhead Point (NO 871769). Phenocrysts are 3 to 8mm.

Of the four clasts, only 3134 and 3220 produce concordant biotite-muscovite-feldspar whole rock isochrons (Fig. 5.9a,b). These give ages of 455.6 ± 2.0 Ma (MSWD = 1.26) and 459 ± 0.3 Ma (MSWD = 0.04) respectively. Initial ratios determined from these mineral-whole rock isochrons are 0.7160 ± 3 and 0.71503 ± 6. Clast 3152 does not produce a concordant isochron for muscovite and biotite separates (Fig.5.10). Mineral-whole rock ages indicate considerable separation of biotite and muscovite closure ages with ages of 428.0 ± 2.2 and 461.1 ± 2.5 Ma for biotite and muscovite respectively. The close approximation of the muscovite age to the mineral-whole rock ages for 3134 and 3220 above suggest the muscovite closed during a widespread muscovite closure event in the source at this time. The younger biotite age is comparable to an age of 421 ± 5 Ma for biotite in a clast of pegmatitic two-mica granite from the Dunnottar Group (Van Breemen and Bluck 1981). These late Silurian ages are inconsistent with the biotite closure reflecting slow uplift and cooling as the evidence from accompanying psammite clasts points to very rapid uplift of the terrane into which the granites were probably emplaced (6.5). It is therefore more likely that the younger age reflects a low temperature alteration effect and has no thermal significance.

The source of scatter in the mineral-whole rock data for clast 3158, the strongly foliated granite, lies in the unrealistic value of the data for the whole rock sample. Rb and Sr isotope dilution results do not concur with duplicated XRF determinations for 3158 whole rock and the sample is therefore rejected as being suspect, the result of a possible error is the isotope dilution. The remaining three points define an isochron with an age of 459.3 ± 7.3 Ma and a initial ratio of 0.7101 ± 3. The high MSWD (14.96) reflects slight discordance of muscovite and biotite, which give mineral-whole rock ages of 468 ± 3.0 and 453 ± 2.4 Ma respectively. Small discordances of biotite and muscovite ages are to be expected where cooling effects are encountered.

The isotopic data above are remarkably consistent with the data of Van Breemen and Bluck (1981) from the Dunnottar Group. Clast 3134 extends the muscovite closure ages to as young as 455 Ma.

The oldest closure age, previously c 465 Ma from a pegmatitic sample (RC 1913) from the Dunnottar Group, now becomes 468 Ma for the foliated sample, 3158. The range of muscovite ages is interpreted as reflecting a pulse of two-mica granite generation and emplacement at c 460 ± 8 Ma. The ages are thought to represent emplacement of the magmas as opposed to metamorphic uplift and cooling ages for three reasons. Firstly the concordance of biotite and muscovite from samples 3134 and 3220 indicate rapid cooling, with intrusion of the magmas into country rocks which were at temperatures of less than 300°C, the estimated blocking temperature of the Rb-Sr system in biotite. Secondly, muscovite and biotite closure ages from metamorphic clasts (largely psammites) which are thought to represent the metamorphic country rocks into which the granites were emplaced generally do not show concordance (6.5). Low Sr micas preserve a significant separation of mica-whole rock ages with biotite consistently c 12 Ma younger than the muscovite, and muscovite ages comparable to those in the granite. The lack of a cooling pattern in several of the granites suggests they were emplaced at depths shallower than the 300°C isothermal surface at c 460 Ma. Separation of muscovite and biotite ages in 3158 may reflect derivation from below this surface, although it is difficult to separate cooling effects from the low temperature alteration which is known to overprint biotites in some of the clasts. It may be significant that 3158 has the oldest muscovite age, and is also strongly foliated. A third criterion whereby emplacement as opposed to uplift ages of the granites are favoured, is the fact that Rb-Sr muscovite systems are known to have survived Caledonian deformation and metamorphism in the Central Highlands (Piasecki and Van Breemen 1979).

On the basis of the observation outlined above, the muscovite closure of both granite and psammite clasts at c 460 Ma is unlikely to reflect bulk isotopic closure of an uplifting and cooling composite granite-metamorphic terrane. The coincidence of inferred granite emplacement ages and regional uplift is however of interest and suggests a possible genetic link between the two. This is more fully discussed in Chapter 6. The occurrence of granites with concordant mica ages suggests the

two-mica granites may have been emplaced high into the metamorphic pile which they intrude. This is confirmed by xenoliths of lower greenschist facies chlorite grade psammite which occur in several two-mica granite clasts. The relationship of the granites to the foliation developed in the psammitic host rocks is seen in several clasts in which two-mica granite veins cut across the foliation in the psammites. In all cases the two-mica granite truncates both the spaced mica foliation and crenulate folds of this fabric.

Initial ratios for the four granite clasts for which isotopic data are available are included in Table 5.4. The initial ratios are comparable to those determined previously by Van Breemen and Bluck (1981) falling within the range 0.710 to 0.716. These are higher than would be expected from a mantle or low Rb/Sr lower crustal source and indicate crustal involvement in the petrogenesis of the granites. The range of initial ratios for two-mica granite clasts from the Dunnottar and Crawton Groups is displaced to slightly lower values than Pankhurst (1974) determined for in-situ c 460 Ma intrusions in Banff. The coarse size of many of the clasts (>1.0m) however precludes derivation from these intrusions as they are in excess of 60km from the depositional basin at present. Two-mica granites in Aberdeenshire are a more attractive source region. Isotopically these rocks are poorly known. Halliday (1984) presents Sr isotopic data for a range of plutons including the Aberdeen Granite. Its initial ratio (assuming an age of 440 Ma) is 0.71151. This is considerably lower than the Banff two-mica granites and very similar to a number of the ratios determined from the clasts of both the Crawton and Dunnottar Groups. It is possible therefore that the Aberdeenshire two-mica granites may be characterised by lower $(^{87}Sr/^{86}Sr)_i$ than contemporary plutons to the north in Banff. The age relationships of these granites however remain unclear.

Whole rock Rb/Sr isotopic data for the three clasts with reliable whole rock determinations (omitting 3158) are plotted, together with the five analyses of two-mica granite clasts from the Dunnottar Group (Van Breemen and Bluck 1981), on an isochron

diagram (Fig. 5.11a). The data fall on a poorly defined isochron with considerable scatter. Regression of the data produces an age of 535 ± 25. If the single pegmatitic clast is ignored, a 7 point York regression age of 521 ± 28 Ma is obtained from the errorchron. The high MSWD (145.8) indicates considerable geological scatter. This is most easily explained in terms of the assumption of initial isotopic homogeneity required by the isochron method not having been met. Initial ratios derived from mineral-whole rock isochrons are plotted in Fig. 5.11b against whole rock Rb/Sr ratios. There is a systematic increase in initial ratio with Rb/Sr over the range of compositions sampled.

5.6.2 Megacrystic Biotite Granite Clasts

Two clasts of the megacrystic biotite granite (G_{2B}) have been investigated with the object of establishing the age relations and provenance of this voluminous suite of granitic clasts. Both clasts were collected from northerly derived conglomerates exposed at Crawton, at the top of the Crawton Group. Both were free from the restitic clots which characterise many clasts of this type, and were larger than 50cm maximum diameter.

Rb-Sr analytical data for biotite, K-feldspar and plagioclase mineral separates, together with whole rock samples, are presented in Table 5.5 for two clasts, 3304 and 3309. An additional clast, 3137, has been included for whole rock analysis only. Details of regression parameters are given in Table 5.5.

Of the two clasts, only 3309 produces an acceptable isochron. Clast 3304 yields a scattered mineral isochron giving an age of 396.3 ± 10.0 Ma and a MSWD of 41.92. This age, largely determined by the biotite point is anomalously young in that the indicated age is younger than the probable age of the sediments in which the clasts occur. This is attributed to low temperature alteration of the biotites during weathering and diagenesis.

Clast 3309, in contrast, gives a good biotite (2)-K-feldspar-whole rock four point isochron (Fig. 5.12) yielding an age of 412 ± 1.7 Ma (MSWD = 1.7) and an initial intercept of 0.70602 ± 7. The two biotite points represent replicate analyses of the same mineral separate. They are treated as individual points during the York regression. The poor reproducibility of the replicate analyses, and the distribution of replicate points along the resulting isochron is thought to reflect sample heterogeneity in the biotite separate. The low MSWD suggests the granite clast has not undergone the low temperature alteration evident in 3304. In addition the biotites have low Sr contents and high Rb/Sr ratios. Consequently, the mineral-whole rock age for the clast is interpreted as reflecting isotopic closure on rapid cooling of a granite emplaced at high level in the source terrane. In addition to voluminous c 460 Ma Ordovician magmatism, the source terrane from which the clasts were derived must therefore also be characterised by Silurian granite plutonism. A pattern of episodic magmatism in the source terrane is indicated.

The late Silurian age for 3309, and by implication, for much of the biotite granite detritus, for the chemistry of these granites shows a close coherence (see 5.7.1), is the first confirmation of an important sediment contribution from late Caledonian granites external to the Midland Valley terrane, to Lower ORS sedimentary basins lying on this terrane. The emplacement age of these granites is only marginally older than the probable absolute age of the sediments which host the clasts. Thirlwall (1983b) established an age of 411 ± 6 Ma for the Lintrathen Porphyry on the basis of Rb/Sr biotite-whole rock data. Patterson and Harris (1969) correlate the Linthrathen Porphyry, which outcrops predominantly to the north of the Highland Boundary Fault north of Blairgowrie, with a single outcrop south of the fault at Glenbervie, where it interfingers with Lower ORS sediments close to the top of the Crawton Group. If this correlation is valid the basal groups of the Lower ORS may be in excess of 410 Ma. The age of the granite clast, 3309, does however suggest that the absolute age of the basal Lower ORS is unlikely to be greatly in excess of c 410 Ma. Estimates for the base of the Devonian include 408 Ma (Harland et al.1982) and 412 Ma (McKerrow et al.

1984).

The isotopic data from the Lower ORS are therefore compatible with a late Silurian age for at least part of the Lower ORS of the northern Midland Valley.

Initial ratios calculated for whole rock samples at 413 Ma are 0.70594 ± 6, 0.70593 ± 6 and 0.70643 ± 11 for the three clasts of megacrystic biotite granite. These values are clearly distinct from the initial ratios determined from the ≤ 460 Ma two-mica granite clasts and suggest a fundamental change in petrogenetic process. A change to less radiogenic Sr isotopic signatures is compatible with a change from a high Rb/Sr to a low Rb/Sr source region, or to a relative young source which has not undergone sufficient time-integrated Rb decay to promote enhanced $^{87}Sr/^{86}Sr$. A migration of the magma source region from an upper crustal to a deeper lower crustal or mantle location would produce the observed transition in chemical and isotopic character.

5.6.3 Quartz-feldspar porphyry clasts

Four clasts of quartz-feldspar porphyry, together with a single feldspar separate, have been analysed. Analytical results are included in Table 5.5. The clasts have high Rb/Sr ratios but a narrow range of compositions when plotted on an isochron diagram. The five clasts produce a good isochron with a MSWD of 0.4. This gives an age of 475.3 ± 7.2 Ma, and an initial intercept of 0.7085 ± 10. Whilst the data yield a good isochron, the narrow range of isotopic compositions mean that it is poorly controlled and caution must consequently be exercised in interpreting the age determined. The isochron age is substantially older than both the two-mica granites and the biotite granite clast, 3309. The initial ratios calculated to 415 Ma are also substantially higher than the biotite granites. The isotopic data therefore confirms that the quartz-feldspar porphyry clasts are probably unrelated to the biotite granite and granophyre clasts. Their exact age relations must however remain unclear.

5.7 DISCUSSION

5.7.1 Geochemical Constraints on the Relationship between Clast Types.

The geochronological data presented in 5.6 establish an episodic history of magmatism within the source terrane which supplied the northerly derived conglomerates. An early phase of anatectic melting produced a group of two-mica granites characterised by homogeneous compositions, relatively low chemical diversity and many `S-type` characteristics. Later magmatism involved a diverse suite of biotite granites, granophyres and associated volcanic rocks which are, in contrast, broadly of `I-type` (Chappell and White 1974). As isotopic and geochronological work on these later granites has been limited, and given the very great diversity of granite types present as clasts, the detailed age relations are unclear. However, the Rb-Sr whole rock-feldspar-biotite age for a clast of porphyritic megacrystic granite (3309) requires a substantial sediment contribution from late-Silurian plutons in the source terrane. Just how large this contribution is is dependent on establishing a genetic link between the dated megacrystic granite and other granite clasts occurring in the conglomerates.

The consanguinity between G_{2A} and G_{2B} is unequivocal. Texturally and chemically the two groups of clasts are very similar and can only be distinguished on the basis of whether or not they contain restitic clots. Restite separation alone cannot explain the chemical variation between the two groups as the uncontaminated clasts do not lie on the extension to more felsic compositions of the contaminated clasts. Rather the two trends overlap and converge at higher silica (e.g. Fig. 5.1). This suggests part of the magma suffered restite contamination whilst the remainder did not. Both underwent differentiation towards more felsic compositions, restite separation being an important process in the contaminated granite type. Restite contaminated clasts probably make up 60-70% of the total G_2 type megacrystic granite clasts.

The relationship between G_2 and G_7, the red equigranular granites

is less clear. These granites do however lie on the extension of the megacrystic granites to more evolved compositions on many plots. LIL modelling suggests derivation of G_7 from G_2 is feasible by a process of K-feldspar fractionation. The K_2O vs SiO_2 plot (Fig. 5.1) shows a significant change in behaviour from broadly increasing K_2O with SiO_2 in the megacrystic granites to decreasing K_2O in the more evolved red equigranular granites. Such behaviour is typical of many felsic magmas and can be explained by crystallisation initially on the quartz + plagioclase cotectic followed by subsequent crystallisation on the quartz + two-feldspar cotectic. Mittlefehldt and Miller (1983) demonstrate a similar initial enrichment followed by subsequent depletion in K_2O in evolved felsic magmas from the Sweetwater Wash Pluton, California. The geochemical data are therefore consistent with a close relationship between the porphyritic and equigranular granite types.

The four clasts of granophyre which have been analysed also show many similarities with the evolved biotite granites and plot on the extension of many of the trace element trends defined by the granitic rocks. There is no reason to suspect therefore that the granophyres are unrelated to the evolved biotite granites and they may represent an undercooled crystal-poor differentiate extracted from the granite magma. In contrast, the high Ba content of the quartz-feldspar porphyry clasts rules out any direct link with the late Silurian magmas. Whole rock and feldspar isotopic evidence from these porphyries suggests an Ordovician age (475 Ma) although the isochron is poorly constrained. No clasts preserving the contact relations of the QF porphyries are found and it is therefore difficult to relate them to the history of magmatism in the source terrane. Their felsic character, depletion in Sr and enrichment in Y suggest they are the product of strong fractionation.

The assorted porphyries grouped as G_{10} cannot be related to the QF porphyries, nor to the evolved biotite granites. They may be late differentiates of the magmas which formed the dacitic and rhyolitic lavas but texturally are hypabyssal rocks. The volcanic rocks show many similarities with the granites although

acid-andesite and dacitic lithologies dominate. Clasts of rhyolite, some with ignimbritic textures, are quite rare. There is therefore a fundamental distinction in the source area between intermediate magmas which were erupted to form volcanic rocks and felsic magmas which underwent low pressure fractionation in shallow magma chambers. These felsic magma chambers did not appear to vent voluminous high silica tuffs at the surface, with the exception of rare ignimbritic clasts and the Lintrathen Porphyry, a single ignimbritic flow of northern provenance which may interfinger with red bed sediments close to the base of the Strathmore Basin.

The relationship of the two clasts of hornblende-biotite granite (G_8) to the more evolved granites is unclear. It is possible they represent a sample of rare more basic magma from which the more evolved granites developed. Volumetrically, they form a minor component of the granite clast assemblage although this may be a function of the level of erosion within the conglomerate source. The chemistry of these rare granodioritic clasts is distinct from granodiorites of southerly derivation and they cannot represent recycled clasts. This is in contrast to the two clasts of suspected southerly derivation (G_9) which do show a marked resemblance to granite clasts occurring in first cycle conglomerates of southerly provenance. This, taken together with the occurrence of `returned` greywacke clasts, is thought to indicate limited mixing of material of southerly provenance with the multicyclic sediment of northerly provenance. This may have either occurred prior to the formation of the Crawton Basin during an earlier phase of sediment dispersal or within the basin as northerly dispersed fan toes were reworked and returned southwards.

The grey equigranular biotite granites (G_6) remain enigmatic. In many respects they chemically resemble clasts of southerly derivation and are distinct from the voluminous late Silurian biotite granites. In the absence of isotopic data the ultimate provenance of this rather rare group of granite clasts is uncertain.

In conclusion, the bulk of the northerly derived granite clasts (70-80%) can be assigned to two distinct magmatic episodes. Ordovician anatectic melting in the source terrane was followed during the late Silurian by shallow level emplacement of highly silicic granites and granophyres.

5.7.2 Provenance of northerly-derived granite and volcanic clasts.

Geochemical and isotopic data presented above have been used to `image` the plutonic and volcanic history of the source terrane which supplied the detritus. Salient features which any prospective source terrane is required to have include a long history of polyphase deformation prior to c 460 Ma, voluminous generation of c 460 Ma anatectic muscovite-biotite granites, coincidence of this Ordovician crustal melting with rapid uplift and cooling of the metamorphic rocks which host the melts, and a widespread and diverse group of late Silurian magmas occurring as both high level permissive evolved granites and closely related more basic volcanic rocks.

Whilst there can be no guarantee that the terrane which shed the detritus will still be exposed within the mosaic of shuffled terranes which compose the final assembly, the Lower ORS occurs sufficiently close to the time of cratonisation of the orogen to infer that the potential for major destruction or masking (for example, by overthrusting) of terranes was low. Bluck (1983) does however demonstrate a possible example of terrane masking in Silurian conglomerates along the southern margin of the Midland Valley. These conglomerates have a provenance which on the basis of the scale of the dispersal system, and the composition of the detritus transported by it, cannot have been in the now adjacent Southern Uplands terrane to the south. One possibility is that this terrane was thrust over a now hidden terrane which originally supplied the detritus to the conglomerates. Support for this hypothesis comes from recent geophysical results which suggest anomalously shallow high density basement at depths of between 1-5km over much of the northern belt of the Southern Uplands tract (Hall et al. 1983). This suggests an allochthonous origin for the low grade sediments and volcanics of the Southern

Uplands which were structurally emplaced over a continental terrane. Given that the youngest sediments in the Southern Uplands are Wenlock in age, there clearly is a possibility that masking of terranes can take place late in the history of orogenic terrane assembly. Accepting the possibility that a correlative terrane showing an identical history of magmatism, from which the clasts may have been originally derived, may not have actually been preserved, it is still important to examine prospective terranes in terms of their potential to supply detritus with the required chemical, chronological and isotopic characteristics. Of particular significance is whether the now adjacent Grampian Highlands terrane has the requisite magmatic history to have been in its present position relative to the Midland Valley during the late Silurian - early Devonian, thereby requiring docking between these terranes substantially earlier than envisaged by Bluck (1984) and Dewey and Shackleton (1984).

Terranes showing episodic Ordovician and Silurian magmatic histories have not been widely recognised along the Caledonian-Appalachian fold-belt. As a detailed compilation of the magmatic histories of the many separate terranes which have been identified within the Caledonides is beyond the scope of the present study, and as in many cases there is insufficient chemical and chronological control to allow the history of magmatism to be accurately characterised, the following discussion centres largely on the suitability of the Grampian Highlands terrane as a source for the detritus. However, some general points can be made with respect to the likelihood of derivation from a terrane now lying outwith the British sector of the Caledonides.

Given the strong evidence for sinistral transcurrent faulting in both the British and Irish, and the Newfoundland Caledonides (Soper and Hutton 1984) during the Silurian and early Devonian, it is likely that a late Silurian source terrane which was subsequently translated laterally and severed from a sedimentary sequence it supplied with detritus, will now be found to the west amongst the terrane collage of the northern Appalachians in Nova Scotia or Newfoundland.

A literature search of chemical and chronological data from plutonic rocks of the Appalachian orogen has failed to identify a comparable sequence of events to that established from the granite and metamorphic clasts of the northerly derived conglomerates. Middle Ordovician (c 460 Ma) plutonic activity has been established in several terranes within Newfoundland. Whalen et al. (in press) demonstrate a mid-Ordovician age for both an amphibole tonalite from the Hungry Mountain Complex, and the Hinds Lake granite, both part of the Topsails Igneous terrane. Tonalites form the tonalite terrane also yield mid-Ordovician ages (Dunning quoted in Whalen et al. in press). Both these terranes are essentially plutonic terranes and show no obvious connection with uplift and cooling of a metamorphic belt. Dallmeyer and Hibbard (1984) demonstrate a probable c 460 Ma age for both the Burlington Granodiorite and the Dunamagon Granite, the latter providing an upper limit for the juxtaposition of the Burlington and Mings Bight terranes (K eppie in press). Rb/Sr isotopic data for the Burlington (Dallmeyer and Hibbard 1984) and Dunamagon (Pringle 1978) plutons show the initial $^{87}Sr/^{86}Sr$ ratios to be less than 0.705. This points to a fundamentally different style of mid-Ordovician plutonism to that recorded in the clasts, in the terranes which logically might be expected to preserve a displaced Lower ORS source terrane, assuming large Lower to Middle Devonian sinistral displacements.

Whalen et al. (in press) argue that the c 460 Ma magmas of the Topsails terrane may have been generated as a direct consequence of superincumbent loading and thermal insulation of an island arc terrane beneath an overthrust ophiolite thrust stack. The complex petrogenesis of many of the mid-Ordovician magmas is seen as reflecting thermal reworking of the island arc rocks. The close association of magmatism and ophiolite obduction is clearly very different to the largely anatectic origin, reflecting rapid post-orogenic decompression, of the c 460 Ma granites occurring as clasts in northerly derived Lower ORS conglomerates.

Analogous Silurian magmas to those occurring as clasts are also lacking in many Newfoundland and Nova Scotian terranes.

Recently, substantial Silurian magmatism has been demonstrated in the Topsails terrane. The granites and related rock types have the required isotopic signature close to bulk earth but chemically are quite distinct with many intrusives having an alkaline or peralkaline affinity (Whalen et al. in press). Peralkaline granite clasts have not been found in the northerly derived conglomerates and the Loch Borolan complex in NW Scotland represents one of the rare occurrences of alkaline magmatism in the Scottish Caledonides (Van Breemen et al.1979).

Stephens and Halliday (1984) demonstrate a gross chemical coherence of c 400 Ma granites of Britain and Ireland which cannot be extended to c 400 Ma granites of the eastern USA, Canada and Newfoundland. The existence of a distinct chemical province in the British Caledonides suggests large terrane displacements cannot have subsequently dismembered the terrane mosaic following the emplacement of the granites.

A further problem with evoking a displaced source for the Lower ORS detritus amongst the terranes of Newfoundland is the fact that many of the Newfoundland terranes which are potential source areas were accreted during the mid-Ordovician Taconic Orogeny to the Long Range. Many prospective source terranes were therefore already bound in the Newfoundland terrane mosaic by the late Silurian and are unlikely to have distributed sediment to the Midland Valley.

The apparent absence of a suitable source terrane for the northerly derived Lower ORS of the Midland Valley amongst the terranes of Newfoundland focusses attention on plutonic-metamorphic terranes closer to the basin of deposition. Of these, the adjacent NE Grampian tract of the Grampian Highlands terrane is the most significant, on account of the proven occurrence here of c 460 Ma two-mica granites (Pankhurst 1974) and late Silurian evolved granites (the Cairngorm suite of Stephens and Halliday 1984). The NE Grampian tract therefore superficially shows a striking resemblance in terms of its magmatic history to that inferred for the source region of the northerly derived clasts in conglomerates which now lie adjacent

to the tract. The magmatic fingerprint of the NE Grampian tract appears to be unique to this area and cannot be extended to encompass other areas of the Grampian Highland terrane. Both the c 460 Ma anatectic granites and the late Silurian granites show distinctive regional variation when traced eastwards from the central Highlands into the NE Grampian tract, a feature possibly not unrelated to the very different thermal histories of the central and NE Grampian tracts during the climax of Grampian metamorphism.

Pankhurst (1974) was the first to demonstrate a distinct suite of mid-Ordovician two-mica granites which post-date both the Younger Basic intrusions and F3 deformation in the NE Grampian tract. Ages ranged from 444 ± 9 Ma for Aberchirder to 462 ± 22 Ma for Strichen. Aftalion et al.(1984) (after Pidgeon and Aftalion 1978) record a nearly concordant monazite age of 476 ± 5 Ma for the Strichen intrusion. Other granites possibly belonging to the same mid-Ordovician episode include the undated Aberdeen granite and related granite vein complexes exposed on the coast south of Aberdeen (Walsworth-Bell 1974). Tourmaline-bearing pegmatites at Belhelvie and Portsoy have yielded Rb-Sr ages of 463 ± 5 Ma (Van Breemen and Boyd 1972, Lappin pers. comm. in Van Breemen and Piasecki 1983).

Two-mica granites also occur outwith the NE Grampian region in the Central Grampian Highlands. Here they occur both as vein complexes e.g. the Strathspey-Laggan complex, and pegmatites associated with muscovite bearing granite and granodiorite plutons e.g. Glen Kyllachy. The Strathspey-Laggan complex is considered to have been derived by crustal anatexis following decompression of the Grampian metamorphic pile due to rapid post-tectonic uplift and erosion (Clayburn et al.1983). Van Breemen and Piasecki (1983) demonstrate muscovite Rb/Sr closure ages of 446-422 Ma from syn-F3 pegmatites of the Glen Kyllachy complex. Whole rock samples from the Glen Kyllachy granite produce a poorly constrained isochron with an age of 443 Ma and initial $^{87}Sr/^{86}Sr$ ratio of 0.7176 ± 4. The high initial ratio, close to values obtained from the surrounding Moine metasediments, suggests derivation from the upper crust by a process of crustal

anatexis at 443 Ma. The central Grampian tract therefore appears to have undergone a similar period of crustal anatexis to the NE Grampian tract albeit some c 20 Ma after melting occurred in the NE.

The hiatus in crustal melting between the two regions is matched by a parallel diachroneity in the timing of deformation. Van Breemen and Piasecki (1983) propose a time integrated change in the geometry of a northwesterly facing subduction zone beneath the Grampian Highlands to have contributed to a westerly migration of crustal melting. A system of deep shear zones of Grampian age which transect the NE Grampian tract may also have been important in uncoupling or compartmentalising the deformation, metamorphism and crustal melting of adjacent Grampian tracts (Ashcroft et al. 1984). In addition lateral displacement on these shear zone structures may have juxtaposed sections of the terrane which were originally more widely separated. A direct consequence of the diachroneity of crustal melting is that clasts of two-mica granite occurring in the conglomerates of northerly derivation in the Crawton Basin can only be derived from the two-mica granites of the NE Grampian tract. Muscovites from clasts derived from the central Grampian Highlands would show closure ages close to 440 Ma whereas observed muscovite ages are in the range 455-468 Ma. The occurrence of two-mica granite clasts which are unfoliated confirms derivation from the central Grampian tract is unlikely, as granites here are syn-F3 and only the latest crosscutting aplites and pegmatites of the Glen Kyllachy complex are unfoliated. Two-mica granites emplaced in the NE Grampian tract are post-F3 and may be both foliated and unfoliated.

Turning to the late Silurian granites of the Grampian terrane, a similar picture of regional variation between different tracts is seen. Stephens and Halliday (1984) use petrographic, geochemical and isotopic data to establish three plutonic suites amongst c 400 Ma granites intruding the Grampian Highlands terrane. A plutonic suite is defined as a regional association of chemically distinct and related plutonic rocks, which may show a range of petrographical types, for example gabbros, diorites and granites

may all belong to the same suite. Boundaries between each of the suites are shown in Fig.5.14. The Cairngorm Suite is distinguished from the Argyll Suite and the South of Scotland Suite (here termed the South Grampian Suite as it includes only those members of the suite intruding the Grampian Highlands terrane) by the highly silicic metaluminous compositions, enrichments in Nb, Rb, and Th, and depletions in Ba and Sr. The suite is dominantly composed of red biotite granites, with few intermediate rock-types and rare appinites. Granodiorites and diorites, rare in the Cairngorm Suite, are in contrast abundant in the Argyll Suite where they are characterised by very high Sr and Ba abundances, low Nb, Th and Rb and lower $^{87}Sr/^{86}Sr$ initial ratios than the granites of the Cairngorm Suite.

The South Grampian Suite also comprises diorites and granodiorites. Pyroxene occurs in the diorites in contrast to hornblende in the diorites of the Argyll Suite. A fundamental distinction between the Argyll Suite and plutons to the south is their lower ε Nd values. Plutons north of the mid-Grampian line, an isotopic boundary coincident with the boundary of the Argyll and South of Scotland Suites, and arrived at independently by Halliday (1984) using coupled U-Pb and Sm-Nd systematics, have ε Nd values of less than -6. La, Ce, Ba, and Sr all tend to be lower in the South of Scotland Suite with respect to the Argyll Suite.

Table 5.6 lists the characteristics of each of the granite suites (from Stephens and Halliday 1984) along with those for the biotite granite clasts. The clasts most closely resemble the granites of the Cairngorm Suite with which they show a close affinity. The clasts show a similar bias towards highly evolved rock types, lakcing any substantial volume of accompanying granodioritic rock-types. Y, Rb and Nb show a similar pattern of enrichment, and Sr and Ba are dpeleted. Initial $^{87}Sr/^{86}Sr$ ratios for granites of the Grampian terrane are plotted on Fig. 5.14. These represent average initial ratios for each of the plutons taken from Harmon and Halliday (1980) and Pankhurst (1974). The initial ratios for $\leq$ 400 Ma granites gradually increase when traced towards the NE away from the SW Highlands where initial

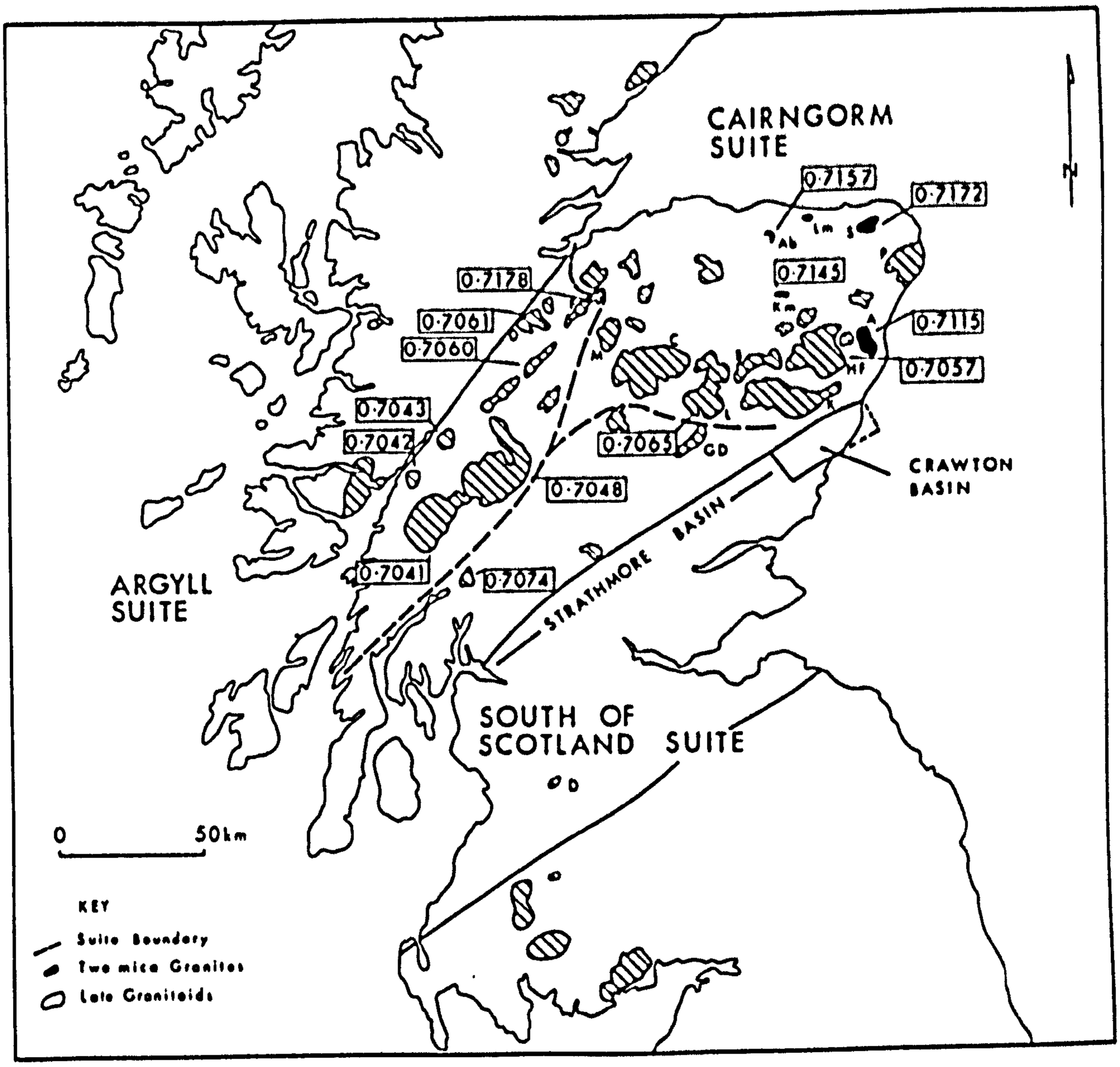

FIGURE 5.14 Distribution of granitoid suites and initial $^{87}Sr/^{86}Sr$ ratios of granites in the Grampian Highlands. Dashed line marks boundary between granites showing coherent geochemical and isotopic characteristics (after Stephens and Halliday 1984). Initial ratios are from Harmon and Halliday (1980) and Pankhurst (1974). Abbreviations are A:Aberdeen, Ab:Aberchirder, B:Ballater, C:Cairngorm, F:Findhorn, GD:Glen Doll, HF:Hill of Fare, K:Kincardine, Km: Kemnay, Lm:Longmanhill, P:Peterhead, S:Stricken.

	ARGYLL SUITE	STH OF SCOTLAND SUITE	CAIRNGORM SUITE	CLASTS
ROCK TYPES	Common granodiorites and diorites; appinites abundant; hornblende characteristic of diorites	Commonly diorites and granodiorites; pyroxene typical of diorites; appinites in N only	Mainly red biotite granites; intermediate types rare; few appinites	Dominantly red biotite granites; few intermediate types; rare appinite clasts
MAJOR ELEMENTS	Calc-alkaline high Na_2O compositions	Calc-alkaline	Highly silicic metaluminous compositions	Highly evolved, many clasts with metaluminous compositions
TRACE ELEMENTS	Very high Sr and Ba Low Nb, Th, Rb	Low La, Ce, Ba, Sr	High Nb, Rb, Th Low Ba, Sr	High Nb, Y, Rb Low Sr, Ba
AGE (Ma)	410-415	390-408	408-415	412
ϵ Sr	-7 to +58	+1 to +54	+24 to +33	+27.3 to +34.5
ϵ Nd	-10 to +3	-4 to +1	-8 to -1	-1.8

Table 5.5 Characteristics of late granitoid suites (from Stephens and Halliday 1984) compared to clasts of northerly provenance.

ratios are close to bulk earth. Late Silurian-early Devonian plutons of the central and NE Grampian tracts have initial ratios in the range 0.7060 ± 5, substantially higher than bulk earth. Significantly, the inital ratios determined for the clasts of megacrystic biotite granite (G_{2B}) also fall in this range. Initial ratios for ≤ 460 Ma granites are also shown in Fig.5.14. These decrease to the south across the NE Grampian tract on the basis of the limited data available.

Taking the regional distribution of ≤ 460 Ma and ≤ 400 Ma granitoids together, the NE Grampian tract can be seen to have a unique chemical, isotopic and chronological fingerprint which cannot be extended to other tracts within the Grampian terrane, or to other terranes in the Caledonian mosaic. Clasts occurring in the adjacent Lower ORS of the Crawton Basin share this unique fingerprint and on the basis of the available data can only be derived from the immediately adjacent metamorphic-plutonic terrane. Sediment and sediment source terrane therefore do not appear to have been displaced relative to one another suggesting that the Grampian terrane and the Midland Valley may have docked with one another by the Late Silurian.

5.7.3 Implications of Late Silurian docking between the Midland Valley and Grampian Highlands Terranes

5.7.3.1 Background

Evidence is presented above establishing a probable provenance for northerly derived granite clasts occurring in conglomerates of the Crawton Basin. Geochemical, isotopic and chronological constraints identify the adjacent NE Grampian tract of the Grampian Highlands terrane as the most likely source. How can the late Silurian docking of the Grampian Highlands and Midland Valley terranes implicit in such a provenance be reconciled with the evidence for a Lower ORS provenance in a terrane other than the `local Dalradian` established by Bluck (1984) ? Bluck cites a number of observations, largely on the basis of Lower ORS outcrops over the western Midland Valley, in support of an alternative source terrane to the local Highlands for the Lower ORS. These observations include :

1. The bulk of the clasts in the Lower ORS of the Strathmore Basin are not in fact metamorphic basement but a range of volcanic, hypabyssal and plutonic rock types.
2. The basement contribution is polycyclic and must be derived from a metamorphic terrane which underwent initial uplift earlier than, and unconnected with the subsidence which accompanied development of the ORS basins.
3. Greenschists or other metamorphic rocks of certain local Dalradian origin have not been recognised in Lower ORS conglomerates.
4. Two sources of quartz-rich metamorphic detritus must logically be considered. Quartzite and psammitic clasts may have been derived from a sequence of conglomerates which mantled the Dalradian where they were concentrated by repeated erosion and redeposition, or, they may have been dispersed from a metamorphic block within the Midland Valley where there is evidence for diverse quartzite basement (Bluck 1969, Wilson 1970, Morton 1976). Difficulties with the first interpretation include the presence of sedimentary quartzites in the Strathmore conglomerates and the evidence for local Dalradian clasts in ORS basins developed on the Grampian Highlands terrane.
5. Lower ORS conglomerates in the outliers north of the Highland Boundary Fault are dispersed to the SE, in which direction across the fault they meet roughly coeval conglomerates of different composition, which are dispersed to the NW.

Bluck (1984) rationalised the above observations in a palaeogeographical reconstruction for the late Silurian-early Devonian in which a terrestrial red-bed basin, a possible subaerial continuation of the Highland Border Basin, extended north of the present position of the Highland Boundary Fault nd received sediment from both a volcanic-metaquartzite source to the south and a crustal block of uncertain affinities to the north. This block, termed Block C, was thought to represent `either a part of the Midland Valley terrane, a hitherto unknown slice of Dalradian terrane, differing in composition from local Dalradian rock, or a totally alien terrane`. The Midland Valley was thought not to have lain adjacent to the Dalradian block of the present Highlands until late Upper ORS times. In the light

of contradictory evidence from the Lower ORS of the NE Midland valley the premise on which this terrane reconstruction is based needs to be re-examined. First, an alternative model is proposed utilising the evidence for a late Silurian docking between the now adjacent Midland Valley and Grampian Highland terranes.

5.7.3.2 An alternative model

Much of the uncertainty involved in establishing the Lower Palaeozoic history of the Midland Valley terrane rests in the poor exposure of Lower Palaeozoic rock-types consequent on a protracted history of Upper Palaeozoic subsidence. However, the Highland Border Complex, a series of faultbounded outcrops of largely Ordovician sediments and volcanic rocks occurring in scattered outcrops along the Highland Boundary from Stonehaven to Arran provide a crucial record of the Arenig to mid-Caradoc history of the Northern Midland Valley.

Curry et al.(1982, 1984) show sediments of the Highland Border Complex to have a provenance in a terrane other than the now adjacent Dalradian, with the posssible exception of greenschist clasts in the Loch Fad conglomerate. The occurrence of Caradocian black shales and limestone in the Highland Border complex is lithologically incompatible with a position for the Highland Border Complex adjacent to the Grampian Highlands at this time, as mica closure ages (Rb-Sr, K-Ar) from Dalradian metamorphic rocks indicate widespread rapid uplift in the period 460-450 Ma (Dempster 1984, 1985).

Large volumes of sediment should have been received by any terrane which was structurally contiguous with the metamorphic belt at this time. This implies a substantial mid-Ordovician separation of the uplifting Grampian Highlands terrane and the now adjacent Midland Valley, as large areas of at least the northern part of the latter must be underlain by rocks laterally equivalent to the Highland Border Complex. The Grampian Highlands terrane therefore underwent isostatic recovery during the Ordovician and early Silurian some distance from the Midland Valley which, as a result, cannot have received first-cycle detritus. The evidence for a late Silurian docking requires the

two terranes to have come together at this time. Bluck (1984, 1985) and Watson (1984) show the Grampian Highlands terrane during the late Silurian to have been close to regaining isostatic equilibrium on the basis of the high intrusion levels of late Caledonian permissive granites and the similarity of the basal Lower ORS unconformity with the present day erosion surface. It follows that if a late Silurian docking is envisaged, the Grampian Highlands must have been juxtaposed against the Midland Valley as an isostatically compensated terrane with little potential for either further uplift or the generation and dispersal of first cycle detritus to the terrane with which it docked.

The mechanism whereby the two terranes converged probably involved a large component of oblique slip translation. Lateral transcurrent emplacement is preferred to orthogonal contraction and over thrusting as envisaged by Leake et al (1984) on the grounds that little first-cycle sediment was generated as direct consequence of juxtaposition of the terranes. This is supported by evidence for a change from regional compressive to regional transcurrent deformation in the British and Irish Caledonides during the Silurian (Soper and Hutton 1984).

Figure 5.15 illustrates a model for the terrane history of the Grampian Highlands and Midland Valley in cartoon fashion. The model hinges on the late Silurian - early Devonian docking inferred from the granite clast data. During the mid-Ordovician the terranes were widely separated and have unconnected magmatic histories. Anatectic magmatism in the Grampian Highlands reflects decompression attendant on rapid uplift which appears to have been diachronous along the terrane. The magmatism is not seen as having a direct link with subduction processes but rather a consequence of crustal thickening by orogenic contraction. Synchronous Ordovician magmatism recorded by granite clasts in fore-arc conglomerates in the SW Midland Valley suggests the Midland Valley at this time was the site of a plutonic arc developed over continental basement (Longman et al. 1979). This arc was uncoupled from the foreland basement by a marginal basin

FIGURE 5.15 Cartoon illustrating possible Late Silurian or Lowermost Devonian docking between the Midland Valley and the now adjacent Grampian Highlands Terrane.
(A)A Caradocian separation is required by the lack of Dalradian detritus in the Highland Border Complex. Dalradian metamorphic rocks are known to have been rapidly uplifted at this time. Molasse from the Grampian Orogeny must have been shed to contiguous foreland basins from which the uplifted core of the orogen was subsequently severed by strike-slip displacement. Granite magmatism occurred in both terranes at this time but only in the case of the Midland Valley is there a direct connection with subduction.
(B)During the Llandovery a change from regional orthogonal to transpressional tectonics has been recognised in the British Caledonides (Watson 1984). Lateral translation of the Midland Valley was accompanied by the collapse of a marginal basin which flanked the terrane on its northwest margin. Earlier molasse basins developed on the Grampian Highlands Terrane were transient in character and reworked by subsequent uplift. However those formed in the possibly extensional regime close to the termination of regional uplift may have had greater preservational potential.
(C)Deposition of the Strathmore Lower ORS was initiated during the Late Silurian and was initially within small pull-apart basins relating to the final phase of terrane juxtaposition. Little first cycle sediment was contributed to the basins from metamorphic sources. Much sediment was however derived from contemporaneous calc-alkaline volcanoes, and from recycled sources. No contemporaneous Caledonian mountain belt is envisaged.

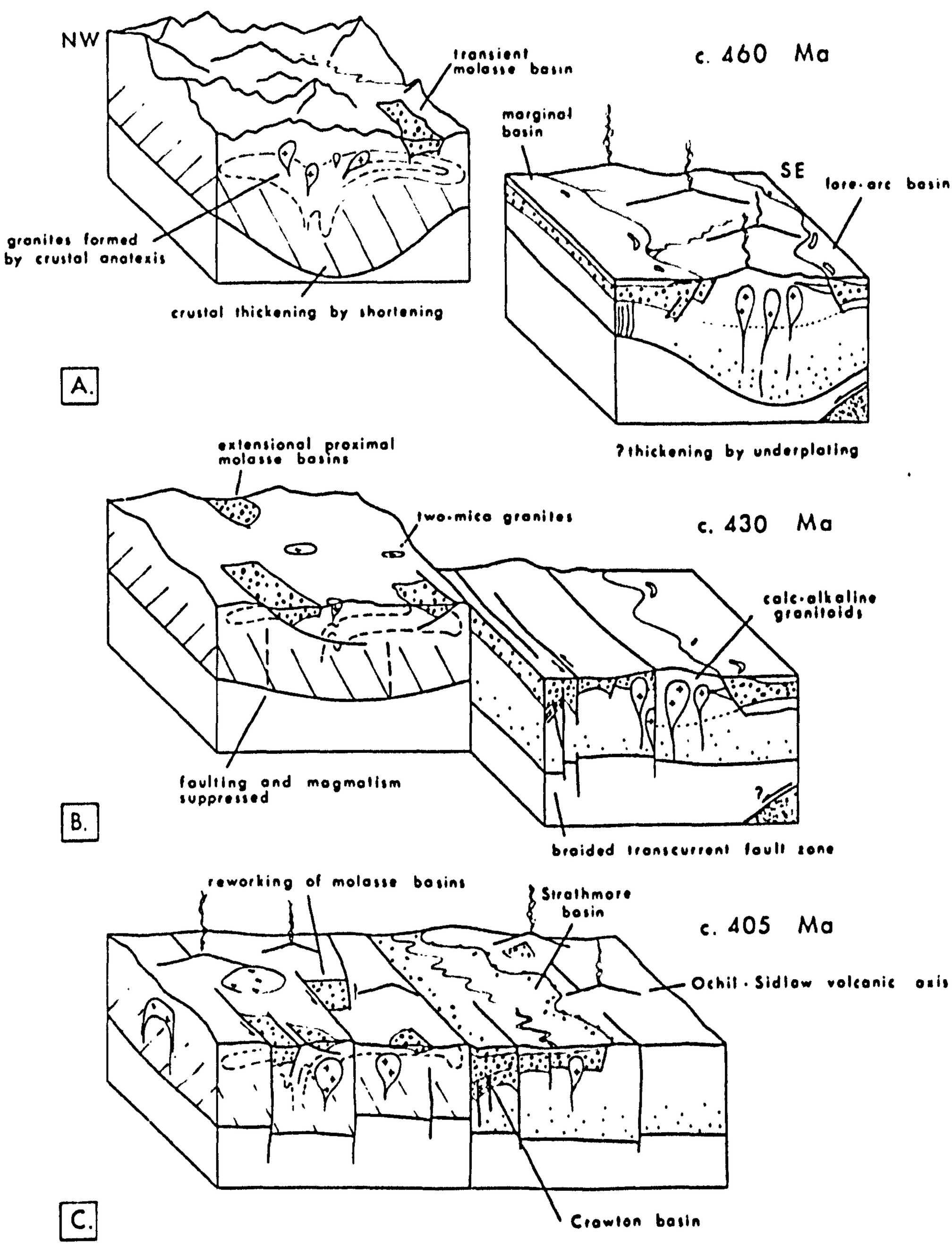
Grampian Highlands Terrane
Midland Valley Terrane
NW
SE
transient molasse basin
marginal basin
fore-arc basin
granites formed by crustal anatexis
crustal thickening by shortening
A.
c. 460 Ma
?thickening by underplating
extensional proximal molasse basins
two-mica granites
calc-alkaline granitoids
faulting and magmatism suppressed
B.
c. 430 Ma
braided transcurrent fault zone
reworking of molasse basins
Strathmore basin
Ochil-Sidlaw volcanic axis
Crawton basin
C.
c. 405 Ma

which may have been up to 100km wide. Rapid uplift of the Grampian Highlands during the mid to late Ordovician would have produced large volumes of unroofed molasse (s.s.). Given the evidence for sinistral transcurrent motion during Silurian terrane translation, the Grampian Highlands terrane would have been displaced some distance to the NE of the Midland Valley terrane. Much of the Grampian molasse may therefore have been dispersed to the Scandinavian Caledonides, or, given a three plate closure model (Dewey and Shackleton 1984, Soper and Hutton 1984), to deep basins at the northeast termination of the British Caledonides in the North Sea (Watson 1984). Alternatively, material may have been shed across the Archaean foreland to basins on a passive margin situated in Arctic Canada.

Molasse basins developed within the orogenic belt during the period of rapid uplift will be transient in character and rapidly reworked. However basins developed on the unroofed terrane towards the end of isostatic recovery will have greater preservational potential. These basins may develop by a process of extensional spreading, in a similar manner to that proposed by Coney and Harms (1984) for the Basin and Range Province. Here evidence for Mesozoic crustal telescoping and thickening is overprinted by Cenozoic extensional tectonics attributed to lateral spreading of the gravitationally unstable mass generated during contraction (England 1981). Extension in the Basin and Range appears to be linked with a mid-Tertiary `plutonic-ignimbrite flare-up` and the development of extensional sedimentary basins and metamorphic core complexes (Davis and Coney 1979). Extension following compression and uplift might therefore result in basins developing on a metamorphic terrane close to the end of isostatic recovery and this may be a mechanism whereby a small component of coarse molasse sediment, the bulk of which is distributed far from the orogen, may be retained in basins actually on the orogenic terrane itself.

The model developed in Figure 5.15 envisages an important role for basins of this type, as a fundamental problem in understanding the underlying control of Lower ORS sedimentation is the abundance of recycled non-igneous material. This requires

a source for the conglomerates not in an uplifting metamorphic terrane but in already existing conglomerates lying in basins on such a terrane. This highlights a fundamental difference between the Lower and Upper ORS. The Lower ORS records a sediment redistribution event as opposed to the production of sediment from contemporaneous uplift adjacent to the basin of deposition. A voluminous contribution of igneous detritus accompanies the recycling of existing conglomerates and reflects the independent role of magmatic processes in producing a direct sediment contribution which was admixed with the pre-existing metamorphic gravels either within the source, or during dispersal to the basin of deposition. An important feature of the Lower ORS is this disharmony between metamorphic and volcanic sediment sources, the latter essentially independent of the tectonic control operating in the redistribution of the former.

In contrast, contemporaneous volcanic or plutonic activity does not accompany the deposition of the Upper ORS in the Firth of Clyde basin, and much of the sediment is of first cycle origin. Northerly derived detritus of certain Dalradian origin (slates and schists closely matching the adjacent Dalradian lithologies) occurs towards the top of the sequence and is interpreted by Bluck (1984) as the first indication of the juxtaposition of the local Dalradian and Midland Valley. However, given the very low production of first-cycle detritus in the Lower ORS, the Upper ORS locally derived conglomerates cannot be taken to be representative of the style of clastic input required to establish juxtaposition of the terranes at some earlier time. A direct consequence of the disparate character of Lower and Upper ORS sedimentation is that the same terrane may have shed very different detritus during the two periods of sediment dispersal. Establishing a pre-Upper ORS link between the Grampian Highlands and Midland Valley terranes is critically dependent upon being able to recognise the product of extensive reworking and recycling of metamorphic detritus temporally removed from the initial unroofing event which introduced the clasts to the post-orogenic sediment mass.

The concept of the Lower ORS as a reworking event combined with

contemporaneous igneous sediment addition is compatible with the evidence suggesting the Grampian Highlands terrane was isostatically inert and transected by active transcurrent faults (the Loch Tay fault set) during the late Silurian. The Lower ORS may therefore be typical of the style of sedimentation expected during the docking of two terranes by lateral translation. It is the product of an event which has no causal relationship with processes of orogenic uplift but reflects a distinct transcurrent overprint of an earlier history of orogenic contraction with which it has no direct connection. The period between c 440 and 415 Ma was a time of magmatic quiescence in the Grampian Highlands terrane although magmatism was abundant in the adjoining northern Highlands and Midland Valley. This suppression of magmatism suggests fracturing may not have transected the terrane until late in the history of translation and magmas were therefore unable to penetrate to the surface. The thick and relatively robust dehydrated orogenic welt produced by metamorphism of the Dalradian sediment pile would have initially inhibited the formation of deep reaching fractures localising the displacements on the boundaries to the terrane. During the late Silurian the structural integrity of the terrane was disrupted as deep-reaching faults propagated through the crust and voluminous magmas were emplaced to high level. Late Silurian disruption of the terrane is thought to have been instrumental in developing Lower ORS basins riding on the terrane, and in initiation reworking of remanent molasse basins to produce the recycled gravels dispersed to the Midland Valley with which by this time the terrane had docked.

To summarise, the model presented in Fig.5.15 integrates a number of features of the Lower ORS as seen in the NE Midland Valley. The model accounts for the late Silurian docking required by the granite clast data by evoking a lateral translation of widely separated terranes during the Ordovician to converge and dock largely by oblique slip motion along a collapsed marginal basin (the Highland Border Complex). The Lower ORS is thought to have been deposited during the final juxtaposition of the terranes and involved a reworking and re-dispersal of proximal molasse basins which were translated with the terrane on which they formed.

Can the model as outlined above accommodate or shed light on the observations cited by Bluck (1984) (5.7.3.1) in favour of a source other than the local Dalradian ? These observation are considered in turn below.

5.7.3.3 The discrepant volume of metamorphic detritus

Should the Grampian Highlands terrane have been adjacent to the Midland Valley during the late Silurian the small volume of metamorphic detritus preserved in the Lower ORS when compared with estimates of the potential sediment yield from the unroofed Grampian Highlands terrane requires explanation (Watson 1984, Bluck 1984). Within the framework of the model outlined above the volume of metamorphic detritus dispersed to Lower ORS basins is related to the volume of proximal molasse trapped in basins overlying the largely planed down Grampian Highlands terrane. Only a small volume of the original unroofed sediment mass will be retained in late basins within the core of the orogen. England (1981) demonstrates a significant feature of the sediment distribution associated with unroofing of the Alpine Orogeny. Over 50% of the unroofed sediment volume is outside the neighbouring along strike basins. A similar situation is seen in the Himalayas where the volume of material in the Bengal Fan is ten times that in basins closer to the orogen (Curray and Moore 1971). England (1981) accounts for the small volume of material adjacent to young orogenic belts as a function of the loading properties of the elastic portion of the lithosphere. Loading of the lithosphere, by a thrust or nappe stack for instance, will cause a flexural depression in an elastic plate in front of the load. Where the scale length of the load is equal to or greater than the flexural wavelength of the lithosphere, the proportion of sediment that can be accounted for in foreland depressions contiguous with the belt is small, and the bulk of the unroofed sediment must be accomodated in basins greater distances from the orogen.

As the Grampian Highlands and Midland Valley terranes were widely separated during the Ordovician when the former underwent rapid post-orogenic uplift, molasse relating to the Grampian Orogeny was probably widely distributed to both contiguous foreland

basins and to successions further afield. Translation of the Grampian Highlnds terrane to dock with the Midland Valley would have severed the metamorphic belt from voluminous molasse sequences that it may have supplied with sediment. The metamorphic conglomerates required to source the recycled sequences of the Lower ORS must have been preserved in deep basins lying on the unroofed terrane and as such can only have developed towards the end of the uplift history . As a result, they will only preserve a fraction of the total volume of sediment originally shed from the orogen and any sequence they are recycled into will inherit this characteristic. The model therefore accords well with the observed very small volume of metamorphic detritus found in Lower ORS basins with respect to the potential sediment yield.

5.7.3.4 Dominance of igneous clast types

Bluck (1984) points out that the provenance of the Lower ORS is dominated by volcanic and plutonic rock types rather than metamorphic basement clasts. This in itself is of little consequence to whether the local Dalradian made a sediment contribution, and is quite compatible with the proposed model which evokes widespread mixing of pre-existing gravels of metamorphic origin with volcanic and plutonic sediment generated during contemporaneous magmatism. It cannot be assumed therefore that the components within a polymict conglomerate have been through the same history of recycling. Mixing of polycyclic and first cycle volcanic sediment can be demonstrated within the basin of deposition (Chapter 2). The abundance of volcanic detritus points to widespread volcanic activity accompanying the docking of the terranes and the redistribution of sediment from remanent molasse basins. Lava flows interfinger with sediments in basins both on the Grampian Highlands terrane and within the Midland Valley. Blanketing of metamorphic basement and conglomerates by lavas in the source area may have been important in suppressing a sediment contribution from some source lithologies. In other cases, large influxes of volcanic material to the basins are accompanied by first-cycle metamorphic detritus indicating volcanic triggering of basement sources independent of the regional tectonic control of sediment dispersal.

5.7.3.5 Lack of metamorphic clasts of certain Dalradian type

Metamorphic clasts which are unequivocally of Dalradian type are not obvious components in Lower ORS conglomerates. As outlined above this is as much a function of the difficulty of removing the bias attendant on a repeated history of recycling as a demonstrable lack of such clast types. There is a danger of accepting only the obvious first cycle material like that dispersed to the top of the Upper ORS in the Firth of Clyde basin as the sole indicator of the structural proximity of the Grampian Highlands terrane to the Midland Valley. The potential for the generation of large volumes of first cycle material from metamorphic basement during the Lower ORS has been shown to be low, so that were the Grampian Highlands and Midland Valley terranes adjacent at this time (as is suggested by the more reliable granite clast data), first cycle metamorphic detritus cannot be expected to occur abundantly in the Midland Valley.

The clasts of metamorphic basement which do occur in the northerly derived conglomerates of the Crawton Basin are treated more fully in the following chapter. It is sufficient to state for the purpose of the present discussion however that the petrographic, chemical and isotopic character of the clasts is entirely compatible with a derivation from the adjacent Dalradian. However, if the Grampian Highlands terrane was adjacent to the Midland Valley the narrow range of lithologies, and restricted chemical and isotopic variability of the metamorphic clasts when compared to the in-situ Dalradian must be explained. Chlorite-grade greenschists are rare components in Lower ORS conglomerates of the Crawton Basin. They do however occur as first-cycle clasts in volcanic units. As the Lower ORS conglomerates are derived from existing conglomerates in the source terrane an explanation for the low diversity must be sought in the processes whereby these initial conglomerates were formed. If these conglomerates represent trapped proximal molasse, as outlined in the model above, they must have filled late basins developed towards the end of the history of uplift. As a result, the material found in these basins will be biased towards sediment generated in the latter stages of regional

uplift and consequently the upper levels of the orogenic pile, including the lower grade metamorphic zones and metamorphic rocks showing the oldest isotopic closure ages, will be poorly represented having already been unroofed and dispersed outwith the immediate confines of the metamorphic belt.

A second process operating to reduce the diversity of the metamorphic detritus reaching Lower ORS basins is the role of selective destruction of the less robust clast types during recycling. This accounts for the total lack of pelitic and semi-pelitic lithologies. This gives a false impression of the metamorphic grade of the terrane from which the clasts were derived as the assemblage of quartzites and psammites found in the conglomerates is relatively inert chemically, and cannot be expected to develop the full range of characteristic metamorphic index minerals. Chlorite, muscovite, epidote, biotite and rare garnet do occur in the psammitic clasts. Campbell (1929) records the occurrence of sillimanite and staurolite bearing gneissose clasts from the Garvock group. Destruction of pelitic lithologies might be expected to liberate diagnostic index minerals to the heavy mineral fraction of the fine sediment that accompanies the conglomerates. Indeed garnet forms the dominant non-opaque heavy mineral phase in northerly derived sands of the Crawton Basin. Braithwaite and Ali (1978) record the occurrence of staurolite as a heavy mineral from three localities in the Strathmore Group of the NE Midland Valley. Whilst heavy mineral populations are potentially of use in establishing lost components in the recycled conglomerates, the aggressive carbonate cements found abundantly in sandstones of the Crawton Basin preclude any quantitative assessment.

5.7.3.6 A Midland Valley metamorphic terrane ?

Bluck (1983,1984) raises the possibility of more than one source of metamorphic detritus associated with clastic successions developed towards the close of the Caledonian Orogeny. There is substantial evidence, both in conglomerate sequences in the southern part of the Midland Valley, and in xenolith suites, for the presence of a separate metamorphic terrane of as yet unknown affinities, lying to the south of the conventional boundary

between the ortho- and para-tectonic zones. Given the evidence for a metamorphic terrane in the Midland Valley, its participation in contributing sediment to the Lower ORS basins cannot be summarily dismissed. Indeed such a provenance may be an important element in the dispersal of sediment to fill Lower ORS basins along the Highland boundary in the western Midland Valley. Bluck (1984) demonstrates a northwesterly dispersal of conglomerates and sandstones from the basal 1km of the Lower ORS which unconformably overlies the Highland Border Complex in the area between Balmaha and Crieff.

In contrast, clasts of psammite and metaquartzite dispersed to the Crawton Basin cannot have been originally derived from a metamorphic source terrane within the Midland Valley. The geometry of dispersal within the basin requires that the recycled psammitic clasts have an original northerly provenance, as first cycle conglomerates dispersed northwards from the southern margin of the basin are dominated by clasts of granite, lithic arenite and greywacke. The absence of metaquartzite and psammite clasts in these southerly derived conglomerates which are demonstrably of first-cycle origin rules out models involving first-cycle derivation from an uplifting Midland Valley metamorphic block followed by returning of the resultant conglomerates southwards to fill Lower ORS basins (Wilson 1970, Morton 1976). The fact that the greywackes of southerly derivation have a petrography dominated by metamorphic detritus which isotopically shows no indication of derivation from the Dalradian does however emphasise the need to escape from the concept of a single all-embracing source of metamorphic detritus in the Scottish Caledonides (Chapter 6). At least three distinct metamorphic sources can be recognised; the Grampian Highlands, the Midland Valley, and the low grade Highland Border rock types. Whilst the Midland Valley cannot be a viable source for the psammitic detritus occurring in the Lower ORS of the Crawton Basin, the possibility remains that metamorphic detritus in the Lower ORS to the west may have a provenance in a Midland Valley metamorphic terrane. This would require a substantial change in the nature of Lower ORS basins along the regional strike.

5.7.3.7 Contrasting Lower ORS basins north and south of the Highland Boundary

Bluck (1984) notes the development of contrasting Lower ORS basins to the north and south of the Highland Boundary. South of the Highland Boundary Fault, in the area between Loch Lomond and Crieff, the basal Lower ORS lies in both faulted and unconformable contact with rocks of the Highland Border Complex. The north-westerly dispersal of the basal conglomerates requires the basin into which the conglomerates were originally dispersed to have extended some distance to the north-west. The basin axis therefore must have been situated to the north of the Highland Boundary Fault, assuming that the palaeocurrents which have largely been determined from cross-stratified sandstones which interfinger with the conglomerates do actually share the same dispersal as the conglomerates. (The sandstones replace the conglomerates when traced laterally in well exposed sections on Conic Hill so this seems a reasonable assumption.) The basin as it is developed south of the Highland Boundary Fault thus appears to have been truncated by subsequent displacements on the Highland Boundary which juxtapose the north-westerly dispersed quartzite-volcanic conglomerates of the Strathmore sequence against conglomerates of Lower ORS age developed in basins overlying the Dalradian. Lower ORS conglomerates north of the Highland Boundary Fault differ from those to the south in that the basal units contain abundant angular locally derived clasts of the underlying Dalradian schists, which on the basis of imbrication and cross-stratification are dispersed to the SE.

The magnitude of the displacement required on either the Highland Boundary Fault, or one of its precursors in the Highland Border Complex (see Bluck 1984), to affect a juxtaposition of the two contrasting Lower ORS sequences is a matter of some conjecture. Bluck (1984) submits the displacement may have been at `terrane scale` with a possible late Devonian docking of the Midland Valley and Grampian Highlands terranes. In the light of the evidence for late Silurian docking, more modest displacements are considered here. It may be that the disharmony in basin structure across the Highland Boundary reflects the different basement substrates on which the basin or basins developed and as

such may not imply a large degree of lateral separation. Comparisons of the compositions and dispersal of basal sequences either side of the Highland Boundary Fault might be expected to magnify local substrate effects as the initial fill to a basin is the most sensitive to local control by basin floor irregularities.

Little is known of the extent to which local basin floor lithological and topographical effects persist both vertically and laterally in the sediment fill to Lower ORS basins. Basins developed on Dalradian substrates tend to have a greater contribution of local material concentrated in the basal conglomerates and breccias than those floored by the Highland Border Complex. In both cases, the basal locally derived angular sediments are replaced up-sequence by a recycled metamorphic and igneous provenance. This suggests the contrast between the Lower ORS north and south of the Highland Boundary Fault has been exaggerated by differential initial subsidence mechanisms controlling the early development of basins floored by very different crustal materials. The contrast between the two sequences is eventually lost when they are traced away from the basal unconformity with their respective substrates.

5.7.3.8 Post late-Silurian uncoupling of the terrane boundary

Docking between the Grampian Highlands and Midland Valley terranes during the late Silurian required by the provenance of Lower ORS conglomerates in the NE Midland Valley is not inconsistent with the observations of Bluck (1984). A number of problems remain however, the possible role of the Midland Valley as a sediment source in the western Midland Valley being perhaps the most important. Accepting a late-Silurian docking, it is evident that the docking process failed to effectively couple the two terranes together, as the junction between the terranes remained an active lineament for over 100Ma subsequent to closure. This compounds the complexity of the sequences occurring close to the terrane boundary and may have been responsible for the aforementioned truncation of the Lower ORS in the western Midland Valley.

The abundant angular blocks of chlorite grade psammite occuring in volcaniclastic units intercalated with polycyclic conglomerates of northerly derivation attest to the former occurrence of widespread low grade psammitic rocks in the source terrane. These cannot have been derived from the adjacent Grampian Highlands terrane in its present configuration, as chlorite bearing metamorphic rocks are very poorly represented. Dewey and Shackleton (1984) and Bluck (1984) show that the Dalradian has been structurally truncated by the Highland Boundary Fault. If the granite clasts occurring in northerly derived conglomerates of the Dunnottar and Crawton Groups are in fact derived from the Grampian Highlands terrane, further structural truncation of the terrane must have occurred subsequent to deposition of the Lower ORS.

Uncoupling of the terrane boundary is also suggested by a fundamental change in the Devonian history of sedimentary basins occurring to the north and south of the boundary. The Middle ORS is absent in basins in the Midland Valley and in red-bed basins southwards to the edge of the ORS continent. This contrasts with the appearance of Middle ORS deposits, unconformably bound, in basins north of the terrane boundary and its probably strike extension in Ireland (Graham et al 1982). This implies that the junction between the Midland Valley and Grampian Highlands terranes acted as a zone of uncoupling during mid-Devonian tectonism.

Bluck (1980) describes a possible pull-apart origin for Upper ORS conglomerates and sandstones outcropping around the Firth of Clyde. The geometry of this late Devonian basin suggests its northwesterly extension is terminated by the present-day trace of the Highland Boundary Fault. Subsequent deformation appears to have partially dismembered the basin. The Firth of Clyde basin is interpreted as having formed close to a major transcurrent fault situated to the north of the basin. This may have been the terrane boundary during Upper Devonian times. During Hercynian deformation the terrane boundary was the site of substantial northwesterly downthrows allowing Carboniferous sediments to accumulate in basins floored by Dalradian rocks. The Highland

Boundary Fault (s.s.) appears to be a late feature recording a high angle reverse displacement between the adjacent terranes (Bluck 1984).

The poor coupling between the terranes reflected in the long history of reactivation and differential tectonics may reflect the very different character of the crustal blocks which were originally juxtaposed. The presence of old Archaean crust to the north and its absence to the south may be one of several features responsible for imparting a sufficiently distinct tectonophysical character to the docked terranes for each to retain a certain independence during subsequent regional deformation.

CHAPTER SIX

PROVENANCE OF SEDIMENTARY AND METASEDIMENTARY CLASTS IN CONGLOMERATES OF THE DUNNOTTAR AND CRAWTON GROUPS

6.1 INTRODUCTION

Sedimentary and metasedimentary lithologies make an important contribution to conglomerates dispersed from both the northern and southern margins of the Crawton Basin. Recycled conglomerates associated with the northern margin of the basin contain abundant metaquartzite and psammite clasts which show evidence of a complex history of polyphase deformation and metamorphism. Conglomerates sourced from the south are characterised by large volumes of greywacke and metagreywacke which superficially bear little resemblance to rocks at similar grade in the northerly derived conglomerates. These varied clasts merit further consideration for a number of reasons.

Firstly, given the evidence for a late Silurian docking between the Midland Valley and Grampian Highlands terranes outlined in the preceding chapter, the clasts of northerly derivation may have been derived ultimately from uplift following the Grampian Orogeny. Petrographic, geochemical and isotopic data are brought to bear on the provenance of these clasts in the following sections, with the emphasis on trying to distinguish whether metamorphic clasts of certain Dalradian origin were contributed to the Midland Valley. Identifying Dalradian molasse, albeit in recycled basins temporally removed from post-orogenic uplift, is important, not only in assessing the Siluro-Devonian terrane configuration, but in constraining models for the mechanism whereby crustal thickening during the Grampian Orogeny took place. Recent models for rapidly producing the very great crustal thickening indicated by PT estimates have favoured overthrusting of exotic terranes. Dewey and Shackleton (1984) propose a progressive northward obduction of a 15km ophiolite stack to generate the necessary thickening. If this was the operative mechanism, post-Grampian molasse should be characterised by abundant ophiolitic detritus. An ophiolitic contribution to molasse basins and to secondary basins to which the sediment is subsequently recycled should be easy to identify chemically, as the distinctive chemistry of ophiolitic rocks should be inherited to a greater or lesser extent by the sediments they source (Hiscott 1984).

A second aspect of the sedimentary and metasedimentary clasts requiring attention concerns the lithic arenite and metagreywacke clasts of southerly derivation. These clasts range from unmetamorphosed lithic arenites to quartz-veined chlorite grade metagreywackes (Plates 6.1,6.2). The apparent transition from unmetamorphosed sediments to lower greenschist facies suggests a substantial sediment pile in the conglomerate source drainage basin. Greywackes occur abundantly in the southern Midland Valley and the Southern Uplands but nowhere are greywackes at higher than prehnite-pumpellyite facies exposed. Oliver et al. (1984) propose that the seismological evidence presented by Hall et al.(1983) in favour of shallow continental basement beneath the Southern Uplands might also be explained by a transition to greenschist facies at depth. There is however independent evidence in favour of continental basement beneath the Southern Uplands and Longford-Down Massif in the form of gneissose xenoliths in Carboniferous volcanics (Upton et al. 1984) and quartzite bearing conglomerates derived from a metamorphic terrrane in the present position of the Southern Uplands (Bluck 1983).

Notwithstanding the equivocal evidence for lower greenschist facies metasediments at depth beneath the Southern Uplands, the lower greenschist facies greywackes occurring as clasts indicate metasediments of anomalously high grade were exposed at surface to the south of the Crawton Basin during the late Silurian. One possibility is that the clasts sample the southerly extension of the coarse fill to the Highland Border Complex marginal basin which is known to underlie the Lower ORS immediately south of the Highland Boundary Fault. The Highland Border Complex is known to be at lower greenschist facies (Ikin and Harmon 1983). If this is the case the greywackes may have inherited some of the characteristics of a metamorphic terrane other than the Dalradian, from which they were originally derived. The greywacke clasts can therefore be used to explore the possibility of metamorphic terranes other than the Grampian Highlands in the Scottish Caledonides.

The low grade metamorphism evident in the greywacke pile may also

PLATE 6.1 Weakly foliated angular clast of lower greenschist facies metagreywacke in south-easterly derived conglomerate at Kings Step (NO 843728). Lens cap 5cm.

PLATE 6.2 Coarse grained veined clast (35cm max. diameter) of microconglomerate in south-easterly derived conglomerates at Kings Step (NO 843728).

PLATE 6.3 Psammitic clast in northerly derived Lithosome 1 conglomerates at Whitehouse (NO 824705). Note characteristic spaced pressure solution cleavage. Lens cap 5cm.

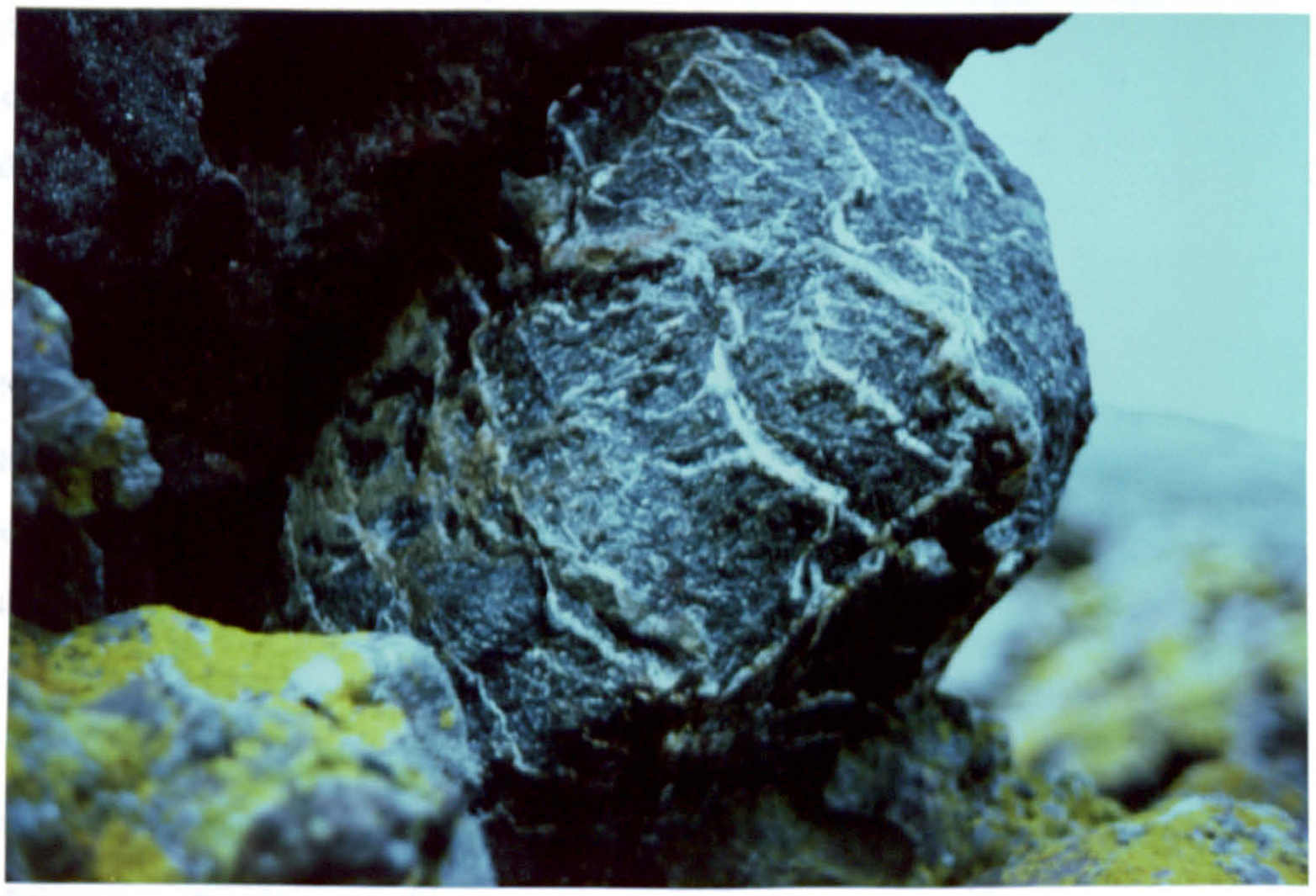

have important implications for low grade metamorphism seen elsewhere in the Highland Border Complex. Ikin and Harmon (1983) argue for a close assocation between the Highland Border Complex and the adjacent Southern Highlands during early Ordovician deformation and metamorphism. They correlate the two units solely on the basis of the similarity in stable isotopic compositions of the metamorphic fluids that the units exchanged with. This is clearly contradictory to stratigraphical and palaeontological evidence for an Ordovician age for much of the Highland Border Complex (Curry et al. 1984). If the clasts have been derived from a proximal equivalent to parts of the Highland Border Complex the indications are that greenschist facies metamorphism may have affected large tracts of northern Midland Valley and that this metamorphism was independent of and unconnected with the thermal history of the Grampian Highlands terrane.

The clasts of greywacke are also important as a sample of a substantial and yet unaccounted for sediment pile occurring within the Midland Valley. Many petrogenetic models for the petrogenesis of Caledonian granites and lavas appeal to a sedimentary component to account for their isotopic character (e.g. Thirlwall 1983, Halliday 1984). The Southern Uplands Ordovician and Silurian sediments, or SULPS (Southern Uplands Lower Palaeozoic Sediment) have been used as a standard sediment end-member for some time. The applicability of SULPS to rock petrogenesis ouside the Southern Uplands, as for example within the Midland Valley, is , given the probable allochthonous nature of the Southern Uplands, suspect. Incorporation of sedimentary material into magma source regions by subduction has been shown to be a viable mechanism whereby a sediment-derived component may be incorporated in orogenic magmas. If the Southern Uplands and Midland Valley were substantially separated, as is suggested by the anomalously small arc-trench gap (Bluck 1983) the sedimentary material preserved in the Southern Uplands accretionary prism may not be representative of sediment subducted beneath the Midland valley. Isotopically characterising the Midland Valley greywacke clasts is therefore important for an understanding of magmatism within the Midland Valley and the adjacent Highlands. The

importance to the latter rests on the possibility that Lower Palaeozoic crust was underthrust beneath the Highlands during Iapetus closure and may have contributed to the complex petrogenesis of Caledonian Granites south of the Mid-Grampian line (Halliday 1984).

A related problem is the provenance of SULPS itself. Given that the conventional derivation from the Highlands is untenable in the light of probable uncoupling along the Highland Border marginal basin, an alternative metamorphic source terrane is required. One possibility is that a Midland Valley plutonic-metamorphic terrane contributed sediment to both a fore-arc accretionary prism sequence to the south and a marginal basin to the north (Longman et al. 1979). A comparison of the isotopic character of the Midland Valley greywacke clasts and SULPS might throw light on whether Ordovician and Silurian flysch sequences were widely sourced from a single terrane or whether the Southern Uplands is truly exotic and sourced from a metamorphic source outwith the Scottish Caledonides.

6.2 FIELD RELATIONS

6.2.1 Northerly Derived Conglomerates

The polymict northerly derived conglomerates of the Dunnottar and Crawton Groups contain an abundance of metamorphic detritus in association with the diverse clasts of igneous origin considered in the previous chapter. The metamorphic contribution is notably mature and is dominated by metaquartzite and psammitic lithologies. Pelitic or semi-pelitic lithologies are absent. As a result, it is difficult to assess the metamorphic grade of much of the detritus as the development of index minerals (e.g. Al_2SiO_5 polymorphs) is suppressed in silica-rich psammitic and quartzitic rock-types. Psammites at chlorite grade can however be distinguished from those containing biotite and muscovite. The latter sometimes contain small garnets e.g. 3204 and probably represent a range of higher metamorphic grades. The former occur almost exclusively in volcaniclastic units and are of first cycle origin.

The distinction between psammitic and metaquartzite clasts appears to be an important one. A gradation between the two lithologies is not seen and the relative proportion of metaquartzite to psammite varies systematically. Metaquartzites are dominant in the lower part of the Dunnottar Group (Downie Point and Carlin Crag Formations) whilst psammitic clasts become more abundant in the granite enriched conglomerates higher in the sequence. In this respect the psammitic clasts show a sympathetic relationship with the abundance of granite clasts and share a similar provenance. This is borne out by a regional overview. The Lower ORS conglomerates of the western Midland Valley in which granite clasts are rare, are characterised by abundant metaquartzite detritus and only contain subdued proportions of psammitic type lithologies.

The metaquartzites range from very pure, white or buff coloured, recrystallised types, to impure lithologies characterised by scattered feldspars. Red weathered skins commonly occur on clast surfaces and serve to distinguish the psammitic clasts from the metaquartzites, as the former do not show this feature. The

metaquartzites are also invariably more well rounded, and more commonly occur as fractured and rerounded clasts. This indicates a longer history of recycling for the metaquartzite clasts, which must have been introduced to transient molasse basins sometime prior to the dispersal of the psammitic clasts to mix with the metaquartzite recycled gravels.

The psammitic clasts are distinguished from the clasts of metaquartzite by the development of chlorite or biotite, together with white mica. The phyllosilicates typically occur in well defined spaced pressure solution cleavage seams, although in many of the low grade rock types chlorite occurs as in intergranular phase with only a weak preferred orientation. The spaced cleavage is itself deformed by a number of ductile folds of varying style indicating a complex history of polydeformation (Plate 6.3). The psammitic clasts have not been as strongly recrystallised as the metaquartzites and relict greywacke textures and graded bedding are apparent in a number of clasts. Detrital feldspar grains are common and blue or lilac quartz grains almost ubiquitous. Blue quartz does not occur in the metaquartzite clasts, but this may in part reflect the strong recrystallisation affecting many of these clasts. Superficially, the psammitic clasts resemble the metagreywackes of the Southern Highland Group, which are also characterised by blue quartz.

6.2.2 Southerly Derived Conglomerates

The sedimentary and metasedimentary clasts occurring in conglomerates of the Crawton Group for which a southerly provenance has been established often dominate the clast assemblage, particularly in the finer grain size fractions. The clasts are readily classified in the field into three categories. These comprise :

1. A group of green weakly foliated, quartz-veined metagreywacke clasts of variable internal grain size ;
2. A subordinate suite of buff to brown coloured unfoliated sandstone clasts, texturally very similar to the green foliated clasts, but lacking quartz veining ;
3. A rare group of grey massive biotite hornfels clasts.

The clasts fall in the angular and sub-angular classes of Powers (1953) indicating that, unlike the clasts of northerly derivation, the conglomerates dispersed from the southern margin of the basin are first cycle in origin. The angularity of the clasts occurring in the southerly derived conglomerates exposed between Gourdon and Whistleberry also suggests that the basin margin from which the conglomerates were dispersed cannot have been situated any great distance to the south. This implies that the clasts represent a sample of material from a sediment sequence which occupied the east-central sector of the Midland Valley.

The clasts provide some constraints on the nature of the sediment sequence from which they were derived. The internal grainsize varies from pebble and micro-conglomerates to medium-grained sands. Although quartz-rich, blue quartz is absent. Sorting is typically poor. The presence of both unfoliated sandstones and weakly deformed low grade metasediments indicates a substantial thickness for the sediment sequence. Bed contacts are seen in some clasts, and graded bedding can frequently be discerned. Occasionally cross-lamination is developed in finer grained sandstone clasts. Coarser grained clasts typically have greywacke textures. Large clasts, in excess of 80cm, in which bed contacts are not observed, require that thick beds were developed in at least part of the sequence. No shale or siltstone clasts accompany the coarser grained sediment clasts suggesting that the sequence was dominated by medium and coarse sandstones.As the conglomerates in which the clasts occur are thought to be first cycle and proximal, the lack of finer grained lithologies is unlikely to reflect preferential destruction during transport and deposition.

From these observations a thick sequence of proximal (i.e. high sand to mud ratio, coarse grained), possibly turbiditic sandstones is inferred to have outcropped extensively directly to the south of the Crawton Basin during the late Silurian. These formed an important source of detritus shed northwards into the subsiding Crawton Basin, but this source was subsequently overstepped or strike-slipped out and buried following the

establishment of the extensive Strathmore Basin and the development of the Ochil-Sidlaw lava pile.

Sandstone clasts similar to those occurring in the southerly derived conglomerates of the Crawton Group also occur as a minor component in northerly derived conglomerates of both the Dunnottar and Crawton Groups (the Haggis Rock clasts of Campbell 1913). A clast of lithic arenite (3145) sampled from the northerly derived conglomerates exposed at Crawton is chemically indistinguishable from those of first-cycle southerly derivation. Significantly, the clasts which occur in the northerly derived units are invariably more well-rounded and are generally finer grained than those of first-cycle origin. This suggests that either the clasts travelled a further distance from the north or were returned southwards following limited mixing of material from both northerly and southerly provenance either prior to subsidence of the Crawton Basin (i.e. during an earlier phase of sediment dispersal across the terrane boundary that the basin overlies), or during basin filling itself. These two alternative models are illustrated in Figure 6.1. Granite clasts of southerly provenance can also be identified as a rare component in the conglomerates of northerly provenance.

(A) SOURCE MIXING IN PRECURSOR BASIN.

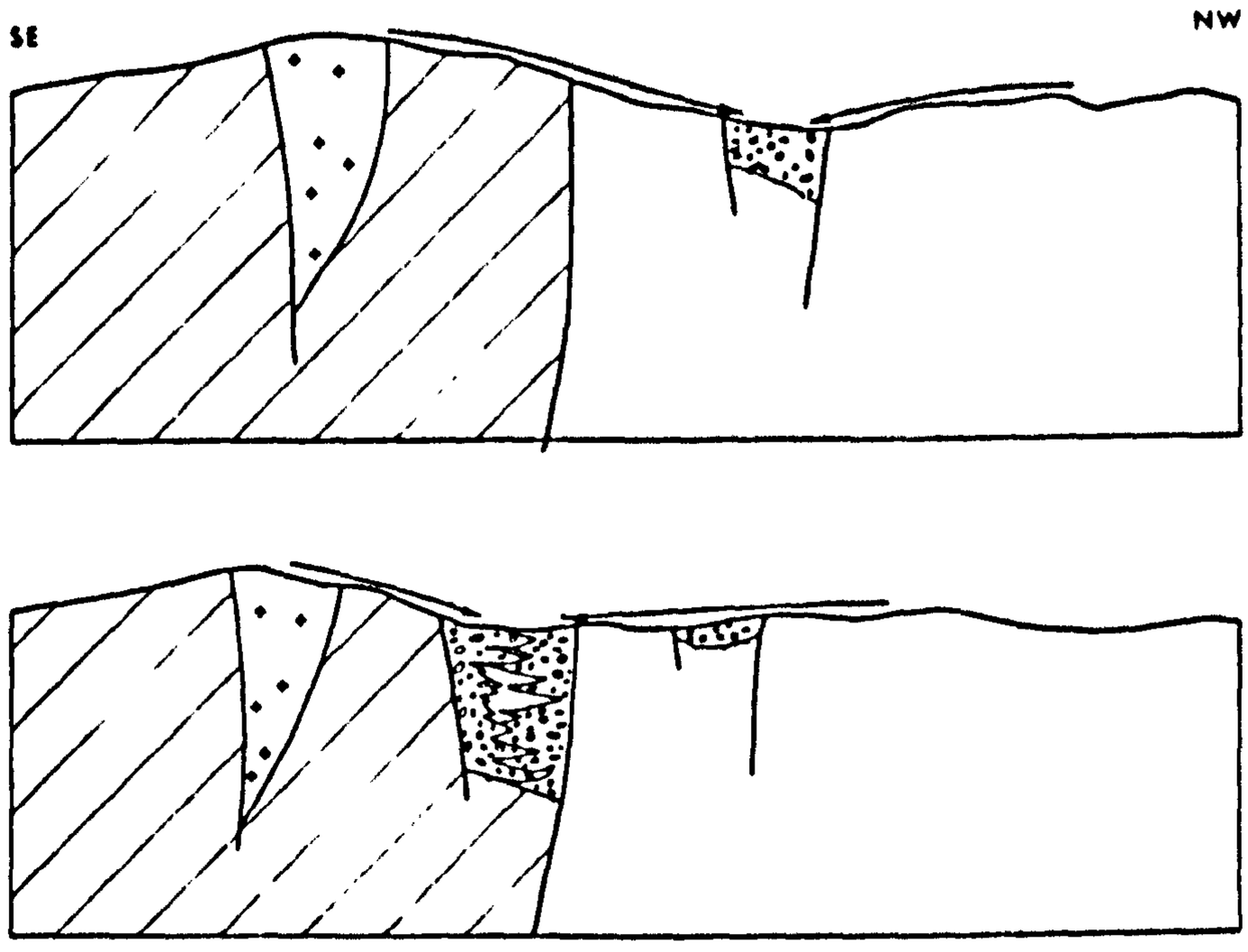

(B) INTRABASINAL SOURCE MIXING

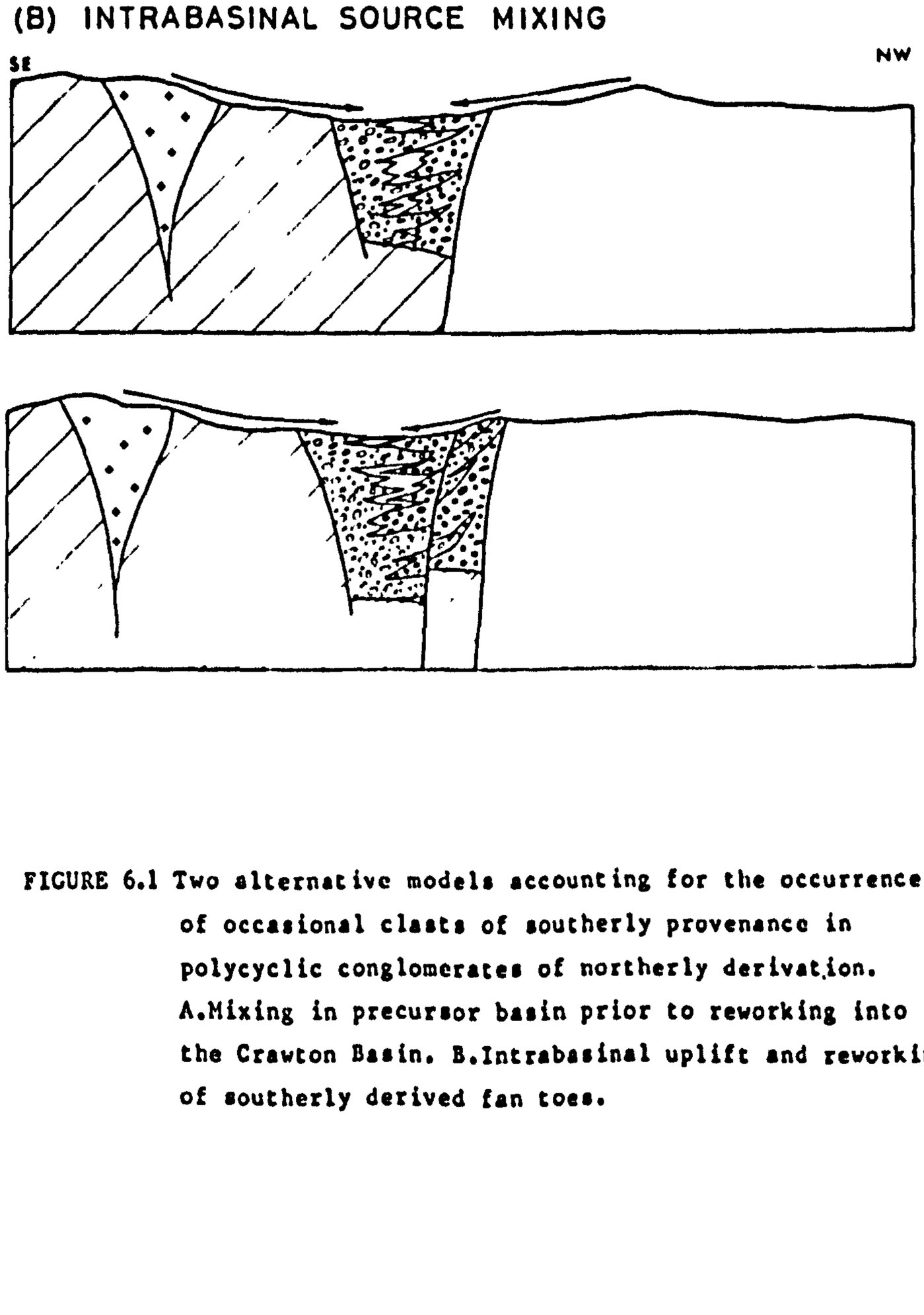

FIGURE 6.1 Two alternative models accounting for the occurrence of occasional clasts of southerly provenance in polycyclic conglomerates of northerly derivation. A.Mixing in precursor basin prior to reworking into the Crawton Basin. B.Intrabasinal uplift and reworking of southerly derived fan toes.

6.3 PETROGRAPHY

6.3.1 Northerly derived chlorite grade psammite (S1)

Clasts of lower greenschist facies psammite have been sampled from thick volcaniclastic units outcropping between Todhead Point and Kinneff (Fig. 4.2). These exposures have been assigned to the Crawton Group by previous workers (Campbell 1913, Armstrong and Paterson 1970), but they may in fact belong to the overlying Arbuthnott Group as indicated in Figs 1.5 and 4.2. This interpretation is favoured by the occurrence of rare clasts resembling the distinctive Crawton lavas in polycyclic conglomerates south of Todhead Point. Analogous chlorite grade psammite clasts do however occur in volcaniclastic units in less equivocal outcrops assigned to the Dunnottar and Crawton Groups.

In this section, the chlorite psammite clasts preserve much of their original detrital textures and are in many instances only weakly foliated. The pressure solution cleavage which characterises clasts at higher grade is notably absent. The original sedimentary protolith appears to have been a poorly sorted quartz rich sandstone with a greywacke texture. The internal grainsize of individual clasts is highly variable, with detrital grains reaching 5mm. Grains of monocrystalline and polycrystalline quartz, feldspar, opaques and quartzo-feldspathic composite grains typically float in a recrystallised matrix of chlorite, white mica and granulated quartz. The largest grains tend to be composite quartz grains which are unusally well rounded. Both mono- and polycrystalline quartz grains typically have strong undulose extinction. Grain boundaries in polycrystalline quartz grains are invariably either granulated or sutured. Attendent elongation of sub-grains produce fabrics which are discordant to any preferred orientation over the psammite clast as a whole.

Feldspar occurs as both single grains and as coarse grained quartzo-feldspathic composite grains, accounting for 10-15% of the overall total. The feldspar is dominantly an albitic plagioclase. Minor perthitic grains are also encountered. Grain outlines tend to be angular and in some cases corroded by the

matrix. Many are fresh and have well developed lamellar twinning. The feldspars tend to be either equant in shape or elongated in a direction normal to the orientation of albite-law twinning. Deformed twinning is seen in some grains whilst others show partial replacement by sericite. Patchy or total recrystallisation, particularly of the larger feldspar grains, is seen in some clasts.

6.3.2 Northerly derived biotite psammite clasts (S2)

The biotite and higher grade psammite clasts occurring in northerly derived Lithosome 1 conglomerates resemble the chlorite psammites in sharing similar relict textures and in containing blue quartz and obvious feldspars. A pervasive spaced pressure solution cleavage is however widely developed, and the clasts were clearly derived from a sequence which was not only originally at a higher metamorphic grade, but also more strongly deformed.

In thin section the S2 psammites are predominantly composed of quartz + albite + biotite + muscovite + opaques ± chlorite ± epidote ± zoisite ± garnet ± zircon. Original detrital textures are generally not discernable. Many of the clasts have a striped appearance, with interbanding of thin quartz-rich and mica-rich stripes. Much of the quartz has been strongly recrystallised. Elongate coarse grained sutured quartz mosaics (relict polycrystalline quartz grains) are frequently set in a matrix of fine grained recrystallised polygonal quartz. Little of the original plagioclase remains intact, with widespread recrystallisation. The micas are concentrated in thin pressure solution cleavage seams. Biotite is dominant and shows pale to dark green pleochroism. Biotites frequently have a bimodal orientation, both parallel to, and at high angle to the striping. Muscovite is finer grained than the accompanying biotite, and is orientated parallel to the striping. Chlorite partially replaces biotite in some clasts.

Subhedral to anhedral inclusion free garnet (up to 200μm) can be recognised as a minor constituent in rare psammite clasts. Other clasts are characterised by the development of epidote and

zoisite, the latter amounting to as much as 5% of the total in some instances (e.g. 3188). Rounded zircon grains occur widely.

6.3.3 Southerly derived sedimentary and metasedimentary clasts

Both metamorphosed and unmetamorphosed sedimentary clasts occur in southerly and easterly derived conglomerates. Superficially, the two groups of clasts share similar textures, quartz-rich compositions, and poor sorting. However in thin section the unmetamorphosed clasts show only minor matrix development and are therefore classified as lithic arenites. The metamorphosed clasts are characterised by the presence of a chlorite and white mica matrix in which the detrital grains are supported. This generally amounts to 10-15% of the total, and the clasts are accordingly termed metagreywackes.

Both the lithic arenite and metagreywacke clasts show a similar range of detrital components. Mono- and polycrystalline quartz dominate, with lithic fragments making up 10-25%. Detrital quartz grains have a range of morphologies. Angular monocrystalline grains with non-undulose extinction are most abundant, although polycrystalline and undulose extinction monocrystalline quartz grains are also well represented. Many composite grains show sutured grain boundaries and evidence for a high strain history. Chlorite inclusions within quartz grains are common. Other detrital mineral grains include microcline, orthoclase, perthite, plagioclase, muscovite, biotite, chlorite, epidote, garnet, calcite and zircon. The feldspars occur as fresh angular grains some of which are mildly sericitised. Perthite and sodic plagioclase dominate with orthoclase (often intergrown with quartz in granophyre fragments) and microcline less commonly encountered.

A wide range of lithic fragments are also present. Igneous fragments include granite, granophyre, quartz porphyry (Plate 6.4), feldspar porphyry, acid and basic volcanics, silicified volcanic rocks and basic hypabyssal types. Mafic phases within basic igneous rock fragments are largely made over to opaques. Metamorphic fragments include coarse grained gneiss, foliated chlorite psammite (Plates 6.5, 6.6), muscovite schist,

Plate 6.4 Acid porphyry and basic volcanic lithic fragments in southerly derived microconglomerate clast. Magnification X30. Cross-polarised light.

Plate 6.5 Fragment of foliated albite-chlorite-muscovite psammite in southerly derived microconglomerate clast. Magnification X30. Plane polarised light.

Plate 6.6 As above. Cross-polarised light.

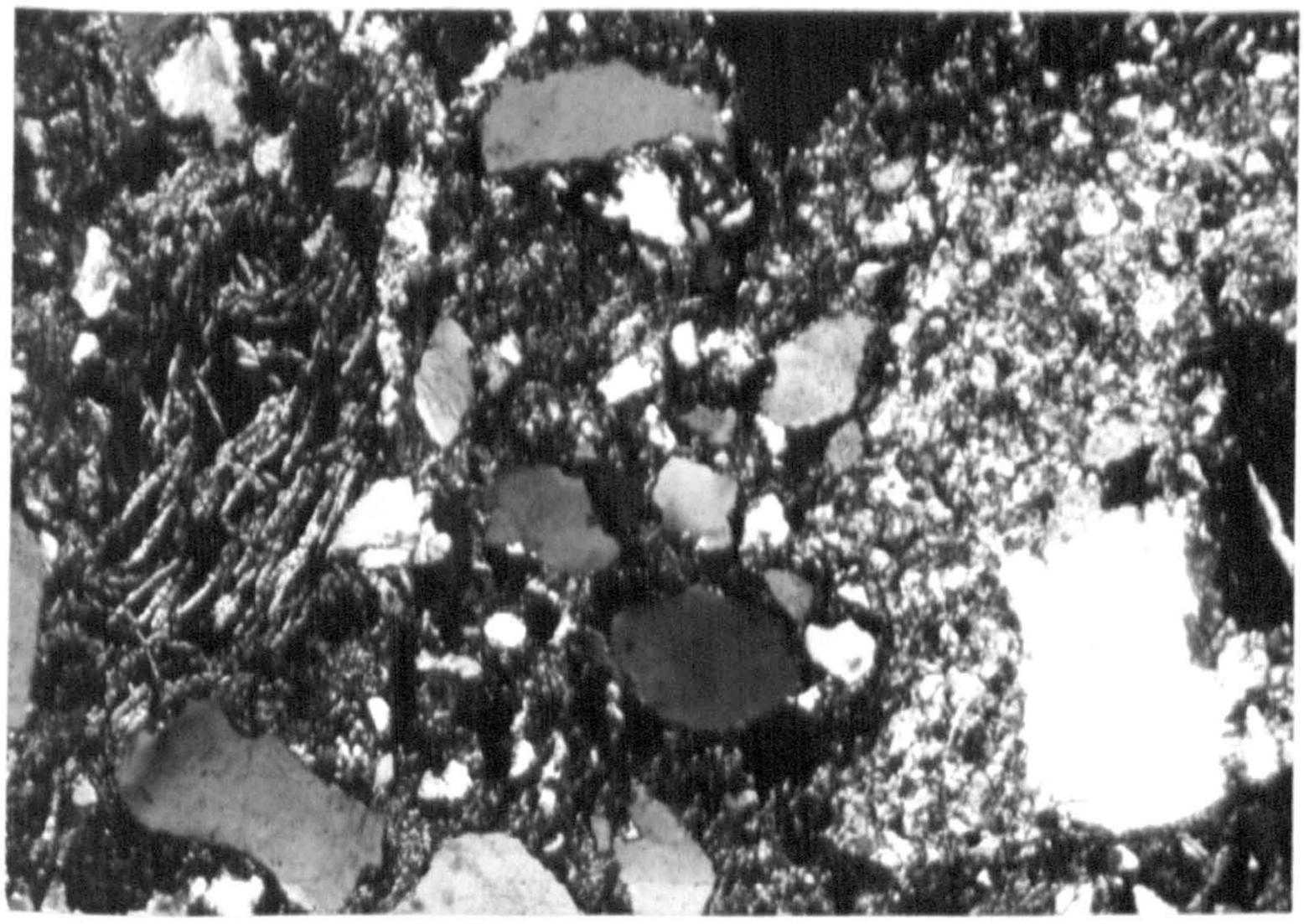

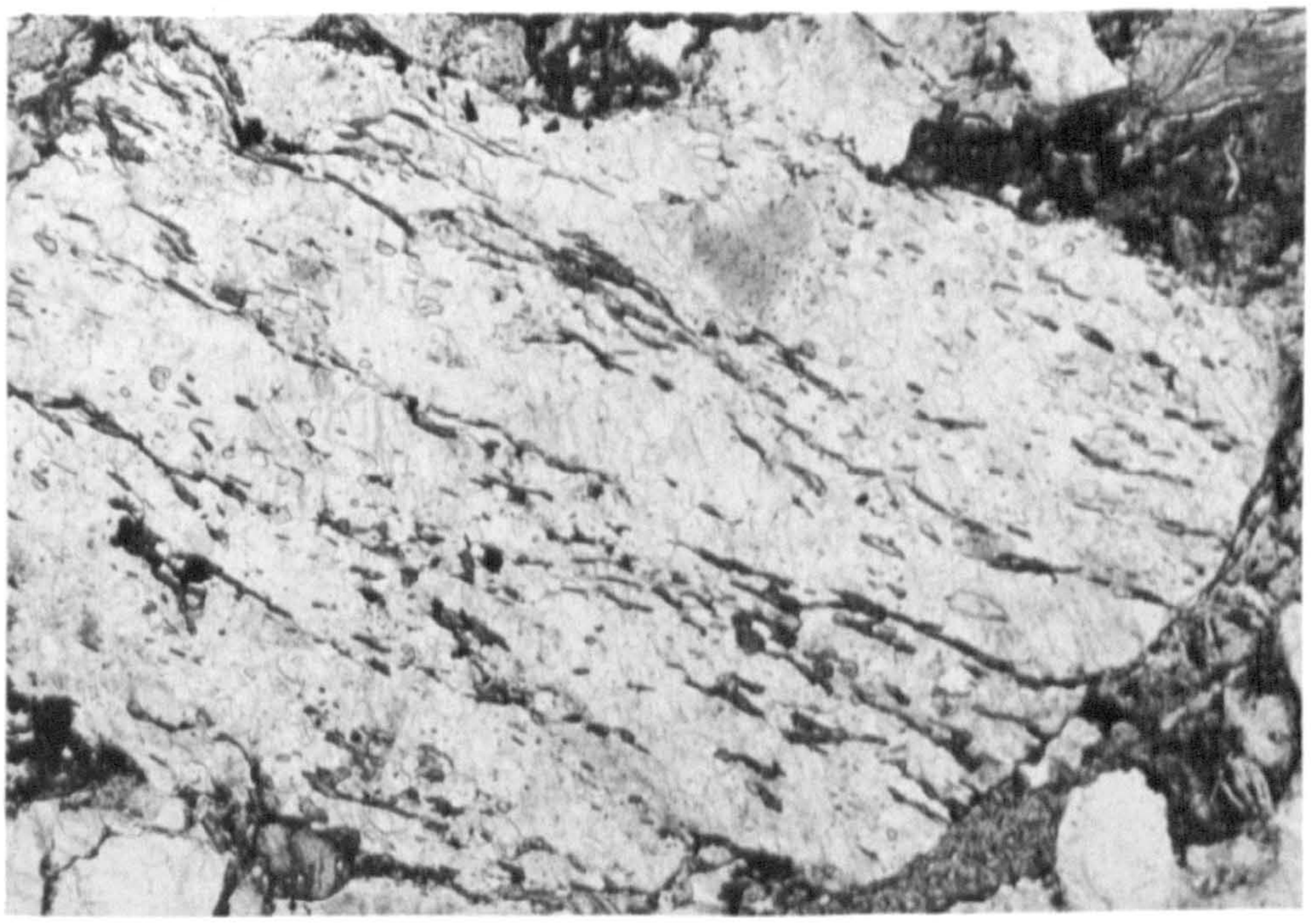

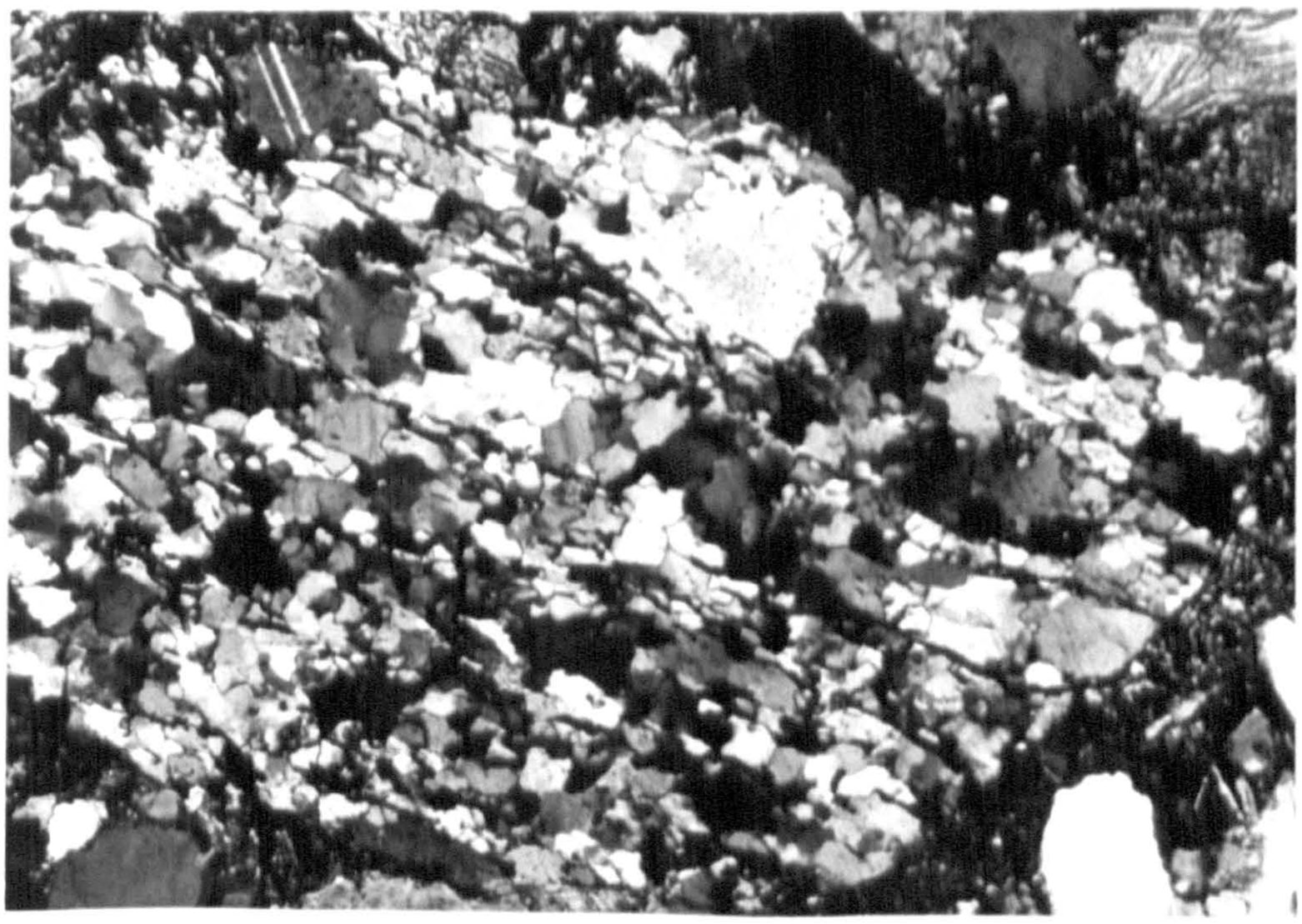

metaquartzite and epidosite (quartz-epidote rock). Some of the schist fragments show a crenulation cleavage. Fragments of sedimentary origin are also common and include shale, siltstone, greywacke, chert, quartz arenite, and red jasper.

The lithic arenite clasts are generally unfoliated, but do show evidence for overcompaction. The metagreywackes typically have weak to moderate grain alignment fabrics. Progressive replacement of the matrix by randomly orientated biotite is seen in a range of clasts which are interpreted as having been thermally overprinted by contact metamorphism.

6.4 SEDIMENTARY GEOCHEMISTRY

6.4.1 Rationale

Representative sedimentary and metasedimentary clasts from both northerly and southerly derived conglomerates have been analysed for both major and trace elements. The geochemistry was undertaken to explore several lines of enquiry in addition to the more general objectives in pursuing the provenance of the clasts outlined in 6.1 above.

Firstly the clast geochemistry addresses the problem of the affinity of the clasts with respect to sedimentary and metasedimentary sequences presently exposed close to the Lower ORS basin of deposition. The northerly derived granite clasts have been shown to closely resemble in-situ granite intrusions exposed in the adjacent Grampian Highlands terrane (5.7). If the granite clasts have indeed been derived from the Grampian Highland terrane, the accompanying psammitic clasts should have a Dalradian chemical signature.

A second and related problem is the relationship between the two clastic sequences sampled by the conglomerates. There are several possibilities. The two sequences may be part of the same sediment pile; one may have contributed or handed on sediment to the other; or they may be completely unrelated. Identifying the relationship between the two sequences places limits on the scale and significance of any crustal break which may underlie the Crawton Basin.

A third consideration is the possibility that the geochemistry of the metasedimentary and sedimentary clasts can be used to constrain the earlier history of the two terranes which were juxtaposed across the basin. Several recent studies (Crook 1974, Schwab 1975, Maynard *et al.* 1982, Bhatia 1983) suggest that the chemical composition of sandstone may be sensitive to the plate-tectonic environment in which the sands were originally deposited. It may be possible therefore to determine the tectonic setting in which the sequences which supply detritus to the Lower ORS were formed originally, allowing the early

evolution of the source terranes to be documented.

6.4.2 Results and Data Presentation

A total of 61 clasts have been analysed for both major and trace elements. These include 14 clasts of chlorite-bearing psammite sampled from volcaniclastic units exposed between Todhead Lighthouse and Whistleberry, 20 biotite psammite clasts from northerly derived conglomerates of both the Dunnottar and Crawton Groups, and 27 sedimentary and metasedimentary clasts of southerly provenance sampled from southerly derived conglomerates of the Crawton Group. Full analytical results are presented in Table 6.1.

6.4.3 Major Element Chemistry

6.4.3.1 Range and Origin of Chemical Diversity.

Some general and recurring features of the major element geochemistry of the clasts are usefully explored using the Al_2O_3 vs SiO_2 plot shown in Fig. 6.2a. Clasts from each of the three main suites sampled are distinguished. Each produce good linear arrays with negative slope. Whilst the strong correlation evident partly reflects closure to 100%, the offset between the clasts of northerly and southerly provenance suggests the operation of other factors. Both the chlorite-bearing and biotite-muscovite-(garnet) psammite clasts fall on a single linear trend, indicating the two northerly derived psammite clast suites are closely related. The three samples which plot off the linear trend defined by the combined psammite clast data either have anomalously high LOI values and high CaO contents indicating secondary alteration, or as in the case of 2117, have a distinctive petrography. The biotite psammites show a broadly comparable range of silica to those at chlorite grade, but whilst the former are skewed to the high SiO_2 end of the range the latter tend to have lower silica contents. This is emphasised in the histograms shown in Figure 6.3.

Clasts of greywacke and metagreywacke of southerly derivation plot with a more restricted distribution on the Al_2O_3 vs SiO_2 plot and are displaced to lower Al_2O_3 at constant SiO_2 than the combined field for the metasediments of northerly provenance.

SAMPLE	3145	4264	4255	4319	4271	4260	4261
GROUP	LA	LA	mG	mG	LA	mG	mG
MAJORS							
SiO_2	75.59	76.98	72.88	70.52	73.43	70.73	73.07
Al_2O_3	9.11	9.26	10.22	11.44	10.75	11.16	10.43
TiO_2	0.67	0.85	0.72	0.78	0.80	0.87	0.68
MnO	0.07	0.07	0.07	0.09	0.08	0.07	0.07
$(Fe_2O_3)^t$	4.76	5.05	5.59	6.71	5.59	6.00	5.17
MgO	2.38	2.26	3.79	3.90	3.69	3.18	3.73
CaO	1.73	0.60	0.28	0.71	0.59	0.64	0.52
Na_2O	1.91	1.79	2.89	3.16	2.15	2.80	2.78
K_2O	1.75	1.33	1.20	0.83	1.48	1.55	1.34
P_2O_5	0.11	0.11	0.11	0.10	0.10	0.13	0.10
LOI	2.69	2.40	2.57	2.65	2.77	2.64	2.72
FeO	nd	nd	nd	nd	nd	nd	nd
Fe_2O_3	nd	nd	nd	nd	nd	nd	nd
TOTAL	100.77	100.70	100.32	100.89	101.43	99.77	100.61
TRACES							
Cr	124	109	546	249	461	231	308
Co	17	11	15	20	17	13	18
Ni	60	30	114	66	104	75	126
Cu	10	11	7	13	9	7	9
Zn	57	61	70	86	80	80	72
Ga	13	10	13	12	13	14	13
Rb	59	48	49	32	59	56	53
Sr	67	78	57	101	57	60	54
Y	25	22	17	22	22	26	16
Zr	350	279	214	154	264	300	220
Ba	328	342	139	133	194	253	185
La	18	24	24	14	30	25	23
Ce	45	53	36	23	39	53	34
Pb	10	9	9	6	3	5	6
Th	9	6	6	1	6	7	7
U	3	2	4	2	3	2	2

TABLE 6.1 SEDIMENT AND METASEDIMENT CLASTS OF SOUTHERLY PROVENANCE. LA: LITHIC ARENITE, mG: METAGREYWACKE, H: BIOTITE HORNFELS.

SAMPLE	4460	4487	4479	4478	4484	4459	4483
GROUP	H	mG	mG	mG	LA	H	mG
MAJORS							
SiO_2	73.17	73.87	71.41	73.51	76.17	77.36	70.53
Al_2O_3	11.00	11.07	11.54	10.53	9.96	9.44	12.28
TiO_2	1.18	0.76	0.94	0.77	0.85	0.93	0.81
MnO	0.12	0.09	0.13	0.12	0.09	0.06	0.09
$(Fe_2O_3)^t$	5.67	5.30	6.23	5.44	5.25	4.83	5.87
MgO	2.40	2.57	3.52	3.49	2.31	2.30	2.93
CaO	1.46	0.70	0.90	1.13	1.16	1.26	0.76
Na_2O	1.85	2.07	2.15	2.27	1.85	1.36	2.29
K_2O	1.32	1.66	1.43	1.29	1.19	0.88	1.71
P_2O_5	0.12	0.10	0.10	0.09	0.10	0.09	0.11
LOI	1.71	2.57	2.81	2.19	2.58	nd	2.48
FeO	nd	nd	4.25	nd	nd	nd	nd
Fe_2O_3	nd	nd	1.50	nd	nd	nd	nd
TOTAL	100.00	100.76	100.68	100.83	101.51	98.51	99.86
TRACES							
Cr	142	138	494	683	107	125	141
Co	8	12	17	14	10	12	15
Ni	39	60	108	104	31	32	72
Cu	9	11	16	11	13	42	15
Zn	54	52	66	60	51	47	64
Ga	12	12	13	12	12	11	14
Rb	46	57	59	49	46	34	65
Sr	133	52	50	158	59	99	61
Y	34	24	25	21	24	29	26
Zr	565	223	301	228	274	308	224
Ba	429	213	270	154	272	244	276
La	41	29	9	17	20	14	6
Ce	70	57	26	36	36	38	22
Pb	10	2	3	8	9	16	4
Th	10	5	7	7	6	7	6
U	3	3	3	3	3	0	3

TABLE 6.1 (cont) SEDIMENT AND METASEDIMENT CLASTS OF SOUTHERLY PROVENANCE

SAMPLE	4481	4488	4490	4491	4492	4493	4494
GROUP	mG	LA	mG	LA	LA	H	mG
MAJORS							
SiO_2	70.91	76.72	73.76	74.48	70.51	74.23	70.85
Al_2O_3	11.18	9.36	11.16	10.44	11.75	10.85	11.40
TiO_2	0.84	0.84	0.77	0.91	0.63	0.91	0.79
MnO	0.10	0.09	0.07	0.07	0.06	0.07	0.06
$(Fe_2O_3)^t$	5.74	5.26	5.33	5.57	4.60	5.01	5.74
MgO	3.72	2.48	2.47	2.44	2.79	2.25	3.18
CaO	0.88	0.62	0.52	0.44	1.58	1.05	0.21
Na_2O	1.70	1.65	2.53	2.14	2.05	1.99	2.09
K_2O	1.82	1.07	1.61	1.22	2.27	1.46	1.79
P_2O_5	0.10	0.08	0.11	0.11	0.12	0.12	0.11
LOI	3.23	2.61	2.24	2.21	3.46	1.51	2.54
FeO	nd	nd	nd	nd	nd	nd	nd
Fe_2O_3	nd	nd	nd	nd	nd	nd	nd
TOTAL	100.22	100.78	100.57	100.03	99.82	99.45	98.76
TRACES							
Cr	487	nd	146	164	136	107	292
Co	16	nd	12	12	9	11	11
Ni	113	26	56	37	63	33	108
Cu	13	13	7	21	18	6	9
Zn	58	48	61	67	67	58	64
Ga	14	11	14	12	16	14	12
Rb	71	38	57	46	84	56	65
Sr	55	62	54	70	74	97	40
Y	22	22	23	21	24	20	19
Zr	257	271	241	314	203	259	249
Ba	381	nd	258	290	345	361	290
La	9	nd	14	18	30	12	14
Ce	17	nd	39	43	56	16	31
Pb	3	8	6	6	7	10	10
Th	8	7	4	5	5	8	7
U	2	3	2	2	1	2	7

TABLE 6.1 (cont) SEDIMENT AND METASEDIMENT CLASTS OF SOUTHERLY PROVENANCE

SAMPLE	4495	4496	4497	4498	4273	4238
GROUP	LA	mG	mG	II	LA	LA
MAJORS						
SiO_2	73.17	74.86	71.38	76.51	77.50	76.09
Al_2O_3	10.41	11.14	10.80	9.90	9.47	8.72
TiO_2	0.87	0.70	0.96	0.98	0.82	0.75
MnO	0.06	0.06	0.08	0.07	0.10	0.09
$(Fe_2O_3)^t$	5.77	4.66	6.37	4.68	4.96	5.42
MgO	3.42	2.13	3.44	1.84	2.10	2.76
CaO	0.43	0.36	0.79	1.19	0.39	1.11
Na_2O	2.65	2.59	1.74	1.96	2.41	2.25
K_2O	0.69	1.59	1.48	1.38	1.18	0.98
P_2O_5	0.13	0.11	0.12	0.12	0.11	0.09
LOI	2.62	1.90	2.84	1.16	2.12	2.26
FeO	nd	nd	nd	nd	nd	nd
Fe_2O_3	nd	nd	nd	nd	nd	nd
TOTAL	100.22	100.1	100.00	99.79	101.16	100.52
TRACES						
Cr	212	118	720	162	109	173
Co	13	8	15	11	11	14
Ni	71	47	94	25	31	43
Cu	15	5	7	9	9	9
Zn	64	56	68	51	62	64
Ga	14	13	14	10	11	9
Rb	29	61	57	54	43	29
Sr	89	60	57	126	76	87
Y	23	21	21	32	22	19
Zr	289	230	315	368	248	168
Ba	146	278	303	344	285	280
La	22	9	14	30	24	17
Ce	38	24	27	59	49	30
Pb	10	2	2	17	2	10
Th	5	6	7	7	4	0
U	3	3	3	3	1	2

TABLE 6.1 (cont) SEDIMENT AND METASEDIMENT CLASTS OF SOUTHERLY PROVENANCE

SAMPLE	2117	2125	2126	3139	3141	3144A	3149
GROUP	bP	bP	bP	bP	bP	bP	bP
MAJORS							
SiO_2	72.14	78.08	84.55	84.37	81.74	83.12	83.12
Al_2O_3	14.52	10.02	6.93	7.28	8.26	7.82	7.86
TiO_2	0.49	0.39	0.38	0.20	0.52	0.46	0.46
MnO	0.07	0.08	0.05	0.07	0.08	0.05	0.06
$(Fe_2O_3)^t$	2.97	2.84	2.16	2.03	3.37	2.93	2.78
MgO	0.77	1.24	0.54	0.43	0.82	1.05	1.08
CaO	1.27	1.70	1.35	1.71	1.06	1.20	1.14
Na_2O	6.25	3.09	1.71	2.52	2.03	2.16	2.36
K_2O	1.30	1.26	1.41	1.34	1.88	1.35	1.29
P_2O_5	0.08	0.06	0.06	0.03	0.04	0.06	0.05
LOI	nd	0.99	0.48	nd	nd	0.36	0.66
FeO	nd	nd	nd	nd	nd	nd	nd
Fe_2O_3	nd	nd	nd	nd	nd	nd	nd
TOTAL	99.86	99.75	99.62	99.98	99.80	100.56	100.86
TRACES							
Cr	76	76	24	32	66	66	65
Co	4	6	2	0	13	6	9
Ni	11	15	2	9	18	15	14
Cu	3	5	3	4	6	6	9
Zn	18	35	26	19	52	46	42
Ga	16	11	9	7	12	10	9
Rb	47	45	55	35	56	42	41
Sr	118	192	71	179	134	123	132
Y	15	11	14	8	11	9	10
Zr	286	193	263	154	235	236	261
Ba	235	399	232	330	471	423	373
La	11	12	7	7	22	19	17
Ce	42	29	27	32	35	32	34
Pb	9	8	4	5	9	9	13
Th	5	5	4	2	5	6	4
U	3	2	3	2	3	3	2

TABLE 6.1 (cont) PSAMMITIC CLASTS OF NORTHERLY PROVENANCE

cP: CHLORITE GRADE PSAMMITE

bP: BIOTITE AND HIGH GRADE PSAMMITE

SAMPLE	2163	3188	3190	3191	3192	3195	3196
GROUP	bP	bP	bP	bP	bP	bP	bP
MAJORS							
SiO_2	78.63	76.15	83.82	81.39	84.15	79.43	77.09
Al_2O_3	9.43	8.20	8.19	8.68	7.45	9.73	10.77
TiO_2	0.43	0.47	0.28	0.37	0.33	0.54	0.59
MnO	0.08	0.13	0.05	0.07	0.05	0.08	0.09
$(Fe_2O_3)^t$	2.74	2.64	2.15	2.63	2.18	2.80	3.93
MgO	1.75	0.62	0.68	1.28	0.41	0.76	1.41
CaO	1.82	6.01	1.13	1.46	1.16	1.14	2.89
Na_2O	3.36	2.39	2.97	2.72	2.67	3.51	1.96
K_2O	1.38	0.71	1.23	0.84	1.00	1.16	1.86
P_2O_5	0.05	0.04	0.05	0.03	0.02	0.05	0.06
LOI	0.28	3.89	0.56	0.77	0.62	1.12	nd
FeO	nd	nd	1.13	1.86	nd	nd	nd
Fe_2O_3	nd	nd	0.89	0.56	nd	nd	nd
TOTAL	99.95	101.25	100.98	100.03	100.04	100.32	100.65
TRACES							
Cr	69	48	38	65	36	59	71
Co	9	4	3	7	1	6	10
Ni	19	8	6	16	6	14	25
Cu	10	19	16	8	4	9	9
Zn	30	30	20	35	20	39	63
Ga	12	8	9	9	8	12	12
Rb	30	25	31	20	29	37	56
Sr	211	349	149	224	126	151	330
Y	11	18	11	10	11	16	12
Zr	230	225	182	237	233	361	241
Ba	519	207	508	403	278	585	709
La	12	25	12	14	9	15	14
Ce	32	51	30	35	35	40	45
Pb	9	12	6	9	9	12	16
Th	4	5	2	5	5	5	8
U	1	2	2	2	2	1	2

TABLE 6.1 (cont) PSAMMITE CLASTS OF NORTHERLY PROVENANCE

SAMPLE	3197	3201	3202	3204	3303	3150
GROUP	bP	bP	bP	bP	bP	bP
MAJORS						
SiO_2	82.64	81.39	79.04	80.27	75.46	75.76
Al_2O_3	7.95	9.34	9.70	9.91	11.27	11.35
TiO_2	0.48	0.30	0.58	0.42	0.60	0.73
MnO	0.03	0.09	0.09	0.12	0.08	0.07
$(Fe_2O_3)^t$	2.74	2.58	3.30	2.99	4.60	4.30
MgO	0.54	0.62	0.66	1.07	1.26	1.35
CaO	1.01	1.31	1.57	1.57	1.36	1.59
Na_2O	2.46	3.17	3.07	3.41	2.91	3.31
K_2O	1.52	1.55	1.25	0.73	1.50	1.62
P_2O_5	0.04	0.04	0.07	0.04	0.05	0.03
LOI	0.93	1.20	0.74	nd	1.02	0.61
FeO	nd	nd	nd	1.93	nd	2.28
Fe_2O_3	nd	nd	nd	0.84	nd	1.76
TOTAL	100.34	101.59	100.07	100.61	100.01	100.46
TRACES						
Cr	31	69	46	13	71	65
Co	4	2	7	9	8	14
Ni	7	11	10	35	18	15
Cu	10	2	8	10	0	10
Zn	23	31	33	35	54	46
Ga	9	11	12	10	14	14
Rb	45	44	45	25	57	53
Sr	107	193	184	269	139	158
Y	12	9	16	10	10	13
Zr	257	174	316	239	222	265
Ba	634	458	403	202	591	490
La	18	12	13	13	19	18
Ce	38	26	53	43	35	36
Pb	13	9	10	10	3	6
Th	8	0	7	4	2	6
U	2	1	3	2	1	3

TABLE 6.1 (cont) PSAMMITE CLASTS OF NORTHERLY PROVENANCE

SAMPLE	4405	4406	4407	4417	4418	4419	4420B
GROUP	cP	cP	cP	cP	cP	cP	cP
MAJORS							
SiO_2	74.41	76.10	75.66	75.70	84.74	71.71	76.72
Al_2O_3	11.66	10.63	9.26	10.97	7.49	12.15	10.67
TiO_2	0.67	0.63	0.58	0.61	0.39	1.06	0.63
MnO	0.08	0.07	0.07	0.07	0.05	0.07	0.07
$(Fe_2O_3)^t$	4.36	3.49	3.40	3.81	2.11	5.44	4.37
MgO	1.80	1.43	1.45	1.90	1.07	2.01	1.69
CaO	0.76	0.56	2.68	0.45	0.39	1.16	0.45
Na_2O	2.51	2.24	1.90	2.25	1.92	1.94	2.52
K_2O	2.11	2.14	1.43	1.93	0.93	2.14	1.14
P_2O_5	0.05	0.03	0.93	0.06	0.03	0.07	0.04
LOI	2.16	1.52	2.32	1.39	1.41	2.13	1.60
FeO	nd	nd	nd	nd	nd	nd	nd
Fe_2O_3	nd	nd	nd	nd	nd	nd	nd
TOTAL	100.57	98.84	99.68	99.14	100.53	99.88	99.90
TRACES							
Cr	63	50	55	58	35	67	92
Co	10	8	6	8	0	11	5
Ni	18	13	9	17	3	23	16
Cu	3	2	0	4	0	1	10
Zn	48	40	32	54	17	73	58
Ga	14	12	10	13	7	16	10
Rb	71	64	53	66	32	76	34
Sr	78	66	118	80	53	80	66
Y	8	7	11	10	7	14	8
Zr	238	232	306	253	201	274	230
Ba	602	616	403	693	356	528	342
La	15	18	15	19	9	13	15
Ce	28	36	38	34	18	33	31
Pb	4	3	1	3	0	4	3
Th	5	4	5	4	2	6	7
U	1	2	3	3	2	2	1

TABLE 6.1 (cont) PSAMMITE CLASTS OF NORTHERLY PROVENANCE

SAMPLE	4408	4409	4410	4412	4413	4415	4416
GROUP	cP	cP	cP	cP	cP	cP	cP
MAJORS							
SiO_2	68.64	80.76	73.56	73.03	75.15	82.86	85.13
Al_2O_3	13.23	8.41	12.39	11.83	11.71	8.50	7.39
TiO_2	0.83	0.48	0.71	0.73	0.61	0.43	0.23
MnO	0.09	0.06	0.08	0.07	0.07	0.04	0.03
$(Fe_2O_3)^t$	5.93	2.27	4.22	4.30	4.41	2.44	1.17
MgO	2.16	1.17	1.98	1.69	1.71	1.17	0.84
CaO	1.02	1.32	0.15	0.84	0.26	0.61	0.42
Na_2O	2.50	2.84	2.75	2.58	2.72	1.75	2.05
K_2O	1.67	0.62	1.74	1.92	1.65	1.26	1.23
P_2O_5	0.06	0.03	0.05	0.05	0.03	0.24	0.01
LOI	3.15	1.60	2.05	2.03	1.76	1.60	1.33
FeO	nd	nd	nd	nd	nd	nd	nd
Fe_2O_3	nd	nd	nd	nd	nd	nd	nd
TOTAL	99.28	99.56	99.68	99.07	100.08	100.90	99.83
TRACES							
Cr	71	57	67	70	63	43	23
Co	12	2	9	6	6	2	nd
Ni	25	5	21	17	19	6	0
Cu	3	2	0	4	3	2	4
Zn	75	24	56	47	48	20	94
Ga	15	8	13	14	14	9	6
Rb	59	24	67	68	57	44	33
Sr	72	68	74	108	69	71	75
Y	10	8	4	8	7	10	5
Zr	249	222	228	294	245	232	141
Ba	454	171	448	553	547	608	453
La	13	16	14	16	3	12	12
Ce	31	35	18	34	18	30	24
Pb	3	5	3	4	3	4	4
Th	7	4	3	8	5	2	5
U	3	2	2	4	4	2	1

TABLE 6.1 (cont) PSAMMITE CLASTS OF NORTHERLY PROVENANCE

FIGURE 6.2 (a)Al_2O_3 vs SiO_2 plot for sedimentary and metasedimentary clasts of both northerly and southerly provenance. Symbols used on this and subsequent plots are:

Northern provenance

- ● biotite and higher grade psammite
- ⊖ chlorite grade psammite
- ⊘ altered chlorite grade psammite clast(high CaO,LOI)
- ▲ microconglomerate clast (2117)

Southern provenance

- □ undeformed lithic and quartz arenite
- ▨ altered lithic arenite clast (high LOI)
- ■ foliated quartz-veined chlorite bearing meta-greywacke
- ◪ biotite hornfels

(b)Plot of log (Na_2O/K_2O) vs log (SiO_2/Al_2O_3) after Pettijohn <u>et al.</u> (1972).

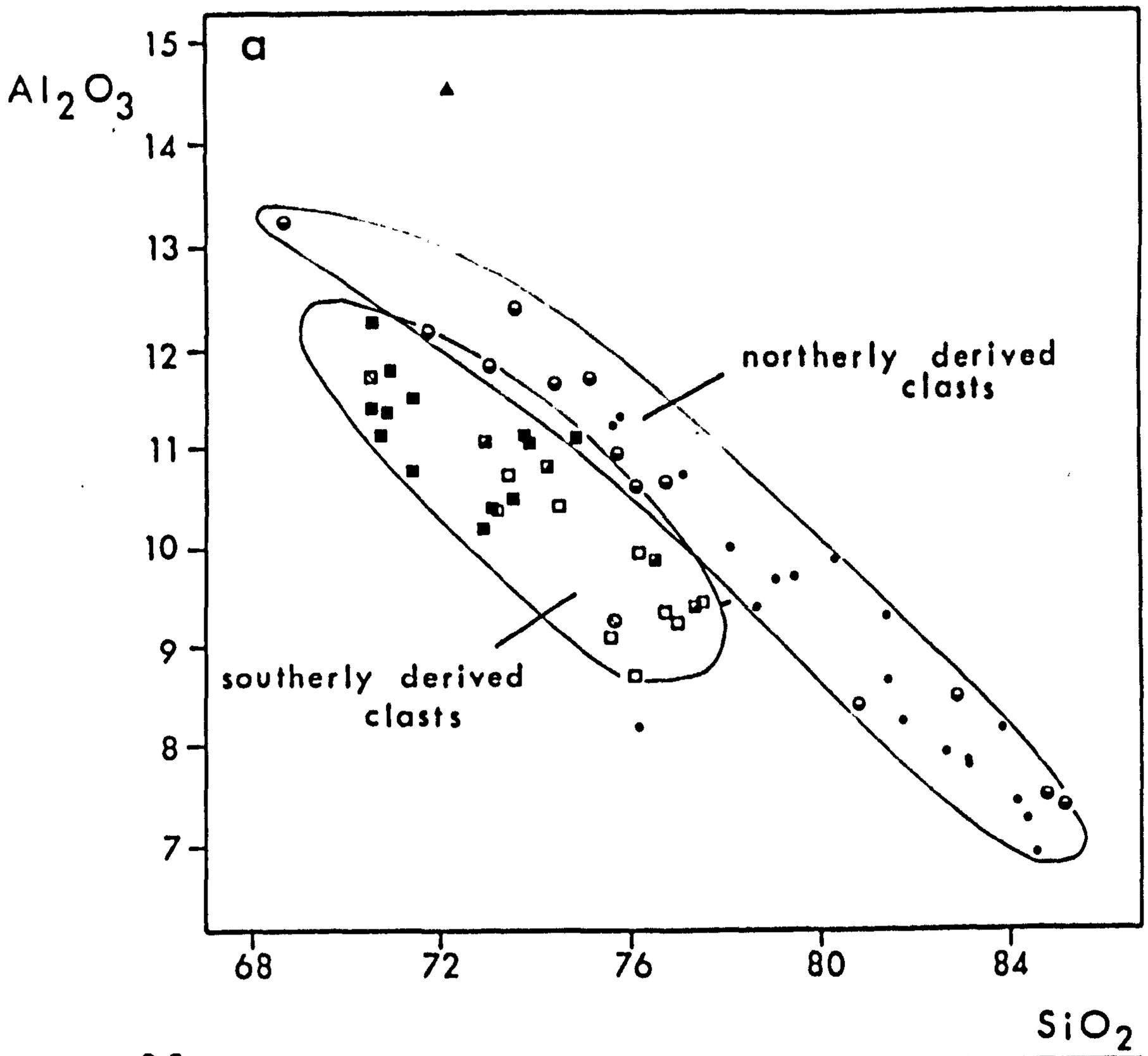
a
Al_2O_3
15
14
13
12
11
10
9
8
7
northerly derived clasts
southerly derived clasts
68
72
76
80
84
SiO_2

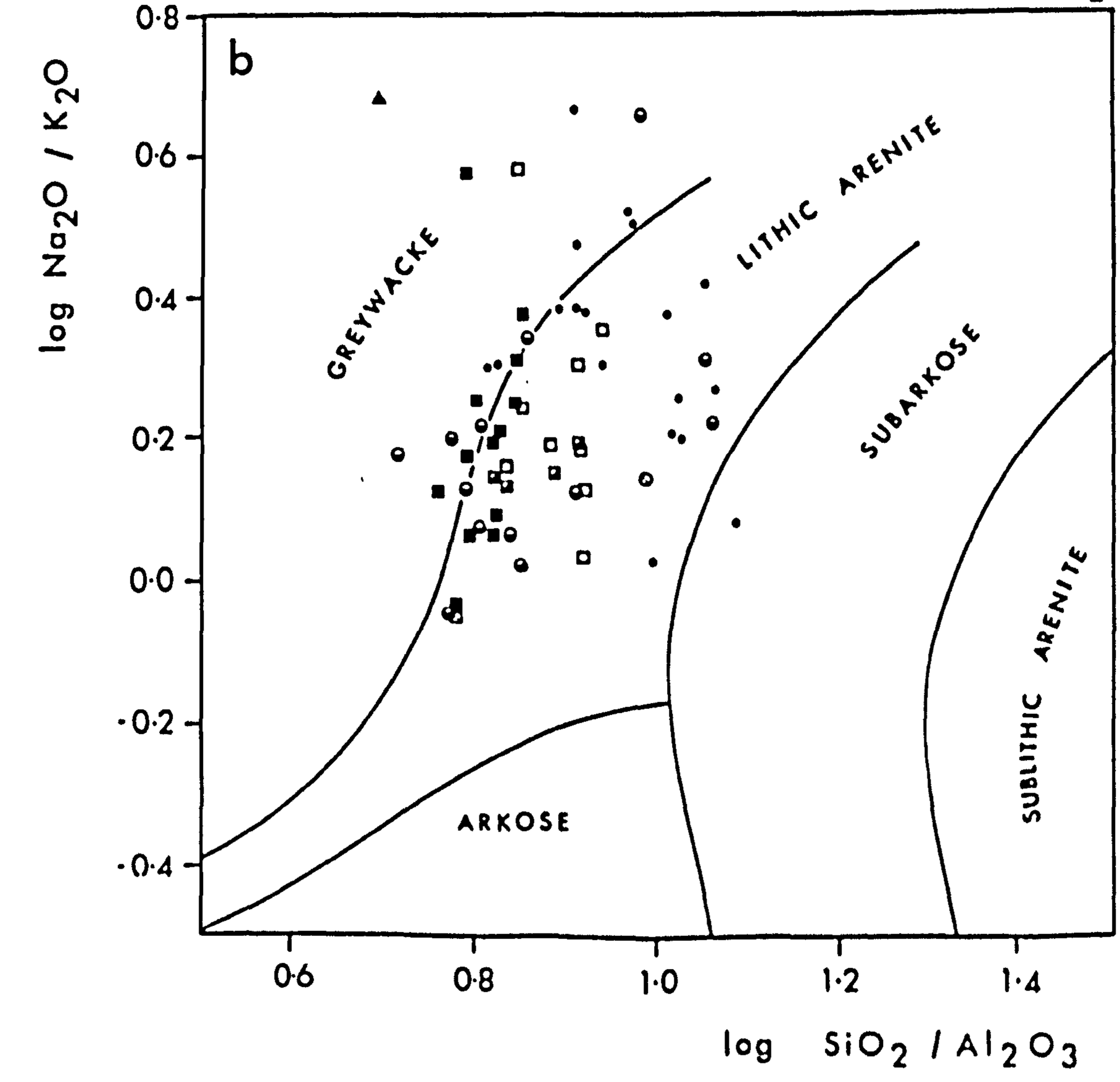
b
log Na_2O / K_2O
0·8
0·6
0·4
0·2
0·0
-0·2
-0·4
GREYWACKE
LITHIC ARENITE
SUBARKOSE
SUBLITHIC ARENITE
ARKOSE
0·6
0·8
1·0
1·2
1·4
log SiO_2 / Al_2O_3

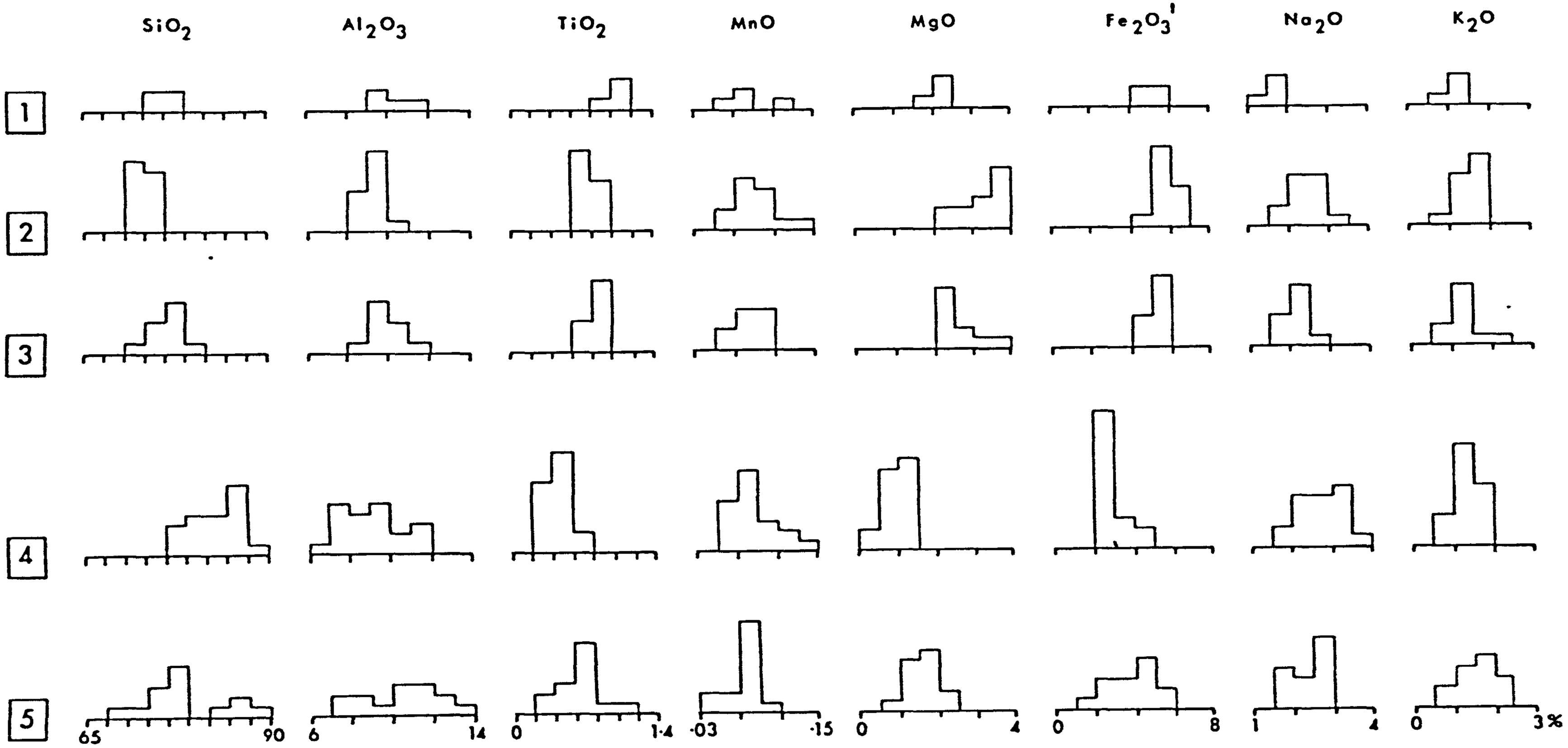

FIGURE 6.3 Comparative histograms of major element distributions in various sedimentary and metasedimentary clasts of northerly and southerly provenance. Groups are (1) hornfels clasts (2) metagreywacke clasts (3) lithic arenite clasts (4) biotite and higher grade psammitic clasts and (5) chlorite grade psammitic clasts.

	BIOTITE PSAMMITE n = 19		CHLORITE PSAMMITE n = 14		BEN LEDI GRIT[b] n = 20	
	$\bar{x}$	σ	$\bar{x}$	σ	$\bar{x}$	σ
SiO_2	80.54	3.06	76.73	4.91	76.02	7.19
Al_2O_3	8.95	1.34	10.45	1.90	10.87	2.93
TiO_2	0.45	0.13	0.61	0.20	0.42	0.18
MnO	0.07	0.2	0.07	0.02	0.03	0.02
$(Fe_2O_3)^t$	2.93	0.71	3.69	1.32	4.20	2.25
MgO	0.93	0.38	1.58	0.40	1.15	0.89
CaO	1.69	1.13	0.79	0.64	0.83	1.16
Na_2O	2.72	0.53	2.32	0.36	2.93	1.07
K_2O	1.31	0.33	1.56	0.48	1.67	0.92
P_2O_5	0.05	0.01	0.12	0.24		
LOI	0.95	0.86[a]	1.86	0.49		
TOTAL	100.59		99.78			
Cr	53.2	18.9	58.1	16.9		
Co	6.3	3.9	6.5	3.6		
Ni	13.8	7.6	13.7	7.8		
Cu	7.8	4.6	2.7	2.5		
Zn	35.7	12.3	49.0	22.0		
Ga	10.4	2.0	11.5	3.1		
Rb	40.6	11.7	53.4	16.9		
Sr	180.0	72.2	77.0	16.9		
Y	11.7	2.6	8.4	2.5		
Zr	238.1	47.3	238.9	39.9		
Ba	432.4	143.2	483.8	137.4		
La	13.6	6.0	19.7	8.0		
Ce	36.2	7.4	29.1	7.0		
Pb	9.05	3.3	3.1	1.3		
Th	4.6	2.1	4.2	1.3		
U	2.01	0.75	2.29	1.0		

a: n=15

b: from Bowes and Convery 1966.

Table 6.2 Comparison of average chlorite and biotite grade psammite compositions.

The discrimination between the two fields is almost complete. The relative enrichment of Al_2O_3 in clasts of northerly provenance is most easily explained by a combination of original source compositional effects and possibly a greater importance for chemical weathering during the pre-depositional history of the sediment which was to make up the thick northerly metasedimentary succession.

The distribution of Al_2O_3 against SiO_2 demonstrates that a considerable but systematic variation in composition can occur in samples thought to share the same provenance, giving rise to linear trends on variation diagrams. Variation in grain-size is probably the most effective mechanism whereby sediment compositional diversity is enhanced. The role of grain size in determining sediment composition has been appreciated for some time in quantitative petrographic studies of sediments. As sediments are often mixtures of many different grain populations, each with their unique size-frequency characteristics, different size fractions may show radically different compositions. The large compositional range of the northerly derived clasts, compared with that for clasts derived from the south, almost certainly in part reflects the wider range of grain sizes present in the former. SiO_2 contents in the chlorite grade psammites of northerly derivation show a progressive increase as the grain size varies from medium to very coarse sand, reflecting the concentration of detrital feldspar in the finer grained sandstones. Although strong recrystallisation has affected many of the biotite psammites, the original detrital grains that can be recognised suggest grain-size alone cannot explain the generally higher SiO_2 contents relative to the chlorite-bearing psammites. The restricted range of compositions observed in the southerly derived clasts is probably a function at least in part of the uniformity of grain size of the analysed clasts which are predominantly medium-grained sandstones.

Within the clasts of southerly provenance there is a systematic compositional difference between the unmetamorphosed clasts and those at lower greenschist facies. The latter consistently plot with lower SiO_2 than the former. There is therefore a consistent

compositional separation of clasts at different metamorphic grades along the linear trends for both northerly and southerly derived clast suites. This suggests that either some form of limited metamorphic reconstitution has taken place or that the metamorphism is overprinting an original compositional gradient. Many studies have shown metamorphism to be a largely isochemical process with little change in the major elements beyond loss of volatiles (Shaw 1954 a,b, 1956, Condie 1967a, Atherton and Brotherton 1982). The latter is therefore more likely to be the case.

As regional metamorphism is a depth related phenomenon, it is quite possible that metamorphic isograds may be superimposed on existing depth-related compositional variation. Atherton and Brotherton (1982), in concluding that metasomatic mechanisms are unnecessary to account for compositional variation between the Barrovian metamorphic zones of the Scottish Dalradian , point out that the isograds tend to parallel the stratigraphy as the major nappe structure is parallel to the original depositional basin, and to the thermal structure of the orogen. As the Dalradian basin shows an upward trend towards less mature sediment with time, it is the youngest and least mature fill to the basin which is most likely to undergo the lowest grade of metamorphism. This may be of some relevance to the compositional variation between the chlorite and biotite-psammite clasts noted above. It is the lower grade clasts which compositionally appear to be the least mature and it is feasible that this reflects an original maturity related compositional gradient in the basin fill prior to metamorphism. Whilst silica loss may accompany the development of pressure solution cleavage, this cannot account for the observed trends, as the biotite psammites which show the strongest cleavage development tend to be the more silicic.

Whilst there is evidence for significant compositional variation between the unmetamorphosed sandstone and the metagreywacke clasts of southerly provenance, the lower SiO_2 contents of the latter may reflect SiO_2 loss during vein segregation. Quartz veins traverse many clasts of metagreywacke but are absent in the unmetamorphosed clasts. The veins are typically parallel walled

with extension directions normal to the vein orientation, and both blocky and microcrystalline quartz fills. Clastic quartz grains in clasts of veined metagreywacke tend to have corroded margins indicating silica was mobilised during the development of a weak penetrative grain alignment fabric. It is possible therefore that the source of the silica filling the quartz veins was not exotic, but came from mild silica dissolution attending grain corrosion. As the samples of metagreywacke selected for chemical analysis were chosen so as to avoid vein material, this may partly account for the depletion in SiO_2 in these clasts with respect to the unveined lithic arenites. Veined clasts are relatively uncommon amongst the metamorphic detritus of northerly provenance, as are vein quartz clasts, indicating a more ductile history of deformation.

Accepting the possibility that the variation in chemical composition of the southerly derived clasts may have been partly enhanced by silica loss during vein segregation, the component of variation relating to the original detrital composition may well be smaller than indicated in Fig.6.2a. This would make the compositional range, already narrow, even more restricted, amplifying the contrast with the rather wide range of compositions established for the clasts of northerly provenance. Whilst this may largely reflect the range of grain size variations in the clast sampled (see above), the remarkable constancy of the clast compositions, in clasts which have been sampled fron conglomerate units separated both laterally and vertically within the Crawton Group, points to the sediment sequence from which the clasts were derived being very well homogenised.

As the lithic arenite and metagreywacke clasts contain detrital volcanic grains they should chemically be very sensitive to any concentration of the volcanic component. The homogeneous compositions argue against a contemporaneous volcanic source during deposition of the thick sequence from which the clasts were derived as this would be expected to produce episodic addition of volcanic material and rather poorly homogenised greywacke sequences. A remanent volcanic source is therefore

favoured.

6.4.3.2 Alkali Distribution

The alkali elements are particularly useful parameters in characterising the chemical composition of sedimentary rocks. The ratio of potassium to sodium has been used extensively in both discriminating tectonic setting (Crook 1974, Maynard et al. 1982, Bhatia 1983) and in attempting to merge chemical and petrological classifications of sedimentary rock (Pettijohn et al. 1972, Blatt et al. 1980). An example of the latter is shown in Figure 6.2b where following Pettijohn et al. (1972) the log ratio (Na_2O/K_2O) is plotted against the log ratio (SiO_2/Al_2O_3). The samples cluster on the boundary between the greywacke and lithic-arenite fields and apart from the displacement of the biotite psammites (S2) towards the lithic arenite field, there is little systematic variation.

A comparison with the fields for Moinian psammitic rocks presented by Winchester et al. (1981) and Haselock (1984) show the biotite psammites are distinct from Moinian rock-types which, with the exception of the basal Morar unit, predominantly have K_2O/Na_2O ratios exceeding 1.0. The psammite clasts are unlikely therefore to have been derived from Moine type metasediments which are more closely related to arkoses. Data for Upper Dalradian Southern Highland Group grits (Bowes and Convery 1966) show an almost identical distribution to the clasts of northerly derivation when plotted on a log (Na_2O/K_2O) vs log (SiO_2/Al_2O_3) plot.

Sodium is plotted against potassium in Figure 6.4. Data for each of the clast groups form a scattered and largely overlapping array with the bulk of the data plotting with K_2O/Na_2O ratios less than 1.0. Only three samples plot below the line representing $K_2O = Na_2O$. The clasts of biotite grade psammite (S2) are displaced to slightly higher Na_2O abundances than the corresponding northerly derived chlorite-bearing psammites. The clasts of southerly derivation show a similar displacement of the metagreywackes, to slightly more enriched Na_2O values than their unmetamorphosed equivalents. Clasts from each of the groups

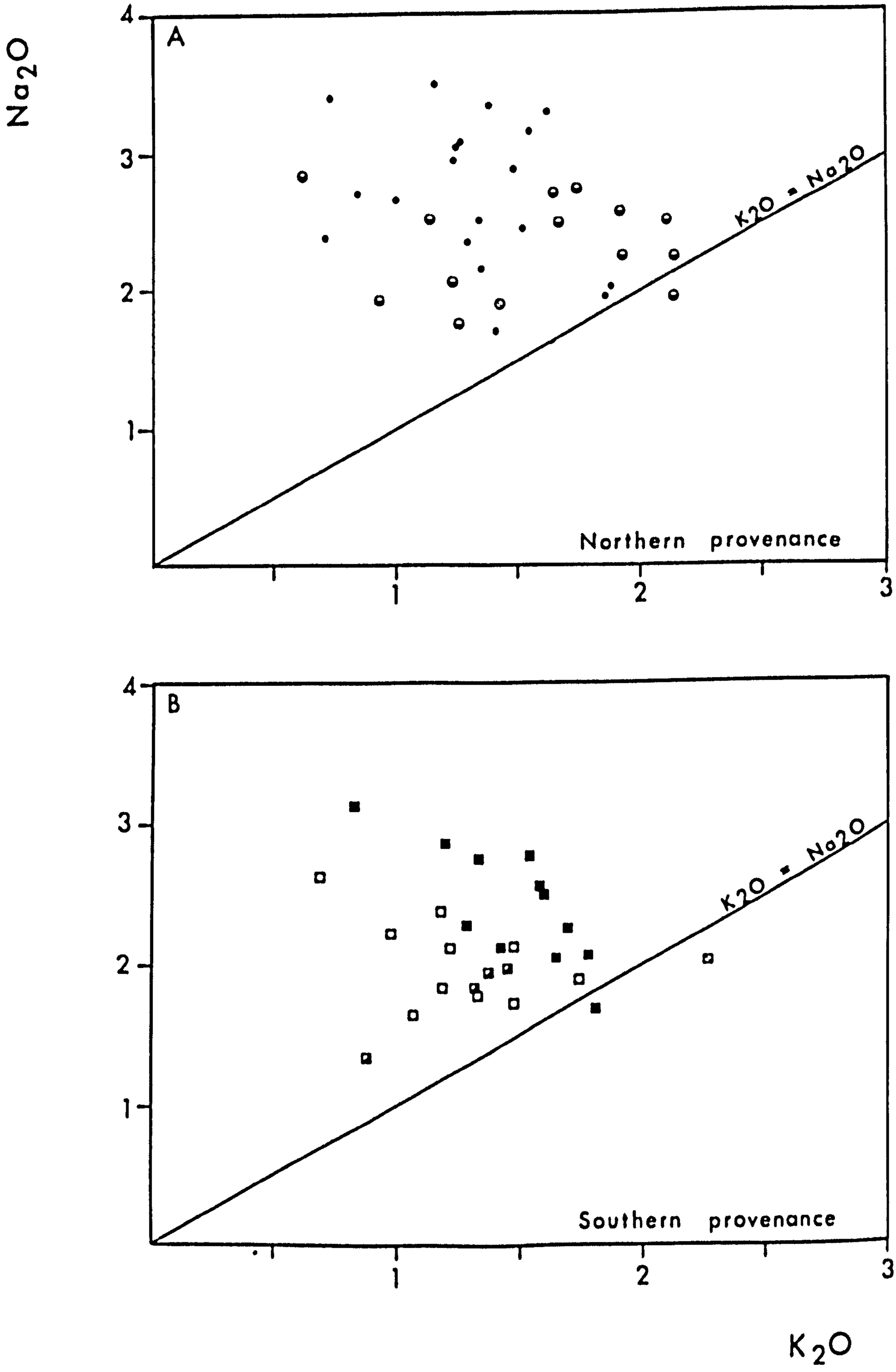

FIGURE 6.4 Na_2O vs K_2O plots for sedimentary and metasedimentary clasts of northerly and southerly provenance. Symbols as in Figure 6.2a.

cannot be distinguished on the basis of K_2O abundances.

High Na_2O contents have been widely recognised in sediments classified as greywackes, particularly those occurring in arc-related and leading edge tectonic settings. The low K_2O/Na_2O ratios observed in the metagreywackes and lithic arenites of southerly provenance are compatible with the petrographic evidence suggesting a mixed provenance in a metamorphic and volcanic terrane. Somewhat more surprising is the Na_2O content of the northerly derived clasts which are unexpectedly high considering the high SiO_2 contents of many of the clasts. Sediments with low SiO_2 contents generally have low K_2O/Na_2O ratios. As the silica content increases the K_2O/Na_2O ratio also shows a concomitant increase. The occurrence of high silica together with low K_2O/Na_2O is therefore anomalous when seen against the background of typical alkali and silica abundances in other sediments. No comparable composition exists amongst the thirty averages of ancient and modern sands compiled by Bhatia (1983).

Figure 6.5 plots the ratio K_2O/Na_2O against SiO_2 for a range of average sediment types largely taken from the compilation of Bhatia (1983). The average values for the chlorite (n = 14) and biotite (n = 20) psammite clasts, together with an average of the data for the Ben Ledi Grits taken from Bowes and Convery (1966) are also shown. The data for the clasts plot well below the field for other high-Q greywackes and sands, as does the average Southern Highland Group grit. The close similarity of the clasts to Upper Dalradian metasediments is particularly significant given the unusual composition they share, and this strengthens the case for a Dalradian source for at least some of the metamorphic detritus preserved in Lower ORS basins of the Midland Valley.

The origin of the high Na_2O content observed in the clasts of northerly provenance is related to the high modal abundance of albite the clasts contain. Albite is the stable plagioclase in rocks at greenschist facies regardless of the CaO content of the host rock (Miyashiro 1973). Sandstones with feldspathic

FIGURE 6.5

Plot of (K_2O/Na_2O) vs SiO_2 for a series of ancient and modern sands. Data largely from compilation of averaged volatile-free analyses in Bhatia (1983). Symbols are : open square, oceanic island arc setting; triangle, continental island arc; circle, active continental margin; diamond, passive margin setting. Half filled symbols are recent sands from Maynard et al (1982); A, G are average arkose and greywacke from Pettijohn (1963). S1 and S2 are average (not volatile free) chlorite and biotite psammite clasts. SHG is average Southern Highland Group grit from Bowes and Convery (1966). Field for normal sediment compositions outlined. Vertical lines divide compositional space into three arbitrary areas; low- , intermediate- and high-quartz greywackes. Horizontal lines separate leading edge from trailing edge sediments (K_2O/Na_2O = 1) and quartz-intermediate from quartz-poor greywackes (K_2O/Na_2O = 0.4), after Crook (1974).

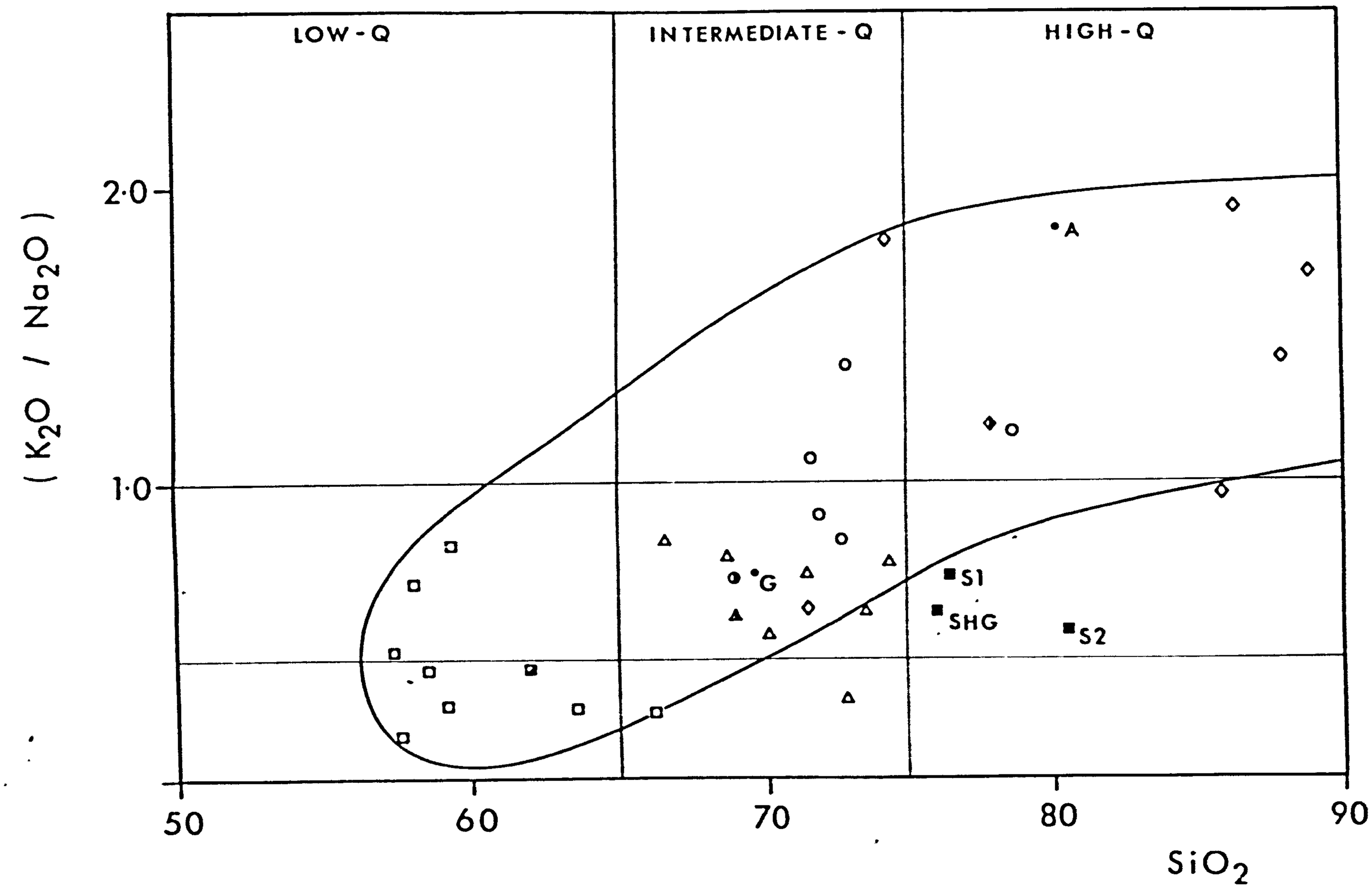
LOW - Q
INTERMEDIATE - Q
HIGH - Q
2·0
1·0
(K2O / Na2O)
A
G
S1
SHG
S2
50
60
70
80
90
SiO2

components dominated by sodic plagioclase occur widely (Ogunyomi et al. 1981) and often are also rich in volcanic detritus. It is sandstones rich in albite but lacking any evidence for volcanic source materials which are more difficult to interpret. Before a detrital origin for the albite can be assumed to account for the high Na_2O content of the clasts secondary processes of albitisation during diagenesis and metamorphism must be ruled out. Detrital textures are well preserved in the lower grade chlorite-bearing psammites but recrystallisation has overprinted the original textures of the biotite psammites obscuring the origin of the feldspar.

In the low grade and least strongly deformed clasts fresh feldspar grains show good detrital textures. Moderate to fresh albite-law twinned sodic feldspars dominate in the finer grain sizes. Some form composite grains with undulose extinction quartz. Very rare larger grains with perthitic exsolution are observed. Coarser grained feldspars are typically untwinned nd almost invariably recrystallised. Occasional coarse twinned grains show deformed twinning. Kastner (1971) reviewed the criteria for the recognition of authigenic feldspar. Authigenic grains are generally euhedral without polysynthetic twinning, often occur as overgrowths and have compositions <1 mol % $CaAl_2Si_2O_8$. The feldspars occurring in the psammitic clasts with their obvious detrital outlines, are unlikely to be of authigenic origin.

Albitisation of detrital feldspar during diagenesis is certainly a possibility. Land and Milliken (1981) showed progressive albitisation of feldspars with depth in a deep borehole. Those non-albitised grains persisting to greater depths were found in martrix rich rocks suggesting hydraulic flow is important in promoting the feldspar alteration. The poorly sorted textures of the psammite clasts and the probable moderate matrix contents (now recrystallised to chlorite) indicate that active hydraulic flow was probably suppressed in the clastic sequence from which the clasts were derived, reducing the likelihood that the high Na_2O contents of the clasts reflects albitisation.

Regional metamorphism, and in particular Na metasomatism, might also be responsible for the unusually sodic character of the psammite clasts. That sodium transfer can take place during progressive metamorphism is shown by the widespread occurrence of albite porphyryoblasts in low grade metamorphic rocks. The detrital grain boundaries, grain elongation normal to the c-axis, and the fact that the albites are, in terms of grainsize, in textural equilibrium with the rest of the sediment (i.e. no porphyroblastic textures) indicate that the Na is unlikely to have been introduced metasomatically, but rather must represent an original feature of the sediments provenance. Bowes and Convery (1966) point out that similar albite rich metasediments occurring in the Southern Highlands Group of the Dalradian Supergroup may in fact be the source of Na during local Na-metasomatism with transfer of sodium from the grit bands to the schistose pelitic bands.

In conclusion, the anomalous Na enrichment and low K_2O/Na_2O observed in the psammitic clasts of northerly derivation are thought to reflect an original detrital albite component in sediments which make up the thick sequence from which the clasts were derived. A similar detrital albitic component has been identified in Upper Dalradian metagreywackes by Bowes and Convery (1966). Significantly, albite and rare oligoclase dominate Cambrian flysch sequences in the Canadian Appalachians (Lajoie et al. 1974) pointing to a widespread development of albite rich sediments associated with rifting and continental breakup in the period 625-555 Ma (Bond et al. 1984).

6.4.3.3 Iron and Magnesium

Maynard et al. (1982) consider the parameter (FeO + MgO) particularly diagnostic of tectonic environment as it is sensitive to the addition of fragmental mafic volcanic material. Harker variation diagrams for MgO and total Fe as Fe_2O_3 are shown in Fig. 6.6a. The MgO plot shows a good discrimination of clasts from each of the three suites with the southerly derived lithic arenites and metagreywackes predictably plotting with the highest MgO abundances. The very low abundances in the biotite-muscovite-(garnet) psammites, many of which contain less than 1%

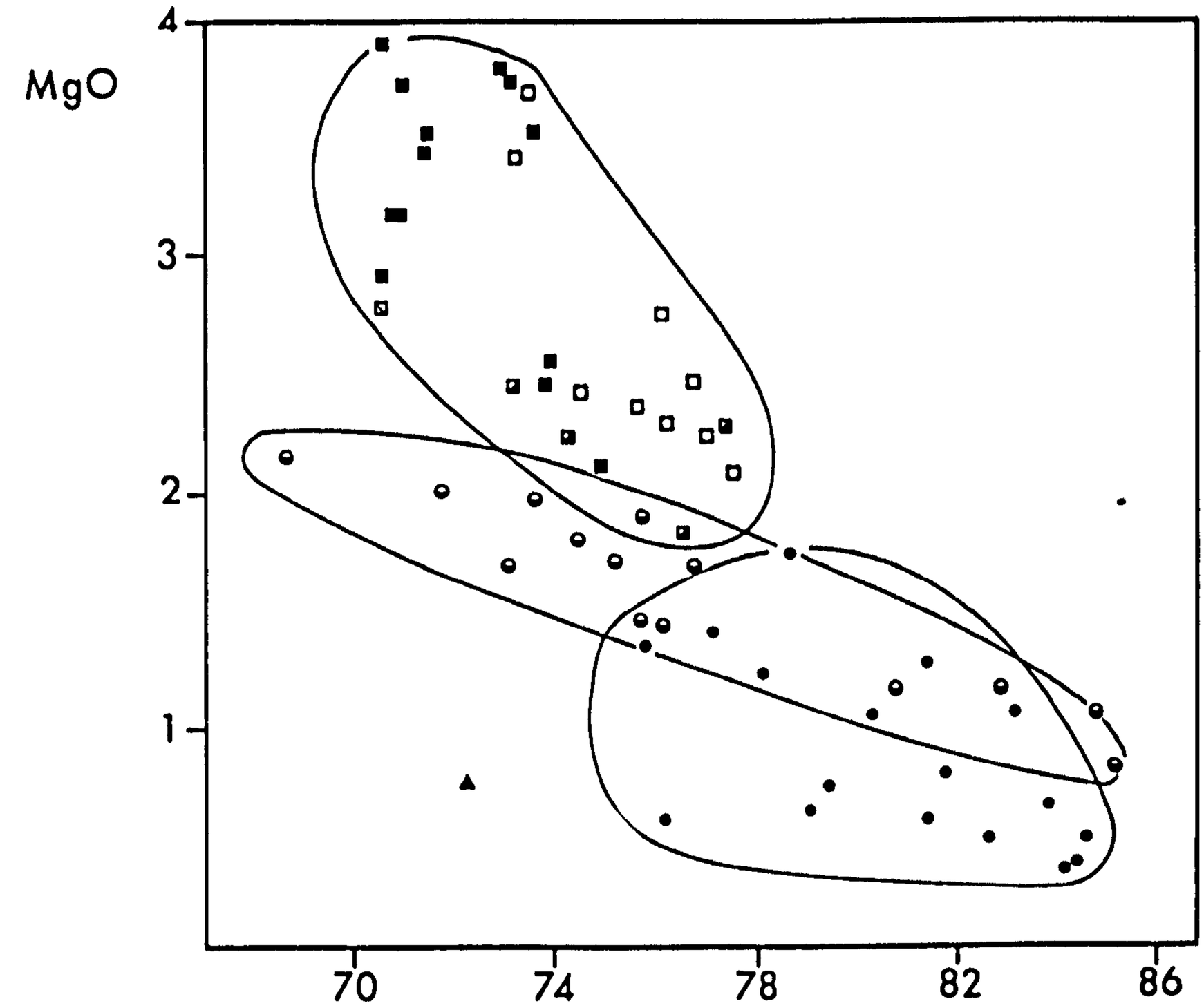

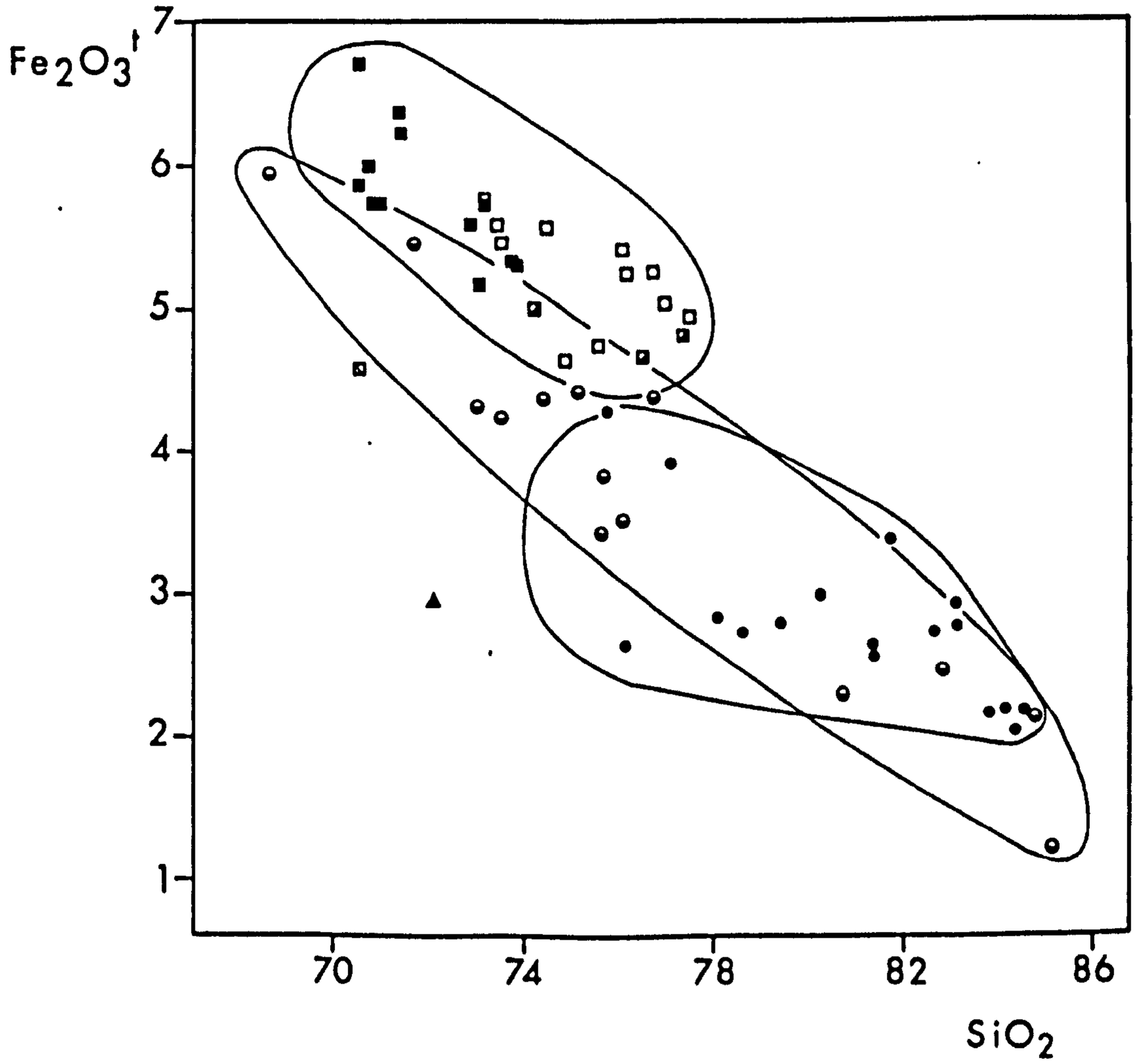

Figure 6.6 MgO and $(Fe_2O_3)^t$ Harker variation diagrams. Symbols as in Fig. 6.2a.

MgO, confirm that volcanic material was unimportant in the provenance of the metasedimentary sequence lying to the north of the Crawton Basin. Unlike the variation of Al_2O_3 and $(Fe_2O_3)^t$ with SiO_2, the MgO vs SiO_2 plot highlights a significant divergence in the trends defined by each of the suites which takes place towards less silicic compositions suggesting the suites are progressively diluted with material which is compositionally distinct. The increase in MgO with decreasing SiO_2 is steeper than would be expected if silica loss to quartz veins was solely responsible for the displacement of the chlorite-bearing metagreywackes to lower SiO_2. An element of original compositional variation must also be involved, with a sequence of greywackes richer in mafic volcanic detritus preferentially undergoing low grade metmorphism. Matrix contents in the chlorite bearing metagreywackes are notably higher than in the unmetamorphosed lithic arenites.

The generally high MgO content of the southerly derived clasts with respect to those of northerly derivation is a direct consequence of the presence of an important mafic component in the former. In the absence of such material in the latter dilution with clay minerals in the less silicic psammite lithologies probably accounts for the mild increase in MgO in the chlorite-bearing psammites. The separation of the chlorite and biotite psammites, with the latter displaced to lower MgO than the former suggests the original composition of the two sequences may have differed significantly. The separation is consistent with the higher grade psammites being compositionally more mature. The two suites cannot be distinguished on the basis of their respective total iron contents, but the southerly derived clasts are displaced to higher $(Fe_2O_3)^t$ at constant SiO_2 forming a linear array paralleling the combined trend for the northerly derived psammites (Fig.6.6b).

6.4.3.4 CaO

The abundance of CaO is sensitive to diagenetic addition of carbonate and is a useful index of alteration. The clast data are plotted on a $CaO-Na_2O-K_2O$ ternary diagram in Figure 6.7 together with average compositions for andesite, granodiorite and

Northern provenance

- • biotite and higher grade psammite
- ⊖ chlorite grade psammite
- ⊘ altered chlorite grade psammite clast(high CaO,LOI)
- ▲ microconglomerate clast (2117)

Southern provenance

- □ undeformed lithic and quartz arenite
- ⧅ altered lithic arenite clast (high LOI)
- ■ foliated quartz-veined chlorite bearing meta-greywacke
- ◪ biotite hornfels

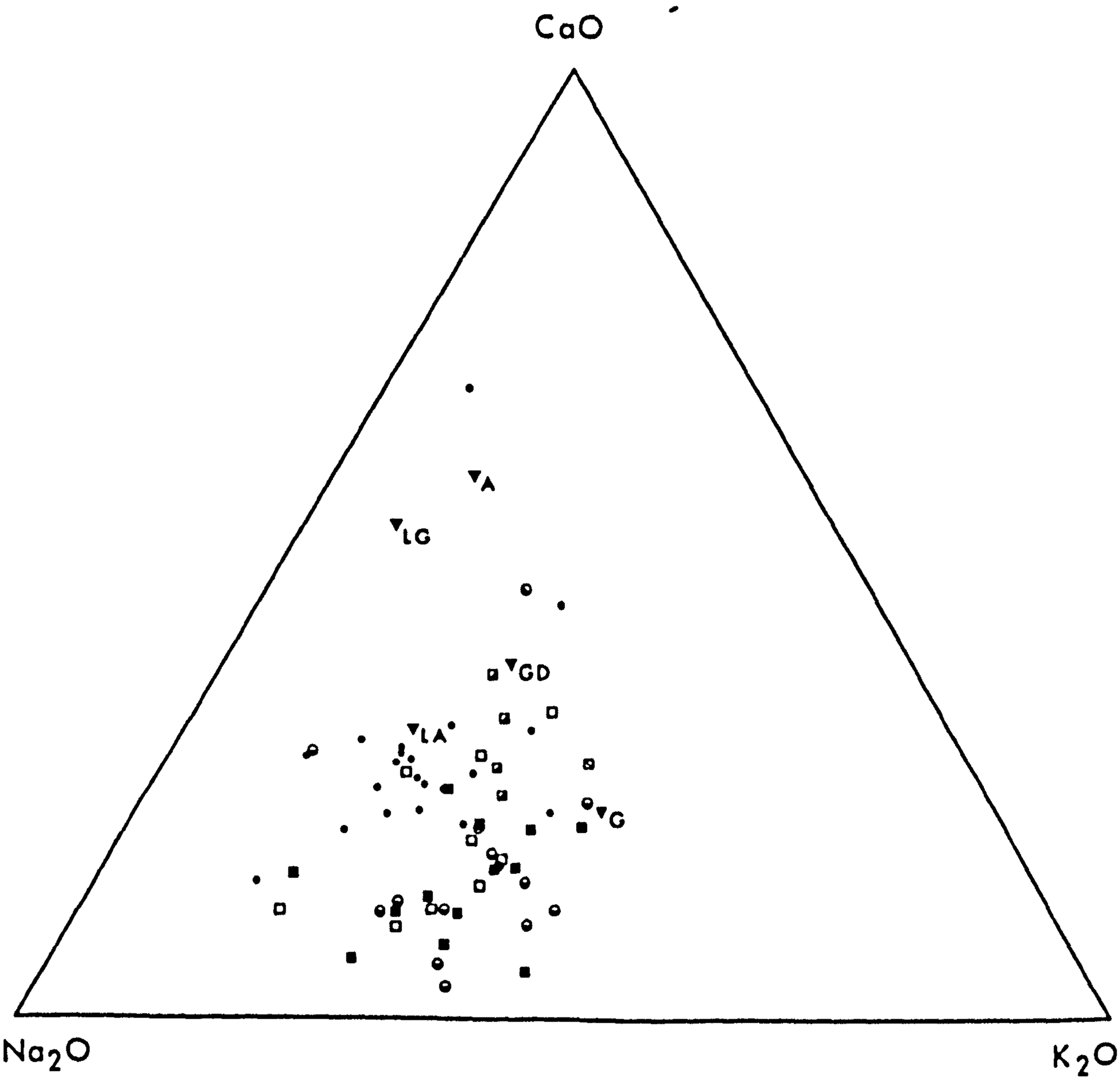

FIGURE 6.7 $CaO-Na_2O-K_2O$ ternary diagram for sedimentary and meta-sedimentary clasts, and average compositions for andesite (A), granodiorite (GD), and granite (G) after Le Maitre (1976). Lewisian granulite (LG) and amphibolite facies (LA) average compositions after Weaver and Tarney (1981).

granite from Le Maitre (1976) and for average Lewisian granulite and amphibolite facies rocks (Weaver and Tarney 1981). apart from a few samples with high LOI which plot towards the CaO apex, the bulk of the clast data plot close to the Na_2O-K_2O base to the ternary diagram indicating low CaO abundances. This is consistent with a minor role for carbonate addition during diagenesis. The data are displaced towards more sodic compositions than the average granite of granodiorite, and less calcic compositions than the average Lewisian granulite or andesite.

One of the more significant distinctions within the data set is that between the chlorite and biotite psammites. The biotite psammite clasts are displace towards the CaO apex relative to the associated chlorite-rich psammite clasts. The enrichment in CaO is revealed in the biotite-psammite petrography by the development of zoisite. Zoisite is a typical constituent of medium grade regionally metamorphosed rocks of marly composition (Deer et al.1966). The origin of the higher CaO content of the biotite psammites is unclear, due to the extent of recrystallisation. It conceivably might reflect either a more calcareous detrital component in the form of more calcic plagioclase, dilution with a carbonate-rich clay phase, or the introduction of a small amount of carbonate during diagenesis.

The large LOI and high CaO content of a number of clasts (e.g.3188) reflects calcite replacement during burial diagenesis of the conglomerates in which the clasts are preserved, and therefore have no relevance to the original clast composition.

6.4.4 Trace Element Geochemistry

6.4.4.1 Introduction

Average trace element abundances for each of the sedimentary/metasedimentary clast suites are given in Table 6.2. As with the major elements, significant differences exist between each of the suites, and are most pronounced with respect to Rb, Sr, Ni, Cr, Y and Ba. The chlorite and biotite grade clasts of northerly derivation show the closest affinity and are distinguished only on the basis of the higher Sr of the biotite

psammites. The southerly derived clasts show striking enrichments in Ni, Cr and to a lesser extent Y, and depletions in Sr and Ba relative to the northerly derived clast suites.

Correlations between trace element abundances and silica are generally poor. Following Senior and Leake (1978), trace elements were plotted against Niggli al-alk (Niggli 1954). The parameter al-alk provides a measure of Al in the original sediment contained in clay minerals and micas as opposed to that residing in detrital feldspar (al-alk in albite and feldspar is zero). A positive correlation between al-alk and trace elements added to the sediment in clays and micas is therefore to be expected. With the exception of Zn in the biotite psammites no such correlation exists for the clasts, and the clay mineral content is consequently not thought to significantly control the abundance of the trace elements. Senior and Leake (1978) show that quartzites and sandstones generally do not conform to al-alk controlled variation in trace element abundances, and they attribute this feature to the rapidity with which sandstones accumulate in marine environments. This inhibits the extraction of trace elements, and Fe and Ti, from seawater. Trace element distributions in sandstones are therefore less likely to be controlled by variation in adsorption on clays and to be more sensitive to primary variation in sediment provenance. Diagenetic dissolution may also exert an important control but is likely to be least effective in sandstones of greywacke type.

6.4.4.2 Ni and Cr

The abundances of Cr and Ni are of particular importance in that they are sensitive to the presence of an ophiolitic component in the provenance of clastic sediment. Cr has been used as a tracer of ophiolitic source rocks by Bjørlykke (1974) and Hiscott (1978, 1984). Cr occurs chiefly in chromite, which can contain 10-45% Cr, whilst Ni occurs in both sulphide minerals and, by substitution, in the lattice sites of the silicates, olivine and pyroxene (Fairbridge 1972). Taylor and McLennan (1985) estimate the average post-Archaean shale to have Ni and Cr abundances of 55 and 110ppm respectively. Average sandstone values are likely to be substantially less than this.

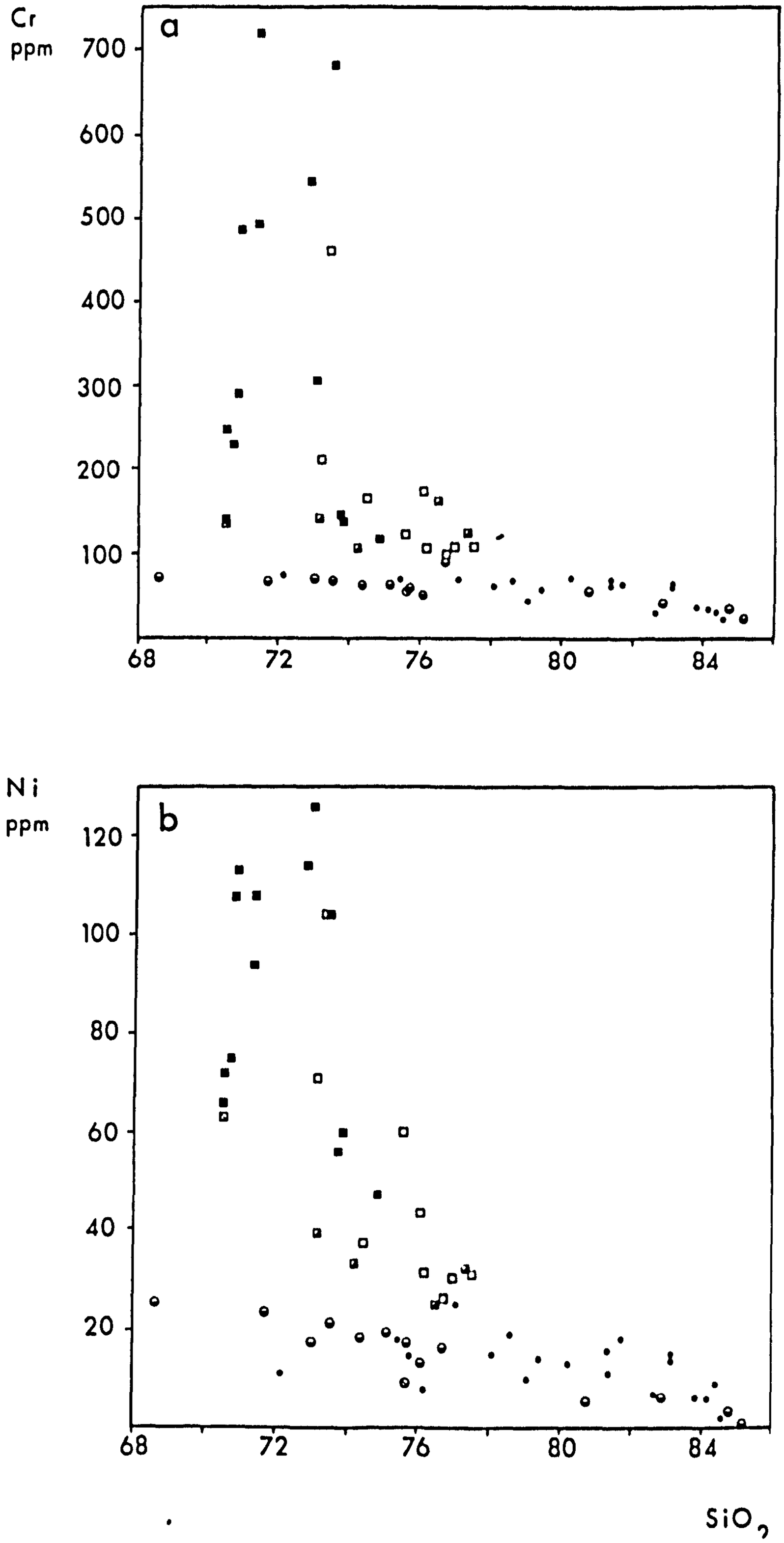

FIGURE 6.8 Harker variation diagrams for Ni and Cr abundances in sedimentary and metasedimentary clasts illustrating unusual enrichment in lithic arenite metagreywacke clasts of southerly provenance. Symbols as in Figure 6.2a.

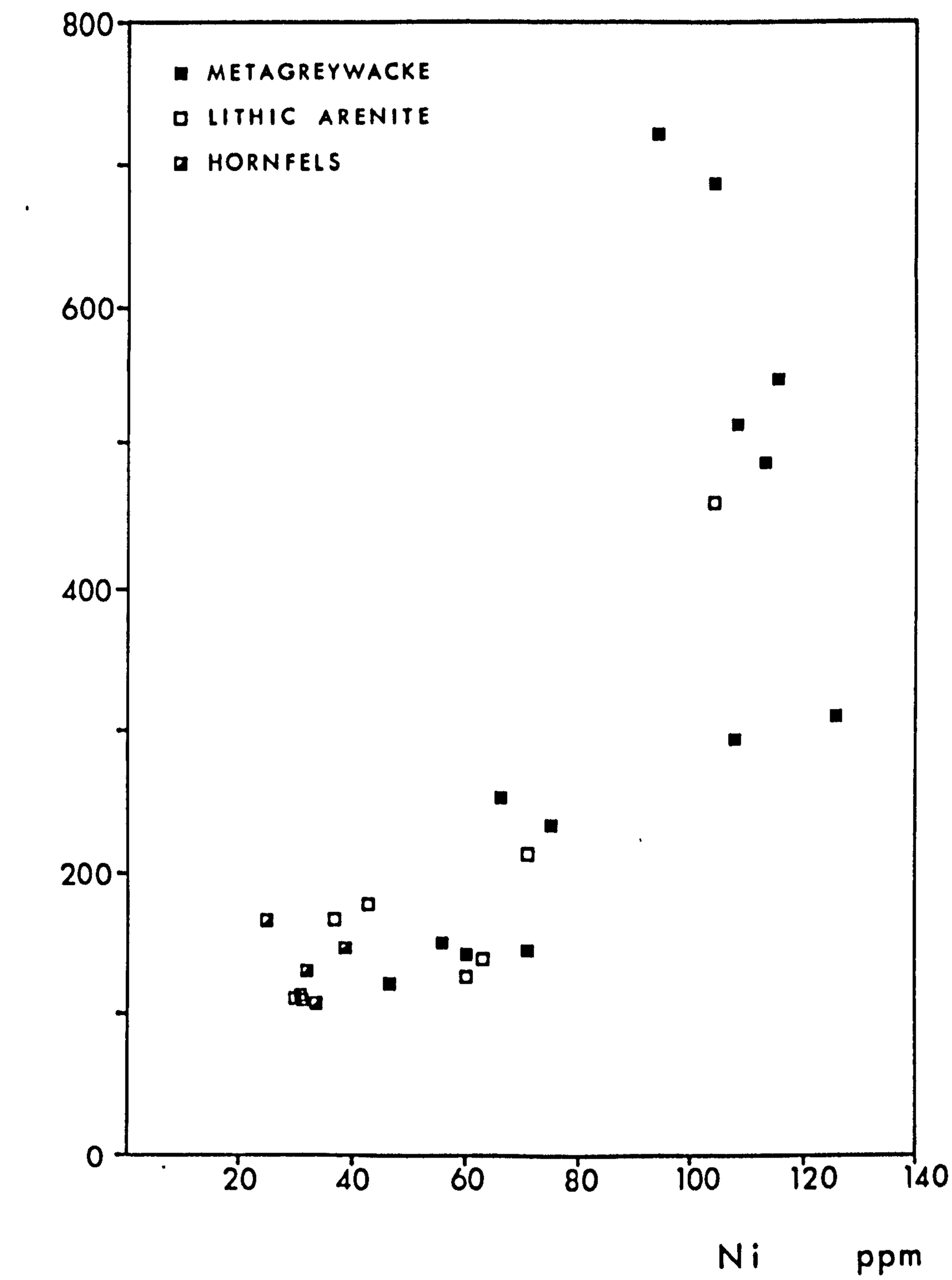

Figure 6.9 Cr vs Ni plot for sedimentary and metasedimentary clasts of southerly provenance. The plot illustrates a strong enrichment of Cr at constant Ni concentrations for the high Ni metagreywacke clasts.

Nickel and chromium abundances are plotted against SiO_2 in Figure 6.8. Both elements show normal post-Archaean abundances in psammite clasts of northerly derivation, but are strongly enriched in the metagreywackes dispersed from a source to the south. Cr concentrations in these clasts reach 700 ppm (mean 350 $\pm$ 212 ppm, n = 13). Whilst both Cr and Ni occur at elevated levels in the metagreywackes, Cr is more strongly enriched than Ni, although the high-Cr samples are accompanied by Ni-enrichment. Figure 6.9 shows a linear trend for Cr vs Ni concentrations from 0 to 100 ppm Ni. At Ni contents >100 ppm, Cr is strongly enriched and the coupling between Ni and Cr breaks down. This suggests the Cr abundance at high concentrations is critically controlled by the presence of a high Cr phase in which Ni is excluded. This is most likely to be chromite, given the very high Cr abundances. (As all samples were crushed in agate the Cr cannot have been introduced as a contaminant during sample preparation. It must represent an original feature of the detrital composition.)

The presence of a Cr bearing detrital phase whose abundance determines the Cr content in samples with Ni >100 ppm explains the lack of correlation between the major element chemistry and Cr enrichment. Should the Cr be controlled by the bulk addition of ultramafic detritus, a correlation between the sediment chemistry and Cr abundance would be expected. If the Cr occurs in a minor phase such as chromite, the major element chemistry should be relatively insensitive (with the possible exception of MgO in high Mg chromite) to the small variations in modal chromite required to explain the Cr abundance. Sr and Nd isotopic compositions also fail to identify the high Cr component confirming that the Cr distribution cannot be related by isotopically distinct primitive ultramafic detritus.

At intermediate Ni concentrations (i.e. 30-100 ppm), Cr correlates well with Ni and their abundance is therefore more likely to be controlled by addition of a small component of basic material containing both Ni and Cr, and a relatively minor role for heavy mineral enrichment. At Ni concentrations <30 ppm, Ni

	LITHIC ARENITE n = 10		METAGREYWACKE n = 13	
	$\bar{x}$	σ	$\bar{x}$	σ
SiO_2	75.06	2.17	72.17	1.52
Al_2O_3	9.92	0.92	11.10	0.53
TiO_2	0.80	0.09	0.80	0.08
MnO	0.08	0.01	0.08	0.02
$(Fe_2O_3)^t$	5.22	0.38	5.70	0.55
MgO	2.62	0.57	3.23	0.56
CaO	0.86	0.49	0.65	0.26
Na_2O	2.08	0.30	2.39	0.45
K_2O	1.32	0.44	1.48	0.27
P_2O_5	0.11	0.01	0.11	0.01
LOI	2.57	0.38	2.57	0.33
TOTAL	100.64		100.28	
Cr	177.2	112.2[a]	350.2	212.0
Co	12.7	2.9[a]	13.54	3.64
Ni	49.6	24.8	87.9	26.2
Cu	12.8	4.1	10.0	3.4
Zn	62.1	9.0	65.9	9.5
Ga	12.1	2.0	12.3	2.9
Rb	48.1	16.3	56.2	9.6
Sr	71.9	11.0	66.1	30.9
Y	22.4	1.7	21.8	3.1
Zr	266.0	51.7	242.8	43.3
Ba	275.8	66.8[a]	241.0	72.6
La	22.5	4.9[a]	15.9	7.2
Ce	43.2	8.4[a]	32.7	11.8

a: n=9

Table 6.3 Comparison of averaged lithic arenite and metagreywacke clast compositions.

and Cr were probably dispersed to the original basin of deposition adsorbed on clays.

Amongst the sediment and metasediment clasts of southerly derivation, the pattern of Cr enrichment highlights an important distinction between the lithic arenite clasts which are unstrained, unmetamorphosed and free of quartz veining, and the metagreywackes which are at lower greenschist facies. The former, with one exception, show only modest Cr enrichment and fall on the broad correlation of Ni and Cr with Ni <100 ppm in Figure 6.9. Detrital chromite therefore is probably largely restricted to the lower greenschist facies clasts, indicating an important compositional variation existed in the sediment pile located to the south of the Crawton Basin.

Table 6.3 compares the mean compositions of the metagreywackes and greywackes/lithic arenites. Ni, Cr, MgO and $(Fe_2O_3)^t$ are the only minor and trace elements which show a statistically significant difference between the two groups. As these elements are characteristically high in basic volcanic rocks and ophiolitic rock associations, an important ophiolitic component is inferred to have been incorporated in the sediments which subsequently underwent lower greenschist facies burial metamorphism. Whilst the unmetamorphosed sediments also received basic or ultrabasic detritus, detrital chromite may not have been as important.

The four clasts of biotite hornfels significantly do not show the anomalous Cr concentrations seen in the lower greenschist clasts and have compositions more akin to the unmetamorphosed greywackes and lithic arenites. This suggests the granites were emplaced largely in the unmetamorphosed part of the sequence.

6.4.4.3 Rb,Sr and Ba

Whilst Rb shows a general decrease in abundance with increasing SiO_2, Sr is enriched in the highly silicic biotite psammites of northerly provenance (Fig. 6.10a). This reflects the higher CaO content of this suite, as Sr readily substitutes for Ca. Both Sr and CaO therefore serve to best discriminate the biotite

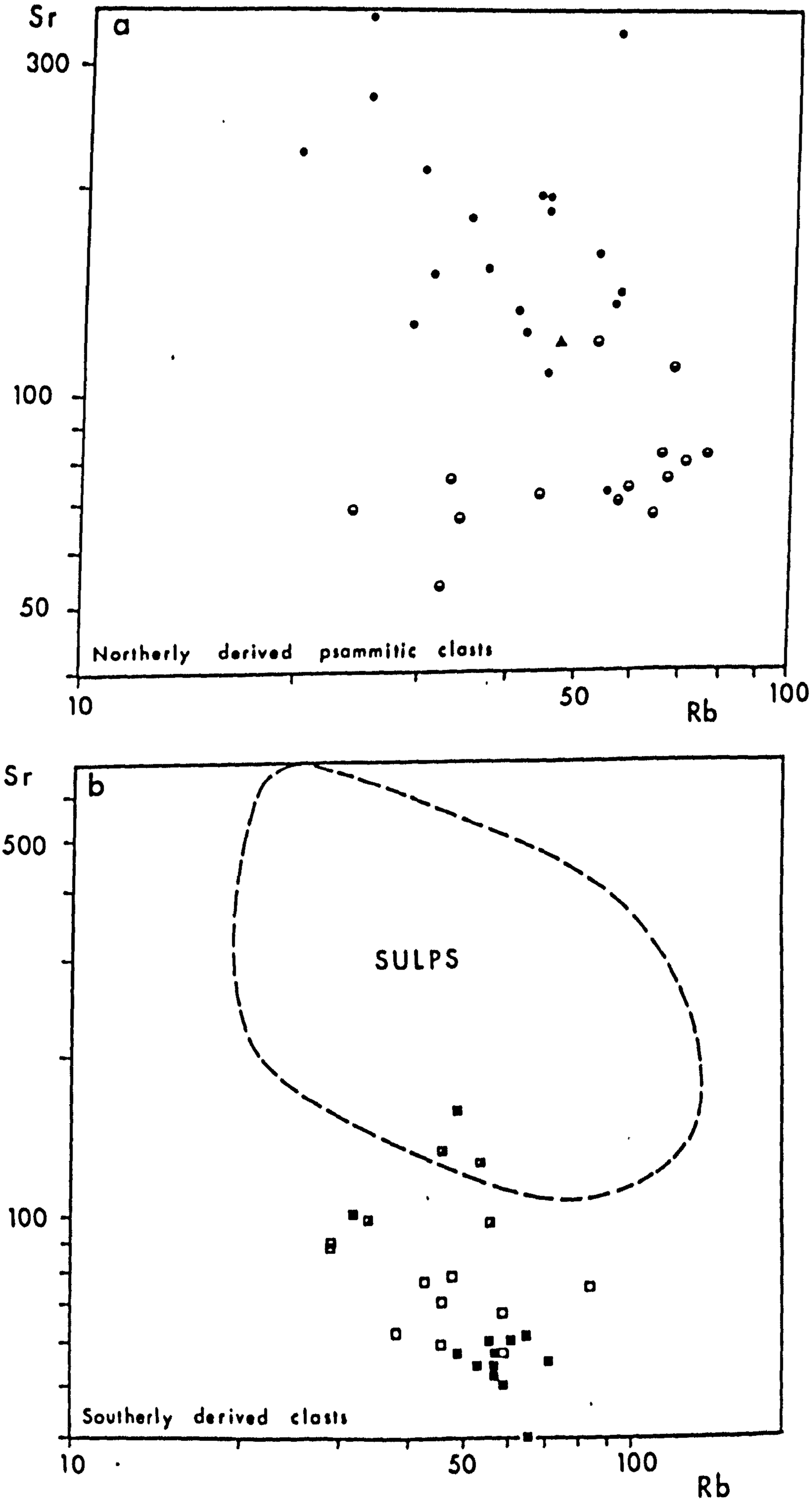

FIGURE 6.10 Rb and Sr (ppm) variation in metasedimentary and sedimentary clasts of northerly (a) and southerly (b) provenance. Symbols as in Figure 6.2a. Field for SULPS from Halliday et al. (1980).

psammites from the accompanying northerly derived chlorite grade psammites. Otherwise the two clast suites show a strong similarity. It is possible the distinction arises from differential diagenetic alteration with the introduction of secondary carbonate to the biotite psammites. The early diagenetic history of these rock types is now however totally obscured by recrystallisation.

Rb and Sr concentrations in the sediment clasts of southerly derivation are plotted in Figure 6.10b, together with Rb-Sr concentration data from the Southern Uplands. Sr concentrations in the clasts depart significantly from the SULPS greywacke data, and are substantially lower. Ba is also depleted in the clasts derived from the south relative to those of northerly provenance. The compositional departure of the southerly derived clasts from SULPS is of some significance in that the latter have been considered to be representative of the sedimentary component involved in the petrogenesis of Midland Valley Lower ORS lavas (Thirlwall 1983). The southerly derived clasts (S3) sample a thick sedimentary sequence developed in the east central Midland Valley which may in part have formed the foundations for the development of the thick Lower ORS Ochil-Sidlaw lava pile. As such, they are a more appropriate sample of material likely to be involved in magma contamination.

6.4.5 Major Element Discrimination of the Plate-tectonic Setting of Sedimentation Associated with Lower ORS Source Terranes

As the chemical composition of sandstones has been shown to be sensitive to the tectonic environment in which they are deposited, the geochemistry of sandstone clasts can potentially be usefully used to establish the tectonic history of the source terrane from which the clasts were derived. In the following section, major element discriminants of tectonic environment are applied to the sedimentary and metasedimentary clasts dispersed to the Crawton Basin in an attempt to further constrain the nature of the source terranes on either margin of the basin.

Bhatia (1983) empirically established a series of major element parameters for the discrimination of the tectonic setting of

Table 6.4 Discriminant scores and discriminant function coefficients

Discriminant scores					
SAMPLE	FUNCTION 1	FUNCTION 2	SAMPLE	FUNCTION 1	FUNCTION 2
4405	-1.09	-0.55	4481	-0.85	2.26
4406	-1.59	-0.10	4483	-0.38	1.18
4407	5.42	6.79	4484	-1.12	0.91
4408	-0.74	0.50	4487	-0.83	0.81
4409	-1.10	2.00	4488	-1.51	1.77
4410	-1.00	1.01	4490	-0.41	0.89
4412	-1.00	0.26	4491	-0.86	1.77
4413	-1.12	-0.07	4492	-0.19	0.81
4415	-0.44	1.89	4493	-0.83	1.30
4416	-1.99	0.80	4494	-0.52	2.15
4417	-1.24	0.58	4495	-0.05	3.89
4418	-2.05	1.13	4496	-0.45	0.98
4419	-1.41	-0.20	4497	-0.74	2.27
4420B	-1.26	0.77	4498	-1.08	1.05
2125	-0.45	0.20	3204	-0.62	0.02
2126	-1.86	-0.53	3303	-0.71	-1.19
3139	-1.33	-1.45	3145	-0.68	0.38
3141	-1.84	-1.68	4238	-0.75	1.89
3144A	-1.46	-0.54	4255	0.10	3.41
3149	-1.43	-0.28	4260	0.15	2.26
3150	-0.86	-0.90	4261	-0.02	3.08
2163	-0.31	0.47	4264	-1.21	1.43
3188	-0.50	-0.98	4271	-0.61	2.23
3190	-1.02	-0.50	4273	-0.91	1.45
3191	-0.99	0.36	4319	0.41	2.81
3192	-1.44	-0.42	4459	-1.60	1.77
3195	-0.60	0.24	4460	-1.14	1.57
3196	-1.14	-2.48	4478	-0.57	2.15
3197	-1.45	-0.98	4479	-0.71	1.99
3201	-0.82	-1.58			
3202	-0.73	-0.48	contd.		

Table 6.4 contd.

Unstandardised discriminant function coefficients used to calculate discriminant scores (Bhatia 1983)

	FUNCTION 1	FUNCTION 2
SiO_2	-0.0447	-0.421
TiO_2	-0.972	1.988
Al_2O_3	0.008	-0.526
Fe_2O_3	-0.267	-0.551
FeO	0.208	-1.610
MnO	-3.082	2.720
MgO	0.140	0.881
CaO	0.195	-0.907
Na_2O	0.719	-0.177
K_2O	-0.032	-1.840
P_2O_5	7.510	7.244
Constant	0.303	43.57

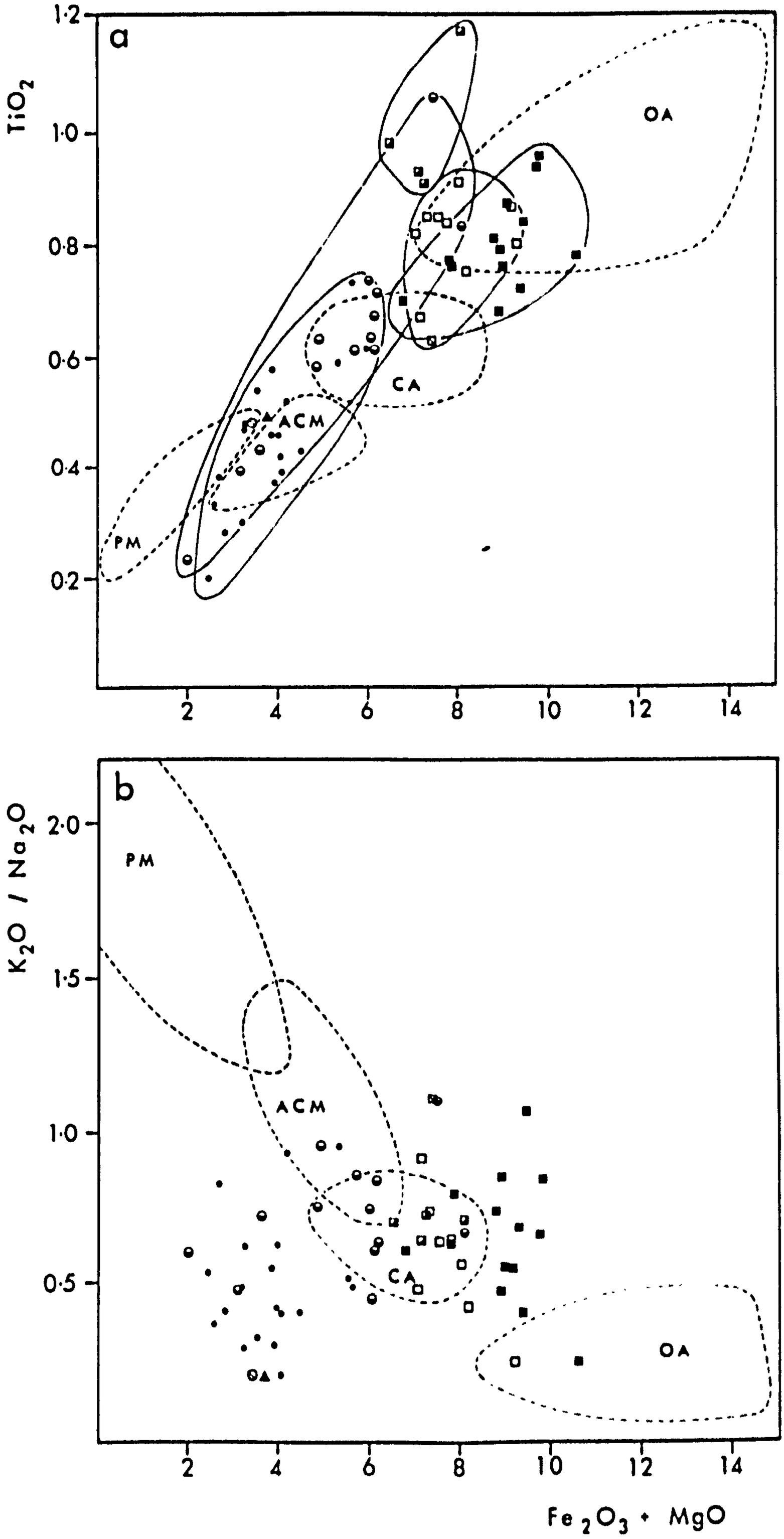

FIGURE 6.11 Bivariate major element plots for the discrimination of the tectonic setting of sandstone deposition (after Bhatia 1983). Symbols as in Figure 6.2a. Dashed lines outline major compositional fields for passive margin (PM), active continental margin, (ACM) continental island arc (CA) and oceanic island arc (OA) sandstones.

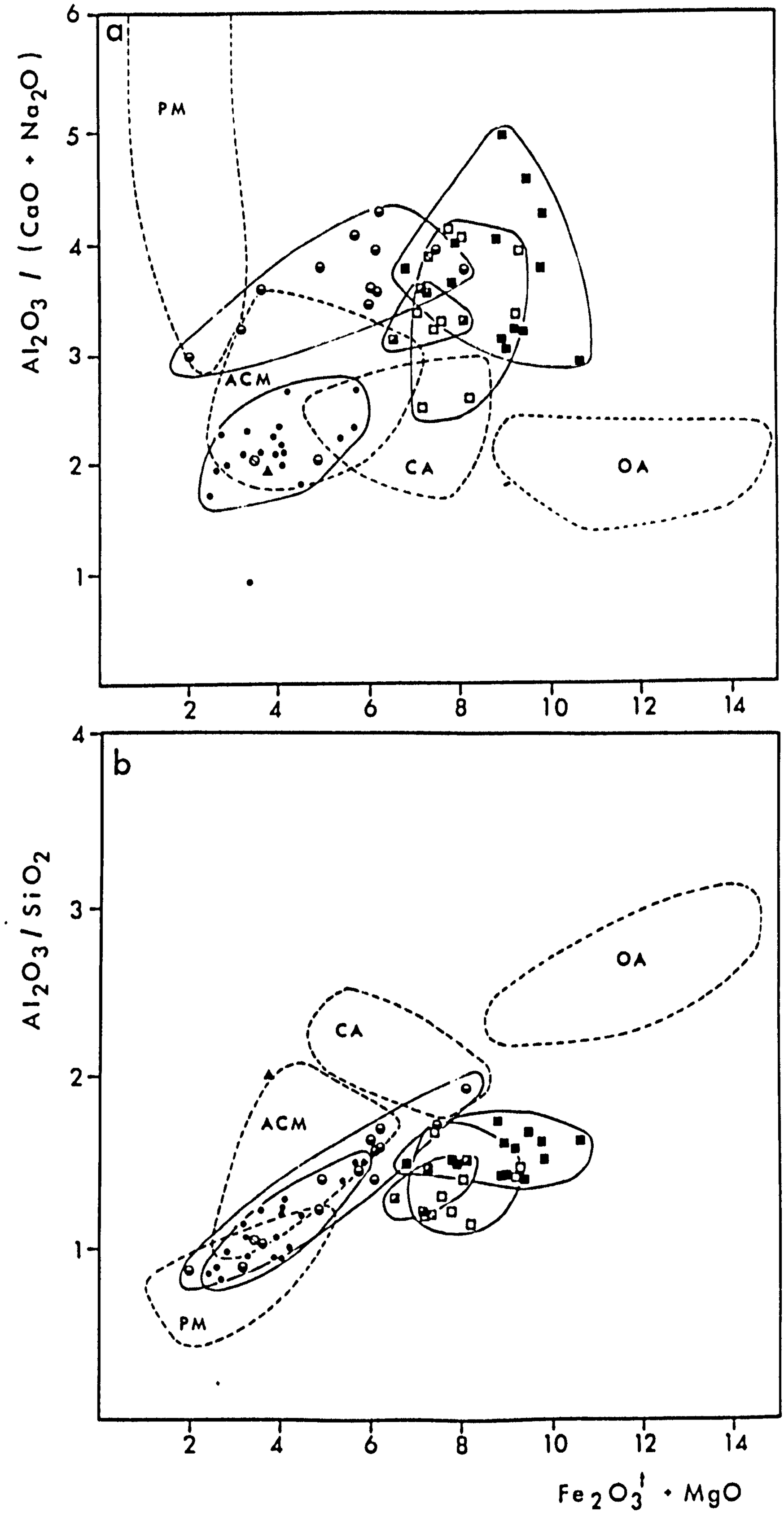

FIGURE 6.12 Tectonic discrimination plots after Bhatia (1983). See Figure 6.11 for abbreviations. Symbols as in Figure 6.2a.

FIGURE 6.13 Plots of discriminant scores calculated using unstandardised discriminant function coefficients shown in Table 6.4 (from Bhatia 1983). The territorial maps are based on data from Australian Palaeozoic sedimentary rock suites. Continuous lines delimit the major tectonic settings and are computer derived (Bhatia 1983). Abbreviations are PM: passive margin, ACM: active continental margin, CA: continental island arc and OA: oceanic island arc. (a)data for northerly derived biotite and higher grade psammite clasts. Open symbols are those samples for which both FeO and Fe_2O_3 analyses are available. Otherwise all scores have been calculated assuming an oxidation ratio of 0.32.

(b)northerly derived chlorite grade psammitic clasts

(c)southerly derived sedimentary and metasedimentary clasts. Symbols as in Figure 6.2a.

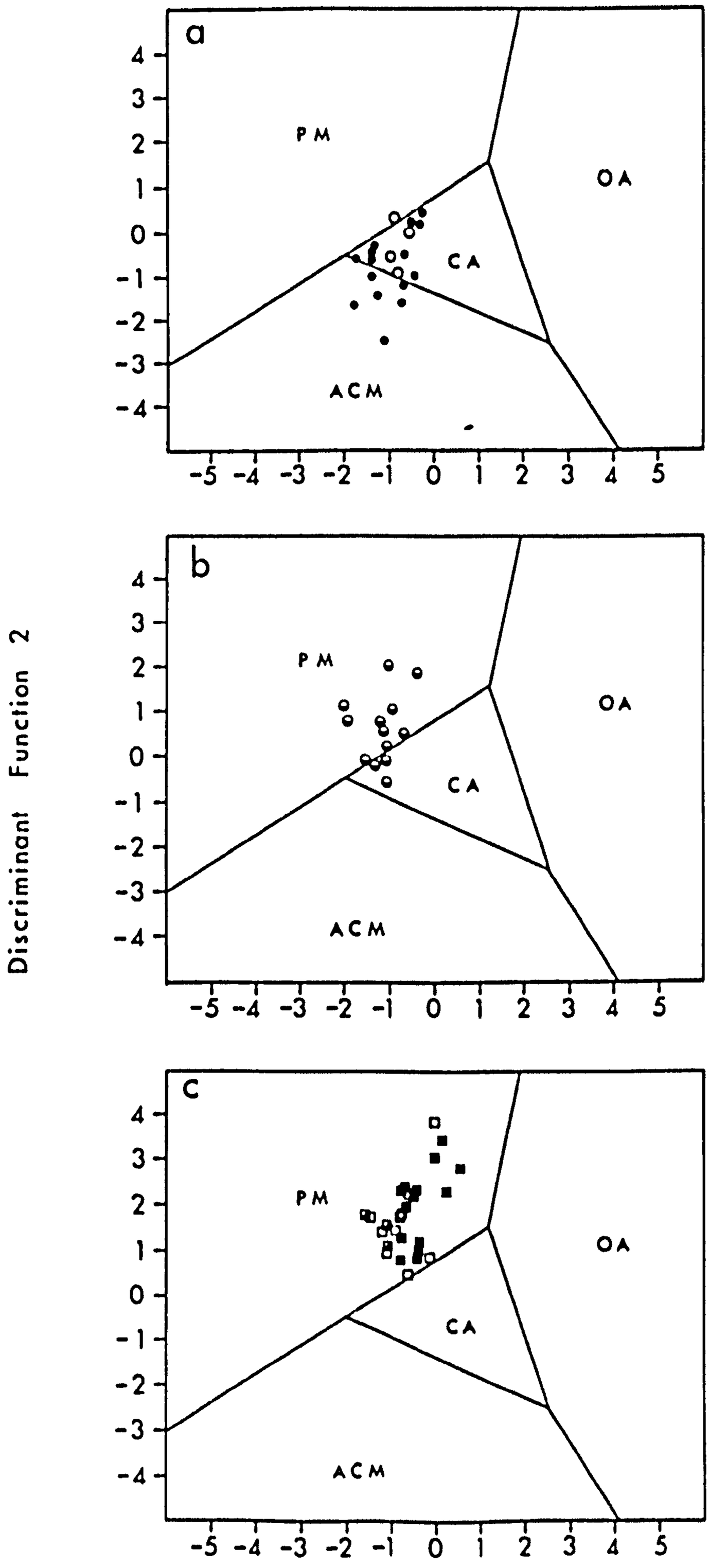
a
b
C
PM
CA
OA
ACM
4
3
2
1
0
-1
-2
-3
-4
-5 -4 -3 -2 -1 0 1 2 3 4 5
Discriminant Function 2
Discriminant Function 1

sandstone deposition. Four plots were found to achieve a separation of sediment compositions from several both known and inferred tectonic settings for both modern and ancient sediments. Figures 6.11 and 6.12 plot the sediment and metasediment clast data on Bhatia`s (1983) composition plots with the major fields for sandstones for various tectonic settings outlined (Bhatia 1983 Fig.6). $(Fe_2O_3)^t$ + MgO is used as the abscissa on all four discriminant plots. TiO_2, K_2O/Na_2O, Al_2O_3/SiO_2 and $Al_2O_3/(CaO + Na_2O)$ form the ordinate parameters. Titanium is useful as it is relatively immobile and has a low residence time in seawater (Taylor and McLennan 1985). Al_2O_3/SiO_2 monitors the degree of quartz enrichment whilst $Al_2O_3/(CaO + Na_2O)$ is a ratio of immobile to highly mobile elements.

From Figures 6.11 and 6.12 it is apparent that the clast data fall broadly between the passive margin and oceanic arc fields, overlapping the compositions of sediments belonging to the continental arc and active continental margin fields. The lower TiO_2 and $(MgO + (Fe_2O_3)^t)$ in the psammites of northerly derivation is consistent with the absence of a detrital volcanic component. The K_2O/Na_2O and $Al_2O_3/(CaO + Na_2O$ plots emphasise the unusual composition of the clasts of northerly provenance which on the basis of their high silica content might be expected to be of passive margin type. The tectonic setting is therefore inconclusive.

Bhatia (1983) also developed more complex discriminant functions using discriminant analysis to classify various sandstone suites. Sandstones from eastern Australia were used to construct a territorial map which was subsequently shown to correctly classify to the expected tectonic setting 90% of the thirty averages of published sandstones and modern sands for which discriminant scores were calculated. Discriminant scores for the clast analyses have been calculated using the unstandardised function coefficients recommended by Bhatia. The results are shown in Table 6.4 together with the unstandardised function coefficients. The scores have been plotted on a series of territorial maps (Fig. 6.13) with boundaries between the fields representing each of the tectonic settings from Bhatia (1983).

Figure 6.13 shows that Function 1 fails to discriminate the three suites despite the fact the clasts of southerly derivation contain a volcanic component. Bhatia proposes that Function 1 is mainly influenced by variation in plagioclase and volcanic fragments. Function 2 however produces a good separation of all three suites. The chlorite bearing clasts of northerly provenance straddle the boundary between passive margin and continental island arc fields and the clasts of southerly derivation plot almost exclusively in the passive margin field.

These results are rather inconclusive and little confidence can be placed in the tectonic settings indicated. This is particularly true of the psammite clasts which, on the basis of their highly silicic compositions, and their close affinity with Dalradian metasediments, might be expected to have formed in a trailing margin setting. It is significant that Bhatia (1983) found that the Cambrian Charney Sandstone of Quebec, an albite-rich passive margin deposit, also plots outwith its expected field on the discriminant diagram, in the field for Continental Island Arc Sandstones. It is possible that the composition of passive margin sands, particularly in syn-rift settings where rift marginal uplifts still dominate the sediment provenance, are too complex to be rationalised by a simple discriminant procedure.

6.4.6 Major and Trace Element Chemistry of Sedimentary and Metasedimentary Clasts - Conclusions

1. The sedimentary and metasedimentary clasts dispersed from opposite flanks of the Crawton Basin are geochemically distinct. As clasts of chlorite grade metasediment occur in conglomerates of northerly and southerly provenance, the geochemical contrast can be established in sediments of similar metamorphic grade and overlapping grain size. The chlorite grade psammites of northerly provenance tend not to show the pervasive pressure solution cleavage seen in psammites of higher grade, and in this respect are similar to the clasts of southerly provenance. The distinction in the chemistry of clasts derived from opposite flanks of the basin must therefore be largely inherited from

original compositional difference between the two sequences which sourced the clasts.The basin must overlie a substantial crustal break along which the two disparate sequences were juxtaposed.

2. The first cycle clasts of chlorite-bearing psammite are compositionally related to the polycyclic metapsammite clasts of biotite and higher grade. Both are thought to have been derived from the same thick sequence of metamorphosed albite-rich sandstones. Slight compositional variation between metapsammites at differing metamorphic grades is possibly the result of an original vertical compositional gradient in the sequence prior to metamorphism. This may have included a sequence which became less mature upwards, but diagenetic effects were also possibly important. The fact that the clasts are of both first-cycle and recycled origin may however have introduced a spurious bias towards more mature clast compositions in the clasts of biotite and higher grade.

3. Psammite clasts of northerly provenance are unusually sodic, given their highly silicic compositions. This probably reflects a high original abundance of detrital Na-rich feldspar as opposed to albitisation or metasomatic Na enrichment. Coarse-grained Upper Dalradian metasediments are also rich in detrital albite and have a similar major element chemistry to the clasts. This is compatible with the psammitic clasts having an ultimate source in metasediments of the Dalradian Supergroup.

4. The lithic arenite and metagreywacke clasts derived from a now buried sequence of sediments located south of the Crawton Basin are characterised by an important mafic component. Compositional variation within the succession is indicated by the enhanced Cr contents (in some cases >700 ppm) and higher MgO in the metagreywackes. Assuming the metagreywackes to be older than the lithic arenites which are unmetamorphosed, the importance of the mafic/ultramafic component appears to be suppressed in the younger sediments. Cr in samples with >100 ppm Ni is assumed to have been largely introduced in high-Cr detrital phase resulting in an uncoupling of the bulk major element chemistry and Cr abundance.

5. The Cr rich metagreywackes are interpreted as having an important ophiolitic component in their provenance. An ophiolitic source also made an important contribution to sediments of the Highland Border Complex (Robertson and Henderson 1984), the Ordovician fore-arc basin at Girvan (Bluck 1983) and the Ordovician of the Southern Uplands (Kelling 1962). The abundance of ophiolitic detritus in Ordovician basins of northern Britain, and in correlative sequences in Newfoundland and the northern Appalachians (Hiscott 1984), indicates that the sedimentary sequence sampled by the clasts may also share this widespread Ordovician ophiolitic provenance.

6. The plate-tectonic setting in which the sediments accumulated to make up the thick metasedimentary succession to the north and south of the Crawton Basin cannot be resolved on the basis of the major element chemistry of the clasts derived from these sequences.

6.5 RB-SR SYSTEMATICS

6.5.1 Rationale

The application of Rb-Sr mineral and whole rock studies to sediments and metasediments has the potential to address three separate problems.

1. Isotopic equilibration is known to take place in both diagenetic and metamorphic environments and it is therefore possible to place age constraints on the time elapsed since isotopic homogenisation of strontium in sedimentary rocks. Many sediment sequences, particularly fine-grained siltstones and mudstones, have been shown to produce acceptable whole rock isochrons (e.g. Moorbath 1969). Without additional criteria it is however difficult to assess with confidence what event the isotopic system is recording, as initial homogenisation is not necessarily associated with deposition but may result from diagenesis, structural deformation or recrystallisation during incipient metamorphism. In addition, equilibration may be incomplete so that older detrital components are not homogenised and yield ages older than the depositional age of the sediment. Another possibility is that coarse-grained rock types less susceptible to complete homogenisation may produce spurious isochrons which reflect internal binary mixing of detritus from two isotopically distinct source regions (Graham 1985).

2. The strontium isotopic composition of coarse-grained sediment can be used to constrain the sediment provenance as the initial $^{87}Sr/^{86}Sr$ ratio is sensitive to the addition of young mantle derived volcanic detritus. The strontium isotopic composition becomes a particularly powerful technique in elucidating sediment provenance when combined with Sm/Nd systematics.

3. The Rb-Sr mica-whole rock system in metasedimentary rocks allows the timing and rate of uplift following deep burial to be established. As uplift produces high relief from which large volumes of sediment may be distributed to basins contiguous with the uplift, establishing the uplift history encoded in the fill to a basin addresses fundamental questions concerning the timing

of vertical movements in the source. Most important of these is whether source uplift and basin filling were contemporaneous, as a major distinction must be drawn between basins which are synchronous with uplift, the traditional molasse basins, and those which are not, reflecting reworking of material introduced to the uncratonised sediment mass (i.e. that part of the total sediment mass not locked up in stable cratonic areas) at some earlier time.

The results of Rb-Sr whole rock and mineral analyses for sedimentary and metasedimentary clasts are presented and discussed below. Four northerly derived clasts of biotite-muscovite psammite were sampled from the top of the Crawton Group at Crawton (3150, 3201) and at Whitehouse, south of Gourdon (3192, 3195). In addition, two further samples are considered, one from the Dunnottar Group at Dunnottar Castle (DUN 1), and an additional sample from Crawton (CR 1). These latter samples were analysed by A.N.Halliday, and together with the data from the present study, and data from other metamorphic clasts from both the Lower and Upper ORS conglomerates of the western Midland Valley, form part of a wider collaborative project in association with B.J.Bluck and R.M.McIntyre (Halliday et al. in prep.). The chlorite grade psammites have not been sampled for isotopic work as although they contain muscovite, a substantial proportion is detrital nd may not have been fully equilibrated. The object of this part of the study was to firstly characterise the uplift history of the metamorphic detritus of northerly provenance filling the Crawton Basin; secondly, to compare the chronology of uplift determined for the detritus with that of the well constrained uplift history of the adjacent Dalradian metamorphic rocks established by Dempster (1984, 1985); and thirdly, to provide a thermal framework for the interpretation of the granite clast data discussed in the previous chapter. As the dating of the granite clasts relies heavily on mineral isochrons it is critically important that the thermal history of the metamorphic rocks into which the granites were emplaced is understood, in order that spurious uplift related cooling effects can be distinguished from emplacement related isotopic closure of the mineral and whole rock systems.

A total of eight greywacke and metagreywacke clasts of southerly provenance have also been analysed for Rb-Sr isotopes. The clasts analysed encompass the full chemical range and therefore should provide a close estimate of the range in strontium isotopic compositions. These can be used to compare the thick sequence which sourced the clasts with other sequences, for example, the Southern Uplands, and also with the clasts of northerly derivation. As the southerly derived granites contain xenoliths of the hornfelsed sediment country rocks, the strontium isotopic composition of the country rocks, when combined with that of the granites, places limits on the volumes of bulk crustal assimilation that the granites can have undergone at high level.

6.5.2 Uplift History of Northerly Derived Metamorphic Detritus

6.5.2.1 Significance of Mica - Whole Rock Closure Ages.

The interpretation of mineral ages from metamorphic rocks relies on the theory of closure or blocking temperatures to predict the temperature, and hence depth that a mineral phase closes to the relevant isotopic exchange. Whilst whole rock systems may record equilibration during peak metamorphism, mineral - whole rock systems are sensitive to the history of uplift following the metamorphic climax, and, providing a range of mineral phases and isotopic systems with different closure temperatures are used, the time-integrated cooling history of an unroofed metamorphic terrane can be established.

Dodson (1973) defined closure temperature as the temperature of a mineral at the time given by its apparent age. The closure temperature therefore records the transition from open to closed system behaviour in a down-temperature direction. Theoretical considerations predict that the temperature at which a mineral phase closes is controlled by activation energy, effective grain size and cooling rate. Consequently it is unrealistic to expect that there is an absolute value for the blocking temperature of a given isotopic system in a specific phase. However, many multi-isotope studies using several mineral phases have shown that the same relative order of closure, indicating that whilst the

closure temperatures may not be absolute (Cliff 1985 notes probable variations up to 100°C in the closure of biotite), the relative closure temperature estimates are reasonably accurate.

Cliff (1985) outlines the basis for biotite closure temperatures. Quantitative estimates are mostly based on geological case studies, many in contact aureoles where thermal gradients can be modelled (Hart 1964, Hanson and Gast 1967), but also in metamorphic belts where metamorphism of varying grade overprints and partially reworks an older mineral closure event (Purdy and Jager 1976, Wagner et al.1977). The latter studies suggest the closure temperatures for both Ar and Sr in biotite are in the range 300°C ± 50°C with little difference between the estimated closure of the two systems. Verschure et al.(1980) argue that the biotite closure temperatures may be higher than those estimated from the Alpine metamorphic rocks as c 870 Ma Sveconorwegian biotite coexist with biotites of Caledonian age (c 400 Ma) in southern Norway. This implies that biotite growth took place actually below the blocking temperature for strontium and argon. This was probalby not lower than 400°C, as biotite growth is unlikely to occur at temperatures much below this. Frey et al.(1980) also propose that biotite may survive to as high as 400°C without being isotopically re-equilibrated.

An underlying assumption in determining the closure age from thermal overprinting relations is that the system behaves similarily in both up- and down-temperature directions i.e. the `opening` temperature is the same as the `closing` temperature. This is not necessarily the case, as even a single kinetic process will be sensitive to the rate at which it is heated or cooled (Cliff 1985), and it is unlikely that the time-integrated up- and down-temperature thermal history will follow exactly the same path. For example, collision related crustal imbrication or ophiolite obduction may lead to rapid crustal thickening and heating whilst subsequent uplift and unroofing may proceed at an altogether slower rate.

For the purposes of this study the biotite and muscovite closure ages presented by Jager (1979) have been adopted. These are

based on the relationship between mineral resetting and metamorphic isograds in the Central Alps. Closure estimates for biotite and muscovite are 300 and 500 ± 50°C respectively for the Rb-Sr system, and 300 and 350 ± 50 respectively for the K-Ar system.

6.5.2.2 Analytical Results

In Table 6.5, the Rb-Sr concentrations and isotopic data are presented for whole rock samples together with their constituent biotites and/or muscovite mineral separates. These include four clasts analysed by A.N.Halliday, one each from the Dunnottar and Crawton Groups, and two from the Lower ORS exposed at Ardmore Point in the western Midland Valley. In addition to the Rb-Sr data, R.M.McIntyre has provided K-Ar mineral-age determinations which have been included in Table 6.5, together with Rb-Sr mineral-whole rock apparent ages calculated for each mineral separate. Rb/Sr ages range from 385 ± 4 Ma to 585 ± 14 Ma.

6.5.2.3 Interpretation of the Rb-Sr mineral-whole rock data

The youngest biotite age, 385 ± 4 Ma for BJB/D, a clast sampled from the Lower ORS at Ardmore Point, is anomalously young and must either reflect a later hydrothermal resetting event or some deficiency in the mineral-whole rock cooling age principle. The latter is suggested by the corresponding K-Ar age of 451 ± 9 Ma. This is comparable to K-Ar mineral ages determined from biotite separates from other Lower ORS clasts and does not appear to have been disturbed during the Devonian. Similarly, the oldest closure age, a muscovite from BJB/C is associated with a normal K-Ar age suggesting the range of Rb-Sr mineral-whole rock ages has been enhanced in a systematic fashion, but the K-Ar system has remained undisturbed.

The calculation of mineral-whole rock ages assumes equilibrium between the mineral in question and the whole rock at the time of closure. The whole rock is therefore used to correct for the common strontium in calculating the closure age of each of the phases. However as the mineral phases close at different temperatures, the true isotopic composition of the strontium that

SAMPLE	Rb(ppm)	Sr(ppm)	$^{87}Rb/^{86}Sr$ (atomic)	$^{87}Sr/^{86}Sr \pm 2\sigma m$	Mineral -wr Apparent age (Ma)	K(wt%)	Rad ^{40}Ar (%)	Rad ($x10^{-9}$mol. g^{-1})	K-Ar age (Ma)
Crawton Group, Lower ORS									
*CR1 wr	36.06	105.0	0.9963	0.73215 ± 2					
*CR1 b	453.2	8.671	167.6	1.81360 ± 5	456 ± 5	7.89	98.5	6.775	438 ± 9
*CR1 m	150.3	17.99	24.58	0.88598 ± 4	458 ± 5	8.26	97.2	7.546	462 ± 9
3150 wr	59.27	129.5	1.327	0.72971 ± 4					
3150 b	348.0	13.17	80.39	1.23129 ± 8	445 ± 5				
3150 m	176.0	54.07	9.489	0.78367 ± 5	464 ± 5				
3195 wr	35.25	153.1	0.6669	0.72296 ± 3					
3195 b	301.2	19.14	46.92	1.02143 ± 6	453 ± 5				
3195 m	95.63	196.6	1.410	0.72916 ± 6	585 ± 14				
3201 wr	38.02	183.9	0.5992	0.72377 ± 7					
3201 b	385.4	35.02	32.53	0.92867 ± 4	450 ± 5				
3192 wr	25.99	124.1	0.6071	0.72400 ± 3					
3192 b	312.4	27.54	33.55	0.93523 ± 6	450 ± 2				
Dunnottar Group, Lower ORS									
*DUN1 wr	49.47	47.36	3.032	0.74099 ± 2					
*DUN1 b	224.3	6.578	105.4	1.39987 ± 5	452 ± 5	6.57	97.6	5.656	438 ± 9
*DUN1 m	180.3	38.12	13.83	0.81345 ± 13	471 ± 6	8.06	94.8	7.034	444 ± 9
Lower ORS, Ardmore Point									
*BJB/Cwr	5.514	19.51	0.8192	0.72712 ± 13					
*BJB/Cm	210.1	66.50	9.220	0.79767 ± 2	589 ± 7	5.93	96.4	5.156	442 ± 8
*BJB/Dwr	24.96	35.88	2.017	0.73168 ± 5					
*BJB/Db	324.9	50.20	18.94	0.82440 ± 12	385 ± 4	5.14	86.9	4.569	451 ± 9
*BJB/Dm	203.6	48.69	12.20	0.79870 ± 15	462 ± 6	7.25	97.4	6.318	443 ± 9

Table 6.5. Mineral and whole rock Rb-Sr and K-Ar results for northerly derived psammitic clasts. * Rb-Sr data from A.N.Halliday. K-Ar data from R.M.MacIntyre. Decay constants used in age calculations are those recommended by Steiger and Jager (1977).

the relevant mineral phase last equilibrated with is never certain. If a rock cools quickly, all the minerals will effectively exchange with Sr of the same $^{87}Sr/^{86}Sr$, and a mineral-whole rock isochron age will correspond to the closure of the system. However, if the rock cools slowly, the mineral-whole rock age is only an approximation of the closure temperature as the sequential closure of phases down-temperature progressively bias the Sr isotopic composition in the phases which remain open to exchange. Muscovite, which closes first for Rb-Sr, probably most closely approximates exchange with the whole rock isotopic composition (Jager 1979).

Bearing in mind the uncertainty in the strontium isotopic composition with which the mineral last equilibrated, the magnitude of the common strontium correction applied to a mineral phase becomes important. If the amount of common strontium in a mineral is small, the apparent age is relatively insensitive to the fact that the whole rock isotopic composition only approximates to the strontium isotopic composition with which the mineral last equilibrated. However, if the amount of common Sr is large, considerable error will be introduced by both the poor control on the whole rock-mineral isochron slope (as the points will plot close together on an isochron diagram) and the possibility that the whole rock does not represent the actual isotopic composition of the strontium with which the mineral last equilibrated.

The influence of the variable importance of the common strontium correction in a set of mica-whole rock closure ages can be assessed by plotting the apparent mica-whole rock age (a two-point isochron age) against the Rb/Sr weight ratio, or the Sr content, of the mica phase used in the age computation (Halliday pers. comm. 1984). Figure 6.14 shows the apparent closure age data for the clasts plotted against both the Rb/Sr ratio and Sr content of the relevant mica phases. Two additional biotite-whole rock points have been included on the plots. These are clasts from the Upper ORS in the Firth of Clyde basin (Halliday et al in prep.). For comparative purposes, mica cooling ages have been plotted for a transect

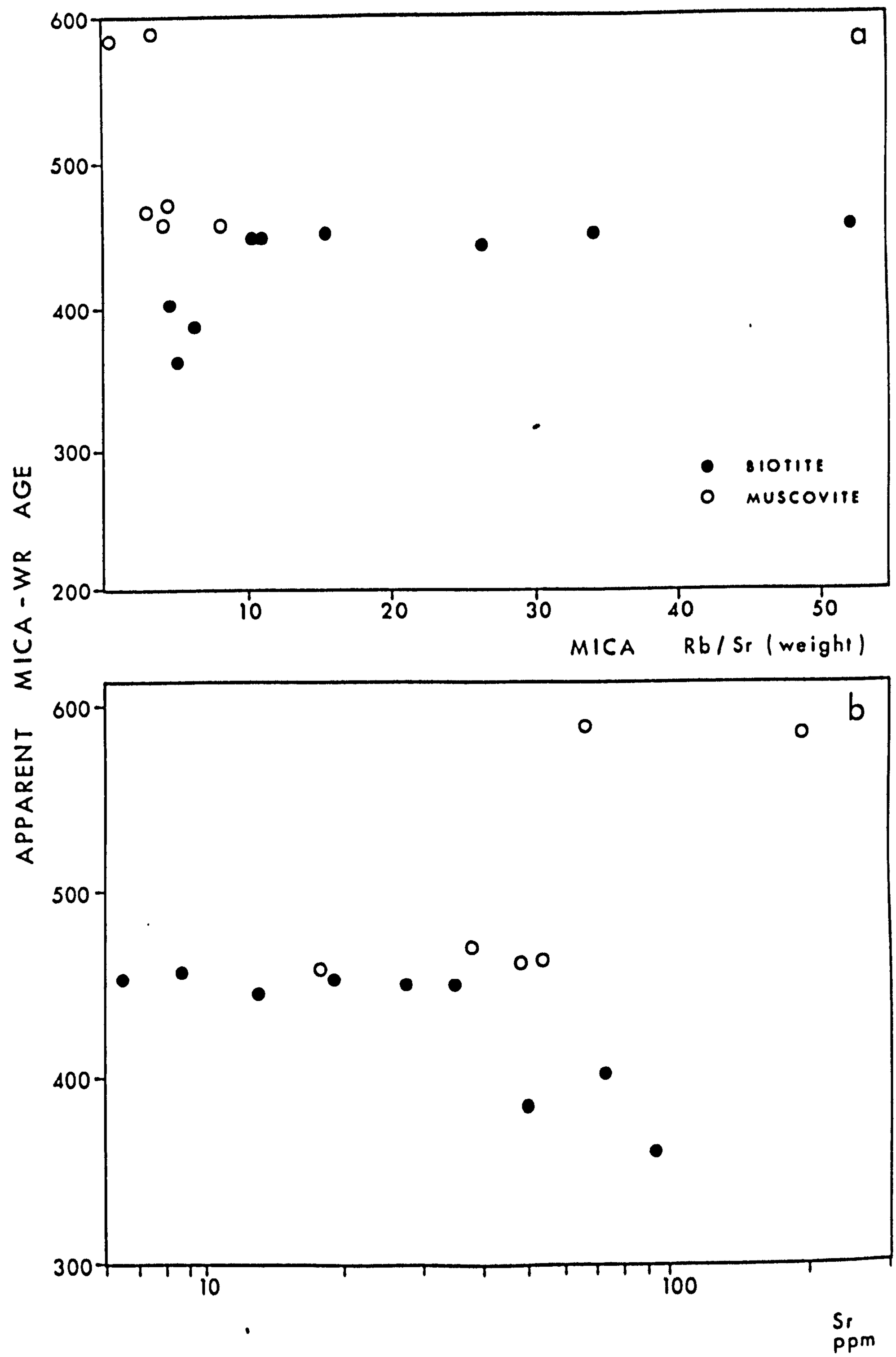

FIGURE 6.14 Apparent mica-whole rock closure ages plotted against the Rb/Sr weight ratio (a) and Sr content (b) of the mica phase used in the age computation.

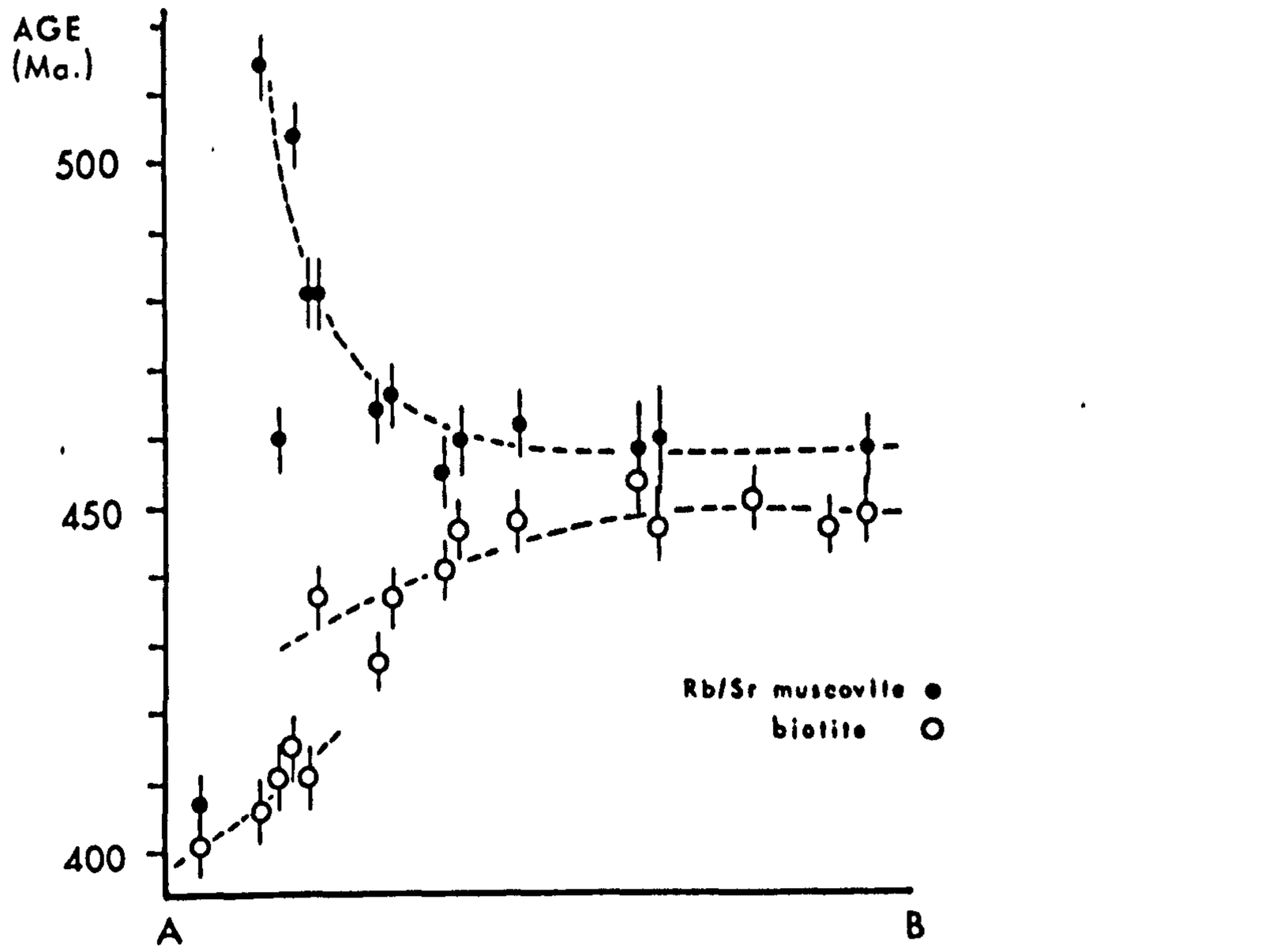

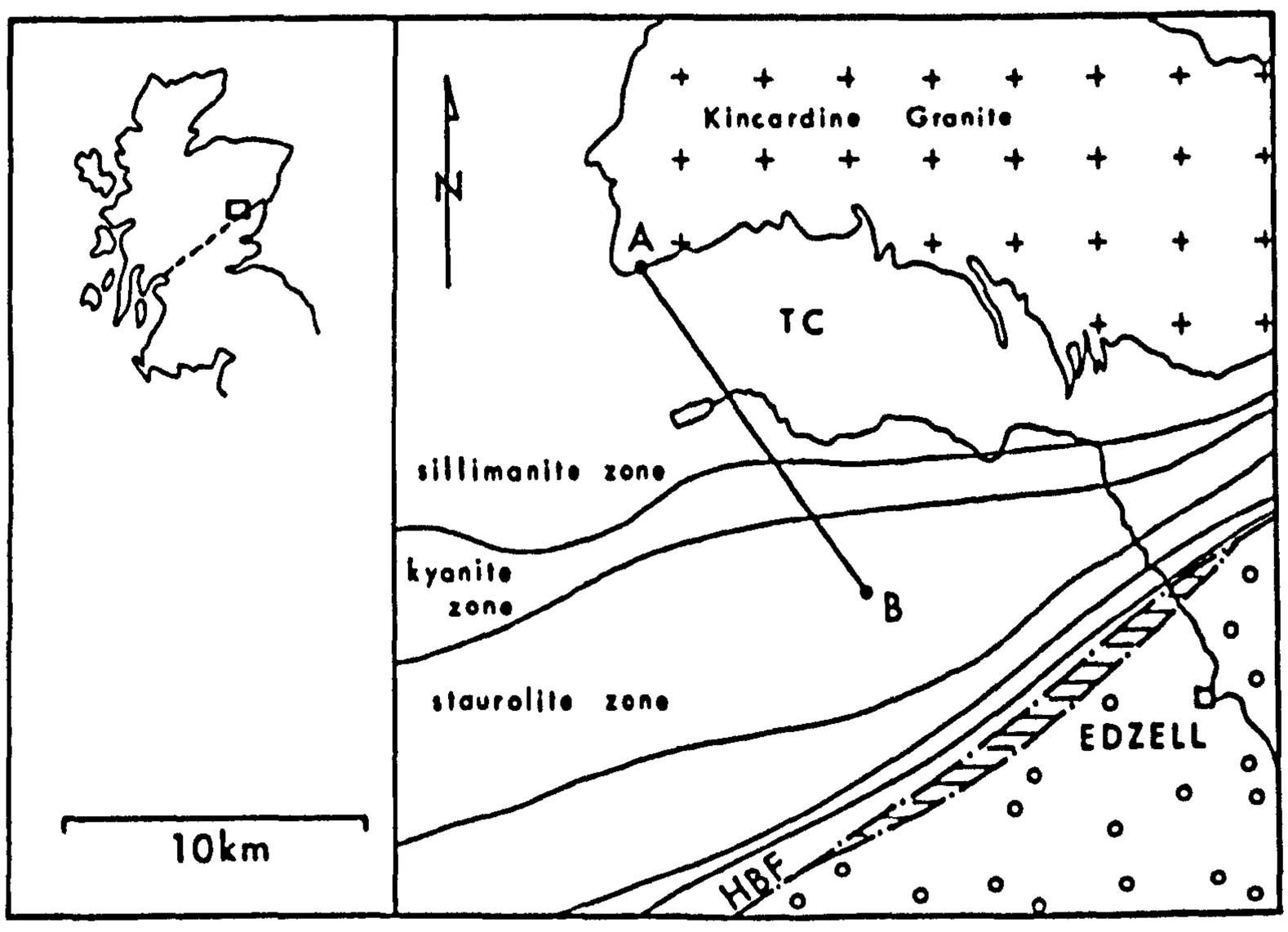

Figure 6.15 Rb-Sr mineral closure ages from a traverse across Dalradian metasediments of the Angus region. Data from Dempster (1984). Abbreviations are: HBF, Highland Boundary; TC, Tarfside Culmination.

across the adjacent Dalradian metamorphic rocks (Dempster 1985), and the resulting graph is shown in Figure 6.15.

The plots of apparent age, against mica Rb/Sr and Sr contents highlights a systematic pattern in the behaviour of the Rb-Sr closure ages. The importance of the common Sr correction is confirmed, with closure ages for micas with low Sr contents and high Rb/Sr ratios tightly clustering about a mid-Ordovician age. In contrast to micas with higher Sr contents and lower Rb/Sr ratios produce a scatter of spurious ages both higher and lower than the more reliable ages given by the low Sr micas. The apparent ages indicated by the high Sr micas do not however scatter about the low Sr mica apparent ages in a random fashion. They show a systematic displacement of muscovite to higher ages and biotites to lower ages, indicating that the scatter is not solely due to the poorer control on the isochron consequent on the micas and whole rocks having comparable Rb/Sr ratios.

The consistently high muscovite closure ages for high Sr micas suggests that the strontium with which the muscovite last equilibrated was more radiogenic in composition than the whole rock, whilst the lower biotite ages must have equilibrated with less radiogenic strontium. This suggests that the muscovite, although it was the first phase to close with Sr exchange, did not equilibrate fully with the whole rock, but must have done so more locally. A striking feature of the psammitic clasts is the almost ubiquitous presence of a well developed spaced pressure solution cleavage in which the micas are concentrated (6.3). These form micaceous laminae which are laterally extensive and show a remarkably constant spacing, separating zones which are dominated by recrystallised mosaics of quartz and feldspar. The anisotropic nature of the rocks may have been instrumental in creating isotopic disequilibrium between the mica-rich cleavage seams and the intervening quartz-feldspar mosaics as the system cooled towards the muscovite closure temperature at 500°C.

A rock containing minerals with a range of Rb/Sr ratios will maintain isotopic equilibrium between the constituent mineral phases only if Sr is being exchanged relatively freely between

the phases, that is, if exchange is more rapid than the rate at which daughter products are generated. The loss of radiogenic isotopes from a mineral phase probably involves volume diffusion in which the rate of loss depends on the size of the mineral grain, or some smaller volume, and the diffusion is controlled by imperfections, dislocations and cleavage fractures in the mineral (Dodson 1979). The process of exchange is probably greatly enhanced by the presence of a fluid phase. The concentration of both biotite and muscovite in laterally extensive micaceous pressure solution seams, through which fluids may have moved, would have facilitated exchange and partial isotopic equilibrium along the micaceous domains prior to closure of muscovite to strontium diffusion. This would account for the more radiogenic strontium compositions the muscovite is inferred to have equilibrated with as it would dominantly have exchanged with biotite with which it is intergrown. Following closure of muscovite, biotite continued to exchange, down to its closure temperature at 300^{o}C, with low Rb/Sr phases unrepresentative of the whole rock composition.

6.5.2.4 Significance of Cooling Ages for Low-Sr Micas

Micas with Sr contents less than 50 ppm Sr are considered to give reliable apparent mineral-whole rock ages free from the complications introduced by the common strontium correction discussed above. The four low Sr muscovites yield a range of ages from 458 to 471 Ma with a mean of 463.7 Ma, whereas the six low Sr biotites have a range of apparent ages from 445 to 456 Ma, with a mean of 451.0. The apparent ages determined from the biotites are significantly younger than those from the muscovites in accordance with the predicted down-temperature closure of the two systems.

Assuming a 30^{o}C/km geothermal gradient, muscovite and biotite closure temperatures of 500 and 300^{o}C respectively, and a 12 Ma interval between closure of the muscovite and biotite phases in the clasts, a crude estimate of the rate of cooling and uplift can be calculated. A cooling rate of 17^{o}C per million years converts to an uplift rate of 0.6mm per year. This is broadly comparable to rates of uplift determined from other orogenic

belts : 0.2-1.0 mm/a for the Himalayas (Zeitler et al.1982), 0.5 mm/a for the Alps (Schaer et al.1975) and 0.2-0.4 mm/a for the Andes. The uplift rates therefore indicated by the cooling ages are the right order of magnitude for orogenic belts.

A comparison of Figures 6.14 and 6.15 demonstrates a comparable pattern of uplift and cooling in both the clasts and the adjacent Dalradian. Dempster (1984, 1985) showed a diachroneity in both metamorphism and cooling across the thermal strike of the Dalradian metasediments of the Angus region. The oldest mineral ages, and hence earliest cooling, occur in rocks found in the highest metamorphic zones, situated to the north. These cooling ages are in excess of 500Ma. Significantly, no reliable older cooling ages have been established from the clast micas. However, south of the Tarfside culmination, the Dalradian rocks do show a pattern of Rb/Sr closure ages for muscovite at 460Ma and biotite at 450Ma. If the psammitic clasts are in fact derived from the Dalradian, the lack of older uplift ages in excess of 500Ma is curious. Two factors may contribute to a bias in the clasts in terms of the uplift history they record.

Firstly, the model presented in Section 5.7 envisages an important role for deep molasse basins in withholding proximal molasse dispersed late in the history of orogenic unroofing. Early molasse sediment cannot be expected to be preserved on the metamorphic terrane itself. The preservational potential of basins located within the confines of the uplifting terrane increases as uplift wanes and extensional spreading takes over. The pre-existing basins from which material was redistributed to the Midland Valley were therefore probably enrichd in detritus associated with the later and youngest phases of post-orogenic uplift. A second factor suggesting the clasts are not unrepresentative of the range of uplift ages seen in the adjacent Dalradian is the relative rarity of uplift ages >500Ma received from the Grampian Highlands.No more than 15% of Dempster`s (1985) Angus transect contains muscovite Rb/Sr ages in excess of 480Ma, whilst the Perthshire traverse shows no muscovite Rb/Sr apparent ages greater than 480Ma apart from those in the chlorite zone which are likely to include a detrital component. It is quite

possible that the small number of analysed clasts has failed to identify an older uplift component which is only present in low abundances. The uplift data, as they stand, are quite compatible with a source for the clasts in the adjacent Dalradian Southern Highlands Group. The comparable uplift ages imply the clasts cannot have been derived from any great distance above the present-day Dalradian surface, as rocks higher in the metamorphic pile would have older uplift ages consequent on their cooling through the relevant closure temperatures at an earlier time. For example, assuming an erosion rate of 0.6 mm/a rocks 6km above the present day surface would have muscovite and biotite closure ages of 470 and 460 Ma respectively (N.B. crude calculations of this nature ignore the very complex pressure-temperature paths of orogenic rocks and assume rates are constant).

The large time interval, some 40-50 Ma, between deposition of the conglomerates containing the metamorphic clasts, at probably no more than 410 Ma, and rapid uplift of the source which supplied the detritus at 450-460 Ma, suggests there is no genetic relationship between orogenic uplift and ORS sedimentation. True molasse basins, i.e. those continuous to mountain belts formed during orogeny, should show a more intimate temporal association of detritus and uplift.

6.5.2.5 Implications for the Accompanying Granite Clasts

The metamorphic clast uplift ages are of some significance to the interpretation of the accompanying two-mica granite clasts. The poorly homogenised initial strontium compositions of the two-mica granites preclude the use of whole rock isochrons to establish their emplacement ages. Mineral-whole rock isochrons are therefore the only viable method of constraining the likely emplacement ages using the Rb-Sr system. Mineral-whole rock studies on single clasts are at any rate preferable to methods using combinations of clasts which cannot be confidently referred to a single comagmatic source.

The coincidence of the metamorphic clast closure ages with the inferred emplacement of the granite clasts at c 460 Ma is significant. There are two possibilities. Firstly, the granites were intruded at some earlier time at deep level, and were subsequently uplifted as an integral part of the metamorphic rocks they intrude. Alternatively, granite emplacement and rapid uplift may have proceeded hand in hand, reflecting an underlying relationship between rapid uplift and granite injection. In the first case, granite mica-whole rock apparent ages will reflect a cooling pattern indistinguishable from the metamorphic rocks they intrude. In the latter case, assuming the granites were intruded into country rocks at less than 300°C, the cooling pattern will be out of phase with the metamorphic rocks, as the granite melt rapidly thermally equilibrates with the cooler country rocks. By comparing the cooling pattern in both metamorphic and granitic clasts it should therefore be possible to distinguish whether the granite magmatism accompanied, or preceded, the uplift.

Figure 6.16 compares the apparent age data for the psammitic and two-mica granite clasts, and includes additional data from the two-mica granites of the Dunnottar Group (Van Breemen and Bluck 1981). Direct comparison of the data is complicated by the much coarser grain size of the granite micas with respect to those in the psammitic clasts which typically range from 100-400 um. As mineral closure to exchange is probably a diffusion controlled process, closure temperatures are likely to be in part controlled by grain size and chemistry. Notwithstanding these non-temperature related effects, some general conclusions can be drawn on the basis of Figure 6.16.

The psammite clasts show a general separation of the muscovite and biotite closure ages in excess of the experimental errors. CR1 is the only exception with muscovite and biotite apparent ages of 458 and 456 Ma respectively. The granites, in contrast, generally have an insignificant separation of muscovite and biotite apparent ages e.g. 3134, 3220 and 1917. Only muscovite analyses are available for 1916 and 1920, and their cooling pattern cannot be resolved. The biotite apparent age in clast 1919 is anomalously low, and Van Breemen and Bluck (1981)

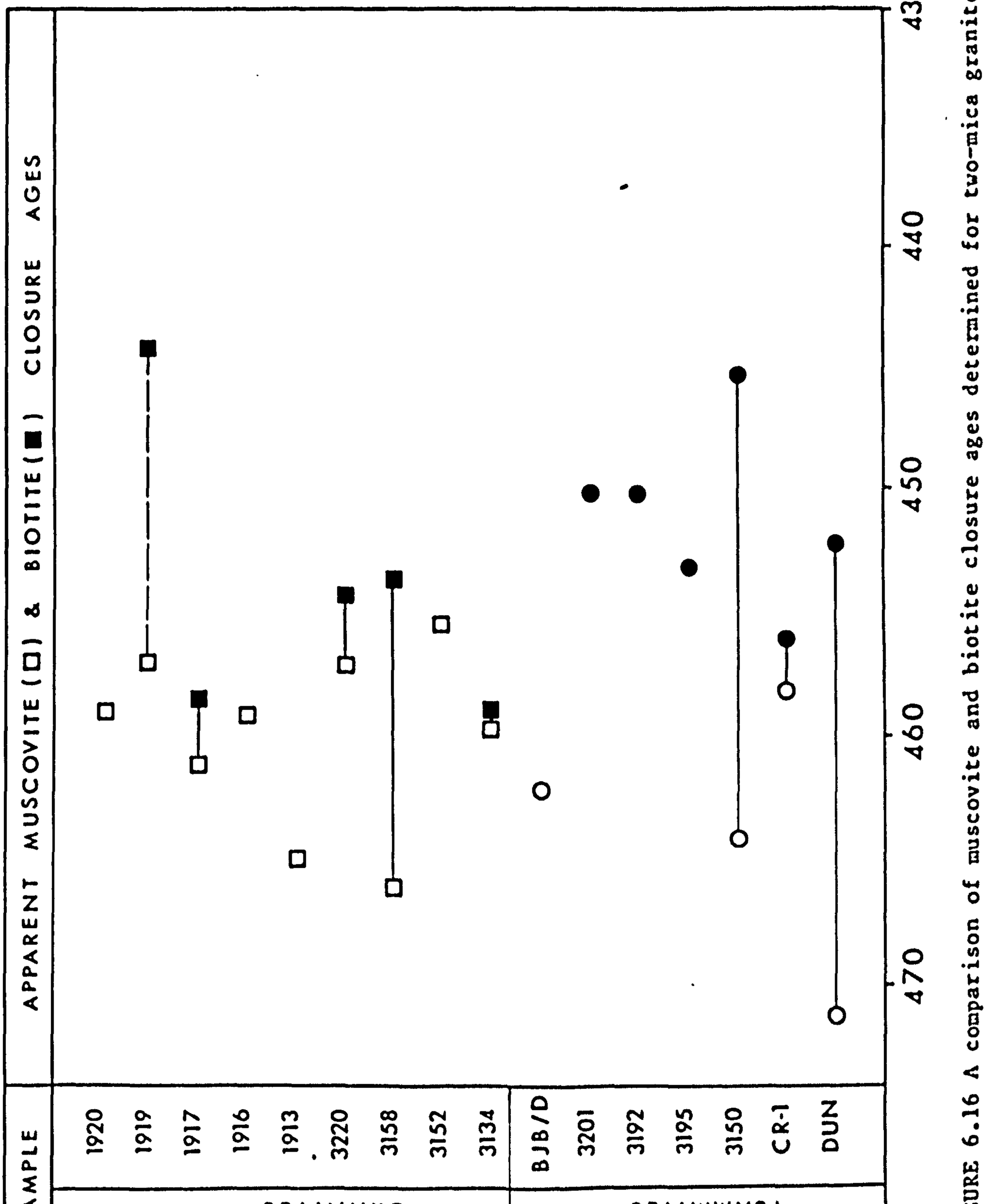

FIGURE 6.16 A comparison of muscovite and biotite closure ages determined for two-mica granite and psammite clasts of northerly provenance.

interpret the younger scattered biotite ages (the biotite in 1913 is also low, at 421 ± 5 Ma), as reflecting partial resetting during chloritisation. These biotites consequently are unlikely to record true closure ages. Clast 3158 stands out amongst the granite clasts in showing a cooling pattern comparable to that shown by the psammite clasts. Significantly, 3158 is the one strongly foliated clast, and it was also the first granite to cool below 500°C.

The concordance of muscovite and biotite ages in clasts 3134, 3220 and 1917 indicates that they must have been emplaced into country rocks which were at temperatures of less than 300°C, the blocking temperature for biotite. Some of the two-mica granite clasts preserve xenoliths of chlorite-rich greenschist facies metasediment, confirming that some of the granites were probably intruded into the metamorphic pile at a higher (and cooler) level than that sampled by the biotite psammite clasts. As they cooled rapidly, in relatively cool country rocks, the concordant mica ages are best interpreted as recording the age of emplacement. The strongly foliated two-mica granite, 3158, was one of the first granites to be emplaced, and may have intruded country rocks which were still at elevated temperatures and consequently its cooling history was controlled by that of the metamorphic rocks it intrudes. The strong foliation confirms a more ductile history.

The uncoupled Rb-Sr cooling histories of granite and psammite clasts allow greater confidence in the interpretation of the granite emplacement ages. These are thought to overlap with a period of rapid uplift of the metamorphic country rocks with granites emplaced both below and above the 300°C isothermal surface at which biotite closes.

6.5.3 Rb-Sr Isotope Geochemistry of Southerly Derived Metagreywacke and Greywacke/Lithic Arenite Clasts

Table 6.6 presents isotope dilution Rb and Sr concentration data, isotope ratios, and initial and epsilon strontium values for the southerly derived clasts. The data include 4 metagreywacke clasts (4260, 4261, 4255, and 4319) and 4 unmetamorphosed lithic

SAMPLE	Rb	Sr	Rb/Sr	$^{87}Rb/^{86}Sr$	$^{87}Sr/^{86}Sr$	$Sr_{i(416)}$	$Sr_{i(460)}$	ϵSr_{416}	ϵSr_{460}
4261	49.15	54.05	0.91	2.637447	0.73235 ±5	0.71672 ±16	0.71507 ±18	180.7	157.9
4260	55.13	59.39	0.93	2.69293	0.73334 ±3	0.71738 ±16	0.71569 ±18	190.1	166.8
4255	44.01	54.40	0.81	2.34554	0.72872 ±4	0.71482 ±14	0.71335 ±16	153.7	133.5
4238	25.97	83.80	0.31	0.89747	0.71633 ±15	0.71101 ±16	0.71045 ±16	99.6	92.3
4273	40.13	70.14	0.57	1.65870	0.72748 ±4	0.71765 ±11	0.71661 ±12	193.9	179.8
4264	45.63	76.45	0.60	1.73002	0.72672 ±4	0.71647 ±11	0.71538 ±12	177.1	162.4
4271	55.70	53.99	1.03	2.99390	0.73677 ±2	0.71903 ±17	0.71715 ±20	213.5	187.5
4319	29.98	104.17	0.29	0.83333	0.71521 ±6	0.71027 ±8	0.70975 ±8	89.1	82.4

Table 6.6. Rb-Sr analytical data and calculated isotopic compositions for lithic arenite and metagreywacke clasts of southerly provenance. Initial isotopic compositions and epsilon strontium values calculated at 416 and 460 Ma. Rb and Sr concentrations in ppm.

arenite clasts (4238, 4264, 4271, and 4273).

The interpretation of the strontium isotopic data is complicated by the uncertainty in the stratigraphic age of the sediments and metasediments from which the clasts were derived. Limestone clasts accompany the lithic arenite and metagreywacke clasts. These are inferred to have an Ordovician age on the basis of their fossil content (Curry pers. comm. 1985). Whilst it is conceivable that the greywackes also share an Ordovician age there is also the possibility that they are considerably older.

The data are plotted on a conventional Sr evolution diagram in Figure 6.17. Available data for Southern Uplands greywackes (Halliday et al. 1980, Halliday 1984, P.Holden pers. comm.), Dalradian metasediments (Frost and O`Nions 1985) and the psammite clasts of northerly derivation (this study) are included for comparison. Reference isochrons for 450, 550, 650, and 750 Ma have been superimposed on the data.

The clasts clearly do not conform to a simple linear distribution indicating that complete equilibration of Sr was never acheived. Six of the eight clasts do however have a pseudolinear distribution with a slope close to the 650 Ma reference line. York regression of the six points gives an errorchron age of 666.5 $\pm$ 19.4 Ma with a MSWD of 28.7. Significantly, the two clasts displaced from the linear array are unmetamorphosed lithic arenites. Coarse-grained lithologies generally do not show early diagenetic-related Sr equilibration with the exception perhaps of some pyroclastic rock types. Priem et al.(1978) note that complete equilibration of Sr isotopes is possible in water-lain pyroclastics consequent on re-ordering and albitisation of feldspar. Dasch (1969) however showed little Sr equilibration in siliciclastic marine sediments, and Chandhari (1976) demonstrated that shales too can inherit source-related isotopic signatures which are not reset in the diagenetic environment. Anchizone and low-grade metamorphism are therefore the more likely processes responsible for complete or partial equilibration of coarser grained sediments. The operation of such processes in equilibrating the Rb-Sr systematics of sedimentary rocks has been

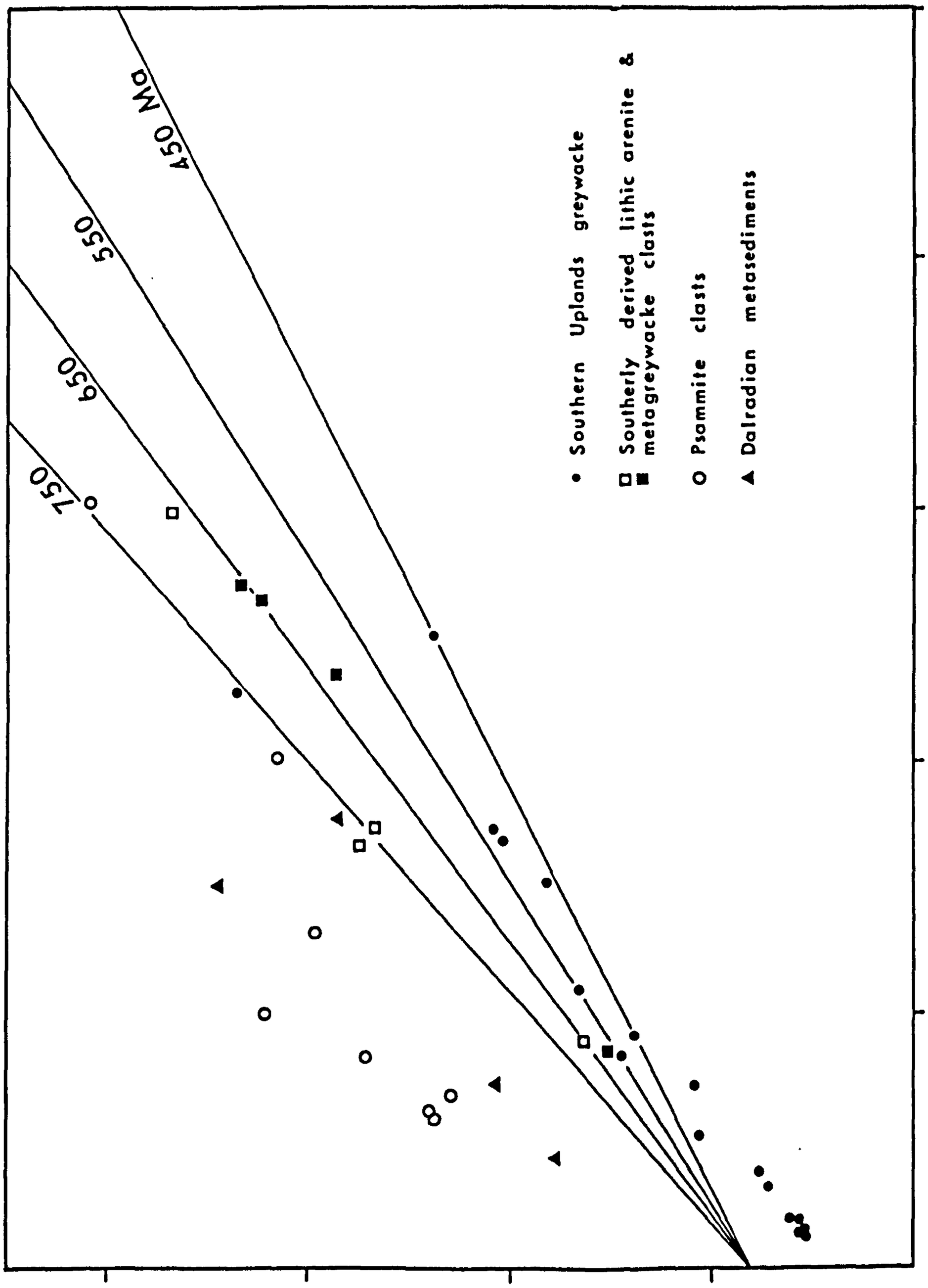

FIGURE 6.17 $^{87}Sr/^{86}Sr$ vs $^{87}Rb/^{86}Sr$ plot for Lower ORS sedimentary and metasedimentary clasts, together with data from the Dalradian (Frost and O'Nions 1985, Dempster 1985) and Southern Uplands (Halliday et al. 1980, Halliday 1984, P.Holden pers.comm.).

demonstrated by Gebauer et al.(1974). They show the least deformed parts of a series of Lower Palaeozoic sediments from the Montagne Noire (southern France) to yield scattered Rb-Sr data, whereas the more strongly deformed parts of the sequence produce linear data arrays on isochron plots, which give ages concordant with established ages for burial metamorphism and deformation. Graham (1985) similarly shows almost complete isotopic equilibration of interbedded argillites and coarse-grained greywackes during prehnite-pumpellyite to lower greenschist facies metamorphism.

The two greywacke clasts displaced to more radiogenic compositions than those lying on the linear trend are notably rich in detrital muscovite, which occurs in varying abundance in almost all the southerly derived greywacke and metagreywacke clasts. Gebauer et al.(1974) showed mineral separates from psammitic rocks at anchimetamorphic grade to have only partly equilibrated detrital micas but fully equilibrated albites. As the four metamorphosed clasts for which data are available scatter about an errorchron it is possible that the recrystallisation of the matrix under lower greenschist facies conditions has partially equilibrated the strontium isotopic compositions. Further sampling from the most strongly recrystallised and deformed clasts is required to explore this possibility further. Should the linear array reflect a recrystallisation event accompanied by partial Sr equilibration, the sediments may possibly be Pre-Cambrian in age.

Strontium equilibration is not however the sole mechanism whereby linear pseudoisochrons can develop. Graham (1985) shows that binary mixing of material from a composite provenance or unmixing of clays during transport and deposition of material from a homogeneous source may both lead to meaningless linear data arrays.

Unmixing of sediment is unlikely to have contributed to isotopic variation seen in the clasts as the samples analysed were all medium-grained greywackes which are poorly sorted, with no systematic covariation of texture with position on the

pseudoisochron. Mixing associated with a binary sediment source may be an important mechanism in combined metamorphic and plutonic or volcanic provenances with evolved quartzo-feldspathic continental detritus variably diluted with young and isotopically primitive volcanic material. As the volcanic material is chemically distinct, volcanic dilution should be relatively easy to identify in the major and trace element chemistry of the sediment.

Figure 6.18 compares the coupled isotopic and chemical variation in both the clasts and sediments from the Southern Uplands. The Southern Uplands data are from Thirlwall (1983) and Halliday et al (1980). The Ordovician and Silurian isotopic data have been normalised to 460 and 430 Ma respectively, to approximate the isotopic composition of the sediment at the time of deposition. An Ordovician age for the sequence from which the clasts were derived has been assumed and $(^{87}Sr/^{86}Sr)^{t}$ ratios recalculated to 460 Ma. Ni, Cr and $((Fe_2O_3)^{t} + MgO)$ are used to identify dilution with a basic volcanic component. $(^{87}Sr/^{86}Sr)^{t}$ correlates negatively with increasing Ni and Cr abundances, and to a lesser extent with increasing $((Fe_2O_3)^{t} + MgO)$, in the Southern Uplands sediments.

This is suggestive of a two component mixing process, with the Ordovician `basic` greywackes dominated by a provenance in a young basic volcanic source, rich in Cr and Ni, and with strontium isotopic compositions close to bulk earth. $(^{87}Sr/^{86}Sr)^{t}$ shows a general overall increase in $(^{87}Sr/^{86}Sr)^{t}$ southwards across the Southern Uplands consistent with an increase in acid-type continental detritus (Halliday et al.1980).

In contrast $(^{87}Sr/^{86}Sr)^{460}$ shows no coherent coupling with Ni or Cr in the clasts of southerly derivation, confirming the probable importance of minor phases in controlling the distribution of these elements. The relationship with $((Fe_2O_3)^{t} + MgO)$ is ambiguous but the clast with the lowest $(^{87}Sr/^{86}Sr)^{460}$ does have the highest $((Fe_2O_3)^{t} + MgO)$, suggesting mixing with a basic volcanic component may be important to the isotopic composition of strontium in the clasts.

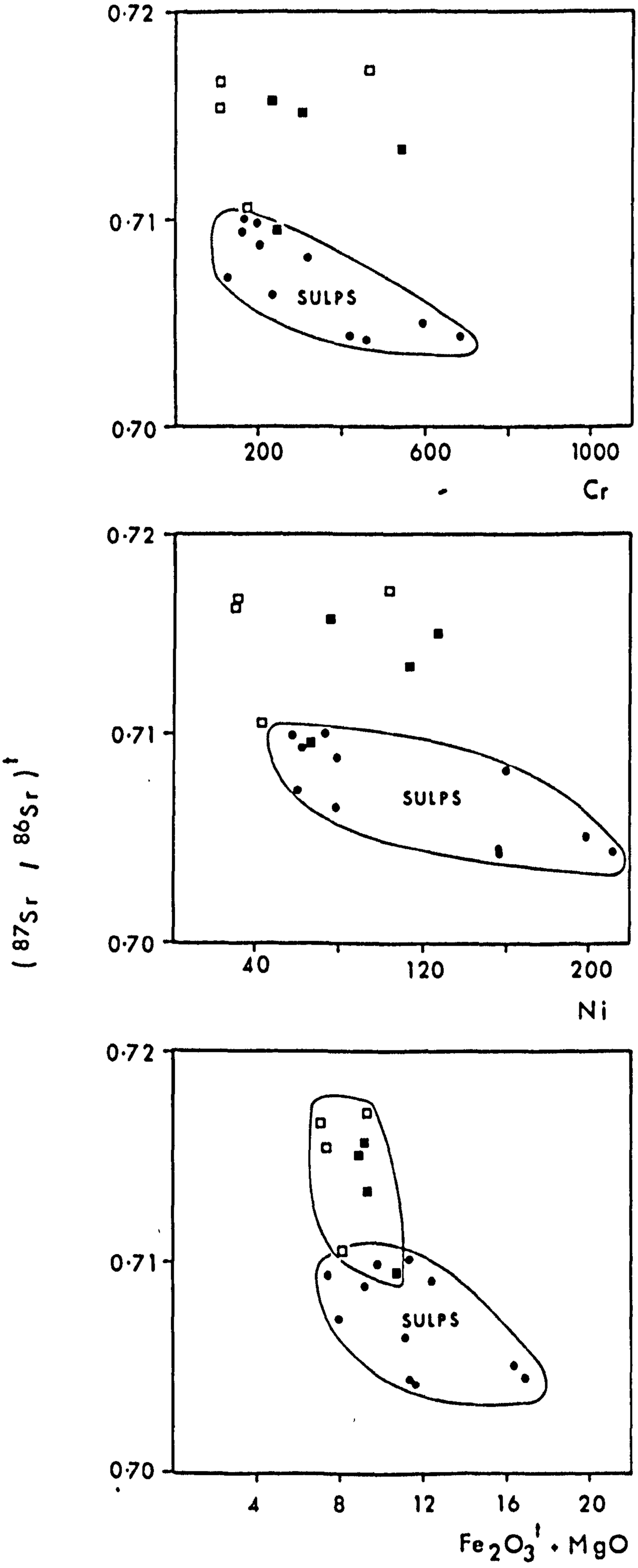

FIGURE 6.18 Coupled Sr isotopic and chemical variation in southerly derived lithic arenite (open square symbols) and metagreywacke (filled square) clasts compared to data for SULPS.

Figure 6.18 also serves to illustrate the generally more radiogenic character of the clasts when compared to the isotopic composition of SULPS. The clast data plot in a position intermediate between SULPS and isotopic data for the Dalradian metasediments. The latter shows a characteristic wide scatter indicating extremely heterogeneous isotopic compositions. The data obtained for the northerly derived psammitic clasts are also shown in Figure 6.18. These show a similar radiogenic and poorly homogenised signature to the Dalradian, strengthening the case for a derivation of the clasts from the Grampian Highlands terrane.

6.5.4 Rb-Sr Systematics - Conclusions

1. Mica-whole rock cooling ages determined from psammitic clasts occurring in northerly derived conglomerates suggest that uplift and cooling of the metamorphic terrane which shed the detritus occurred during the period 465-445 Ma. Micas yield average apparent ages of 463.7 Ma (n=4) and 451.0 Ma (n=6) for muscovite and biotite respectively. The uplift rate implied is typical of rates of uplift determined in other orogenic belts.

2. The mica closure ages for the clasts closely parallel the cooling pattern of Dalradian metasediments north of the Highland Boundary Fault. Should the clasts have been derived from the Dalradian, the data require that the clasts were sourced from close to the present-day erosion surface truncating the Grampian Highlands. The absence of clasts with older mica-closure ages (>500 Ma) may reflect either insufficient sampling to identify an older uplift component which is rare in the Dalradian cooling pattern, or a bias in the recycling process towards clasts with younger uplift ages.

3. The uplift pattern established for the metamorphic clasts cannot be recognised in the bulk of the two-mica granite clasts. This suggests that the granites do not record regional uplift of a terrane which they were emplaced into at some earlier time. The generation and emplacement of the two-mica granites is inferred to be synchronous with, and possibly triggered by, a

phase of rapid uplift and cooling.

4. The southerly derived lithic arenites and greywackes have more radiogenic Sr isotopic compositions than greywackes from the Southern Uplands, and less radiogenic compositions than the clasts of northerly derivation. The latter are isotopically comparable to Dalradian metasediments. Six of the clasts of southerly derivation fall on a pseudoisochron which gives an age of 666.4 Ma. This is most likely to reflect binary mixing and is of little significance.

6.6 SM-ND ISOTOPIC CONSTRAINTS ON SEDIMENT PROVENANCE

6.6.1 Concept

Different elements show a range of divergent behaviour as a consequence of varying degrees of fractionation during weathering, erosion and transport. The rare earth elements however show consistent distribution patterns in a variety of fine-grained clastic sediments indicating minimal fractionation of Sm/Nd during the formation of sedimentary rocks from their precursors (O`Nions et al.1983 and references therein). Major chemical fractionation (40%) of Sm/Nd is therefore only likely to accompany differentiation of material from the mantle and its incorporation into the continental crust. Minor fractionation of Sm and Nd is also expected during intracrustal melting events but this is subordinate to the fracitonation following initial extraction of the material from the mantle, and generally follows crustal formation by 100-200 Ma (Taylor and McLennan 1985). As the major fractionation of Sm and Nd can be attributed to a single discreet event, given both the present-day Sm/Nd ratio and the isotopic composition of a sample, and assuming various mantle parameters, a model age for the elapsed time since extraction of the material from the mantle can be calculated.

Both samarium and neodymium are rare earth elements. The ^{147}Sm isotope of samarium decays to ^{143}Nd with a half-life of 1.06 x 10^{-11} years (McCulloch and Wasserburg 1978). The $^{143}Nd/^{144}Nd$ ratio measured in a sample at the present time comprises both an original component inherited during the initial fractionation event, and a component derived from time-integrated accumulation of radiogenic ^{143}Nd since that event. This is described by the conventional radioactive decay equation:

$$(^{143}Nd/^{144}Nd)_p = (^{143}Nd/^{144}Nd)_i + (^{147}Sm/^{144}Nd)_p.(e^{\lambda T}-1) \qquad (1)$$

where p denotes the ratio measured in the rock today, T the elapsed time and λ the ^{147}Sm decay constant. If the evolution of $^{143}Nd/^{144}Nd$ isotopic compositions in the source reservoir is known or can be estimated, the time elapsed since extraction of the material, the crustal residence age, can be calculated.

Variations in the Nd isotopic compositions of terrestrial samples were first studied by DePaolo and Wasserburg (1976) who showed that $^{143}Nd/^{144}Nd$ compositions in the source of continental rocks of known stratigraphic age evolved with only minor deviation from the expected evolution of a reservoir with a chondritic Sm/Nd ratio.

This was taken to imply that the mantle reservoir which is the source of crustal rocks has a Sm/Nd ratio very close to the relative abundance found in a chondritic uniform reservoir or CHUR. This forms the basis for a widely used model age calculation, the t_{CHUR} age. The value of $^{143}Nd/^{144}Nd$ in CHUR at the present time is given by :

$$(^{143}Nd/^{144}Nd)^{P}_{CHUR} =$$

$$(^{143}Nd/^{144}Nd)^{T}_{CHUR} + (^{147}Sm/^{144}Nd)_{CHUR} (e^{\lambda T}-1) \qquad (2)$$

where $(^{143}Nd/^{144}Nd)^{P}_{CHUR} = 0.512638$, $(^{143}Nd/^{144}Nd)^{T}_{CHUR}$ is the $^{143}Nd/^{144}Nd$ ratio in CHUR at any time T in the past and $(^{147}Sm/^{144}Nd)_{CHUR} = 0.1966$. If a rock has been extracted from a chondritic uniform reservoir at time T, its initial Nd isotopic composition will be that of the reservoir at time T, but assuming the rock remains a closed system, and that the extraction of the rock from the reservoir involved a relatively large fractionation of Sm/Nd from the chondritic ratio, the isotopic composition of the rock and its CHUR source will show a divergent evolution.

Assuming a CHUR model applies to the mantle reservoir from which the continental crust is extracted the time of fractionation and deviation from a CHUR reservoir is given by :

$$T_{CHUR} = \frac{1}{\lambda} \ln\left[1 + \frac{\varepsilon_{Nd(o)}.(^{143}Nd/^{144}Nd)^{P}_{CHUR}.10^{-4}}{f_{Sm/Nd}.(^{147}Sm/^{144}Nd)_{CHUR}}\right] \qquad (3)$$

where

$$f_{Sm/Nd} = \frac{(Sm/Nd)_{P}}{(Sm/Nd)_{CHUR}} - 1 \qquad (4)$$

$$\epsilon_{Nd(o)} = \left[\frac{(^{143}Nd/^{144}Nd)_p}{(^{143}Nd/^{144}Nd)_{p_{CHUR}}} - 1 \right] \times 10^4 \qquad (5)$$

The assumption that the Sm/Nd ratio of the mantle growth curve is chondritic (McCulloch and Wasserburg 1978) and constant through time is at variance with the evidence for differentiation of the continental crust from that part of the mantle which is the source of MORB which is depleted relative to CHUR (DePaolo 1981b, Allegre and Ben Othman 1980). Model ages calculated relative to a CHUR type bulk earth ($\epsilon^T_{Nd} = 0$) may therefore be unrealistic, a fact confirmed by the occurrence of Archaean rocks with $\epsilon^T_{Nd} > 0$ (O`Nions et al. 1983). Allegre and Rousseau (1984) calculate sediment model ages of shales using a growth curve for oceanic mantle as a reference. The model ages are calculated from the intersection of two curves given by the equations for $^{144}Nd/^{143}Nd$ evolution (eq.1), and a depleted mantle curve defined by the data for MORB, ophiolites, PreCambrian mafic volcanics, komatiites, Isua supracrustals and meteorites. The equation has the form :

$$(^{143}Nd/^{144}Nd)_{DM} = A^2 + BT + C \qquad (6)$$

where $A = 1.53077 \times 10^{-5}$

$B = -0.22073 \times 6.54 \times 10^{-3}$

$C = 0.513078$

A third type of model age calculation has been used in the literature, particularly by the Cambridge group (Goldstein et al. 1984, Miller and O`Nions 1984, Frost and O`Nions 1985). This is the t_{CR} crustal residence age estimate described by Goldstein et al. (1984). Again this incorporates the evidence for a non-chondritic evolution of the mantle, but in this case a linear depleted mantle curve is preferred, simplifying the calculation. Mantle evolution is constrained by CHUR at 4.5 Ma, initial $^{143}Nd/^{144}Nd$ ratios of Archaean terranes and present day oceanic basalts ($\epsilon_{Nd} + 10$). The t_{CR} age calculation is given by :

$$t_{CR} = \frac{1}{\lambda} \ln \left[1 + \frac{0.513151 - ^{143}Nd/^{144}Nd}{0.21362 - ^{147}Sm/^{144}Nd} \right] \qquad (7)$$

Both t^{Nd}_{CHUR} and t^{Nd}_{DM} ages have been calculated for the data considered in the present study. The t^{Nd}_{CHUR} calculations follow equation (3) whilst t^{Nd}_{DM} ages have been calculated relative to the mantle evolution curve described by DePaolo (1981) given by the equation :

$$\epsilon_{Nd}(T) = 0.25T^2 - 3T + 8.5 \qquad (8)$$

where T is the age. As the crust is not formed with $\epsilon_{Nd} = 0$ (DePaolo 1981) the t^{Nd}_{DM} age is preferred to the t^{Nd}_{CHUR} estimate of crustal residence.

Whilst the Sm/Nd isotopic system is sensitive to the generation of continental crust, model ages calculated from sedimentary rocks do not as a rule indicate discreet episodes of continental growth. O`Nions et al.(1983) show that mixing of sediment from different crustal segments may produce averaged crustal residence ages of no direct significance to addition of material to the crust. Sm/Nd provenance ages therefore generally provide an estimate for the mean crustal residence age of the exposed continental crust from which the sediment was eroded. This is of considerable significance to constraining sediment provenance, particularly when alternative sediment source areas are associated with distinctive residence ages which may be inherited by the sedimentary sequences they source.

6.6.2 Sample Selection

Sm-Nd isotopic data have been obtained for a total of eight greywacke and lithic arenite clasts of southerly derivation. In addition A.N.Halliday has determined Sm-Nd provenance ages for three psammite clasts of northerly derivation (Halliday et al. in prep.). The Sm-Nd data allow some constraints to be placed on the early history and affinity of the sedimentary sequences which supplied the detritus to the ORS basin of deposition. The data also isotopically characterise a thick and previously unrecognised portion of the British sedimentary mass, which may have played an important role in magma petrogenesis. Halliday (1984) suggests that underthrusting of young crust might explain the high ϵ_{Nd} values in granites between the Highland Boundary Fault and the Mid-Grampian Line.

Shales have been conventionally used in Sm-Nd isotope studies on sediments. Shales are derived from fine particulates associated with continental erosion and as such probably encompass large source areas. Taylor and McLennan (1985) conclude that only a few chemical elements in fine-grained terrigenous clastic sediments preserve a direct relationship between their abundance in the upper crust and their abundance in the sedimentary record, but the REE are among these. Shales probably therefore represent averaged samples of the REE content of large continental segments, and on this basis, their Sm-Nd isotopic compositions can be used to both document large scale changes in sediment source areas relating to the relative position of the continental masses (Miller and O`Nions 1984), and show the evolution of continental growth through geological time (Allegre and Rousseau 1984).

Often, however, the investigation of sediment provenance requires that more specific problems are addressed, within a more restricted spatial framework than that represented by the continental masses. This is particularly so in reconstructing the history of terrane accretion in orogenic belts where sediment dispersed from one terrane to another often may be the only record of docking or lateral displacement between adjacent terranes. In this respect, the Sm-Nd systematics of coarser grained sediments are of interest. These are more likely to escape the crustal averaging seen in many shales and particulates and thereby retain a unique isotopic image of their source regions. A further advantage is that the constituent detrital components are easily identified in thin section, allowing the range of source components to be identified, and the isolation of possible mixing effects.

Can the assumption of minimal fractionation of Sm and Nd during formation of shales be reasonably extended to encompass greywackes? Taylor and McLennan (1985) show that REE patterns in greywackes and sands are similar to the upper crustal abundances as indicated by PAAS or in some cases are intermediate between those of andesite and the upper crust. Volcanogenic greywackes and immature sands derived from island arcs deviate from the

upper crustal composition as might be expected. Sandstones generally have lower REE abundances than shales but the shape of the chondrite-normalised plots is generally similar (Nance and Taylor 1976, Cullers et al. 1979, Basu 1982). This indicates that sandstones can be treated in much the same way as shales in terms of Sm-Nd provenances studies. A possible complication however is the greater abundance of heavy minerals in coarser grained sediments which if hydraulically concentrated can dominate the rare earth element budget. That greywackes can yield reliable Sm-Nd provenance ages is confirmed by the concordance of crustal residence ages from greywacke-shale pairs in the Southern Uplands (O`Nions et al.1983).

6.6.3 Sm-Nd Isotopic Data

The analytical procedure is outlined in full in Appendix 3. Sm and Nd concentrations were determined by isotope dilution. Separations were performed using standard cation exchange columns with 2.5N HCl as the elutant followed by separation of the rare earth elements on PTFE columns. Nd blanks at SURRC are less than 1ng. All isotopic analyses were performed on a fully automated V.G. Isomass 54E mass spectrometer. Sm and Nd were run as the metal species on triple filament assemblies, with the load on a Ta side filament and a Re centre filament. All isotopic data are corrected for machine discrimination using $^{146}Nd/^{144}Nd = 0.7219$. The precision on the $^{147}Sm/^{144}Nd$ ratio is better than 0.1%($2\sigma_m$), with the exception of samples 4255 and 4273 where the spiked Sm isotope dilution runs did not achieve target precisions and the Sm concentrations are only known to a precision of 1%.

Isotopic ratios, Sm and Nd concentration data, ϵ values and model ages are presented in Table 6.7. Bulk-earth ages parameters used to calculate ϵ values are $^{143}Nd/^{144}Nd = 0.512638$ and $^{147}Sm/^{144}Nd = 0.1966$. ϵ^{t}_{Nd} have been calculated assuming a stratigraphic age of 450 Ma. Sample 4260 has been analysed in duplicate. The unspiked $^{144}Nd/^{143}Nd$ ratios agree within the 2σ experimental errors although the error for 4260 - 1 (4.5 E-5) is in excess of the target precision of better than 3.5 E-5 ($2\sigma_m$). Duplicate isotope dilution results show a slight discrepancy (0.9% for Sm, 2.0% for Nd), but higher Sm concentrations accompnay higher Nd

Table 6.7. Sm-Nd analytical results

SAMPLE	Sm(ppm)	Nd(ppm)	$^{147}Sm/^{144}Nd$	$^{143}Nd/^{144}Nd \pm 2\sigma_m$	$\epsilon_{Nd}450$	t_{CHUR}	t_{DM}
4238	3.318	14.60	0.13733	0.512139 ± 24	-6.3	1.28	1.80
4255	3.992*	20.28	0.11898	0.511838 ± 22	-11.1	1.57	1.94
4260-1	5.464	27.67	0.11937	0.511897 ± 46	-10.0	1.46	1.85
4260-2	5.514	28.23	0.11806	0.511842 ± 18	-11.0	1.54	1.91
4261	3.568	18.82	0.11460	0.511831 ± 30	-11.0	1.50	1.86
4264	4.464	20.30	0.13294	0.512045 ± 26	-7.9	1.41	1.88
4271	4.505	24.53	0.11097	0.511852 ± 25	-10.4	1.39	1.76
4273	4.427*	22.25	0.12025	0.511878 ± 19	-10.4	1.51	1.90
4319	3.388	14.85	0.13789	0.512099 ± 16	-7.14	1.40	1.89

a ± 0.1%, except 4255, 4273 (*) ± 1%

b ϵ_{Nd} calculated relative to CHUR parameters, at estimated stratigraphic age of 450 Ma

c model age calculated relative to CHUR

d model age (in Ga) calculated relative to depleted mantle model (DePaolo 1981)

such that the variation in Sm/Nd ratio is small, at 1%. This is interpreted as the result of slight sample heterogeneity.

6.6.4 Results

Values for ϵ_{Nd}, the deviation in parts per 10^4 of the initial $^{144}Nd/^{143}Nd$ from CHUR, vary from -6.3 to -11.1 at 450 Ma, and are distinct from ϵ^t_{Nd}, as indicated by data for the Bay of Islands ophiolite, Newfoundland (Jacobsen and Wasserburg 1979), lavas, gabbros and trondhjemites of the Ballantrae ophiolite (Hamilton et al. 1984, Thirlwall and Bluck 1983), and Arenig/Llanvirn pillow lavas in the Southern Uplands (Hooker et al.1981, Thirlwall and Bluck 1983 Fig.3). As C_{Nd} values are age dependent, uncertainty in the true age of the sediments introduces an uncertainty into the ϵ_{Nd} values determined. An increase in the estimated age of deposition to 550 Ma produces a shift towards slightly higher ϵ_{Nd} values of the order of one epsilon unit. Crustal residence ages (t_{DM}) calculated relative to the depleted mantle model range from 1.76 to 1.94 Ga, with a mean of 1.87 $\pm$ 0.06 (1σ) Ga. The striking feature of the crustal residence age data is the narrow range of the depleted mantle ages, in rocks which show a wide range of $^{147}Sm/^{144}Nd$ from 0.11097 to 0.13789.

6.6.5 Discussion

Figure 6.19 compares $^{147}Sm/^{144}Nd$ ratios of the clasts with those measured from other sedimentary rock suites in Britain and Ireland, and with Caledonian granites (Halliday 1984, Hamilton 1980, Frost and O`Nions 1985) and Lower ORS lavas. Sm/Nd ratios vary in different rock types and the Sm/Nd ratio of sediment is consequently sensitive to provenance (Goldstein et al. 1984). Geological provinces in which basaltic magmatism is dominant (island arcs, continental flood basalts, mid ocean ridges, oceanic islands) are characterised by higher Sm/Nd ratios than the average Sm/Nd ratio of 0.19 for the upper continental crust as estimated by the study of atmospheric dusts and particulates from major river systems (Goldstein et al.1984). Consequently sediments derived from such provinces show a commensurate shift towards higher Sm/Nd ratios and $^{147}Sm/^{144}Nd$. The histograms in Figure 6.19 show the range of $^{147}Sm/^{144}Nd$ ratios in the clasts to

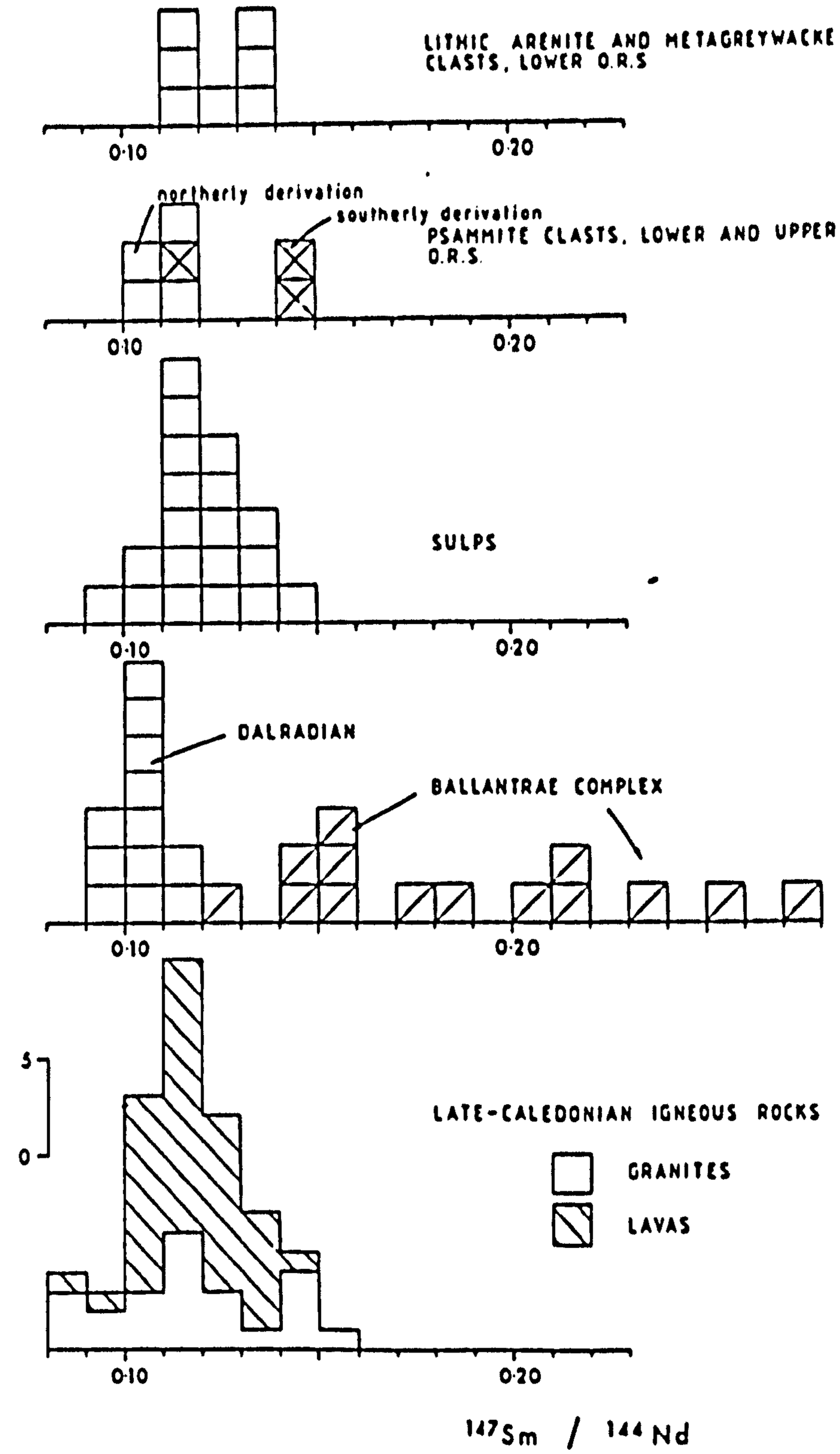

FIGURE 6.19 $^{147}Sr/^{144}Nd$ ratios determined in Lower ORS sedimentary and metasedimentary clasts compared with the isotopic composition of SULPS (O'Nions et al, 1983, Halliday 1984), Dalradian metasediments (O'Nions et al, 1983), the Ballantrae complex (Thirlwall and Bluck 1983, Hamilton et al, 1984), and late Caledonian granite (Halliday 1984) and volcanic rocks (Thirlwall 1982).

have a comparable range to those in SULPS and both are displaced to higher $^{147}Sm/^{144}Nd$ values relative to the Dalradian metasediments reported by O`Nions et al.(1983) and Frost and O`Nions (1985).

O`Nions et al. (1983) attributed the generally higher $^{147}Sm/^{144}Nd$ ratios of the Southern Uplands sediments to the presence of a basic volcanic component which may amount to 20-30% of the total sediment volume. Miller and O`Nions (1984) argue that a provenance for the Southern Uplands sediments from Dalradian metasediments, together with dilution with a contemporaneous basaltic source, cannot be accommodated by the Sm-Nd data. This is on account of the rather narrow range of crustal residence ages despite the wide range of measured Sm/Nd ratios. The restricted model ages point to well homogenised sediment compositions, but the variation in Sm/Nd ratios show that homogenisation cannot have been complete. They argue that this requires the endmembers in a bimodal basaltic-acid provenance to have similar crustal residence ages, such that mixing in varying proportions, to give a range of Sm/Nd ratios, does not produce a significant reduction in the bulk crustal residence age of those samples most strongly diluted with the high Sm/Nd basaltic component. Miller and O`Nions (1984) conclude that a binary source for the Southern Uplands sediments must have had both a component with higher than average Sm/Nd values, yet with similar crustal residence ages to a more evolved component with lower Sm/Nd, and that this source was a crustal segment extracted from the mantle 1.7-1.9 Ga ago.

The greywacke and metagreywacke clasts of southerly derivation resemble SULPS in that a range of $^{147}Sm/^{144}Nd$ ratios suggestive of source heterogeneity do not produce a corresponding range of t_{DM} ages, nor a correlation between t_{DM} and Sm/Nd. Instead, as noted above the t_{DM} ages are remarkably uniform. This is illustrated in the epsilon Nd evolution diagram plotted in Figure 6.20, on which the data can be seen to radiate from a narrow distribution of t_{DM} ages on the depleted mantle curve to a wide range of $\epsilon_{Nd}(o)$ values. Following the logic of Miller and O`Nions (1984) it can be argued that the data require mixing of

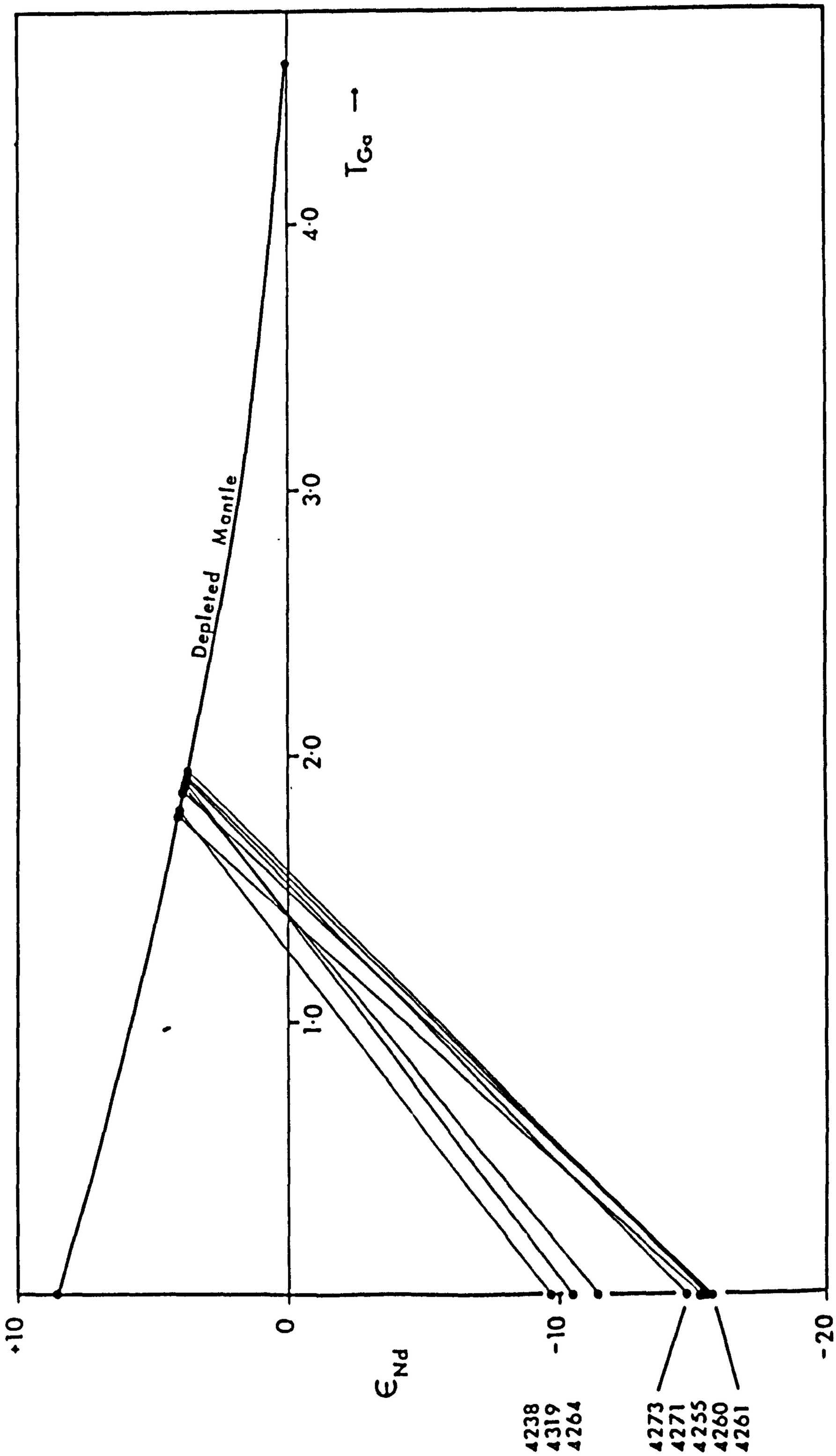

FIGURE 6.20 ε Nd evolution diagram for lithic arenite and metagreywacke clasts of southerly provenance.

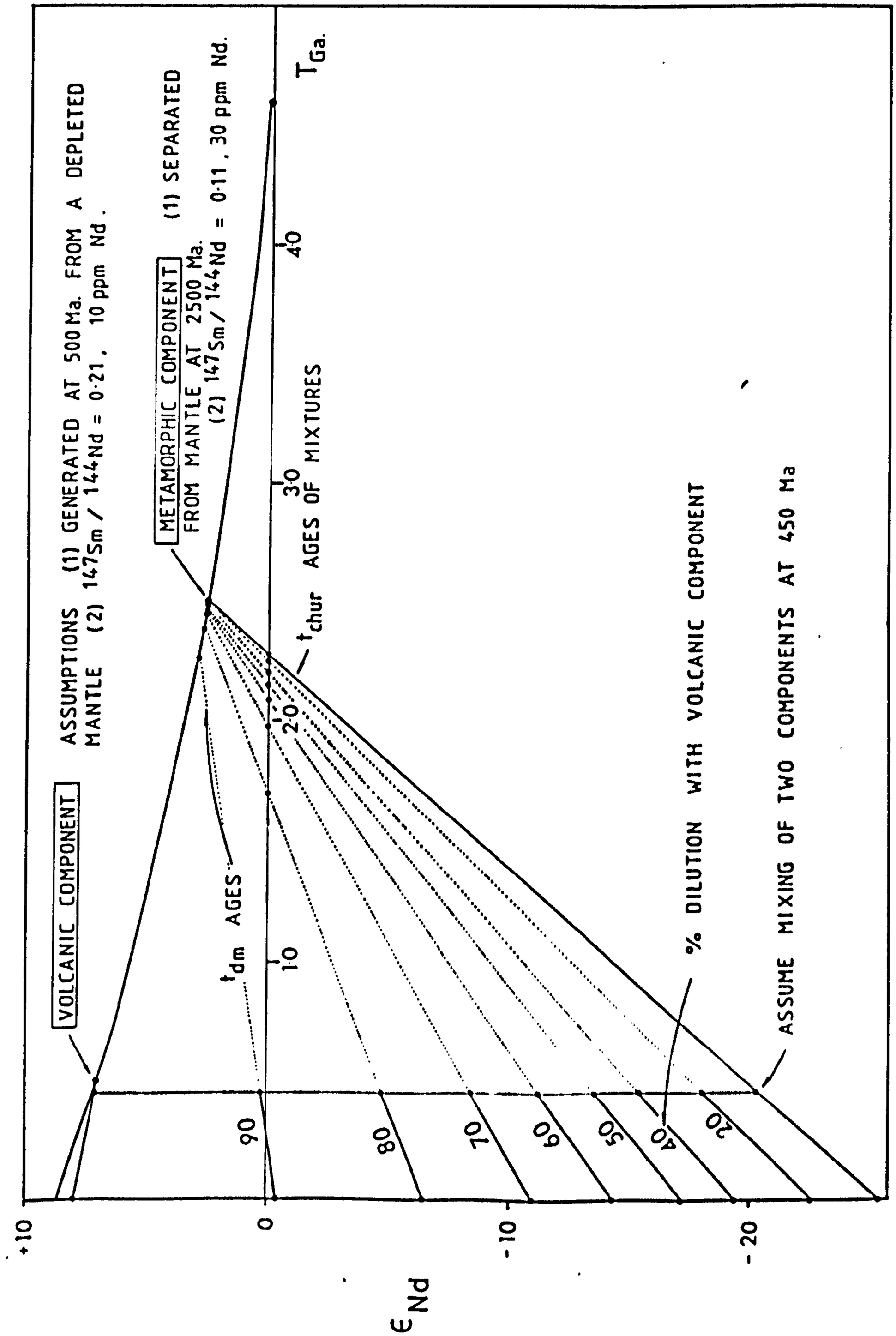

FIGURE 6.21 ϵ_{Nd} evolution for hypothetical mixing calculations discussed in text.

material with variable rare earth distributions but similar crustal residence ages, in order that the wide range of $^{147}Sm/^{144}Nd$ ratios with almost constant t_{DM} ages can be accounted for. This would require a source terrane with both a basaltic, and a low Sm/Nd metamorphic source, with depleted mantle residence ages for both components of approx. 1.85 Ga, somewhat older than that required to source the Southern Uplands sediments.

However, before a role for dilution with material derived from contemporaneous or young basaltic rocks can be ruled out, it is necessary to look a little more closely at the effects of sediment mixing on Sm-Nd systematics, and in particular at the assumption that the crustal residence age of sediment from two sources with residence ages t^1 and t^2 will yield a combined residence age directly proportional to the ratio in which the two components are mixed (O'Nions et al. 1983).

Figure 6.21 illustrates the modelled t_{CHUR} and t_{DM} ages for a hypothetical two-component sediment mixture. A metamorphic source with $^{147}Sm/^{144}Nd$ = 0.110 and a t_{DM} age of 2.5 Ga is assumed to have been mixed with a young volcanic component at 450 Ma. The volcanic sediment source is modelled as having been derived from MORB like basaltic volcanics which separated from a depleted mantle at 500 Ma with a $^{147}Sm/^{144}Nd$ ratio of 0.210. The low Sm/Nd metamorphic component evolves from a depleted mantle $^{143}Nd/^{144}Nd$ ratio of 0.509528 to 0.511012 (ϵ^{450}_{Nd} = -20.42) at 450 Ma. The basaltic component is modelled as having been extracted from a depleted mantle at 500 Ma ($^{143}Nd/^{144}Nd$ = 0.512355, ϵ^{500}_{Nd} = 7.06) and evolves to have a ϵ^{450}_{Nd} value of 7.14 at 450 Ma, the time at which both volcanic and metamorphic components are mixed in varying proportions during sediment dispersal and deposition. Epsilon Nd evolution lines for various mixtures are shown in Figure 6.21 for the time interval 450 Ma to the present, together with back projections to intersect the t_{DM} curve. The resulting t_{DM} crustal residence ages are tabulated in Table 6.8.

From both Figure 6.21 and Table 6.8 it is obvious that the

Table 6.8 Mixing calculations based on dilution of old low Sm/Nd sediment with young high Sm/Nd basaltic detritus.

Endmembers: (1) Metamorphic component originally separated from a depleted mantle at 2.5 Ga with Sm/Nd = 0.11. At 450 Ma, $\epsilon_{Nd} = -2^{0.42}$, $^{143}Nd/^{144}Nd = 0.5111012$. (2) Basaltic detritus, fractionated from a depleted mantle at 500 Ma with Sm/Nd = 0.21 $\epsilon^{500}_{Nd} = 7.06$. At 450 Ma $\epsilon^{450}_{Nd} = 7.14$, $^{143}Nd/^{144}Nd = 0.512424$.

% dilution with volcanic component at 450 Ma	ϵ^{450}_{Nd}mixture	$(^{143}Nd/^{144}Nd)^{450}_{mx}$	$(^{147}Sm/^{144}Nd)_{mx}$	$(^{143}Nd/^{144}Nd)_p$	$\epsilon_{Nd}(o)$	t_{CHUR} Ga	t_{DM}
0	-20.42	.511012	.1100	.511336	-25.39	2.28	2.52
20	-18.30	511121	.1177	511468	-22.82	2.24	2.51
40	-15.41	.511269	.1281	.511646	-19.34	2.19	2.50
50	-13.53	.511365	.1350	.511763	-17.07	2.15	2.49
60	-11.23	.511483	.1433	511905	-14.29	2.08	2.48
80	-4.67	.511819	.1671	512311	-6 37	1.68	2.41
90	+0.25	.512071	.1850	.512616	-0.42	0.28	2.28
100	+7.14	.512424	.2100	.513043	+7.89		0.52

Calculations assume Nd concentrations of 30ppm and 10ppm for crustal and MORB derived sediment reservoirs respectively.

crustal residence age of a mixture cannot simply be related to the proportion in which the components are mixed i.e. for a sediment comprising a 50% contribution from crustal segments with distinct crustal residence ages (t^1_{DM}, t^2_{DM}), the resulting composite residence age will only be a straightforward average $(t^1_{DM} + t^2_{DM})/2$, in situations in which the Sm/Nd ratios of the two components are similar.

The variable Sm/Nd ratios of the components in a mixed basaltic-metamorphic provenance therefore have a number of important implications for the interpretation of the residence ages of sediment mixtures. Figure 6.21 emphasises that dilution with a young basaltic component will not necessarily result in a shift to lower t_{DM} ages in direct proportion to the extent of volcanic dilution. In fact t_{DM} ages in mixtures in which the volcanic dilution is low (20%) may well be comparable to the t_{DM} ages of the low Sm/Nd component itself. This is because dilution with basaltic components can significantly alter the Sm/Nd ratio of the sediment mixture.

If the volcanic component admixed is young in comparison to the residence age of the older low Sm/Nd component the assumption that the Sm/Nd ratio measured at the present time can be used to single-stage correct the present day $^{143}Nd/^{144}Nd$ ratio to the appropriate model mantle value is unjustified. Whilst the Sm/Nd ratio appears to be a robust feature during crustal evolution, dilution of sediment with a basaltic component appears to be an important and overlooked mechanism whereby net fractionation of Sm and Nd can take place during evolution of the sedimentary mass. Dilution with a basaltic component can increase the Sm/Nd ratio of the sediment such that computation of model ages assuming the enhanced Sm/Nd ratio pertained throughout the crustal history of the material involved results in misleading estimates of the length of crustal residence.

As only basaltic rock-types, e.g. MORB, OIB, and continental flood basalts, show high Sm/Nd ratios and can induce the effects documented in Figure 6.21, sequences which receive large volumes of basaltic detritus are those most likely to show complex

provenance age relationships. Many arc-related volcanic rocks, for example Andean andesites (Hawkesworth et al. 1979), do not have Sm/Nd ratios which depart significantly from average crustal values and consequently mixing of an arc-related andesitic component with an older metasedimentary component will not produce complex mixing effects. The role of the volcanic dilutant is emphasised on the $^{143}Nd/^{144}Nd$ vs $^{147}Sm/^{144}Nd$ plot shown in Figure 6.22 on which data from the clasts, Southern Uplands and Dalradian are superimposed on compositional fields for various different rock-types taken from Goldstein et al. (1984). Both the southerly derived clasts and SULPS plot with linear distributions which are most easily explained in terms of binary mixing between a basaltic component and a low Sm/Nd phase. Mixing with andesitic arc related detritus is ruled out by the generally low $^{147}Sm/^{144}Nd$ ratios of these rock-types.

Figure 6.22 also serves to illustrate the distinction between the southerly derived clasts and SULPS. Whilst both show a similar behaviour in terms of mixing with a high Sm/Nd basaltic component, the two sets of data fall on distinct but sub-parallel trends with the SULPS data displaced to more radiogenic isotopic compositions. A number of conclusions follow from this and preceding observations.

1. The southerly derived greywacke clasts cannot have been derived from the Southern Uplands greywacke sequence, as they are isotopically distinct. Rather the greywacke clasts must have been derived from a thick proximal sediment pile previously unrecognised in the Scottish sediment mass.

2. The distinction in isotopic composition between SULPS and the clasts suggests the two sequences were originally derived from different source terranes, and were both diluted with young basaltic volcanic detritus. The displacement of the clast data to lower $^{143}Nd/^{144}Nd$ values is compatible with an older lower Sm/Nd component than that which contributed to SULPS. This is in agreement with the generally lower t_{DM} ages determined for SULPS (O`Nions et al. 1983). The average of SULPS t_{DM} ages is 1.53 $\pm$ 0.3 (2σ) Ga (n=16) compared with 1.87 $\pm$ 0.12 (2σ) Ga for the

FIGURE 6.22 Comparison of the fields of $^{147}Sr/^{144}Nd$ and $^{143}Nd/^{144}Nd$ for the lithic arenite and metagreywacke clasts (filled circle symbols) and potential source materials. Mixing on this diagram is linear. Variations in Sm/Nd primarily reflect magmatic and mixing processes whilst $^{143}Nd/^{144}Nd$ ratios reflect both Sm/Nd and time. Fields are from compilation by Goldstein et al. (1984) with the addition of data from Southern Uplands sediments (O`Nions et al. 1983, Halliday 1984), the Byne Hill Trondhjemite (Hamilton et al. 1984) and Southern Uplands basalts (Hooker et al. 1981). Abbreviations are BT: Byne Hill Trondhjemite, SULPS: Southern Uplands Lower Palaeozoic Sediment (open circle symbols). See text for discussion.

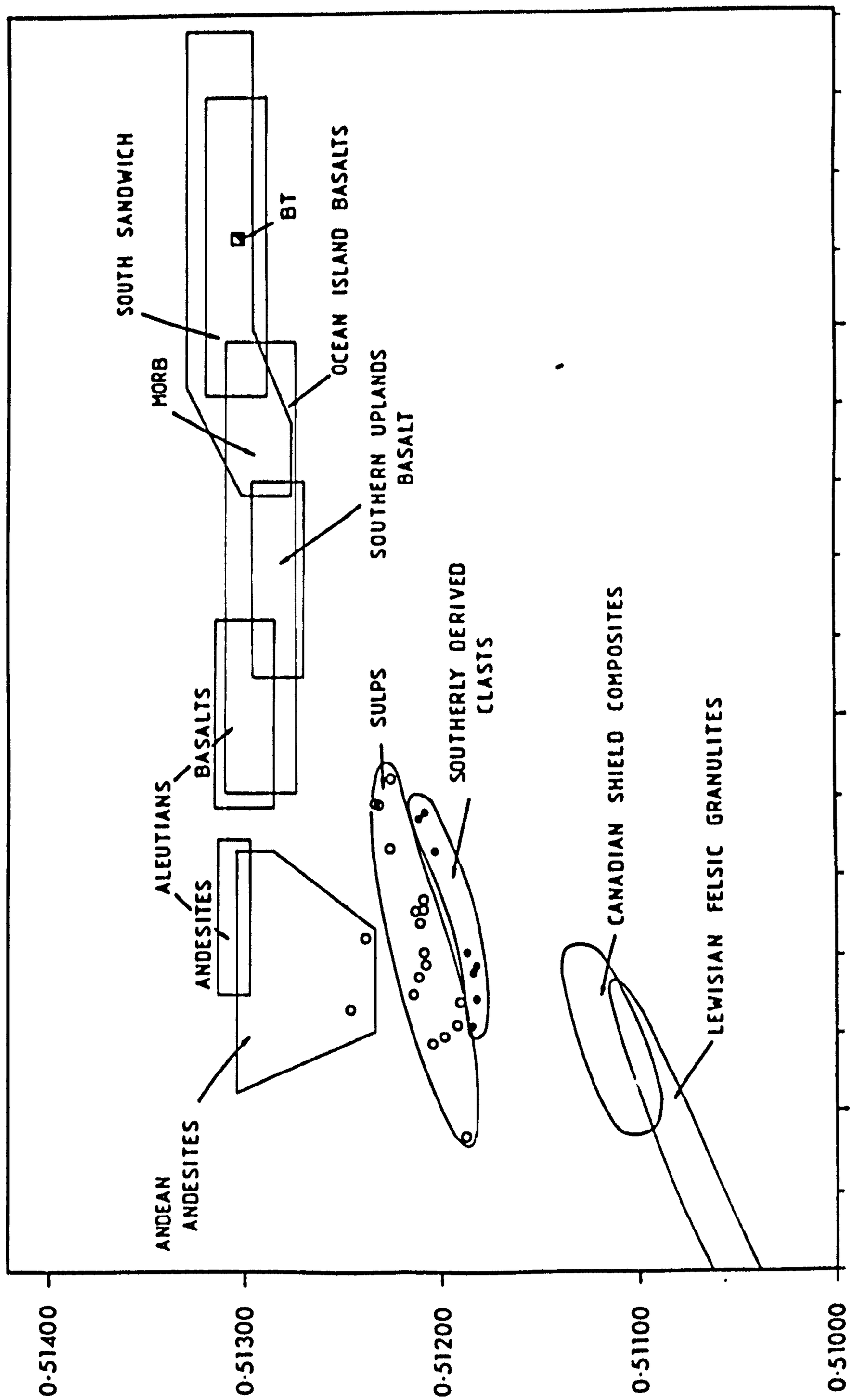
^{147}Sm / ^{144}Nd
0·20
0·15
0·10
^{143}Nd / ^{144}Nd
0·51400
0·51300
0·51200
0·51100
0·51000
BT
SOUTH SANDWICH ISLAND BASALTS
MORB
OCEAN ISLAND BASALTS
SOUTHERN UPLANDS BASALT
SULPS
SOUTHERLY DERIVED CLASTS
BASALTS
ALEUTIANS
ANDESITES
ANDEAN ANDESITES
CANADIAN SHIELD COMPOSITES
LEWISIAN FELSIC GRANULITES

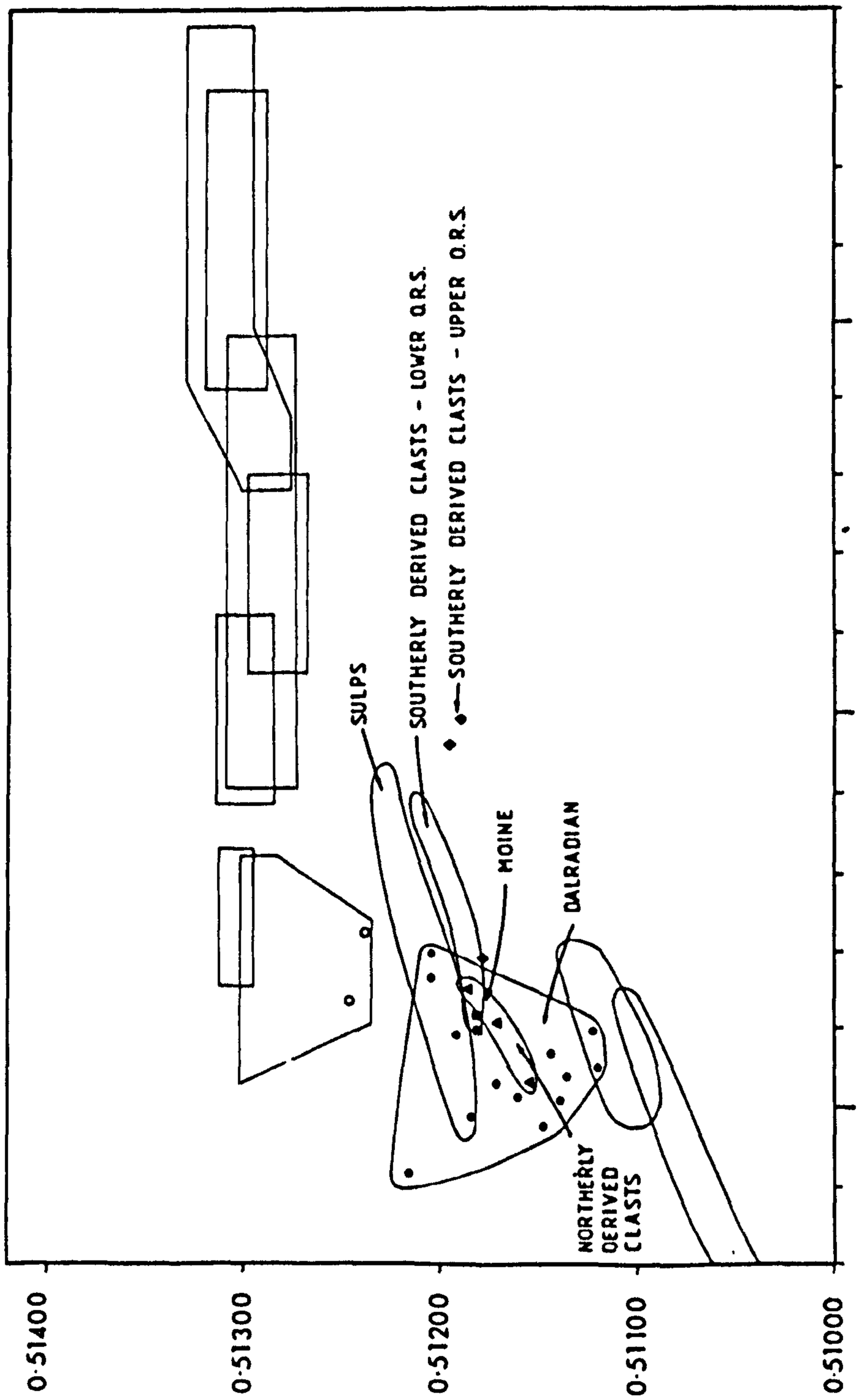

FIGURE 6.23 Sm-Nd isotopic data for the Dalradian (O'Nions et al. 1983, Frost and O'Nions 1985), Moine (Van Breemen and Hawkesworth 1980), and southerly derived psammitic clasts in the Upper and Lower ORS (Halliday et al. in prep.) superimposed on compositional fields shown in Figure 6.22. Symbols are: filled circle, Dalradian; filled square, Moine; open triangle, northerly derived psammite clasts from the Dunnottar and Crayton Groups; filled diamond, south-westerly derived psammite clasts from the Upper ORS at Rosneath.

clasts. That this is not solely a function of the greater volcanic dilution evident in SULPS is shown by Figure 6.22 in which the clast data consistently plot with lower $^{143}Nd/^{144}Nd$ at constant $^{147}Sm/^{144}Nd$, a crude index of volcanic addition.

3. The coherent behaviour and linear trends evident for the clasts and SULPS on the $^{143}Nd/^{144}Nd$ vs $^{147}Sm/^{144}Nd$ plot is at variance with the data for the Dalradian plotted in Figure 6.23. The Dalradian data do not plot with a linear distribution and show no relationship between $^{143}Nd/^{144}Nd$ and $^{147}Sm/^{144}Nd$. Frost and O`Nions (1985) draw attention to the highly variable Sm-Nd systematics which typify the Dalradiam metasediments and serve to distinguish them from other sedimentary and metasedimentary sequences. The field for Dalradian isotopic compositions overlaps the low Sm/Nd end of both the SULPS and the southerly derived clast linear arrays and must be considered as a potential source of low Sm/Nd detritus in both sediment sequences. That the Dalradian is unlikely to have made such a contribution is suggested by the absence of scatter in the low Sm/Nd part of the trends for each of the sediment suites. Unless the sediment derived from the Dalradian was very well homogenised during erosion and transportation, sediment sequences sourced by these isotopically heterogeneous metasediments should inherit the variable isotopic signature of their source materials.

The poor sorting, coarse grain size and angular grain boundaries of the southerly derived greywacke clasts all suggest that the potential for large scale homogenisation and mixing was probably low and that the absence of scatter in the low Sm/Nd samples, which contain the largest metamorphic component, may be significant. It should be noted, however, that a wide range of Nd isotopic compositions was established in a relatively restricted area of Dalradian metasediments surrounding the Etive Complex by Frost and O`Nions (1985). Whilst the scale of isotopic heterogeneity in the Dalradian remains uncertain through paucity of data, it is possible that the heterogeneity in Nd isotopic compositions is developed at a relatively small scale allowing homogenisation during erosion and transportation of detritus in small scale dispersal systems.

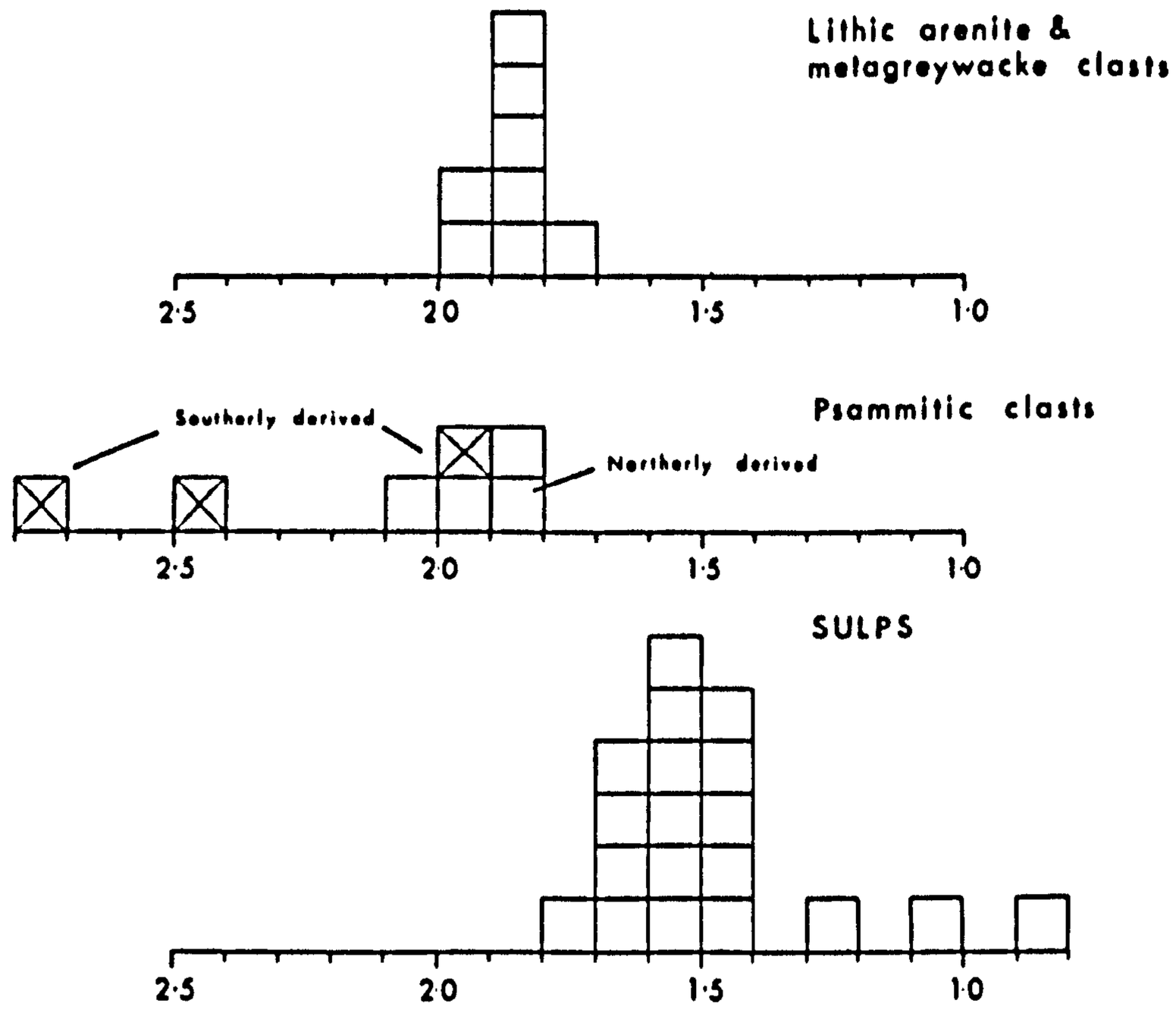

FIGURE 6.24 A comparison of t_{DM} (depleted mantle) crustal residence ages determined for the southerly derived lithic arenite and metagreywacke clasts, psammitic clasts from the Lower and Upper ORS (Halliday et al. in prep.), SULPS (O'Nions et al. 1983, Halliday 1984) and Lewisian (L), Torridonian (t), Moinian (m), and Dalradian (d) sediments and metasediments (O'Nions 1983, Van Breemen and Hawkesworth 1980).

Less equivocal evidence against a Dalradian contribution to the sequence sampled by the southerly derived clasts is provided by the absence of detrital blue quartz in all southerly derived sediment and metasediment clasts. Blue quartz is particularly abundant towards the top of the Dalradian sequence, and should also occur in sediments derived by recycling of these materials. The absence of t_{DM} ages in excess of 2.0 Ga in the lithic arenite and metagreywacke clasts contrasts with the common occurrence of Dalradian metasediments with t_{DM} provenance ages >2.0 Ga and up to 2.6 Ga (Fig.6.24). This is taken to indicate that a metamorphic terrane other than the Dalradian contributed sediment to the greywacke pile lying directly to the south of the Crawton Basin in the east central sector of the Midland Valley. This metamorphic terrane had a bulk depleted mantle crustal residence age of close to 1.85 Ga, substantially younger than metamorphic terranes to the north, but probably older than the metamorphic terrane which supplied detritus to the Southern Uplands. One possibility is that the terrane represents part of the continental root to a Lower Palaeozoic volcanic-plutonic arc which was active in the Midland Valley, particularly during the Ordovician (Longman et al.1979, Bluck 1983).

4. Nd isotopic data for seven further clasts pertinent to identifying and constraining the sources of metamorphic detritus in the Scottish Caledonides are given in Table 6.9. These have been analysed by A.N.Halliday and form part of a wider collaborative project. Four are northerly derived psammitic clasts from the Lower ORS exposed in the Crawton Basin (Dunl, CR-1 and 3195) and at Ardmore Point (BJB/D). The remaining three samples are metasedimentary clasts from the Upper ORS at Rosneath where they have a south-westerly provenance from a source terrane within the Midland Valley (Bluck 1983, 1984). The three northerly derived psammitic clasts from the Dunnottar and Crawton Groups have t_{DM} ages of 1.84, 1.98 and 2.06. These are compatible with a provenance for the clasts in the adjacent Grampian Highlands terrane, but the wide range of provenance ages determined for the Grampian Highlands (Fig.6.24) detracts from identifying a unique source for the clasts on the basis of Sm-Nd data alone.

Sample Number	Sm (ppm)	Nd (ppm)	$^{147}Sm/^{144}Nd$ (atomic)	$^{143}Nd/^{144}Nd$ $\pm 2\sigma m$	εNd at t	t_{DM} (Ga)
Crawton Group, Lower ORS t = 400 Ma						
CR1	1.845	10.84	0.1029	0.511544 ± 22	-16.6	2.06
3195	3.523	19.24	0.1107	0.511706 ± 35	-13.8	1.98
Dunnottar Group, Lower ORS t = 400 Ma						
DUN 1	1.794	9.432	0.1150	0.511850 ± 43	-11.2	1.84
Lower ORS, Ardmore Point t = 400 Ma						
BJB/D	2.662	14.73	0.1092	0.511748 ± 20	-12.9	1.89
Upper ORS, Roseneath Point t = 370 Ma						
GN1	1.979	10.05	0.1190	0.511808 ± 20	-12.5	1.99
GN3	1.329	5.503	0.1460	0.511966 ± 27	-10.7	2.44
GN4	1.904	7.722	0.1490	0.511903 ± 21	-12.1	2.72

TABLE 6.9 SM-ND ISOTOPIC DATA FOR METAMORPHIC CLASTS FROM ORS CONGLOMERATES, SCOTTISH MIDLAND VALLEY. $\lambda^{147}Sm = 6.54 \times 10^{-12}y^{-1}$, BULK EARTH $^{147}Sm/^{144}Nd = 0.1966$, $^{143}Nd/^{144}Nd = 0.512638$. DATA FROM HALLIDAY ET AL IN PREP.

The southerly derived clasts at Rosneath have older Sm-Nd model ages than those derived from the north and also have anomalously high $^{147}Sm/^{144}Nd$. The metasediment clasts dispersed northwards from sequences within the Midland Valley are therefore isotopically distinct when traced from NE to SW (Fig.6.25) suggesting the Midland Valley zone may be underlain by a collage of tectonically assembled, disparate metamorphic blocks. Evidence from the northerly dispersed conglomerates filling the Crawton Basin indicates the involvement of a metamorphic terrane with a t_{DM} age of less than 2.0 Ga, whilst the Rosneath data require a terrane in excess of 2.0 Ga with anomalously high Sm/Nd. Leake et al.(1984) attribute the tectonic position of the Dalradian rocks of Connemara to southerly directed overthrusting and it is possible that an older provenance component was incoporated in the western Midland Valley and its extension into Ireland by this mechanism.

5. A volcanic component has been shown to be important in producing the linear correlation between $^{143}Nd/^{144}Nd$ and $^{147}Sm/^{144}Nd$, and the high $^{147}Sm/^{144}Nd$ in the clast data. Sm/Nd ratios for various igneous rock-types require that this component is basaltic (MORB, OIB, continental flood basalts) and cannot be derived from arc-related andesites of Andean type. Situations conducive to the generation and dispersal of large volumes of basaltic sediment are likely to be rare in the geological record. Basaltic volcanism typifies extensional environments in which subsidence is rapid. The rheology of basalt magma is such that basaltic landforms are of low relief and volcaniclastic sediment production suppressed. The potential for the production of voluminous basaltic sediment is therefore likely to be low with one important exception - ophiolite obduction. Sedimentary basins associated with the obduction of oceanic crust can be expected to receive substantial volumes of basaltic and related detritus with high Sm/Nd, and the sediment fill to these basins is therefore likely to depart significantly from average upper crustal Sm/Nd.

The Sm-Nd isotope systematics, when combined with the trace-element evidence presented above, argue for an important

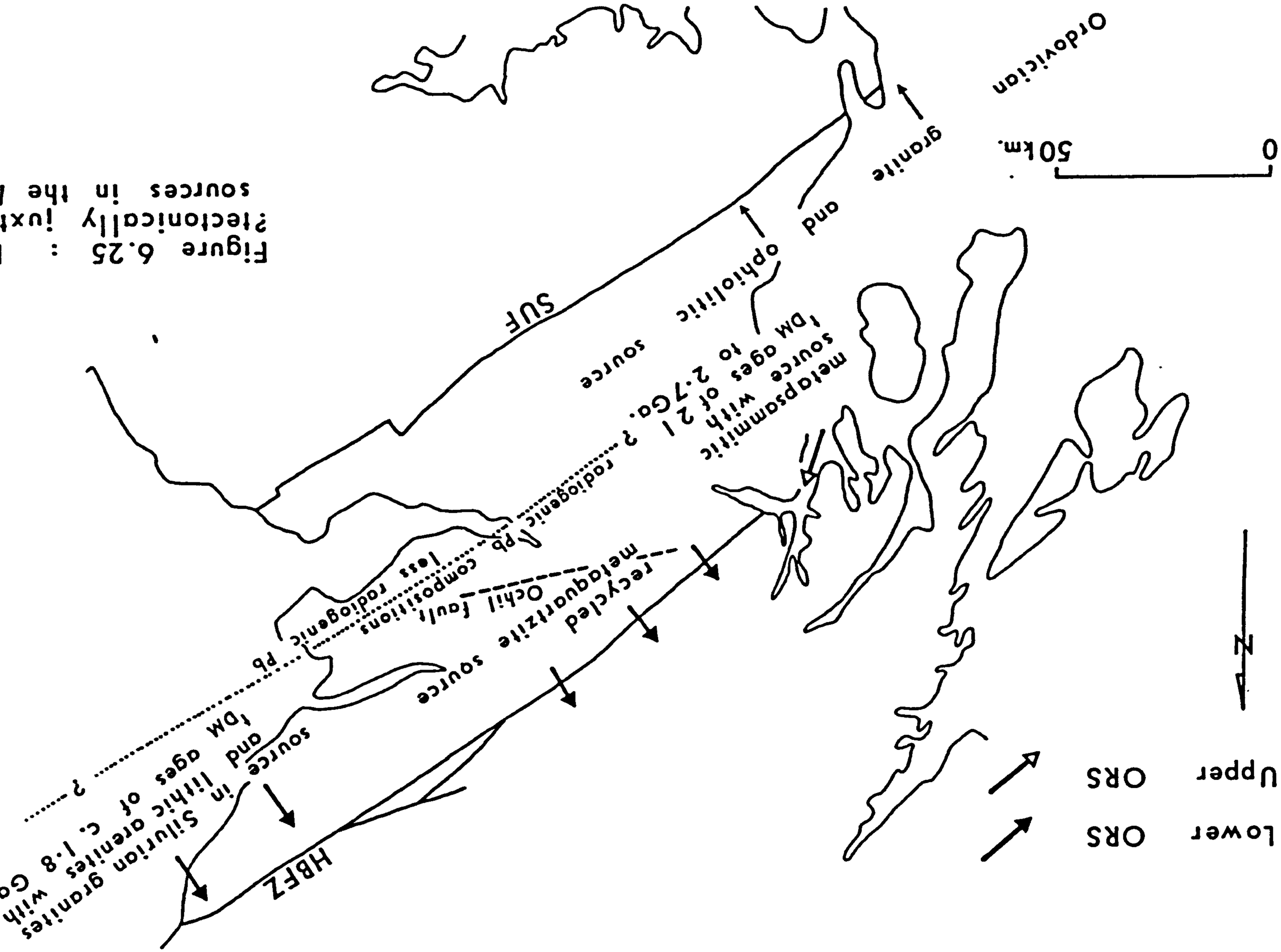

Figure 6.25 : Evidence for diverse ?tectonically juxtaposed sediment sources in the Midland Valley.

ophiolitic component in the lithic arenite and metagreywacke sequence occurring in the east-central sector of the Midland Valley. High Cr greywackes also typify the northern belt of the Southern Uplands (Thirlwall 1983), and clastic units in the Highland Border Complex (Robertson et al. 1984), attesting to the wider occurrence of sedimentary successions to which ophiolites have made an important sediment contribution along the northern Iapetus margin (see also Hiscott 1984).

CHAPTER SEVEN

PB ISOTOPIC STUDIES ON GRANITIC DETRITUS

7.1 INTRODUCTION

Spatial variations in Pb isotopic compositions have been shown to characterise the continental crust in several regions (Zartman 1974, Michard-Vitrac et al.1981, Gariepy et al.1985). Two sets of processes are likely to contribute to these systematic regional variations. The first is a lateral segmentation of the crust by juxtaposition of continental segments or terranes having unique age relations, chemical and isotopic compositions, and petrological histories. The second is a lateral expression of an important vertical zonation of the continental crust into a K, Rb, and U enriched upper crustal reservoir and a depleted unradiogenic lower crustal reservoir.

Several studies have shown the potential of Pb isotopic studies to mapping variation in the structure of the continental crust and to defining isotopic provinces characterised by an internal coherence in isotopic composition. Zartman (1974) showed a correlation between the Pb isotopic signature of Mesozoic and Tertiary magmatic rocks and ore leads from the western United States on the one hand and geotectonic setting on the other. Less radiogenic Pb compositions were observed in areas underlain by thick PreCambrian crust, whereas comparatively radiogenic leads were found in granites and hydrothermal ore deposits associated with a thick (>15 km) sequence of miogeosynclinal sediments. Michard-Vitrac et al.(1981) showed a clear geographical distribution of Pb isotopic compositions in Hercynian granitic K-feldspars in western Europe at a smaller scale than was observed by Zartman in the western U.S. The isotopic provinces are considered to reflect crustal melting across a previously differentiated continental crust. Gariepy et al.(1985) demonstrate the presence of granitoid rocks defining two distinct Pb-isotopic provinces in Southern Tibet with a sharp compositional divide which coincides with the Indus-Zangpo suture zone. The two Pb-isotopic provinces can be shown to have undergone a complex history of U-Th-Pb fractionation and are thought to represent discrete continental segments juxtaposed during large-scale intracontinental thrusting events.

The presence of Pb-isotopic zonation in the continental crust is of some significance to provenance studies. Granite clasts should preserve in their feldspar Pb isotopic compositions a fingerprint for the crustal segment from which they were derived. Basins which overlie or are associated with the juxtaposition of discrete continental segments or terranes might be expected to receive isotopically distinct detritus from sources in both terranes. It is argued elsewhere that the Crawton Basin overlies a substantial crustal break along which the Midland Valley and Grampian Highlands terranes were juxtaposed during the late Silurian. The basin receives large volumes of granitic detritus, from source terranes flanking the basin to both north and south, providing an ideal opportunity to test the significance of the inferred crustal structure on which the basin is nucleated. The following chapter presents and explores the implications of preliminary Pb-isotopic data for feldspars separated from granite clasts of both northerly and southerly derivation. The emphasis is on delineating compositional variation and characterising the source terranes as opposed to presenting detailed, multi-stage models for the evolutions of lead in each of the granite-clast suites.

7.2 THEORY

The isotopic composition of Pb measured in continental rocks often reflects a complex history of evolution in several reservoirs. The term `common lead` refers to a lead developed in environments with U/Pb and Th/Pb ratios that never greatly exceeded the range observed in average crustal rocks (U/Pb = 0.05-1.0, Th/Pb = 1-1.0), (Koppel and Grunenfelder 1979). The isotopic composition of common lead is a mixture of both primeval and radiogenic components. Single stage growth of Pb isotope ratios can be described by the following equations :

$$(^{206}Pb/^{204}Pb)_t = (^{206}Pb/^{204}Pb)_o + \mu(e^{\lambda_1 T} - e^{\lambda_1 t}) \quad (1)$$

$$(^{207}Pb/^{204}Pb)_t = (^{207}Pb/^{204}Pb)_o + \frac{\mu}{137.88}(e^{\lambda_2 T} - e^{\lambda_2 t}) \quad (2)$$

$$(^{208}Pb/^{204}Pb)_t = (^{208}Pb/^{204}Pb)_o + W(e^{\lambda_3 T} - e^{\lambda_3 t}) \quad (3)$$

where T = age of the earth (4570 Ma)

$(^{206}Pb/^{204}Pb)_o = 9.307$

$(^{207}Pb/^{204}Pb)_o = 10.294$

$(^{208}Pb/^{204}Pb)_o = 29.479$

(derived from the primordial Pb composition of Canyon Diablo Troilite - Oversby 1974);

$u = {}^{238}U/{}^{204}Pb$

$W = {}^{232}Th/{}^{204}Pb$

$^{238}U/^{235}U = 137.88$

and λ_1, λ_2 and λ_3 are the decay constants of ^{238}U, ^{235}U and ^{232}Th respectively. These are :

$\lambda_1 = 1.55125 \times 10^{-10}\ yr^{-1}$

$\lambda_2 = 9.8485 \times 10^{-10}\ yr^{-1}$ (Jaffey et al 1971)

$\lambda_3 = 0.49475 \times 10^{-10}\ yr^{-1}$ (Le Roux and Glendenin 1963)

These equations assume the lead isotopic compositions have developed since T in a closed U-Th-Pb system with u and W values

that have changed only as a result of radioactive decay. As U, Th, and Pb fractionate during many geochemical processes, and as crustal and mantle reservoirs are characterised by differing U/Pb and Th/Pb ratios, the assumptions inherent in the single-stage evolution of lead (the Holmes-Houtermans model) are unrealistic in most geological situations. Nonetheless, the single stage equations have been widely used to describe to a first approximation the evolution of common lead.

In an effort to more accurately constrain the origin of variation in Pb-isotopic systems, attempts have been made to model the evolution of Pb isotopic ratios through more complex multistage histories. These take into account the likelihood that lead may have been associated with several reservoirs having different U/Pb and Th/Pb ratios, and that it may have resided in these reservoirs for varying lengths of time. Doe and Zartman (1979) and Zartman and Doe (1981) consider three major terrestrial reservoirs; the mantle, the upper continental crust and the lower continental crust. They establish growth curves for each of these long-term reservoirs using fields defining the present day lead isotopic compositions of each as the major external control. The evolution of lead in the three reservoirs is modelled to include dynamic interaction between the upper and lower continental crust, and the mantle, during recurrent orogenic events which generate a fourth short-term reservoir, the orogene. In the orogenic environment, leads from each of the three long-term reservoirs are homogenised by a combination of `sedimentation, volcanism, plutonism, metamorphism and rapid erosional turnover` (Doe and Zartman 1979). The composition of leads in the orogene therefore contains a component from the mantle, the upper crust and to a lesser extent the lower continental crust. The emphasis on dynamic interaction between the crustal and mantle reservoirs and the role of orogeny in acheiving this interaction make the `plumbotectonic` model a useful framework for interpreting regional variation in Pb isotopic compositions, and relating these compositions to source regions at depth.

7.3 PREVIOUS WORK

Pb isotopic compositions have been determined for a range of whole rocks, feldspars, and galenas from the Scottish crust. Moorbath et al.(1969) and Chapman and Moorbath (1977) determined Pb isotopic compositions for metamorphic rocks from the Lewisian basement complex lying to the west of the Moine Thrust. Uranium concentrations were found to be strongly depleted relative to the crustal average, a feature of granulite facies terranes attributed to a combination of fluid migration following dehydration reactions and/or melt extraction (Fyfe 1973). Isotope ratios from Lewisian rocks fall on linear arrays on $^{207}Pb/^{204}Pb$ vs $^{206}Pb/^{204}Pb$ plots which intersect the two-stage terrestrial lead evolution curve of Stacey and Kramers (1975) at c 2.7-2.8 Ga.

Pankhurst (1978) presented data for age corrected Pb isotopic compositions in four granite whole rocks from the Foyers intrusion. These formed a tight cluster on a $^{207}Pb/^{204}Pb$ vs $^{206}Pb/^{204}Pb$ Pb evolution diagram well removed from contemporary mantle compositions estimated using the linear increase model for the mantle source of ore leads proposed by Cumming and Richards (1975). Pankhurst (1978) interpreted the data in terms of mixing of Lewisian-type lower crustal Pb with juvenile Caledonian Pb. No systematic relationship was found between Sr and Pb isotopes with the more evolved adallemites having lower initial $^{87}Sr/^{86}Sr$ and more radiogenic Pb isotopic compositions than the less evolved tonalites and granodiorites.

Blaxland et al.(1979) published the first common Pb study of feldspars separated from Scottish Caledonian granites. Eleven K-feldspar separates from granite intrusions emplaced into the northwest Highlands, Grampian Highlands, the Midland Valley and the Southern Uplands crustal segments, were analysed. These plotted with a linear alignment on a $^{207}Pb/^{204}Pb$ vs $^{206}Pb/^{204}Pb$ diagram with the best-fit regression line suggesting a lower intercept age of c 2.7 Ga with both single-stage and two-stage (after Stacey and Kramers 1975) growth curve models. Blaxland et al.(1979) interpret the linear trend as a mixing lime between a

Lewisian basement component and a younger mantle or orogene component. Halliday (1981) shows the contribution from Lewisian-derived Pb must be low and in addition it does not necessarily need to have been derived directly from Lewisian basement. Sedimentary sequences having a provenance in Lewisian rock-types may have inherited the Pb isotopic characteristics of their source. Dickin et al.(1981) show the Pb isotopic composition of the Dalradian to define a steep array close to the 2680 Ma isochron formed by Lewisian gneisses and they interpret this to be a possible indication of a Lewisian provenance for the Dalradian. The Dalradian Pb-isotopic compositions are however notably radiogenic.

Blaxland et al. (1979) also noted an important regional zonation in Pb isotopic compositions across the Scottish crust. Granite feldspars from the Southern Uplands were found to be considerably more radiogenic than those further north, plotting close to the modelled composition of the orogene at 400 Ma. As the granites are traced northwards they become progressively more radiogenic. Van Breemen and Bluck (1981) interpret the consistent downward trend of $^{206}Pb/^{204}Pb$ ratios when traced away from the Iapetus suture in terms of an increasingly unradiogenic Pb input to the granites from the lower crust. Granites from the Southern Uplands in the south have Pb isotopic compositions close to the predicted orogene compositions of Zartman and Doe (1981).

Halliday (1981) demonstrated a positive correlation between the U content in zircon and initial lead isotope ratios for Scottish Caledonian granites. These correlations suggest the source(s) of U in the zircons are also the source(s) of Pb in the granite magmas, and from this it was argued that the granite Pb isotopic compositions are dominated by crustal Pb.

Pb isotopic data for the Etive complex have been presented by Clayburn et al.(1983) and Frost and O`Nions (1985). A similar range of isotopic compositions was reported in both studies. Clayburn et al.(1983) showed a steep trend for Etive complex $^{206}Pb/^{204}Pb$ compositions when plotted against $(^{87}Sr/^{86}Sr)_i$. The data define a sub-linear array of points trending away from

contemporary mantle towards the estimated field for Middle Proterozoic (Grenville) and Archaean lower crust. Late Proterozoic upper crustal metasediments (Dalradian, Moine) do not appear to have played an important role in determining the Pb- or Sr- isotopic compositions of the magmas.

Thirlwall (1983) determined the Pb isotopic composition of Lower ORS lavas from Fife in the east central Midland Valley. These were found to have a narrow range of variation little greater than the errors introduced by mass fractionation and the large age correction. The data plot in a position intermediate between the feldspar Pb compositions of Southern Uplands granites to the south and the less radiogenic compositions of Grampian and northern Highland granites to the north. The composition of the andesites was found to be marginally more radiogenic than the more primitive basalts. The absence of the relatively unradiogenic Pb compositions characteristic of Highland granites suggests U-depleted lower crustal granulites have not made a significant contribution to the Pb in Lower ORS lavas of the Midland Valley. Thirlwall (1983) drew an analogy between the relatively high $^{207}Pb/^{204}Pb$ ratios and the steep $^{207}Pb/^{204}Pb$ vs $^{206}Pb/^{204}Pb$ correlation seen in the lavas, and similar features in modern arc volcanic rocks.

Pb isotopic compositions of galenas from the Scottish crust were first reported by Moorbath (1962). Kennan et al.(1979) combine Moorbath`s early determinations with more recent Pb isotopic studies on Irish galenas. They calculate single stage μ values and show that these vary systematically showing a progressive increase southwards from Scotland to England. A more detailed study of galena isotopic compositions from the Midland Valley of Scotland and adjacent regions is reported by Parnell and Swainbank (1984). They find lead isotope compositions to vary markedly between different regions with the regional pattern diverging from the simple southerly increase in isotope ratios reported in earlier studies (Kennan et al.1979). Galenas from the northern Midland Valley were found to be more radiogenic than those from both the southern Grampian Highlands and the southern Midland Valley. The change in isotopic composition across the

Highland Boundary Fault was attributed to the presence or absence of Dalradian rocks as opposed to any major change in the deep basement. The radiogenic nature of galenas in the northern Midland Valley was assumed to be a feature directly inherited from primary variation in the host Lower ORS lavas.

7.4 ANALYTICAL PROCEDURE

Igneous K-feldspars are particularly suited to lead-evolution studies because, having generally high Pb/U ratios, their lead is expected to closely approximate the initial isotopic composition of their host rocks, and to be relatively insensitive to age correction. Whilst K-feldspar is an abundant phase in granite clasts of northerly provenance, it is less common in the tonalite and granodiorite clasts which share a southerly provenance. As a result it proved to be impractical to separate K-feldspar from the foliated tonalite clasts (G1) and the less evolved biotite granodiorites (G2) of southerly derivation. Plagioclase separates were consequently used in lieu of K-feldspar for common Pb determinations for these clasts. As Pb substitutes for K, Pb concentrations in plagioclase are not as high as in K-feldspar. Uranium concentrations are however low (<1 ppm).

Feldspars for Pb analysis were concentrated using conventional heavy liquid and magnetic separation techniques (Appendix 2). The separates were cleaned in acetone and leached in 1N HCl (twice distilled) for one hour. They were subsequently rinsed several times in x3 distilled water.

Splits of 2-300 mg were dissolved in distilled HF using screw-top PFA vessels placed on a hotplate at 150°C. Complete dissolution took several days. Each sample was subsequently dried down, taken up in 6N HNO_3 and part aliquoted into a small screw-top PFA teflon vessel to which was added $\underline{c}$ 0.2g of a mixed ^{254}U-^{206}Pb spike. The samples were subsequently dried down under evaporators and taken up in 6N HCl (x2 distilled).

Pb was separated from spiked and unspiked aliquots using a two stage ion exchange technique. The samples were taken up in HBr and loaded onto pre-washed anion exchange columns. These columns were freshly made up using Bio-rad anion exchange resin (AG1-X8, 200-400 mesh). After initial washing with 4 column volumes of HBr, followed by three column volumes of 2N HCl, Pb was eluted with 3 column volumes of 6N HCl. The samples were dried down and the procedure was then repeated to clean up the Pb recovered

during the first elution. U was recovered from the washings collected during the first stage of the Pb separation. These were dried down and loaded on a second set of anion exchange columns. The samples were loaded onto the columns in 7N HNO_3 and washed with 2N HCl. U was recovered by flushing with ten column volumes of x3 H_2O.

All operations, except initial weighing, aliquoting and spiking were performed in a clean air laboratory. All reagents were x2 distilled (except HF which was once distilled). Overall blanks were <10ng Pb.

Pb, after evaporation in a drop of HNO_3 was loaded onto a single Re filament assembly with silica gel and H_3PO_4. U was also loaded on a Re filament using Ta_2O_5 dust and H_3PO_4. All mass spectrometry was performed on a VG Isomass 54E machine.

Pb isotope ratios are subject to fractionation during mass spectrometry runs for which it is impossible to correct by reference to a standard ratio. Machine discrimination and fractionation effects must therefore be corrected for after analysis by normalising the data against a common Pb standard.

NBS SRM 981 was analysed in position 1 of each sample barrel allowing the run conditions to be standardised. Results for three separate analyses of NBS 981 made during this study are given in Table 7.1. When these are fractionation corrected by 0.1% amu^{-1} they closely agree with recommended values for the NBS standard. A fractionation correction of 0.1% amu^{-1} has therefore been applied to all Pb ratios determined.

Between 15 and 50 sets, each based on 10 peak scans were measured and the ratios $^{208}Pb/^{204}Pb$, $^{207}Pb/^{204}Pb$ and $^{206}Pb/^{204}Pb$ averaged. $^{208}Pb/^{204}Pb$ and $^{207}Pb/^{204}Pb$ ratios were determined for both spiked and unspiked samples providing an external control on fractionation. Between 10 and 40 sets, based on 10 scans each of the ratio $^{254}U/^{251}U$, were measured during uranium runs.

Analytical data for 12 feldspar separates are listed in Table

7.2. Both raw data and fractionation corrected ratios are shown, together with age corrected values for $^{208}Pb/^{204}Pb$, $^{207}Pb/^{204}Pb$ and $^{206}Pb/^{204}Pb$. These have been calculated using the U and Pb concentrations determined by isotope dilution and assuming a Th/U ratio of 4.0. An age of 420 Ma has been assumed. In addition, three samples for which U and Pb concentrations are unavailable are included in Table 7.2.

Table 7.1

PB STANDARDS

		2σ	
	$^{206}Pb/^{204}Pb$	$^{207}Pb/^{204}Pb$	$^{208}Pb/^{204}Pb$
981-1	16.896 ± 3	15.444 ± 3	36.557 ± 7
981-2	16.894 ± 4	15.442 ± 8	36.538 ± 25
981-3	16.893 ± 6	15.442 ± 5	36.561 ± 12
FRACTIONATION CORRECTED			
981-1	16.930 ± 3	15.490 ± 3	36.703 ± 7
981-2	16.928 ± 4	15.488 ± 8	36.684 ± 25
981-3	16.927 ± 6	15.488 ± 5	36.707 ± 12
RECOMMENDED			
SRM981	16.937	15.491	36.720

						AGE CORRECTED RATIOS (420 Ma)		
SAMPLE	U	Pb	$^{206}Pb/^{204}Pb$	$^{207}Pb/^{204}Pb$	$^{208}Pb/^{204}Pb$	$^{206}Pb/^{204}Pb$	$^{207}Pb/^{204}Pb$	$^{208}Pb/^{204}Pb$
4366	0.10	6.76	18.276 ± 3	15.556 ± 2	37.887 ± 8[a]	18.250	15.599	37.958
				(15.550 ± 2)	(37.856 ± 8)[b]			
			18.313 ± 3	15.603 ± 2	38.039 ± 8[c]			
4328	0.15	21.29	18.246 ± 1	15.541 ± 2	37.867 ± 7	18.253	15.586	37.981
				(15.548 ± 2)	(37.881 ± 8)			
			18.283 ± 1	15.588 ± 2	38.019 ± 7			
4279	0.90	45.35	18.329 ± 2	15.601 ± 5	38.067 ± 14	18.281	15.643	38.111
				(15.605 ± 6)	(38.071 ± 20)			
			18.366 ± 2	15.649 ± 5	38.220 ± 14			
4329	0.85	34.42	18.362 ± 7	15.590 ± 2	38.164 ± 21	18.293	15.631	38.181
				(15.564 ± 7)	(38.053 ± 28)			
			18.399 ± 7	15.637 ± 2	38.317 ± 21			
4282			18.274 ± 1	15.561 ± 2	37.949 ± 6			
			18.310 ± 1	15.608 ± 2	38.101 ± 6			

Table 7.2a. Isotopic data for feldspar separates. Uncorrected isotope ratios[a], replicate $^{207}Pb/^{204}Pb$ and $^{208}Pb/^{204}Pb$ ratios from isotope dilution determinations[b], mass fractionation corrected data[c], and age corrected data. Errors are 2σ.

						AGE CORRECTED RATIOS (420 Ma)		
SAMPLE	U	Pb	$^{206}Pb/^{204}Pb$	$^{207}Pb/^{204}Pb$	$^{208}Pb/^{204}Pb$	$^{206}Pb/^{204}Pb$	$^{207}Pb/^{204}Pb$	$^{208}Pb/^{204}Pb$
4311	0.14	9.06	18.282 ± 1	15.570 ± 2	37.982 ± 9	18.253	15.613	38.050
				(15.544 ± 3)	(37.882 ± 8)			
			18.319 ± 1	15.617 ± 2	38.135 ± 9			
4462	0.46	11.04	18.418 ± 6	15.569 ± 7	38.178 ± 19	18.277	15.606	38.102
				(15.569 ± 6)	(38.196 ± 13)			
			18.455 ± 6	15.616 ± 7	38.331 ± 19			
4278	0.11	9.85	18.253 ± 7	15.562 ± 4	37.933 ± 9	18.242	15.606	38.024
				(15.603 ± 68)	(37.974 ± 203)			
			18.290 ± 7	15.609 ± 4	38.085			
4331	0.15	1.67	18.892 ± 9	15.537 ± 9	38.276 ± 23	18.543	15.562	37.932
				(15.547 ± 7)	(38.276 ± 23)			
			18.930 ± 9	15.584 ± 9	38.430 ± 23			
3134	0.98	48.40	17.883 ± 1	15.434 ± 1	37.785 ± 6	17.834	15.476	37.827
				(15.409 ± 3)	(37.706 ± 9)			
			17.919 ± 1	15.480 ± 1	37.937 ± 6			

Table 7.2b.

SAMPLE	U	Pb	$^{206}Pb/^{204}Pb$	$^{207}Pb/^{204}Pb$	$^{208}Pb/^{204}Pb$	$^{206}Pb/^{204}Pb$	$^{207}Pb/^{204}Pb$	$^{208}Pb/^{204}Pb$
3304	0.65	34.74	18.083 ± 3	15.487 ± 6	37.806 ± 16	18.040	15.529	37.856
				(15.491 ± 2)	(37.806 ± 8)			
			18.119 ± 3	15.534 ± 6	37.958 ± 16			
3309	0.20	41.61	17.945 ± 8	15.467 ± 10	37.734 ± 23	17.961	15.512	37.859
				(15.437 ± 1)	(37.655 ± 12)			
			17.981 ± 8	15.514 ± 10	37.886 ± 23			
3220	1.00	53.72	17.873 ± 5	15.438 ± 4	37.805 ± 10	17.831	15.480	37.856
				(15.435 ± 4)	(37.800 ± 17)			
			17.909 ± 5	15.484 ± 4	37.957 ± 10			
3152			17.874 ± 2	15.429 ± 2	37.648 ± 9			
				(15.435 ± 2)	(37.667 ± 6)			
			17.910 ± 2	15.475 ± 2	37.799 ± 9			
4286			18.264 ± 7	15.573 ± 2	37.924 ± 14			
				(15.566 ± 2)	(37.892 ± 29)			
			18.301 ± 7	15.620 ± 2	38.076 ± 14			

Table 7.2c.

7.5 RESULTS

Fractionation and age corrected $^{207}Pb/^{204}Pb$ and $^{206}Pb/^{204}Pb$ ratios are plotted on a conventional evolution diagram (Fig. 7.1). Present day and age corrected isotopic compositions are joined by tie lines. Pb isotopic compositions of Caledonian granite feldspars are included for reference. These are from Blaxland et al (1979) and have not been fractionation corrected. A number of features are evident in this diagram.

1. There is a clear distinction in the feldspar Pb isotopic compositions of granite clasts derived from a southerly source within the Midland Valley, and those of northerly derivation; the former are significantly more radiogenic than the latter.

2. The granite clasts of southerly derivation plot to the right of the present day geochron and are unusually radiogenic; they show a small range in $^{206}Pb/^{204}Pb$ (18.242-18.293) and a correspondingly wide range in $^{207}Pb/^{204}Pb$ (15.586-15.643) resulting in a steep correlation between age corrected $^{207}Pb/^{204}Pb$ and $^{206}Pb/^{204}Pb$.

3. The granite clasts with a southerly provenance have feldspar Pb isotopic compositions close to the estimated composition of the orogene at 400 Ma (Zartman and Doe 1981). $^{206}Pb/^{204}Pb$ ratios are comparable to values obtained from Southern Uplands granites (Blaxland et al 1979) but the $^{207}Pb/^{204}Pb$ ratios are substantially higher than previously recorded from Caledonian igneous rocks.

4. The wide range in $^{207}Pb/^{204}Pb$ in the granite clasts of southerly derivation shows no systematic relationship with $(^{87}Sr/^{86}Sr)^{i}_{420}$; apart from 4279 (G4), the Pb isotopic compositions of each of the suites G1, G2 and G3 broadly overlap within the errors introduced by the fractionation correction.

5. The three two-mica granite clasts of northerly provenance (3134, 3152, 3220) have uniform Pb isotopic compositions despite the range in initial $^{87}Sr/^{86}Sr$ ratios. These overlap, within

Figure 7.1 $^{207}Pb/^{204}Pb$ vs $^{206}Pb/^{204}Pb$ plot for feldspars from granite clasts of northerly and southerly provenance. Tie-lines connect fractionation corrected (open circles) and age corrected (filled circles) isotopic compositions. Samples 4329, 4279, 4462, 4311, 4278, 4282, 4286, 4382 and 4366 are representative southerly derived clasts belonging to the four main granite types (G1-G4). Samples 3220, 3134 and 3152 are northerly derived two-mica granites. 3309 and 3304 are northerly derived biotite granites. Data for Caledonian granites (square symbols) from Blaxland et al. (1979). Note these have not been fractionation corrected. Abbreviations are: A, Aberdeen; D, Distinkhorn; L, Lochnagar; ST, Strontian; LD, Loch Doon; F, Fleet; C, Criffel. Growth curves for orogene and mantle from Zartman and Doe (1981).

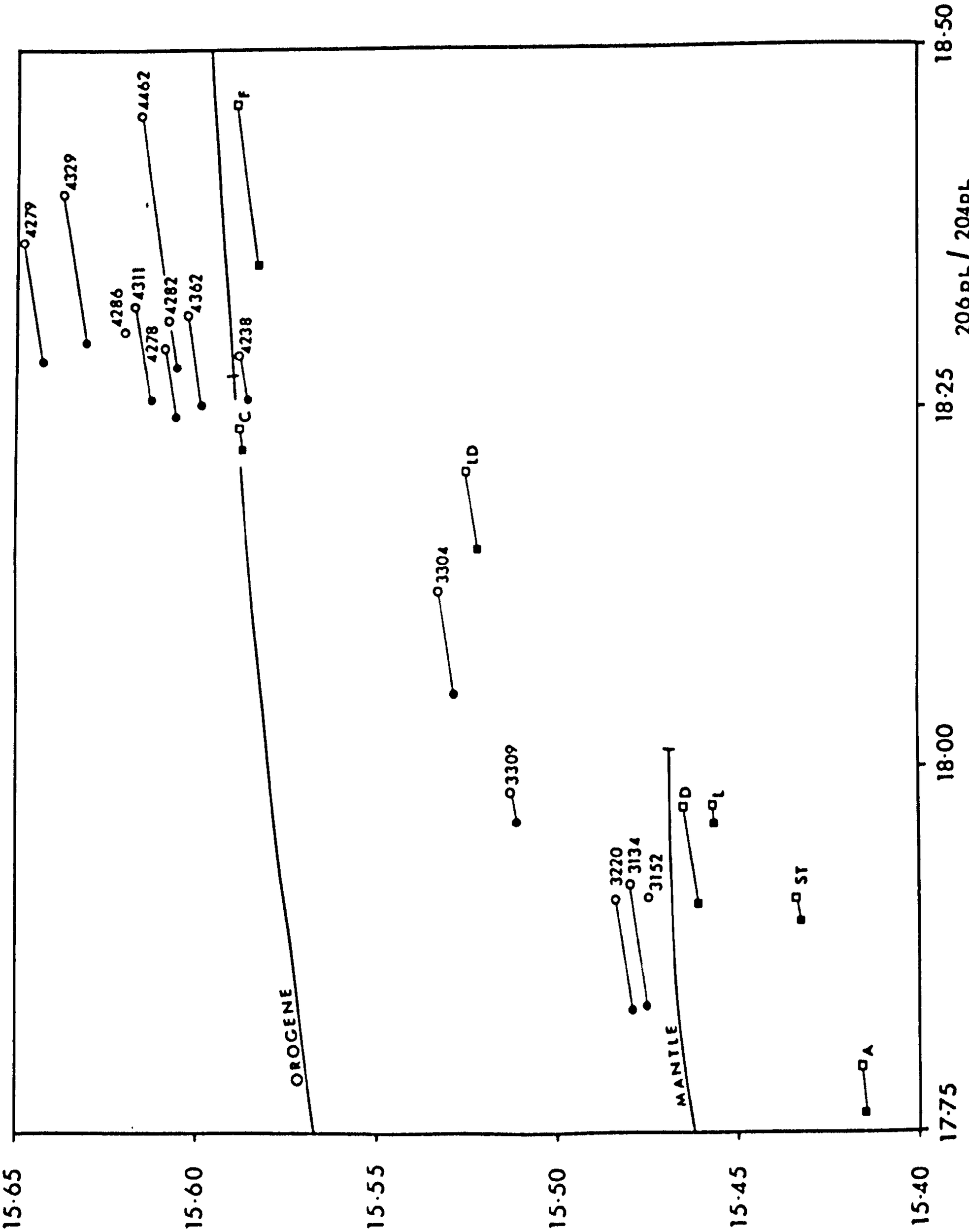
18·50
18·25
18·00
17·75
206Pb/ 204Pb
15·65
15·60
15·55
15·50
15·45
15·40
207Pb/204Pb
4462
4329
4279
4286
4311
4278
4282
4362
4238
F
C
1D
3304
3309
3220
3134
3152
D
L
ST
A
OROGENE
MANTLE

fractionation errors, the more radiogenic of the Highlands granites (e.g. Lochnagar, Strontian, Aberdeen), and the Distinkhorn tonalite which outcrops in the southwest Midland Valley.

6. The two biotite granite clasts (G2) of northerly provenance (3309, 3304) have slightly more radiogenic Pb isotopic compositions than the two-mica granites. The radiogenic character of 3304 almost certainly is a secondary effect as the Sr isotopic systematics of this clast have clearly been disturbed.

Before the data can be interpreted, it is first necessary to consider whether the age corrected feldspar compositions are representative of the magmas at the time of crystallisation. It is possible the Pb compositions have been modified since crystallisation by loosely bound U subsequently removed from the feldspar lattice, or by migration of radiogenic Pb into the feldspar lattice from discordant zircons (Faure 1977). Ludwig and Silver (1977) show that some Precambrian feldspars have unsupported radiogenic lead which is pure ^{206}Pb derived from long-term migration and accumulation of radioactive daughters of ^{238}U. It is possible that the unusually radiogenic compositions of the granite clasts of southerly provenance reflect secondary alteration and consequently it may be mislaeding to use the feldspar data to image primary variation in magmatic lead. That this is unlikely to be the case is suggested by the following evidence.

1. The southerly derived granite clasts are inferred to have been sourced by plutons which were emplaced at high level, and which were post-tectonic and unaffected by metamorphism.

2. That weathering, erosion and burial of the granite clasts has not overprinted their isotopic composition is suggested by the fact that intertongueing conglomerates dispersed from opposite margins of the basin retain their distinct isotopic fingerprint.

3. Although oxidation ratios for the southerly derived clasts are

higher than those of northerly provenance, there is no correlation between degree of alteration and isotopic composition. In fact the clast which has the highest $^{207}Pb/^{204}Pb$ ratio (4279) is one of the freshest petrographically. This is mirrored in its LOI value of 0.44% and its low oxidation ratio of 0.32.

4. It is unlikely that secondary alteration could induce the steep correlation between $^{207}Pb/^{204}Pb$ and $^{206}Pb/^{204}Pb$, and the narrow range in $^{206}Pb/^{204}Pb$.

5. The clasts of northerly derivation are isotopically similar to in-situ granites exposed in the Grampian Highlands. Should the clasts have been derived from these or related plutons (as is suggested by independent chemical and isotopic data) the Pb isotopic compositions clearly do not deviate from what are interpreted to be true magmatic compositions.

7.6 DISCUSSION

7.6.1 Southerly Derived Granite Clasts

The granite clasts of southerly provenance have unusually radiogenic Pb compositions and are displaced to higher $^{207}Pb/^{204}Pb$ ratios than the bulk of the late Caledonian granites. The age corrected data show a steep correlation between $^{207}Pb/^{204}Pb$ and $^{206}Pb/^{204}Pb$. Similar steep $^{207}Pb/^{204}Pb$ - $^{206}Pb/^{204}Pb$ arrays at high $^{207}Pb/^{204}Pb$ have been shown to characterise island arc volcanic rocks. Sun (1980) attributed such behaviour to mixing between a mantle component and subducted sediment. Some Cordilleran-style batholiths show a similar pattern. Gariepy et al. (1985) record steep $^{207}Pb/^{204}Pb$ - $^{206}Pb/^{204}Pb$ trends and high $^{207}Pb/^{204}Pb$ from the Trans-Himalayan plutonic complex, a Cretaceous-Palaeocene batholith interpreted to have developed during northward subduction of Mesozoic ocean crust beneath Tibet. Gariepy et al.(1985) interpret the Pb isotopic compositions of Trans-Himalayan complex feldspars as reflecting mixing between a mantle-like component and a radiogenic crust-like end-member. They favour crustal contamination during magma ascent to account for the mixing trend and the high $^{207}Pb/^{204}Pb$ (in all cases significantly higher than MORB ratios).

The relationship between $^{207}Pb/^{204}Pb$ and $(^{87}Sr/^{86}Sr)_i$ for the clasts of southerly provenance is shown in Figure 7.2a. Whilst the tonalites and granodiorites making up G1, G2 and G3 can generally be distinguished on the basis of their Sr systematics, the Pb compositions reveal no such distinction. $^{207}Pb/^{204}Pb$ ratios broadly overlap in clasts of G1, G2 and G3 type pointing to probable widespread homogenisation of Pb in the reservoir which contributed Pb to the magmas. The uniform Pb ratios for clasts from each of the suites suggest a close relationship between the plutons which gave rise to the various clast types. The range in $^{207}Pb/^{204}Pb$ is considerably enhanced by two samples, 4329 and 4328, which have $^{207}Pb/^{204}Pb$ ratios both higher and lower than the narrow range of compositions defined by the rest of the clasts.

FIGURE 7.2 (A) Relationship between age corrected $^{207}Pb/^{204}Pb$ and $(^{87}Sr/^{86}Sr)_i$ for southerly derived granite clasts. Note $^{207}Pb/^{204}Pb$ ratios are not age corrected for samples 4286 and 4282. (B) Relationship of $^{206}Pb/^{204}Pb$ and $(^{87}Sr/^{86}Sr)_i$ for granite clasts compared with the estimated compositional fields for depleted mantle; late Proterozoic upper crust (Dalradian, Moine); Archaean lower crust (Lewisian granulites and amphibolites); the Etive and Laggan-Strathspey complexes; granites from the Southern Uplands; and SULPS. Data from Clayburn et al.(1983), Halliday et al.(1980), Thirlwall (1983) and Frost and O`Nions (1985). Average composition of southerly derived granite clast types G1-G4 shown with conventional open symbols. Solid diamonds are northerly derived two-mica granite clasts.

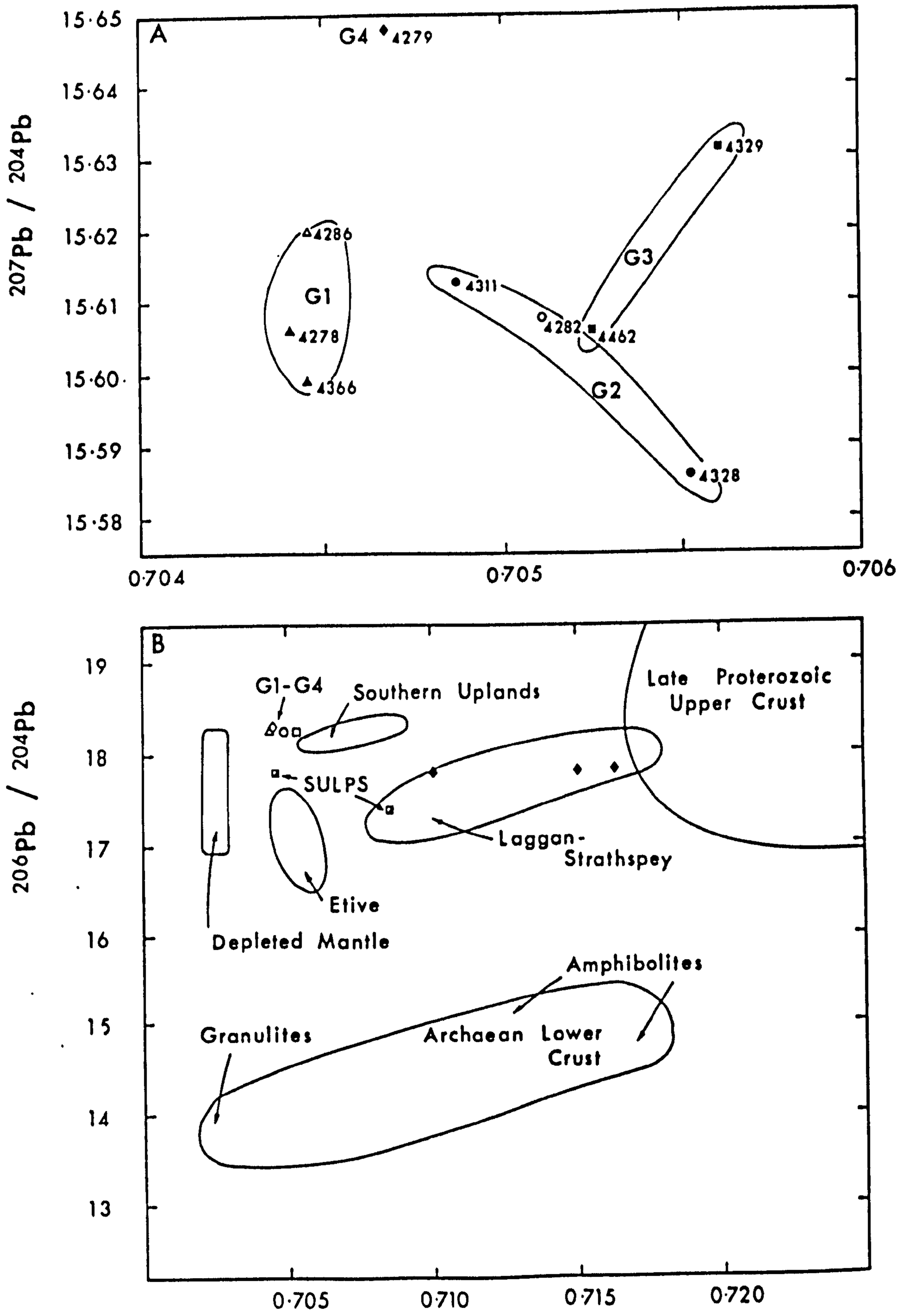
A
G4 ♦4279
G1
▲4278
△4286
▲4366
G3
■4329
●4311
○4282
■4462
G2
●4328
15·65
15·64
15·63
15·62
15·61
15·60
15·59
15·58
207Pb / 204Pb
0·704
0·705
0·706
B
G1-G4
Southern Uplands
SULPS
Laggan-
Strathspey
Late Proterozoic
Upper Crust
Etive
Depleted Mantle
Amphibolites
Granulites
Archaean Lower
Crust
19
18
17
16
15
14
13
206Pb / 204Pb
0·705
0·710
0·715
0·720
(87Sr / 86Sr)i

FIGURE 7.3 $^{208}Pb/^{204}Pb$ vs $^{206}Pb/^{204}Pb$ plot for feldspars from granite clasts of northerly and southerly provenance. Tie-lines connect fractionation corrected (open circles) and age corrected (filled circles) isotopic compositions. Samples 4329, 4279, 4462, 4311, 4278, 4282, 4286, 4382, and 4366 are representative southerly derived clasts belonging to the four main granite types (G1-G4). Samples 3220, 3134 and 3152 are northerly derived two-mica granites. 3309 and 3304 are northerly derived biotite granites. Fields outline predominant isotopic compositions of galenas from the Midland Valley (north and south), the Southern Uplands and the Grampian Highlands. Data from Parnell and Swainbank (1984). Data for Lower ORS lavas from the Midland Valley from Thirlwall (1983) and for late Caledonian granites from Blaxland *et al.* (1979). Note the latter have not been fractionation corrected. Abbreviations are Ab: Aberdeen; D: Distinkhorn; LG: Lochnagar; LD: Loch Doon; F: Fleet; CF: Criffell. Growth curves for orogene and upper crust from Zartman and Doe (1981).

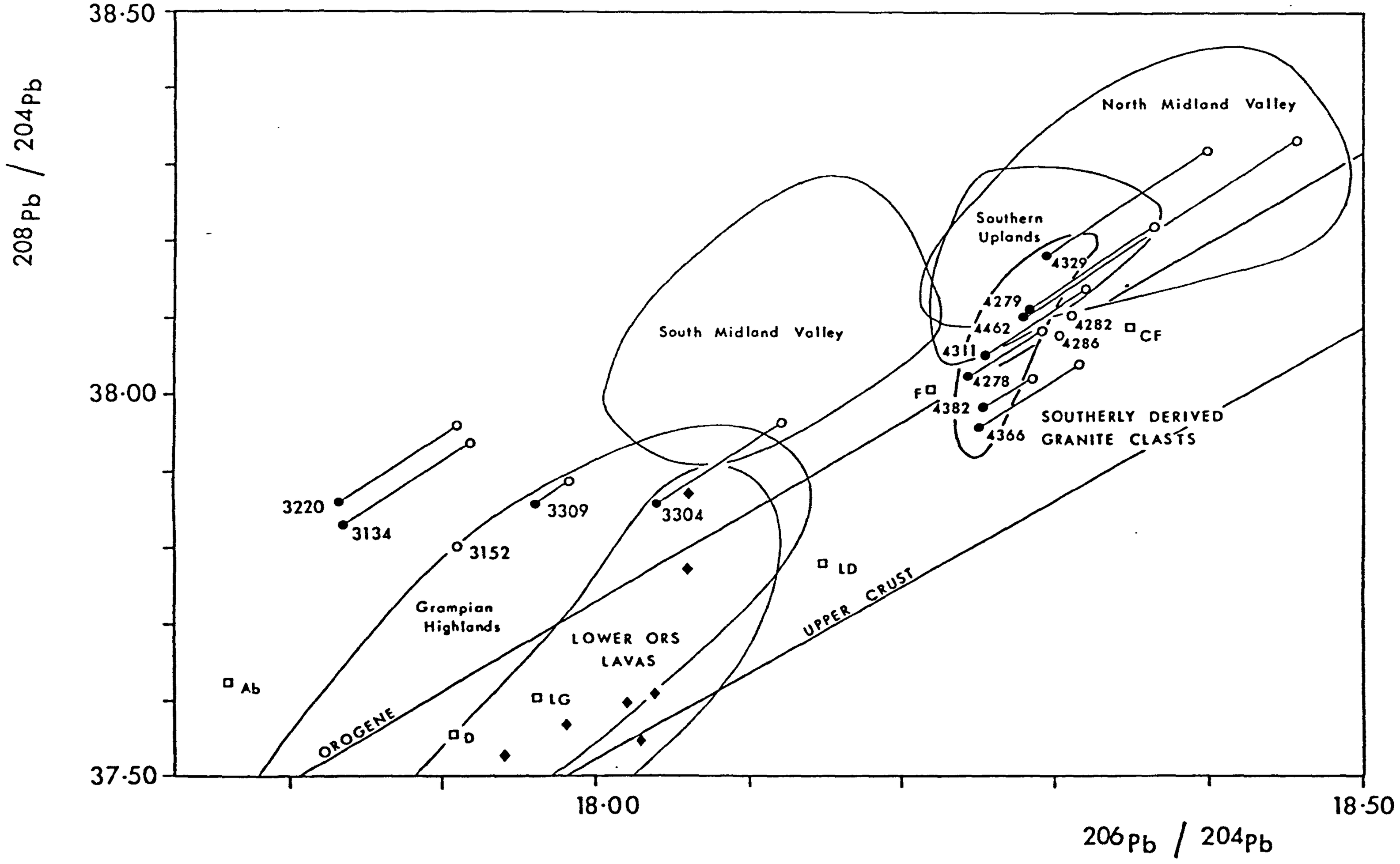
38·50
38·00
37·50
18·00
18·50
208Pb / 204Pb
206Pb / 204Pb
North Midland Valley
Southern Uplands
South Midland Valley
Grampian Highlands
LOWER ORS LAVAS
OROGENE
UPPER CRUST
SOUTHERLY DERIVED GRANITE CLASTS
4329
4279
4462
4282
CF
4311
4286
4278
F
4382
4366
3220
3134
3309
3304
3152
LD
Ab
LG
D

4329 (G3) has the highest initial $^{87}Sr/^{86}Sr$ ratio of any G3 clast analysed. The clast contains metasedimentary xenoliths and these are thought to have contributed to the enriched $(^{87}Sr/^{86}Sr)_i$. The age corrected $^{207}Pb/^{204}Pb$ ratio determined for 4329 is also more radiogenic than in the uncontaminated G3 clast, 4462. The apparent coupling of $(^{87}Sr/^{86}Sr)_i$ and $^{207}Pb/^{204}Pb$ suggest the more radiogenic Pb composition of 4329 may reflect contamination of the G3 magma at high level during emplacement. This implies the sediment pile into which the magma rose had high $^{207}Pb/^{204}Pb$ such that contamination could produce a shift to enhanced $^{207}Pb/^{204}Pb$ in a magma which already had radiogenic Pb isotopic compositions. As $^{207}Pb/^{204}Pb$ appears to be sensitive to high level contamination constraints can be placed on the variation in $(^{87}Sr/^{86}sr)_i$ between each of the granite clast suites. As G1, G2 and G3 have broadly comparable $^{207}Pb/^{206}Pb$ ratios irrespective of $(^{87}Sr/^{86}Sr)_i$, the observed increase in $(^{87}Sr/^{86}Sr)_i$ between the granite clast types in the order G3>G2>G1 cannot be explained by high level contamination alone. Each of the granite suites must have largely inherited their unique Sr isotopic compositions from deeper crustal levels.

4328 is a sample of one of the more evolved granite clasts of G2 type. $(^{87}Sr/^{86}Sr)_i$ appears to increase with increasing SiO_2 and A/CNK amongst the variable granites of this group. The sympathetic increase of A/CNK with $(^{87}Sr/^{86}Sr)_i$ has been shown in 4.5 to be compatible with a model involving an increasing metasedimentary contribution to the magma. The $^{207}Pb/^{204}Pb$ ratio determined for 4328 is however the least radiogenic of the feldspar lead compositions measured in granite clasts of southerly derivation. On the basis of the limited data available, $^{207}Pb/^{204}Pb$ therefore appears to have a negative correlation with initial $^{87}Sr/^{86}Sr$ in clasts of G2 type. Should this be substantiated by further analyses, the metasedimentary component inferred to be present in more evolved G2 clast types would have to be isotopically distinct from the metasediments contaminating the G3 magma at high level. It must be emphasised however that the difference in $^{207}Pb/^{204}Pb$ ratios between 4328 and 4329 is close to the limit of errors introduced by mass fractionation and the interpretation of the data must therefore

be necessarily cautious.

The most radiogenic Pb composition determined from granite clasts of southerly provenance is for 4279. This clast is both chemically and isotopically distinct from the rest of the southerly derived clasts and it appears to record an early phase of late Ordovician plutonism. 4279 is strongly peraluminous but has a low $^{87}Sr/^{86}Sr$ ratio (0.70448 at 443 Ma).

If the generally high $^{207}Pb/^{204}Pb$ of the southerly derived clasts is to be explained in terms of mixing between mantle-like and crustal-like reservoirs, the uncoupled behaviour of Sr and Pb must be explained. Two processes may contribute to the uncoupling of Sr and Pb systematics. Firstly, largely independent reservoirs of Pb and Sr may have contributed to the magmas. Halliday et al.(in press) argue that magmas originating in the mantle may obtain the bulk of their Sr from their mantle source regions where plagioclase is unstable. As Pb is enriched in the continental crust minor crustal contamination can however dominate the isotopic composition of Pb in the magmas. The implication is that Sr and Pb have very different sensitivities to contamination. A second mechanism for producing uncoupling of Sr and Pb is large scale circulation of fluids and regional equilibration of Pb isotopes. Several studies have shown Pb isotopes to be remarkably uniform on a regional scale, irrespective of rock type, and despite the fact that the Sr and O isotopes may show a correspondingly large range (Michard-Vitrac et al.1981, Gariepy et al.1985). This has been taken to indicate widespread homogenisation of lead isotopes by large scale mobilisation and circulation of fluids. Fluid circulation fails to equilibrate Sr regionally allowing regional variation in Sr isotopes to persist. The narrow range of $^{207}Pb/^{204}Pb$ ratios for the granite clasts suggests regional equilibration of Pb isotopes may have been an important factor in uncoupling Pb from Sr variation.

The unusually high $^{207}Pb/^{204}Pb$ ratios of the granite clasts of southerly provenance distinguish them from other Caledonian granites. Only the Fleet and Criffel plutons in the Southern

Uplands show comparable radiogenic compositions. The radiogenic character of the clasts precludes the involvement of U-depleted granulites in the magma petrogenesis. The similarity in composition and behaviour of Pb isotopic variation between the clasts and volcanic and plutonic rocks associated with subduction of oceanic crust (see above) argues for a destructive margin setting for the magmas sampled by the conglomerates. Several mechanism have been proposed for producing steep mixing trends and high $^{207}Pb/^{204}Pb$ ratios in arc environments. These include melting of pelagic sediments within the down-going slab, subduction and melting of continental detritus shed into the trench, and assimilation of continental crust.

Judging from the composition of modern pelagic sediments (Stacey and Kramers 1975) the $^{207}Pb/^{204}Pb$ ratios of Iapetus pelagic sediments are likely to have been lower than those required to produce the granite Pb compositions by mixing. Subduction of pelagic sediment is therefore unlikely to be the mechanism whereby the magmas achieved high $^{207}Pb/^{204}Pb$. Subduction and melting of continental detritus shed into the trench might explain the data if the detritus was eroded from a continental terrane which was both sufficiently old, and enriched in U, to impart high $^{207}Pb/^{206}Pb$ ratios to the sediment eroded from it.

Little is known of the Pb isotopic composition of Caledonian sediments, not least on account of the considerable uncertainties involved in determining reliable U/Pb ratios for sedimentary rocks. Thirlwall (1983) presents two analyses of Southern Uplands greywackes which prove to be substantially less radiogenic than that required to explain the Pb variation in the granite feldspars. Harmon et al. (1984) point out that the Southern Uplands sediments may either be very heterogeneous with respect to Pb, or that they have been contaminated by U-Pb alteration and therefore may not be representative of the sediment involved in the petrogenesis of Caledonian igneous rocks. They propose that `type II` western U.S. leads (Zartman 1974) may be a more realistic estimate of sedimentary upper crustal Pb south of the Highland Boundary Fault. These are

of the Dalradian metamorphic pile (Clayburn et al 1983). The Pb data for the two-mica granite clasts are therefore compatible with a provenance for the clasts in the adjacent Grampian Highlands terrane as outlined in 5.7.3.

The biotite granites 3304 and 3309 have slightly more radiogenic Pb compositions than the two-mica granites. 3304 is altered but 3309 has probably retained its original magmatic Pb composition. 3309 has a composition similar to the more radiogenic granites emplaced in the Highlands and cannot have a large unradiogenic lower crustal Pb component. This is confirmed by the relatively high $(^{87}Sr/^{86}Sr)_i$ ratio of 0.70602 for 3309, suggesting a degree of crustal interaction. As the biotite granites of northerly derivation are highly evolved, it is likely they crystallised from strongly fractionated magmas pooled in high level magma chambers. Crustal contamination and modification of Sr and Pb isotopic compositions may have taken place in these high level magma chambers.

Initial $^{87}Sr/^{86}Sr$ ratios in the evolved granites of the Cairngorm suite (Stephens and Halliday 1984) appear to be more radiogenic than those in granites of the Argyll and SW Highlands suites to the west (Fig.5.14). Variation in the Pb isotopic compositions of the Highland granites between the chemical and isotopic suites recognised by Halliday (1984), and Stephens and Halliday (1984) are less well known. Blaxland et al.(1979) analysed a single Cairngorm suite pluton, Lochnagar. Significantly, it is the most radiogenic of the granites from north of the Highland Boundary Fault, and has a similar $^{206}Pb/^{204}Pb$ ratio to 3309. It may be that granites of the Cairngorm suite generally have enhanced $^{206}Pb/^{204}Pb$ ratios in accordance with Sr evidence for a greater degree of upper crustal contamination. The greater importance of upper crustal contamination may suppress the unradiogenic lower crustal Pb component seen regionally in other Highland granites.

7.6.3 Implications for Crustal Structure

The Pb isotopic data presented above show the granite detritus dispersed from opposite flanks of the Crawton Basin to be isotopically distinct. The basin overlies a boundary between

granites which to the south have more radiogenic Pb compositions than those to the north. Similar junctions in the regional variation of feldspar Pb isotopic compositions have been attributed to variations in crustal structure (Zartman 1974, Michard-Vitrac et al. 1981, Gariepy et al. 1985). It is likely therefore that the isotopic variation recorded across the basin reflects an important crustal break on which the basin nucleated. This break is inferred to be the terrane boundary along which the Midland Valley and a granite-metamorphic terrane were juxtaposed during the late Silurian-early Devonian. The Pb isotope data are compatible with the latter being the Grampian Highlands terrane. The change in Pb isotopic ratios in granites intruding the crust on opposite margins of the basin reflects the lack of a component of unradiogenic lower crustal Pb in granites emplaced in the Midland Valley. The southerly derived granites also have an important radiogenic Pb component in their petrogenesis, which by analogy with destructive margin magmas elsewhere, may be subducted sediment. Alternatively the magmas may have derived their Pb from an unusually radiogenic deep crustal reservoir homogenised by large scale fluid circulation.

The regional variation in feldspar Pb isotopic compositions across the Scottish crust needs to be reconsidered in the light of the present data. Van Breemen and Bluck (1981) interpreted the available feldspar data in terms of a progressive increase in $^{206}Pb/^{204}Pb$ from north to south. This can no longer be the case as the data from the clasts of southerly derivation establish that granites emplaced in the east central Midland Valley during the Silurian were more radiogenic than the Southern Uplands granites. Only a single granite is known from the intervening ground, the Distinkhorn tonalite in the SW Midland Valley. This is less radiogenic than either the granites which are thought to have pssed through the northern Midland Valley crust, or the Southern Uplands granites. The Scottish crust therefore appears to be segmented into a series of crustal blocks characterised by distinct Pb isotopic compositions. Granites intruding the Highlands have the least radiogenic Pb whilst granite clasts in the NE Midland Valley attest to the former presence of Silurian plutons with unusually radiogenic Pb. It is unclear whether the

crustal block into which these latter granites were emplaced was subsequently removed by strike-slip faulting, or whether it forms part of the present basement to the northern Midland Valley. The fact that the lead isotopic composition of the Distinkhorn tonalite is less radiogenic than the granites sampled by the clasts indicates that there may be a distinction in terms of isotopic composition between granites emplaced in the northern and southern Midland Valley. There is a tendency to view the Midland Valley as a single terrane where in fact it may be that it represents a composite of separate terranes, with important crustal structures located within the Midland Valley itself.

The galena and granite feldspar data are compared in Figure 7.3. The compositional variation of the galenas closely parallels that for the feldspar data. Parnell and Swainbank (1984) showed the most radiogenic galenas to occur in the northern Midland Valley. They attribute the origin of the radiogenic compositions to scavenging from Lower ORS lavas. Some of the galenas are notably more radiogenic than the range of Pb isotopic compositions determined for Lower ORS lavas by Thirlwall (1983). It is possible that radiogenic sediments and granites similar to those sampled by the southerly derived conglomerates lie beneath much of the Strathmore Lower ORS sequence and may have contributed to the composition of Pb in the galenas. The galenas show a marked compositional variation across the Midland Valley with galena occurrences to the north being substantially more radiogenic than those to the south.

CHAPTER EIGHT

CONCLUSIONS

1. Two contrasting conglomerate lithosomes have been identified in coastal exposures of the Dunnottar and Crawton Groups in Kincardineshire. These are not only distinguished by their gross structure, but also by mutually exclusive clast assemblages and contraposed palaeoflows. Conglomerates having an important recycled component and a derivation from the north and north-east are dominated by metaquartzite, psammite and granite detritus. Angular conglomerates of southerly and easterly provenance are of first cycle derivation and include clasts of lithic arenite, metagreywacke, granite, vesicular basalt and rare limestone. Andesitic and dacitic detritus occurs in conglomerates of both northerly and southerly provenance, and also makes up discreet volcanogenic units which comprise a subordinate third lithosome type.

2. The structure of the two conglomerate lithosomes is in both instances consistent with fluvial deposition. Lateral textural and grainsize transitions have a direct analogy in gravel bars in modern gravel-bed rivers. The lithosomes are distinguished by the greater abundance of cross-stratification and channelled erosion surfaces in the first-cycle conglomerates of southerly provenance. Northerly derived conglomerates have a sheet-like geometry and were evidently generated in an unconfined fluvial regime with a low bed topographic contrast. The different lithosome structure and contraposed dispersal of coeval conglomerates are attributed to deposition on fluvial dominated fans prograding from opposite margins of a small laterally filled basin.

3. The difference in lithosome structure on opposite margins of the basin may be a consequence of two unrelated processes. Basins developed between two active fault strands generally show evidence for basin floor tilting, as vertical displacements on the boundary faults are unlikely to be exactly matched. This is commonly expressed by variation in marginal fan structure across the basin. Scale considerations however suggest intrabasinal and fault margin processes may not be wholly responsible for the difference in fan behaviour in this case. The contrast in structure may in part reflect the distinction which must be made

between a large antecedent drainage system captured by the basin, and a smaller scale system initiated by the basin itself.

4. Several features of the Dunnottar and Crawton Groups require that the depositional setting was substantially different from that in which the widely correlated upper levels of the Strathmore succession accumulated. A significant change in the nature of Lower ORS sedimentation is implied. The Strathmore succession has previously been considered as the fill to a single elongate basin which gradually extended south-westwards by lateral overstep. An alternative interpretation evokes vertical amalgamation of essentially separate basins in response to a changing tectonic framework. The Dunnottar and Crawton Groups are interpreted as having accumulated within a small tectonically active sub-basin (the Crawton Basin) to the laterally more extensive and overlying Strathmore Basin. In this respect thickness variation in the Strathmore succession may largely be a function of sub-basin development.

5. The Crawton Basin has many of the attributes normally thought to characterise basins of pull-apart type. These include a thick fill relative to the small size of the basin, high rates of sedimentation, asymmetrical facies patterns, and textural cycles which probably reflect tectonic activity. Other features lending support to a pull-apart interpretation include the very different provenance of sediment derived from opposite margins of the basin, the evidence for widespread sinistral transpression in the zones flanking the basin during its formation, and some internal features of the sediment fill. The available radiometric and biostratigraphic data suggest the Strathmore succession has a two stage subsidence history with the rate and pattern of subsidence resembling subsidence curves for established pull-apart basins. The Crawton Basin is interpreted as a small laterally filled pull-apart basin which preceded the development of a more extensive finer grained axial filled basin. The dominant control on the latter is thought to have been thermal subsidence following the crustal extension which generated the earlier pull-apart.

6. The transition from a small laterally filled extensional basin to a large axial filled basin significantly coincides with the acme of Lower ORS volcanism. Lower ORS volcanic rocks in the Midland Valley have generally been ascribed to the operation of a volcanic arc above a north-west facing subduction zone which persisted into the lowermost Devonian. This is however difficult to reconcile with evidence for the cessation of subduction during the Silurian. Given the evidence for widespread transpressional tectonics it is possible that lineament controlled volcanism is a more realistic mechanism for the generation of the voluminous suite of Lower ORS volcanic rocks. Leaky transcurrent faults are one of the few settings outside of island and continental arc regimes where orogenic andesites may occur.

7. Granite clasts preserved in first-cycle conglomerates of southerly provenance are a unique sample of granites which can no longer be found in outcrop. The clasts were derived from a source terrane which during the late Silurian - early Devonian occupied the east central Midland Valley. Four distinctive granite suites can be identified on the basis of field appearance and petrography. The subdivision into suites is substantiated by major and trace element analyses for the clasts. Compositional variation between the granite clasts can be resolved into two components. Amongst clasts assigned to the same suite, chemical variation is generally continuous and produces linear or sub-linear trends on variation diagrams. Internal variation of this type is overprinted by a compositional separation of each of the suites. This is best seen for K_2O with the granite clasts spanning the full spectrum of orogenic magma compositions from low- to high-K magmas. This is unusual for Caledonian granites which tend to be highly potassic and have a restricted range of K_2O at constant silica. The clasts however show Na enrichment comparable to that seen in other Caledonian granites, and have a similar calc-alkaline affinity.

8. Rb-Sr mineral-whole rock isochrons for representative clasts establish that the bulk of the granitic detritus is derived from plutons of Silurian age. A single clast of a distinctive biotite-garnet granite (G4) appears to have been derived from a

late Ordovician granite pluton. Otherwise clasts from the remaining three suites produce a narrow range of ages (420 ± 5 Ma), despite the wide variation in chemical composition. These are interpreted as emplacement ages, although there necessarily must be some uncertainty in the interpretation of the data for the foliated tonalite clasts. Although the age determinations depend upon a single method (U-Pb geochronology is currently in progress) some confidence can be placed in the results in that they concur with circumstantial evidence also favouring a Silurian age. The Silurian ages for granite clasts derived from high level plutons located within the Midland Valley establish that granites of calc-alkaline affinity were emplaced in the Midland Valley at a time when magmatism was suppressed in the Grampian Highlands. In this respect the Midland Valley is more closely affiliated with the Northern Highlands. In the wider context of Lower Palaeozoic magmatism in the Midland Valley, the clasts occurring in the Crawton Basin fill a gap in a record of what can now be seen as a long history of continuous magmatism extending over an interval of greater than 150 Ma. The clasts also record an important transition in the style of Midland Valley magmatism from dominantly intrusive to dominantly effusive.

9. Whilst high level differentiation may largely account for the compositional variation within each of the granite clast suites, the wide compositional separation of the suites at constant silica cannot be explained by such a mechanism. Isotopic data suggest that the three Silurian clast suites are closely related, despite their major and trace element compositional separation. Initial $^{87}Sr/^{86}Sr$ ratios for the clasts are low indicating a mantle or low Rb/Sr crustal source for the magmas. The peraluminous foliated tonalites significantly have the lowest $(^{87}Sr/^{86}Sr)_i$ indicating the peraluminous composition cannot in this case be ascribed to crustal assimilation. Although each of the three Silurian clast suites have distinctive Sr isotopic compositions, the range in $(^{87}Sr/^{86}Sr)_i$ is smaller than would be anticipated were the compositional separation of the magmas to reflect differential contamination. Pb isotopic data show that the southerly derived granite clasts are anomalously radiogenic

with each of the granite suites having comparable Pb isotopic compositions. Preliminary Sm-Nd data confirm that the three Silurian granite suites share a similar isotopic signature. ϵ_{Nd} values for representative clasts of G1, G2 and G3 are +0.6 (4366), +0.2 (4311), and +1.1 (4462) respectively. When combined with the relevant ϵ_{Sr} data, the data plot on the negatively correlated ϵ_{Sr} - ϵ_{Nd} trend for Lower ORS Midland Valley lavas (Thirlwall 1983).

10. The wide range in major and trace element compositions developed in magmas which isotopically appear to be closely related suggests deep-level fractionation may have been important. The role of magmatism within a framework of oblique slip tectonics may have implications for the variable chemistry of the clasts. Shear zones are likely to be particularly effective sites for filter pressing in that local compression and extension can take place simultaneously in the shear zone environment. The strongly foliated tonalite clasts may have been derived from a pluton channelled to the surface along a deep reaching shear zone in which pumping of the magma resulted in deep level fractionation of hornblende and biotite, stripping the melt of K_2O, Ni, Cr and a range of other major and trace elements. The unfoliated granodiorite clasts may have been derived from a pluton emplaced in the extensional zone between adjacent shear zones, and which retained a more primitive chemistry.

11. Granite clasts also occur in polycyclic conglomerates having a northerly provenance. These are chemically and isotopically distinct from those simultaneously dispersed from the southern margin of the basin. Previously these northerly derived granite clasts were considered to be invariably primary muscovite bearing, but this has not been substantiated by more detailed study. Although two-mica granite clasts are locally abundant, they are subordinate to a diverse assemblage of biotite K-feldspar granites and acid porphyries over the sequence as a whole.

12. Chemical and isotopic data define an episodic magmatic

history for the terrane from which the clasts of northerly provenance were derived. Two-mica granite clasts from the top of the Crawton Group have Rb-Sr mineral-whole rock ages of c. 460 Ma pointing to the persistence of the 460 Ma two-mica granite source first established by Van Breemen and Bluck (1981) in the Dunnottar Group. An age of 412 ± 2 Ma for a clast of porphyritic K-feldspar biotite granite however suggests that late Silurian granites also made an important contribution to the conglomerates. These late Silurian granite clasts are geochemically quite distinctive, having highly evolved compositions, evidence for extensive high-level feldspar fractionation, and intermediate $^{87}Sr/^{86}Sr$ ratios.

13. The magmatic history of the adjacent NE Grampian tract bears a striking resemblance to that established for granite clasts in northerly derived conglomerates in the contiguous Crawton Basin. Two-mica granite plutons with ages of c. 460 Ma outcrop in Banff but are both too distant, and have the wrong Sr isotopic compositions, to be the source of the clasts. However, other two-mica granite occurrences probably also belonging to the same mid-Ordovician episode include the undated Aberdeen Granite and related granite vein complexes exposed on the coast south of Aberdeen. These have the requisite isotopic compositions to have sourced the clasts. Halliday (1984) measures an ϵ_{Nd} value of -12.7 for the Aberdeen Granite. Preliminary data for a single clast of two-mica granite from the Crawton Group indicates an ϵ_{Nd} value of -12.6. Sr and Pb isotopic data for two-mica granite clasts are also closely comparable to that for the Aberdeen Granite. Late Silurian biotite granites also occur in Aberdeenshire forming part of a regionally anomalous suite of highly evolved fractionated granitoids, the Cairngorm Suite of Stephens and Halliday (1984). The Silurian granite clasts closely resemble the granites of the Cairngorm Suite. When the regional distribution of c. 460 Ma and c. 400 Ma granitoids are considered together, the NE Grampian tract can be seen to have a unique chemical, isotopic and chronological fingerprint which cannot be extended to other tracts within the Grampian terrane, or to other terranes in the Caledonian mosaic. The fact that clasts occurring in the adjacent Lower ORS of the Crawton Basin

share this unique fingerprint suggests that the Crawton Basin has not been subsequently displaced from the source terrane from which it received sediment during the late Silurian and Lowermost Devonian.

14. The granite clast data for northerly derived conglomerates preserved in the Crawton Basin appear to require a late Silurian docking of the Midland Valley and Grampian Highlands terranes. That the two terranes were once widely separated is suggested by the lack of Grampian style metamorphic detritus in the Ordovician Highland Border Complex. Rapid post-Grampian uplift operated throughout much of this period and basins originally contiguous with the orogen might be expected to have received much detritus. The evidence for late Silurian docking of the Midland Valley and Grampian Highlands terranes is contrary to recent proposals favouring a late Devonian terrane juxtaposition (Bluck 1984, Dewey and Shackleton 1984). Much of the evidence advanced in favour of a post-Lower ORS docking history can be accommodated within the late Silurian docking model. Thus the relatively small volume of the metamorphic detritus involved, its anomalous metamorphic grade and uplift history, and the lack of metapelites, may reflect a complex history of sediment recycling through earlier successor basins. The concept of the Lower ORS as a molasse type deposit flanking the emerging Caledonian mountains (Mykura 1983) clearly needs to be re-examined. Much of the Lower ORS metamorphic detritus was handed on through reworking of pre-existing conglomerates. No major contemporaneous uplift of metamorphic basement is required. First cycle sediment dispersed to Lower ORS basins in the Midland Valley is dominantly volcanogenic pointing to the autonomous role of volcanism in generating relief which is independent of the tectonic framework.

15. Sedimentary and metasedimentary clasts in conglomerates of northerly and southerly provenance serve to emphasise the significance of the substantial crustal break over which the Crawton Basin must have formed. In addition, psammitic clasts of northerly and northeasterly provenance show clear indications of having an ultimate source in Grampian style metamorphic rocks.

Metasediment clasts at similar metamorphic grade dispersed from opposite margins of the basin are geochemically distinct and cannot have been sourced from the same metamorphic pile. Psammitic clasts of northerly provenance are unusually sodic, given their silicic compositions. This probably reflects a high original abundance of detrital albite. Coarse grained Upper Dalradian metasediments of the Southern Highland Group are also notably rich in detrital albite and have a similar major element chemistry to the clasts. Clasts derived from the east central Midland Valley include lithic arenites and metagreywackes which have an important mafic detrital component. High Cr metagreywackes are interpreted as having a provenance in ophiolitic and metamorphic rock-types. Ophiolitic detritus is common in Ordovician sedimentary basins of Northern Britain, and in correlative sequences in Newfoundland and the northern Appalachians, suggesting the clasts may be derived from a sedimentary sequence which shared this widespread Ordovician ophiolitic provenance. The occurrence of lower greenschist facies metasediments within the Midland Valley indicates that low grade metamorphism may have affected large tracts of the northern Midland Valley. Low grade metamorphism is also seen in the Highland Border Complex, a potential lateral equivalent of the sequence sampled by the clasts. The metamorphism must have been independent of, and unconnected with, the thermal history of the Grampian Highlands terrane.

16. Mica-whole rock cooling ages determined from psammitic clasts occurring in northerly derived conglomerates suggest that uplift and cooling of the metamorphic terrane which shed the detritus occurred during the period 465-445 Ma. The mica closure ages closely parallel the cooling pattern for Dalradian metasediments north of the Highland Boundary Fault. Should the clasts have been derived from the Dalradian, the data require that the clasts were sourced from close to the present day erosion surface. The absence of clasts with older mica-closure ages (>500 Ma) may reflect either insufficient sampling to identify an older uplift component which is rare in the Dalradian cooling pattern, or a bias in the recycling process towards clasts with younger uplift ages. The uplift pattern established for the metamorphic clasts

cannot be recognised in the bulk of the two-mica granite clasts. The generation and emplacement of the two-mica granites is inferred to be synchronous with, and possibly triggered by, a phase of rapid uplift and cooling.

17. Sm-Nd data show that the southerly derived lithic arenite and metagreywacke clasts cannot have been derived from the Southern Uplands. The clasts must have had a source in a thick sediment pile previously unrecognised in the Scottish sediment mass. The isotopic distinction between this sequence and SULPS suggests they were both originally derived from different metamorphic source terranes. The bulk crustal residence age of the source which contributed to the Midland Valley sequence appears to have been substantially older than that which supplied sediment to the Southern Uplands, but not sufficiently old to indicate a provenance in the Grampian Highlands. In contrast, southerly derived metasediment clasts from the Upper ORS at Rosneath do have old (>2.0 Ga) model ages suggesting the Midland Valley may be underlain by a collage of tectonically assembled, disparate metamorphic blocks.

18. Pb isotopic data establish that granite detritus dispersed from opposite flanks of the Crawton Basin is isotopically distinct. The basin overlies a boundary between granites which to the south have more radiogenic Pb compositions than those to the north. The northerly derived Ordovician and Silurian granites have Pb isotopic compositions which are compatible with a source in granites of the NE Grampian region. Granite clasts of southerly provenance however have unusually radiogenic Pb compositions and have a steep correlation between $^{207}Pb/^{204}Pb$ and $^{206}Pb/^{204}Pb$. These are features which have been described from subduction related arc settings. The variation in Pb isotopic composition across the basin is thought to reflect an important variation in crustal structure on which the basin was originally nucleated. This break is inferred to be the complex terrane boundary along which the Midland Valley and a granite-metamorphic terrane were juxtaposed during the late Silurian - early Devonian. The Pb isotope data are consistent with the latter being the Grampian Highlands terrane.

REFERENCES

AFTALION,M.,VAN BREEMEN,O.and BOWES,D.R.1984.Age constraints on basement of the Midland Valley of Scotland. Trans.R.Soc. Edinb. 75,53-64.

AGGASIZ,L.1835.On the fossil fishes of Scotland. Rep.Br.Ass.Advmt Sci. 4,646-649.

ALLAN,D.A.1928.The geology of the Highland Border from Tayside to Noranside. Trans.R.Soc.Edinb. 56,57-87.

-----,D.A.1929.A preliminary account of certain Lower Old Red sandstone conglomerates in Perthshire and Forfar.Rep.Br.Ass. Advmt.Sci. 96,555.

-----,D.A.1940.The geology of the Highland Border from Glen Almond to Glen Artney. Trans.R.Soc.Edinb. 60,171-193.

ALLEGRE,C.J.and BEN OTHMAN,D.1980.Nd-Sr isotopic relationship in granitoid rocks and continental crust development: a chemical approach to orogenesis. Nature 286,335-342.

-------,C.J.and ROUSSEAU,D.1984.The growth of the continents through geological time studied by Nd isotope analysis of shales. Earth Planet.Sci.Lett. 67,19-34.

ALLEN,J.C.,MODRESKI,P.J.,HAYGOOD,C.and BOETTCHER,A.L.1972.The role of water in the mantle of the earth: the stability of amphiboles and micas.Proc.24th Int.geol.Congr. 2,231-240.

ALLEN,J.R.L.1965.Fining-upward cycles in alluvial successions. Geol.J. 4,229-246.

APPLETON,J.D.1972.Petrogenesis of potassium-rich lavas from the Roccamonfina volcano, Roman region, Italy. J.Petrology 13, 425-456.

ARCULUS,R.J.and JOHNSON,R.W.1978.Criticism of generalised models for the magmatic evolution of arc-trench systems. Earth Planet.Sci.Lett. 39,118-126.

ARMSTRONG,M.and PATERSON,I.B.1970.The Lower Old Red Sandstone of the Strathmore Region. Rep.Inst.geol.Sci. No.70/12,24pp.

---------,M.,PATERSON,I.B.and BROWNE,M.A.E.1985.Geology of the Perth and Dundee district. Mem.Br.geol.Surv. Sheets 48W,48E, 49. 108pp.

ARTH,J.G.1976.Behavior of trace elements during magmatic processes-a summary of theoretical models and their applications.J.Res.U.S.G.S. 4,41-47.

----,J.G.and BARKER,F.1976.REE partitioning between hornblende and dacitic liquid and implications for the genesis of

trondhjemitic-tonalitic magmas. Geology 4,534-536.

----,J.G.and HANSON,G.N.1972.Quartz diorites derived by partial melting of eclogite or amphibolite at mantle depths.Contrib. Mineral.Petrol. 37,161-174.

----,J.G.and HANSON,G.N.1975.Geochemistry and origin of the early PreCambrian crust of northeastern Minnesota.Geochim. cosmochim.Acta 39,325-362.

----,J.G.,BARKER,F.,PETERMAN,Z.E.and FRIEDMAN,I.1978. Geochemistry of the Gabbro-Diorite-Tonalite-Trondhjemite Suite of southwest Finland and its implications for the origin of tonalitic and trondhjemitic magmas. J.Petrology 19,289-316.

ASHCROFT,W.A.,KNELLER,B.C.,LESLIE,A.G.and MUNRO,M.1984.Major shear zones and autochthonous Dalradian in the northeast Scottish Caledonides. Nature 310,760-762.

ATHERTON,M.P.and BROTHERTON,M.S.1982.Major element composition of the pelites of the Scottish Dalradian. Geol.J. 17,185-221.

--------,M.P.,MCCOURT,W.J.,SANDERSON,L.M.and TAYLOR,W.P.1979. The geochemical character of the segmented Peruvian Coastal Batholith and associated volcanics. In ATHERTON,M.P.and TARNEY,J.(eds) Origin of Granite Batholiths: Geochemical Evidence. Shiva, Cheshire,45-64.

AYDIN,A.and NUR,A.1983.Evolution of pull-apart basins and their scale independence.Tectonics 1,91-106.

BAKER,V.R.1973.Palaeohydrology and sedimentology of Lake Missoula flooding of eastern Washington.Spec.Pap,geol.Soc.Am. 144,69pp.

BARTH,T.F.W.1959.Principles of classification and norm calculations of metamorphic rocks. J.Geol. 67,135-152.

BASU,A.,BLANCHARD,D.P.and BRANNON,J.C.1982.Rare earth elements in the sedimentary cycle: a pilot study of the first leg. Sedimentology 29,737-742.

BATEMAN,P.C.and DODGE,F.C.W.1970.Variations of major chemical constituents across the central Sierra Nevada batholith. Bull,geol.Soc.Am. 81,409-420.

--------,P.C.,CLARK,L.D.,HUBER,N.K.,MOORE,J.G.and RINEHART,C.D. 1963.The Sierra Nevada batholith-a synthesis of recent work across the central part.Prof,Pap,U.S,geol,Surv. 414D,46pp.

BAYLY,B.1968.Introduction to Petrology. Prentice-Hall, New Jersey.

BECKINSALE,R.D.1979.Granite magmatism in the tin belt of south-east Asia. In ATHERTON.M.P.and TARNEY,J.(eds) Origin of

Granite Batholiths: Geochemical Evidence.Shiva,Cheshire,34-44.

BEST,M.G.1975.Migration of hydrous fluids in the upper mantle and potassium variation in calc-alkaline rocks. Geology 3,429-432.

BHATIA,M.R.1983.Plate tectonics and geochemical composition of sandstones. J.Geol. 91,611-627.

BLATT,H.,MIDDLETON,G.V.and MURRAY,R.1980.Origin of Sedimentary Rocks. Prentice-Hall, New Jersey.

BLAXLAND,A.B.,AFTALION,M.and VAN BREEMEN,O.1979.Pb isotopic composition of feldspars from Scottish Caledonian granites, and the nature of the underlying crust.Scott.J.Geol. 15, 139-151.

BLUCK,B.J.1969.Old Red Sandstone and other Palaeozoic conglomerates of Scotland. In KAY,M.(ed.) North Atlantic - Geology and Continental Drift. Mem.Am.Ass.Petrol.Geol. 12, 771-723.

-----,B.J.1974.Structure and directional properties of some valley sandur deposits in southern Iceland.Sedimentology 21,533-554.

-----,B.J.1976.Sedimentation in some Scottish rivers of low sinuosity.Trans.R.Soc.Edinb. 69,425-456.

-----,B.J.1978.Sedimentation in a late orogenic basin:the Old Red Sandstone of the Midland Valley of Scotland. In BOWES,D.R. and LEAKE,B.E.(eds) Crustal Evolution in North western Britain and adjacent Regions. Geol.J.Spec.Iss. 10.

-----,B.J.1979.Structure of coarse-grained stream alluvium. Trans.R.Soc.Edinb. 70,181-221.

-----,B.J.1980a.Evolution of a strike-slip fault-controlled basin, Upper Old Red Sandstone, Scotland.Spec.Publ.int.Ass. Sediment. 4,63-78.

-----,B.J.1980b.Structure,generation and preservation of fining upwards,braided stream cycles in the Old Red Sandstone of Scotland. Trans.R.Soc.Edinb. 71,29-46.

-----,B.J.1982a.Hyalotuff deltaic deposits in the Ballantrae ophiolite of SW Scotland: evidence for crustal position of the lava sequence.Trans.R.Soc.Edinb. 72,217-228.

-----,B.J.1982b.Texture of gravel bars in braided streams.In HEY, R.D.,BATHURST,J.C.and THORNE,C.R.(eds) Gravel-bed Rivers. John Wiley and Sons Ltd.

-----,B.J.1983.Role of the Midland Valley of Scotland in the

Caledonian orogeny.Trans.R.Soc.Edinb. 74,119-136.

-----,B.J.1984.Pre-Carboniferous history of the Midland Valley of Scotland.Trans.R.Soc.Edinb. 75,275-296.

BJORLYKKE,K.1974.Geochemical and mineralogical influence of Ordovician island arcs on epicontinental clastic sedimentation - A study of Lower Palaeozoic sedimentation in the Oslo region, Norway.Sedimentology 21,251-272.

BOND,G.C.,NICKESON,P.A.and KOMINZ,M.A.1984.Break-up of a supercontinent between 625 Ma and 555 Ma: new evidence and implications for continental histories.Earth Planet.Sci.Lett. 2,325-345.

BOWES,D.R.and CONVERY,H.J.E.1966.The composition of some Ben Ledi Grits and its bearing on the origin of albite schists in the southwest Highlands.Scott.J.Geol. 2,67-75.

BRADLEY,D.C.1982.Subsidence in late Palaeozoic basins in the northern Appalachians.Tectonics 1,107-123.

BRAITHWAITE,C.J.R.and JAWAD ALI,A.1978.Heavy mineral distribution in the Old Red Sandstone of the northeastern Midland Valley of Scotland.Scott.J.Geol. 14,273-288.

BRETZ,J.H.,SMITH,H.T.U.and NEFF,G.E.1956.Channelled scabland of Washington: new data and interpretations.Bull.geol.Soc.Am. 957-1049.

BROOKS,C.,HART,S.R.and WENDT,I.1972.Realistic use of two-error regression treatments as applied to rubidium-strontium data. Rev.Geophys. 10,551-577.

BROWN,G.C.and HENNESSY,J.1978.The initiation and thermal diversity of granite magmatism.Phil.Trans.R.Soc.A, 288, 631-643.

-----,G.C.and LOCKE,C.A.1979.Space-time variations in British Caledonian granites - some geophysical correlations.Earth Planet.Sci.Lett. 45,69-79.

-----,G.C.,CASSIDY,J.and LOCKE,C.A.1981.Caledonian plutonism in Britain: A summary.J.geophys.Res. 86,10502-10514.

BRYHNI,I.1964.Migrating basins on the Old Red continent. Nature, Lond. 202,384-385.

BUDDINGTON,A.F.1959.Granite emplacement with special reference to North America.Bull.geol.Soc.Am. 70,671-747.

BURNHAM,C.W.1979.Magmas and hydrothermal fluids.In BARNES,H.L. (ed.) Geochemistry of Hydrothermal Ore Deposits,Wiley, New

York.

BUSSELL,M.A.1983.Crystallisation history of granophyric intrusives from the Peruvian Coastal Batholith.Lithos 16,169-184.

CAILLEUX,A.1945.Distinction des galets marins et fluviatiles. Bull.Soc.geol.Fr. 15,375-404.

CAMERON,T.D.J.1981.The history of Caledonian deformation in east Lecale, County Down.J.Earth Sci.R.Dubl.Soc. 4,53-74.

CAMPBELL,R.1913.The geology of south-eastern Kincardineshire. Trans.R.Soc.Edinb. 48,923-960.

--------,R.1967.Lamina, lamina set, bed, bedset.Sedimentology 8,7-26.

--------,R.1929.The composition of the conglomerates of the Downtonian and Lower Old Red Sandstone of the Stonehaven District.Rep.Br.Ass.Advmt.Sci. 96,554-555.

CANN,J.R.1970.Upward movement of granitic magma.Geol.Mag. 107, 335-340.

CAWTHORN,R.G.and O`HARA,M.J.1976.Amphibole fractionation in calc-alkaline magma genesis.Am.J.Sci. 276,309-329.

--------,R.G.,STRONG,D.F.and BROWN,P.A.1976.Origin of corundum-normative intrusive and extrusive magmas.Nature 259,102-104.

CHAPMAN,H.J.and MOORBATH,S.1977.Lead isotope measurements from the oldest recognised Lewisian gneisses of north-west Scotland.Nature 268,41-42.

CHAPPELL,B.W.1984.Source rocks of I- and S-type granites in the Lachlan Fold Belt, southeastern Australia.Phil.Trans.R.Soc. Lond. A,310,693-707.

--------,B.W.and WHITE,A.J.R.1974.Two contrasting granite types. Pac.Geol. 8,173-174.

CHAUDHURI,S.1976.The significance of rubidium-strontium age of sedimentary rock.Contrib.Mineral.Petrol. 59,161-170.

CLARKE,F.1924.The data of geochemistry.Bull.U.S.geol.Surv. 770,841pp.

CLAYBURN,J.A.P.,HARMON,R.S.,PANKHURST,R.J.and BROWN,J.F.1983.Sr, O, and Pb isotope evidence for origin and evolution of Etive Igneous complex, Scotland.Nature 303,492-496.

CLIFF,R.A.1985.Isotopic dating in metamorphic belts.Jl geol. Soc.Lond. 142,97-110.

COBBING,E.J.and PITCHER,W.S.1972.The coastal Batholith of central

Peru.Jl geol.Soc.Lond. 128,421-460.

--------,E.J.and PITCHER,W.S.1983.Andean plutonism in Peru and its relationship to volcanism and metallogenesis at a segmented plate edge. Mem.geol.Soc.Am. 159,277-292.

CONDIE,K.C.1967.Geochemistry of early PreCambrian greywackes from Wyoming.Geochim.cosmochim.Acta 31,2135.

CONEY,P.J.and HARMS,T.A.1984.Cordilleran metamorphic core complexes: Cenozoic extensional relics of Mesozoic compression.Geology 12,550-554.

COX,K.G.,BELL,J.D.and PANKHURST,R.J.1979.The Interpretation of Igneous Rocks.Allen and Unwin, London.

CROOK,K.A.W.1974.Lithogenesis and geotectonics: the significance of compositional variation in flysch arenites (graywackes). In DOTT,R.H.and SHAVER,R.H.(eds) Modern and ancient geosynclinal sedimentation.Spec.Publs Soc.econ.Palaeont.Miner. Tulsa.19,304-310.

CROUGH,S.T.1983.Apatite fission-track dating of erosion in the eastern Andes, Bolivia.Earth Planet.Sci.Lett. 64,396-397.

CULLERS,R.L.,CHAUDHURI,S.,KILBANE,N.and KOCH,R.1979.Rare-earths in size fractions and sedimentary rocks of Pennsylvanian-Permian age from the mid-continent of the U.S.A.Geochim. cosmochim.Acta 43,1285-1301.

CUMMING,G.L.and RICHARDS,J.R.1975.Ore lead isotope ratios in a continuously changing earth.Earth Planet.Sci.Lett. 28,155-171.

CURRAY,J.R. and MOORE,D.G.1971.Growth of the Bengal deep sea fan and denudation in the Himalayas.Bull.geol.Soc.Am. 82,563-572.

CURRY,G.B.,INGHAM,K.J.,BLUCK,B.J.and WILLIAMS,A.1982.The significance of a reliable Ordovician age for some Highland Border rocks in Central Scotland.Jl geol.Soc.Lond. 139,451-454

-----,G.B.,BLUCK,B.J.,BURTON,C.J.INGHAM,K.J.SIVETER,D.J.and WILLIAMS,A.1984.Age,evolution and tectonic history of the Highland Border Complex, Scotland.Trans.R.Soc.Edinb. 75,113-134.

DALLMEYER,R.D.and HIBBARD,J.1984.Geochemistry of the Baie Verte Peninsula, Newfoundland: implications for the tectonic evolution of the Humber and Dunnage Zones of the Appalachian orogen.J.Geol. 92,489-512.

DASCH,E.J.1969.Strontium isotopes in weathering profiles, deep-sea sediments and sedimentary rocks.Geochim.cosmochim.Acta 33,

1521-1552.

DAVIS,G.H.and CONEY,P.J.1979.Geologic development of the Cordilleran metamorphic core complexes.Geology 7,120-124.

DAWSON,J.W.1890.On certain Devonian plants from Scotland. Nature, Lond. 61,537.

DEANS,T.,GARSON,M.S.and COATS,J.S.1971.Fenite-type soda metasomatism in the Great Glen, Scotland. Nature,Phys.Sci. 234,145-147.

DEER,W.A.,HOWIE,R.A.and ZUSSMANN,J.1966.An Introduction to the rock-forming minerals.Longman,London.

DEMPSTER,T.J.1984.Localised uplift in the Scottish Dalradian. Nature 307,156-159.

--------,T.J.1985.Uplift patterns and orogenic evolution in the Scottish Dalradian.Jl geol.Soc.Lond. 142,111-128.

DEPAOLO,D.J.1981.Neodymium isotopes in the Colorado Front range and crust-mantle evolution in the Proterozoic.Nature 291, 193-196.

-------,D.J.and WASSERBURG,G.J.1976.Nd isotopic variations and petrogenetic models.Geophys.Res.Lett. 3,249-252.

DEWEY,J.F. and SHACKLETON,R.M.1984.A model for the evolution of the Grampian tract in the early Caledonides and Appalachians. Nature 312,115-120.

DICKIN,A.P.MOORBATH,S.and WELKE,H.J.1981.Isotope, trace element and major element geochemistry of Tertiary igneous rocks, Isle of Arran, Scotland.Trans.R.Soc.Edinb. 72,159-170.

DODSON,M.H.1973.Closure temperatures in cooling geochronological and petrological systems.Contrib.Mineral.Petrol. 40,259-274.

------,M.H.1979.Theory of cooling ages.In JAGER,E.and HUNZIKER, J.C.(Eds) Lectures in Isotope Geology. Srpinger-Verlag,New York.194-202.

DOE,B.R.and ZARTMAN,R.E.1979.Plumbotectonics 1, The Phanerozoic. In BARNES,H.L.(ed.)Geochemistry of Hydrothermal Ore Deposits 2nd edn Wiley-Interscience, New York, 22-70.

DUNHAM,A.C.1965.The nature and origin of the groundmass textures in felsites and granophyres from Rhum, Inverness shire.Geol.Mag. 102,8-23.

EGGLER,D.H.1972.Amphibole stability in H_2O-undersaturated calc-alkaline melts.Earth Planet.Sci.Lett. 15,28-34.

------,D.H.and BURNHAM,C.W.1973.Crystallisation and fractionation

trends in the system andesite-H_2O-CO_2-O_2 at pressure to 10Kb. Bull.geol.Soc.Am. 84,2517-2532.

ELIAS,P.and STRONG,D.F.1982.Palaeozoic granitoid plutonism of southern Newfoundland: contrasts in timing, tectonic setting and level of emplacement.Trans.R.Soc.Edinb. 73,43-57.

ENGLAND,P.1981.Metamorphic pressure estimates and sediment volumes for the Alpine Orogeny: an independent control on geobarometers.Earth Planet.Sci.Lett. 56,387-397.

EVANS,A.L.,MITCHELL,J.G.,EMBLETON,B.J.J.and CREER,K.M.1971. Radiometric age of the Devonian polar shift relative to Europe Nature Phys.Sci. 229,50-51.

EWING,T.E.1980.Paleogene tectonic evolution of the Pacific northwest.J.Geol. 88,619-638.

EYNON,G.and WALKER,R.G.1974.Facies relationships in Pleistocene outwash gravels, southern Ontario: a model for bar growth in braided rivers.Sedimentology 21,43-70.

FAIRBRIDGE,R.W.(ed.)1972.The Encyclopedia of Geochemistry and Environmental Sciences. Reinhold,New York.

FAURE,G.1977.The Principles of Isotope Geology.Wiley, New York.

FISHER,R.V.and SCHMINKE,H.U.1984.Pyroclastic Rocks. Springer, Berlin.

FLEMING,J.1831.On the occurrence of scales of vertebrated animals in the Old Red Sandstone of Fifeshire. Edinb.Jnl nat.geogr. Sci. 3,81-86.

FLOYD,P.A. and WINCHESTER,J.A.1975.Magma type and tectonic setting discrimination using immobile elements.Earth Planet. Sci.Lett. 27,211-218.

------,P.A.and WINCHESTER,J.A.1978.Identification and discrimination of altered and metamorphosed volcanic rocks using immobile elements.Chem.Geol. 21,291-306.

FODEN,J.D.and VARNE,R.1980.The petrology and tectonic setting of Quaternary-Recent volcanic centres of Lombok and Sumbawa, Sunda Arc.In LE MAITRE,R.W.(principal editor) Chemical Characterisation of Tectonic Provinces.Chem.Geol. 30,201-226.

FRANCIS,E.H.1982.Magma and sediment-I.Emplacement mechanism of late Carboniferous tholeiite sills in northern Britain.Jl geol.Soc.Lond. 139,1-20.

--------,E.H.,FORSYTH,R.H.,READ,W.A.and ARMSTRONG,M.1970.The Geology of the Stirling District.Mem.geol.Surv.Gt.Br.

FRIEND,P.F.1969.Tectonic features of Old Red Sandstone sedimentation in North Atlantic borders.Mem.Ass.Am.Petrol.Geol. 12,703-710.

------,P.F.1981.Devonian sedimentary basins and deep faults of the northernmost Atlantic borderlands.Mem.Can.Soc.Petrol.Geol. 7,149-165.

------,P.F.and MACDONALD,R.1968.Volcanic sediments, stratigraphy and tectonic background of the Old Red Sandstone of Kintyre, West Scotland. Scott.J.Geol. 4,265-282.

------,P.F.and WILLIAMS,B.P.J.1978.International Symposium on the Devonian System,(P.A.D.S.78) September 1978.Palaeontol. Assoc.

------,P.F.,HARLAND,W.B.and HUDSON,J.D.1963.The Old Red Sandstone and the Highland Boundary in Arran, Scotland.Trans. R.Soc.Edinb. 19,363-425.

FREY,M.,BUCHER,K.,FRANK,E.and MULLIS,J.1980.Alpine metamorphism along the geotraverse - Basel-Chiasso: a review.Eclog.geol. Helv. 72,527-546.

FROST,C.D.and O`NIONS,R.K.1985.Caledonian magma genesis and crustal recycling.J.Petrology 26,515-544.

FYFE,W.S.1973.The granulite facies, partial melting and the Archaean crust.Phil.Trans.R.Soc.A, 273,457.

GABRIELSE,H.1985.Major dextral transcurrent displacements along the Northern Rocky Mountain Trench and related lineaments in north-central British Columbia.Bull.geol.Soc.Am. 96,1-14.

GANDY,M.K.1975.The petrology of the Lower Old Red Sandstone lavas of the eastern Sidlaw Hills, Perthshire, Scotland.J.Petrology 16,189-211.

GARIEPY,C.,ALLEGRE,C.J.and XU,R.H.1985.The Pb-isotope geochemistry of granitoids from the Himalaya-Tibet collision zone: implications for crustal evolution.Earth Planet.Sci. Lett. 74,220-234.

GARSON,M.S.,COATS,J.S.,ROCK,N.M.S.and DEANS,T.1984.Fenites, breccia dykes, albitites and carbonatitic veins near the Great Glen Fault, Inverness, Scotland.Jl geol.soc.Lond. 141,711-732.

GEBAUER,D.and GRUNENFELDER,M.1974.Rb-Sr whole-rock dating of late diagenetic to anchimetamorphic, Palaeozoic sediments in southern France (Montagne Noire).Contrib.Mineral.Petrol. 47,113-130.

GEORGE,T.N.1960.The stratigraphical evolution of the Midland Valley. Trans.geol.Soc.Glasg. 23,32-107.

GILL,J.1981.Orogenic Andesites and Plate Tectonics (Minerals and Rocks 16).Springer-Verlag, New York.

GLOPPEN,T.G.and STEEL,R.J.1981.The deposits, internal structure and geometry in six alluvial fan-fan delta bodies (Devonian, Norway)- a study in the significance of bedding sequences in conglomerates.In ETHERIDGE,F.G.and FLORES,R.M.(eds).Recent and Ancient Non-marine Depositional Environments: Models for Exploration.Spec.Publ.Soc.Econ.Paleont.Mineral. 31,49-69.

GOLDICH,S.S.and GAST,P.W.1966.Effects of weathering on the Rb-Sr and K-Ar ages of biotite from the Morton gneiss, Minnesota. Earth Planet.Sci.Lett. 1,372-375.

GOLDSTEIN,S.L.,O`NIONS,R.K.and HAMILTON,P.J.1984.A Sm-Nd isotopic study of atmospheric dusts and particulates from major river systems.Earth Planet.Sci.Lett. 70,221-236.

GRAHAM,I.J.1985.Rb-Sr geochronology and geochemistry of Torlesse metasediments from the Central North Island, New Zealand.Chem. Geol.(Isot.Geosci.Sect.) 52,317-331.

GRAHAM,J.R.,RICHARDSON,J.B.and CLAYTON,G.1983.Age and significance of the Old Red Sandstone around Clew Bay, NW Ireland.Trans.R.Soc.Edinb. 73,245-249.

GREEN,T.H.1977.Garnet in silicic liquids and its possible use as a P-T indicator.Contrib.Mineral.Petrol. 65,59-67.

GROOME,D.R. and HALL,A.1974.The geochemistry of the Devonian lavas of the Northern Lorne Plateau, Scotland.Mineralog.Mag. 39,621-640.

HALL,A.1967.The chemistry of appinitic rocks associated with the Ardara pluton, Donegal, Ireland.Contrib.Mineral.Petrol. 16, 156-171.

HALL,J.,POWELL,D.W.,WARNER,M.R.,EL-ISA,Z.H.M.,ANESANYA,O.and BLUCK,B.J.1983.Seismological evidence for shallow crystalline basement in the Southern Uplands of Scotland.Nature 305, 408-420.

HALLIDAY,A.N.1981.On the sources of uranium in some Scottish Caledonian granites.Mineralog.Mag. 44,437-442.

---------,A.N.1984.Coupled Sm-Nd and U-Pb systematics in late Caledonian granites and the basement under northern Britain. Nature 307,229-233.

---------,A.N.and STEPHENS,W.E.1984.Crustal controls on the genesis of the 400 Ma old Caledonian granites.Phys.Earth & Planet.Interiors. 35,89-104.

---------,A.N.,STEPHENS,W.E.and HARMON,R.S.1980.Rb-Sr and O isotopic relationships in 3 zoned Caledonian granite plutons, Southern Uplands, Scotland: evidence for varied sources and hybridisation of magmas.Jl geol.Soc.Lond. 137,329-346.

---------,A.N.,STEPHENS,W.E.and HARMON,R.S.1981.Isotopic and chemical constraints on the development of peraluminous Caledonian and Acadian granites.Can.Mineralogist 19,205-216.

---------,A.N.,STEPHENS,W.E.,HUNTER,R.H.,MENZIES,M.A.,DICKIN,A.P., and HAMILTON,P.J.1985.Isotopic and chemical constraints on the building of the deep Scottish lithosphere.Scott.J.Geol. In press.

HAMILTON,P.J.,O`NIONS,R.K.and PANKHURST,R.J.1980.Isotopic evidence for the provenance of some Caledonian granites. Nature 287,279-284.

---------,P.J.,BLUCK,B.J.and HALLIDAY,A.N.1984.Sm-Nd ages from the Ballantrae complex, SW Scotland.Trans.R.Soc.Edinb. 75, 183-188.

HANSON,G.N.1978.The application of trace elements to the petrogenesis of igneous rocks of granitic composition.Earth Planet. Sci.Lett. 38,26-43.

---------,G.N.and GAST,P.W.1967.Kinetic studies in contact metamorphic zones.Geochim.cosmochim.Acta 31,1119-1153.

HARLAND,W.B.,COX,A.V.,LLEWELLYN,P.G.,PICKTON,C.A.G.,SMITH,A.G. and WALTERS,R.1982.A geologic time scale. Cambridge University Press, Cambridge.

HARMON,R.S.and HALLIDAY,A.N.1980.Oxygen and strontium isotope relationships in the British late Caledonian granites.Nature 283,21-25.

-------,R.S.,HALLIDAY,A.N.,CLAYBURN,J.A.P.and STEPHENS,W.E.1984. Chemical and isotopic systematics of the Caledonian intrusions of Scotland and northern England. A guide to magma source region and magma crust interaction.Phil.Trans.R.Soc.Lond. A,310,709-742.

HARRIS,P.G.,KENNEDY,W.Q.and SCARFE,C.M.1970.Volcanism vs plutonism - the effect of chemical composition.In NEWALL,G. and RAST,N. (eds) Mechanisms of Igneous Intrusion Spec.Iss.

Geol.J. 2,187-200.

HART,S.R.1964.The petrology and isotopic mineral age relations of a contact zone in the Front Range, Colorado.J.Geol. 72, 493-525.

HARVEY,P.K.,TAYLOR,D.M.,HENDRY,R.and BANCROFT,F.1972.An accurate fusion method for the analysis of rocks and chemically related materials by X-ray flourescence spectrometry.X-ray spectrometry 2,33-44.

HASELOCK,P.J.1984.The systematic geochemical variation between two tectonically separate successions in the southern Monadhliaths, Inverness-shire.Scott.J.Geol. 20,191-206.

HAWKESWORTH,C.J.,NORRY,M.J.,RODDICK,J.C.,BAKER,P.E.,FRANCIS,P.W. and THORPE,R.S.1979.$^{143}Nd/^{144}Nd$, $^{87}Sr/^{86}Sr$ and incompatible element variations in calc-alkaline andesites and plateau lavas from South America.Earth Planet.Sci.Lett. 42,45-57.

HEMPTON,M.R.and DUNNE,L.A.1984.Sedimentation in pull-apart basins -active examples in eastern Turkey.J.Geol. 92,513-530.

-------,M.R.,DUNNE,L.A.and DEWEY,J.F.1983.Sedimentation in an active strike-slip basin, southeastern Turkey.J.Geol. 91,401-412.

HENDERSON,S.M.K.1932.Notes on Lower OLd Red Sandstone plants from Callander, Perthshire. Trans.R.Soc.Edinb. 57,277-285.

HEWARD,A.P.1978.Alluvial fan sequence and megasequence models: with examples from Westphalian D-Stephanian B coalfields, northern Spain.In MIALL,A.D.(ed.)Fluvial Sedimentology Mem. Can.Soc.Petrol.Geol. 5,669-702.

HICKLING,G.and DON,A.W.R.1915.On Parka decipiens. Q.Jl geol. Soc.Lond. 71,648-663.

HIETANEN,A.1943.Uber das Grundgebirge des Kalantigebietes im sudwestlichen Finnland.Comm.Geol.Finlande,Bull. 130,105pp.

--------,A.1975.Generation of potassium-poor magmas in the northern Sierra Nevada and the Svecofennian of Finland. J.res. U.S.G.S. 3,631-645.

HISCOTT,R.N.1978.Provenance of Ordovician deep-water sandstones, Tourelle Formation, Quebec and implications for initiation of the Taconic Orogeny.Can.J.Earth Sci. 15,1579-1597.

-------,R.N.1984.Ophiolitic source rocks for Taconic-age flysch: trace element evidence.Bull.geol.Soc.Am. 95,1261-1267.

HOLDER,M.T.1979.An emplacement mechanism for post-tectonic

granites and its implications for their geochemical features. In ATHERTON,M.P. and TARNEY,J.(eds) Origin of Granite Batholiths: Geochemical Evidence,Shiva,Cheshire,116-128.

HOOKE,R.LeB.1972.Geomorphic evidence for late-Wisconsin and Holocene tectonic deformation,Death Valley,California.Bull. geol.Soc.Am. 2073-2098.

HOOKER,P.J.,HAMILTON,P.J.and O`NIONS,R.K.1981.An estimate of the Nd isotopic composition of Iapetus seawater from c 490 Ma metalliferous sediments.Earth Planet.Sci.Lett. 56,180-188.

HUGHES,C.J.1982.Igneous Petrology.Amsterdam,Oxford.

HUTCHISON,A.G.1928.A lava flow at the base of the Kincardine-shire Downtonian. Trans.Edinb.geol.Soc. 12,69-73.

HUTTON,D.H.W.1982.A tectonic model for the emplacement of the Main Donegal Granite, NW Ireland.Jl geol.Soc.Lond. 139,615-631

IGS 1982.Sheet 77. Aberdeen.

IKIN,N.P.and HARMON,R.S.1983.A stable isotope study of serpentinisation and metamorphism in the Highland Border Suite, Scotland, U.K.Geochim.cosmochim.Acta 47,153-167.

JACK,R.L.and ETHERIDGE,R.1877.On the discovery of plants in the Lower Old Red Sandstone of the neighbourhood of Callander. Q.Jl geol.Soc.Lond. 33,213-222.

JACOBSEN,S.B.and WASSERBURG,G.J.1979.Nd and Sr isotopic study of the Bay of Islands ophiolite complex and the evolution of the source of mid-ocean ridge basalts.J.geophys.Res. 84, 7429-7445.

JAFFEY,A.H.,FLYNN,K.F.,GLENDENIN,L.E.,BENTLY,W.C.and ESSLING,A.M. 1971.Precision measurements of half lives and specific activities of ^{235}U and ^{238}U.U.Phys.Rev. C4,1889-1906.

JAGER,E.1979.Introduction to geochronology.In JAGER,E.and HUNZIKER,J.C.(eds) Lectures in isotope geology1-12. Springer, Berlin.

KASTNER,M.1971.Authigenic feldspars in carbonate rocks.Am.Miner. 56,1403-1442.

KELLING,G.1962.The petrology and sedimentation of Upper Ordovician rocks in the Rhinns of Galloway, south-west Scotland.Trans.R.Soc.Edinb. 65,107-137.

KENNAN,P.S.,PHILLIPS,W.E.A.and STROGEN,P.1979.Pre-Caledonian basement to the paratectonic Caledonides in Ireland.In HARRIS, A.L.,HOLLAND,C.H.and LEAKE,B.E.(eds) The Caledonides of the

British Isles - reviewed.Spec.Publ.geol.Soc.Lond.8,157-161.

KEPPIE,J.D.In press.The Appalachian collage.In GEE,D.C.and STURT,B.(eds) The Caledonide Orogen, Scandinavia and Related Areas. Wyllie and Sons.

KIDSTON,R.1893.On the occurrence of Arthrostigma gracile Dawson, in the Lower Old Red Sandstone of Perthshire. Proc.R.phys. Soc.Edinb. 12,102-111.

-------,R. and LANG,W.H.1924.Notes on fossil plants from the Lower Old Red Sandstone of Scotland. Trans.R.Soc.Edinb. 52, 601-611.

KIRKPATRICK,R.J.1976.Towards a kinetic model for the crystallisation of magma bodies.J.geophys.Res. 81,2565-2571.

KOPPEL,V.and GRUNENFELDER,M.1979.Isotope geochemistry of lead.In JAGER,E.and HUNZIKER,J.C.(Eds) Lectures in Isotope Geology. Springer-Verlag, New York.134-153.

KRAUSKOPF,K.B.1967.Introduction to Geochemistry,McGraw-Hill.

KUNO,H.1966.Lateral variation of basalt magma type across continental margins and island arcs.Bull.volcan. 29,195-222.

LAJOIE,J.1973.Albite of secondary origin in Charny Sandstones, Quebec: discussion.J.sedim.Petrol. 43,575-576.

------,J.,MEROUX,Y. and MATHEY,B.1974.The PreCambrian shield and the Lower Palaeozoic Shelf: the unstable provenance of the Lower Palaeozoic flysch sandstones and conglomerates of the Appalachians between Beaumont and Bic, Quebec.Can.J.Earth Sci. 11,951-963.

LAMBERT,I.B. and WYLLIE,P.J.1974.Melting of tonalite and crystallisation of andesite liquid with excess water to 30 kb. J.Geol. 82,88-97.

LAMBERT,R.ST.J.and HOLLAND,J.G.1974.Yttrium geochemistry applied to petrogenesis utilising calcium-yttrium relationships in minerals and rocks.Geochim.cosmochim.Acta 38,1393-1414.

LAMING,D.J.C.1966.Imbrication, palaeocurrents and other sedimentary features in the Lower New Red Sandstone, Devonshire, England.J.Sedim.Petrol. 36,940-959.

LAMONT,A.1952.Ecology and correlation of the Pentlandian - a new division of the Silurian system in Scotland. Rep.XVIII Int. geol.Congr.,Gt Br. 10,27-32.

LAND,L.S.and MILLIKEN,K.1981.Feldspar diagenesis in the Frio Formation, Brazoria County, Texas Gulf Coast.Geology 9,314-318

LANG,W.H.1927.Contributions to the study of the Old Red Sandstone flora of Scotland.VI.Zosterophyllum myretoninnum Penhallow and some other plant remains from the Carmyllie Beds of the Lower Old Red Sandstone. Trans.R.Soc.Edinb. 55,443-452.

----,W.H.1932.Contributions to the study of the Old Red Sandstone flora of Scotland.VIII.On Arthrostigma, Psilophyton and some associated plant remains from the Strathmore Beds of the Caledonian Lower Old Red Sandstone. Trans.R.Soc.Edinb. 57, 491-518.

LARSEN,O.and SORENSEN,H.1960.Principles of classification and norm calculations of metamorphic rocks: a discussion.J.Geol. 68,681-683.

LEAKE,B.E.1978.Granite emplacement: the granites of Ireland and their origin.In BOWES,D.R.and LEAKE,B.E. (eds) Crustal evolution in northwestern Britain and adjacent regions. Spec. Iss.Geol.J. 10,221-248.

-----,B.E.,TANNER,P.W.G.,MACINTYRE,R.M.and ELIAS,E.1984.Tectonic position of the Dalradian rocks of Connemara and its bearing on the evolution of the Midland Valley of Scotland.Trans.R. Soc.Edinb. 75,165-174.

-----,B.E.,HENDRY,G.L.,KEMP,A.,PLANT,A.G.,HARVEY,P.K.,WILSON,J.R. COATS,J.S.,AUCOTT,J.W.,LUNEL,T.and HOWARTH,R.J.1969.The chemical analysis of rock powders by automatic X-ray flourescence.Chem.Geol. 5,7-86.

LEEDER,M.R.1978.A quantitative stratigraphic model for alluvium, with special channel deposit density and interconnectedness. In MIALL,A.D.(ed.) Fluvial Sedimentology.Mem.Can.Soc.Petrol. Geol. 5,587-596.

LEEMAN,W.P. and PHELPS,D.W.1981.Partitioning of rare earth elements and other trace elements between sanidine and co-existing volcanic glass.J.geophys.Res. 86,10193-10199.

LE FORT,P.1981.Manaslu leucogranite: a collision signature of the Himalaya. A model for its genesis and emplacement.J.geophys. Res. 86,10545-10568.

LE MAITRE,R.W.1976.The chemical variability of some common igneous rocks.J.Petrology 17,589-637.

LE ROUX,L.J.anD GLENDENIN,L.E.1963.Half-life of Thorium 232. Proc.Natl.Conf.Nucl.Energy, Pretoria 82-94.

LIPMAN,P.W.and MEHNERT,H.H.1979.The Taos Plateau volcanic field,

northern Rio Grande rift, New Mexico. In: Rio Grande Rift: Tectonics and Magmatism, 289-311.

LONGMAN,C.D.1980.Age and affinity of granitic detritus in Lower Palaeozoic conglomerates, SW Scotland: implications for Caledonian evolution. Unpub.Ph.D. thesis, Glasgow University.

--------,C.D.,BLUCK,B.J.and VAN BREEMEN,O.1979.Ordovician conglomerates and the evolution of the Midland Valley.Nature 280,578-581.

--------,C.D.,BLUCK,B.J.,VAN BREEMEN,O.and AFTALION,M.1982. Ordovician conglomerates: constraints on the timescale.In ODIN G.S.(ed.) Numerical dating in stratigraphy Wiley, New York, 807-809.

LUDWIG,K.R.and SILVER,L.T.1977.Lead-isotope inhomogeneity in Precambrian igneous K-feldspars.Geochim,cosmochim,Acta 41,1457-1471.

LUTH,W.C.,JAHNS,R.H.and TUTTLE,O.F.1964.The granite system at pressures of 4 to 10 kb.J.geophys.Res, 69,759-773.

LYELL,C.Elements of Geology. 6th edn.London, John Murray.

MCCARTHY,T.S.1976.Chemical interrelationships in a low-pressure granulite terrain in Namaqualand, South Africa, and their bearing of granite genesis and the composition of the lower crust.Geochim.cosmochim.Acta 40,1057-1068.

---------,T.S.and HASTY,R.A.1976.Trace element distribution patterns and their relationship to the crystallisation of granitic melts.Geochim.cosmochim.Acta 40,1351-1358.

---------,T.S.and ROBB,L.J.1978.On the relationship between cumulus mineralogy and trace and alkali chemistry in an Archaean granite from the Barberton Region, South Africa. Geochim.cosmochim.Acta 42,21-26.

MCCOURT,W.J.1981.The geochemistry and petrography of the Coastal Batholith of Peru, Lima segment.Jl geol,Soc,Lond, 138,407-420.

MCCULLOCH,M.T.and WASSERBURG,G.J.1978.Sm-Nd and Rb-Sr chronology of continental crust formation.Science 200,1003-1011.

MCINTIRE,W.L.1963.Trace element partition coefficients-a review of theory and applications to geology.Geochim,cosmochim,Acta 27,1209-1264.

MCKERROW,W.S.,LAMBERT,R.ST.J.,and COCKS,L.R.M.1984.The Ordovician Silurian and Devonian periods (in press).

MCKENZIE,D.1978.Some remarks on the development of sedimentary

basins.Earth Planet.Sci.Lett. 40,25-32.

MANN,P.,HEMPTON,M.R.,BRADLEY,D.C.and BURKE,K.1983.Development of pull-apart basins.J.Geol. 91,529-554.

MARSTON,R.J.1971.The Foyers granitic complex, Inverness-shire, Scotland.Jl geol.Soc.Lond. 126,331-368.

MAYNARD,J.B.,VALLONI,R.and YU,H.1982.Composition of modern deep sea sands from arc-related basins.Spec.Publ.geol.Soc.Lond. 10,551-561.

MEIJER,A.and REAGAN,M.1983.Origin of K_2O-SiO_2 trends in volcanoes of the Mariana Arc.Geology 11,67-71.

MICHARD-VITRAC,A.,ALBAREDE,F.and ALLEGRE,C.J.1981.Lead isotopic composition of Hercynian granitic K-feldspars constrains continental genesis.Nature 291,460-464.

MIDDLETON,G.V.1972.Albite of secondary origin in Charny Sandstones,Quebec.J.sedim.Petrol. 42,341-349.

MILLER,C.F.and BRADFISH,C.J.1980.An inner Cordilleran belt of muscovite-bearing plutons.Geology 8,412-416.

------,C.F.and MITTLEFEHLDT,D.W.1982.Depletion of light rare-earth elements in felsic magmas.Geology 10,129-133.

MILLER,H.1841.The Old Red Sandstone. Thomas Constable,Edinburgh.

MILLER,R.G.and O`NIONS,R.K.1984.The provenance and crustal residence ages of British sediments in relation to palaeogeographic reconstructions.Earth Planet.Sci.Lett. 68,459-470.

MITCHELL,H.1860.Notice on new fossils from the Lower Old Red Sandstone. The Geologist 3,273-275.

--------,H.1861.On the position of the beds of the Old Red Sandstone developed in the counties of Forfar and Kincardine. Q.Jl geol.Soc.Lond. 17,145-151.

MITTLEFEHLDT,D.W.and MILLER,C.F.1983.Geochemistry of the Sweet-water Wash pluton, California: implications for `anomalous` trace element behaviour during differentiation of felsic magmas.Geochim.cosmochim.Acta 47,109-124.

MIYASHIRO,A.1973.Metamorphism and Metamorphic Belts.Allen and Unwin, London.

MOORBATH,S.1962.Lead isotope abundance studies on mineral occurrences in the British Isles and their geological significance.Phil.Trans.R.Soc.Lond. 254,295-360.

---------,S.1969.Evidence for the age of deposition of the

Torridonian sediments of north-west Scotland. Scott.J.Geol. 5,154-170.

---------,S.,WELKE,H.and GALE,N.H.1969.The significance of lead isotope studies in ancient, high-grade metamorphic basement complexes, as exemplified by the Lewisian rocks of northwest Scotland. Earth Planet.Sci.Lett. 6,245-256.

MORTON,D.J.1976.Lower Old Red Sandstone sedimentation in the north-west Midland Valley and north Argyll areas of Scotland. Univ.Glasgow Ph.D.Thesis (Unpub.)

------,D.J.1979.Palaeogeographical evolution of the Lower Old Red Sandstone basin in the western Midland Valley. Scott.J.Geol. 15,97-116.

MURCHISON,R.I.1859.On the succession of the older rocks in the northern-most counties of Scotland, with some observations on the Orkney and Shetland Islands. Q.Jl geol.Soc.Lond. 15, 353-417.

MURPHY,F.C.1985.Non axial planar cleavage and Caledonian sinistral transpression in eastern Ireland. Geol.J. 20,257-279.

MYKURA,W.1983.Old Red Sandstone. In CRAIG,G.Y.(ed.)The Geology of Scotland. Scottish Academic Press.205-251.

NANCE,W.B.and TAYLOR,S.R.1976.Rare earth element patterns and crustal evolution - 1.Australian post-Archaean sedimentary rocks. Geochim.cosmochim.Acta 40,1539-1551.

NIGGLI,P.1954. Rocks and Mineral Deposits. Freeman, San Francisco.

NOYES,H.J.,WONES,D.R.and FREY,F.A.1983.A tale of two plutons: petrographic and mineralogic constraints on the petrogenesis of the Red Lake and Eagle Peak plutons, Central Sierra Nevada, California. J.Geol. 91,353-379.

ODIN,G.S.1982.The Phanerozoic time scale revisited. Episodes 1982, 3-9.

OGUNYOMI,O.,MARTIN,R.F.and HESSE,R.1981.Albite of secondary origin in Charney Sandstones, Quebec: a re-evaluation. J. sedim.Petrol. 51,597-606.

OLIVER,G.J.H.,SMELLIE,J.L.,THOMAS,L.J.,CASEY,D.M.,KEMP,A.E.S., EVANS,L.J.,BALDWIN,J.R.and HEPWORTH,B.C.1984.Early Palaeozoic metamorphic history of the Midland Valley, Southern Uplands-Longford-Down massif and the Lake District, British Isles. Trans.R.Soc.Edinb. 75,245-258.

O`NIONS,R.K.,HAMILTON,P.J.and HOOKER,P.J.1983.A Nd isotope

investigation of sediments related to crustal development in the British Isles.Earth Planet.Sci.Lett. 63,229-240.

ORE,T.H.1964.Some criteria for recognition of braided stream deposits.Contrib.Geol.Univ.Wyoming 3,1-14.

OVERSBY,V.M.1974.New look at the lead isotope growth curve.Nature 248,132-133.

PANKHURST,R.J.1974.Rb-Sr whole rock chronology of Caledonian events in north-east Scotland.Bull.geol.Soc.Am. 85,345-350.

---------,R.J.1979.Isotope and trace element evidence for the origin and evolution of Caledonian granites in the Scottish Highlands.In ATHERTON,M.P.and TARNEY,J.(eds)Origin of Granite Batholiths: Geochemical Evidence, Shiva,Cheshire,18-33.

---------,R.J.and PIDGEON,R.T.1976.Inherited isotope systems and the source region pre-history of early Caledonian granites in the Dalradian Series of Scotland.Earth Planet.Sci.Lett. 31,55-68.

PARNELL,J.and SWAINBANK,I.1984.Interpretation of Pb isotope compositions of galenas from the Midland Valley of Scotland and adjacent regions.Trans.R.Soc.Edinb. 75,85-96.

PATERSON,I.B.and HARRIS,A.L.1969.Lower Old Red Sandstone ignimbrites from Dunkeld, Perthshire.Rep.No.69/7,Inst.geol. Sci.,6pp.

PEACOCK,M.A.1931.Classification of igneous rock series.J.Geol. 39,54-67.

PEARCE,J.A.and CANN,J.R.1973.Tectonic setting of basic volcanic rocks determined using trace element analysis.Earth Planet. Sci.Lett. 19,290-300.

------,J.A.and NORRY,M.J.1979.Petrogenetic implications of Ti,Zr Y, and Nb variation in volcanic rocks.Contrib.Mineral.Petrol. 69,33-47.

------,J.A.,HARRIS,N.B.W.and TINDLE,A.G.1984.Trace element discrimination diagrams for the tectonic interpretation of granitic rocks.J.Petrol. 25,956-983.

PECCERILO,A.and TAYLOR,S.R.1976.Geochemistry of Eocene calc-alkaline volcanic rocks from the Kastamonu area, northern Turkey.Contrib.Mineral.Petrol. 58,63-81.

PETRO,W.L.,VOGEL,T.A.and WILBRAND,J.T.1979.Major-element chemistry of plutonic rock suites from compressional and extensional plate boundaries.Chem.Geol. 26,217-235.

PETTIJOHN,F.J.1963.Chemical composition of sandstones, excluding carbonate and volcanic sands.In FLEISCHER,M.(ed.) Data of Geochemistry, U.S.Geol.Surv.Prof.Paper 440-S,19p.

---------,F.J.1973.Sedimentary Rocks (2nd edn).Harper and Row.

---------,F.J.,POTTER,P.E.and SIEVER,R.1972.Sand and Sandstone Springer-Verlag, New York.

PHILLIPS,W.E.A.,STILLMAN,C.J.and MURPHY,T.J.1976.A Caledonian plate tectonic model.Jl geol.Soc.Lond, 132,579-609.

PIASECKI,M.A.J.and VAN BREEMEN,O.1979.A Morarian age for the `younger Moines` of central and western Scotland.Nature 278,734-736.

PIDGEON,R.T. and AFTALION,M.1978.Cogenetic and inherited zircon U-Pb systems in granites: Palaeozoic granites of Scotland and England.In BOWES,D.R.and LEAKE,B.E.(eds) Crustal evolution in Northwestern Britain and Adjacent Regions.Geol.J.Spec. Issue 10,183-220.

--------,R.T.and JOHNSON,M.R.W.1974.A comparison of zircon U-Pb and whole rock Rb-Sr systems in three phases of the Carn Chuinneag granite, northern Scotland.Earth Planet.Sci.Lett. 24,105-112.

PITCHER,W.S.1978.The anatomy of a batholith.Jl geol.Soc.Lond. 135,158-182.

--------,W.S.1979.The nature, ascent and emplacement of granitic magmas.Jl geol.Soc.Lond. 136,627-662.

--------,W.S.and BERGER,A.R.1972.The geology of Donegal: a study of granite emplacement and unroofing. Wiley Interscience, London.

PIWINSKII,A.J.1973a.Experimental studies of granitoids from the Central and Southern Coast Ranges, California.Tschermaks miner.petrogr.Mitt. 20,107-130.

---------,A.J.1973b.Experimental studies of igneous rock series, central Sierra Nevada batholith, California: Part II.Neues Jb. Miner.Mh. 5,193-215.

---------,A.J.and WYLLIE,P.J.1970.Experimental studies of igneous rock series: felsic body suite from the Needle Point Pluton, Wallowa batholith, Oregon.J.Geol.Chicago 78,52-76.

POWERS,M.C.1953.A new roundness scale for sedimentary particles. J.Sedim.Petrol. 23,117-119.

POWRIE,J.1864.On the fossiliferous rocks of Forfarshire and their

contents. Q.Jl geol.Soc.Lond. 20,413-429.

PRESNALL,D.C.and BATEMAN,P.C.1973.Fusion relations in the system $NaAlSi_3O_8$ - $CaAl_2Si_2O_8$ - $KAlSi_3O_8$ - SiO_2 - H_2O and generation of granite magmas in the Sierra Nevada batholith.Bull.geol. Soc.Am. 84,3181-3202.

PRIEM,H.N.A.,BOELRIJK,N.A.I.M.,HEBEDA,E.H.,SCHERMERHORN,L.J.G., VERDURMEN,E.A.Th.and VERSCHURE,R.H.1978.Sr isotopic homogenisation through whole-rock systems under low-greenschist racies metamorphism in Carboniferous pyroclastics at Aljustrel (southern Portugal).Chem.Geol. 21,307-314.

PRINGLE,I.R.1978.Rb-Sr ages of silicic igneous rocks and deformation, Burlington Peninsula, Newfoundland.Can.J.Earth Sci. 15,293-300.

PROPACH,G.1976.Models of filter differentiation.Lithos 9,203-209.

PURDY,J.W. and JAGER,E.1976.K-Ar ages on rock forming minerals from the Central Alps.Mem.1st geol.mineral.Univ.Padova 30,1-31

RAMSAY,D.M.1964.Deformation of pebbles in Lower Old Red Sandstone conglomerates adjacent to the Highland Boundary Fault. Geol. Mag. 101,228-248.

REID,J.and MACNAIR,P.1896.On the genera Lycopodites and Psilophyton of the Old Red Sandstone Formation of Scotland. Trans.geol.Soc.Glasg. 10,323-330.

----,J.,GRAHAM,W.and MACNAIR,P.1897.Parka decipiens, its origin, affinities and distribution.Trans.geol.Soc.Glasg. 11,105-121.

RICHARD,P.,SHIMIZU,N.and ALLEGRE,C.J.1976.$^{143}Nd/^{144}Nd$, a natural tracer: an application to oceanic basalts.Earth Planet.Sci. Lett. 31,269-278.

RICHARDS,J.R., BARKAS,J.P.and VALLANCE,T.G.1977.A Lower Devonian point in the geological time scale.Geochem.J.(Japan) 11,147-153.

RICHARDSON,J.B.1967.Some British Lower Devonian spore assemblages and their stratigraphic significance. Rev.Palaeobotan.Palynol. 1,111-129.

----------,J.B.,FORD,J.H.and PARKER,F.1984.Miospores, correlation and age of some Scottish Lower Old Red Sandstone sediments from the Strathmore region (Fife and Angus). J.micropalaeontol. 3,109-124.

RINGWOOD,A.E.1955.The principles governing trace element behaviour during magmatic crystallisation, part II: the role

of complex formation.Geochim,cosmochim,Acta 7,242-254.

ROBERTSON,A.H.F.and HENDERSON,W.G.1984.Geochemical evidence for the origins of igneous and sedimentary rocks of the Highland Border, Scotland.Trans.R.Soc.Edinb. 75,135-150.

RODDICK,J.A.and HUTCHINSON,W.W.1974.Setting of the coast plutonic complex, British Columbia. Pac.Geol. 8,91-108.

ROLFE,W.D.I.and BECKETT,E.C.M.1984.Autecology of Silurian Xiphosurida, Scorpionida, Cirripedia, and Phyllocarida. Spec. Pap.Palaeont. 32,27-37.

ROSS,R.J.,NAESER,C.W.and IZETT,G.A.1977.Fission track dating of Lower Palaeozoic bentonites in British stratotypes.U.S.geol. Surv.Open file report. 77-348.

RUST,B.R.1975.Fabric and structure of glaciofluvial gravels.In JOPLING,A.V.and MCDONALD,B.C.(Eds)Glaciofluvial and Glaciolacustrine Sedimentation Spec.Publs Soc.econ.Paleont. Miner.Tulsa, 23,238-248.

----,B.R.1978.Depositional models for braided alluvium.In MIALL, A.D.(ed.) Fluvial Sedimentology.Mem.Can.Soc.Petrol.Geol. 5,605-625.

----,B.R.1984.Proximal braidplain deposits in the Middle Devonian Malbaie Formation of Eastern Gaspe, Quebec, Canada. Sedimentology 31,675-695.

SCHAER,J.P.,REIMER,G.M.and WAGNER,G.A.1975.Actual and ancient uplift rate in the Gotthard region, Swiss Alps: a comparison between precise levelling and fission-track apatite age. Tectonophys. 29,293.

SCHWAB,F.L.1975.Framework mineralogy and chemical composition of continental margin-type sandstone.Geology 3,487.

SCLATER,J.G.,ROYDEN,L.,HORVATH,F.,BURCHFIEL,B.C.,SEMKENS,S.and STEGEN,A.L.1980.The formation of the intra-Carpathian basins as determined from subsidence data.Earth Planet.Sci.Lett. 51,139-162.

SENIOR,A.and LEAKE,B.E.1978.Regional metamorphism and the geochemistry of the Dalradian metasediments of Connemara, western Ireland.J.Petrology 19,584-625.

SHAW,D.M.1954a.Trace elements in pelitic rocks. Part 1: variations during metamorphism.Bull.geol.Soc.Amer. 65, 1151-1166.

----,D.M.1954b.Trace elements in pelitic rocks. Part II:

geochemical relations.Bull.geol.Soc.Amer. 65,1167-1182.

----,D.M.1956.Geochemistry of pelitic rocks. Part III: Major elements and general geochemistry.Bull.geol.Soc.Amer. 67, 919-934.

SIMON,J.B.and BLUCK,B.J.1982.Palaeodrainage of the southern margin of the Caledonian mountain chain in the northern British Isles.Trans.R.Soc.Edinb. 73,11-15.

SIMPSON,P.R.,BROWN,G.C.,PLANT,J.and OSTLE,D.1979.Uranium mineralisation and granite magmatism in Britain.Phil.Trans.R. Soc. 291A,385-412.

SMITH,D.I.1961.Pattern of minor faults in the south central Highlands of Scotland.Bull.geol.Surv.Gt Br. 17,145-152.

SMITH,J.V.1974.Feldspar Minerals,I. Crystal Structure and Physical Properties;II. Chemical and Textural Properties. Springer-Verlag, New York.

SOPER,N.J.and HUTTON,D.H.W.1984.Late Caledonian sinistral displacments in Britain: implications for a three-plate collision model.Tectonics 3,781-794.

STACEY,J.S.and KRAMERS,J.D.1975.Approximation of terrestrial lead isotope evolution by a two-stage model.Earth Planet. Sci.Lett. 26,207-221.

STEEL,R.J.and THOMPSON,D.B.1983.Structures and textures in Triassic braided stream conglomerates (`Bunter` Pebble Beds) in the Sherwood Sandstone Group, north Staffordshire, England. Sedimentology 30,341-367.

-----,R.J.,MAEHLE,S.,NILSEN,H.,ROE,S.L.and SPINNANGR,A.1977. Coarsening upward cycles in the alluvium of Hornelen Basin (Devonian) Norway: Sedimentary response to tectonic events. Bull.geol.Soc.Am. 88,1124-1134.

STEIGER,R.H.and JAGER,E.1977.Subcommission on geochronology: convention on the use of decay constants in geo- and cosmo-chronology.Earth Planet.Sci.Lett. 36,359-362.

STEPHENS,W.E.and HALLIDAY,A.N.1979.Compositional variation in the Galloway plutons.In ATHERTON,M.P. and TARNEY,J.(eds) Origin of Granite Batholiths : Geochemical Evidence. Shiva, Cheshire,9-17.

--------,W.E.and HALLIDAY,A.N.1984.Geochemical contrasts between late Caledonian granitoid plutons of northern, central and southern Scotland.Trans.R.Soc.Edinb. 75,259-274.

STERN,C.R.,HUANG,W.L.and WYLLIE,P.J.1975.Basalt-andesite-rhyolite -H_2O: crystallisation intervals with excess H_2O and H_2O-undersaturated liquidus surfaces to 35Kb, with implications for magma genesis.Earth Planet.Sci.Lett. 28,189-196.

STRECKEISEN,A.L.1976.To each plutonic rock its proper name.Earth Sci.Rev. 12,1-33.

SUN,S.S.1980.Lead isotopic study of young volcanic rocks from mid-ocean ridges, oceanic islands and island arcs.Phil.Trans. R.Soc. A,297,409-445.

SWANSON,S.E.1977.Relation of nucleation and crystal growth rate to the development of granitic textures.Am.Miner. 62,966-978.

TARNEY,J.and SAUNDERS,A.D.1979.Trace element constraints on the origin of Cordilleran batholiths.In ATHERTON,M.P. and TARNEY, J.(eds) Origin of Granite Batholiths : Geochemical Evidence. Shiva, Cheshire, 90-105.

TAYLOR,S.R.and MCLENNAN,S.M.1985.The Continental Crust: Its Composition and Evolution. Blackwell, Oxford.

THIRLWALL,M.F.1981.Implications for Caledonian plate tectonic models of chemical data from volcanic rocks of the British Old Red Sandstone.Jl geol.Soc.Lond. 138,123-138.

---------,M.F.1982.Systematic variation in chemistry and Nd-Sr isotopes across a Caledonian calc-alkaline volcanic arc: implications for source materials.Earth Planet.Sci.Lett. 58,27-50.

---------,M.F.1983.Discussion on implications for Caledonian plate tectonic models of chemical data from volcanic rocks of the British Old Red Sandstone.Jl geol.Soc.Lond. 140,315-318.

---------,M.F.1983a.Isotope geochemistry and origin of calc-alkaline lavas from a Caledonian continental margin volcanic arc.Jl Volc.Geoth.Res. 18,589-631.

---------,M.F.and BLUCK,B.J.1983.Sr-Nd isotope and chemical evidence that the Ballantrae `ophiolite`,SW Scotland is polygenetic.In GASS,I.G.,LIPPARD,S.J.and SHELTON,A.W.(eds) Ophiolites and Oceanic Lithosphere,Blackwell,Oxford,215-230.

THORPE,R.S.and FRANCIS,P.W.1979.Petrogenetic relationships of volcanic and intrusive rocks of the Andes.In ATHERTON,M.P.and TARNEY,J.(eds) Origin of Granite Batholiths: Geochemical Evidence. Shiva,Cheshire,65-75.

TINDLE,A.G.and PEARCE,J.A.1981.Petrogenetic modelling of in situ

fractional crystallisation in the zoned Loch Doon pluton, Scotland.Contrib.Mineral.Petrol. 78,196-207.

------,A.G.and PEARCE,J.A.1983.Assimilation and partial melting of continental crust: evidence from the mineralogy and geochemistry of autoliths and xenoliths.Lithos 16,185-202.

TRAQUAIR,R.H.1902.Note on the fossil fishes of the Old Red Sandstone of Scotland. In The Geology of Lower Strathspey. Mem.geol.Surv.Gt Br.

UPTON,B.G.J.,ASPEN,P.and HUNTER,R.H.1984.Xenoliths and their implications for the deep geology of the Midland Valley of Scotland and adjacent regions.Trans.R.Soc.Edinb. 75,65-70.

VAN BREEMEN,O.and BLUCK,B.J.1981.Episodic granite plutonism in the Scottish Caledonides.Nature 291,113-117.

--- -------,O.and BOYD,R.1972.A radiometric age for pegmatite cutting the Belhelvie mafic intrusion, Aberdeenshire.Scott. J.Geol. 8,15-120.

--- -------,O.and PIASECKI,M.A.J.1983.The Glen Kyllachy granite and its bearing on the nature of the Caledonian Orogeny in Scotland.Jl geol.Soc.Lond. 140,47-62.

--- -------,O.,AFTALION,M.PANKHURST,R.J.and RICHARDSON,S.W.1979. Age of the Glen Dessary syenite, Inverness-shire: diachronous Palaeozoic metamorphism across the Great Glen.Scott.J.Geol. 15,49-62.

VARNE,R.1985.Ancient subcontinental mantle: a source of K-rich orogenic volcanics.Geology 13,405-408.

VERNIERES,J.,JORON,J.L.,TREUIL,M.,COULON,C.and DUPUT,C.1977. Coefficient de partage de qualques elements en trace entre plagioclase et verre dans les ignimbrites-implications petrogenetiques.Chem.Geol. 19, 309-325.

VERSCHURE,R.H.,ANDRIESSAN,P.A.M.,BOELRIJK,N.A.I.M.,HEBEDA,E.H., MAIJER,C.,PRIEM,H.N.A.and VERDURMEN,E.A.Th.1980.On the thermal stability of Rb-Sr and K-Ar biotite systems: evidence from co-existing Sveconorwegian (c. 870 Myr) and Caledonian (c. 400 Myr) biotites in SW Norway.Contrib.Mineral.Petrol. 74,245-252.

WAGNER,G.A.,REIMER,G.M.and JAGER,E.1977.Cooling ages derived by apatite fission track, mica Rb-Sr and K-Ar dating: the uplift and cooling of the central Alps.Mem.Ist geol.petrol.Univ. Padova 30,1-27.

WALSWORTH-BELL,E.B.1974.Some studies of various Aberdeenshire granitic rocks. Unpub.Ph.D. thesis, Univ.Aberdeen.

WATERSTON,C.D.1965.In CRAIG,G.Y.(ed.) The Geology of Scotland Oliver and Boyd, Edinburgh. pp270-310.

WATSON,E.B.1976.Two liquid partition coefficients: experimental data and geochemical implications.Contrib.Mineral.Petrol. 56,119-134.

------,E.B. and CAPOBIANCO,1981.Phosphorous and the rare earth elements in felsic magmas: an assessment of the role of apatite.Geochim.cosmochim.Acta 45,2349-2358.

WATSON,J.V.1984.The ending of the Caledonian orogeny in Scotland. Jl geol.Soc.Lond. 141,193-214.

WEAVER,B.L.and TARNEY,J.1981.Lewisian gneiss geochemistry and Archaean crustal development models.Earth Planet.Sci.Lett. 55, 172.

WESTOLL,T.S.1945.A new cephalaspid fish from the Downtonian of Scotland, with notes on the structure and classification of ostracoderms. Trans.R.Soc.Edinb. 61,341-357.

-------,T.S.1951.The vertebrate-bearing strata of Scotland. Rep.XVIII Int.geol.Congr.Gt Br. 11,5-21.

-------,T.S.1977.Northern Britain.In HOUSE,M.R.,RICHARDSON,J.B., CHALONER,W.G.,ALLEN,J.R.L.,HOLLAND,C.H.and WESTOLL.T.S. A correlation of the Devonian Rocks of the British Isles.Geol. Soc.Lond.,Special Report 8,110pp.

WHALEN,J.G.1983.The Ackley City batholith, southern Newfoundland: evidence for liquid-state fractionation.Geochim.cosmochim.Acta 47,1443-1458.

WHALEN,J.B.,CURRIE,K.L.and VAN BREEMEN,O.(in press).Episodic Ordovician-Silurian plutonism in the Topsails igneous terrane, western Newfoundland.

WHITE,A.J.R.and CHAPPELL,B.W.1977.Ultrametamorphism and granitoid genesis.Tectonophys. 43,7-22.

-----,A.J.R.and CHAPPELL,B.W.1983.Granitoid types and their distribution in the Lachlan Fold Belt, southeastern Australia. In RODDICK,J.A.(ed.) Circum-Pacific Plutonic Terranes Mem. geol.Soc.Am. 159.

WILSHIRE,H.G.1959.Deuteric alteration of volcanic rocks.J.Proc. R.Soc.N.S.W. 93,105-120.

WILSON,A.C.1971.Lower Devonian sedimentation in the north-west

Midland Valley of Scotland. Univ.Glasgow Ph.D.Thesis (unpub.)

------,A.C.1980.The Devonian sedimentation and tectonism of a rapidly subsiding, semi-arid fluvial basin in the Midland Valley of Scotland.Scott.J.Geol. 16,291-313.

WINCHESTER,J.A.,LAMBERT,R.ST.J.and HOLLAND,J.G.1981.Geochemistry of the western part of the Moinian Assemblage.Scott.J.Geol. 17,281-294.

WINKLER,H.G.F.1979.Petrogenesis of Metamorphic Rocks. Springer-Verlag, New York.344pp.

-------,H.G.F.and BREIBART,R.1978.New aspects of granitic magmas. Neues Jahrb.Mineral.Monatsch. 10,463-480.

-------,H.G.F.,BOESE,M.and MARCOPOULOS,T.1975.Low temperature granitic melts.Neues Jb.Miner.Mh. 6,245-268.

WRIGHT,A.E. and BOWES,D.R.1979.Geochemistry of the appinite suite.In HARRIS,A.L.,HOLLAND,C.H.,and LEAKE,B.E.(eds) The Caledonides of the British Isles - reviewed.Spec.Publ.geol. Soc.Lond.8,699-703.

YORK,D.1969.Least squares fitting of a straight line with correlated errors.Earth Planet.Sci.Lett. 5,320-324.

ZARTMAN,R.E.1974.Lead isotope provinces in the Cordillera of the western United States and their geological significance.Econ. Geol. 69,792-805.

ZARTMAN,R.E.and DOE,B.R.1981.Plumbotectonics - the model. Tectonophys. 75,135-162.

ZEITLER,P.K.,JOHNSON,N.M.,NAESER,C.W.and TAHIRKHEL,I.1982. Fission-track evidence for Quarternary uplift of the Nanga Parbat region, Pakistan.Nature 298,255.

ZHOU,J.1985.The timing of calc-alkaline magmatism in parts of the Alpine-Himalayan collision zone and its relevance to the interpretation of Caledonian magmatism.Jl geol.Soc.Lond. 142,309-317.

ZINDLER,A.,HART,S.R.,FREY,F.A.and JACOBSEN,S.P.1979.Nd and Sr isotope ratios and rare earth element abundances in Reykjanes Peninsula basalts: evidence for mantle heterogeneity beneath Iceland.Earth Planet Sci.Lett. 45,249-262.

ZINGG,Th.1935.Beitrage zur Schotteranalyse.Schweizerische Mineralogische u. Petrographische Mitt. 15,39-140.

APPENDIX 1

SAMPLE INDEX

A1.1 SOUTHERLY DERIVED GRANITE AND VOLCANIC CLASTS

SAMPLE	CODE	DERIVATION	LOCALITY	GRID REFERENCE
4237	G1-B	S	WHITEHOUSE SOUTH	NO 82277021
4278	G1-A	S	GOURDON EAST	NO 83257090
4286	G1-A	SE	KINGS STEP	NO 84477297
4366	G1-A	S	YELLOW ARK	NO 84647326
4369	G1-A	S	LITTLE JOHNSHAVEN	NO 85547526
4371	G1-A	S	LITTLE JOHNSHAVEN	NO 85547526
4382	G1-B	S	YELLOW ARK	NO 84627323
4383	G1-B	S	YELLOW ARK	NO 84667328
4392	G1-A	S	YELLOW ARK	NO 84577323
4395	G1-A	S	YELLOW ARK	NO 84577323
4398	G1-A	SE	RICH MADAM	NO 84517301
4230	G2	SE	KINGS STEP	NO 84487294
4232	G2	SE	KINGS STEP	NO 84487294
4282	G2	SE	KINGS STEP	NO 84487297
4311	G2	SE	KINGS STEP	NO 84487294
4321A	G2	SE	KINGS STEP	NO 84487297
4328	G2	SE	KINGS STEP	NO 84307273
4363	G2	S	LITTLE JOHNSHAVEN	NO 85527427
4373	G2	S	LITTLE JOHNSHAVEN	NO 85527428
4374	G2	S	LITTLE JOHNSHAVEN	NO 85527427
4375	G2	S	LITTLE JOHNSHAVEN	NO 85527426
4376	G2	S	YELLOW ARK	NO 84697347
4377	G2	S	YELLOW ARK	NO 84697347
4378	G2	S	YELLOW ARK	NO 84577323
4391	G2	S	YELLOW ARK	NO 84577323
4393	G2	S	YELLOW ARK	NO 84577323
4397	G2	SE	RICH MADAM	NO 84517301
4384	G2	S	YELLOW ARK	NO 84677330
4386	G2	S	YELLOW ARK	NO 84677330
4314	G2	SE	KINGS STEP	NO 84467294
4254	G2X	S	GOURDON EAST	NO 83257090

4242	G3	S	WHITEHOUSE SOUTH	NO 82287014
4243	G3	S	WHITEHOUSE SOUTH	NO 82287014
4275	G3X	S	GOURDON EAST	NO 83087085
4280	G3	SE	KINGS STEP	NO 84487298
4281	G3	SE	KINGS STEP	NO 84487298
4285	G3	SE	KINGS STEP	NO 84487298
4315	G3	E	KINGS STEP	NO 84447295
4316	G3	SE	KINGS STEP	NO 84457293
4322	G3	SE	KINGS STEP	NO 84447295
4325	G3	S	BERVIE MOUTH	NO 83657242
4329	G3X	S	KINGS STEP	NO 84307269
4335	G3	S	WHITEHOUSE NORTH	NO 82427052
4350	G3	SE	KINGS STEP	NO 84457293
4364	G3	S	YELLOW ARK	NO 84667327
4365	G3	S	YELLOW ARK	NO 84667327
4368	G3	S	LITTLE JOHNSHAVEN	NO 85577428
4370	G3	S	LITTLE JOHNSHAVEN	NO 85577429
4379	G3	S	YELLOW ARK	NO 84587323
4380	G3	S	YELLOW ARK	NO 84587323
4381	G3	S	YELLOW ARK	NO 84877323
4385	G3	S	YELLOW ARK	NO 84677330
4386A	G3	S	YELLOW ARK	NO 84647328
4388	G3	S	YELLOW ARK	NO 84647328
4389	G3	S	YELLOW ARK	NO 84667329
4390	G3	S	YELLOW ARK	NO 84587323
4394	G3	S	YELLOW ARK	NO 84587323
4396	G3	S	YELLOW ARK	NO 84587323
4462	G3	S	YELLOW ARK	NO 84677332
4312	G3b	SE	KINGS STEP	NO 84487297
4313	G3b	SE	KINGS STEP	NO 84487297
4321	G3b	SE	KINGS STEP	NO 84477292
4279	G4	SE	KINGS STEP	NO 84477292
4231	Vs	SE	KINGS STEP	NO 84447297
4283	Vs	SE	KINGS STEP	NO 84467292
4284	Vs	SE	KINGS STEP	NO 84457292
4288	Vs	SE	KINGS STEP	NO 84457292
4289	Vs	-	KINGS STEP	NO 84387292

4318	Vs	SE	KINGS STEP	NO 84467292
4327	Vs	-	KINGS STEP	NO 84317275
4330	Vs	-	KINGS STEP	NO 84317275
4331	Vs	-	KINGS STEP	NO 84357275
4332	Vs	-	KINGS STEP	NO 84357275
4399	Vs	SE	RICH MADAM	NO 84517302
4400	Vs	SE	RICH MADAM	NO 84517302
4401	Vs	SE	RICH MADAM	NO 84517302
4402	Vs	SE	RICH MADAM	NO 84517302
4403	Vs	SE	RICH MADAM	NO 84517302
4458	Vs	-	KINGS STEP	NO 84587299
4461	Vs	-	KINGS STEP	NO 84317287
4464	Vs	-	YELLOW ARK	NO 84677332
4465	Vs	-	YELLOW ARK	NO 8467732
4477	Vs	-	YELLOW ARK	NO 8467732
4480	Vs	?NE	LITTLE JOHNSHAVEN	NO 85547429
4482	Vs	SE	KINNEFF	NO 85727454
4485	Vs	-	KINNEFF	NO 85727465

A1.2 NORTHERLY DERIVED GRANITE AND VOLCANIC CLASTS

SAMPLE	CODE	DERIVATION	LOCALITY	GRID REFERENCE
3134	G_1	N	CRAWTON	NO 88087978
3142	G_1	N	CRAWTON	NO 88087978
3152	G_1	N	CRAWTON	NO 87927960
3156	G_1	N	CRAWTON	NO 88087978
3158	G_1	N	WHISTLEBERRY	NO 86127525
3220	G_1	N	CRAWTON	NO 88067976
3301	G_1	N	CRAWTON	NO 87927958
3305	G_1	N	CRAWTON	NO 87927958
3306	G_1	N	CRAWTON	NO 87927958
3307	G_1	N	CRAWTON	NO 87927958
2177	G_{2A}	NE	CASTLEHAVEN BAY	NO 88088430
2180	G_{2A}	NE	CASTLEHAVEN BAY	NO 88088430
2215	G_{2A}	NE	BOWDUN ROCKS	NO 88448445
2454-2	G_{2A}	NE	BOWDUN ROCKS	NO 88418449
2455	G_{2A}	NE	BOWDUN ROCKS	NO 88438447
2473	G_{2A}	NE	BOWDUN ROCKS	NO 88438441
2475	G_{2A}	NE	BOWDUN ROCKS	NO 88448442
2475A	G_{2A}	NE	BOWDUN ROCKS	NO 88448442
2130	G_{2B}	NE	BOWDUN ROCKS	NO 88438451
3137	G_{2B}	N	CRAWTON	NO 88087978
3244	G_{2B}	N	WHITEHOUSE	NO 82377036
4272BR	G_{2B}	NE	BOWDUN ROCKS	NO 88408440
3309	G_{2B}	N	CRAWTON	NO 87927958
3422	G_{2B}	NE	TODHEAD	NO 86957679
3423	G_{2B}	NE	TODHEAD	NO 86957679
3424	G_{2B}	NE	TODHEAD	NO 86957679
3304	G_{2C}	N	CRAWTON	NO 87927958
2467	G_{2C}	NE	OLDHALL BAY	NO 88048369
2109	G_3	NE	STRATHLETHAN BAY	NO 88248460
2160	G_3	NE	DOWNIE POINT	NO 88278529
2162	G_3	NE	DOWNIE POINT	NO 88278529
2181	G_3	NE	DOWNIE POINT	NO 88278529

3132	G_4	N	CRAWTON	NO 88077978
3138	G_4	N	CRAWTON	NO 88077978
3144	G_4	N	CRAWTON	NO 88077978
3185	G_4	N	WHITEHOUSE	NO 82387041
3199	G_4	N	WHITEHOUSE	NO 82387041
3200	G_4	N	WHITEHOUSE	NO 82367036
3219	G_5	N	WHITEHOUSE	NO 83377034
2112	G_6	NE	BOWDUN ROCKS	NO 88438448
3155	G_6	N	CRAWTON	NO 88077977
3159	G_6	N	WHISTLEBERRY	NO 86127525
2129	G_7	NE	BOWDUN ROCKS	NO 88448430
2178	G_7	NE	CASTLEHAVEN BAY	NO 88088430
3436	G_7	N	TODHEAD	NO 86847657
2445	G_7	NE	BOWDUN ROCKS	NO 88418451
2449	G_7	NE	BOWDUN ROCKS	NO 88428445
2450	G_7	NE	BOWDUN ROCKS	NO 88418451
2451	G_7	NE	BOWDUN ROCKS	NO 88418451
2457	G_7	NE	BOWDUN ROCKS	NO 88438448
2474	G_7	NE	BOWDUN ROCKS	NO 88438443
2179	G_{7B}	NE	CASTLEHAVEN BAY	NO 88088432
3421	G_8	N	TODHEAD	NO 86957679
3435	G_8	N	TODHEAD	NO 86847657
2468	G_9	N	OLDHALL BAY	NO 88028363
2476	G_9	NE	BOWDUN ROCKS	NO 88458444
3187	G_{10}	N	WHITEHOUSE	NO 82387037
3193	G_{10}	N	WHITEHOUSE	NO 82387040
3194	G_{10}	N	WHITEHOUSE	NO 82387040
2118		N	TREMUDA BAY	NO 88088310
2171		NE	DOWNIE POINT	NO 88278529
2470		NE	OLDHALL BAY	NO 88028367

2101	V_N	-	STRATHLETHAN BAY	NO 88208461
2102	V_N	-	STRATHLETHAN BAY	NO 88208461
2106	V_N	-	STRATHLETHAN BAY	NO 88228462
2183	V_N	NE	DOWNIE POINT	NO 88278528
2208	V_N	-	STRATHLETHAN BAY	NO 88208461
2210	V_N	-	STRATHLETHAN BAY	NO 88208461
2466	V_N	-	OLDHALL BAY	NO 88028362
2469	V_N	-	OLDHALL BAY	NO 88018362
2471	V_N	-	OLDHALL BAY	NO 88018362
2472	V_N	-	OLDHALL BAY	NO 88018362

A1.3 SEDIMENTARY AND METASEDIMENTARY CLASTS

SAMPLE	CODE	DERIVATION	LOCALITY	GRID REFERENCE
4405	S1	-	ROUEN BAY	NO 86467592
4406	S1	-	ROUEN BAY	NO 86447589
4407	S1	-	ROUEN BAY	NO 86447589
4408	S1	-	ROUEN BAY	NO 86447589
4409	S1	?N	BURIAN HOLE	NO 86397569
4410	S1	?N	BURIAN HOLE	NO 86397569
4412	S1	-	GREEN HEUGH	NO 86267537
4413	S1	-	GREEN HEUGH	NO 86267537
4415	S1	-	GREEN HEUGH	NO 86267537
4416	S1	-	POWDAM HEAD	NO 86707633
4417	S1	-	POWDAM HEAD	NO 86707633
4418	S1	-	POWDAM HEAD	NO 86627618
4419	S1	-	POWDAM HEAD	NO 86677624
4420B	S1	-	POWDAM HEAD	NO 86717629
2117		NE	BOWDUN ROCKS	NO 88418448
2125	S2	N	OLDHALL BAY	NO 88048366
2126	S2	N	OLDHALL BAY	NO 88048366
3139	S2	N	CRAWTON	NO 88077974
3141	S2	N	CRAWTON	NO 88077976
3144A	S2	N	CRAWTON	NO 88077976
3149	S2	N	CRAWTON	NO 87897961
3150	S2	N	CRAWTON	NO 87897961
2163	S2	NE	DOWNIE POINT	NO 88278529
3188	S2	N	WHITEHOUSE	NO 82397038
3190	S2	N	WHITEHOUSE	NO 82397038
3191	S2	N	WHITEHOUSE	NO 82397038
3192	S2	N	WHITEHOUSE	NO 82397038
3195	S2	N	WHITEHOUSE	NO 82397038
3196	S2	N	WHITEHOUSE	NO 82257005
3197	S2	N	WHITEHOUSE	NO 82257005
3201	S2	N	CRAWTON	NO 88007983
3202	S2	N	CRAWTON	NO 88007983
3204	S2	N	CRAWTON	NO 88007983
3303	S2	N	CRAWTON	NO 88007983

3145	S3(LA)	NE	CRAWTON	NO 88077976
4238	S3(LA)	S	WHITEHOUSE	NO 82257015
4264	S3(LA)	S	GOURDON EAST	NO 83207075
4271	S3(LA)	S	GOURDON EAST	NO 83207075
4273	S3(LA)	S	GOURDON EAST	NO 83207075
4484	S3(LA)	S	KINNEFF	NO 85647454
4488	S3(LA)	S	BERVIE MOUTH	NO 83737240
4491	S3(LA)	SE	KINGS STEP	NO 84447293
4492	S3(LA)	SE	KINGS STEP	NO 84447293
4495	S3(LA)	S	GOURDON EAST	NO 83487090
4255	S3(mG)	S	GOURDON EAST	NO 83207075
4260	S3(mG)	S	GOURDON EAST	NO 83207075
4261	S3(mG)	S	GOURDON EAST	NO 83207075
4319	S3(mG)	SE	KINGS STEP	NO 84447293
4478	S3(mG)	S	LITTLE JOHNSHAVEN	NO 85537429
4479	S3(mG)	S	LITTLE JOHNSHAVEN	NO 85517427
4481	S3(mG)	S	LITTLE JOHNSHAVEN	NO 85427430
4483	S3(mG)	S	KINNEFF	NO 85647454
4487	S3(mG)	S	BERVIE MOUTH	NO 83737240
4490	S3(mG)	SE	KINGS STEP	NO 84447292
4494	S3(mG)	S	GOURDON EAST	NO 83207075
4496	S3(mG)	S	KINGS STEP	NO 84447293
4497	S3(mG)	SE	KINGS STEP	NO 84447293
4459	S3(H)	SE	KINGS STEP	NO 84457295
4460	S3(H)	SE	KINGS STEP	NO 84457295
4473	S3(H)	SE	KINGS STEP	NO 84457295
4498	S3(H)	S	GOURDON EAST	NO 83177085

APPENDIX 2

SAMPLE PREPARATION AND MAJOR AND TRACE ELEMENT ANALYSIS

A2.1 SAMPLE PREPARATION

A2.1.1 Sample preparation procedure for major and trace element analysis

Large (>30cm maximum diameter) clasts were crudely trimmed in the field and brought back to the laboratory intact. They were then reduced to 1kg chunks using a hydraulic rock splitter. Two or three fresh chunks selected from the core of each clast were washed in distilled water prior to reduction to 1cm chips in a tungsten steel jaw crusher. The sample was then cone and quartered and a representative fraction crushed for 4 minutes to 100 mesh (142 μm) in a chalcedony Tema mill. Half of this was bottled and retained for major element analysis, whilst the remainder was further crushed in a chalcedony ball mill for 20 minutes. The resulting 250 mesh (61μm) powder was stored for use in trace element analysis. The quality of the powders was checked by periodic seiving. All crushing equipment was flushed out prior to use with a representative sample to reduce the likelihood of passed on contamination.

A2.1.2 Sample preparation for isotopic analysis

Between 5 and 10 kg of sample was used for whole rock-mineral analysis. This was selected from the core of clasts which had maximum diameters >40cm and which were free of fractures. Both sample preparation and mineral separating were performed using facilities at SURRC, East Kilbride. The sample was initially reduced to 1-2 kg chunks using a hydraulic splitter. These were washed in distilled water and coarse crushed to chips in a tungsten steel jaw crusher. The sample was then quartered and a fraction further ground for 30 seconds in a Tema-mill. The resulting powder was thoroughly washed in water and acetone to remove fine clays and then sieved to 100-160 mesh (sometimes 160-215 mesh) using cloth sieves.

Mineral separation was by both conventional heavy liquid/magnetic separation methods and by hand picking under a binocular

microscope. Biotite was separated using tetrabromoethane followed by magnetic separation. In most cases it was possible to separate biotite from the main impurity, amphibole, using fine current and side-slope adjustment of a standard Franz isodynamic magnetic separator. Occasionally, biotite and amphibole had overlapping magnetic susceptibilities and the heavy fraction was returned to heavy liquid, this time methylene iodide, and this was diluted with analar grade acetone until a density separation was achieved. The biotite separate was examined optically under transmitted light for purity. In several cases the initial coarse biotite separate appeared opaque in transmitted light. Thin sections show this to be due to thin opaque films developed along biotite cleavage planes. The biotite separates were recrushed for 10-15 seconds in a small tungsten carbide Tema mill in a suspension of distilled water. They were subsequently thoroughly washed in twice distilled water and analar acetone, and gently dried under a heat lamp. Excessive heating was avoided since it can lead to static problems during subsequent weighing into teflon. The samples were further magnetically purified and re-examined optically in transmitted light. Purity was estimated >98% with most grains translucent. Samples were stored in labelled prewashed glass phials ready for analysis. Chloritisation of biotite is minimal in the rocks under study, but nonetheless, every effort was made to ensure no chlorite appeared in the biotite separates.

Feldspar separates were purified from the light fraction floated off in the initial tetrabromoethane separation. A grain of feldspar from the rock in question and a standard quartz grain were used to dilute the tetrabromoethane liquid, using acetone, to the density required to achieve separation of the two phases. The light fraction was then placed in the diluted heavy liquid and the feldspar fraction either floated or sunk off. The strongly zoned feldspars meant plagioclase densities were quite variable and in several cases two or more fractions were sunk off using progressive dilution of the liquid. K-feldspar was floated from quartz in the three clasts of southerly derived G3 type granite. As the K-feldspar is intergrown with quartz in granophyric intergrowths the separates do contain appreciable

amounts of quartz impurities. All the feldspar separates were thoroughly washed in acetone to remove any trace of heavy liquid and further purified by passing several times through the magnetic separator with low side slope and high current (1.5 amps). This effectively removed all coated grains and any remaining magnetic impurities.

Muscovite was magnetically purified from the light fraction floated off in the initial tetrabromoethane separation. Separates of high purity were achieved for clasts of two-mica granite, but the finer grained muscovites in northerly derived psammitic clasts proved more difficult to separate. Problems with composite grains required recrushing of the separate in the case of 3195, and pure muscovite separates could not be achieved for samples 3192 and 3201. The low K_2O content of the muscovite for 3195 (Table 6.5) suggests sample purity may be poor.

All heavy liquid was recycled by reclaiming liquid from acetone washings. The liquid was filtered twice before use through Whatman`s No.1 or No.4 filter paper, and once after use. Heavy liquid separations were performed in a customised separating funnel with a ground glass tap. It was therefore unnecessary to use grease which can be dissolved by, and contaminate the heavy liquids.

A2.2 MAJOR AND TRACE ELEMENT GEOCHEMISTRY

A2.2.1 Method

Ten major (SiO_2, TiO_2, Al_2O_3, $Fe_2O_3{}^t$, MnO, MgO, CaO, Na_2O, K_2O, P_2O_5) and sixteen trace elements (Ba, Ce, Co, Cr, Cu, Ga, La, Ni, Pb, Rb, Sr, Th, Y, Zn, Zr and U) were determined for all samples by X-ray flourescence analysis (XRF). In addition, Nb was measured for selected samples. The major elements were determined on fused beads made from dehydrated rock powder (<142 μm) and a lithium tetraborate flux (Spectraflux 105). The flux and rock powder were combined in a weight ratio of 1:5.3 and fused in a platinum-gold crucible. The weight prior to and following fusion for 20 minutes in a furnace at 1000°C was used to calculate the percentage loss on ignition (LOI). This approximates to the volatile content and was used in lieu of H_2O and CO_2 measurements in totalling the data to 100%. The trace elements were measured on pressed powder pellets comprising a thoroughly homogenised mixture of the rock powder (<61μm) and a thermal binder (phenol formaldehyde) in a weight ratio of 6:1.

All major and trace elements were analysed using a Philips PW1450 sequential automatic X-ray spectrometer. Major element analyses were made on duplicate beads and were subsequently averaged. The method follows that of Harvey et al. (1972). Peak-background measurements for each element were ratioed against a standard monitor pellet, and absolute concentrations calculated with reference to internal and international calibration standards. The calculation of absolute abundances and the conversion to weight percent oxide were performed by an on-line Superbrain microcomputer using a program devised by C.Farrow. Trace elements were determined following the methods of Leake et al. (1969) using the Compton peak ratio to correct for absorption and matrix effects. FeO determinations for representative samples were made by titration against standard dichromate solution after dissolution of the whole rock in sulphuric and hydrofluoric acids.

A2.2.2 Analytical Precision

Five internal (Glasgow) standards were continuously monitored

during major and trace element analysis. These allow a check on data quality and reproducibility. The means and standard deviations of trace element analyses obtained for these standards during the period of the present study are shown in Table A2.2. In addition duplicate major element analyses for each of the samples indicate the level of uncertainty introduced during bead and pellet preparation. K_2O and Na_2O have been independently determined by a `wet chemical` procedure for several representative samples, with good agreement between the two techniques.

Rb and Sr have been determined by isotope dilution analysis. Rb and Sr concentrations obtained by isotope dilution are compared with those measured by X-ray flourescence in Table A2.1. There is generally a good agreement between the two methods. Slight discrepancies may reflect the fact that the isotopic determinations were made on non-dehydrated rock powders. The whole rock powders analysed in the case of samples from which mineral phases were separated were independently crushed, and it is possible slight heterogeneity may contribute to small differences in XRF and isotope dilution results for these samples.

The sum of the major element oxides and LOI values mostly fall in the range 99-101%. The few analyses which fell substantially outside this range, or for which the replicate analyses showed a poor agreement, were re-analysed.

The wet chemical determinations for FeO show good agreement between replicates and reproduced standard values.

SAMPLE	RbXRF ppm	RbID ppm	SrXRF ppm	SrID ppm
3309	123	122.2	419	409.5
3304	88	84.6	443	414.4
3137	115	113.5	407	401.9
3219	121	127.1	98	88.9
3132	155	155.6	48	42.4
3138	163	162.1	53	46.4
3185	151	145.4	42	37.8
3200	164	155.2	51	48.9
3134	213	188.7	95	83.8
3220	206	218.5	95	91.4
3152	136	155.9	166	158.0
4261	53	49.1	54	54.0
4260	56	55.1	60	59.4
4255	49	44.0	57	54.4
4238	29	26.0	87	83.8
4273	43	40.1	76	70.1
4264	48	45.6	78	76.4
4271	59	55.7	57	54.0
4319	32	30.0	101	104.2
3192	29	26.0	126	124.1
3195	37	35.2	151	153.1
3201	44	38.0	193	183.9
3150	53	59.3	158	129.5
4237	33	30.6	477	475.3
4382	30	26.6	461	464.1
4383	57	55.3	478	479.3
4278	34	32.7	449	461.6
4366	29	27.3	531	518.2
4392	28	25.8	468	482.5
4286	38	36.1	493	487.9
4311	94	99.3	446	456.9
4282	91	92.9	414	432.1

TABLE A2.1 Comparison of XRF and isotope dilution analyses for Rb and Sr concentrations. (contd overleaf)

SAMPLE	RbXRF ppm	RbID ppm	SrXRF ppm	SrID ppm
4314	73	70.9	449	443.6
4321a	80	80.5	451	451.7
4232	69	65.0	403	407.5
4393	84	83.3	424	424.2
4378	89	88.0	427	430.4
4242	81	80.1	502	523.5
4329	89	84.2	559	577.3
4462	98	95.6	590	576.6
4281	85	85.7	515	526.6
4280	104	102.0	532	534.8
4243	81	79.5	567	571.5
4322	76	74.3	537	547.0
4328	59	56.9	470	474.2
4279	121	122.5	138	140.5

TABLE A2.1 contd.

Table A2.2 Internal standard pellets replicated during period of present study.

	σ	$\bar{x}$	n
7500			
Ba	27.9	1260.5	24
Ce	2.40	36.21	24
Co	1.56	1.125	24
Cr	1.1	15.6	24
Cu	1.7	5.8	25
Ga	1.1	18	25
La	3.85	22.7	24
Ni	1.6	5.9	25
Pb	2.2	23.6	25
Rb	1.6	79	25
Sr	11.6	881.2	25
Th	1.72	7.2	25
U	0.91	2	25
Y	0.84	8.84	25
Zn	1.43	29	25
Zr	4.42	140.6	25
7510			
Ba	14.2	599.5	24
Ce	2.75	22.4	24
Co	1.75	3.84	24
Cr	2.85	135.0	24
Cu	2.0	8.1	27
Ga	1.0	15.5	27
La	3.0	13.5	24
Ni	2.2	43.6	27
Pb	1.9	4.3	27
Rb	0.89	27.9	27
Sr	5.3	308	27
Th	1.4	1.5	27
U	0.92	1.3	27
Y	0.92	7.5	27
Zn	2.4	25.7	27
Zr	3.0	112.0	27

Table A2.2 contd.

	σ	$\bar{x}$	n
7520			
Ba	16.9	446	25
Ce	4.9	101	25
Co	0.5	0.1	25
Cr	-	-	-
Cu	-	-	-
Ga	1.3	21.8	27
La	4.4	54	25
Ni	1.8	3.3	27
Pb	1.9	6.8	27
Rb	2.0	102.9	27
Sr	1.2	41	27
Th	1.5	8.4	27
U	0.9	2.9	27
Y	1.2	39.6	27
Zn	1.4	41.7	27
Zr	9.7	516.6	27
7530			
Ba	26.4	787.3	22
Ce	6.4	95.8	22
Co	3.8	33.8	22
cr	2.4	17.1	22
Cu	3.0	21.5	23
Ga	2.0	22.0	23
La	6.0	49.8	22
Ni	6.7	20.1	23
Pb	2.9	6.9	23
Rb	0.9	26.7	23
Sr	7.2	545.8	23
Th	1.8	2.6	23
U	1.2	1.5	23
Y	1.2	43.8	23
Zn	3.6	127.6	23
Zr	4.4	268.0	23

Table A2.2 contd.

7540

	σ	$\bar{x}$	n
Ba	25.6	662.7	15
Ce	4.3	48.4	15
Co	2.3	34.8	15
Cr	2.9	26.0	15
Cu	3.8	105.9	18
Ga	1.7	21.6	18
La	3.8	27.8	15
Ni	3.2	49.8	18
Pb	1.7	2.3	18
Rb	1.5	37.8	18
Sr	13.2	606.7	18
Th	1.5	1.4	18
U	0.7	1.2	18
Y	1.2	30	18
Zn	2.1	84.8	18
Zr	4.3	156.5	18

APPENDIX 3
METHODS OF ISOTOPIC ANALYSIS

A3.1 STRONTIUM ISOTOPES

A3.1.1 Chemistry

Rb and Sr concentrations were determined by isotope dilution. Aliquots of the samples (typically 0.05-0.1g) and ^{87}Rb and ^{84}Sr enriched spike solutions were accurately weighed (to 0.01mg) into teflon beakers or PFA screw-top vessels. The amount of spike added was determined by the Rb and Sr abundances in the sample or mineral separate analysed. Considerable static problems, particularly with mica separates, were overcome by using an anti-static gun, and by wrapping vessels and spike bottles in aluminium foil during weighing. Dissolution and isotopic equilibration were achieved by treatment with HF (Merck Suprapur) followed by HNO_3 and HCl dissolutions. All were performed on a hot-plate at 150-200°C.

Separation of Rb and Sr was by elution through cation exchange columns containing AGI-X8 (200-400 mesh) resin, using 2.5N HCl as the eluting agent. Sample solutions were checked for complete solution before centrafugation and loading on the columns. The Rb and Sr cuts were collected in teflon beakers, dried down either on a hot plate, or under evaporators, and stored for a short time prior to mass spectrometry.

All operations, apart from initial weighing and spiking, were performed in a clean-air laboratory. All acids used in the isotope dilution (apart from the HF) were twice distilled analar grade, where necessary diluted by the addition of twice pyrex distilled H_2O. Blank Sr levels in the various reagents are periodically checked by isotope dilution. Blanks and international NBS standards were also included in the batches of samples processed through the chemical procedure. All teflon and PFA lab-ware was rigorously cleaned between samples by boiling in 50% HNO_3 followed by 50% HCl and finally twice distilled H_2O.

A3.1.2 Mass Spectrometry

Sr was loaded as a phosphate on a single tantalum filament bead, and Rb as a chloride on one side of a triple-filament assembly. Mass analyses were performed on both MM30B and Isomass 54E mass spectrometers at SURRC, East Kilbride. Greater than 90% of the Sr analyses were made on the MM30B machine, a semi-automated mass-spectrometer incorporating a 30cm tube, and a VGCA2 collector amplifier and digital integrator connected initially to an on-line Nova 3 mini-computer, but in the latter part of the study, to a digital Rainbow 100 microcomputer. Computer programs controlling the magnet switching routines, peak centring and on-line data processing were devised by J.Hutchinson.

Five peaks and a zero mass (89.5) were collected during each mass scan for Sr. The collecting order was normally 86, 87, 88, 84, 85, 89.5. The peak sequence is scanned ten times and the mean 87/86 ratio and percentage error printed for each set. Machine fractionation is corrected for by normalising the 87/86 ratio against a standard 88/86 ratio of 8.37521. At least 30 sets of data were normally collected, with the run proceeding until the target precision of 0.00002 (1σ) was approached. The 85 peak was used to monitor Rb contamination early in the run allowing the 87/86 to be modified accordingly. Rb has only two natural isotopes, 85 and 87, and it is therefore impossible to correct for machine fractionation during analysis. The effect of fractionation has therefore to be minimised by running at the lowest possible temperature, and by rejecting analyses which systematically drift.

During the latter part of the present study the data collecting routine during Sr mass analysis on the MM30B was modified to accommodate a significant divergence in mass ratios measured in up and down mass directions. Both up- and down-mass peak scans were subsequently incorporated in the data collection routine and the $^{87}Sr/^{86}Sr$ ratio calculated from the combined up- and down-mass scans.

A3.1.3 Analytical precision

Blanks analysed during the present study were less than 5ug for

Rb and Sr and no blank corrections were made on any of the presented analyses. Internal laboratory precision is checked by regular measurement of standards 86035, NBS607 and NBS981. Isotopic results for the standards NBS607 and 86035 determined in the course of the present study are shown in Table A3.1, together with average standard measurements compiled from several operators over the same period.

Replicate and standard analyses are used to estimate the reproducibility of the isotopic determinations, and hence the experimental errors assigned to the points used in the isochron regressions. Blanket errors of 0.5% for $^{87}Rb/^{86}Sr$ and 0.01% for $^{87}Sr/^{86}Sr$ are adopted in this study in calculating the regression parameters. Whilst individual errors on each analysis are considerably better than this, the blanket errors encompass possible errors introduced during the isotope dilution procedure and are therefore considered to be more realistic. The isochron regression procedure used is that of York (1969) with errors expressed at the 2σ level. The scatter about the regression line is measured by the MSWD parameter, the mean square of the weighted deviates (equivalent to SUMS/n-2 where n = no. of points. Brooks et al. 1972). A value close to unity for MSWD indicates that all observed scatter about the isochron can be accounted for in terms of analytical uncertainty inherent in the data. A value significantly greater than unity would indicate real geologic scatter. The decay constant used in all calculations is $\lambda^{87}Rb = 1.42 \times 10^{-11} y^{-1}$.

STANDARDS ANALYSED DURING PERIOD OF STUDY

86035A (EAST KILBRIDE INTERNAL WHOLE ROCK STANDARD)

	Rb(ppm)	Sr(ppm)	$^{87}Rb/^{86}Sr$	$^{87}Sr/^{86}Sr$
86035A-1	223.1	19.4	35.1255	1.27996
86035A-2	225.1	19.5	35.2630	1.28348
86035A-3	223.6	19.3	35.3359	1.28042

NBS 607 K-FELDSPAR STANDARD

607-1	513.3	64.1	24.2707	1.20076
607-2	523.3	66.1	24.0142	1.20110
607*			24.06 $\pm$ 0.11	1.2008 $\pm$ 0.0002

*Mean NBS 607 (n=9) by various operators during period October 1983 to October 1985.

Errors are 2σ.

The mean NBS 987 $^{87}Sr/^{86}Sr$ during the period of study was 0.710296 $\pm$ 14 (2σ) for nineteen determinations by various operators.

BCR-1 analyses on the Isomass 54E given in Hamilton et al. (1984) yielded $^{143}Nd/^{144}Nd$ ratios of 0.512612 $\pm$ 0.000021 and 0.512642 $\pm$ 0.000015 (2σ).

TABLE A3.1 Isotope standard data.

A3.2 SM-ND ISOTOPIC ANALYSIS

A3.2.1 Chemistry

Aliquots of 0.05g were accurately weighed (to 0.01mg) into pre-washed screw-top PFA vessels. These were digested in HF for 48 hours at 150°C, before they were dried down (under evaporators) and taken up again in twice distilled HNO_3. After a further 24 hours on the hot plate, the solutions were checked for complete dissolution. Each sample was subsequently split into two aliquots, one of which was spiked with ^{145}Nd and ^{149}Sm spike solutions. The spiked aliquots were shaken and homogenised on a hot plate before both spiked and unspiked aliquots were dried down and converted to chloride.

A two column separation procedure was used for Sm and Nd separation. The rare earth elements (REE) were first separated by conventional cation exchange chromatography using similar columns to those used in the Rb and Sr separation. The REE remain on the columns after elution with 2.5N HCl. They are subsequently recovered with 3N HNO_3. After drying down and conversion to chloride, Sm and Nd were separated from the spiked and unspiked aliquots using dilute hydrochloric acid elution on a bed of PTFE beads coated with Di-2 ethylhexyl phosphate. The technique is similar to that outlined by Richard *et al.* (1976) and Zindler *et al.* (1979).

3.2.2 Mass Spectrometry

All isotope measurements were made using a fully automated V.G. Isomass 54E mass spectrometer. Nd and Sm were run as the metal species on triple filament assemblies loading on Ta side filaments with a Re centre filament. Isotope ratios were corrected for machine discrimination using a standard $^{146}Nd/^{144}Nd$ ratio of 0.7219. The target precision for $^{143}Nd/^{144}Nd$ ratios on unspiked runs was 0.00001 (2σ). Whilst this was not achieved, precisions were generally better than 0.00003 (2σ). Normally 130 sets comprising 10 scans each of the peaks 144, 145, 146 and 143 were collected during unspiked Nd runs. Peaks at masses 140 (Ce) and 138 (Ba) were monitored in order to identify possible peak interference. Mass 147 was also initially measured as a check on

Sm contamination. This was corrected for using a contamination ratio of 4.8763.

Sm and Nd concentrations were determined by isotope dilution. The spiked Sm and Nd runs had target precisions of 0.0001 (2σ). Typically 50 sets of data each comprising 10 scans of masses 147, 149, 152 and 145 were made during Sm isotope dilution runs, whilst masses 143, 145 and 146 were measured during spiked Nd analyses.

A single replicate analysis on sample 4260 was made during the present study. The $^{143}Nd/^{144}Nd$ ratios determined agree within the 2o experimental errors. Analyses of BCR-1 by other operators during the course of this work are included in Table A3.1.